UNIVERSITÀ DEGLI STUDI DI MILANO

Facoltà di Scienze Matematiche, Fisiche e Naturali

Dipartimento di Chimica Organica e Industriale
Corso di Dottorato di Ricerca in Chimica Industriale (XXIII ciclo)
Settore disciplinare: CHIM/06

CHIRAL LEWIS BASES ACTIVATION OF TRICHLOROSILYL DERIVATIVES

Tutor: Prof. Maurizio Benaglia

Co-Tutor: Prof. Laura Maria Raimondi

Coordinatore: Prof. Dominique Roberto

Tesi di Dottorato di

Sergio Rossi

Matr. R07820

Anno Accademico 2009-2010

To my family

INDEX

Introduction

"Chemists – the transformers of matter". This sentence, taken from the book "The Periodic Table" by Primo Levi, well defines one of the major achievements of present day actual chemistry: to provide, in a controlled and economic fashion, valuable products from readily available starting materials.

It is very difficult to define what chemistry actually is. Looking at the past, chemistry must be inevitably connected to alchemy, born in the II century B.C. in Egypt, where the transformations of the matter (the conversion of a metal in another one) were connected to philosophical and esoterism. Only after the introduction of the scientific method and the chemistry revolution that takes place at the end of the XVIII century, modern chemistry began its development, giving day by day a most real and precise structure for the transmutation of the matter.

So, chemistry keeps evolving, new discoveries expand and amplify the interest fields and the employed method. The study of properties and structures of the constituent of the matter (atoms, molecules) and their interactions become the new chemical target: not only the properties and the structures in a static instant, but also in its transformations, that is chemical reactions.

The knowledge of the atomic electronic structure is the basis of chemistry and it is responsible for the transformations of the matter; for these reasons, chemistry can be defined as a "*central science*", because it has connections with many other disciplines, as natural science, physics, material science, biology and geology.

Over the past 10 years, scientific research has been increasingly directed towards the study and application of new chemical processes that were environmental friendly and

less dangerous for human life. This approach, that is currently enjoying a lot of attention, is defined sustainable or, more precisely, "*green chemistry*"**.**

Nowadays it is important to develop a consciousness: chemical consequences are not only limited at the properties of a given molecule or at the efficiency of a given reagent, but they interest also many other aspects about the impact of the environment where these products are employed. That's why, it is important to consider a comprehensive vision of the process of production including not only the application of the products, but also its byproducts and wastes.

Green chemistry then, implies the design of chemical products and processes that reduce or eliminate the use or generation of hazardous substances. *Green chemistry* is applied across the life cycle of a chemical product, including its design, manufacture, and use.[1] To do that, twelve principles are defined:

1. **Prevention**: it is better to prevent waste than to treat or clean up waste after it has been created;
2. **Atom Economy**: synthetic methods should be designed to maximize the incorporation of all materials used in the process into the final product;
3. **Less hazardous chemical syntheses**: wherever practicable, synthetic methods should be designed to use and generate substances that possess little or no toxicity to human health and the environment;
4. **Designing Safer Chemicals**: chemical products should be designed to affect their desired function while minimizing their toxicity.
5. **Safer Solvents and Auxiliaries**: the use of auxiliary substances (e.g., solvents, separation agents, etc.) should be made unnecessary wherever possible and innocuous when used;
6. **Design for Energy Efficiency**: energy requirements of chemical processes should be recognized for their environmental and economic impacts and should be minimized.
7. **Use of Renewable Feedstocks**: a raw material or feedstock should be renewable rather than depleting whenever technically and economically practicable;
8. **Reduce Derivatives**: unnecessary derivatization (use of blocking groups, protection/ deprotection, temporary modification of physical/chemical processes) should be minimized or avoided if possible, because such steps require additional reagents and can generate waste;

9. **Catalysis**: the use of catalytic reagents (as selective as possible) is superior to that of stoichiometric reagents;
10. **Design for Degradation**: chemical products should be designed so that at the end of their function they break down into innocuous degradation products and do not persist in the environment;
11. **Real-time Analysis for Pollution Prevention**: analytical methodologies need to be further developed to allow for real-time, in-process monitoring and control prior to the formation of hazardous substances;
12. **Inherently Safer Chemistry for Accident Prevention**: substances and the form of a substance used in a chemical process should be chosen to minimize the potential for chemical accidents, including releases, explosions, and fires.

It is not so simple to comply with all these principles. In our studies, we focused on the ninth principle, and in particular on the use of stereoselective organic catalysts versus that of the more traditional organometallic catalysis[2]. The organocatalytic approach fulfils many of requirements listed in the twelve principles of the green chemistry. A process based on a catalytic methodology in fact is already "green" by definition, since it is clearly stated that "catalysts are preferable to stoichiometric reagents", because they minimize wastes and increase energy efficiency. Obviously, a catalytic transformation provides the best "atom economy", since the stoichiometric introduction and then removal of stereocontrolling auxiliaries can be avoided, or, at least, minimized[3]. A catalyst often allows to run a reaction in milder experimental conditions, once again improving the efficiency of a process from the economic and energetic point of view. Specifically, organocatalysts may lead to the design of "safer chemicals and products", as expected by modern synthetic chemists, also with the goal to use less hazardous solvents or reaction conditions. The replacement of metal-based catalysts with equally efficient metal-free counterparts is very appealing in view of possible applications in the future of non toxic, low cost, and more environmentally friendly promoters on industrial scale with obvious advantages from the environmental and economic point of view.[4]

In this framework, stereochemical control remain one of the main issues among the problems of control in chemistry. For example, the possibility to synthesize only one out of all the possible stereoisomers of a compound is an essential feature in the pharmaceutical industry, also for economical reasons.

Recent market analysis showed that global revenues from chiral technology soared from $6.63 billion in 2000 to $16.03 billion in 2007, growing at a compound annual rate of 13.4% during that period. Approximately 80% of all products currently in development for the pharmaceutical industry are based on chiral building blocks; as clear demonstration why Chiral Technology has become of fundamental importance not only for pharmaceutical companies.[5]

Today, the number of methods available for high-yielding and stereoselective transformations of organic compounds has increased enormously, and most of the newly introduced reactions are catalytic in nature.

There are many methods to synthesize enantiomerically pure organic compounds and they generally employ transition-metal complexes and enzymes. As a crowning achievement, in 2001 the Nobel Prize in Chemistry was awarded to William R. Knowles and Ryoji Noyori "for their work on chirally catalyzed hydrogenation reactions", and to K. Barry Sharpless "for his work on chirally catalyzed oxidation reactions".

The quite recently published Wiley – VCH book "Asymmetric Catalysis on Industrial Scale"[6] shows the highly competitive head-to-head race between transition metal catalysis and enzymatic catalysis in contemporary industrial production of enantiomerically pure fine chemicals. At the same time, the complementary character of both types of catalyst becomes obvious. In the past, synthetic chemists have scarcely used small organic molecules as catalysts because the few examples of organocatalytic reactions were considered not competitive with the traditional approach.

Today, however, organocatalysis has more advantages than in the past. The discovery of the first organocatalytic reaction is attributed to J. von Liebig, who found, accidentally, that dicyan is transformed into oxamide in the presence of an aqueous solution of acetaldehyde[7]. The term "Organic Catalysts" ("Organische Katalysatoren") was coined in 1932 by the German chemist Wolfgang Langenbeck[8]. In 1912, Bredig and Fiske[9] reported the first asymmetric organocatalytic reaction: the addition of HCN to benzaldehyde was accelerated by the alkaloids quinine and quinidine, thus resulting in cyanohydrins that were enantiomerically enriched and of opposite configuration. Unfortunately, the stereoselectivity of the reaction was less than 10% and therefore insufficient for preparative purposes. Pioneering work by Pracejus et al.[10] in 1960, again using alkaloids as catalysts, afforded a quite remarkable 74% ee in the addition of methanol to phenylmethylketene.

Another landmark reaction in the history of asymmetric organocatalysis is due to Hajos and Wiechert[11] that reported the first highly enantioselective Robinson annulation reaction, carried out by using the simple amino acid L-proline as the catalyst, in the early 1970s. This reaction, that can be catalogued as an intramolecular aldol reaction, allowed the access to some of the key intermediates for the synthesis of natural products, making the organocatalysis competitive with traditional chemistry.

Since then, many other examples of organocatalysis were reported in the literature and during the last few years a change in perspective has occurred: organic molecules could be as highly effective and remarkably enantioselective catalysts as the metal catalysts, that dominated the chemistry of the last century.

Hence, organocatalysis can be considered as a third approach to the catalytic production of enantiomerically pure organic compounds that is situated at the borderline between the transition metal catalysis and enzymatic transformations[12].

But what are the features of an organic catalyst? In this field, chemist have dissenting opinions. One of the first definitions describe the organic catalyst (or organocatalyst) as a purely "organic" molecule, that is composed of (mainly) carbon, hydrogen, nitrogen, oxygen, sulphur and phosphorus. Clearly, this definition is inadequate and incomplete, because does not consider what these molecules are able to do; so, a more recent one defines an organic catalyst as "an organic compound (of relatively low molecular weight and simple structure) capable of promoting a given transformation in substoichiometric quantity".[13] The term "organic" emphasizes the advantages of performing a catalytic reaction under metal-free conditions.

These advantages might include, *inter alia*, the possibility of working in wet solvents and under an aerobic atmosphere, dealing with a stable and robust catalyst, and avoiding the problem of the leaching of a (possibly toxic) metal into the organic product. Because of the absence of transition metals, organocatalytic methods seem to be especially attractive for the preparation of compounds the use of which can't tolerate metal contamination, (e.g. pharmaceutical products) or in processes where the purification and the elimination of metals are one of the main expensive synthetic steps.

Unlike to organometallic catalysts, organic catalysts are usually more stable, more readily available, less expensive and more easily amenable to anchoring on a support, in order to facilitate their recovery and recycling.

These factors contribute to a superior efficiency, avoiding the protection of the substrates and deprotection of the products, and allowing the direct synthesis of structurally complex molecules, even through asymmetric multicomponent reactions[14] including domino,[15] tandem[16] or cascade transformations.[17]

Consequently, it can be anticipated that this methodology will enjoy a relevant role in industry, due to its versatility and its favourable environmental impact.[18]

Several comprehensive publications, that give a full account of the organocatalysis field, are available.[19] Here, in order to show the scope of organocatalysis and its possible synthetic applications, the five different modes of activation by which most organocatalysts work are shown:

- secondary amine catalysis via enamines;
- secondary amine catalysis via iminium ions;
- phase-transfer catalysis;
- nucleophilic catalysis and Brønsted base catalysis;
- hydrogen bonding catalysis.

A description of these five different modes of catalysis and examples of synthetic methods for assembling useful molecules with high enantiomeric purity are discussed below.[20]

Secondary amine catalysis via enamines

The first example of asymmetric enamine catalysis was the above mentioned Robinson annulation reaction (also called Hajos – Parrish – Eder – Sauer – Wiechert reaction, by the names of the authors). In this transformation, proline operates as a bifunctional catalyst: the amine functionality activates the aldol donor molecules by converting them into enamines, whereas the carboxylic acid moiety provides an activation by hydrogen bond to the acceptor, that is the carbonyl electrophile. The activation by formation of an enamine intermediate is reminiscent of that of the Type 1 aldolases[21], metal-free enzymes that also mediate aldol reactions via enamine intermediate. The stereocontrol crucially depends on the formation of a hydrogen bond between the carboxylic group of the catalyst and the oxygen of the electrophile. This elegant asymmetric transformation has proven useful in the synthesis of a variety of steroids and terpenes. The proposed mechanism is shown in Figure 1.[22]

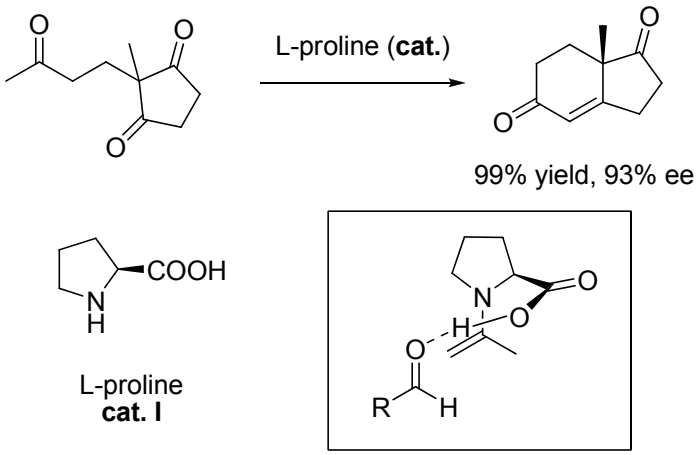

Figure 1: *Hajos – Parrish – Eder – Sauer – Wiechert reaction.*

However, despite the inherent simplicity and huge potentiality of this approach, it took 25 years from this discovery for a new alternative use of proline to be reported. In 2000, List, Barbas and Lerner, followed by other research groups, published proline-catalyzed enantioselective intermolecular aldol reactions (Scheme 1a),[23] Mannich reactions (Scheme 1b)[24] and Michael additions,[25] opening up new areas for enamine catalysis.[26] This approach has also been extended to highly enantioselective α-functionalization of aldehydes and ketones such as amination (Scheme 1c),[27] hydroxylation (Scheme 1d),[28] alkylation (Scheme 1e),[29] chlorination (Scheme 1f)[30] and C-C bond formation by intramolecular Michael reaction (Scheme 1g).[31]

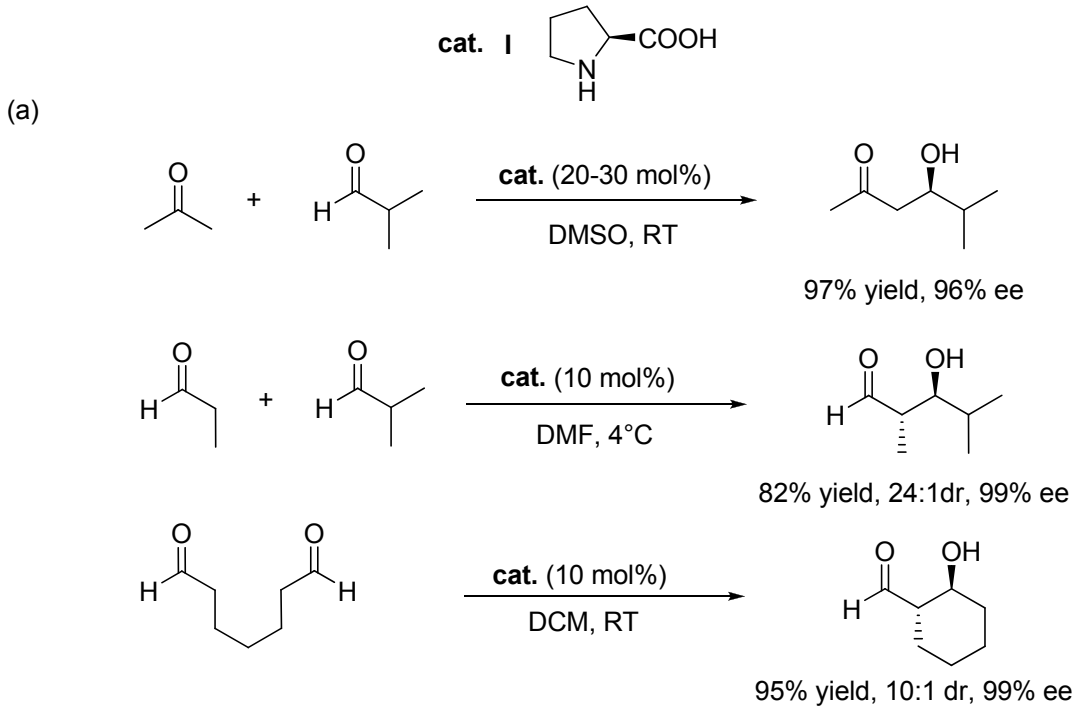

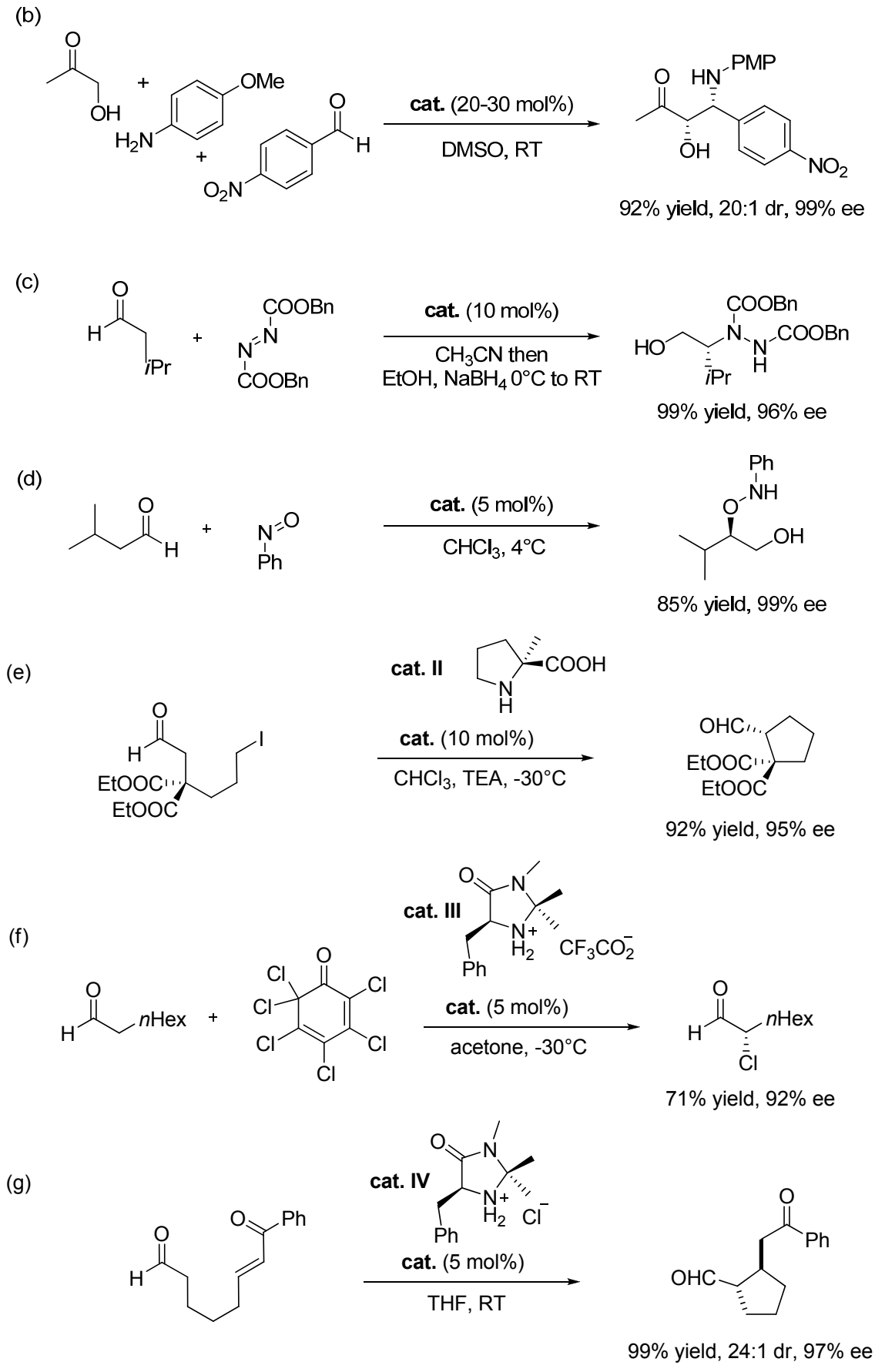

***Scheme 1**: examples enamine catalysis.*

Many processes can be catalyzed via the formation of enamines and not all of them are discussed here. However, it is likely that many processes remain to be discovered. To achieve this, a better understanding of the reactions is essential, especially for the kinetic parameters of the processes, which will help in the design of better catalysts for new and existing strategies.[22]

Secondary amine catalysis via iminium ions

The use of chiral secondary amines as catalysts to activate enals via iminium ion was reported during the late 1990s by MacMillan and co-workers.[32]. The almost simultaneous reporting of the initial proline aldol research and MacMillan's iminium ion catalysis concept, set the scene for an explosion of organocatalytic research over the next years.

This strategy can be considered as an organocatalytic alternative to conventional Lewis acid catalysis of α,β-unsaturated compounds, where mechanistic hypothesis is founded on the reversible formation of an unsaturated iminium ion from a chiral amine catalyst and an α,β-unsaturated carbonyl substrate (figure 2).

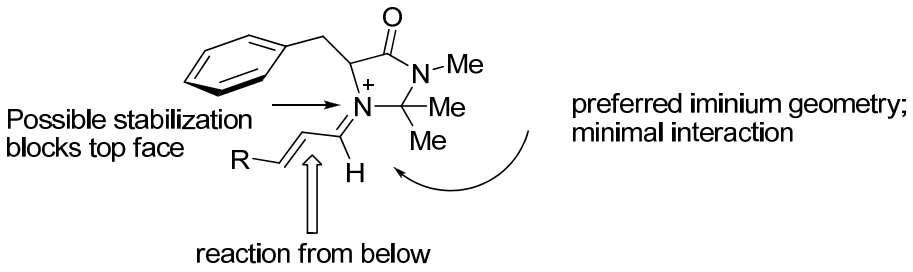

***Figure 2**: proline iminium ion.*

In this way, the energy of the LUMO orbital of the iminium species is lowered, making possible the interaction with suitable coupling partners, through either pericyclic reactions or conjugate addition. The operational simplicity of these processes makes them attractive alternatives to Lewis acid catalysis. The higher reactivity of the iminium ion compared to the carbonyl species is used to promote reactions such as Knoevenagel condensations, cyclo- and nucleophilic additions and cleavage of σ-bonds adjacent to the α-carbon.

The pioneering example of modern iminium catalysis is MacMillan's enantioselective Diels-Alder reaction of α,β-unsaturated aldehydes and ketones with dienes, using the chiral imidazolidinone catalyst (Scheme 2a). The condensation between the α,β-unsaturated aldehydes with the enantiopure amine catalyst leads to the formation of the activated iminium ion with lowered LUMO energy, which reacts with the diene leading to the Diels-Alder adduct.

This type of approach is responsible for numerous highly enantioselective transformations with α,β-unsaturated carbonyl compounds, namely [3+2] cycloaddition of nitrones (up to 98% yields, dr 98:2 and ee 99%),[33] Friedel-Crafts alkylation of pyrroles,[34] indoles,[35] and benzenes (Scheme 2b, up to 97% yields and 99% ee),[36] Mukaiyama-Michael reactions (up to 93% yields and 98% ee),[37] and hydrogenation reactions.[38] Other relatively recent examples involving iminium ion catalysis are the Michael addition of malonates[39] and nitronates[40] to enones, using *L*-proline or a similar catalyst system that presumably activates the enone (Michael acceptor) by forming an iminium intermediate.

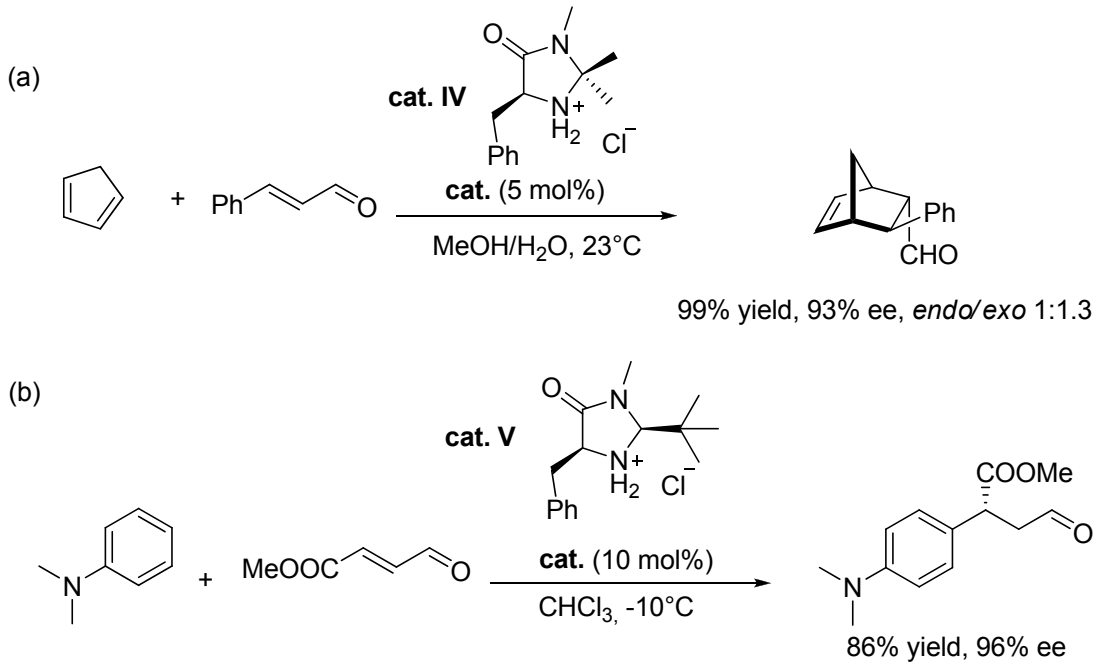

***Scheme 2**: (a) enantioselective Diels-Alder reaction, (b) Friedel-Crafts alkylation.*

Ideally, a process involving the C–C bond formation as part of the iminium and enamine-mediated steps would be a powerful method in synthesis: combining the two catalysis principles in tandem sequences is obviously attractive and worth pursuing. It is clear that tandem sequences can be quite powerful for the generation of molecular

complexity in a simple one-flask operation. In this way, a range of heterocycles can be added to the iminium-activated enal and the resulting enamine intercepted with an electrophilic chlorinating reagent, to form useful aldehydes building blocks. Moreover, a similar process can be performed using a Hantzsch ester conjugate reduction of the iminium species, followed by either chlorination or fluorination: the valuable compounds obtained would be formally the products of asymmetric HCl or HF addition across a C=C double bond.[41] It is difficult to find a comparably simple way to synthesize such molecules using conventional organic and organometallic methods.

Iminium ion catalysis of enals with secondary amines has become a general synthetic paradigm over the past years. Its expansion has accelerated the progression of enantioselective organocatalysis and, although many of the obvious reactions have now been developed, the challenge has been set to design and discover new processes. This exciting area of synthetic chemistry promises the continued development of new and useful methodologies.

Phase-transfer catalysis

Another important class of organic catalysts is represented by phase-transfer catalysts, that can be considered the organic Lewis acids. The use of chiral phase-transfer catalysts has had a major impact on synthesis of unnatural amino acid derivatives via asymmetric alkylation reactions. The first examples of phase-transfer reactions were carried out with quaternary ammonium salts derived from Cinchona alkaloids, but today there is an enormous profusion of structures (both from natural products and fully synthetic) that can be used with good enantioselectivies. Despite significant progress, however, low reactivity (in particular at low temperature), as well as substrate incompatibility, are commonly encountered problems. Derivatives of the Cinchona alkaloids that don't present these problems are Cinchonium salts. These compounds can be considered as the first efficient phase-transfer asymmetric catalysts: in fact, the majority of the most recent work is based on the use of this class of compounds.

It was early recognized that the substituents on both the oxygen and the nitrogen atom of the quinuclidine moiety of the Cinchona alkaloids play a key role on enantioselectivity. Whereas the influence of the substitution pattern of the secondary

alcohol is a matter of controversy, it is clearly recognized that a bulky substituent at the quaternary nitrogen atom increases the enantioselectivity of the catalyst. This observation led to the synthesis of a number of *N*-benzyl and *N*-anthracenylmethyl derivatives, generally referred to as second- and third- generation catalysts. In 1984, Merck scientists reported the use of the quaternarized derivatives of cinchonine and cinchonidine as the first efficient chiral phase-transfer catalysts for the highly enantioselective alkylation of indanone (Scheme 3).[42]

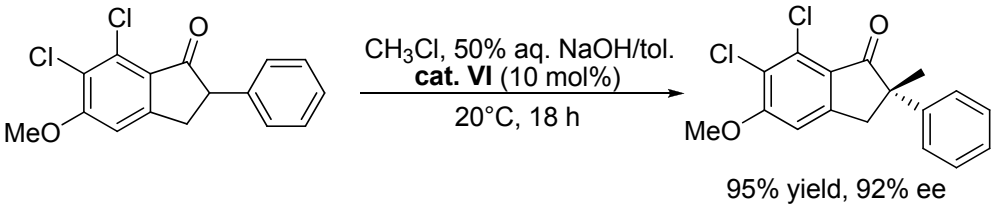

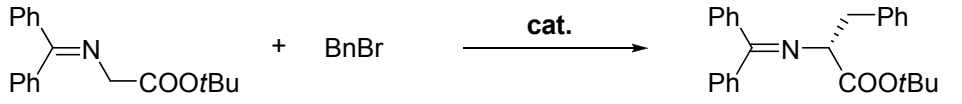

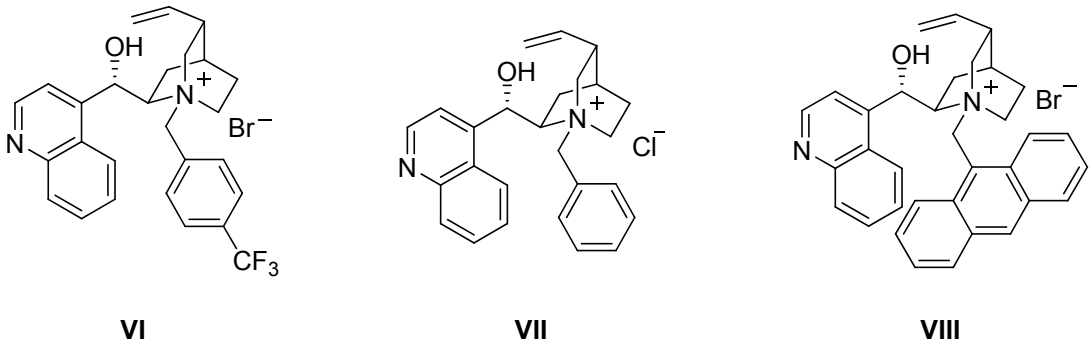

VI **VII** **VIII**

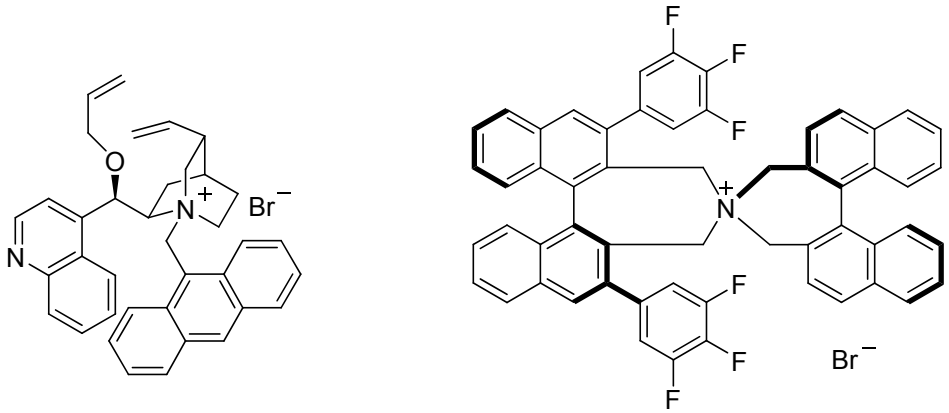

IX **X**

cat. (mol%)	base/solvent	T (°C)	yield (%)	ee (%)
VII (10%)	aq. NaOH/DCM	20	75	66 (*R*)
VIII (10%)	aq. KOH/toluene	20	68	91 (*R*)
X (10%)	aq. CsOH/DCM	-78	87	94 (*S*)
X (1%)	aq. NaOH/benzene	0	90	99 (*R*)

***Scheme 3**: examples of phase-transfer catalysts.*

In 1989, using similar cinchonine and cinchonidine salts, O'Donnell and his research group[43] achieved the α-alkylation of protected glycine derivatives, to furnish α-amino acids in an enantioselective fashion. Later on, the research groups of Lygo[44a] and Corey[43b] developed simultaneously *N*-anthracenylmethyl Cinchoninium salts **VIII** and **IX**, as third generation chiral phase-transfer catalysts, achieving remarkably high asymmetric inductions (up to 99.5%) in the α-alkylation of glycine derivatives.

Recently, Maruoka and co-workers[45] developed some highly efficient and enantioselective C_2-symmetric chiral spiro-ammonium salt catalysts, such as **X**, derived from commercially available (*S*)- or (*R*)-1,1'-bi-2,2'-naphthol, and successfully applied them to enantioselective α-alkylations as well as aldol and Michael reactions (Scheme 3, table).

The ready accessibility of phase-transfer catalysts and the mild experimental conditions make asymmetric phase-transfer reactions appealing both for academic research and for industrial applications.

Nucleophilic catalysis and Brønsted base catalysis

Nucleophilic catalysts have had a wide-ranging role in the development of new synthetic methods.[46] In particular, the Cinchona alkaloids catalyze many useful processes with high enantioselectivities and Cinchona derivatives can be employed in the kinetic resolution of several organic molecules due to the presence of their bridgehead *N*-atom. Cinchona alkaloids are bases able to deprotonate substrates with relatively acidic protons (e.g. malonates and thiols), forming a contact ion pair between the resulting anion and protonated amine. This interaction leads to a chiral environment around the anion and allows enantioselective reactions with electrophiles.

Deng et al. showed that thiols could undergo asymmetric 1,4-addition to cyclic enones forming the β-mercaptoketones in excellent enantioselectivities, using the $(DHQD)_2PYR$ catalyst (Scheme 4a).[47] Subsequently, they used this concept to develop C–C bond-forming processes including additions of stabilized enolates to nitroalkenes (Scheme 4b) and vinyl sulfones (Scheme 4c).[48] Important in many of these processes is the possibility to control the formation of quaternary stereogenic centres with high enantiomeric excesses.[49]

(a) Cinchona alkaloid-catalyzed thiol conjugate addition to enones

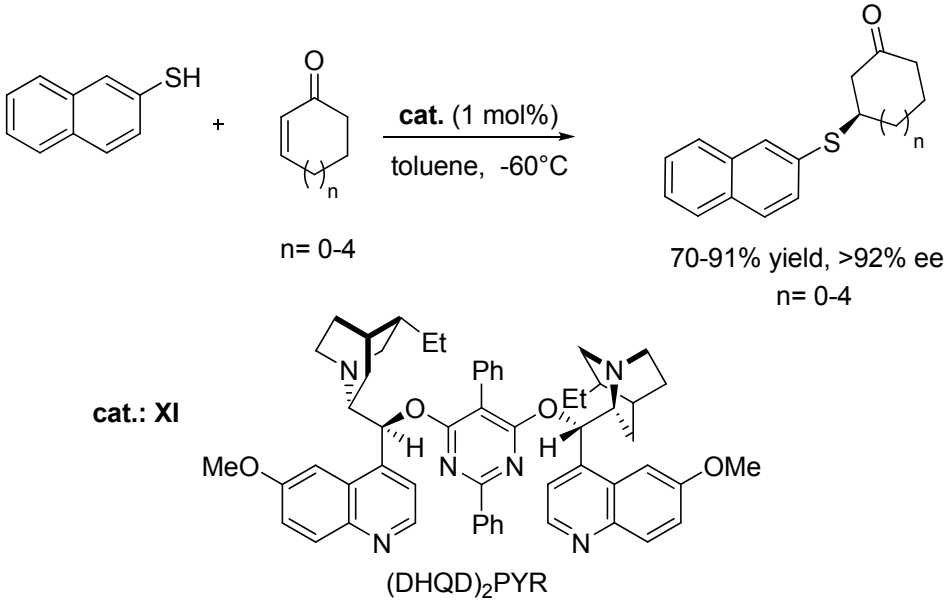

(b) Cinchona alkaloid-catalyzed conjugate addition to nitroalkenes

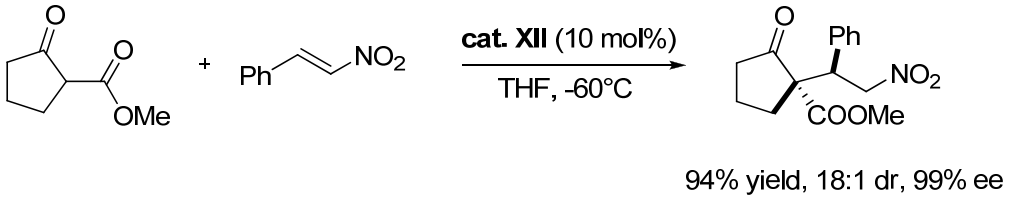

(c) Cinchona alkaloid-catalyzed conjugate addition to vinyl sulphones

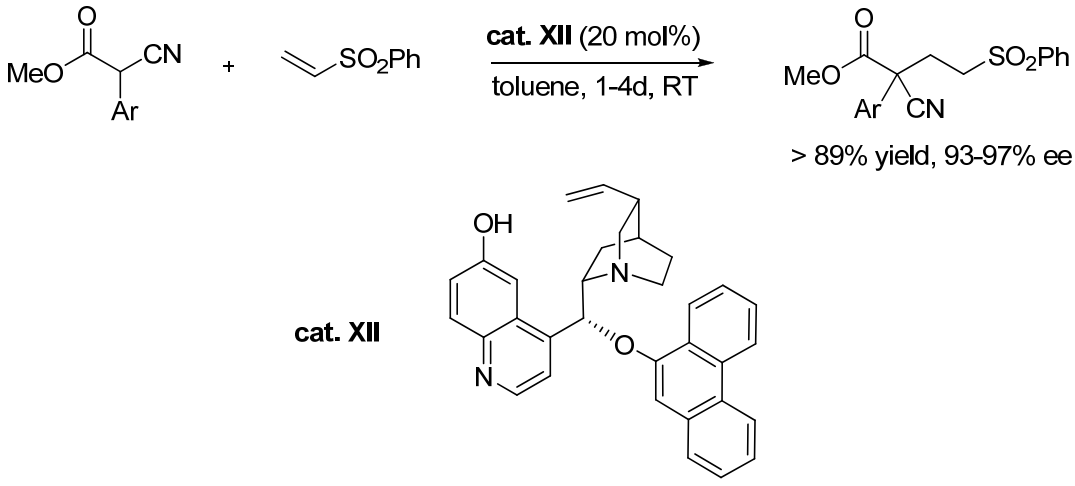

***Scheme 4**: Cinchona alkaloid-catalysts in organic reaction.*

Cinchona alkaloids can also be used as nucleophilic catalysts in other processes through a different mechanism: probably, the best known is the Baylis-Hillman reaction.[50] This reaction is traditionally problematic: although many tertiary amines catalyze the Baylis-Hillman reaction, only few amines impart high level of enantioselectivity. Some polycyclic Cinchona derivatives are able to promote the reaction with both aldehydes and tosyl imines with moderate to excellent enantiomeric excesses[51,52] (Scheme 5). Unfortunately, this method selectively produces only one enantiomer, because the corresponding quinine-derived catalyst cannot be synthesized. Despite this limitation, this strategy remains one of the best way of achieving an asymmetric Baylis-Hillman reaction.

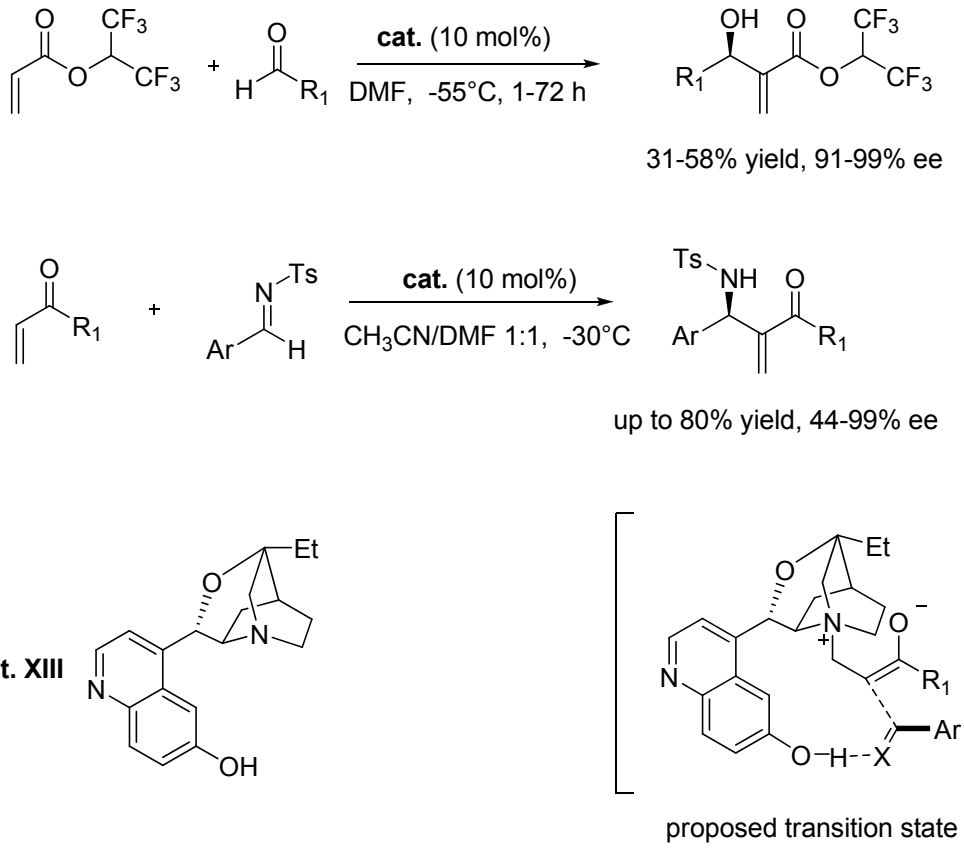

***Scheme 5**: Cinchona alkaloids in Baylis-Hillman reaction.*

Cinchona alkaloids can also be used, in combination with Lewis acids as co-catalysts, to promote the formation of β-lactones and lactams, from ketenes and aldehydes or imines, respectively. For example, Nelson and co-workers reported that lithium perchlorate assisted the Cinchona alkaloid-catalyzed addition of ketenes (generated *in situ*

from acid chlorides) to aldehydes, to form β-lactones in excellent yields, diastereoisomeric ratios and enantiomeric excesses.[53] Lectka also reported that the indium(III) complex of a salicylic-derived quinine derivative effectively forms the β-lactam structure by reaction between a ketene and an imine, again with excellent stereoselectivity.[54]

Cinchona alkaloids can also be used to generate asymmetric ammonium ylides. Gaunt and co-workers have used this concept to develop a catalytic enantioselective cyclo-propanation process, that is general over a range of substrates.[55]

The use of nucleophilic carbene catalysts is a rapidly emerging and exciting area for organocatalysis: Rovis and co-workers reported that a chiral *N*-heterocyclic carbene catalyst induces excellent enantioselectivity in the intramolecular Stetter reaction, over a broad range of cyclic products with very good yields and enantiomeric excesses (Scheme 6).[56]

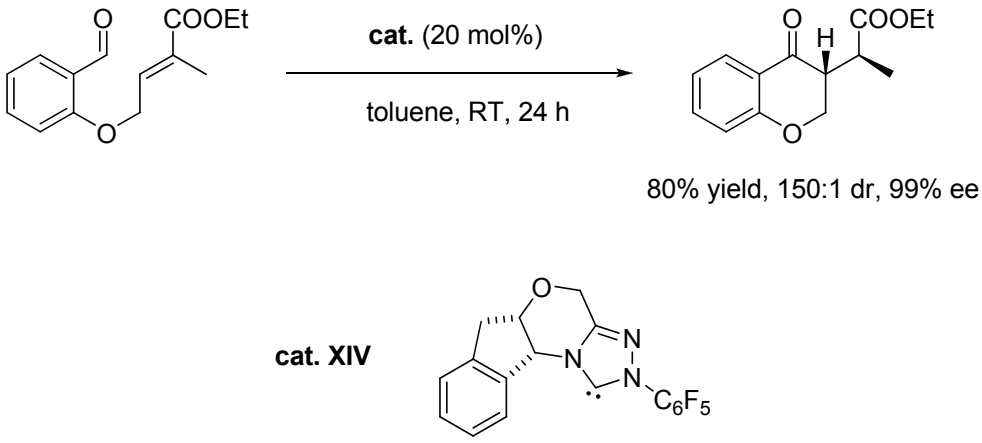

***Scheme 6**: nucleophilic carbene catalyzed intramolecular Stetter reaction.*

In 2005, Fu and co-workers have reported the use of a chiral monophosphine as an organic catalyst for the [4+2]-type annulation of imines with allenes. The *cis*-substituted piperidine products are formed in excellent yields, diastereoisomeric ratios and enantiomeric excesses, thus providing an efficient method for the synthesis of this key heterocyclic motif (Scheme 7).[57]

There are many processes to be developed, based on nucleophilic catalysis, and the concept of generating asymmetric anions through contact ion pairs is a methodology with wide-ranging possibilities. Furthermore, other reactive species, such as chiral

ammonium enolates and ammonium ylides, have great potential for the development of new chemistry.

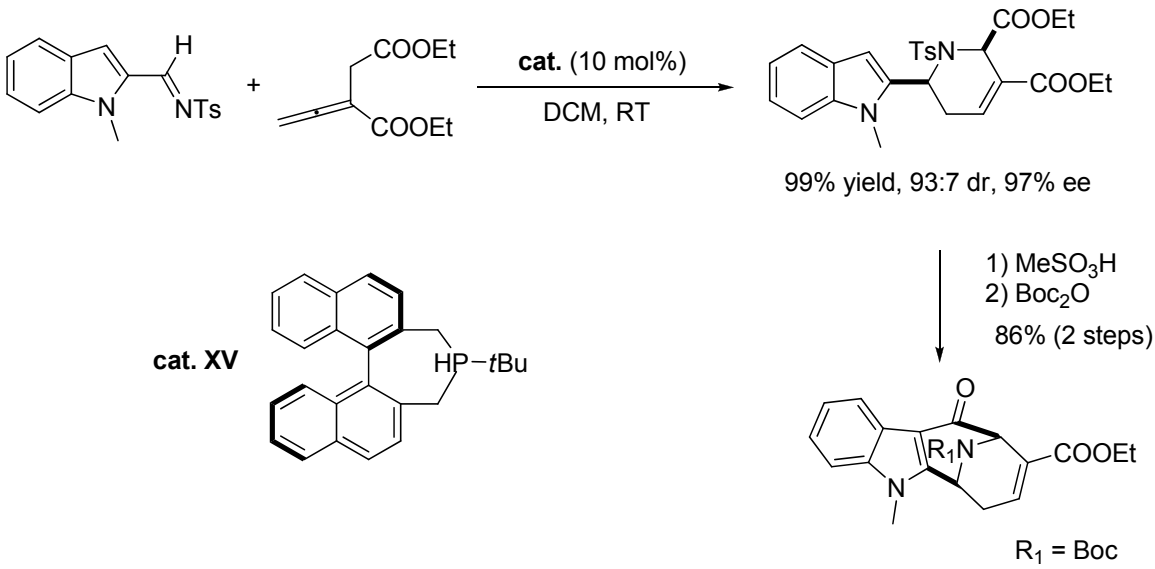

***Scheme** 7: [4+2]-type annulation of imines with allenes catalyzed by chiral monophosphine.*

Hydrogen bonding catalysis

Hydrogen bonding is responsible for the structure of much of the world around us, even if its energetic value is very low (about 5 kcal/mol). Indeed, hydrogen bonding acts like an ubiquitous “glue” that holds matter together providing, for example, the complex properties of bulk water; the intricate architecture and functionality of proteins; and many supramolecular assemblies. In addition to its primacy as a structural determinant, hydrogen bonding plays a crucial role in catalysis.[58]

The hydrogen bonding catalysis is similar to the enzymatic one, and can be described as an acidic catalysis, where the transition state presents less electron density than the starting materials on some atoms, permitting the nucleophilic attack.

In the last few years, organic chemists have studied this type of electrophilic activation in small molecule to apply this methodology in synthetic catalytic systems.

The ability of well-defined achiral hydrogen bond donors to catalyze useful organic transformations was discovered in pioneering studies at the beginning of the mid 1980s. Rapid progress in other areas of organocatalysis, which occurred simultaneously

with early development in chiral hydrogen bond donor catalysis, rendered chemists keenly aware of the potential of simple organic molecules in asymmetric catalysis.

Although the concept of hydrogen donor catalysts has been widely accepted, less is known about the mechanism and the different modes by which they effect the rate acceleration by hydrogen bond donation. Nevertheless, a classification has been proposed by Jacobsen et al.; this type of catalysts are divided into three categories according to their features:[59]

- double hydrogen bond donor catalysts, such as ureas, thioureas, as well as guanidinium and amidinium ions;
- bifunctional hydrogen bond donor catalysts, such as proline and amino thioureas;
- single hydrogen bond donor catalysts, such as BINOL-derived phosphoric acids.

General evolution from biphenylene diols to efficient N,N'-diarylthio(urea)catalysts

In preliminary studies, Hine and co-workers demonstrated that 1,8-biphenylene diols can be used to activate epoxides towards nucleophilic attack: they reported the successful addition of diethylamine to phenyl glycidyl ether (Scheme 8).[60a] The authors proposed that the enhanced activity of the biphenylene diol (**XVI**) in solution, with regard to phenol, is due to the simultaneous donation of two hydrogen bonds to the electrophile; this model was strongly supported by a solid-state 1:1 structure of the catalyst with the substrate.[60b]

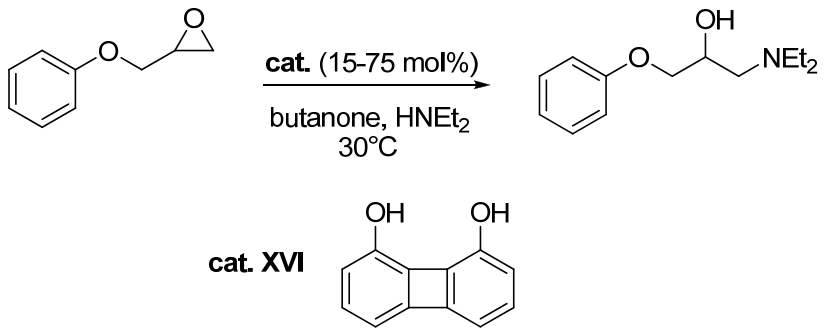

***Scheme 8**: Addition of diethylamine to phenyl glycidyl ether catalyzed by 1,8-biphenylene diol.*

Later on, in 1990 Kelly et al. extended this concept to the carbonyl domain and reported the promotion of the Diels-Alder reaction between cyclopentadiene and α,β-unsaturated aldehydes and ketones by biphenylene diol derivatives: they also proposed a

double hydrogen bond donation to the dienophile (**XVII**, Scheme 9) as an explanation for the observed catalysis.[61] This was consistent with a theory proposed by Jørgensen, based on computational studies, to rationalize the observed acceleration of Diels-Alder reactions and Claisen rearrangements in water with respect to non-protic solvents (**XVIII**, Scheme 9). Although the biphenylene diol catalysts possessed only moderate reactivity, the pioneering work of Hine and Kelly established that general acid catalysis by conformationally restricted metal-free diprotic acids is a valid strategy upon which organocatalyst design could be based.

In this period, Etter and co-workers observed that electronpoor diaryl ureas (in particular 3,3'-dinitrocarbanilide (**XIX,** Scheme 9) can be co-crystallized, by formation of a double hydrogen bond, with a wide variety of Lewis basic functional groups, such as nitroaromatics, ethers, ketones and sulfoxides.[62] In each case, the bidentate nature of the binding interaction is particularly attractive, because it removes some conformational degrees of freedom. To avoid entropic loss upon coordination, this also means that the hydrogen bond donor must be relatively rigid.

The studies of efficient catalysis by rigid bidentate hydrogen bond donors and the demonstration of binding between thioureas and Lewis bases provided the basis for the development of thiourea-based organocatalysis.

The first example was reported by Curran et al.. They found that substoichiometric amounts of diarylurea **XX** enhanced both the yield and the diastereoselectivity of the allylation of cyclic α-sulfinyl radicals. Later, the same group reported the promotion of the Claisen rearrangement by using catalytic amounts of **XXa** (Scheme 9).[63] For the first time thiourea derivatives, e.g. **XXb**, were also shown to hold promise as hydrogen bonding catalysts.

Based on Curran's studies, Schreiner and co-workers developed a remarkable array of thiourea catalysts: the advantages outlined by the authors are their solubility in a variety of solvents and the simplified preparation. In addition, the thiocarbonyl group is a much weaker hydrogen bond acceptor than the urea oxygen. As expected, thioureas bearing electron-withdrawing substituents at the *meta*- and *para*- positions have a significant accelerating effect, due to their rigid conformation; this observation is also in line with the fact that co-crystals with 1,3-bis(*m*-nitrophenyl) urea are of higher quality when trifluoromethyl groups are present in the thiourea derivatives.[64]

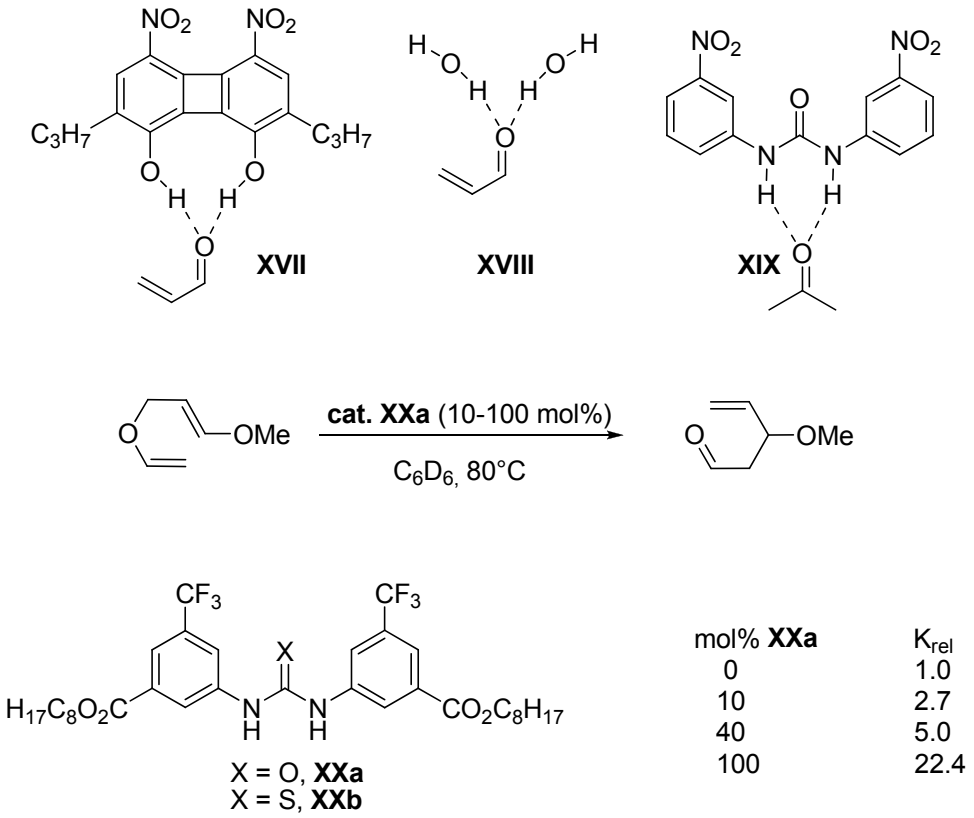

***Scheme 9**: Diels-Alder reaction catalyzed by hydrogen bonding.*

After a systematic study, they identified thiourea **XXI**, which has two trifluoromethyl groups at the 3,5-positions of the aromatic rings, as the most active catalyst in the promotion of Diels-Alder and dipolar cycloaddition reactions, even in water as the solvent (Scheme 10).

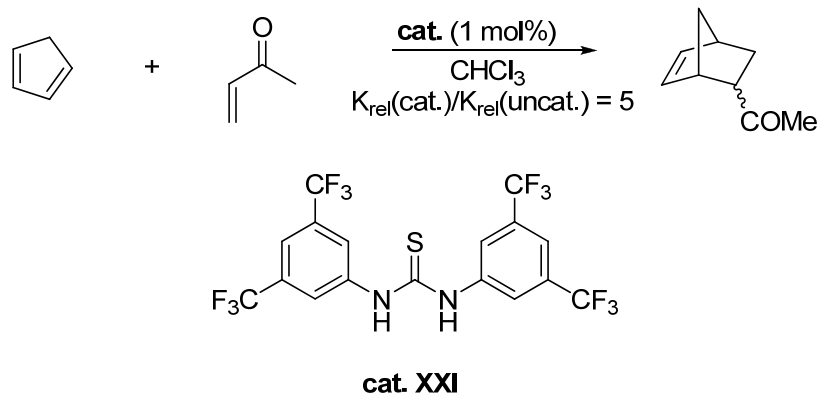

***Scheme 10**: Thiourea catalyzed Diels Alder reaction.*

The *meta*-CF_3 substituents would significantly increase the acidity of the N–H protons. Thiourea **XXI** has been used in a wide range of useful transformations, such as nucleophilic addition, Baylis-Hillman reaction, Friedel-Crafts alkylation, acetalization, epoxide opening, acyl-Strecker reaction, as well as transfer hydrogenations. Moreover, by incorporation of the electronpoor 3,5-bis(trifluoromethyl)phenyl thiourea moiety, various achiral/chiral mono- and bifunctional organocatalysts have been developed for a broad spectrum of reactions through hydrogen bond activation.

Enantiopure thioureas for stereoselective organocatalysis

The synthesis of chiral thiourea catalysts was greatly facilitated by the ready availability of enantiopure chiral building blocks bearing primary amino groups, derived from the chiral pool or other sources. Therefore, it is not surprising that a wide variety of chiral analogues have been developed so far and still are: thanks to their great versatility, functional group tolerance and easy preparation, they have been utilized in a great number of synthetically useful transformations.

The most remarkable advances in this field were achieved by Jacobsen's group. [65] They studied the activation of alkyl- or acyl-substituted imines, identifying and optimizing a series of urea- and thiourea-containing Schiff bases that are able to catalyze various type of asymmetric reactions: Strecker, Mannich, hydrophosphonylation, nitro-Mannich and acyl Pictet-Spengler reactions.

The discovery that Schiff bases **XXIIa-c** catalyze asymmetric hydrocyanation reactions of a wide variety of imine substrates, revealed for the first time that chiral urea and thiourea derivatives were capable of promoting highly enantioselective transformations (Scheme 11). These compounds were originally intended as potential ligands for Lewis acidic metals: the observation that the best enantioselectivities were obtained in the absence of the metal was unexpected.

Thus, the mechanism of the activation of the imines by these catalysts was investigated, by using different approaches, such as structural modification, NMR, kinetic and computational studies. The data obtained were all consistent with the formation of a double hydrogen bond between the acidic N–H protons and the imine lone pair activating the electrophile towards the attack by the cyanide.

After systematic optimization, catalyst **XXIIc** was also found very effective in the Strecker reaction; its versions **XXIIe** and **XXIIf**, immobilized on a polystyrene bead, facilitate Strecker product purification, by simple filtration and solvent removal. Furthermore, the catalyst can be reused without loss of either activity or enantioselectivity.

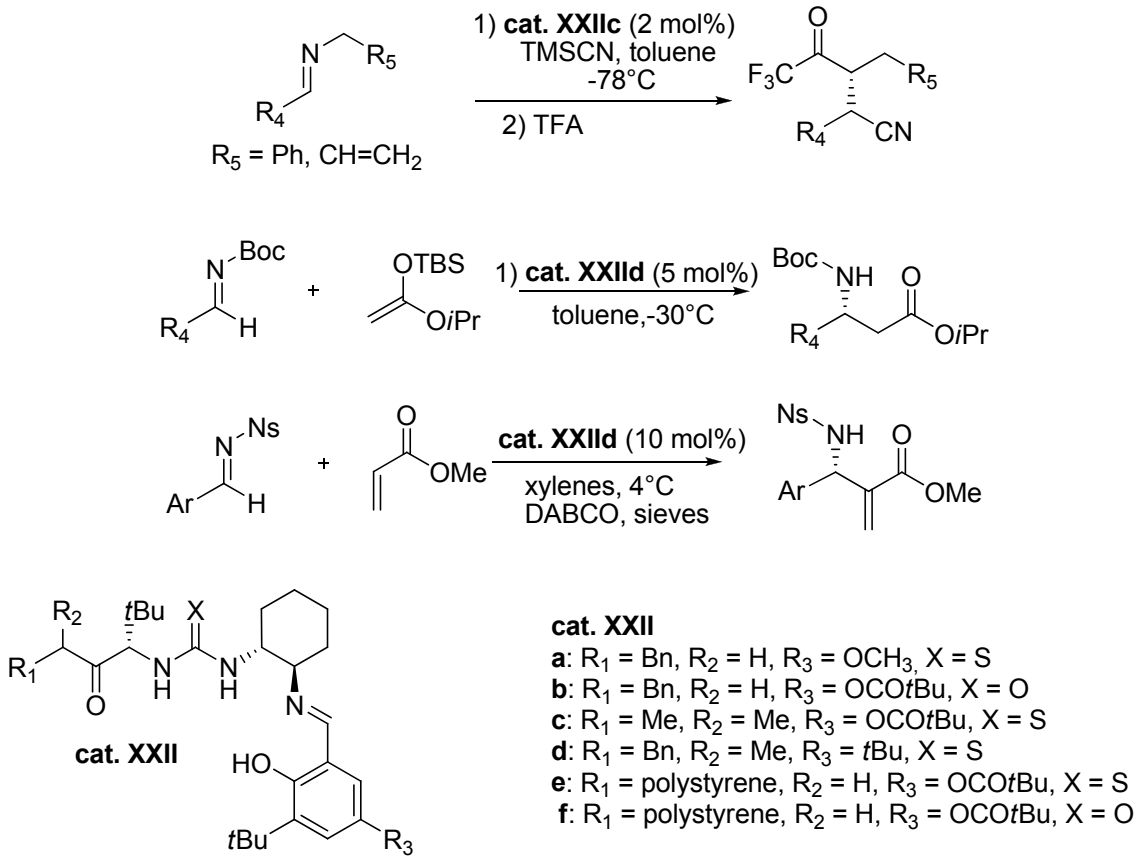

***Scheme 11**: thiourea-catalysts developed by Jacobsen.*

In addition to hydrogen cyanide, a wide variety of nucleophiles undergo enantioselective addition to *N*-benzyl imines in presence of catalysts **XXII**; for example, an efficient asymmetric synthesis of amino phosphonic acids involved the addition of di-(2-nitrobenzyl) phosphite to imines derived from both aliphatic and aromatic aldehydes, followed by hydrogenolysis of the *N*- and *O*-benzyl groups. However, it is remarkable that highly enantioselective additions to such a broad range of functionally diverse electrophiles are promoted by thiourea catalysts. The first indications of this ability came from studies of Mannich reactions of *N*-*tert*-butoxycarbonyl (Boc) imines, a reaction that has a great interest for the preparation of enantioenriched β-amino acid derivatives.

Thiourea **XXIId**, for example, catalyzes this reaction with high enantiomeric excess, despite the significant steric and electronic differences between *N*-Boc imines and the *N*-benzyl and *N*-allyl imines employed in the Strecker reaction.

The ability of thiourea catalysts to activate imines bearing a wide variety of protecting groups forms the basis for several enantioselective C–C bond forming methodologies. Recently, the scope of the thiourea catalysis was extended to include *N*-(4-nitrobenzene)sulfonyl (nosyl, Ns) imines, that are useful substrates due to their high electrophilicity and the easy removal of the nosyl group. These imines undergo enantioselective aza-Baylis-Hillman reactions with methyl acrylate, in presence of the catalyst **XXIId** and a stoichiometric amount of DABCO as the nucleophilic activator (Scheme 11).

Among the most reactive imine derivatives are *N*-acyl iminium ions: a few methodologies based upon these intermediates have been developed and extensively applied to the synthesis of nitrogen containing compounds. Jacobsen and co-workers reported the first example of a highly enantioselective acyl-Pictet-Spengler reaction, catalyzed by the pyrrole-containing thiourea **XXIII**, between indoles and *N*-acyl iminium ions, generated in situ from imines and acetyl chloride (Scheme 12a).[65e]

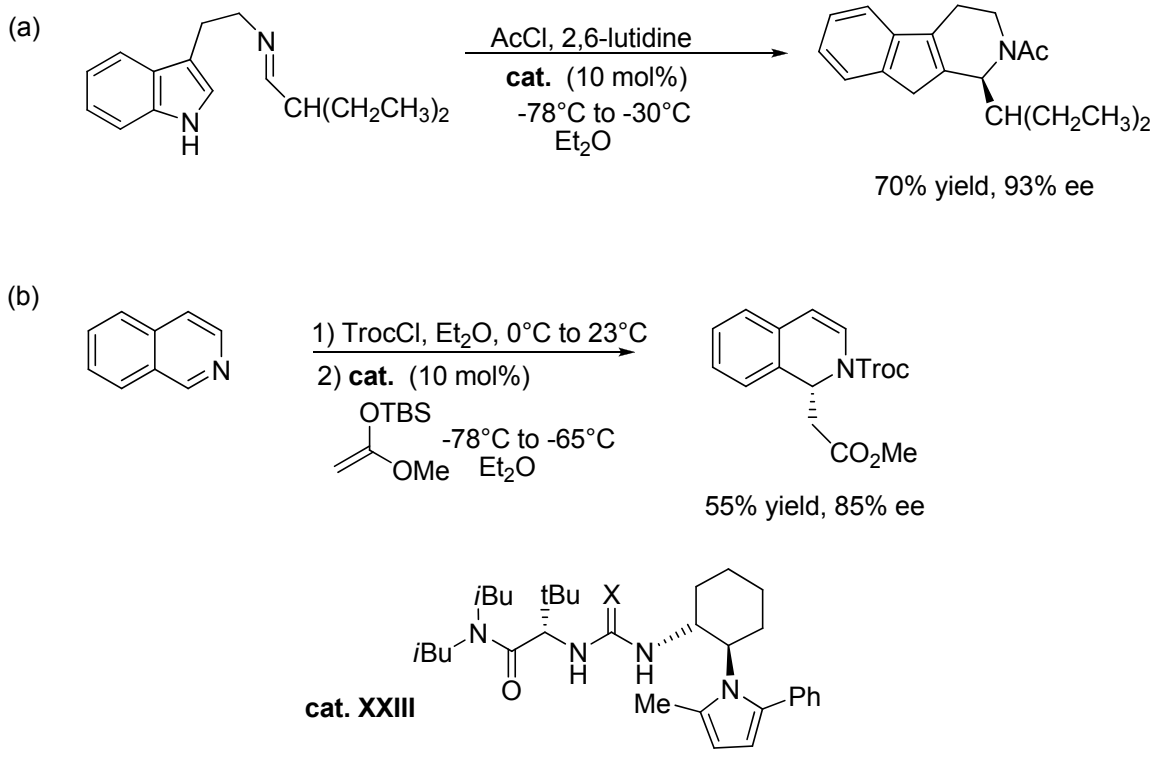

***Scheme 12**: Imine activation with thiourea-catalyst.*

Afterwards, the same group found that catalyst **XXIII** was also effective for Mannich-type additions of silyl ketene acetals to isoquinolines, in the presence of 2,2,2-trichloroethyl chloroformate, giving access to enantioenriched dihydroisoquinoline products (Scheme 12b).[65f]

In 2003, Takemoto and co-workers reported the first bifunctional thiourea catalyst **XXIV**, which bears a dimethylamino group, able to promote the efficient addition of malonate esters to nitroolefins, with excellent enantioselectivity (Scheme 13).[66]

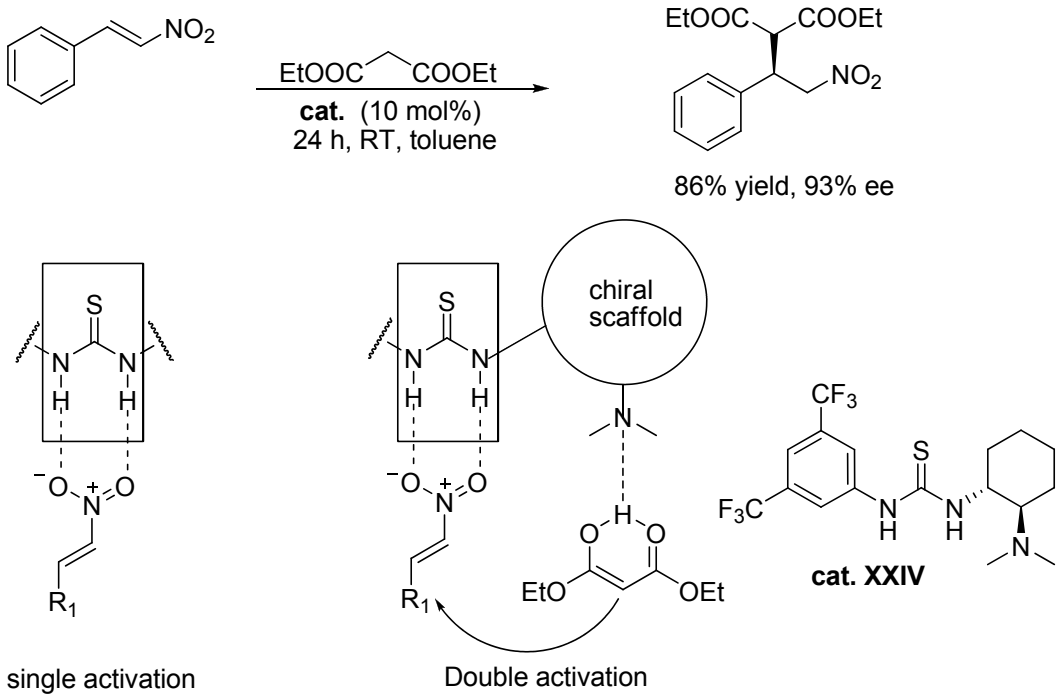

***Scheme 13**: Bifunctional thiourea-based catalyst.*

The authors found that both the tertiary amine and the thiourea moieties were necessary for efficient and selective catalysis. By studying the reaction kinetic and by performing catalyst modification, effects consistent with the mechanistic proposal of the authors were observed: the catalyst activates both the nucleophile, by general base catalysis, and the electrophile, by hydrogen bonding to the nitro group.

Recently, the scope of the Takemoto catalyst **XXV** has been expanded to encompass reactions involving nucleophiles and electrophiles substantially different from those initially reported. The field concerning the design of thiourea-based bifunctional catalysts has widely been developed. In this introduction only some examples of new chiral urea derivatives are reported.

Highly enantioselective transformations involving the donation of a single hydrogen bond as the only mechanism of activation are significantly less common than those employing either double hydrogen bonding interactions or bifunctional catalysis. The major difficulty in this field is due to the moderate strength and directionality of an isolated hydrogen bond, and, consequently, the limited rigidity of the catalyst-substrate complex. One example of single hydrogen bond activation is represented by TADDOL-, BINOL- and phosphoric acid- derivatives, that are able to catalyze several interesting processes involving imines. In a seminal work published in 2004 by the group of Akiyama, the use of a phosphoric acid as an effective catalyst in the Mannich-type addition of silyl ketene acetals to aldimines has been proposed (scheme 14).[67]

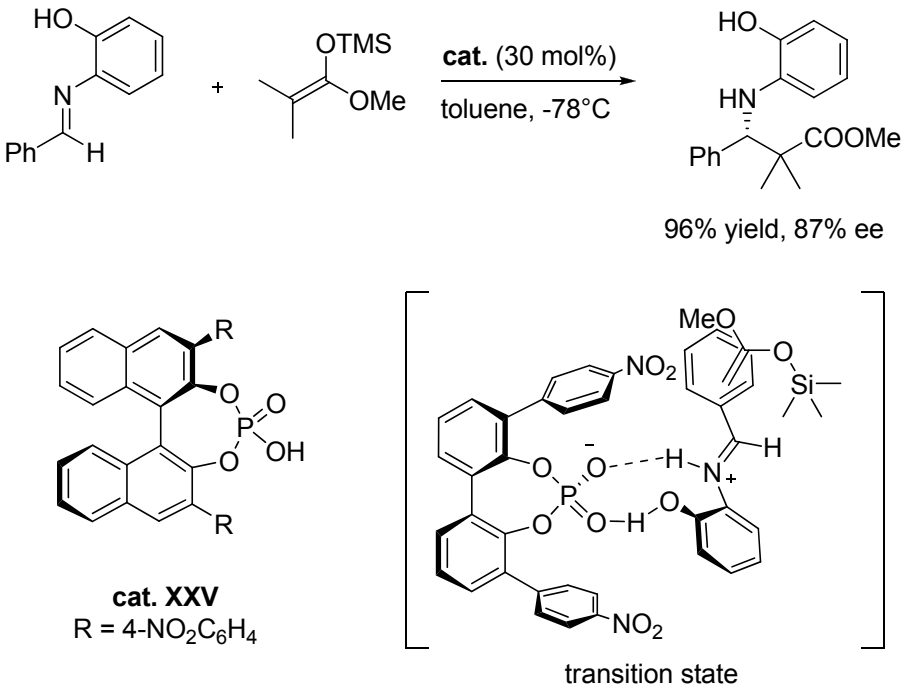

***Scheme 14**: Mannich-type addition of silyl ketene acetals to aldimines catalyzed by BINOL-derivative.*

The selectivity of this system was tentatively rationalized via formation of a nine-membered cyclic structure featuring an aromatic stacking interaction between the 4-nitrophenyl group and the N-aryl group fixing the geometry of aldimine.

Mannich reactions seem to be ideally suited to this class of organocatalysis, and the BINOL phosphoric acid catalyzes both the addition of β-diketone and silyl enol ethers to imines in excellent yield and enantiomeric excess.

Other important processes have been extensively studied: among these Friedel-Crafts alkylation, Pictet-Spengler reaction, reductive amination, transfer hydrogenation, only to cite a few. Most of these reactions are expected to have a major impact on industrial fine chemistry.

In the present doctoral thesis, a series of novel chiral Lewis bases was firstly designed and synthesized, and their potential applications as organocatalysts were investigated in several important synthetic transformations.

The development of Lewis-bases catalyzed reactions for regio- and stereoselective bond formation is a topic of primary importance in modern organic chemistry. As shown before, chiral small molecules able to donate electron-pairs have been reported to promote a wide variety of stereoselective reactions.

Moreover, a very new and recent type of catalytic method was developed, that could be called as "Lewis base catalyzed Lewis acid mediated reaction", where a chiral Lewis basis catalyzes the reaction while one or more starting materials are activated by an achiral Lewis acid, for example trichlorosilyl derivative.

For these reasons, in Chapter 1 a brief description of silicate-mediated stereoselective reactions catalyzed by chiral Lewis bases is reported.

In Chapter 2 novel examples of phosphoramides and their use in stereoselective catalysis are discussed.

In Chapter 3 a few examples of stereoselective transformations organocatalyzed by chiral phosphine oxides in the presence of Lewis acid are introduced.

In Chapter 4 highly stereoselective direct aldol-type condensations of ketones to aromatic aldehydes catalyzed by biheteroaromatic diphosphine oxides are described.

In Chapter 5 basic principles of molecular modeling are showed, and in Chapter 6 the experimental section is reported.

CHAPTER 1

Silicate-mediated stereoselective reactions catalyzed by chiral Lewis bases

"*The number of different hypotheses erected*
to explain a given chemical phenomenon
is inversely proportional to the available knowledge."
Edington's Theory

The chemistry of penta and/or hexavalent silicon compounds has recently attracted much attention because of the possibility to develop organocatalyzed enantioselective reactions in the presence of cheap, low toxic and environmental friendly species such as hypervalent silicates.[68] Even if the discovery of silicon compounds with a coordination number greater than four dates back to 1809, when the adduct $SiF_4 \bullet 2\ NH_3$ was reported by Gay-Lussac,[69] only in the last forty years the distinctive reactivity displayed by penta- and hexavalent silicon compounds has been increasingly studied, and organosilicon compounds have become more and more important intermediates in organic synthesis.[70]

More recently, the possibility to develop organocatalytic silicon-based methodologies has given even new impulse to the studies in this field. The tremendous growth of the interest in what is currently referred to as the "organocatalytic" approach toward enantioselective synthesis, is strongly indicative of the general direction toward which modern stereoselective synthesis is moving.

In the last few years, stereoselective versions of several reactions promoted by silicon-based catalysts have been developed,[71] especially promoted by hypervalent silicate intermediates used as chiral Lewis bases.[72] Before entering in the discussion of

these different reactions, it is important to summarize the mechanism that is responsible of the formation of silicon hypervalent states.

1.1 Hypervalent bonding analysis

The theory of acid–base interactions, pioneered by G. N. Lewis at the beginning of the 20th century, is at the basis for the state of knowledge about hypervalent silicon; indeed, hypervalent compounds are adducts generated by an interaction between a Lewis base and a Lewis acid.

When a Lewis base interacts with a Lewis acid, a new bond is formed, because of the interaction between the two molecules; citing Lewis "*the basic substance furnishes a pair of electrons for a chemical bond; the acid substance accepts such a pair*".[73] Related to Lewis's definition of the acid–base interaction, the octet rule defines that each atom must have eight electrons in its valence shell, giving it the same electronic configuration of a noble gas. Generally, when the formation of an acid–base adduct is favorable, the donor and acceptor atoms reach their octets through the formation of a dative bond that leads to enhanced thermodynamic stability. In this way, a decrease in the reactivity of the acid and the base occurs, by a reaction called neutralization.

However, there are also many exceptions to Lewis assumptions about the octet rule, where stable acid–base adducts show enhanced reactivity, as in the case of hypervalent silicon species. Lewis base, at variance from a Lewis acid, can indeed enhance its chemical reactivity by modifying the nucleophilicity or the electrophilicity of molecules, by modulating their electrochemical properties.[74]

In a reaction catalyzed by a Lewis base, the rate of reaction is accelerated by the action of a catalytic amount of an electron-pair donor on a electron-pair acceptor, that could be the substrate or a reagent. The binding of the Lewis base to a Lewis acid generates a transfer of electron density from the base to the acid, and a new adduct is formed. This electron change is the principal factor responsible of the chemical reactivity of a Lewis base. The most common effect of this transfer is the enhancement of the nucleophilicity of the acceptor, but in some rare cases, the binding of a Lewis base enhances the electrophilic character of the Lewis acid. To visualize this concept clearly, it is important examine the nature of the newly formed dative bond.

In this respect, Jensen has classified all the possible types of interactions on the basis of the involved orbitals, and nine type of bonding phenomena were identified.[75] They are shown in table 1.1:

Donor	Acceptor		
	*n**	σ*	π*
n	*n* - *n**	*n* - σ*	*n* - π*
σ	σ - *n**	σ - σ*	σ - π*
π	π - *n**	π - σ*	π - π*

***Table 1.1**: Jensen's orbital analysis of molecular interactions.*

Although each of these combinations could represent a productive interaction, in practice, only three of these interactions are significant in terms of catalysis.[76]
These are the:

1) interaction between nonbonding electron pairs and antibonding orbitals with π character (n–π* interactions),
2) interaction between nonbonding electron pairs and antibonding orbitals with σ character (n–σ* interactions),
3) interaction between nonbonding electron pairs and vacant nonbonding orbitals (n–n* interactions).

The first one is the most common interaction and represents almost all the examples of Lewis basis catalysis. The nonbonding electron pairs of the donor interact with the antibonding orbitals with π character, contained in alkynes, alkenes, carbonyls, azomethines, or other common unsaturated functional groups. One example of this n–π* interaction is the 1,4-addition to α,β-unsaturated compounds (scheme 1.1).

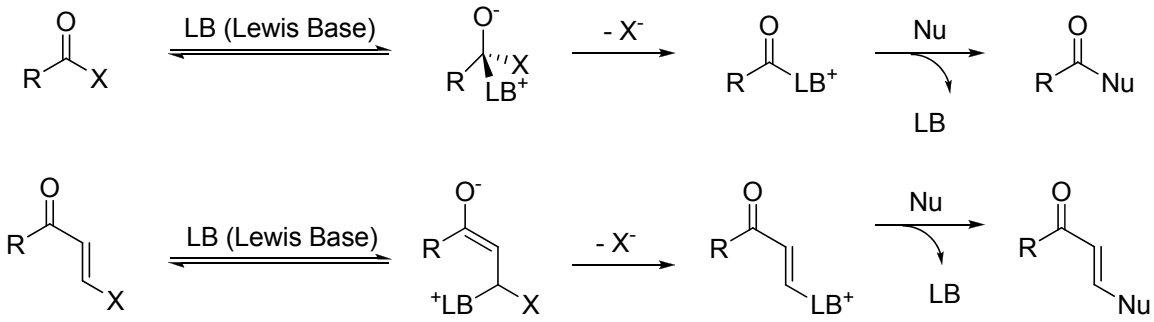

***Scheme 1.1**: example of n–π* interactions.*

The second and third interactions, n–σ* and n–n* are less known, but activate the dative bond in the same way. The difference is correlated to the type of acceptor orbital involved in the interaction; in the case of boron and other group 13 elements this is an n* orbital, whereas, for group 14 elements, is a σ* orbital. An important requirement for these types of interactions is that the Lewis acidic acceptor must be able to expand its coordination sphere giving a "hypervalent" state.[77] When the dative bond is formed, the preference of nucleophilic or electrophilic character of the new specie depends on the polarizability of the new generated bond, as predict by Gutmann empirical analysis.[78] When an acid–base adduct is generated, the electron density in the acceptor fragment increases. However, its distribution is not equal among the constituent atoms; so the redistribution of the electron density in the adduct to compensate the electronic changes results in the lengthening of some bonds, and the contraction of other bonds. As a consequence, the coordination number of the Lewis acid increases, and an expansion of the coordination sphere occurs (scheme 1.2).

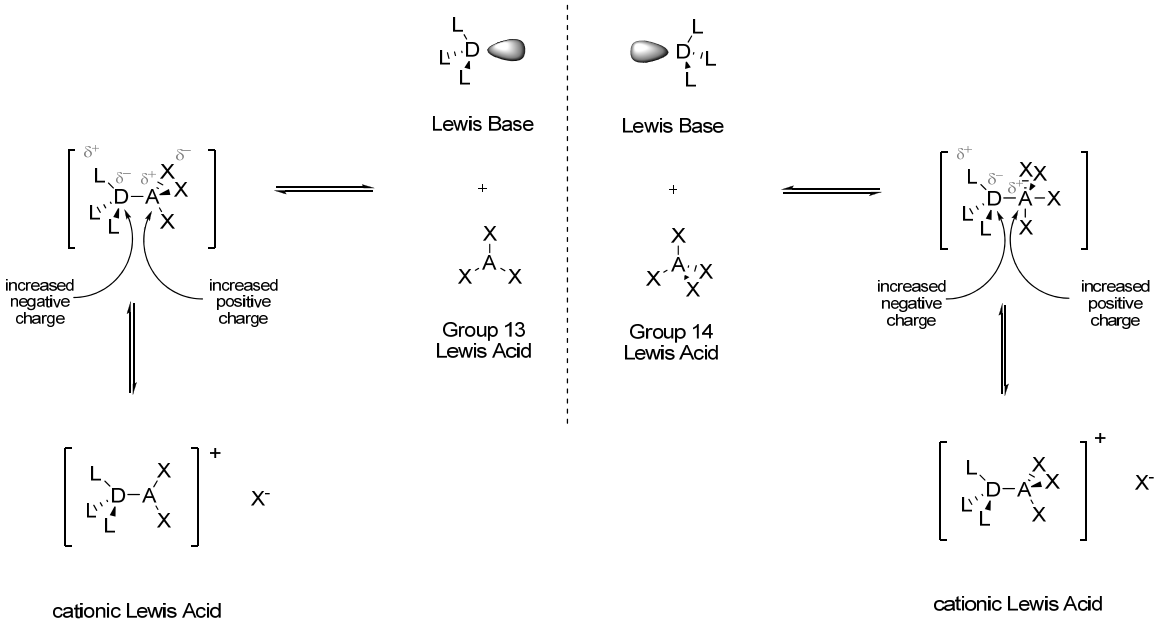

Scheme 1.2*: electronic redistribution resulting from Lewis acid-base complexation.*

Support to this conclusion can be derived from calculations performed with relevant Lewis acid-base adducts of silicon tetrachloride (Scheme 1.3). Gordon and co-workers have studied the binding of chloride ion to $SiCl_4$ to form penta- and hexacoordinate silicates at the 6-311^{++}G(d,p) level of theory and observed changes in

bond lengths and electron densities consistent with the Gutmann analysis.[79] The addition of the first chloride ion is exothermic by 40.8 kcal/mol, but, more interestingly, leads to an increase in the partial positive charge at silicon by +0.051. A corresponding increase in the partial negative charge at the chlorine atoms accompanies this change. A greater degree of the negative charge accumulates at the axial chlorine atoms when compared to the equatorial chlorine atoms due to their involvement in a hypervalent three-center/four electron bond. Binding of the second chloride ion, although now an endothermic process by 48.3 kcal/mol, further accentuates this polarization, as the partial positive charge at silicon increases by another +0.310 kcal/mol.

So, the polarization of the adjacent bonds in the metal fragment of the adduct leads to ionization of one of the other ligands and generation of a cationic metal center.

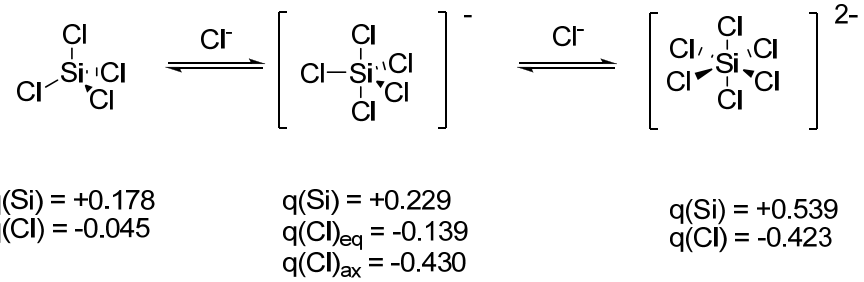

***Scheme 1.3**: Gordon analysis of $SiCl_4$*

Contrary to carbon (its first row group 14-analogue), silicon displays the ability to form more bonds than the four necessary for fulfilling the octet rule: in the presence of donor molecules or ions it is possible the formation of five-, six- and even seven-coordinated silicon species, some of which have been isolated and/or characterized.[80]

In order to explain this behaviour, two main different theories have been formulated: the first invokes the participation of the silicon 3d orbitals in the expansion of the coordination sphere[81] as shown in scheme 1.4; the second proposes instead a so-called "hypervalent bonding" (showed in scheme 1.5).

The first theory asserts that in the five-coordinated species the silicon orbitals would have a sp^3d hybridization (with trigonal-bipyramidal geometry), while in the six-coordinated species the hybridization would be sp^3d^2 (with octahedral geometry). The reduced s-character of the silicon orbitals in the hypercoordinated species would explain their increased Lewis acidity and the transfer of electron density to the ligands.

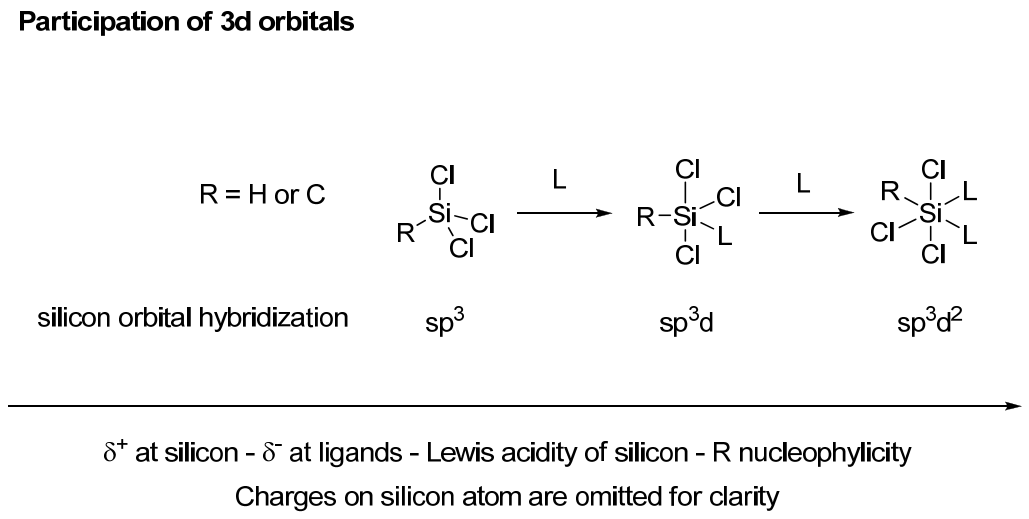

***Scheme 1.4**: expansion of the coordination sphere of silicon atom.*

The second theoretical approach in contrast, rules out the participation of the 3d orbitals in the bonding process and hypothesizes instead a so-called "hypervalent bonding" (scheme 1.5).[82] The ability of main-group elements to form compounds which appear to break the Langmuir–Lewis octet rule was originally explained by invoking an availability of d orbitals (such as 3d for silicon) by using an analogy to transition-metal complexation. However, silicon is not a transition metal, and it is now generally accepted that the 3d orbitals on silicon are too diffuse to engage in meaningful bonding.[83a]

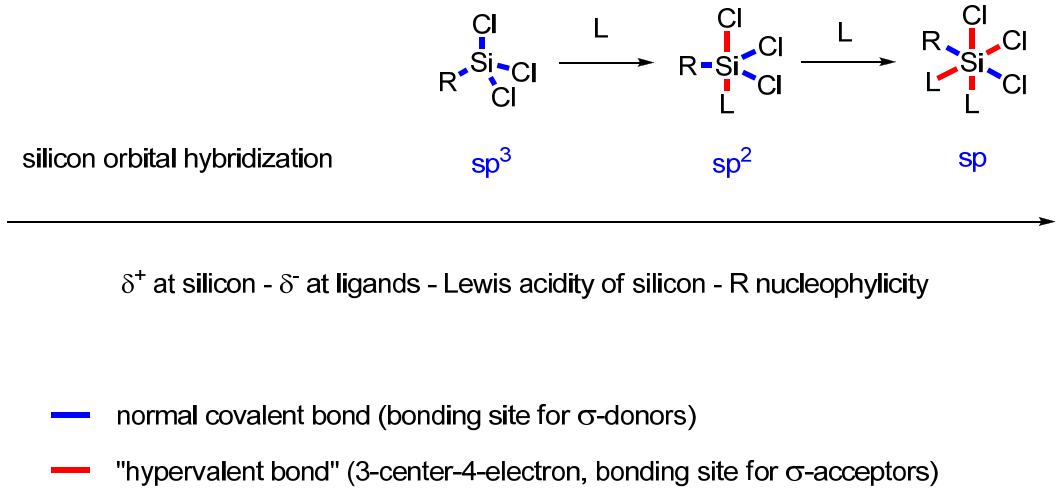

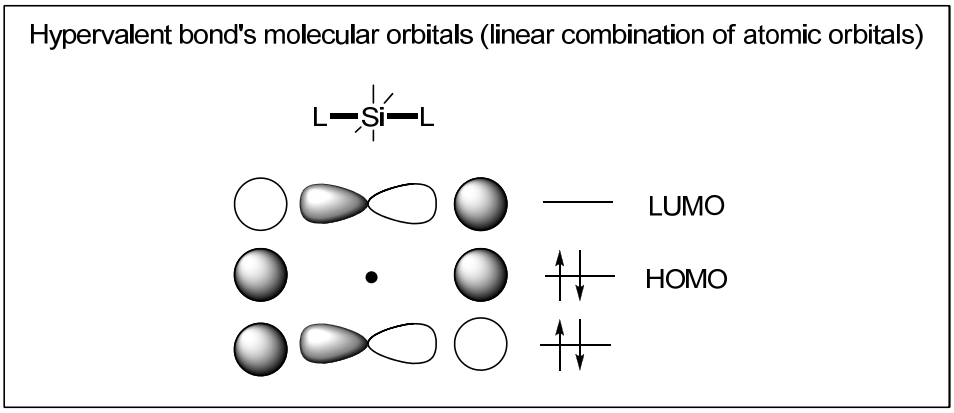

***Scheme 1.5**: hypervalent bonding theory.*

The ability of silicon to expand its coordination sphere (leading to hypervalent bonding) is due to the ability of the silicon 3p orbitals to engage in electron-rich three-center-four-electron bonding. Therefore the formation of a penta- or hexa-coordinated silicon species would involve respectively one or two 3-center-4-electron molecular bonds, each formed by a silicon p-orbital and two p-orbitals of electronegative ligands featuring a relative trans-disposition. An important consequence is the non-equivalence of the ligand positions in five- and six-coordinated silicon species, the σ-acceptor ligands preferring "hypervalent" bonds and the σ-donors forming preferentially normal covalent bonds with the sp^2 (for pentacoordianted compounds) or sp (for hexacoordinated compounds) silicon orbitals.

The presence of hypervalent bonds imposes some stereochemical constraints (like the *trans*-disposition of the most electronegative ligands) and allows to formulate predictions about the positions of the other ligands on the basis of their electronic properties. Accordingly, the number of possible configurations of the silicon ligands to be considered in the elaboration of a stereoselection model is actually restricted, as shown in a recent paper by Denmark and co-workers.[83b]

Both theories are helpful in the interpretation of the fundamental properties of hypervalent silicon species, that clearly distinguish their reactivity from that of four-coordinated compounds, such as the increased Lewis acidity of the silicon atom and the transfer of electronic density to the ligands, which confer to silicon-bound R groups (carbanion or hydride equivalent) marked nucleophilic properties. The hypervalent silicon species involved in synthetically useful processes are generally formed in situ by reaction between a four-coordinated species and a Lewis base in what is often called the

"activation step".[82,84] The so-formed five- or six-coordinated silicon species is able to promote the desired reaction in a catalytic process if the base can dissociate from silicon after the product is formed.

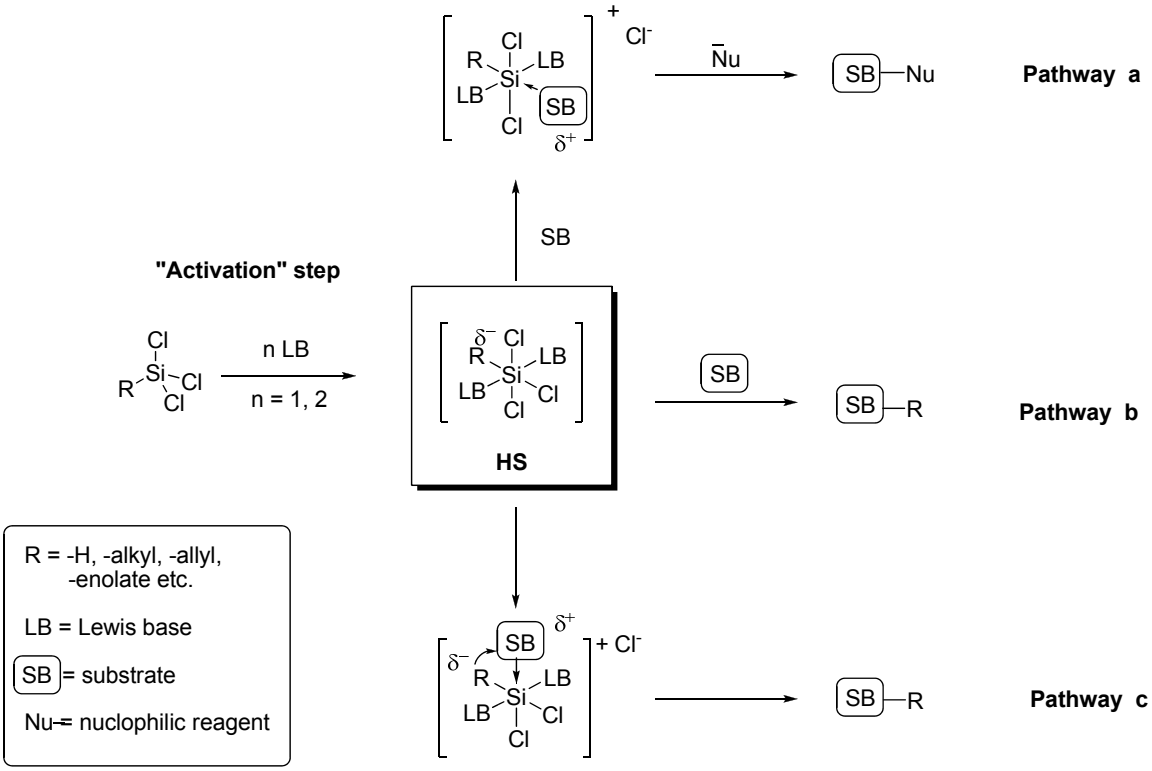

***Scheme 1.6**: three different pathways depending of the role of hypervalent specie.*

Three general kinds of reaction mechanism can be envisaged depending on the role played by the hypervalent species (scheme 1.6):

1. the hypervalent species (HS) may act as a Lewis acid coordinating the substrate and activating it towards the attack of an external nucleophile (Figure 1.3, pathway a);
2. a nucleophilic silicon ligand is transferred to the substrate which is not coordinated by silicon (Figure 1.3, pathway b);
3. the hypervalent species coordinates the substrate transferring at the same time one of its ligands to it (Figure 1.3, pathway c).

In the last case both of the peculiar properties of hypervalent silicon species are so exploited at the same time. When a mechanism of type C is operating, the cyclic transition state allows an efficient control of the relative stereochemistry of the product.

This classification should be helpful for a more immediate comprehension of the mechanicistic details that are discussed in the following sections, where the mechanism of several reactions promoted by hypervalent silicon species is reported.

Reductions will be discussed first, followed by carbon-carbon bond formations and opening of epoxides and other miscellaneous reactions. Trimethylsilyl cyanide addition to carbon-nitrogen double bonds will not be discussed, because the mechanism of this reaction is not fully understood.[76,82]

1.2 Achiral C-H bond formation from reduction with $HSiCl_3$

Among the metal-free reductive methodologies recently developed,[85] the procedure that involve the use of $HSiCl_3$ as reducing agent is particularly attractive. This cheap reagent is a colourless liquid, commercially available and abundant byproduct of the industrial Rochow process, it is volatile and can be removed under reduced pressure; alternatively, after workup with dilute aqueous saturated $NaHCO_3$, $HSiCl_3$ and its byproducts are converted into harmless hydroxysilanes.

One of the first examples of achiral C-H bond formations involves the use of $HSiCl_3$ with tertiary amine combinations. These are able to remove the carbonyl oxygen from a wide variety of compounds. Aromatic ketones, aldehydes, acid chlorides, amides, and aromatic acids are preferred substrate for this reaction, defined “reductive silylation”. In a general view, the reaction can be represented as the replacement of a carbonyl oxygen by the H and $SiCl_3$ moieties of trichlorosilane (Scheme 1.7).

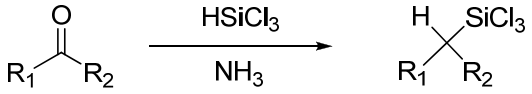

Scheme 1.7: *reductive silylation.*

In 1982, Benkeser et al. found unexpected results when this approach was extended to carbon-nitrogen double bond. *N*-(benzylidene) aniline was treated with this system yielding the amine rather than the cleavage product toluene after hydrolysis.[86] The reaction proceeded well under reflux conditions in acetonitrile (Scheme 1.8).

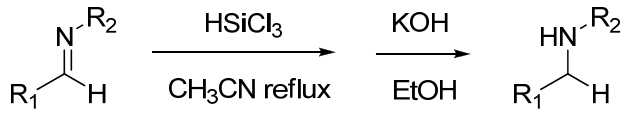

Scheme 1.8: *reduction of C-N double bond.*

Another efficient reducing agent was developed by Kobayashi and co-workers,[87] where the use of the trichlorosilane dimethylformamide adduct ($HSiCl_3$-DMF), was able to promote the reduction of aldehydes to alcohols, imines to amines, and also the reductive amination of aldehydes under mild conditions (scheme 1.9).

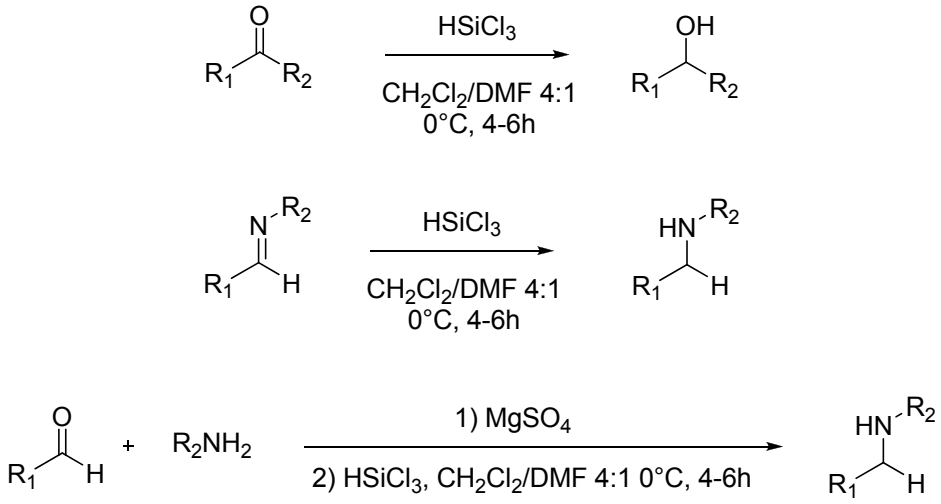

Scheme 1.9*: reductions mediated by $HSiCl_3$-DMF.*

Some years later, Sakurai and Kira reported that bis(1,2-benzenediolate)-hydridosilicate, prepared from trichlorosilane and dilithium catecholate, reduced aldehydes and ketones affording the corresponding alcohols. Also the use of biphenyl-2,2'-diol, gave good results (scheme 1.10).

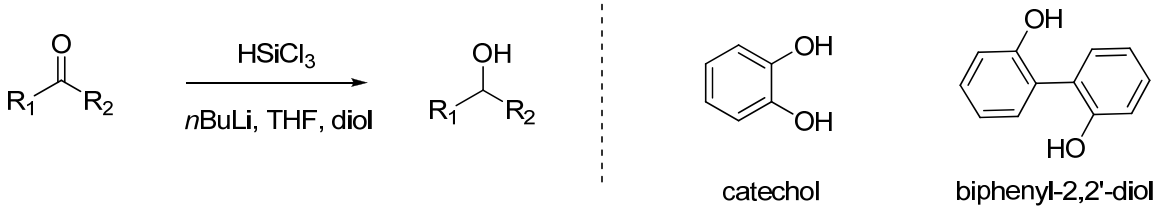

Scheme 1.10: *reduction mediated by diols in the presence of $HSiCl_3$*

These examples showed that trichlorosilane needs to be activated by coordination with Lewis bases, such as *N*,*N*-dimethylformamide, acetonitrile, trialkylamines, to generate hexacoordinated hydridosilicate, the active reducing agent that operates under mild conditions. For these reasons, the use of chiral Lewis bases was investigated to obtain stereoselective reduction products in a stereoselective fashion.

1.3 Stereoselective C-H bond formation

The use of chiral Lewis bases offers the possibility to control the absolute stereochemistry of the process and it has been widely explored in the last few years, leading to the development of some really efficient catalytic protocols. The catalytic systems may be classified as ***N*-formyl derivatives**, which may be historically considered the first class of compounds developed as chiral activators of trichlorosilane, **chiral picolinamides**, a second class extensively investigated in the last few years and other **Lewis basic compounds**.

1.3.1 Reactions catalyzed by N-formyl derivatives

The first example of stereoselective catalytic reduction with $HSiCl_3$ was reported in 1999; Matsumura and co-workers reported *N*-formyl cyclic amine compounds derived from (*S*)-proline scaffold that are able to enantioselectively reduce ketones in the presence of trichlorosilane.[88a] A catalytic amount of these Lewis bases was used for obtaining enantiomerically enriched secondary alcohols in up to 51% ee (Scheme 1.11).

Two years later the same group found that trichlorosilane, activated with the same chiral Lewis basic *N*-formylproline, is an effective reagent for chemo- and stereoselective reduction of imines (Scheme 1.11). The corresponding amines were isolated in moderate yields with up to 66% ee.[88b]

Matsumura contribution in designing *N*-formyl pyrrolidine derivatives as $HSiCl_3$ activators can be considered as a milestone for the asymmetric reduction of ketones and imines using $HSiCl_3$ as reducing agent and paved the road to the synthesis of other related systems. Since then, considerable efforts have been devoted to the development of

efficient catalysts for the reduction of carbon-nitrogen double bonds, and remarkable progress has been made.

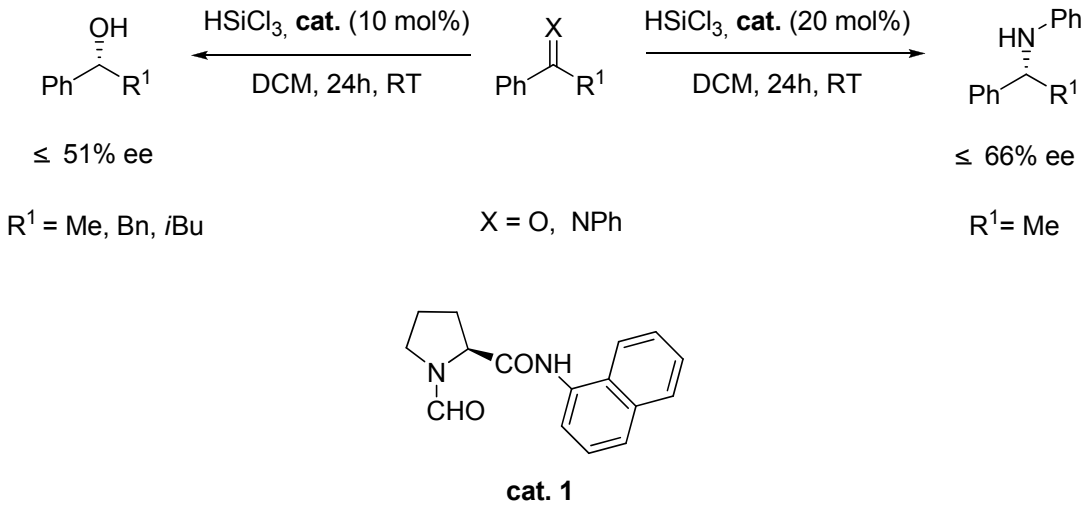

***Scheme 1.11**: N-formyl proline as chiral promoter of $HSiCl_3$-mediated reactions.*

One important breakthrough in the field was achieved by Malkov and Kočovský in 2004, when they developed the first highly enantioselective catalytic system; the compounds of choice are *N*-methyl-(*S*)-valine-derived Lewis basic organocatalysts of type **2**, commercially available since 2009 (Scheme 1.12).[89]

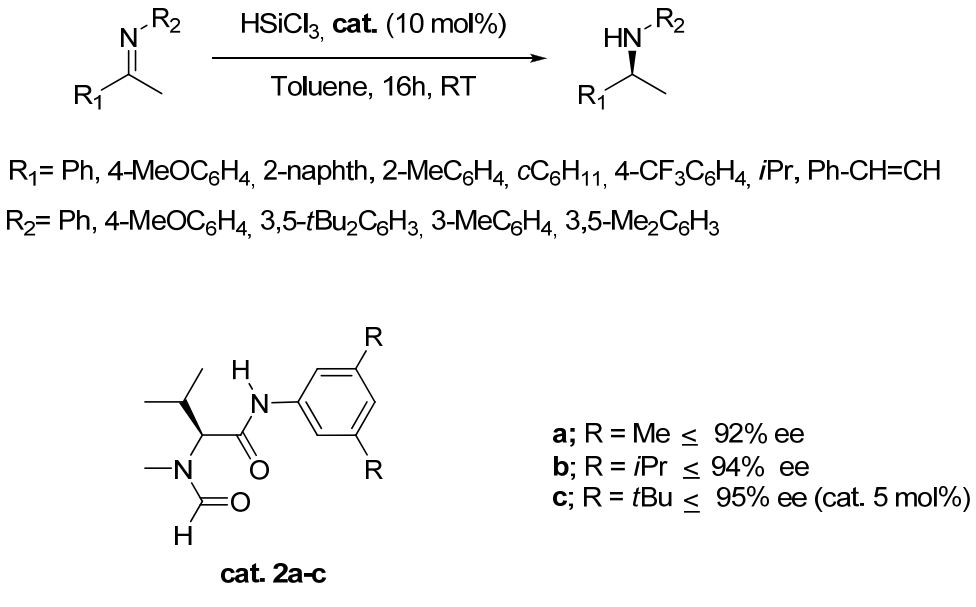

***Scheme 1.12:** N-formyl derivative of- N methyl-(S)-valine.*

In 2006, the same authors reported a detailed investigation of the reduction of imines with $HSiCl_3$ catalyzed by *N*-methyl-(*S*)-aminoacid derivatives.[90] A library of chiral *N*-formylated aminoacids was designed and synthesized, with structural variations at the carboxyamide group, provided by either aromatic or aliphatic substituents. The reaction was carried out in non-polar solvents; toluene was chosen for its relatively low environmental impact. Different substituted *N*-aryl ketimines have been tested as substrates.

After screening of a variety of *N*-methyl-(*S*)-amino acid in the reduction of ketomines, valine was selected as chiral element of choice to perform stereocontrol and a few conclusions were proposed: (*i*) the *N*-methyl formamide moiety of the catalyst is fundamental for the enantioselectivity; (*ii*) arene-arene interactions may play an important role in determining the stereoselectivity of the catalyst; (*iii*) the anilide moiety of the catalyst has to be a secondary amide retaining an NH group; (*iv*) the silicon atom is activated by coordination with the formamide moiety; (*v*) the configuration of the resulting product depends on the nature of the aminoacid side chain, (*vi*) bulkier groups in the 3,5-positions of the aromatic ring (diisopropyl and ditertbutyl) determine an increase of enantioselectivity in the reduction of aromatic and non-aromatic ketoimines.

Catalyst-substrate hydrogen bonding and coordination of the silicon atom by the two carboxyamide groups were suggested to play a fundamental role in determining the stereoselectivity of the reaction. In the proposed transition state an additional element of stereocontrol is the formation of a hydrogen-bond between the secondary amide group of the catalyst and the substrate (Scheme 1.13).

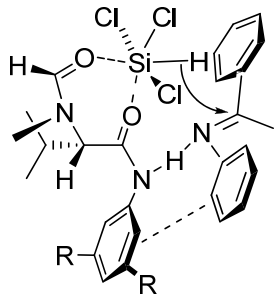

Scheme 1.13: *model of stereoselection for (S)-valine-derived organocatalyst.*

The stereocontrolling ability of the catalyst **2c** (called Sigamide, Scheme 1.12) was then investigated in the reduction of multifunctionalized ketoimines bearing heterocyclic and aliphatic substrates.[91] The reaction exhibited high enantioselectivities with ketimines derived from aromatic amines and aromatic, heteroaromatic conjugated and nonaromatic ketones with an appreciable steric difference between the alkyl groups R_1 and R_2. Introduction of a heteroatom into the aromatic system (pyridyl derivatives) afforded the products with almost no enantioselection, probably due to the competition of the substrate pyridine nitrogen with the catalyst in the coordination of the silicon atom of $HSiCl_3$.

Recently two new (*S*)-valine-derived organocatalysts (**3a**, **3b** Scheme 1.14) bearing a bulky aromatic substituent at the amidic nitrogen were synthesized.[92] The efficiency of the new compounds was tested in the model reduction of ketoimines derived from aryl methyl ketones and it was found to be slightly inferior compared with that of Sigamide **2c**.

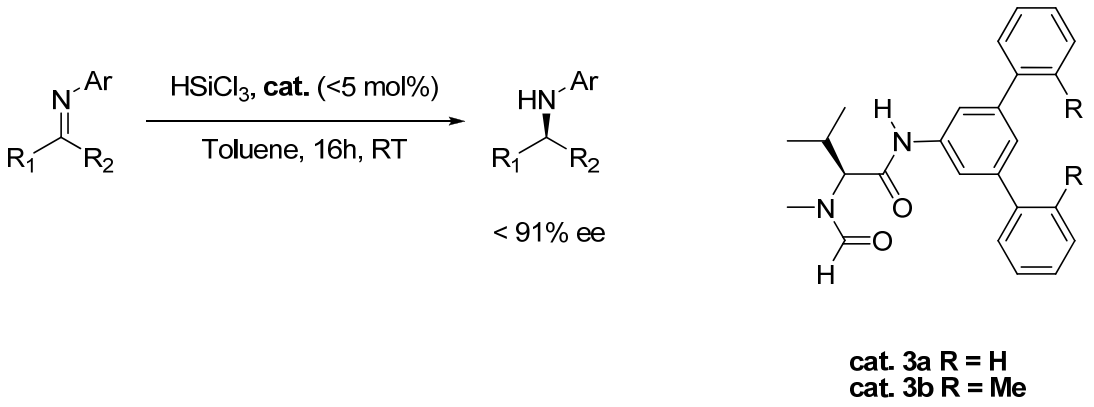

***Scheme 1.14**: new (S)-valine-derived organocatalysts.*

The recoverability of this family of catalysts has also been studied. A fluorous-tagged catalyst was shown to operate in solution, with very little difference in terms of catalytic efficiency with respect to the untagged version.[93a] The products were separated from the catalyst by filtration though a pad of fluorous silica and the catalyst was easily recovered and recycled.

Recently another study on the development of a polymer-anchored version of the same catalyst was reported; different supports such as Merrifield and extended Merrifield, Wang, TentaGel, Marshall resins, were all employed to immobilize the organocatalysts

through an ethereal bond.[93b] The enantioselective reduction of *N*-aryl ketoimines in the presence of trichlorosilane was performed by employing typically 15-25% mol amount of the supported catalyst, a higher loading than the one used with the non supported system (typically 5-10% mol cat). The immobilized catalysts showed a remarkable dependence on the reaction solvent; while the non-supported organocatalyst works well in toluene, the polymer-anchored species behaves much better in chloroform. By operating under the best experimental condition, with the Merrifield-anchored catalyst, the product was isolated in good yield and in 82% ee, about 10% lower than that obtained with the non-supported catalyst. After filtration of the immobilized organocatalysts, it was possible to reuse it five times maintaining the same level of stereoselectivity; however, a catalyst's reactivation step was required.

The use of (*S*)-valine-derived formamide was extended also to the reduction of α-chloro-imines. These compounds were generated *in situ* from corresponding α-chloro-ketones and aniline derivatives. The reduction in the presence of $HSiCl_3$ at room temperature gave the α-chloro-amines with high enantioselectivities (up to 96% ee) and good yields and, after cyclization, the corresponding aziridines as final products (Scheme 1.15).[94]

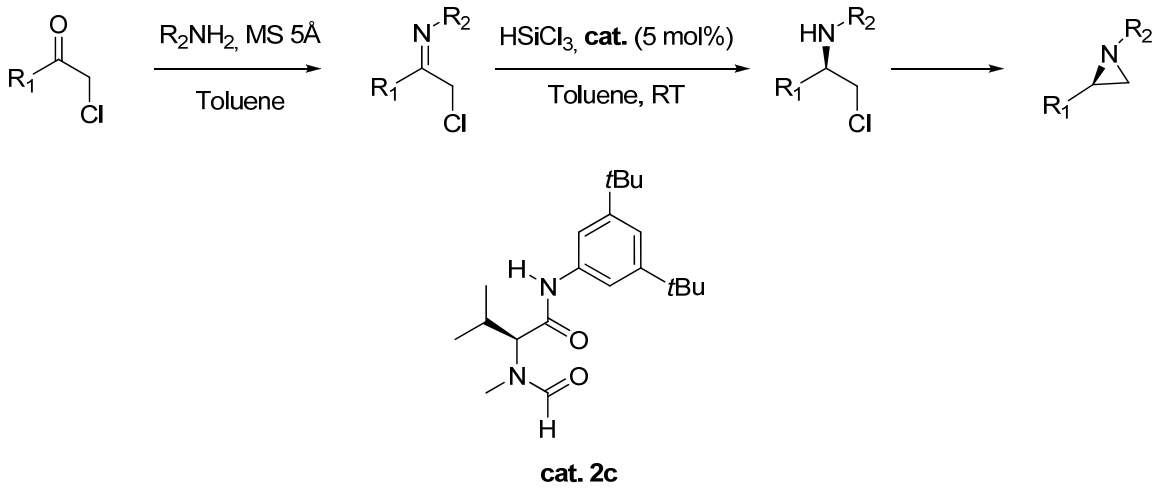

Scheme 1.15: *stereoselective synthesis of aziridine.*

Very recently catalyst **2c** proved to be suitable also for the development of a new protocol for the enantioselective synthesis of β-aminoacids derivatives from enamine precursors.[95] Treatment of the β-ketoester or β-ketonitrile with *p*-anisidine afforded enamines, which as such cannot be reduced by $HSiCl_3$. Because the enamine-imine

equilibration is facilitated by Brønsted acids, a number of acid additives were examined, among which AcOH (one equivalent mol) proved a good compromise between reactivity and selectivity. Enamine was reduced to give the amino ester in high yield and 89 % ee. The enantiomerically pure product could be obtained by a single crystallization. Nitriles exhibited the same behavior as the esters in terms of reactivity. The authors then focused on the synthesis of β-amino acids. In this case, since the starting achiral enamines are in fast equilibrium with the corresponding chiral racemic imines, the reaction can be considered as a dynamic kinetic resolution (Scheme 1.16). The corresponding amino esters and amino nitriles were prepared in good yields high, enantioselectivities (≤ 90% ee) and diastereoselectivities (≤ 99 % de).

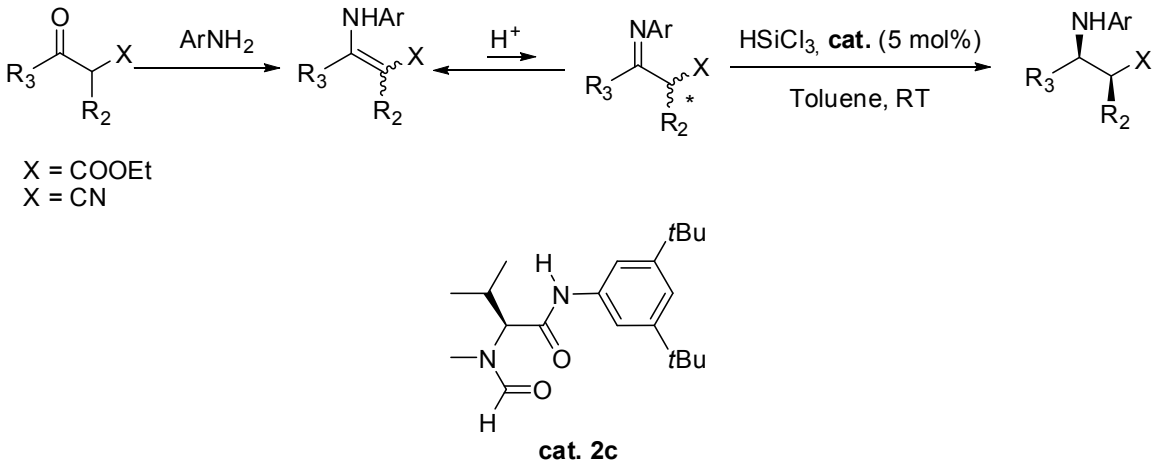

Scheme 1.16*: stereoselective reduction of enamines.*

Following his previous studies with prolinamides, in 2006 Matsumura reported the activity of *N*-formyl proline derivatives in the reduction of ketones in the presence of trichlorosilane.[96] Secondary alcohols could be synthesized with high enantioselectivity (up to 97%, Scheme 1.17) employing a catalytic amount of *N*-formyl-α'-(2,4,6-triethylphenyl)-(*S*)-proline (catalyst **4**). The selection of the best performing compound was the result of the screening of a series of α'-arylproline derivatives. Both carbonyl group at the α-position and a 2,4,6-triethylphenyl group at the 5 position in the proline ring play an important role for determining the high enantioselectivity.

More recently the use of *N*-formyl-*L*-pipecolinic acid derivatives as organocatalysts was also explored in the reduction of aromatic and aliphatic ketones.[97] The best catalyst for the reduction of carbonyl compounds was found to be amide **5**,

characterized by the presence of the methoxy group on carbon C2' of the chiral aminoalcohol moiety (Scheme 1.17). The methoxy functional group on that position turned out to be crucial for obtaining alcohols with high enantioselectivity. Indeed the replacement of this moiety with either a bigger alkoxy group or a group with a less electron-rich 2'-oxygen led to a decreased reactivity and/or enantioselectivity. According to the authors catalyst **5** works as a tridentate activator and promotes the hydrosilylation of ketones through transition structure featuring a heptacoordinate silicon species.

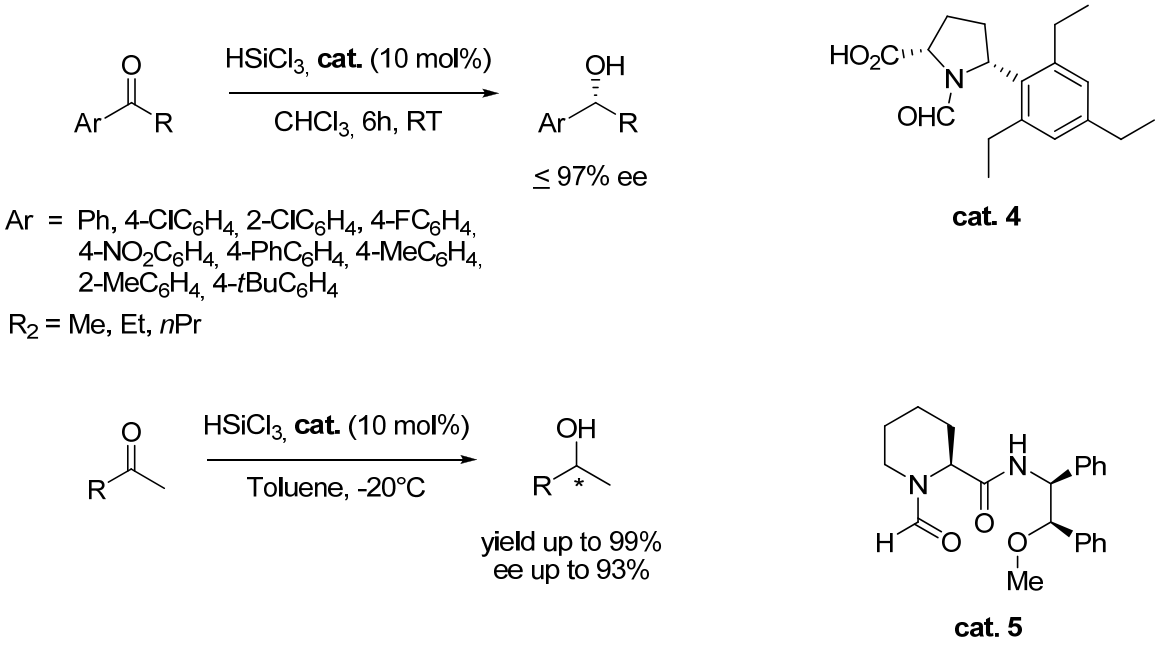

Scheme 1.17: *stereoselective reduction of ketones.*

In 2007 Tsogoeva's research group reported the use of new chiral formamides in the reduction of ketoimines in the presence of trichlorosilane.[98] A second element of stereocontrol, such as a chiral amine, was added to the proline moiety. Catalyst **6**, the *N*-formyl prolinamide of (*R*)-α-methyl amine, activated trichlorosilane in the ketoimine reduction affording the product in 75 % yield and 81% ee in the presence of an additive. HMPA and *p*-nitrobenzoic acid were tested as additives, and, quite surprisingly, the former turned out to be the more effective.

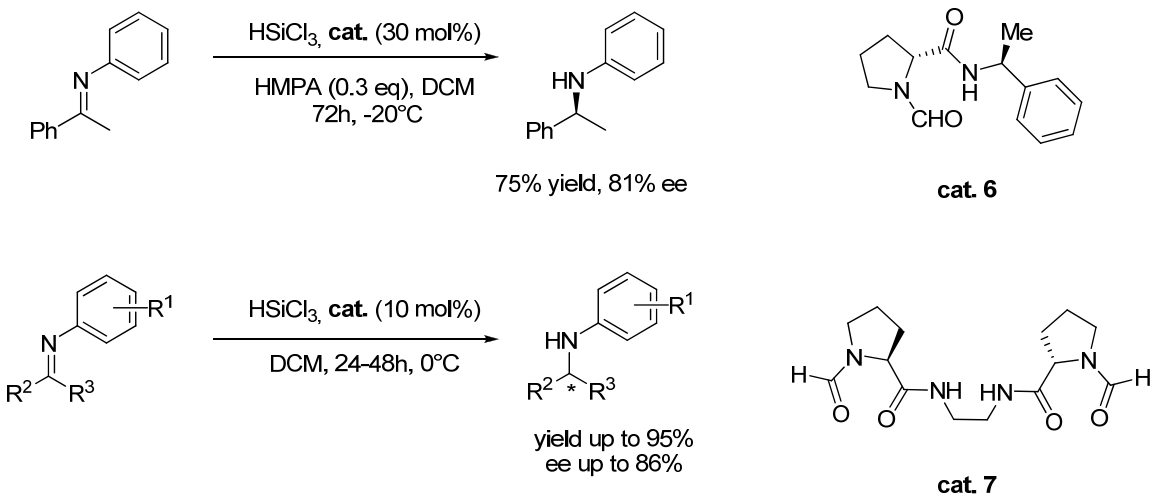

***Scheme 1.18**: novel N-formyl chiral Lewis bases.*

In the same year the Sun group reported the (*S*)-proline-derived C_2-symmetric chiral tetraamide **7** (Scheme 1.18) as a novel catalyst in the enantioselective hydrosilylation of ketomines. [99] The choice of catalyst **7** is the result of the screening of a series of C_2-symmetric chiral tetraamide derivatives where the linkage of the two proline diamide units proved to have a significant impact on the enantioselectivity. Either a shorter or longer linkage and aromatic linkages provided products with much lower enantioselectivities.

The reaction products were isolated in high yields (up to 95%) and moderate to high enantioselectivities (up to 86% ee) for a broad range of substrates, including aromatic and aliphatic imines. The two diamide units in the chiral Lewis base work cooperatively, showing a synergistic effect.

In 2006 Sun reported that switching from the five-membered ring of proline to a six-membered ring had a beneficial effect on the enantioselectivity. The first catalyst[100] derived from *L*-pipecolinic acid, compound **8**, promoted the reduction of *N*-aryl ketoimines with trichlorosilane with high yields and good enantioselectivities. (Scheme 1.19).

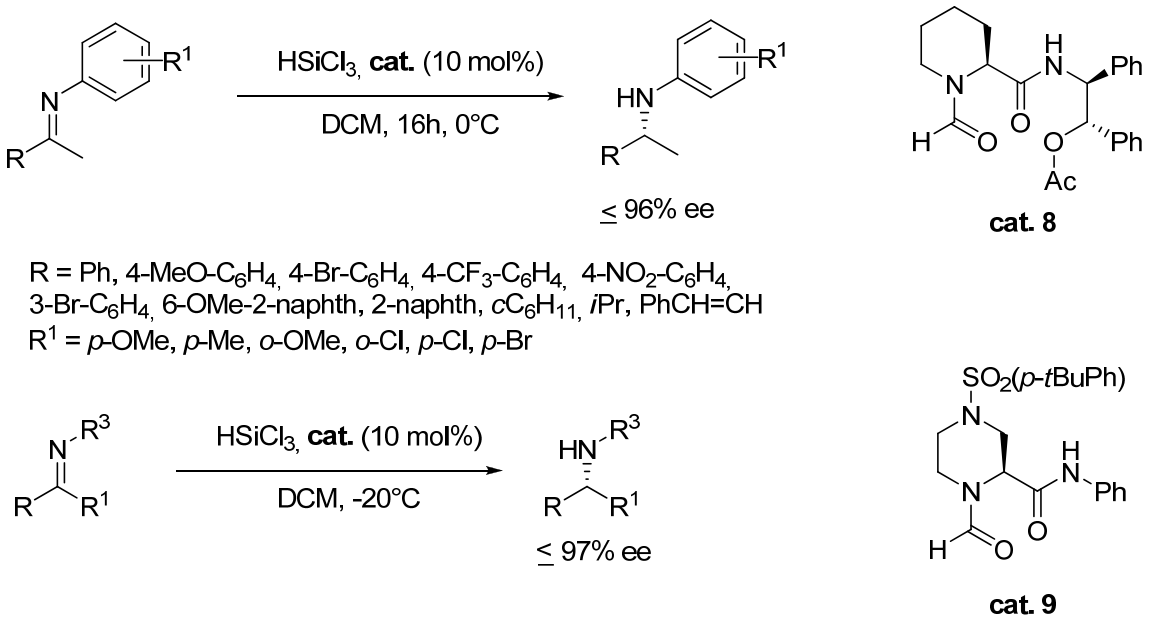

***Scheme 1.19**: chiral pipecolinic acid derivatives.*

Later a piperazinyl backbone was employed as building block for the construction of a new catalyst.[101] The arenesulfonyl group on the 4-position group has been shown to be a key element for obtaining a high level of enantiocontrol (Scheme 1.19). Catalyst **9** promoted the reduction of a broad range of imines with good yields and enantioselectivities.

Very recently Schreiner has published a detailed investigation of the influence that non aromatic groups in *N*-formylprolinamide may have on the enantiomeric excesses of ketimine reductions, by employing also computational methods in the attempt to get some mechanistic insights of the process.[102] By working with a series of novel chiral organocatalysts derived from proline, valine, and pipecolinic acid, the dominant role of the amino acid scaffold in the enantiodifferentiating step was demonstrated. Mechanistic studies by DFT computations seem to confirm that the catalyst not only coordinates to trichlorosilane, but also reacts as a proton donor in the crucial transition structure; indeed the importance of the presence of acidic NH proton of a secondary amide group, able to bind to the basic nitrogen of the reacting imine has been demonstrated. Although the authors suggest that the enantiodifferentiating steps for proline, pipecolinic acid, and valine-derived catalysts may be different, based on the computational studies they propose a general picture for the catalytic reduction of ketimines with trichlorosilane, that could be described as a formal H^+/H^- transfer to the C=N double bond.

1.3.2 Reactions catalyzed by chiral picolinamides

In 2006, Matsumura employed chiral picolinamides as a novel class of catalysts for trichlorosilane-mediated reductions. His group reported that *N*-picolinoylpyrrolidine derivatives may activate trichlorosilane in the reduction of aromatic imines, showing that the *N*-formyl group is not always essential for catalytic activity.[103]

N-picolinoyl-(2*S*)-(diphenylhydroxymethyl)-pyrrolidine **10** gave the best results, leading to enantioselectivities up to 80%. It was proposed that both the nitrogen atom of picolinoyl group and the carbonyl oxygen play a fundamental role in the coordination of silicon atom, while the hydrogen of the hydroxy group is supposed to be involved in a hydrogen bond with the nitrogen atom of the imine (Scheme 1.20).

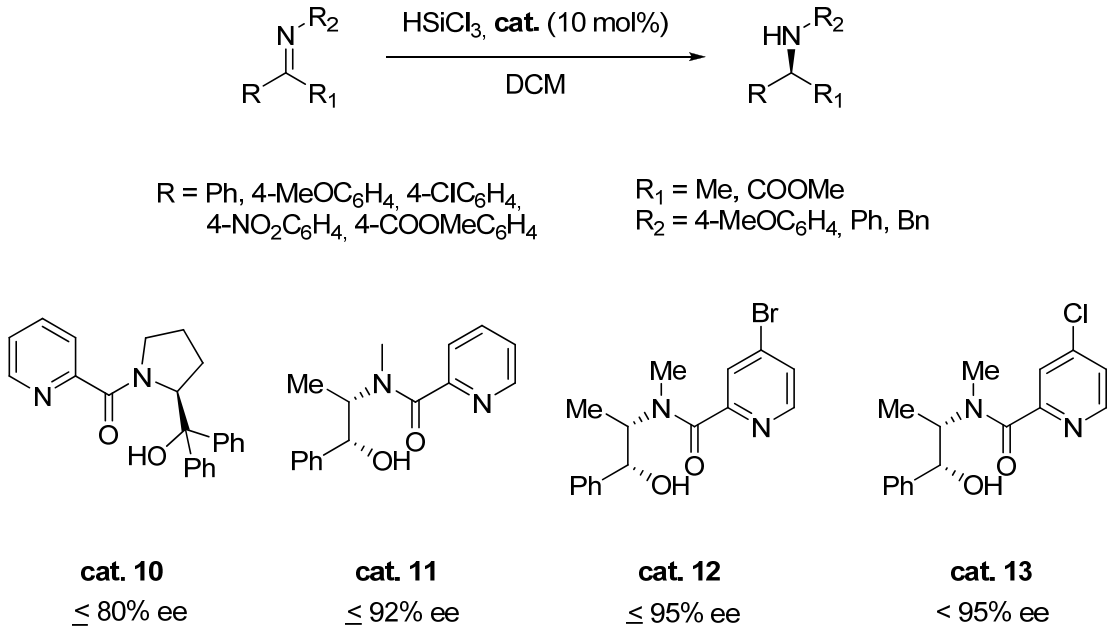

***Scheme 1.20**: chiral N-picolinoyl derivatives.*

Based on these seminal works, our group has recently focused onto the design and synthesis of a wide class of catalysts prepared by simple condensation of a chiral aminoalcohol with picolinic acid or its derivatives. While our investigation led to a patent deposit,[104] at the same time Zhang independently reported, in a preliminary communication, the use of ephedrine and pseudoephedrine-derived picolinamides in the reduction of *N*-aryl and *N*-benzyl ketimines promoted by trichlorosilane.[105] With catalyst **11** easily prepared from 2-picolinic acid and (1*R*,2*S*)-ephedrine, a variety of *N*-aryl

ketimines and *N*-benzyl ketimines were reduced with trichlorosilane in high yields (<93%) and moderate to excellent ee (< 92%) under mild conditions (Scheme 1.20).

Our group systematically investigated this class of organocatalysts.[106] In a single step procedure several catalysts were synthesized simply by reaction of picolinic acid and different enantiomerically pure amino alcohols mediated by condensing agents or by reaction of picolinoyl chloride with an amino alcohol. The pyridine ring, the free hydroxyl group and *N*-alkyl substitution in the aminoalcohol portion were identified as key structural elements, necessary to secure good stereocontrol; the effect of different substituents at the nitrogen atom and at the two stereocenters was also studied. By studying several differently substituted derivatives it was shown that the introduction of a proper substituent in 4 position of the pyridine moiety could improve catalyst efficiency.

Indeed 4-bromo and 4-chloro picolinic derivatives **12** and **13** showed remarkable catalytic properties. Working at 0°C in dichloromethane with catalyst **13** the chiral amine was obtained in quantitative yield and 83% enantiomeric excess; enantioselectivity was increased up to 88% by working in chloroform. A further improvement was observed by performing the reaction at -20°C when enantioselectivity reached 95% with no erosion of the chemical yield, being the reduction product isolated in quantitative yield. Even by working with 1% mol amount catalyst **13** promoted the reduction in 90% yield after only 2 hours.

Systematic screening of modified organocatalysts of this family led to identify the key structural factors that influence their catalytic properties and to propose a tentative model of stereoselection. In this model pyridine nitrogen and CO amidic group of picolinamide activate trichlorosilane by coordination; the hydrogen atom of hydroxyl group plays a fundamental role in coordinating the imine through hydrogen bonding. The presence of two stereogenic centers on the aminoalcohol moiety with the correct relative configuration such as in (1*R*,2*S*)-(-)-ephedrine is necessary to efficiently stereodirect the imine attack by trichlorosilane. The methyl groups on the amide nitrogen and on the stereocenter in position 2 of the aminoalcohol chain apparently have the optimum size for maximizing the enantioselection of the process. In the proposed stereoselection model **A** (scheme 1.21), leading to the major enantiomer, the steric interaction between the pyridine ring and *N*-aryl group is much less significant than that observed in adduct **B**, that is thus disfavored.

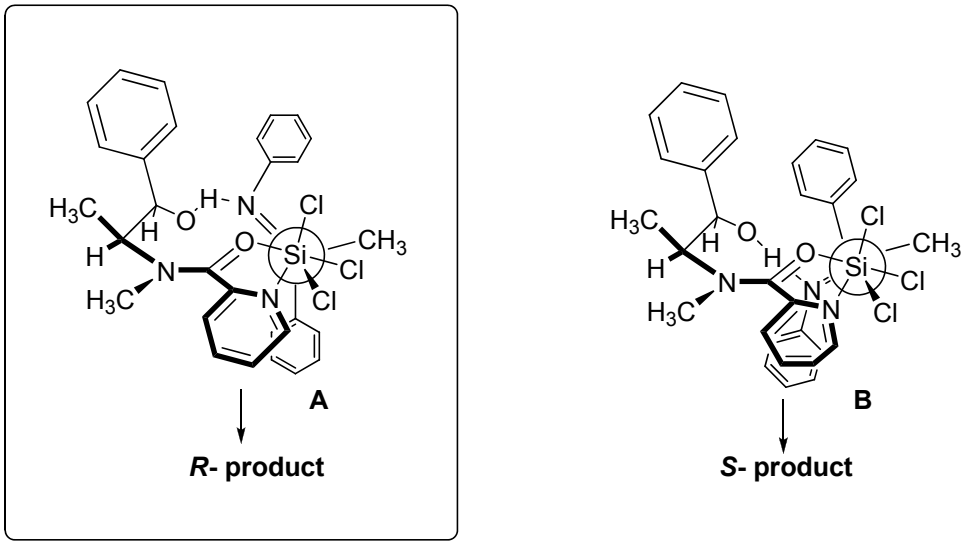

***Scheme 1.21**: proposed model of stereoselection for reduction of N-aryl ketoimines.*

Good results were obtained also in the enantioselective reduction of *N*-alkyl imines,[107] a transformation that only recently has been accomplished organo-catalytically.[108] Ephedrine-based picolinamides promoted the reaction of *N*-butyl imine of acetophenone in excellent yields and high stereoselectivities: under the best conditions (chloroform, 0°C, 24 hours) 4-chloropicolinic derivative **13** promoted the reduction in 98% yield and 91% ee.

These organocatalysts have several convenient features: they are easily prepared, by a single condensation step, between commercially available compounds; they are low cost catalysts, the source of stereocontrol being a very cheap and largely available aminoalcohol, such as ephedrine; the reduction of carbon-nitrogen double bond is performed under very mild reaction conditions and with an extremely simple experimental procedure that allows to obtain a highly pure product after an aqueous work up. A very convenient enantioselective organocatalytic three-component methodology was also developed; the reductive amination process, starting simply from a mixture of a ketone and an aryl amine, opens an easy access to chiral amines with a straightforward experimental methodology. All these features make the present catalytic method suitable, in principle, also for large scale applications; its synthetic potentiality was indeed demonstrated by successfully employing the present metal-free catalytic procedure in the preparation of (*S*)-metolachlor, a potent and widely used herbicide.[106]

In order to further improve the selectivity of the process, the trichlorosilane mediated reduction was accomplished on ketoimines derived from (*R*)-1-phenyl-ethyl amine (Scheme 1.22). It was found that a catalytic amount of *N*,*N*-dimethyl formamide was able to promote $HSiCl_3$ addition with good stereoselectivity, although in low yield.[109] By optimizing the reaction conditions it was shown that best results were obtained at -50°C in chlorinated solvents by performing the reduction with 6 equivalents of DMF. In these conditions *N*-α-methyl benzyl imines of methyl-aryl ketones of different electronic properties were effectively reduced to the corresponding secondary amines in quantitative yields, with 90-99% diastereoselectivity. However when chiral picolinamide **13** was employed as a catalyst, the control of the stereoselectivity was total, as demonstration of the presence of a cooperative effect of Lewis basic catalyst with the (*R*)-residue at the imine-nitrogen.[110]

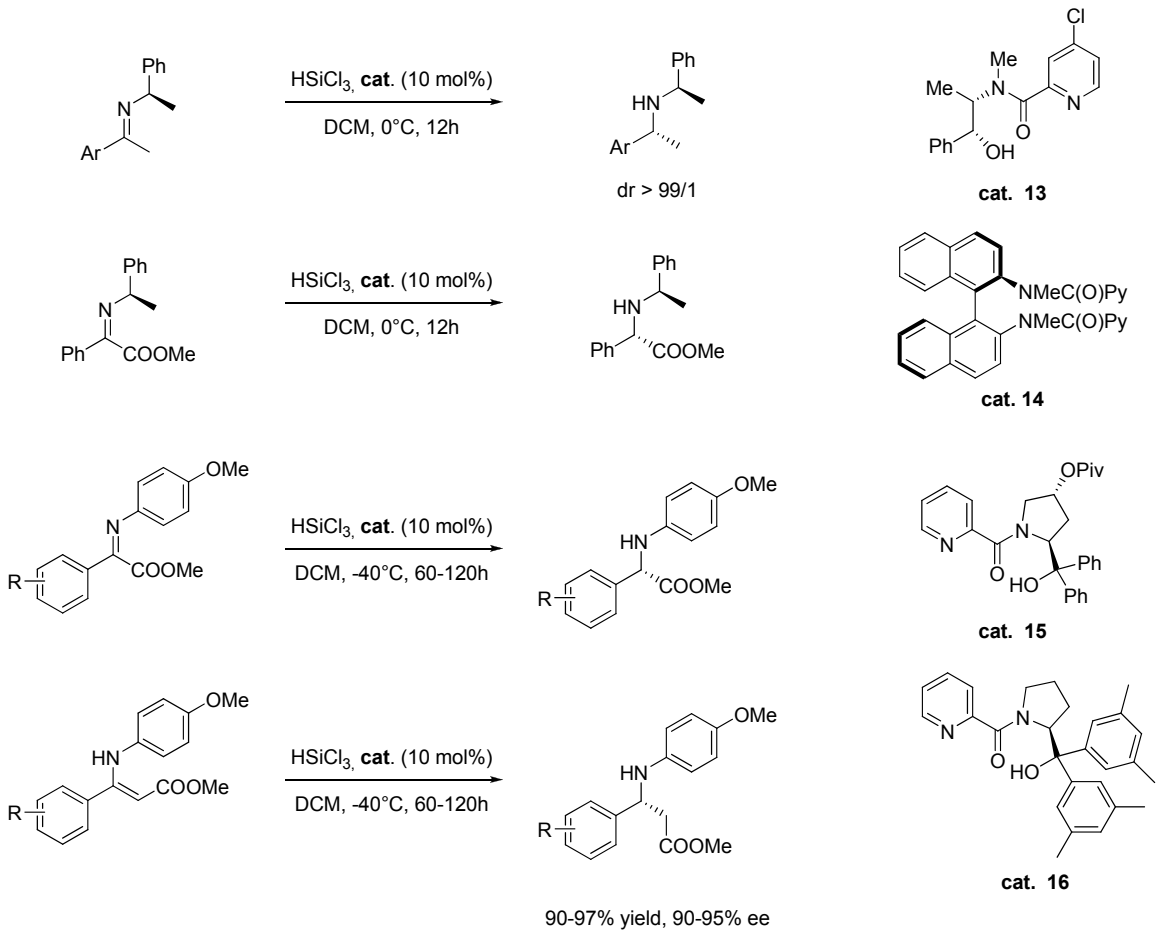

Scheme 1.22*: stereoselective catalytic reduction of chiral imines and imino esters.*

The methodology was extended to the synthesis of an enantiomerically pure secondary amine with both C_1 or C_2 symmetry. Also the imine derived from methyl isobutyl ketone was readily reduced in >98% yield in the presence of catalyst **13** to afford an enantiomerically pure direct precursor of (*R*)-isopropyl methyl amine. The methodology is attractive since the combination of low cost, easy to make metal-free catalyst and an inexpensive chiral auxiliary allowed to reduce ketimines with different structural features often with total control of the stereoselectivity.

The wide applicability of this method was demonstrated also in the preparation of α-amino esters (Scheme 1.22). Catalyst **13** promoted the reduction of *N*-benzyl iminoester in quantitative yield and up to 71% ee. However with the same catalyst the reduction of *N*-α-methylbenzyl imine of methyl-phenyl glyoxylate at 0°C in dichloromethane afforded the corresponding chiral aminoester in 73% yield and 91% diastereoisomeric excess.

Our group developed also a second class of chiral picolinamides as efficient chiral organocatalysts for trichlorosilane-mediated reactions. Picolinic acid was condensed with (*R*)-*N*,*N*'-dimethyl amino binaphthyl diamine to afford catalyst **14** in 73% yield after chromatographic purification. Noteworthy binaphthyldiamine-derived bis-picolinamides showed a remarkable activity in performing the reduction of *N*-aryl (up to 83% ee), *N*-benzyl (up to 87% ee) and *N*-alkyl ketoimines (up to 87% ee), by working typically at 0°C.[111] Furthermore catalyst **14** was employed also in the imine reduction of *N*-benzyl imine of ketoesters, although with less success (71% ee).[112]

Zhang, very recently, also reported an efficient protocol for the organocatalytic synthesis of α-amino esters.[113] A novel class of chiral Lewis base organocatalysts derived from *trans*-4-hydroxy-*L*-proline was developed (Scheme 1.22); noteworthy the catalyst of choice, compound **15**, exhibited only moderate enantioselectivities in the hydrosilylation of *N*-aryl β-enamino esters, but it promoted the hydrosilylation of α-imino esters with high enantioselectivities (up to 93% ee). The introduction of a bulky group at C4 of the pyrrolidine ring was decisive in order to obtain high stereoselectivities. The hydroxy group was functionalized with various bulky groups; while benzyl, trimethylsilyl, and isovaleryl protection of the hydroxy group only caused marginal changes in the enantioselection, an increase in enantioselectivity was observed when *O*-pivaloyl catalyst **15** was employed. In exploring the applicability of the catalyst to imines of differently substituted aryl glyoxylates it was found that both *para* and *meta*

functionalized substrates could be reduced with good enantioselectivity (80-93% ee), while *ortho* substitution caused a decrease of stereoselection (50-60% ee).

The same group has employed picolinamide derivatives of prolinol to realize also an efficient reduction of enamine.[114] Chiral *N*-picolinoylpyrrolidine derivatives and *N*-picolinoylephedrine were evaluated in hydrosilylation of (*Z*)-methyl-3-phenyl-3-(phenylamino)acrylate, leading to the corresponding reduction product in good enantioselectivities in chloroform at 0°C. The enantioselectivity increased slightly with increasing size of the aryl groups in the catalyst. The best yield and enantioselectivity were obtained with catalyst **16** at -30°C for 48h. Under the optimized conditions, the generality of the Lewis base organocatalyzed hydrosilylation of various β-enamino esters were examined. In the presence of 10 mol% of Lewis base, β-enamino esters were reduced in high yields and enantioselectivities typically ranging from 90% to 95%. It is worth mentioning that *N*-acyl β-enamino esters were totally inactive in the present organocatalytic system. The reaction is supposed to proceed through the imine tautomer rather than its enamine counterpart. In the proposed mechanism the nitrogen atom of the pyridine ring and the carbonyl oxygen atom of the catalyst are coordinated to $HSiCl_3$, while the imine is activated by the hydroxy group of the Lewis base through hydrogen bonding. It has also been hypothesized, even thought not demonstrated, that a stabilization due to arene-arene interactions between the aromatic systems of the catalyst and the substrate may occur.

1.3.3 Reactions catalyzed by other chiral Lewis bases

In 2006 a novel chiral Lewis basic system was reported by Malkov and Kočovský: chiral oxazolines bearing an isoquinoline fragment. Catalyst **17** has been employed in the reduction of aromatic ketones and imines with trichlorosilane providing the products with a good level of enantioselectivity (Scheme 1.23).[115]

The best enantiomeric excess reached in the reduction of ketones was 87%, while even better results were achieved in the ketoimines reduction (92% ee). The authors hypothesized that coordination of the trichlorosilane by the catalyst would generate a chiral hexacoordinated silicon species that would be the actual reducing species. When a ketone is the reactive substrate, further activation would be provided by coordination of a molecule of trichlorosilane by the carbonyl oxygen.

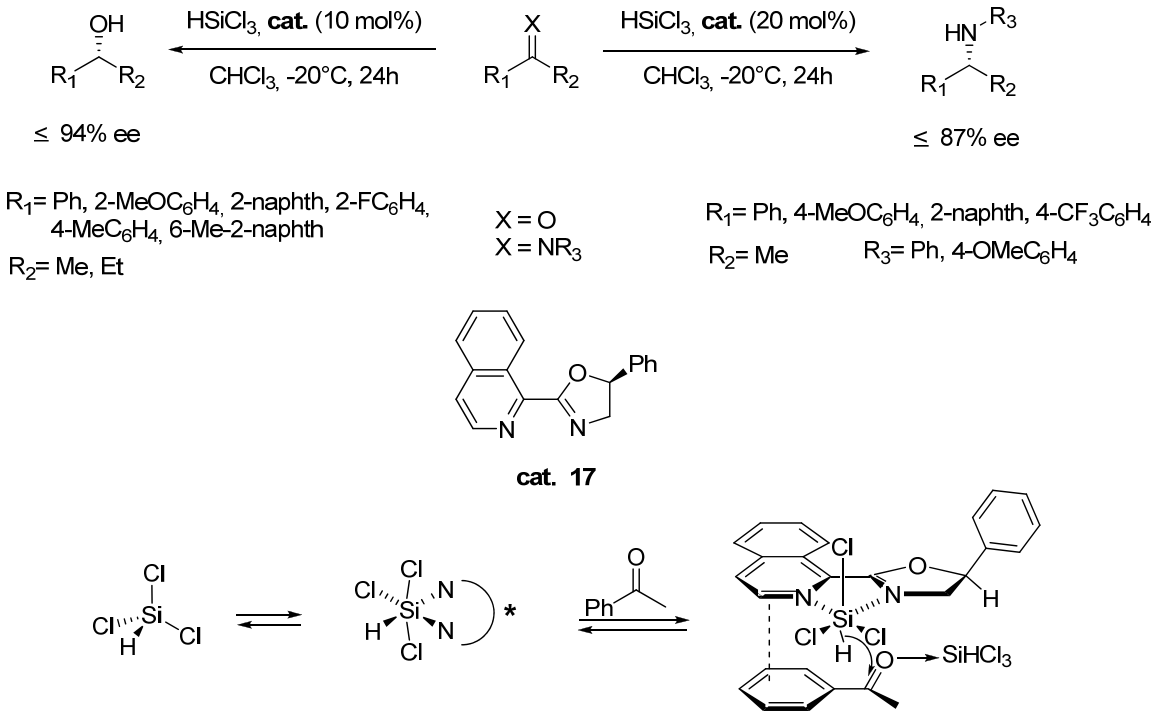

***Scheme 1.23**: stereoselective catalytic reduction promoted by oxazoline-based chiral catalyst.*

Almost at the same time, Sun published a novel designed catalyst featuring a sulfinamide group as the chiral element.[116] This family of organocatalysts was found to be able to activate trichlorosilane for the stereoselective reduction of *N*-aryl ketimines with good yield and enantioselectivity, catalyst **18** being the most successful compound in terms of stereoselection (Scheme 1.24).

Based on the assumption that the mechanism would involve two molecules of Lewis base for the activation of $HSiCl_3$, a novel chiral bis-sulfinamide was then developed. After a screening of different derivatives, the compound of choice was found to be a bis-sulfinamide bearing a spacer containing five methylene groups. Catalyst **19** promoted the reduction of the model substrate, *N*-phenyl imine of acetophenone, with 96% ee (Scheme 1.24). Sulfinamide **20** represents the most recent catalyst prepared by Sun group.[117] This derivative incorporates two different elements responsible for the stereochemical control of the process: a sulfinamide group with a stereogenic sulphur atom and a *N*-aryl prolinamide. This system has been employed in the reduction of aromatic *N*-alkyl ketimines in the presence of trichlorosilane providing the corresponding amines with good enantioselectivities (up to 99.6% ee) and high yields.

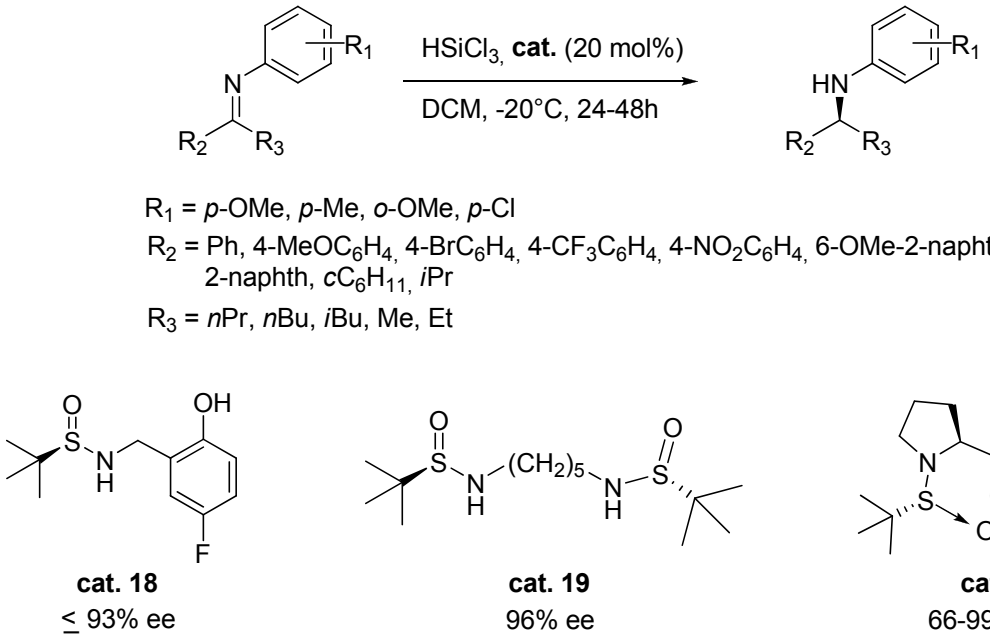

***Scheme 1.24**: chiral sulfinamides as promoters of imine reductions.*

A clearly innovative catalytic system was reported by Nakajima, who introduced chiral phosphine oxides as suitable Lewis bases for activating trichlorosilane in stereoselective transformations. Indeed trichlorosilane has been used in the conjugate reduction of α,β-unsaturated ketones in the presence of a catalytic amount of a chiral Lewis base. The reduction of 1,3-diphenylbutenone promoted by catalytic amounts of 2,2'-bis(diphenylphosphanyl)-1,1'-binaphthyl dioxide **21** ((*S*)-BINAPO) at 0°C was successfully accomplished leading to the corresponding saturated compound in 97% yield and a somehow surprising, but very good, 97% ee.[118] An alternative methodology for organocatalytic conjugate reduction of enones and subsequent reaction with aldehydes, to perform a reductive aldol reaction was developed. The idea was to activate the silane with a suitable Lewis base to perform the 1,4-reduction via a six-membered transition state; then, with the assistance of the same Lewis base, the generated trichlorosilyl enolate should react with the electrophilic aldehyde. (Scheme 1.25).

Triphenylphosphine oxide was shown to be able to catalyze the three-component reaction of chalcone, benzaldehyde and trichlorosilane (reductive aldol reactions) to afford the corresponding aldol product in 78% yield. Preliminary experiments with (*S*)-BINAPO as chiral Lewis base were very promising in term of stereocontrol.

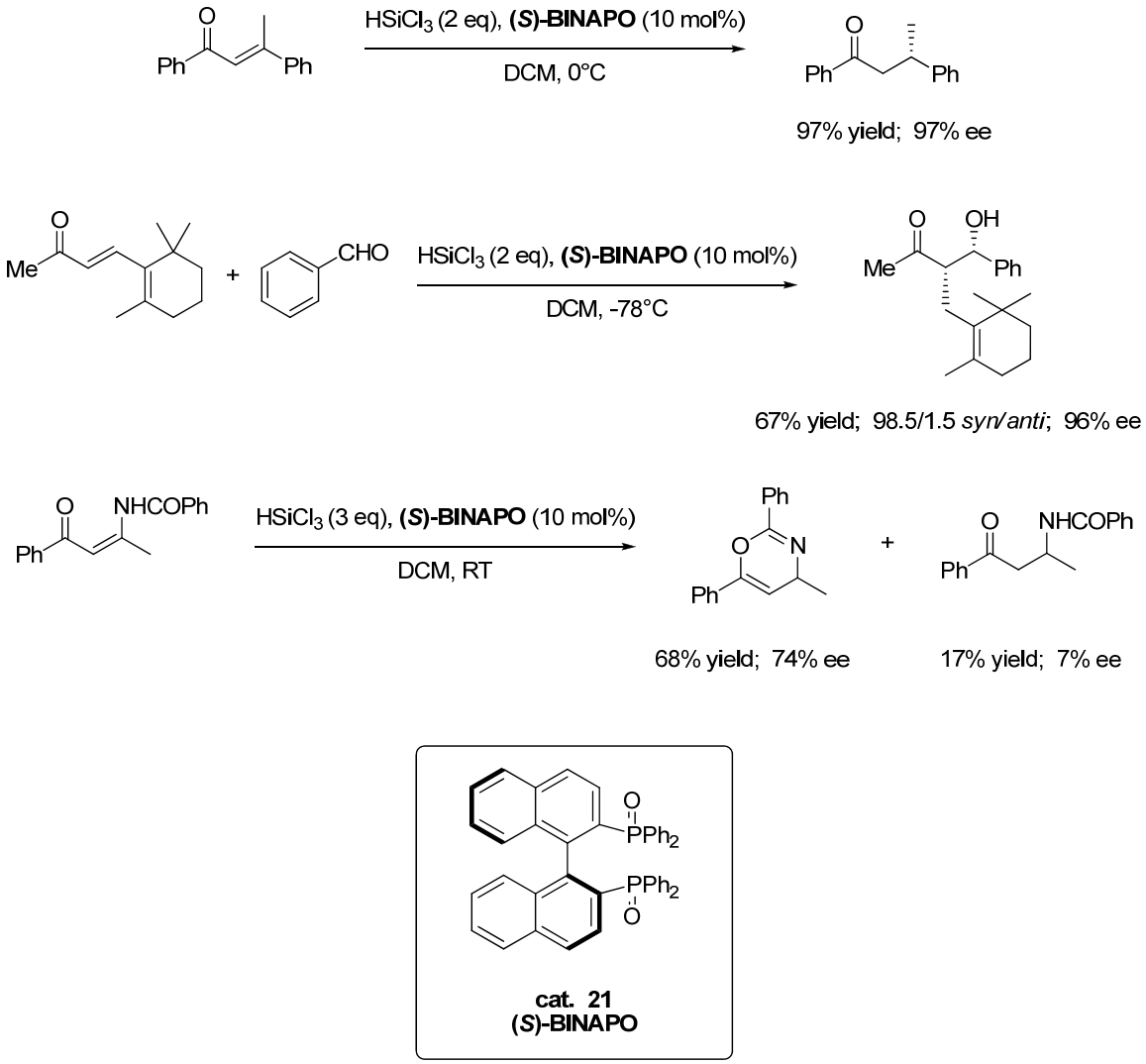

***Scheme 1.25**: chiral phosphine oxide-catalyzed reductions.*

The phosphine dioxide **21** gave even more appealing results in the reductive aldol reduction of β-ionone with benzaldehyde, where a very high *syn* stereoselectivity was observed along with 96% enantioselectivity for the *syn* isomer.

A great variety of Lewis-base catalyzed stereoselective transformations are currently under investigation, and novel synthetic methodologies are currently being developed. An example comes from a very recent report where, by studying the stereoselective synthesis of *N*-acylated β-amino ketones, it was unexpectedly found that optically active 4*H*-1,3-oxazines could be directly obtained via reductive cyclization of *N*-acylated β-amino enones using trichlorosilane and chiral Lewis base catalysts.[119] The reaction of trichlorosilane in the presence of catalytic amounts of (*S*)-BINAPO with (*Z*)-*N*-benzoyl enone derived from 3-amino-1-phenylbutane-1,3-dione, surprisingly

afforded the 4*H*-1,3-oxazine as major product in 68% yield and 74% enantioselectivity (Scheme 1.25). Similar yields and stereoselectivity (up to 81% ee) were obtained by extending the reaction to other five substrates; among different chiral phosphine oxides investigated BINAPO was found to secure the best performances. From some preliminary experiments it was observed that trichlorosilane acts not only as a reductant, but also as a dehydrating agent. In the reaction different ratios of oxazine and the expected β-keto amide were formed, depending on the experimental conditions. Interestingly, it was observed that the two products were obtained with different levels of stereoselection, and sometimes even with a different absolute configuration.

The result was tentatively explained by assuming that the oxazine was not derived from the ketoamide by simple dehydration. It was proposed that 4H-1,3-oxazine was generated via the conjugate reduction of *N*-acylated β-amino enone, followed by cyclization of the resulting enolate and elimination of $HOSiCl_3$, whereas the ketoamide originates from the 1,2-reduction of the *N*-acyl imine generated via equilibration of the enamide. Further studies will be necessary to fully understand the reaction mechanism, in order to design more efficient catalysts.

1.4 Stereoselective C-C bond formation

The coordination of a Lewis base to a tetracoordinated silicon atom leads to hypervalent silicate species of increased Lewis acidity at the silicon centre. As a consequence, such extracoordinated organosilicon compounds become very reactive carbon nucleophiles or hydryde donors with a strong electrophilic character at silicon and an enhanced capability to transfer a formally negative charged group to an acceptor. (See scheme 1.4 and 1.5). When a hypervalent silicon atom is involved as the reactive site in a transformation, carbon-carbon as well as carbon-heteroatom bond formation can occur. On the contrary, when a tetracoordinated silicon atom is exclusively involved in the reaction mechanism, a carbon-silicon as well as heteroatom-silicon bond formation may occur (but not a carbon-carbon formation). Along these lines several asymmetric catalytic systems have been explored in order to develop new stereoselective substoichiometric methodologies for carbon-carbon bond construction.

Here we have reported a general overview on the allyltrichlorosilane addition to C=O and C=N bonds and on the aldolic condensation in the presence of silyl compounds. The stereoselective C-C bond formation catalyzed by phosphine oxides in presence of tetrachlorosilane require particular attention, and it will be discussed in Chapter 3.

1.4.1. Allyltrichlorosilane addition to C=O and C=N bonds

Allylation of C=N group

The synthesis of enantiomerically enriched homoallylic amines is a topic of paramount importance since they represent useful synthetic intermediates that may be converted into different classes of compounds. However, while the catalytic enantioselective allyl addition to carbonyl compounds is well developed, only a few examples of the analogous reaction with imines and imino esters are known, despite their utility in organic synthesis.[120]

In 2004 Kobayashi reported the first example of allyltrichlorosilane addition to *N*-benzoyl hydrazones a reaction promoted by a chiral phosphine oxide as Lewis base.[121] Phosphine oxide **21** ((*S*)-BINAPO) was employed in the reaction of α-hydrazono esters, (obtained from ethyl glyoxylate and benzhydrazide) with allyltrichlorosilane, affording the product in high yields and enantioselectivities at -78°C in dichloromethane (Scheme 1.26). The reaction is stereospecific, in that (*E*)-crotyltrichlorosilanes afford exclusively the *syn* isomers, and (*Z*)-crotyltrichlorosilanes their *anti* counterparts.

It must be noted that a more than stoichiometric amount of what was called NCO (Neutral Coordinate-Organocatalyst) was necessary in order to achieve high stereoselectivities, while 0.2 equivalent of BINAPO catalyzed the reaction in only 11% yield and 56% ee. Another drawback of the methodology is represented by the reductive cleavage of the N-N bond (accomplished by using SmI_2) required in order to obtain synthetically useful compounds. Even if the chiral source could be recovered without loss of stereochemical integrity, it is obvious that the reaction cannot be considered catalytic; however it has some merit, since it represents the first example, and still one of the few cases, of enantioselective allylation of a carbon-nitrogen double bond involving a metal-free promoter.[122]

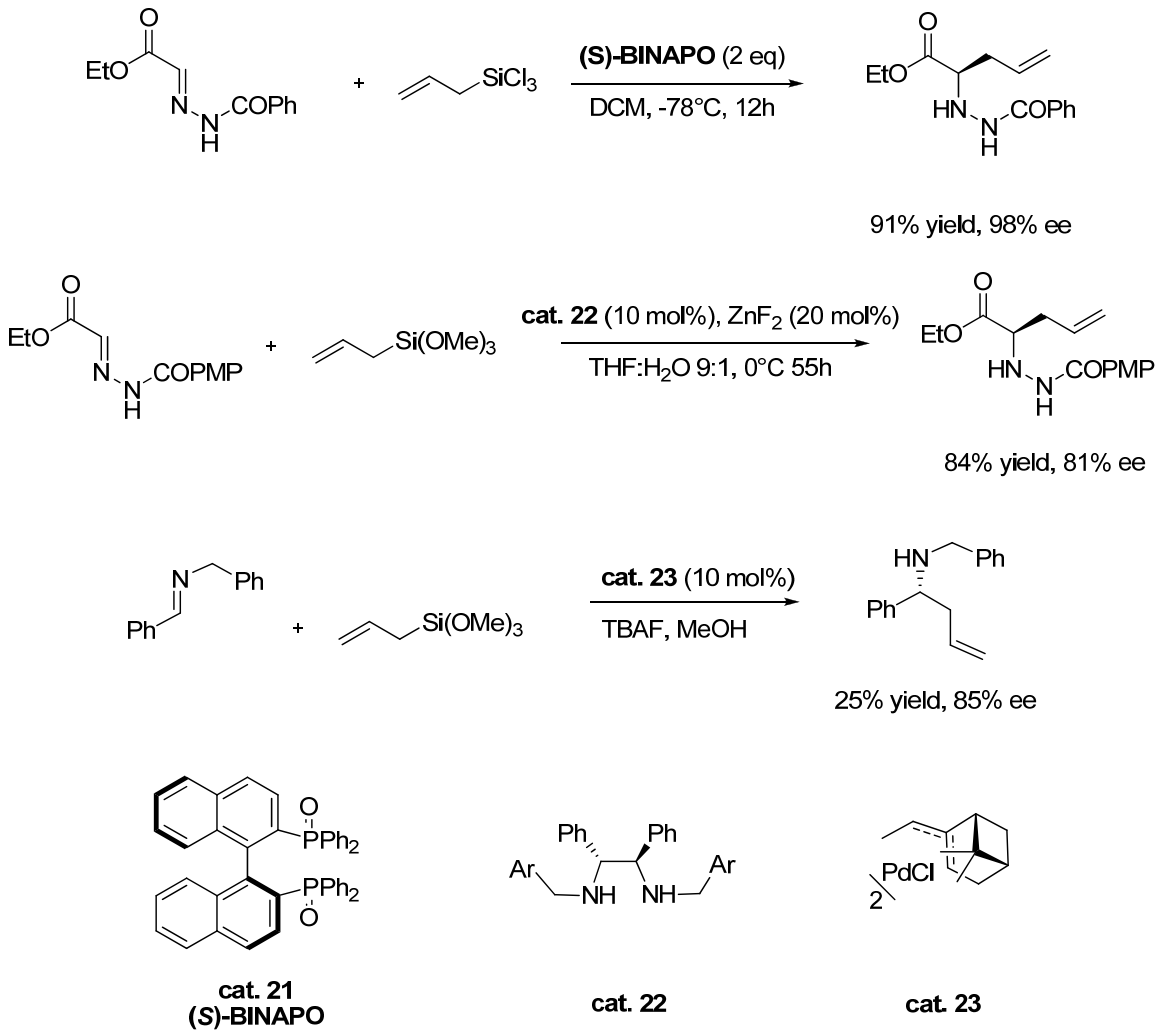

***Scheme 1.26**: stereoselective addition of carbon-nitrogen double bond.*

Recently Kobayashi has also developed a zinc fluoride catalyzed addition of allyltrimethoxy silane[123] to acylhydrazono esters, in the presence of a chiral diamine ligand **22** (Scheme 1.26).[124] Water plays a determinant role in affording the product of reaction, that suffers anyway of substrate limitations. Recently Yamamoto and Fernandes have reported the addition of allyltrimethoxysilane to simple imines mediated by a dual activation /promotion process that involves the use of TBAF and the chiral complex of palladium **23**; the product is isolated in 84% ee but very low yields.(Scheme 1.26).[125]

Allylation of C=O group

Previously promoted by chiral Lewis acids, this reaction, that may lead to the formation of two new stereocenters, can currently be carried out in the presence of a variety of organic Lewis bases as catalysts. Since a few reviews have recently covered the topic,[76,82] in the present section only the most important contributions in the field will be discussed as representative examples of different classes of catalysts; in addition, the more recent achievements in the allylation reaction of carbonyl compounds will be included. In 1994 Denmark reported the first enantioselective, non catalytic, addition of allyltrichlorosilane to aldehydes promoted by chiral phosphorotriamides.[126] A series of detailed studies demonstrated that two pathways were possible; one involving an octahedral cationic silicon atom, coordinated by two Lewis bases molecules leading to a good selectivity,[127a] and another less selective one, where only one phosphoroamide was bound to a pentacoordinated silicon centre.[127b] In view of these mechanicistic considerations several chiral bidentate phosphoroamides were prepared and studied in the test allylation of benzaldehyde; a catalyst loading as low as 5 mol% of compound **24** was found to promote the reaction affording the product in high yield and enantioselectivity up to 72% (Scheme 1.27).[128]

Based on these results, that clearly indicated the beneficial effect of combining two phosphoramide units through a diamminoalkyl chain, new bidentate catalysts derived from 2,2'-bispyrrolidine and 2,2'-bis piperidine units were investigated.

Compound **25** was found to be a really efficient promoter for the allylation reaction of benzaldehyde with allyltrichlorosilane and afforded the homoallylic alcohol in 85% yield and 87% ee.[127] Various γ-substituted allyltrichlorosilanes were employed leading to the products in high yields and up to 96% ee, showing a good correlation between the configuration of the C=C double bond in the reagent and the *syn/anti* diastereoisomeric ratio of the products. A rationalization of the behaviour of catalyst **25** was also proposed (Scheme 1.27). In the chairlike, cyclic **TS A** the aldehyde ring is located in an unfavorable position occupied by a forward-pointing pyrrolidine ring, creating destabilizing steric interactions. In the diastereoisomeric chairlike arrangement of **TS B** the aldehyde ring does not have any unfavorable interaction with the backward-pointing pyrrolidine unit, leading to the experimentally observed product of *S*-configuration.

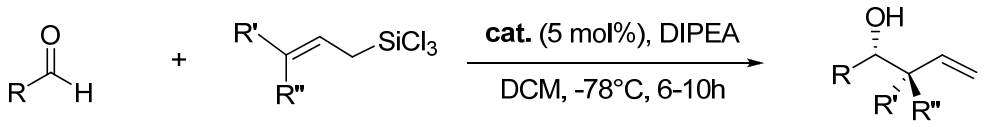

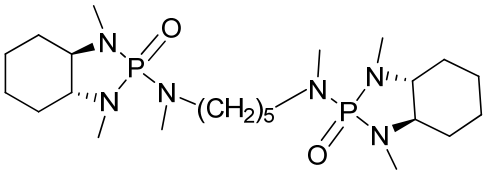

cat. 24

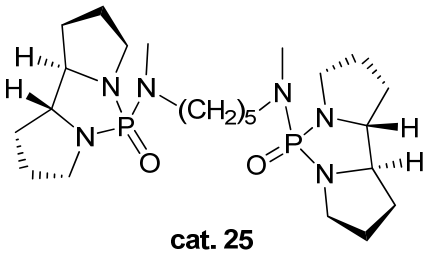

cat. 25

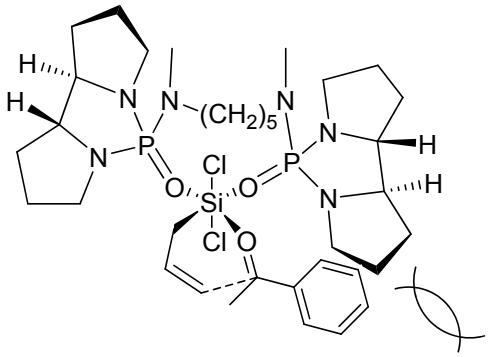

TS A

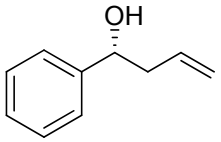

(*R*) unfavoured

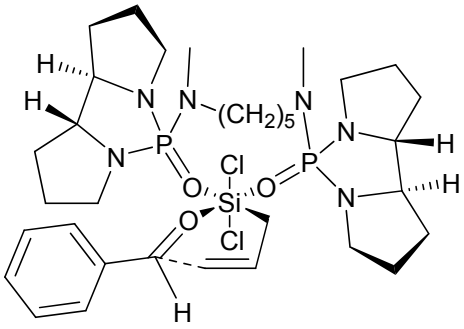

TS B

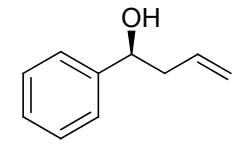

(*S*) favoured

Scheme 1.27*: allylation reactions promoted by chiral phosphoroamides.*

Among Lewis basic catalysts, another class of compounds that deserve a special attention is represented by amine *N*-oxides.[129] The high nucleophilicity of the oxygen in *N*-oxides, coupled with the high affinity of silicon for oxygen, represents ideal properties for the development of synthetic methodology based on nucleophilic activation of organosilicon reagents. The first asymmetric addition of trichlorosilane to aldehyde catalyzed by biquinoline *N,N'*-dioxides **26** was reported in 1998 by Nakajima.[130] The reaction was accelerated by the addition of diisopropylethylamine and afforded the products in high yields and enantioselectivities (up to 92%) with aromatic and heteroaromatic aldehydes. Lower yields and stereocontrol were observed with non conjugated aldehydes (Scheme 1.28).

Later, Hayashi developed another chiral catalyst, **27**, with a stereogenic axis as key element of stereocontrol, leading to comparable enantioselection with catalyst **26** (56-98% ee).[131] Remarkably, Hayashi's catalyst was found to be effective at 0.1 mol% level (-40°C, acetonitrile) and retains moderate activity even at 0.01 mol% loading, which makes this organocatalyst the most reactive one reported to date. More recently, a simple synthesis of unsymmetric atropoisomeric bipyridine *N,N'*-dioxides in three steps from commercially available material was reported.[132] The key step of this reaction sequence is the cobalt-catalyzed heterocyclotrimerization of 1-pyridyl-1,7-octadiynes with nitriles to provide unsymmetrical bipyridines, followed by oxidation and resolution into enantiomers. Catalyst **28** promoted the addition of allyltrichlorosilane to aromatic aldehydes in up to 80% ee.

Another class of catalysts was actively studied by Malkov and Kočovský, which have shown that the terpene-derived bipyridine *N*-monoxides Me_2PINDOX, **29** (cat. 10 mol%, -78°C, CH_2Cl_2) was extremely enantioselective (up to 98% ee), although the reaction was sluggish.[133] Such catalyst combines the effects of both stereogenic centers and axis, the rotation about the bond connecting the two pyridine moieties is restricted by the two methyl groups and the N-O residue.

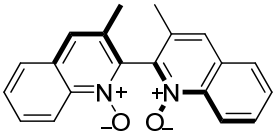

cat. 26

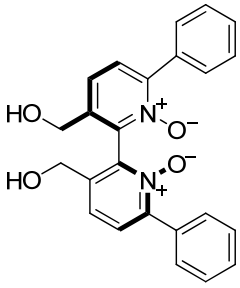

cat. 27

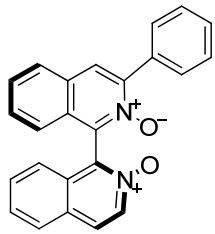

cat. 28

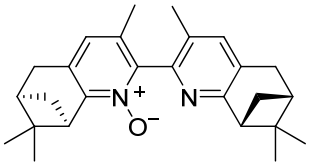

cat. 29

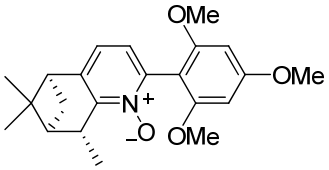

cat. 30

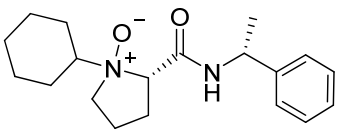

cat. 31

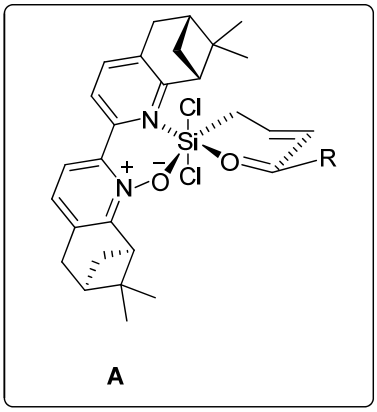

A

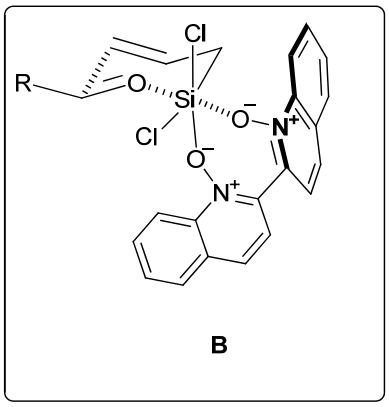

B

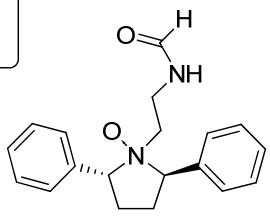

cat. 32

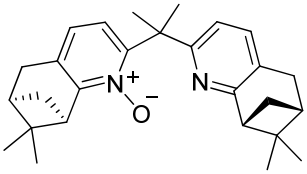

cat. 33

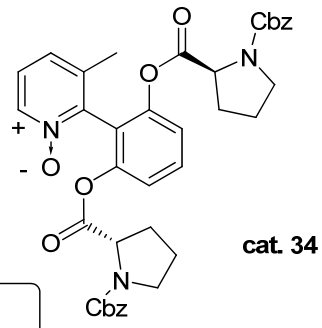

cat. 34

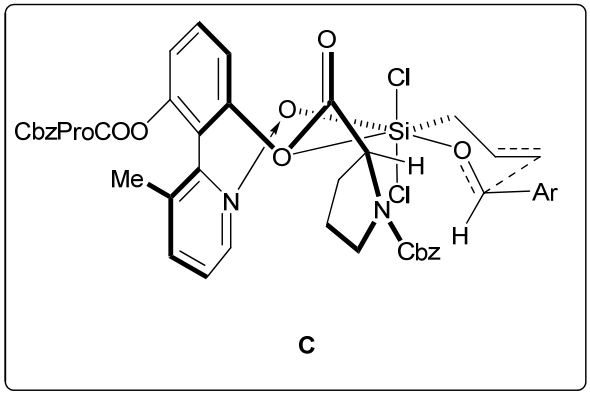

C

Scheme 1.28: *chiral N-oxides as catalysts for allylation of carbonyl compounds.*

In analogy to the previously proposed model, chelation of the silicon in allyltrochlorosilane by the O and N atoms was also proposed for **29**. (Scheme 1.28)

In another important contribution, Malkov and Kočovský showed that two *N*-oxide groups are not necessary, but one *N*-oxide and a second coordination element (such as in the new developed catalyst **30**)[134] are enough to guarantee high levels of stereocontrol, The proposed transition structure for the mono-*N*-oxide derivatives **A** is very similar to that proposed for bis-*N*-oxide compounds, **B**. (Scheme 1.28)

In catalyst **30** arene-arene interactions between the catalyst and the substrate have been suggested to account for the high reactivity and selectivity. Furthermore, it was shown that the axial stereogenicity, whether predetermined or induced during the reaction, is not an absolute prerequisite for attaining high enantioselectivity in the allylation reaction.[135] As further demonstration of these considerations, Hoveyda developed the *N*-oxide **31**, the only representative of aliphatic tertiary amine *N*-oxides so far reported in this series, that presents a stereogenic center at the nitrogen.[136] It is pertinent to note that catalysts **30** and **31** secure high enantioselectivity even at room temperature.

The only other example of chiral non-pyiridinic *N*-oxide used as promoter of the allylation reaction has been recently developed by our group.[137] A new class of amine *N*-oxides derived from *trans*-2,5-diphenylpyrrolidine were synthesized in enantiomerically pure form and tested as catalysts in the reaction of aldehydes with allyltrichlorosilane to afford homoallylic alcohols. The products were obtained in fair to good yields and up to 85% ee. Noteworthy a catalyst capable of promoting the allylation of aliphatic aldehydes with an almost unprecedent and unusually high enantioselectivity, up to 85%, was identified in **32**.

Based on these studies other systems characterized by the absence of stereogenic axis were recently developed.[138] For example, new chiral dipyridine *N*-monoxides and *N,N′*-dioxides, which possess an isopropylidene backbone between two pyridine rings, have been prepared from naturally occurring monoterpenes, the more efficiently being compound **33** (Scheme 1.28).[139] Its utility as organocatalyst has been demonstrated in the enantioselective addition of allyltrichlorosilane to aldehydes, where enantioselectivities up to 85% ee have been obtained.

A series of structurally simple pyridine *N*-oxides have readily been assembled from inexpensive aminoacids and tested as organocatalysts in the allylation of aldehydes

with allyltrichlorosilane to afford homoallylic alcohols.[140] (*S*)-Proline based catalyst **34** afforded the products derived from aromatic aldehydes in fair to good yields and up to 84% ee. By implementing the results of conformational analysis with those of a few control experiments, transition structure **C** shown in Scheme 1.28 can be proposed to tentatively explain the stereochemical result of the allylation reaction. In this model, the hypervalent silicon atom is coordinated by the pyridine *N*-oxide oxygen and the phenolic oxygen of one side arm. The bulky proline residue effectively blocks one side of the adduct and accomodates the aldehyde better than the sterically more requiring allyl residue as its *cis* substituent.

In 2005 for the first time it was demonstrated that also chiral phosphine oxides, such as BINAPO, can act as organocatalysts in the enantioselective addition of allyltrichlorosilane to aldehydes.[141] In the presence of 10% mol of (*S*)-BINAPO **21** the homoallylic alcohol was obtained in DCM in only 32% yield and 36% ee (Scheme 1.29).

By employing a proper additive such as $Bu_4N^+I^-$ and 5 equiv. of DIPEA the yield was improved to 92% after only 4 hours at room temperature, even if with still modest enantioselectivity (43% ee), definitely lower than that obtained with the best phosphoroamide-derived catalysts. The reduced chemical activity might be ascribed to the different electronic properties of the ligands. However, for this kind of reactions it had been already suggested that the effectiveness of a catalyst is determined not only by the donor properties of the Lewis base but also by the steric hindrance at the oxygen atom. For example, dimethylphosphinic *N,N*-dimethylamide is a better promoter for the allylation of benzaldehyde than methylphosphonic di-(*N,N*-dimethylamide) that, in its turn, is better than HMPA (hexamethylphosphoric triamide). However if in dimethylphosphinic *N,N*-dimethylamide a methyl group is replaced by a isopropyl group, the chemical efficiency of the catalyst dramatically decreases, clearly pointing at the importance of the steric accessibility of the oxygen atom for co-ordination.

A marked improvement of the catalytic efficiency of chiral phosphine oxides was obtained by our group exploring the characteristics of heteroaromatic systems.[142] The advantages offered by the biheteroaryldiphosphine oxides, with respect to carbocyclic aromatic derivatives, reside in their greater synthetic accessibility and in the possibility of testing a series of catalysts displaying different electronic properties, where the influence of both the electronic availability of the heterocyclic system and of the position of the phosphorus atoms on the latter may be investigated.

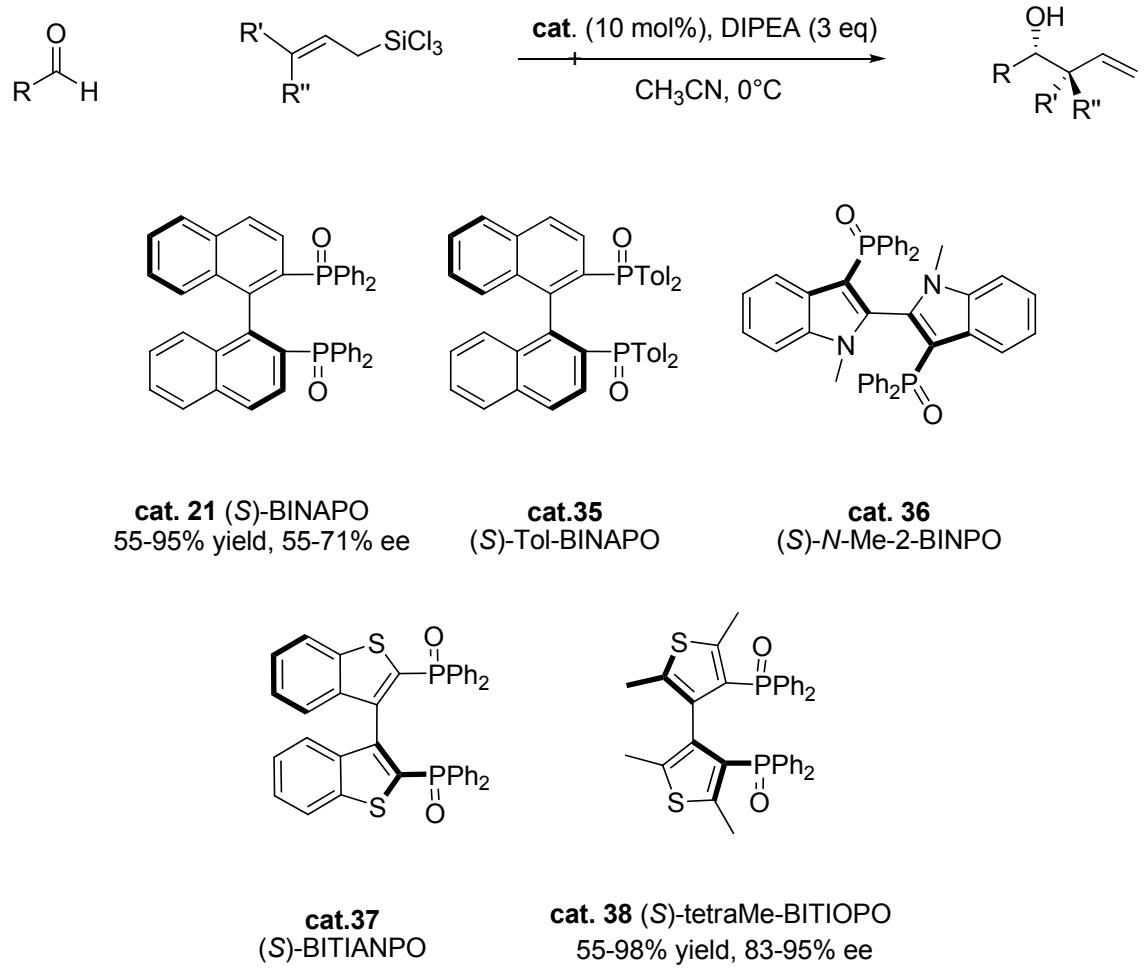

***Scheme 1.29**: chiral phosphine-oxide-catalyzed addition of allyltrichlorosilane to aldehydes.*

While the most electron deficient diphosphine oxide BITIANPO did not promote the reaction in appreciable yields, more electron-rich compounds showed a significant catalytic activity, promoting the addition of allyltrichlorosilane to benzaldehyde at 0°C in higher yield (85%) than medium electron rich diphosphine oxide Tol-BINAPO. Biheteroaromatic diphosphine oxides showed also an extraordinary ability in determining the stereochemical outcome of the reaction, being (*S*)-*N*-Me-2-BINPO able to catalyze the reaction in 81% ee, a result clearly higher than that obtained with Tol-BINAPO (51%).

The catalyst of choice was found to be (*S*)-tetramethyl-bithiophene phosphine oxide, (*S*)-TetraMe-BITIOPO, **38**, which promoted the allylation of benzaldehyde in 93% ee, a very high level of enantioselectivity, comparable to those obtained with the best known organocatalysts. The same catalyst efficiently promoted the addition of allyltrichlorosilane to aromatic aldehydes bearing electron-withdrawing groups as well as electron-donating groups with enantioselectivities constantly higher than 90%.

1.4.2 Aldol condensation reaction

Since the structure and the reaction mode of allylsilane may recall that of silyl enol ether (C-Si bond cleavage vs O-Si bond cleavage), the addition of trichlorosilyl enol ethers to carbonyl derivatives catalyzed by Lewis bases was studied. However since silyl enol ethers have a higher nucleophilicity compared to the corresponding allylsilanes, the aldol addition of trichlorosilyl enol ethers to aldehydes proceeds readily at room temperature even without a catalyst and it exhibits simple first-order kinetics in each component. Nevertheless, the fact that the reaction is substantially accelerated by Lewis bases, sets the scene for the development of an asymmetric variant. Denmark introduced a range of efficient chiral phosphoramides as nucleophilic activators for enantioselective C-C bond aldol formation and also carried out a detailed mechanistic investigation.[143]

In 1996 the first example of aldol condensation of trichlorosilyl enol ethers was reported.[144]

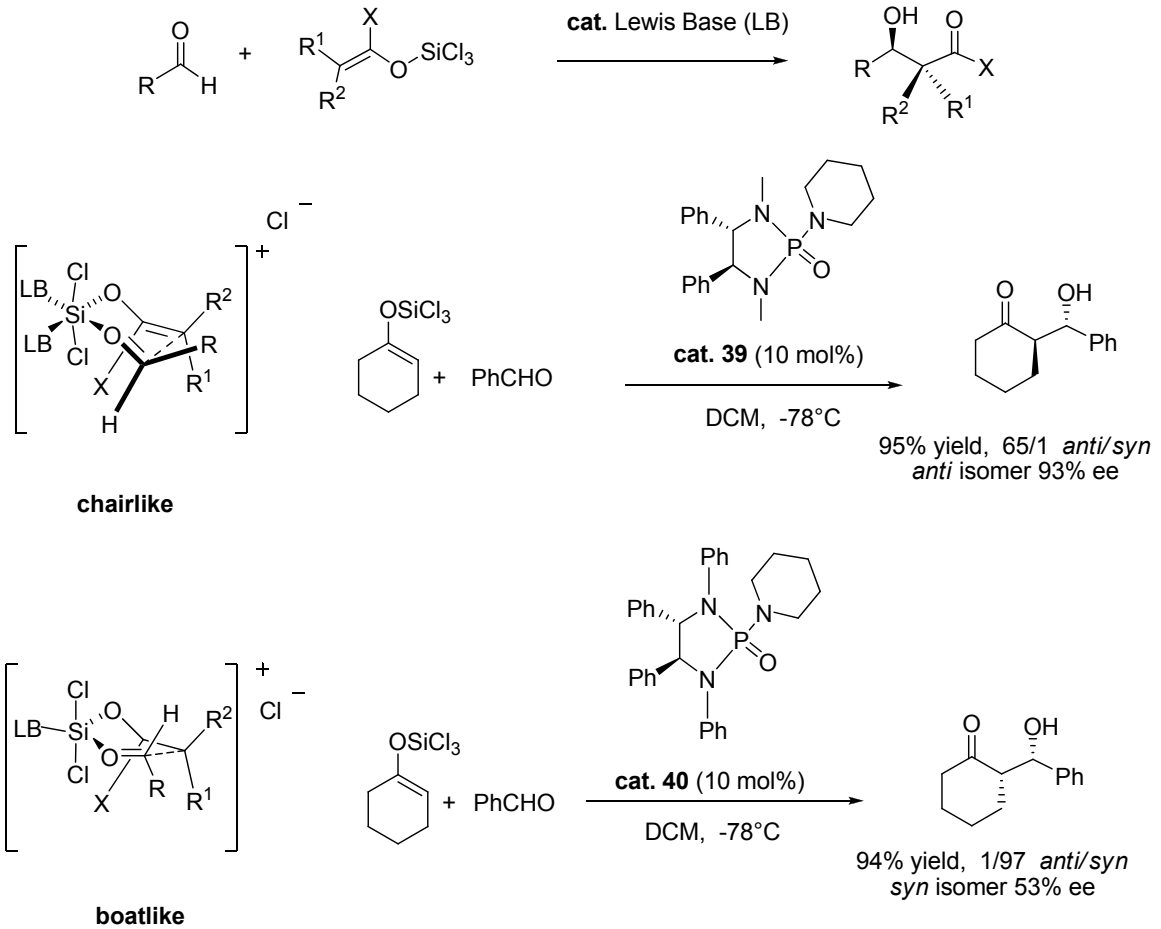

***Scheme 1.30**: aldol condensation promoted by chiral phosphoroamides.*

The chiral phosphoroamide **39** derived from 1,2-diphenyl-ethylendiamine successfully promoted at 10 mol% the addition of the trichlorosilyl enol ether of cyclohexanone to benzaldehyde in 95% yield, 65:1 *syn:anti* ratio and 93% ee (Scheme 1.30). However it was demonstrated that the diastereoselectivity was largely dependent on the structure of the chiral catalyst. After carrying a detailed mechanicistic study bidentate and smaller monodentate catalysts were shown to react through a cationic chair-like transition state, similar to that usually proposed for the allylation reaction, involving octahedral extracoordinate silicon. According to this scheme, (*Z*)-enol ethers produced *syn* adducts, whereas (*E*) derivatives provides *anti* diastereoisomers. In the case of a bulky monodentate activator, where coordination of the second catalyst molecule is precluded by steric factors, the diastereoselectivity of the reaction was reversed. Here, the reaction presumably proceeds via the cationic boat-like TS, in which the silicon is pentacoordinate. According to this scheme, the cyclohexanone-derived enol ether with a fixed (*E*) configuration of the double bond gave rise to the *syn* product with sterically demanding catalyst **39** and to the *anti* isomer with catalyst **40**.[145]

Also pyridine *N*-oxides were demonstrated to work as catalysts in the aldol reaction. In the absence of an activator, addition of trichlorosilyl ketene acetal to acetophenone slowly takes place at 0°C, but it can be accelerated by a Lewis base (Scheme 1.31). Bis-*N*-oxide **41** emerged as the most promising in terms of reactivity and enantioselectivity (cat. 10 mol%, -20°C, CH_2Cl_2), affording the β-hydroxy ester, with a quaternary stereocenter, in 94% yield and 84% ee.[146] A new procedure for the synthesis of atropoisomeric bis-*N*-oxide has also been developed. An X-ray crystal structure of the complex between the catalyst and silicon tetrachloride has been obtained. Extensive computational analysis were conducted to propose a stereochemical rationale for the observed trends in enantioselectivities.

Other chiral *N*-oxides were employed, but with less success; for example Nakajima reported that catalyst **42** promoted the addition of trichlorosilyl enol ethers to aromatic aldehydes in decent diastereoselectivity and enantioselection up to 82%.[147] (Scheme 1.31). Also phosphine oxide **21** was able to catalyze the addition of cyclohexanone-derived silyl enol ether with activated aromatic aldehydes in high stereoselectivity.[148] The aldol adduct was obtained in moderate yield and diastereoselectivity, with 82% of enantioselectivity for the *anti* isomer (Scheme 1.31).

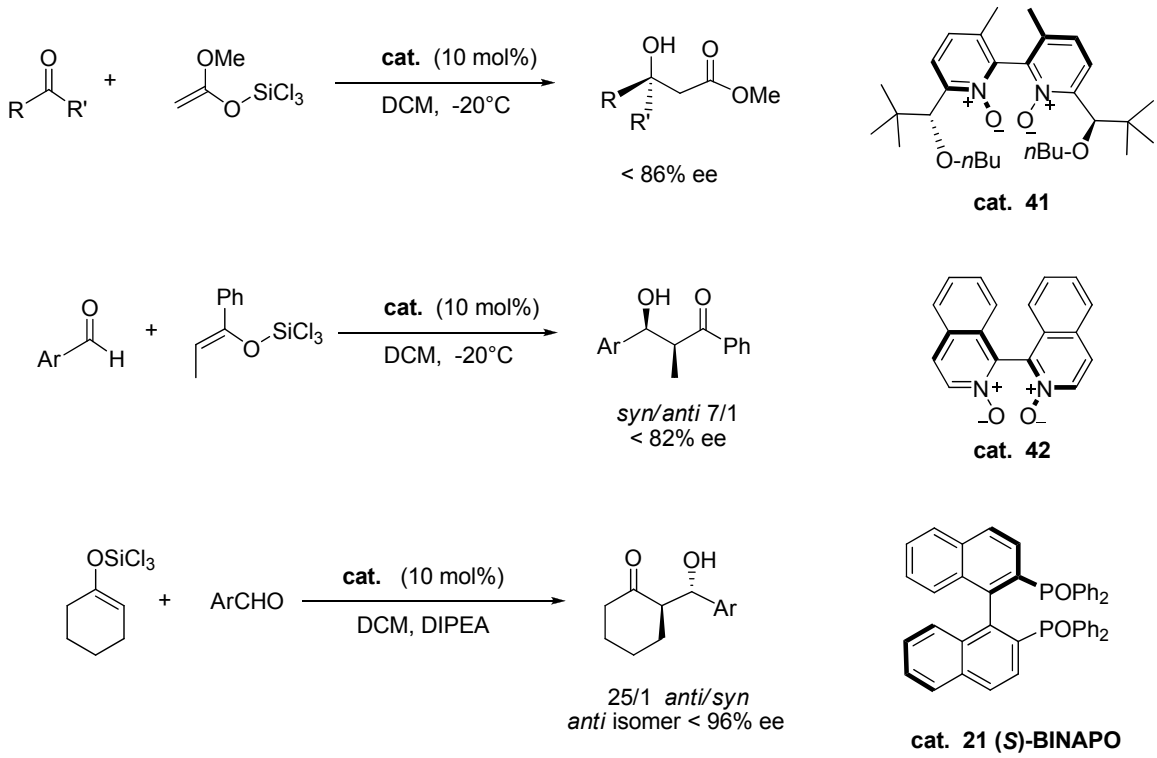

Scheme 1.31*: aldol reactions catalyzed by chiral N-oxides and phosphine-oxides.*

By the addition of DIPEA both chemical and stereochemical efficiency was increased, the product being isolated (-78°C, DCM) in 94% yield, 86% of *anti* diastereoselectivity and 87% ee for the *anti* isomer. It was proposed that the tertiary amines additive not only may work as acid scavenger to neutralize the hydrogen chloride produced by adventitious hydrolysis of trichlorosilyl enolethers, but also accelerates the reaction rate by promoting the dissociation of phosphine oxide from the silicon atom. The Lewis-base promoted condensation afforded *anti* adducts starting from (*E*)-silanes and *syn*-adducts from (*Z*)-silanes, confirming the hypothesis that similarly to allylation reaction, a cyclic, six membered transition state is involved.

1.5 Ring opening reaction of epoxides

The first catalytic enantioselective opening of *meso*-epoxides with tetrachlorosilane in the presence of the chiral phosphoramide **43** as a Lewis base (Scheme 1.32) was reported by Denmark.[149] The mechanicistic hypothesis is that the Lewis base reacts with tetrachlorosilane forming a pentacoordinate silicate complex which coordinates the oxygen atom of the substrate activating it towards nucleophilic substitution. The attack of the chloride ion proceeds in an S_N2 fashion. The enantioselectivity depends on the substrate's structure. A higher level of enantiomeric excess was obtained for acyclic substrates, whereas for cyclic substrates the ee also depends on ring size.

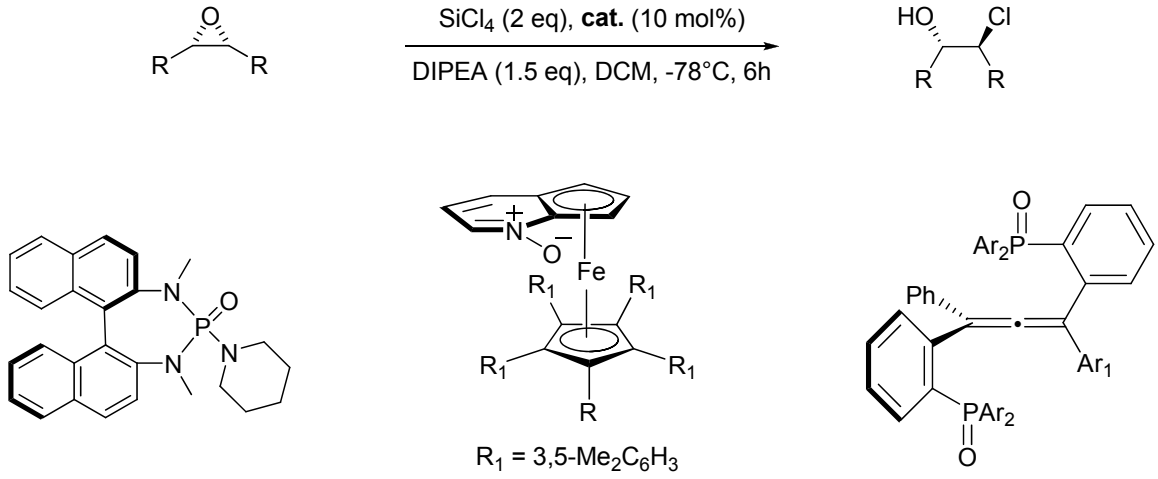

cat. 43 87% ee

cat. 44 < 98% ee

cat. 45 < 94% ee

Scheme 1.32: *catalytic stereoselective epoxide-opening reactions.*

Denmark investigated different aspects of the reaction[150] as the use of different chlorosilane sources and stoichiometry, catalyst loading, internal quench and kinetic and non-linear effect. This survey highlights that only silicon tetrachloride affords the product with high level of stereocontrol: only one chlorine is released and in the course of the reaction the nature of silicon reagent does not change; the selectivity does not change with catalyst loadings ranging from 100 mol% to 4 mol%, but it decreases with a 2 mol% loading. This behaviour suggests that a single pathway mechanism is active in the

100 mol% - 4 mol% range. The authors conclude that probably more than one molecule of catalyst is involved in the stereochemistry determining step.

Fu and co-workers reported[151] a new family of chiral catalysts capable of promoting the opening of *meso*-epoxides with high enantioselectivity (up to 98% ee) in the presence of tetrachlorosilane via a hexacoordinate silicate (Scheme 1.32). The choice of catalyst **44** is the result of the screening of a series of enantiopure pyridine *N*-oxides for which the authors show that the level of stereocontrol increased with steric hindrance. An electron-poor aromatic group on the substrate leads to the chlorohydrin with the highest selectivity: the enantiomeric excess depends on electronic effects. A positive nonlinear correlation between the enantiomeric excess of the catalyst and the enantiomeric excess of the product was observed.

Later, Nakajima's group showed[152] that also the chiral posphine oxide (*S*)-BINAPO provided the product of ring opening of *meso*-epoxides with high enantioselectivity (up to 90% ee) in the presence of tetrachlorosilane and DIPEA, whose presence seems to be necessary in order to obtain a good level of stereocontrol. More recently a novel catalytic system has been reported: optically active mono- and bis-phosphine oxides containing an allene backbone were prepared in enantiomerically pure form and used as organocatalysts (Scheme 1.32).[153] The novel chiral allenes were tested in the opening of *meso* epoxides by addition of silicon tetrachloride. It was observed that bis-phosphine oxides performed much better than mono- phosphine oxide. It must be said that in the solid state, bisphosphine oxide adopt a conformation characterized by π-stacking interactions involving two phenyl rings of the phosphine oxides and one of the backbone phenyl rings. As a consequence of this arrangement the two oxygen atoms project in roughly the same direction. The selected catalyst **45** was found to be a really effective promoter that could be employed at 0.1% mol cat loading, clearly indicating that a completely unexplored novel class of chiral phosphine oxide are now available as suitable catalysts.

1.6 Miscellaneous

Propargyl trichlorosilane (prepared by CuCl-catalyzed reaction between propargyl chloride and $HSiCl_3$) and allenyl trichlorosilane (synthesized analogously in the presence of $Ni(acac)_2$), were shown to react with aromatic aldehydes under activation of a Lewis base, similarly to the addition of allyltrichlorosilane to carbonyl compounds.[154]

The addition of propargyl trichlorosilane to aldehydes leads to allenyl alcohols (Scheme 1.33), while the reaction of allenyl trichlorosilane affords the corresponding homopropargyl alcohol. An asymmetric version has been reported by Nakajima,[155] who employed the chiral biquinoline bis-*N*-oxide **17** as a catalyst; however the enantioselectivities were rather modest (40-62 % ee).

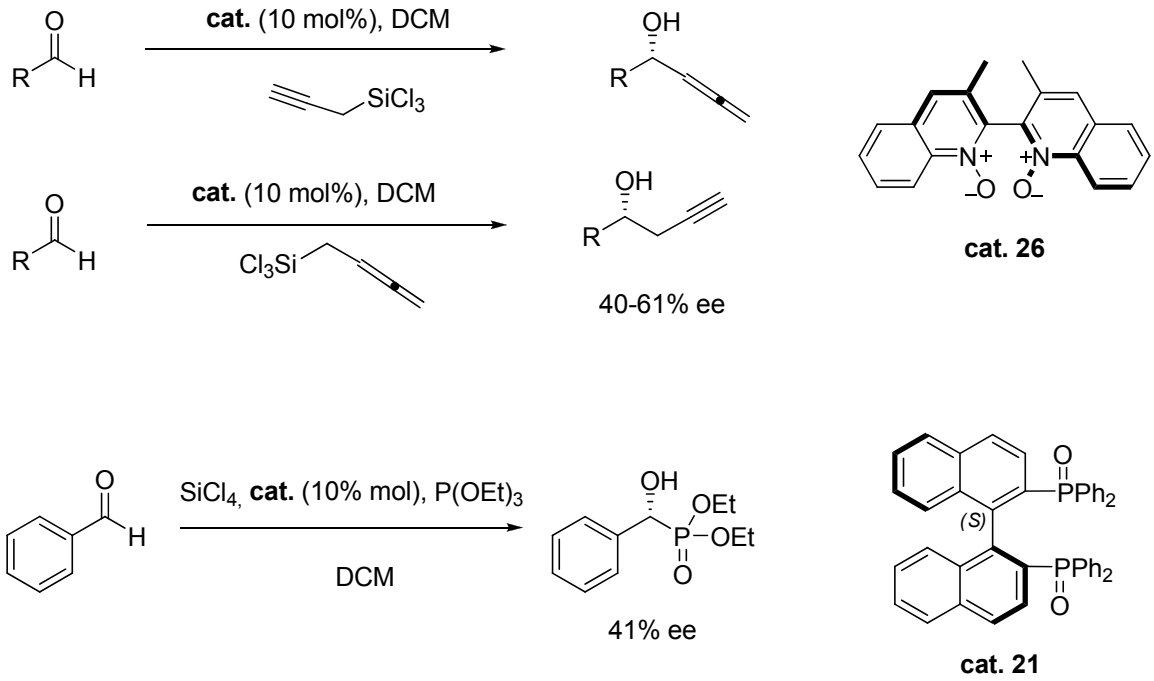

***Scheme 1.33**: organocatalytic miscellaneous reactions.*

In the attempt to further explore new synthetic methodologies based on the use of trichlorosilyl derivatives activated by chiral Lewis bases, the enantioselective addition of trialkylphosphites to achiral aldehydes was investigated.[141]

However, the catalytic Abramov-type phosphonylation of carbonyl compounds promoted by tetrachlorosilane in the presence of catalytic amounts of (S)-BINAPO was met with limited success, affording the corresponding α-hydroxyphosphonate in 86%

yield but only 41% enantioselectivity (Scheme 1.15). Once again the use of diisopropylethylamine as additive was decisive to achieve high chemical yields, but did not improve the stereocontrol. Even if the level of stereoselectivity is unsatisfactory the work is worth of mentioning because it represents the first organocatalytic enantioselective Abramov-type phosphonylation of aldehydes and the first report where different classes of chiral phosphine oxides other than the bis-(diarylphosphanyl)-binaphthyl dioxides were taken in consideration, although without success, in this kind of reaction.

CHAPTER 2

New phosphoramides and phosphoramidates as catalysts in trichlorosilyl compounds-mediated reactions

"No experiment is ever a complete failure;
it can always serve as a bad example"
Law of compensation

Phosphoramides have found extensive applications in organic chemistry.[156] Their Lewis basicity and their strong donor proprieties make them very important ligands in organometallic chemistry, for their capability to modulate the reactivity at the metal center.[78,157] Phosphoramides have a very strong and polarized P-O double bond where the phosphorous atom is connected to one or more nitrogen subunit; these characteristics are responsible of their Lewis basic character. For a long time, only mono-phosphoramides were known. Recently bis-phosphoramides (where two phosphorous atoms are connected by a nitrogen linker) were developed.[127]

The best known phosphoramide is hexamethylphosphoric triamide (HMPA), that is commonly prepared by reacting phosphorus oxychloride and an excess of dimethylamine in an inert organic solvent. It has variety of applications, for example, as a solvent in polyacrylonitrile spinning operations and in processes for removing acetylene from gas streams. In organic chemistry HMPA is often used as additive to improve the selectivity of lithiation reactions by breaking up the oligomers of lithium bases such as butyllithium.

In recent years chiral phosphoramides have attracted a lot of attention because of their ability to promote stereoselettive reactions in organocatalysis, as showed in chapter 1 (scheme 1.27). The most important examples of phosphoroamides as chiral

organocatalysts were developed by Denmark, using monodentate and bisdentate phosphoroamides obtained from chiral diamines. A few examples of Denmark's mono- and bis- phosphoramides are shown in scheme 2.1.

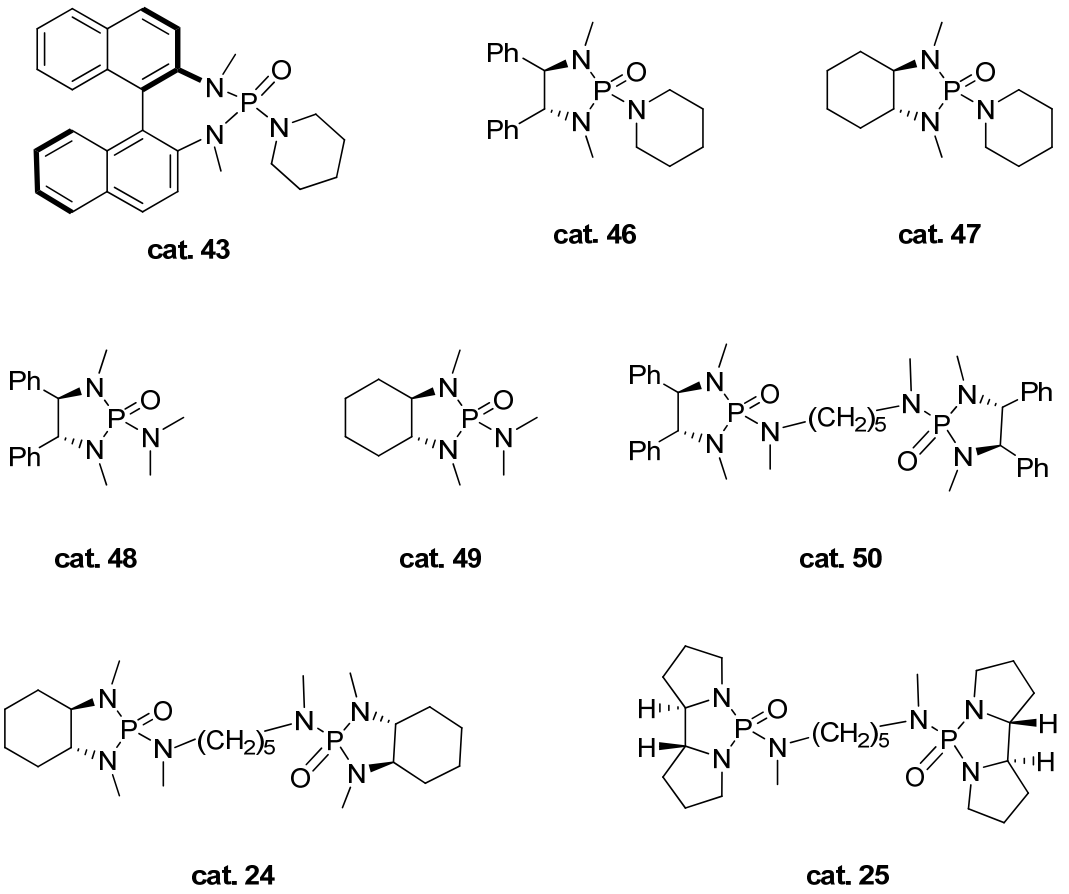

***Scheme 2.1**: Denmark's phosphoramides.*

These compounds were employed as organic catalysts to promote two types of organic reactions: Mukaiyama aldol addition of silylenol ethers to carbonyl compounds;[158] and allylation of aldehydes with allyltrichlorosilanes.[126a, 127]

The most important results are reported in scheme 2.2. The addition of silyl enolethers to benzaldehyde takes place with good yields and a good level of stereocontrol. The allylation of benzaldehyde in the presence of allyl trichlorosilane, instead, requires a stoichiometric amount of phosphoramide to promote the reaction with modest yields and discrete stereocontrol. In the best case it's possible to obtain a product with 60% enantiomeric excess with the phosphoramide **47**. Only the use of bis-phosphoramides allowed to perform the reaction in a catalytic way, but the addition of DIPEA is required.

When catalyst **25** is employed in fact, the stereoselectivity of the process improved and the allyl alcohol was obtained with 87% ee that increased to 95% when crotyl trichlorosilane was employed.

a) Mukaiyama aldol addition of silylenolethers to carbonylic compounds

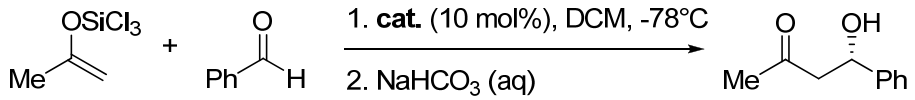

cat. **43**, y= 71%, ee= 62%
cat. **46**, y= 92%, ee= 85%
cat. **47**, y= 76%, ee= 53%

b) Allylation of aldehydes with allyltrichlorosilane

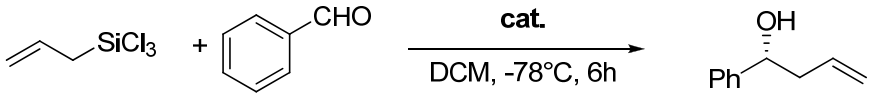

cat.	mol%	additive	y (%)	ee (%)
43	100	-	43	20
48	100	-	78	32
49	100	-	78	60
50	50	DIPEA	82	20
24	10	DIPEA	54	72
25	5	DIPEA	85	87

***Scheme 2.2**: stereoselective reactions with phosphoramides.*

In order to explain the stereocontrol of the process, Denmark et al. investigated the mechanism of allylation of benzaldehyde, and they found that the reaction was first order in trichlorosilane and aldehyde. Surprisingly however, the reaction order in the phosphoramide was 1.77.[126a] This fact can be explained only with two simultaneous operation of two pathways involving first and second order dependence on catalyst, where more than one phosphoramide is involved in the stereochemistry-determining transition structure. To account for this phenomenon, the transition structure requires that the silicon expels one chloride anion to produce a hexacoordinate octahedral cationic silicon species. A transition state that involves the formation of a Zimmerman-Traxler

like six member ring has been proposed, where the phosphoramide activates the allyl trichlorosilane by coordination to the silicon atom (scheme 2.3).

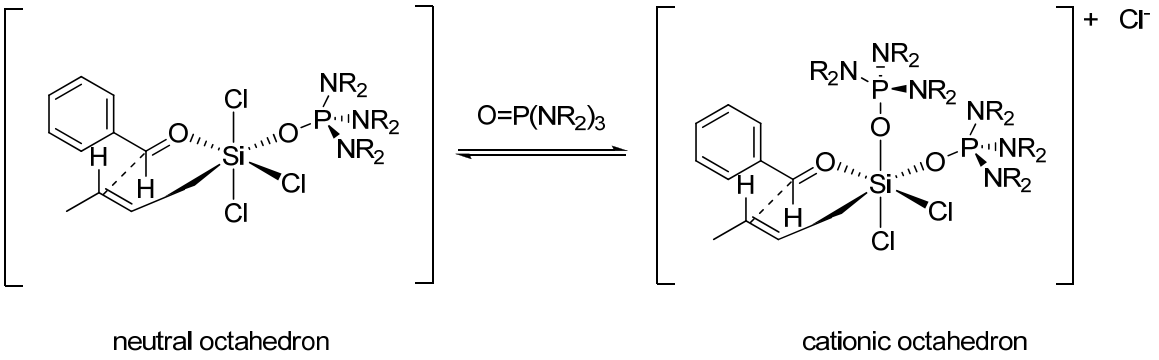

Scheme 2.3: *transition structures with one or two phosphoramides.*

The involvement of ionic species as intermediates is also supported by the effect of ammonium salts on the reactivity. For instance the addition of 1.0 equiv of *n*-Bu_4NI enhances the reaction rate. However, it's well known that the allyl addition is the rate determining step of the reaction, so the reaction rates for these pathways would depend on the reactivities of these complexes but not on the rate of their formation.[159] It has been also demonstrated that the prevailing pathway in the allylation reaction involves two phosphoramides in a cationic octahedral specie, and then bidentate systems work better than monodentate catalysts.

The operation of dual mechanistic pathways has significant implications on the asymmetric catalysis, and suggests a direction for the development of highly selective, reactive catalysts. Denmark bis-phosphoroamides are very efficient catalysts, but their synthesis requires long and not trivial sequence of synthetic steps; often with resolution of racemic mixture. For this reason we have decided to synthesize new chiral mono-phosphoramide more easily accessible than Denmark's and possibly obtained from readily available chiral molecules.

Despite their large use in chemistry, only few and not so well rationalized methods to generate phosphoramides are known;[160] the general strategy for the synthesis of these compounds involves the reaction of an amine with a phosphorus reagent. To obtain asymmetric phosphoramides, different chiral diamines can be employed during this process.

Three different synthetical methodologies have been proposed in order to obtain enantiopure phosphoroamides (scheme 2.4):

1. a diamine is coupled to a dialkylaminophosphoric dichloride,
2. a diamine is coupled to a dialkylaminophosphorus dichloride to afford the corresponding phosphorus triamide followed by *in-situ* oxidation to give the desired phosphoramide;
3. PCl_3 is combined first with a hindered diamine and then a secondary amine, followed by in-situ oxidation.

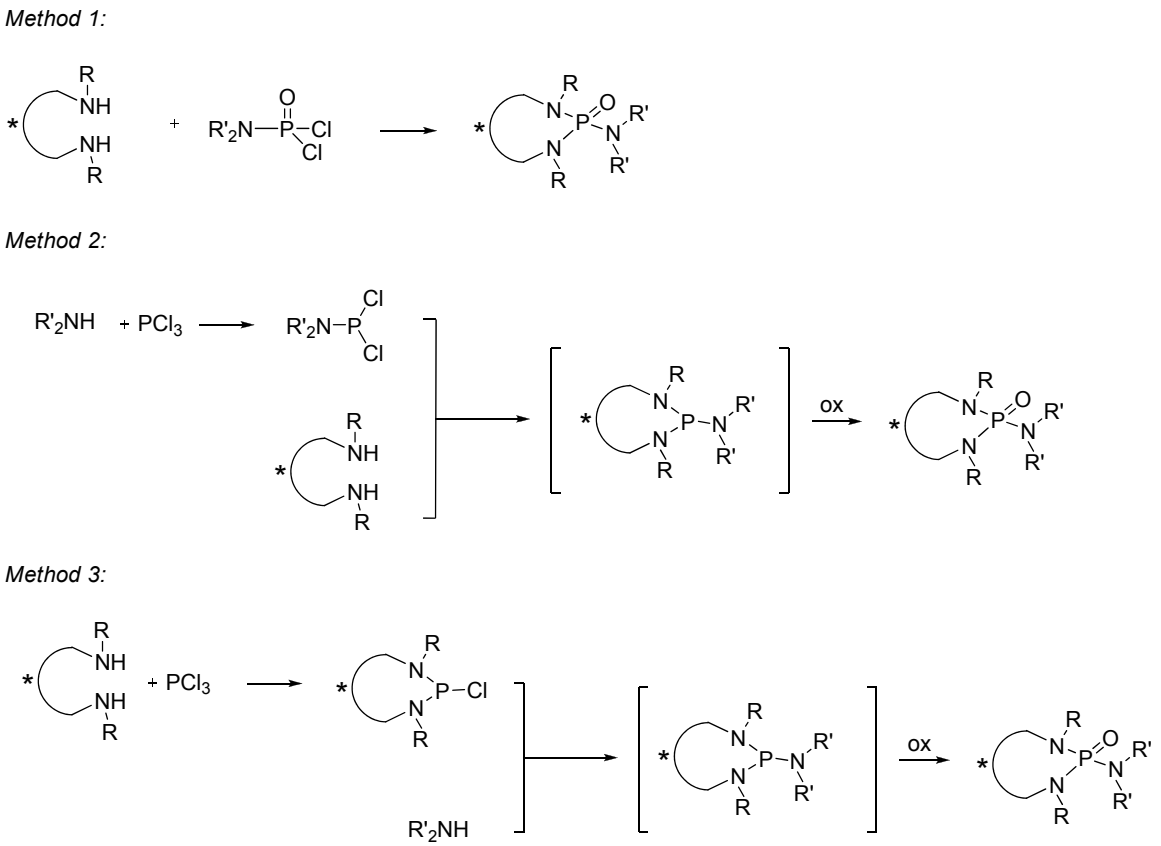

Scheme 2.4: *general strategy for the synthesis of phosphoramides.*

Method 1 is applicable when both coupling partners are not sterically demanding. Methods 2 is applicable when one amine is sterically hindered, and method 3 (derived from method 2) could be used when both coupling partners are sterically hindered. Generally, method 1 is preferred while methods 2 and 3 are employed only when the first one gave less satisfactory results.

While designing new chiral Lewis basic organocatalysts, with different residues connected at the phosphorous atom, we decided to pursue the highest structural simplicity. Accordingly, the catalysts should be obtained by modification of an inexpensive, commercially available, enantiopure material whose manipulation must be kept to minimum. In this context, the first class of catalysts was prepared starting from (*R*)-1,1'-binaphthyldiamine (BINAM) and a flexible secondary amines such as *N*-methyl-benzylamine.

Based on previous work,[161] we decided not to employ dialkylaminophosphoric dichloride (method 1), because when it's linked to an amine residue its reactivity decreases, and no other substitution occurs. So, the general synthetic pathway for the synthesis of compound **51** was derived from the second method, and is reported in scheme 2.5.

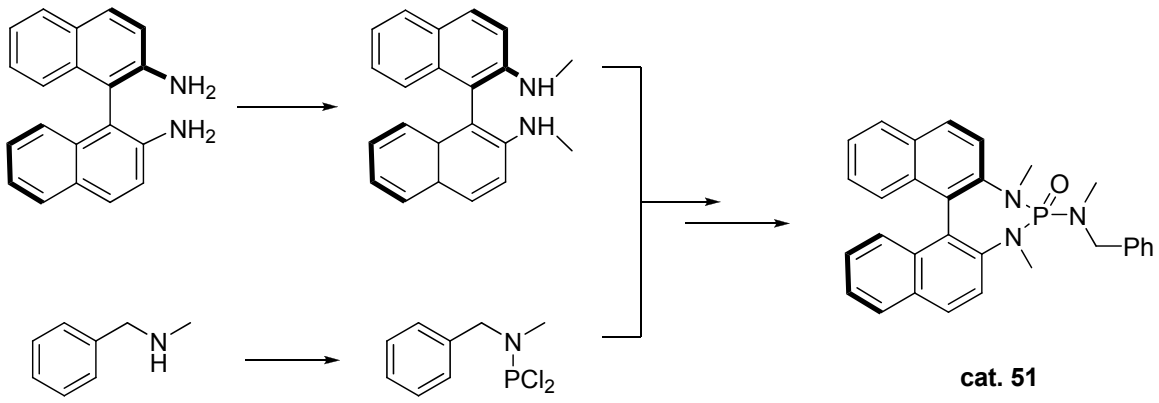

Scheme 2.5.

The first step consist in the methylation of (*R*)-BINAM by reaction with ethylchloroformiate followed by reduction with lithium aluminium hydride in quantitative yield (scheme 2.6).

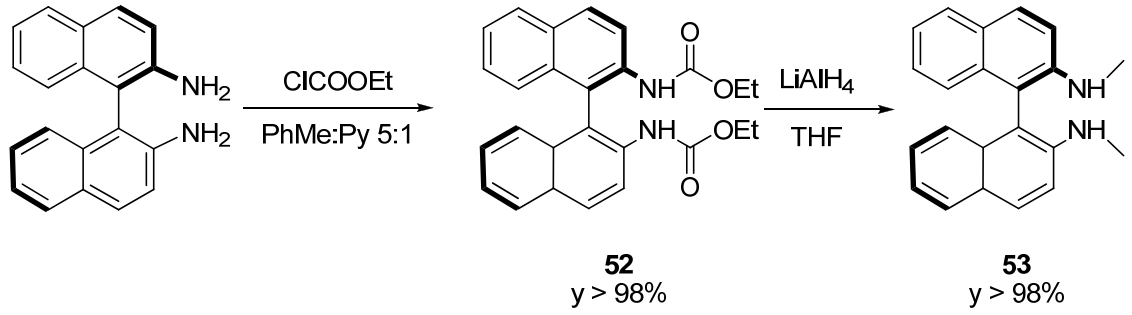

***Scheme 2.6**: synthesis of Me_2-BINAM.*

The aminophosphin dichloride derivative can be obtained by reaction between *N*-methyl-benzylamine and phosphorus trichloride. This reaction requires a long time (12h) using PCl_3 in the presence of TEA in exane, but by generating the anion of the amine using butyllithium the rate reaction increases, and the product can be obtained with good yields, after distillation, as shown in scheme 2.7.

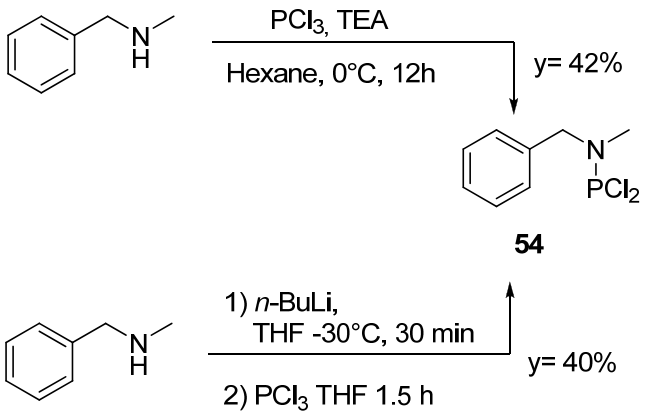

Scheme 2.7: *synthesis of diaminophosphinic dichloride.*

This product is very air sensitive and unstable, so it was synthetized under strict conditions of nitrogen atmosphere and immediately used in the next step. Bis lithiation of *N,N*-dimethyl-1,1'-binaphthyldiamine with *t*-butyllithium and reaction with dichloride **54** afforded a phosphorotriamidite that was oxidized *in situ* with *m*-chloro perbenzoic acid (*m*-CPBA) to give the enantiomerically pure phosphoramide **51** with 13% yield after chromatographic purification (scheme 2.8).

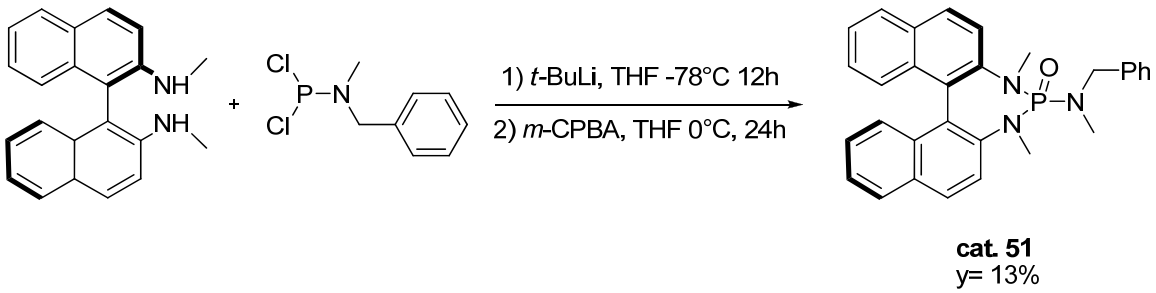

Scheme 2.8.

Similarly, we tried to introduce a further stereogenic element close to the catalitic site thus to improve the stereoselectivity of the allylation process. To obtain this goal, we

have first synthesized the two chiral dichlorides **59** and **60** in enantiopure form, starting from chiral α- and β-phenylethylamine, that was acetylated, reduced, and treated with PCl_3 following the same procedures reported above for adduct **54** (scheme 2.9). These products were obtained with good yield, but attempts to synthesize the catalysts **61** and **62** were not successful and only the two starting materials were recovered.

Probably the increased steric hindrance around the phosphorous atom is responsible of this failure. Attempt to isolate the phosphinic precursor after oxidation of **59** and **60** with *m*-CPBA also failed.

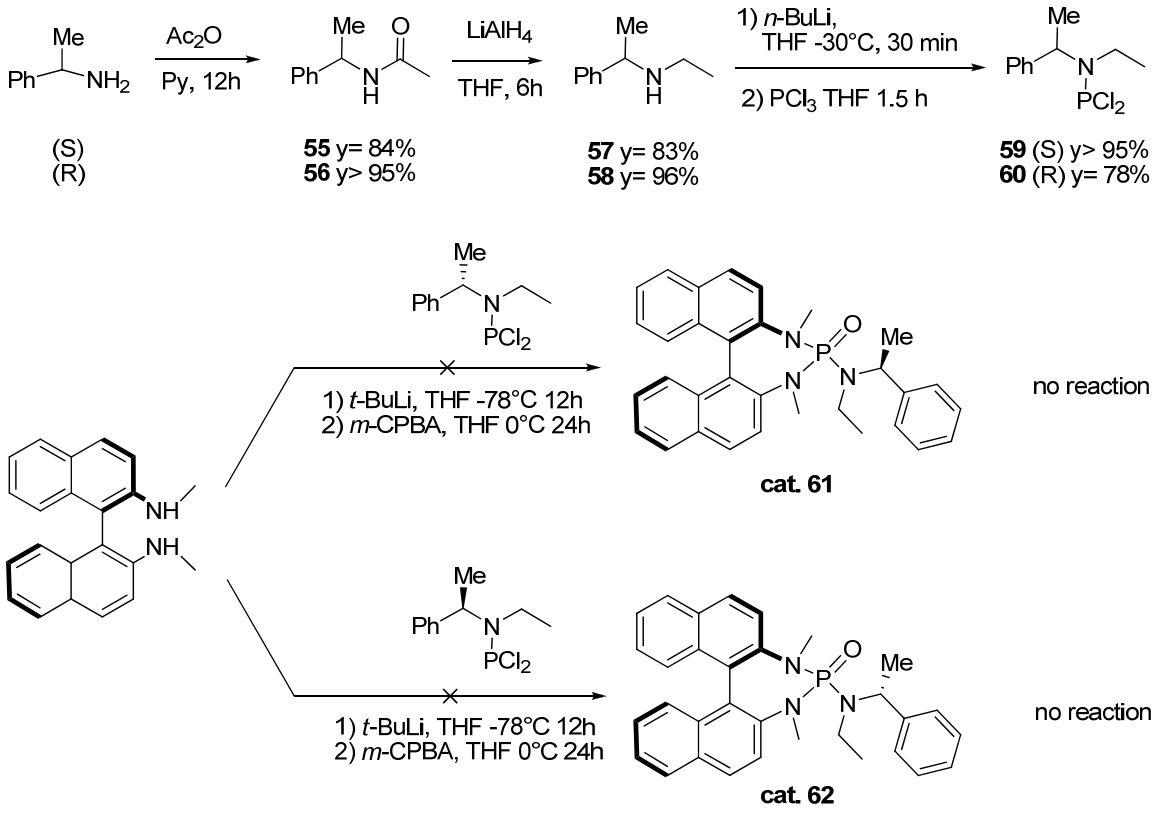

Scheme 2.9.

In order to provide more flexibility around the catalytic site we also changed the chiral scaffold. Starting from (*R*,*R*)-1,2-diphenyl-1,2-ethylendiamine we prepared compound **65** (scheme 2.10), with a synthesis similar to that of the previous analogue. The desired enantiomeric pure product was obtained with 30% yield after chromatographic purification.

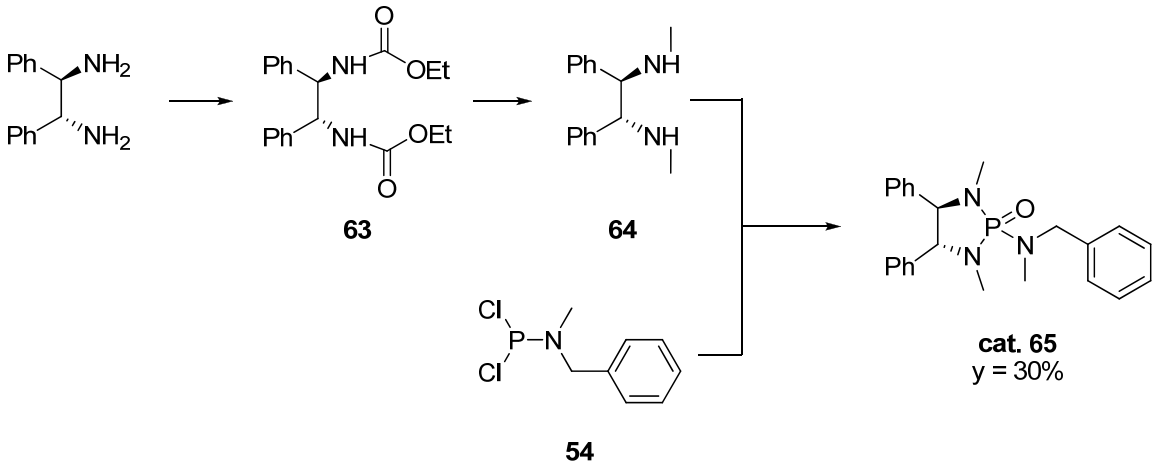

Scheme 2.10.

Compounds **51** and **65** were employed as catalysts in two types of model reactions mediated by trichlorosilyl compounds: the allylation of benzaldehyde with allyltrichlorosilane and the asymmetric reduction of keto-imines with trichlorosilane.

In the first case, the reaction was performed in the presence of 10 mol% of catalyst, at 0°C in dichlorometane and with an excess of *N,N*-diisopropylethyldiamine to neutralize the formation of HCl (scheme 2.11); the starting materials were freshly distilled before use. Unfortunately, neither of the catalysts **51** and **65** was able to promote the reaction.

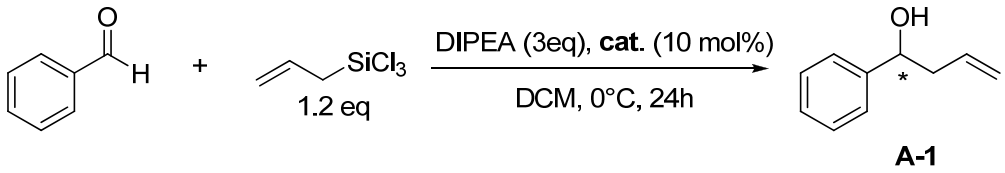

Scheme 2.11*: experimental conditions in allylation reaction.*

The asymmetric reduction of keto-imine **66** with trichlorosilane was performed in the presence of 10 mol% of catalyst, at 0°C in dichlorometane (scheme 2.12b). The imine was prepared with a microwave-promoted reaction between acetophenone and aniline in toluene in the presence of K10 clay as activator (scheme 2.12a); a prolonged reaction time was necessary in order to obtain a good yield.

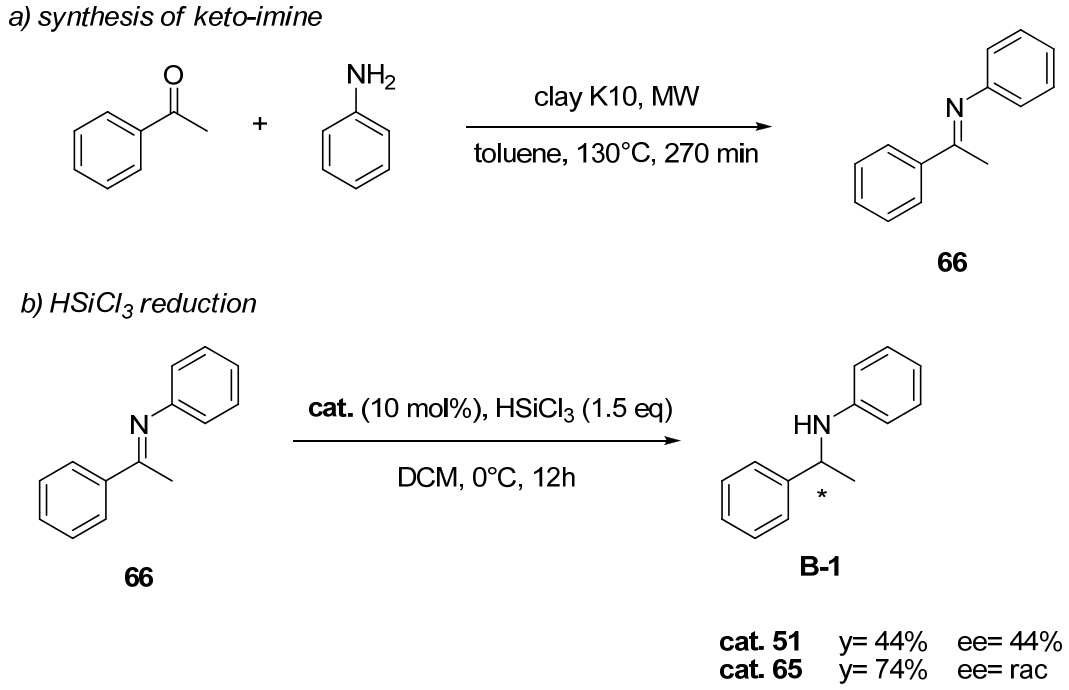

Scheme 2.12.

Analyzing the results we can observe that phosphoramide **51** derived from (*R*)-BINAM gives a product with 44% yield and 44% enantiomeric excess, while phosphoroamide **65** gives the product with 74% yield but no stereocontrol; it is possible that a major conformational liberty of the catalyst secures a better yield but a lower enantiomeric excess.

On the light of these modest results, we turned our attention to a different chiral scaffold. Inspired by Feringa's work, that employed 1,1'-binaphtol derived C_1 symmetric phosphoroamidites as ligands in a copper-catalyzed enantioselective coniugate addition of dialkylzinc reagents to cyclic enones,[162] we decided to replace BINAM with 1,1'-bi-2-naphthol (BINOL). The synthetic procedure of these phosphoramidates is shown in scheme 2.13, where the first step is the reaction between phosphoryl chloride and chiral 1,1'-bi-2-naphthol (BINOL), followed by addition of a secondary amine to generate the desired product.

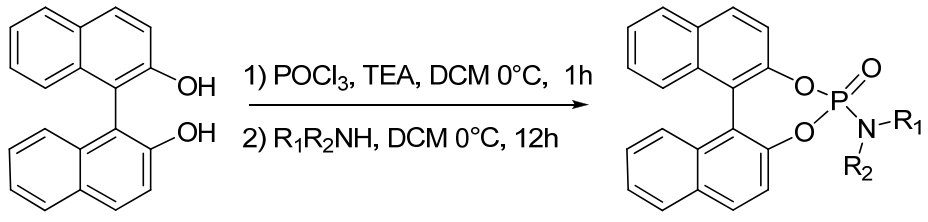

Scheme 2.13: *general procedure for the synthesis of phosphoramidates.*

We prepared a set of eight enantiomerically pure compounds that were purified by chromatography. Three catalysts were synthesized starting from (*R*)-BINOL and achiral amines: diethyl amine, *N*-methyl-benzylamine and piperidine (compounds **67**, **68** and **69**). Catalyst **70** instead presents a further stereogenic center coming from (*S*)-*N*-ethyl-1-phenylethanamine. The remaining four catalysts derive from *L*-proline *t*-butylester (compounds **71** and **73**) and *L*-proline carboxyamide (compounds **72** and **74**) with (*R*)- and (*S*)-BINOL (scheme 2.14).

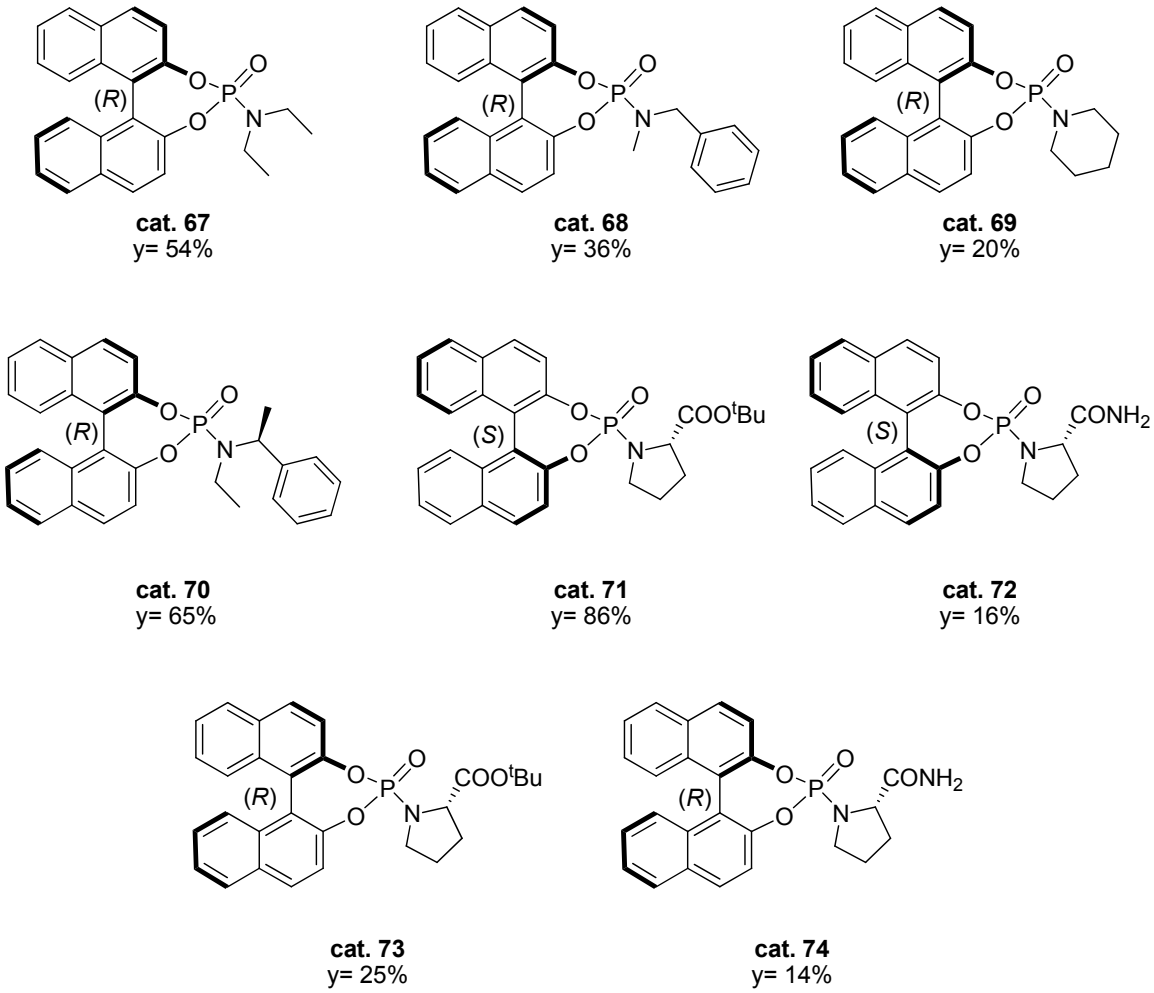

cat. 67
y= 54%

cat. 68
y= 36%

cat. 69
y= 20%

cat. 70
y= 65%

cat. 71
y= 86%

cat. 72
y= 16%

cat. 73
y= 25%

cat. 74
y= 14%

Scheme 2.14.

All these molecules were tested in the allylation of benzaldehyde with allyltrichlorosilane (scheme 2.11) and in the asymmetric reduction of keto-imines with trichlorosilane (scheme 2.12). The results of the addition of allyltrichlorosilane are reported in table 2.1.

cat	conc (M)	yield (%)	ee (%)
67	0.67	54	rac
68	0.13	12	12
68	0.67	31	rac
69	0.40	66	rac
70	0.13	23	7
71	0.40	-	-
72	0.40	30	rac
73	0.40	-	-
74	0.40	40	rac

Table 2.1

This screening shows that all catalysts are less chemically and stereoselectively efficient than Denmark's catalysts. The variation of concentration of the catalyst does not influence the results of reaction, so only one phosphoroamide seem to be coordinated to the silicon atom.

While catalyst **51** is not able to promote the reaction, the corresponding binaphtol compound **68** gives the product with 31% of yield but without stereoselection. The presence of a stereogenic center on the phosphoramidic residue (**70**) slightly increases yield and enantiomeric excess.

Using the bis-coordinating catalysts (**71** and **73**) it's not possible to obtain the desired compound, but if **72** and **74** are employed, we can observe the formation of the racemic product with moderate yields. Since these catalysts are not very different from **68** and **70**, we can hypothesize that the coordination occurs on the amidic nitrogen atom, and not on the expected P=O catalytic site.

The use of catalyst **69**, that is very similar to phosphoramide **43**, does not lead to the desired product under Denmark's conditions. However, it promotes the reaction in 30% yield without stereoselection at 0°C for 24 hours. This result confirm that phosphoramidites are less reactive than phosphoramides.

The results of the reduction of keto-imines with trichlorosilane (table 2.2) show that binaphthyl diamine derived catalyst **51** is more stereochemically efficient then the corresponding binaphtol derived catalyst **68**.

cat	Conc (M)	yield (%)	ee (%)
51	0.15	44	44
65	0.15	74	rac
68	0.3	19	rac
69	0.3	45	28
71	0.3	8	n.d.
72	0.3	18	rac
73	0.3	18	Rac
74	0.3	8	n.d.

Table 2.2

Since catalysts **51** and **65** are more active than other catalysts we can imagine that the presence of the nitrogen atom close to the catalytic site is very important. Moreover, if we compare the binaphthyl derivative (**51**) with diphenyl ethylendiamine derivative (**65**) we can observe that to a major conformational liberty corresponds a better yield but a lower enantiomeric excess.

Catalysts **68-74** instead, give products with low yields and no stereocontrol, with the exception of **69** that inexplicably affords the product with 45% yield and 28% ee.

In conclusion, a novel class of chiral Lewis basis has been explored in reactions with trichlorosilane reagents. The results show that phosphoramides derived from binaphthyldiamine are better catalyst than those derived from binaphtol, but they are more difficult to sinthesize. However, in both cases chemical and stereochemical efficiencies are modest. For these reasons, we turned our attention to different classes of catalysts.

CHAPTER 3

Chiral phosphine oxides in present-day organocatalysis

"The flowers have been growing thorns for millions of years.
For millions of years the sheep have been eating them just the same.
And is it not a matter of consequence to try to understand why the flowers
go to so much trouble to grow thorns which are never of any use to them?"
The little prince - Antoine de Saint-Exupery

The design and synthesis of new chiral Lewis bases is a field of extraordinary activity, the result of the never ending research towards new catalytic systems of improved efficiency and novel synthetic methodologies. Small organic Lewis bases able to promote a wide variety of synthetic transformations become protagonists of an incredible rich chemistry.[76] They include different classes of compounds, such as naturally-occurring alkaloids and aminoacids, but also synthetic amine-based catalysts and *N*-oxides. Also phosphines have witnessed a renewed importance as Lewis basic organic catalysts because they are less basic but more nucleophilic than structurally related amines and endowed with easily adjustable electronic properties by a judicious choice of substituents. Triarylphosphines are much less nucleophilic than trialkylphosphine, which are about 100 times stronger nucleophiles than trialkylamines, even if they are 100 times less basic.[163] It has been demonstrated that these unique properties of phosphines and amines may lead to different mechanistic pathways, so that the nature of the Lewis base may allow to orient the course of reaction.[164]

While *N*-oxides derived from both heteroaromatic systems and aliphatic amines[165] have found widespread application in organocatalysis, quite surprisingly

phosphine oxides have been scarcely used. This is even more surprising if one thinks that very often chiral phosphine oxide derivatives are well known compounds, prepared in enantiomerically pure form mostly through resolution processes, as precursors of the corresponding phosphines, widely employed as chiral ligands in organometallic catalysis.[166] If one considers the abundance of current commercial chiral phosphines it becomes immediately clear how many phosphine oxides are easily available and ready to be investigated in Lewis bases-organocatalyzed reactions.

Only a few examples of chiral phosphine oxide catalysts are known in literature; the first example of a reaction promoted by a chiral phosphine oxide[167] as chiral Lewis base may be considered the just cited allyltrichlorosilane addition to *N*-benzoyl hydrazones. This reaction, reported by Kobayashi, involves the use of (*S*)-BINAPO in stoichiometric amounts (scheme 1.26).[121] The first true organocatalytic reaction promoted by chiral phosphine oxides was reported by Nakajima[141] in 2005, when (*S*)-BINAPO promoted in catalytic quantities the addition of allyltrichlorosilane to aldehydes (scheme 1.29). In the same year, an enantioselective ring opening of *meso*-epoxides catalyzed by (*S*)-BINAPO to give optically active chlorohydrins was also reported.[152] The ring opening of *meso*-stilbene oxide with a solution of tetrachlorosilane in dichloromethane using 10 mol% (*S*)-BINAPO at -78 °C afforded smoothly the corresponding chlorohydrin in high yield and 59% ee. Only an extensive screening of the reaction conditions allowed to identify diisopropylethylamine as the best additive capable of increasing enantioselectivity up to 90% ee. (*S*)-Tol-BINAPO catalyzed the reaction in 82% ee, a level of stereoselection comparable to that obtained with (*S*)-TetraMe-BITIOPO, that promoted the opening of cis-stilbene oxide in DCM at -78°C in the presence of DIPEA, in quantitative yield and 81% ee (scheme 3.1).[142]

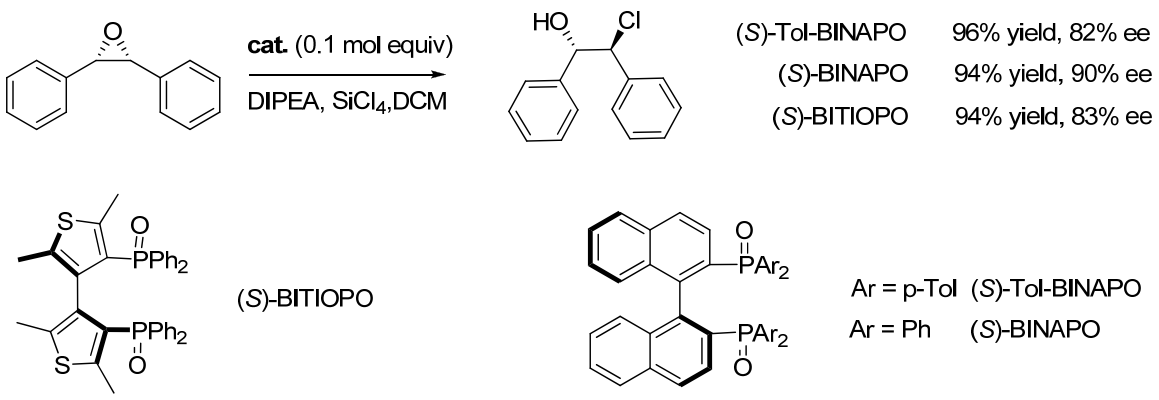

Scheme 3.1*: Lewis base-catalyzed stereoselective ring opening of epoxides.*

(*S*)-BINAPO was also employed as organocatalyst in the stereoselective aldol reaction of trichlorosilyl enolethers. After seminal work by Denmark[168] with phosphoroamide-based catalysts (scheme 1.30), where it was demonstrated that the reaction proceeds via a chair-like transition state involving a hypervalent silicate, Nakajima showed that also phosphine oxides may promote the condensation.[169]

The aldol adduct was obtained in moderate yield and diastereoselectivity, with 82% of enantioselectivity for the *anti* isomer. (Scheme 3.2) By the addition of DIPEA both chemical and stereochemical efficiency was increased, the product being isolated in 94% yield, 86% of *anti* diastereoselectivity and 87% ee for the *anti* isomer at -78°C in DCM. DIPEA accelerates the reaction rate by promoting the dissociation of phosphine oxide from the silicon atom, and scavenges the hydrogen chloride produced by adventitious hydrolysis of trichlorosilyl enolethers.

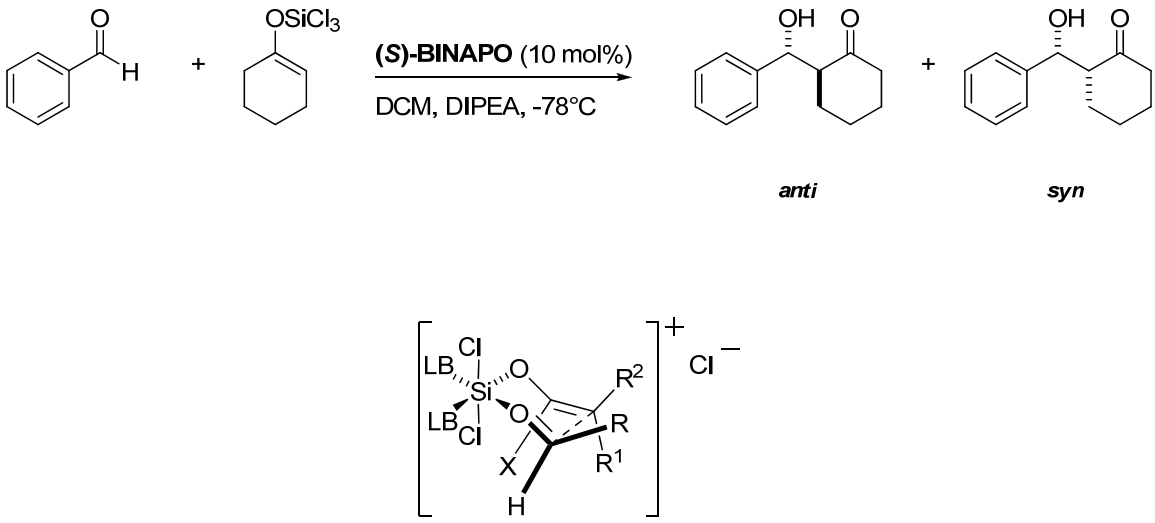

Scheme 3.2: *Aldol reaction catalyzed by phosphine oxides.*

In 2008, Nakajima and Sugiura[170] investigated the enantioselective addition of trialkylphopshite to achiral aldehydes in the presence of different phosphine oxides (scheme 3.3). This reaction gives the corresponding α-hydroxyphosphonate with modest yield and lower enantioselectivity. This is probably due to the strong background reaction, that is competitive with the stereoselective mechanism.

When aldehydes with different electronic properties and sterically hindrance were tested, it was found that aldehydes substituted with withdrawing groups or sterically congested aldehydes give the product with lower yield and poor level of stereocontrol.

However, even if the level of stereoselectivity of this reaction is not very high, this work represents the first organocatalytic enantioselective Abramov-type phosphonylation of aldehydes promoted by phosphine oxides.

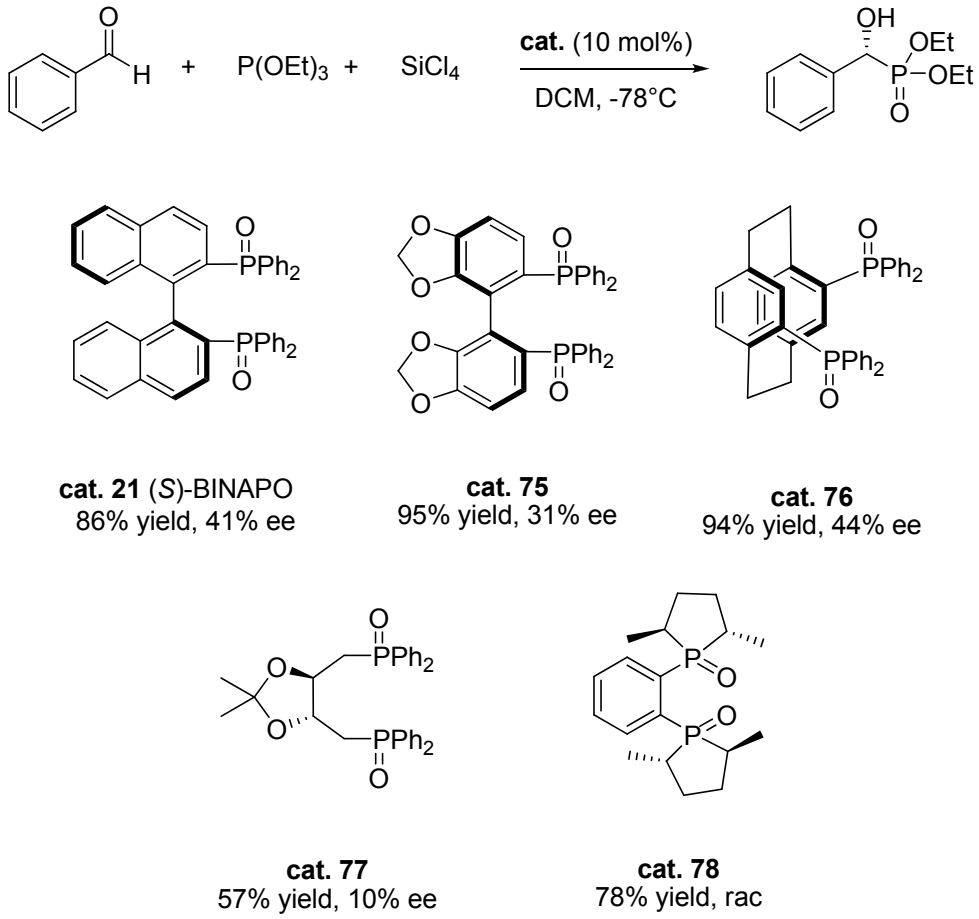

Scheme 3.3: *Abramov-type phosphonylation of carbonyl compounds.*

Last year, phosphine oxides and phosphoramides were employed in a novel class of reactions, that could be considered as "Lewis base-catalyzed Lewis acid-mediated reactions". A significant breakthrough in the field was accomplished by Denmark who explored the possibility to develop chiral hypervalent silicates to be used as Lewis acids, according to the mode of activation described in chapter 1 and proposed in scheme 1.31.[83a]

The weakly acidic species, silicon tetrachloride ($SiCl_4$), can be activated by binding of a strongly Lewis basic chiral phosphoramide or phosphine oxide, leading to *in situ* formation of a chiral Lewis acid. This species has proven to be an efficient catalyst

for the aldol addition of acetate-, propioneate-, and isobutyrate-derived silyl ketene acetals to conjugated and nonconjugated aldehydes.

Catalytic amounts of binaphthyldiamino-based phosphoramide **79** (1 mol%, scheme 3.4) in the presence of stoichiometric amount of tetrachlorosilane promoted the addition of silyl ketene acetals to aromatic aldehydes in high enantioselectivities.

In the proposed mechanism a basic ligand is employed to enhance the activity of a Lewis acid. The coordination of a Lewis base to a Lewis acid makes it more electrophilic; since a cationic species is generated, the result is a significantly increased Lewis acidity of the new adduct. In this aspect the combination of a chiral Lewis base and silicon tetrachoride to generate a strong Lewis acid is different from most of the other chiral Lewis acid-promoted reactions. Lewis base coordination to $SiCl_4$ activates the Lewis acid, while complexation of a basic chiral ligand to a Lewis acid precursor normally decreases the reactivity of the chiral complex. It is correct to say that these are not Lewis acid-catalysed reactions; the fact that the aldol products are trichlorosilyl ethers, as demonstrated by NMR analysis, demonstrates that each molecule of tetrachlorosilane partecipating to the catalytic cycle, is incorporated into the product.

By exploiting the same concept, and always by using catalyst **79**, other reactions were performed, such as the addition of silyl enol ethers to aldehydes.

This reaction is a synthetically powerful transformation in organic synthesis, and different strategies have been developed for controlling the stereochemical course of the addition. In this sense, it is possible use chiral Lewis acids,[171] transition metal enolates,[172] amino acids[173] and chiral Lewis base as catalysts[143,158] to promote this type of reaction. All these methodologies have met considerable success, but the use of chiral Lewis acids has received so far more attention. Generally, an achiral metal species is transformed by ligand substitution with a chiral adjuvant into a chiral metal complex. A consequence of ligand binding is however a decrease in the inherent electrophilicity of the metal atom, thus requiring either a high association constant or preformation of the complex to avoid competition from an achiral background reaction.

Interestingly, not all Lewis acid-base interactions lead to diminished electrophilicity; indeed, when a catalytic amount of a chiral phosphoramide is employed, the weak Lewis acid $SiCl_4$ can be activated to form a strongly Lewis acidic chiral species through coordination and subsequent ionization of a chloride ligand. Only after coordination of phosphoramide is $SiCl_4$ sufficiently Lewis acidic to promote addition of

silyl ketene acetal of *t*-butylpropionate to benzaldehyde with good yield and high enantiomeric excess. Further studies demonstrated also that the presence of ammonium salts (TBAI) improves the chemical activity, without loss of stereoselection.

The hypothesized catalytic cycle involves the chiral trichlorosilyl cation **A** that binds the aromatic aldehyde to give adduct **B**, which is attacked by the silyl ketene acetal to afford the intermediate **C**. This intermediate, after dissociation from the catalyst leads to the product as trichlorosilyl ether (Scheme 3.4).

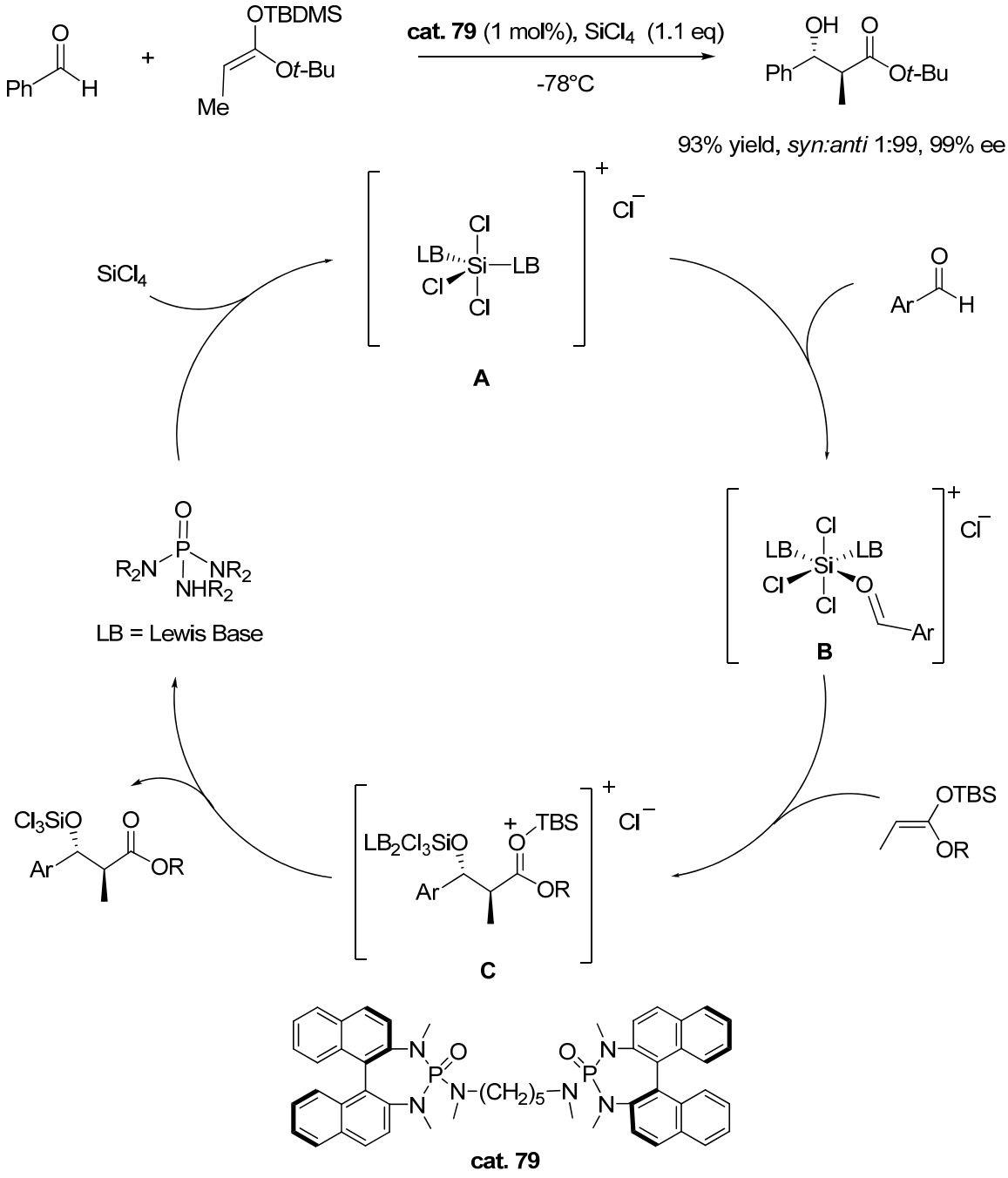

***Scheme 3.4**: Lewis base-catalyzed Lewis acid-mediated reactions.*

Not only the reaction is *anti* selective, but is also diastereoconvergent, affording the same stereoisomer independently from the geometry of the starting enolate. This behavior was tentatively rationalized by proposing that the decisive factor responsible for the observed trend in diastereoselectivity is the interaction between the α-substituent and the bound silyl cation complex in an open, acyclic transition structure. Analysis aimed at explaining the sense of the enantioselectivity of the process was less conclusive, but it showed that the catalyst pocket is quite congested and the stereo and enantiocontrol was possibly dominated by steric factors.

When an aliphatic rather than an aromatic aldehyde was employed, the reactivity enormously decreased and no product is formed. IR and NMR investigations demonstrated that in the presence of equimolar amounts of aliphatic aldehyde and $SiCl_4$ and of a catalytic amount of HMPA at -78 °C, the signals of the aldehyde disappeared, and new signals corresponding to alkylchloro silyl ether appeared. Similar experiments with benzaldehyde only revealed a slight broadening of the aldehydic proton without the appearance of any new signal. The resistance of such conjugated aldehydes to chloride addition may be due to the unfavorable loss of resonance stabilization in the extended, conjugated system.

With this new information, the proposed model was modified, and a new equilibrium between the activated aldehyde **B** and the alkylchloro silyl ether **D** was formulated. (scheme 3.5)

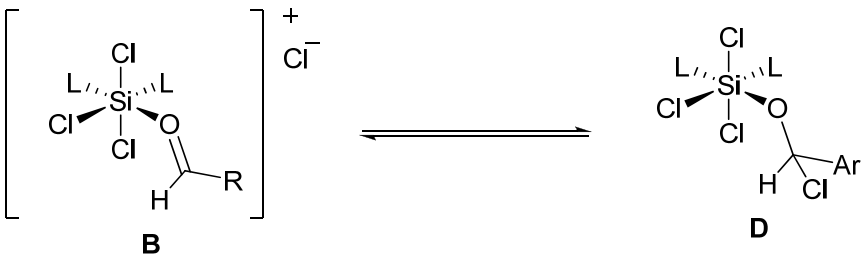

Scheme 3.5: *equilibrium between activated aldehyde and the correlated alkylchloro silyl ether.*

The discovery that a catalytic amount of a chiral phosphoramide could activate silicon tetrachloride in order to promote stereoselective reactions opened the way to a novel application to many other reactions promoted by a Lewis acids. According to this general mechanism, these reactions can be properly defined as phosphoroamide-catalyzed and $SiCl_4$-mediated transformations, as proposed by Denmark.[76]

By exploiting the same concept and always using catalyst **79**, other reactions were performed, such as the allylation with allyltributylstannane, the propargylation of aldehydes,[174] and vinylogous aldol reactions.[175] Recently also the vinylogous aldol addition of conjugated *N,O*-silyl ketene acetals to aldehydes showed in scheme 3.6 was reported.[176]

a) allylation whith allyl tributyl tin

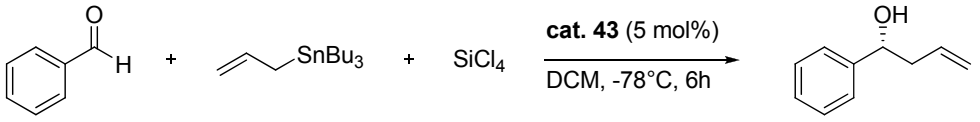

y= 91%, ee= 94%

b) Propargylation of aldehydes

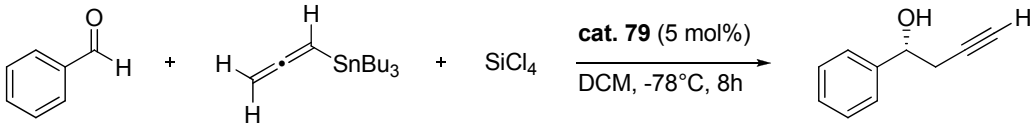

y= 81%, ee= 97%

c) vinylogous aldol reaction

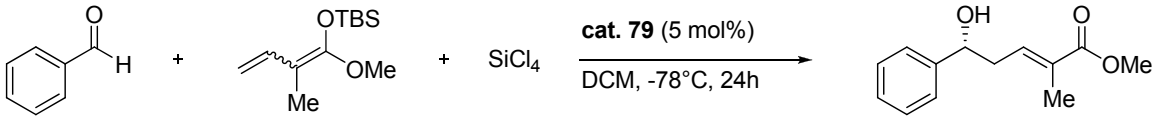

only γ-addition
y= 93%, ee= 99%

d) vinylogous aldol addition of conjugated N,O-silyl ketene acetals

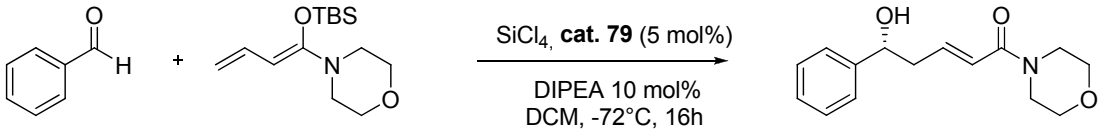

only γ-addition
y= 95%, ee= 95%

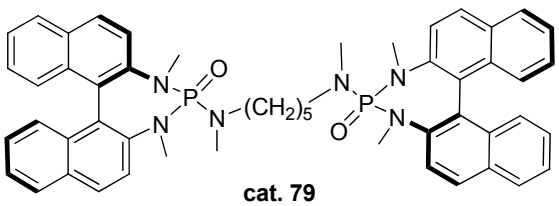

cat. 79

Scheme 3.6: *Lewis based catalyzed Lewis acid mediated reactions*

Very recently it was demonstrated that also chiral phosphine oxides are able to promote the silyl ketene acetals addition to aromatic aldehydes in the presence of a stoichiometric amount of silicon tetrachloride (Scheme 3.7).[141] The reaction of benzaldehyde with the trimethylsilyl ketene acetal derived from methyl isobutyrate in the presence of 1.5 eq of tetrachlorosilane and 0.1 eq of chiral phosphine oxide BINAP dioxide ((*S*)-BINAPO **21**) smoothly afforded the aldol adduct in high yield but moderate enantioselectivity (52% ee, scheme 3.8).

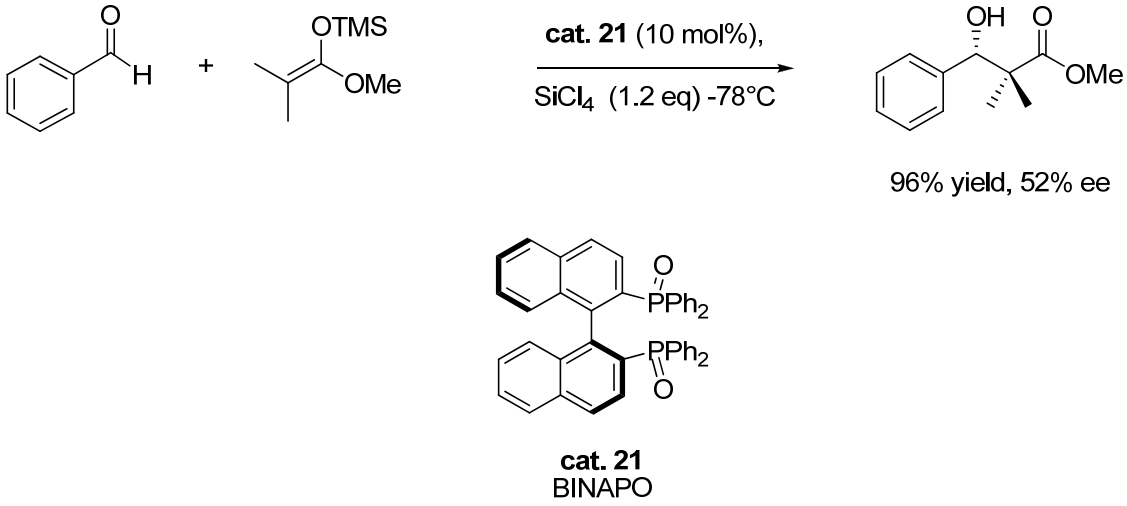

Scheme 3.8: *reaction of aldehyde with trimethylsilyl ketene acetal in presence of (S)-BINAPO.*

A more interesting work has been recently reported by the group of Nakajima where the *in situ* preparation of trichlorosilyl enol ether was investigated.[177] The aldol reaction of trichlorosilyl enolethers developed by Denmark suffers from the major drawback of requiring the preparation of the trichlorosilyl derivatives according to an environment-unfriendly procedure that involves the use of mercuric salts. To improve the efficiency of the methodology, the direct synthesis of the enolethers from the carbonyl compounds with tetrachlorosilane in the presence of phosphine oxides was realized; the resulting trichlorosilyl enol ether was simultaneously activated by phosphine oxide to add to aldehydes and afford a β-hydroxy ketone in a direct aldol-type reaction. After the usual screening of several experimental conditions, propionitrile was found to be the solvent of choice; under the best conditions the adduct was isolated in high yield with a good diasteroselectivity but moderate enantioselectivity (0°C, 2 h, 81% yield, *syn:anti* = 17:83, 54% ee for *anti* isomer, scheme 3.9).

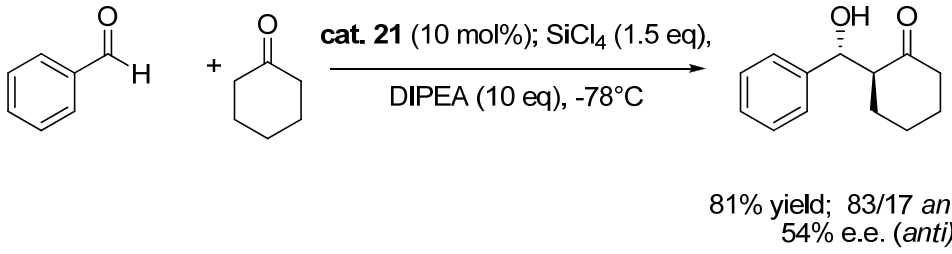

Scheme 3.9: *Direct aldol-type reaction catalyzed by phosphine oxide.*

Taking advantage of the poor reactivity of aliphatic aldehydes as electrophiles, a direct aldol-type reaction between two different aldehydes was also successfully accomplished. The reaction between benzaldehyde and isobutyraldehyde in the presence of (*S*)-BINAPO **21** leads to the expected β-hydroxy aldehyde that was reduced to the corresponding diol in order to facilitate the isolation of the product. Also in this case the enantioselectivity was not satisfactory (55% ee scheme 3.10).

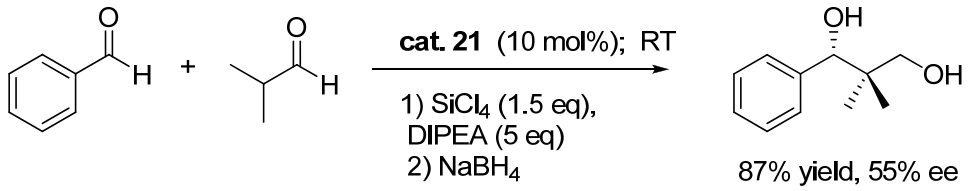

Scheme 3.10: *cross-aldol reaction catalyzed by phosphine oxide.*

The very promising results of these studies paved the way towards the application of this methodology to other nucleophilic attacks to activated C=O, C=N and even C=C promoted by chiral hypervalent silicon Lewis acids.

A very nice example came last year from Nakajima group, that reported an alternative methodology for organocatalytic conjugate reduction of enones and subsequent reaction with aldehydes, to realize a reductive aldol reaction. The method employs phosphine oxides as Lewis base-catalysts and trichlorosilane as a reductant.[118] The idea was to activate the silane with a suitable Lewis base to perform the 1,4-reduction via a six-membered transition state; then, with the assistance of the same Lewis base, the generated trichlorosilyl enolate should react with the electrophilic aldehyde. (Scheme 3.11). Triphenylphosphine oxide was shown to be able to catalyze the three-component reaction of chalcone, benzaldehyde and trichlorosilane (reductive aldol reaction) to afford the corresponding aldol product in 78% yield.

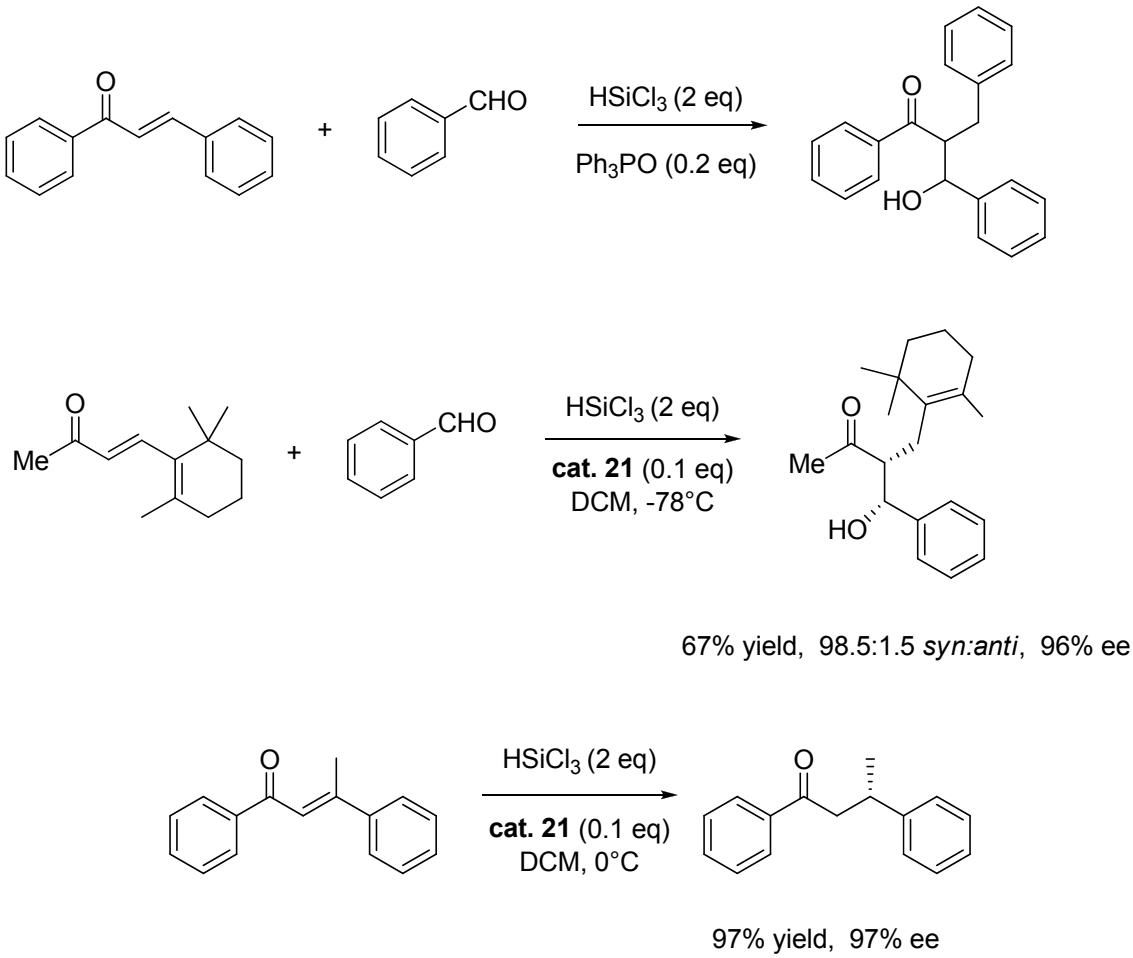

Scheme 3.11: *reductive aldol reaction catalyzed by phosphine oxides.*

Preliminary experiments with (*S*)-BINAPO as chiral Lewis base were very promising in term of stereocontrol. The reduction of 1,3-diphenylbutenone promoted by catalytic amounts of (*S*)-BINAPO at 0°C in the presence of two equivalents of trichlorosilane was successfully accomplished leading to the corresponding saturated compound in 97% yield and a somehow surprising, but very good, 97% ee. (*S*)-BINAPO gave even more appealing results in the reductive aldol reduction of β-ionone with benzaldehyde, where a very high *syn* stereoselectivity was observed along with 96% enantioselectivity for the *syn* isomer.

A great variety of Lewis-base catalyzed stereoselective transformations are currently under investigation, and novel synthetic methodologies are being developed as well. An example comes from a very recent report where, by studying the stereoselective synthesis of *N*-acylated β-amino ketones, it was unexpectedly found that optically active 4*H*-1,3-oxazines could be directly obtained via reductive cyclization of *N*-acylated β-

amino enones using trichlorosilane and chiral Lewis base catalysts (Scheme 3.12).[119] The reaction of trichlorosilane in the presence of catalytic amounts of (*S*)-BINAPO with (*Z*)-*N*-benzoyl enone derived from 3-amino-1-phenylbutane-1,3-dione, surprisingly afforded the 4*H*-1,3-oxazine as major product in 56% yield and 71% enantioselectivity. Similar yields and stereoselectivity (up to 81% ee) were obtained by extending the reaction to other five substrates; among different chiral phosphine oxides investigated (*S*)-BINAPO was found to secure the best performances. From some preliminary experiments it was observed that trichlorosilane act not only as a reductant, but also as a dehydrating agent. In the reaction different ratios of oxazine and the expected β-keto amide were formed, depending on the variation of experimental conditions. Interestingly, it was observed that the two products were obtained with different levels of stereoselection, and sometimes even with a different absolute configuration. The result was tentatively explained by assuming that the oxazine was not derived from the ketoamide by simple dehydration. It was proposed that 4*H*-1,3-oxazine was generated via the conjugate reduction of *N*-acylated β-amino enone, followed by cyclization of the resulting enolate and elimination of $HOSiCl_3$, whereas the ketoamide originates from the 1,2-reduction of the *N*-acyl imine generated via equilibration of the enamide. Further studies will be necessary to fully understand the reaction mechanism, in order to design more efficient catalysts.

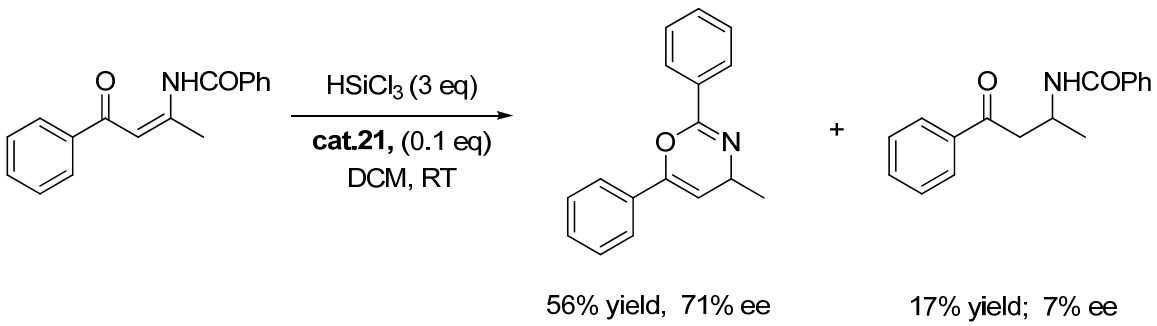

***Scheme 3.12**. (S)-BINAPO-catalyzed synthesis of oxazines.*

The great variety of structurally different chiral phosphine oxides, directly derived from the corresponding enantiomerically pure phosphines, was further enriched by a late report where optically active mono- and bis-phosphine oxides containing an allene backbone were prepared in enantiomerically pure form and used as organocatalysts (Scheme 3.13).[153] The novel chiral allenes were tested in the opening of *meso*-epoxides

by addition of silicon tetrachloride. Generally, BPO work better than MPO (scheme 1.32). When Ar = Ar_1 = Ph, only 0.1 mol% of catalyst is sufficient to promote the reaction to give the chlorohydrine with high yield (up to 97%) and high enantiomeric excess (94%).

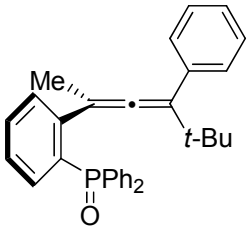

MONO - PHOSPHINE OXIDES (**MPO**)

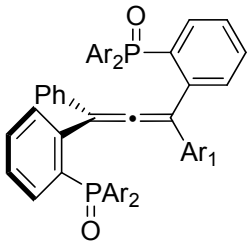

BIS - PHOSPHINE OXIDES (**BPO**)

Scheme 3.13: *chiral allenes phosphine.oxide.*

Finally, it is worth mentioning that the phoshine oxide group could be part of a multifunctional chiral catalyst. The search for a system that exhibits simultaneous activation of two separate reactants is extremely active. However, it should be noted that only bifunctional catalysts bearing a phosphine oxide group and Lewis acid metal sites were reported so far. No example of "metal-free" bifunctional catalyst containing phoshine-oxide as Lewis base has been reported. In this context, of particular interest is the work by the Shibasaki group, who described the activity of the new bifunctional catalyst based on a titanium complex generated *in situ* from the phosphine-oxide **80** and titaniumtetraisopropoxide in the cyanosilylation of ketones (Scheme 3.14).

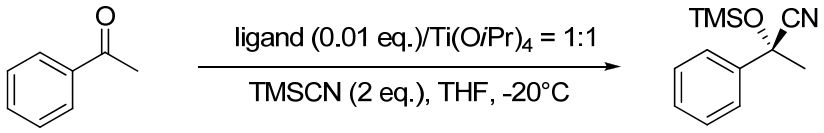

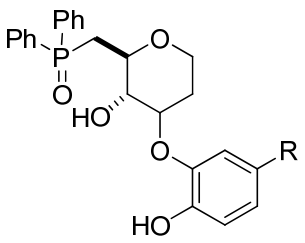

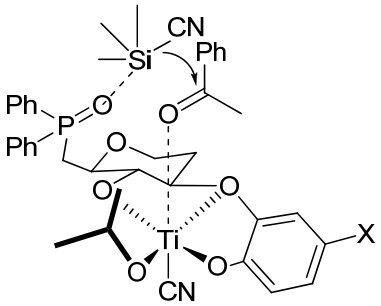

ligand 80, R=H 130h, 31%yield, 84% ee
ligand 81, R=COPh 88h, 92% yield, 94% ee

Scheme 3.14: *chiral phoshine oxide in a multifunctional catalyst.*

The products of this reaction are obtained with high enantioselectivity.[178] In 2001 the novel catalyst **81** was developed. This differed from **80** for the presence of a benzoyl group at the catechol moiety.[179] The benzoyl substituent has a positive effect in terms of enantioselectivity and yield, probably due to steric and electronic factors. Since the benzoyl group can enhance the acidity of the phenol hydroxy group, these results seem to point to an involvment of this group in the catalytic cycle. With aryl ketones ligand **81** has been used with a loading of 1 mol%, while in the case of aliphatic ketones a loading of 2.5 mol % is required. Under both conditions the cyanohydrines have been obtained in high yield and with excellent enantioselectivity. The authors have proposed the transition state showed in scheme 3.14: the titanium atom acts as a Lewis acid on the ketone, while the phosphine-oxide oxygen coordinates the silicon atom of TMSCN generating a pentacoordinated silicon species and thus increasing the nucleophilicity of the cyanide group.

In 2001 the bifunctional catalyst **82**, characterised by the simultaneous presence of one Lewis-acidic site (the metal) and two Lewis-basic sites (the phosphine-oxide oxygen atoms), was described.[180] In this case, the stereoselective cyanosilylation of aldehydes is promoted via a dual activation: the aldehyde is activated by coordination with the metal, while the silicon reagent (trimethylsilyl cyanide), that in this process acts just as a nucleophilic species, is activated by the Lewis basic centers, c.e. the phosphine oxides. Quite inexplicably the best results have been obtained using an additive: $Bu_3P(O)$ for aliphatic and α-β-unsaturated aldehydes and $MeP(O)Ph_2$ for aromatic aldehydes (Scheme 3.15).

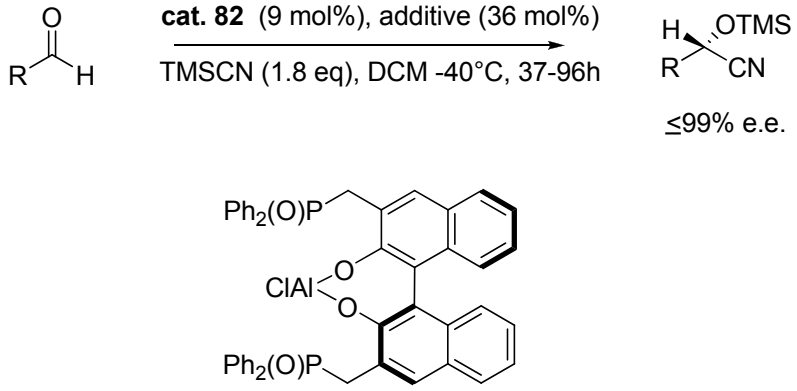

Scheme 3.15: *Stereoselective cyanosilylation of aldehydes promoted by a bifunctional catalyst.*

It is easy to predict that further studies about phosphine oxides and more detailed investigations for the development of innovative synthetic methodologies will appear soon.

Indeed, so far only a few classes of phosphine oxides have been investigated, and the major part of these studies were based on the use of bis-(diphenylphosphinoyl)-binaphthyl dioxides (BINAPO). Only in two works other phosphine oxides have been screened as promoters in stereoselective reactions although with no success. [119,170]

It should be noted however that not only aromatic but also heteroaromatic phosphine oxides may be considered.[141] These compounds offer new possibilities of development, since the electronic and steric properties of the ligands could be modulated by a proper choice of substituents.

In this line, also our group has been involved in the development of new reactions promoted by catalytic amounts of chiral phosphine oxides derived from biheteroaromatic systems, already employed with success in the allyltrichlorosilane addition (scheme 1.29).

A more detailed study on the use of (*S*)-tetraMe-BITIOPO will be discussed in the next chapter.

CHAPTER 4

Biheteroaromatic diphosphine oxides as catalysts in organic reactions

"Look up at the sky. Ask yourselves: is it yes or no?
Has the sheep eaten the flower?
And you will see how everything changes…"
The little prince - Antoine de Saint-Exupery

In the last few years, enantiomerically pure Lewis bases have attracted an increasing attention as chiral organocatalysts promoting stereoselective reactions. Among the different classes of Lewis bases, phosphine oxides are specially interesting because of the availability of several compounds in enantiomerically pure form.

Recently our attention has been devoted to the study of (*S*)-TetraMe-BITIOPO, a new C_2-symmetric chiral diphoshine oxide employed as promoter in organic reactions involving trichlorosilyl compounds. This compound is simply obtained by oxidation of TetraMe-BITIOP [2,2',5,5'-tetramethyl-4,4'-bis(diphenylphosphino)-3,3'-bithiophene], a chelating ligand for transition metals. The complexes of this electronrich diphosphine with Ru(II) and Rh(I) are very useful catalysts for some enantioselective homogeneous hydrogenation reactions. The synthesis of TetraMe-BITIOPO, starting from inexpensive materials, is reported in scheme 4.1 and consists of only five steps (including resolution). The very good synthetic accessibility make this compound very interesting from a industrial point of view, and in the last few years, TetraMe-BITIOPO is commercially available in both enantiomeric forms from Chemi S.p.A.[181]

Analyzing the structure from an electronic point of view, it's possible to observe that the two diphenylphosphino groups are located in the electronrichest position (the β-

position) of an inherently electronrich heterocyclic ring (the thiophene ring). To guarantee configurational stability to the ligand through consistent hindrance to rotation around the interanular bond, four methyl group were introduced in α- and δ-position of the two thiophene rings. While the methyl group adjacent to the biaryl bond gives direct contribution to the stability of the system, the other one develops a consistent buttressing effect on the phosphine group.

The steric hindrance around the biaryl bond makes the bistiophene scaffold similar to a biphenyl backbone, but with lower bite-angle. The biaryl bond coincides with the stereogenic axis, and this structure exist in two enantiomeric forms that can be separated using chiral dibenzoyltartaric acid.

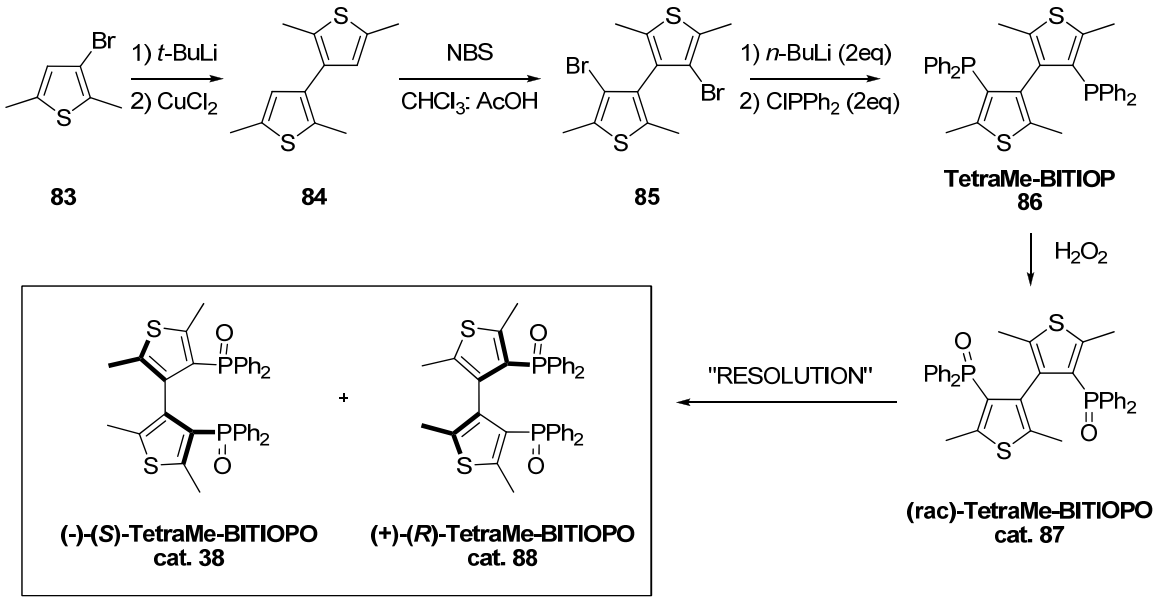

***Scheme 4.1**: synthetic scheme of TetraMe-BITIOPO.*

X-ray studies allowed to assign the absolute configuration to the two enantiomers: (*R*)-(-)-TetraMe-BITIOP and (*S*)-(+)-TetraMe-BITIOP. The oxidation of dextrorotatory (*S*)-(+)-TetraMe-BITIOP gives the levorotatory phosphine oxide (*S*)-(-)-TetraMe-BITIOPO.[182] This phosphine oxide is able to promote the enantioselective opening of *meso*-epoxides and the allylation of aldehydes in the presence of allyl trichlorosilane as BINAPO (see chapter 1 and 3), providing better chemical efficiency and higher stereochemical control. Inexplicably, no other reactions promoted by TetraMe-BITIOPO were reported in literature; so we decided to test this phosphine oxide as catalyst in other organic reactions promoted by phosphine oxides.

4.1 Biheteroaromatic diphosphine oxides-catalyzed stereoselective reactions

The possibility to investigate reactions promoted by a chiral Lewis acid generated through coordination to trichlorosilyl compounds by an enantiomerically pure phosphine oxide was obviously very attractive. Since electron-rich TetraMe-BITIOPO had already shown higher performances than BINAPO in the allylation we thought that such a Lewis base could successfully generate the chiral cationic hypervalent silicon species acting as efficient catalyst for numerous reactions.

For these reasons, TetraMe-BITIOPO was tested as a catalyst in a series of organic reactions, to assess its reactivity and to collect suggestions for further elaborations. On the basis of Nakajima work[119] we used (*S*)-TetraMe-BITIOPO in the asymmetric synthesis of oxazines by reductive cyclization of *N*-acylated β-amino enones with $HSiCl_3$ (scheme 4.2).

a) Synthesis of N-acylated β-amino enones

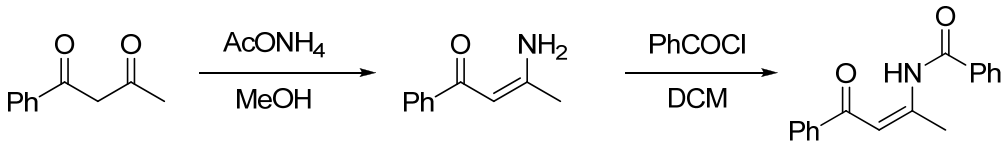

b) Asymmetric synthesis of 4H-1,3-oxazines

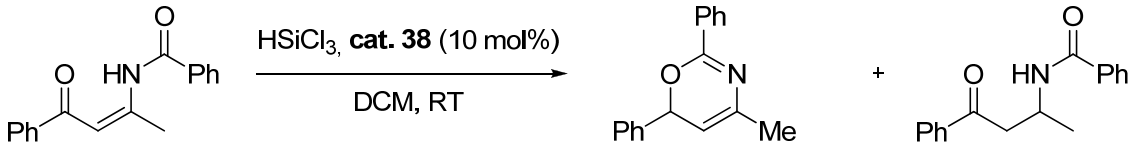

Cat	Time (h)	C-1 yield (%)	C-1 ee (%)	D-1 yield (%)	D-1 ee (%)
(S)-BINAPO	24	68	74	13	7
(S)-TetraMe-BITIOPO	24	46	22	24	16
(S)- TetraMe-BITIOPO	72	44	nd	14	nd

Scheme 4.2

The data showed that while the activities of TetraMe-BITIOPO and BINAPO were comparable in this reaction, the level of stereoselectivity was not very satisfactory. However these results represent only preliminary data and more studies on the substrate and on the experimental conditions are needed.

We also studied the reduction of keto-imines promoted by trichlorosilane (scheme 4.3).

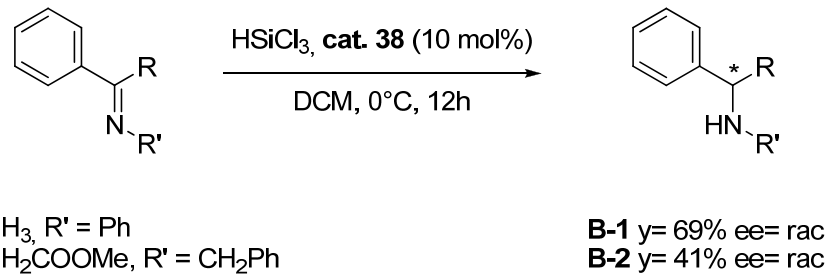

66 R = CH_3, R' = Ph
92 R = CH_2COOMe, R' = CH_2Ph

B-1 y= 69% ee= rac
B-2 y= 41% ee= rac

Scheme 4.3

Also in this case, the chemical efficiency was good, but the stereoselection was low, both the products **B-1** and **B-2** being obtained in racemic form. Other types of keto-imines were studied, but the results was very unsatisfactory.

Interesting results were obtained when $SiCl_4$ was employed as Lewis Acid. The possibility to investigate reactions promoted by a chiral Lewis acid generated through coordination to $SiCl_4$ by an enantiomerically pure phosphine oxide are very attractive. As explained in the previous chapter, upon coordination to a Lewis base, the silicon atom of $SiCl_4$ become more electrophilic and generates a cationic specie, with significantly increased Lewis acidity.

The first reaction investigated was the allylation of *p*-NO_2-benzaldehyde with allyltributil tin (0°C, 16 hours), that gave the allylic alcool in 41% yield and 13% enantiomeric excess (scheme 4.4).

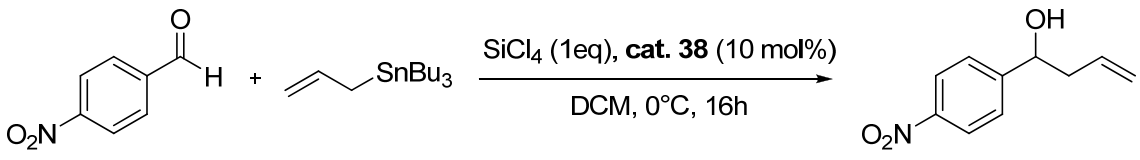

A-2
y = 41%, ee= 10%

Scheme 4.4

Also the the enantioselective addition of trialkylphopshite to achiral aldehydes was investigated (scheme 4.5). Again, TetraMe-BITIOPO was able to promote the reaction with chemical efficiency similar than BINAPO, but with lower stereocontrol.

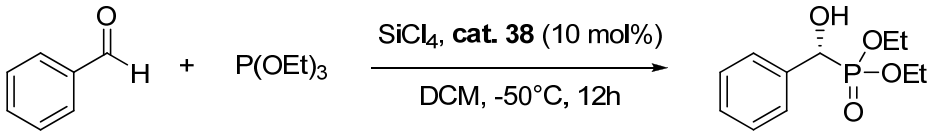

E-1
y= 22%, ee= 22%

Scheme 4.5

Particular attention was given to the enantioselective aldol reaction of silyl ketene acetals promoted by a Lewis base-activated Lewis acid catalyst. The addition of silyl ketene acetals to benzaldehyde was conducted in the presence of 10 mol% of catalyst, at different temperatures for 20 hours. The results are reported in scheme 4.6 and shown that TetraMe-BITIOPO was able to promote the reaction with high yield and modest but encouraging stereocontrol.

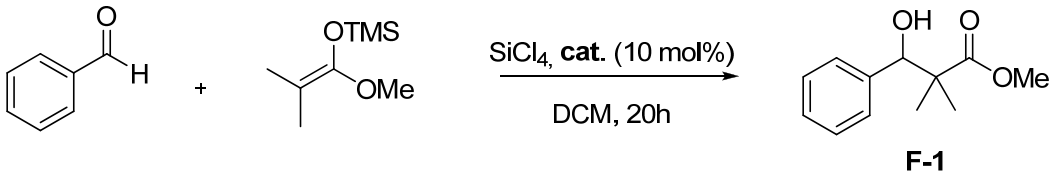

F-1

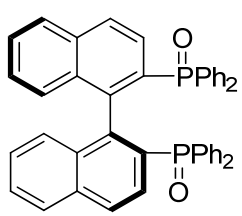

cat. 21 (*S*)-BINAPO
-78°C, 96% yield, 52% ee

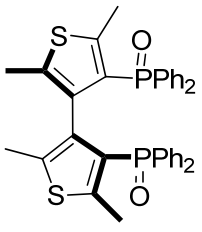

cat. 38 (*S*)-tetraMe-BITIOPO
0°C, 78% yield, 39% ee

Scheme 4.6

The chiral adduct generated by coordination of (*S*)-TetraMe-BITIOPO with $SiCl_4$ catalyzed also the addition of cyclohexanone to benzaldehyde with a good

diastereostereoselectivity (7:93 sy*n*:*anti* ratio) and a high enantioselectivity (88%) for the *anti* enantiomer. This results are better those obtained with BINAPO,[177] although the yields are lower (scheme 4.7).

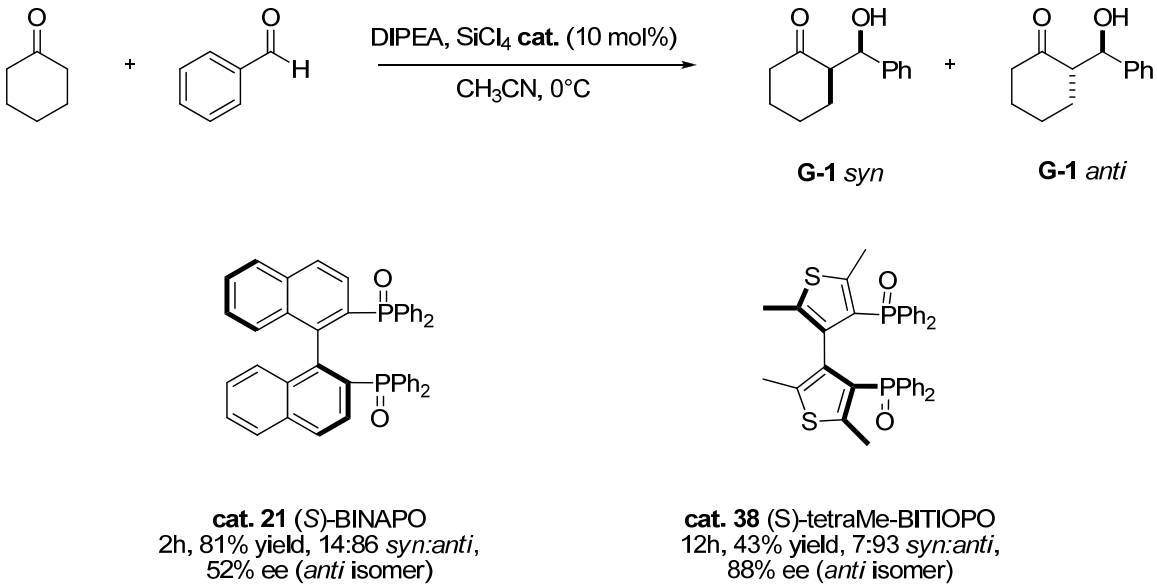

Scheme 4.7

The obtained results are obviously interesting, and considering the importance of this reaction in synthetic organic chemistry for its simple experimental procedure, we decided to concentrate our studies on the direct aldol addition of a ketone to aromatic aldehydes promoted by the chiral biheteroaryl-diphosphine oxide TetraMe-BITIOPO.

4.1.1 The direct aldol reaction of ketones with aromatic aldehydes

The direct aldol reaction of a ketone with aromatic aldehydes reaction is very appealing, because the synthetic procedure does not involve the preparation of enol ethers or ketene acetals. The trichlorosilyl enol ether is generated *in situ* in the presence of tetrachlorosilane and it is activated by phosphine oxide to react with an aldehyde, that in its turn is coordinated by the chiral cationic hypervalent silicon species.

The reaction between cyclohexanone and benzaldehyde was first investigated in the presence of stoichiometric amounts of $SiCl_4$ without phosphine oxide at 0°C for 16h in dichloromethane, in order to evaluate the presence of a background reaction. Under these conditions, we were pleased to find that no product was formed.

Subsequently, different experimental conditions (solvent, temperature and additives) were screened in order to optimize the performance of phosphine oxide.

The direct condensation of 1 mol equiv of cyclohexanone with 1 mol equiv of benzaldehyde in the presence of 3 mol equiv of silicon tetrachloride, 10 mol equiv of DIPEA and 0.1 mol equiv of (*S*)-TetraMe-BITIOPO afforded the corresponding β-hydroxy ketone **G-1** after 15 hours at 0°C in CH_3CN in 53% yield, as mixture of *anti:syn* isomers (92:8) and 60% enantioselectivity for the major *anti* isomer after chromatographic purification (entry 1, Table 4.1).

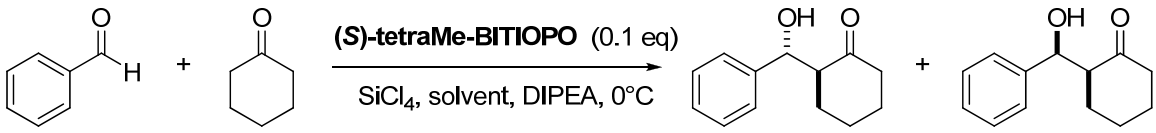

(1 eq) (2 eq) **G-1** *anti* **G-1** *syn*

entry	solvent	time (h)	yield (%)	*anti:syn*	ee *anti* (ee *syn*) (%)
1[a]	CH_3CN	15	53	92:8	60 (33)
2[b]	CH_3CN	15	91	90:10	69 (37)
3	DCM	15	63	88:12	75 (42)
4	Toluene	15	50	25:75	31 (7)
5	THF	15	70	84:16	61 (17)
6	$CHCl_3$	15	40	88:12	67 (41)
7	DCM	2	51	89:11	70 (31)
8	CH_3CN	2	65	90:10	53 (15)

[a] 1 mol equiv of ketone was used; [b] 20% mol of catalyst

Table 4.1

By optimization of the experimental conditions, the reaction was found to proceed better in dichloromethane, by employing 2 mol equiv of ketone for 1 mol equiv of aldehyde; in this case the *anti* diastereoisomer was isolated as major product (88:12 *anti:syn*) in 75% ee (entry 3, Table 4.1). Operating in $CHCl_3$ the diastereoselection was comparable with DCM, but yields and enantioselections were lower.

The use of other solvents was deleterious for the enantioselectivity of the process, even if an interesting switch of the sense of the diastereoselectivity was observed when

the reaction was conducted in toluene, where a modest *syn* selectivity was obtained (entry 4, Table 4.1). Shorter reaction times instead, did not bring any appreciable variation of the stereochemical outcome of the reaction (entries 7-8).

Then, a variation of temperature reaction was studied. A lower reaction temperature had a positive effect on the stereocontrol of the aldol reaction, but it was detrimental for the chemical efficiency (Table 4.2).

entry	solvent	temp (°C)	yield (%)	*anti:syn*	ee *anti* (ee *syn*) (%)
1	CH_3CN	-25	30	81:19	65 (27)
2	DCM	-25	70	93:7	83 (49)
3[b]	DCM	-45	44	79:21	86 (11)

[b] 20% mol of catalyst

Table 4.2

When the reaction temperature was decreased to -45°C, in fact, longer reaction times and 20 mol% of tetraMe-BITIOPO catalyst were necessary in order to obtain satisfactory chemical yields (entry 3, table 4.2). Once again DCM secured better performances than acetonitrile: after 36 hours in DCM at -25°C, the product was obtained in 70% yield, 93:7 *anti:syn* ratio and 83% enantioselectivity for the *anti* isomer (entry 2, table 4.2). Enantioselection was further improved by running the reaction at -45°C, when the major diastereoisomer was produced with 86% ee. (entry 3, table 4.2).

Other bases than DIPEA were also investigated, but *N*-methylmorpholine (NMM) or DABCO did not bring any significative change (table 4.3).

entry	solvent	base	temp (°C)	yield (%)	*anti:syn*	ee *anti* (ee *syn*) (%)
1	DCM	DABCO	-25	42	76/24	57 (10)
2	DCM	NMM	-25	40	91/9	65 (18)

Table 4.3

On the basis of these results we decided to compare the performances of BINAPO and tetraMe-BITIOPO under the same conditions. By performing the reaction under the conditions reported in the literature[177] (CH_3CN, 0°C, 2 hours) in our hands BINAPO promoted the reaction in 64% yield, 89:11 *anti:syn* ratio and 40% ee for the *anti* isomer, lower than enantioselection observed with BITIOPO (53% ee., entry 2 vs 1, Table 4.4).

At lower temperature bithiophene-based phosphine oxide confirmed to perform better than binaphthyl-derived diphenylphosphine, affording the aldol adduct in 93:7 *anti:syn* ratio and 80% ee, while BINAPO led to the *anti* isomer with 60% enantioselectivity and lower *anti* selectivity (entries 3 and 4, table 4.4).

entry	solvent	catalyst	time (h)	temp (°C)	yield (%)	*anti:syn*	ee *anti* (ee *syn*) (%)
1	CH_3CN	BINAPO	2	0	64	89:11	40 (5)
2	CH_3CN	BITIOPO	2	0	65	90:10	53 (15)
3	DCM	BINAPO	30	-25	40	79:21	60 (3)
4	DCM	BITIOPO	30	-25	70	93:7	83 (49)

Table 4.4

These results show that tetraMe-BITIOPO is a good catalyst in the direct aldol condensation of benzaldehyde with cyclohexanone. In order to expand this synthetic procedure, the use of other aromatic aldehydes with different electronic properties was investigated.

First aldehydes with electron withdrawing substituents were tested (table 4.5). When cyclohexanone was reacted at -25°C with 4-nitrobenzaldehyde in the presence of a catalytic amount of Lewis base the product was isolated in 87:13 diastereoisomeric ratio and 93% of enantiomeric excess for the major *anti* isomer (entry 1, Table 4.5). A further decrease of the reaction temperature did not improve the stereoselection (entry 3, Table 4.5).

The use of trifluoromethyl substituted aldehydes led to a better diastereoselection than that observed with 4-nitrobenzaldehyde, but a slightly lower enantioselection. Also *ortho*-substituted aromatic aldehydes may be suitable substrates for the reaction, as shown by the case of 2-chlorobenzaldehyde, where the product **G-4** was formed in 90:10 *anti:syn* ratio and 87% ee for the major isomer.

Aromatic aldehydes bearing electron-withdrawing groups reacted with high *anti* selectivity at -25°C in fair yields and enantioselectivity often higher than 80%.

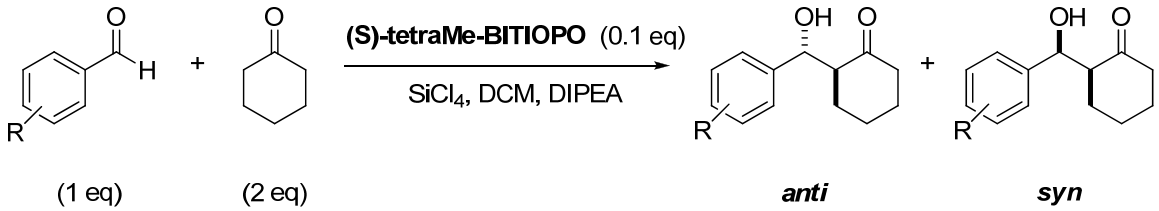

entry	R	product	temp (°C)	yield (%)	*anti:syn*	ee *anti* (ee *syn*) (%)
1	4-NO_2	**G-2**	-25	71	87:13	93 (65)
2[a]	4-NO_2	**G-2**	-25	51	90:10	85 (71)
3[b]	4-NO_2	**G-2**	-45	50	86:14	92 (67)
4[b]	4-Cl	**G-3**	-45	41	81:19	88 (11)
5	4-Cl	**G-3**	-25	56	98:2	71 (n.d.)
6	2-Cl	**G-4**	-25	55	90:10	87 (27)
7	4-CF_3	**G-5**	-25	57	92:8	77 (33)
8	3,5-CF_3	**G-6**	-25	65	94:6	83 (n.d.)

[a] reaction was run in CH_3CN; [b] with 20% mol of BITIOPO.

Table 4.5

The same high level of stereoselection was maintained also with aromatic aldehydes featuring electron-donating residues (table 4.6). For example the reaction of cyclohexanone with 4-methoxybenzaldehyde led to the corresponding hydroxy ketone **G-10** in 87% enantioselectivity for the *anti* isomer at -45°C (entry 5, Table 4.6). The condensation of 2-methyl-benzaldehyde afforded the corresponding aldol **G-7** in high diastereoselectivity (94:6) but lower enantioselectivity (73% ee, entry 1, Table 4.6). However, the position of the electron-donor substituent seemed to influence only the yield of the reaction and not its stereoselection, as shown by entry 1-3 table 4.6.

entry	R	product	Time (h)	yield (%)	*anti:syn*	ee *anti* (ee *syn*) (%)
1	2-Me	**G-7**	-25	56	94:6	73 (31)
2	3-Me	**G-8**	-25	36	98:2	71 (n.d.)
3	4-Me	**G-9**	-25	55	98/2	77 (n.d.)
4	4-OMe	**G-10**	-25	22	94:6	66 (n.d.)
5[a]	4-OMe	**G-10**	-45	42	92/8	87 (22)
6	1-Naph	**G-11**	-25	40	97:3	77 (n.d.)

[a] with 20% mol of BITIOPO.

Table 4.6

Heteroaromatic aldehydes were also used in the direct aldol condensation, and were shown to be suitable substrates for this methodology. Satisfactory levels of *anti* selectivity were reached, but only modest enantioselection was observed both with 2-thiophene carboxyaldehyde and 2-furfurol (table 4.7).

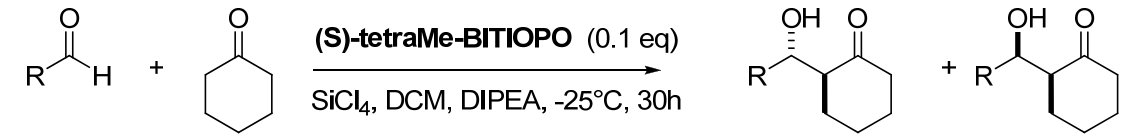

(1 eq) (2 eq) ***anti*** ***syn***

entry	R	product	yield (%)	*anti:syn*	ee *anti* (%)
1	2-Thioph	**G-12**	55	98:2	53
2	2-Furyl	**G-13**	36	98:2	51

Table 4.7

Finally, the aldol condensation was attempted with non aromatic aldehydes; as expected, aliphatic aldehydes did not react (see scheme 3.5), even at 0°C, while cynnamic aldehyde reacted with cyclohexanone in 41% yield 90:10 *anti:syn* ratio but only 37% enantioselectivity of the major isomer (table 4.8).

Entry	R	product	Temp (°C)	yield (%)	*anti:syn*	ee *anti* (%)
1	PhCH=CH	**G-14**	-25	41	90:10	37
2	$Ph(CH_2)_2$	**G-15**	0	-	-	-
3	$C(CH_3)_3$	**G-16**	0	-	-	-

Table 4.8

After the screening of different aldehydes, different cyclic ketones were then investigated in the direct aldol condensation with electron poor aldehydes (scheme 4.8). Interesting results were obtained in the aldol condensation of cyclopentanone with benzaldehyde; TetraMe-BITIOPO catalyzed the transformation with higher stereoselectivity than BINAPO (83% ee vs 53% ee)[177] and with very high *anti* selectivity (94%). Lower selectivity was observed in the reaction of cycloheptanone, where no diastereoselectivity and a modest enantioselectivity were observed.

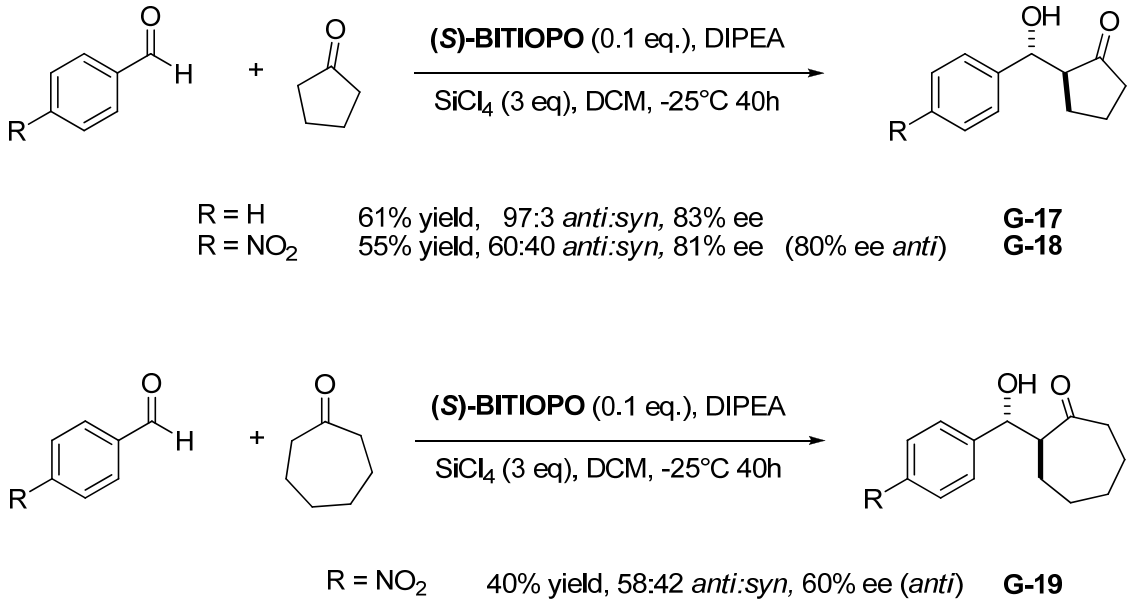

Scheme 4.8

Also heterocyclic ketones as well as 4,4-disubstituted cyclohexanone may react as aldol donors in this Lewis base-catalyzed $SiCl_4$-mediated direct aldol condensation (scheme 4.9).

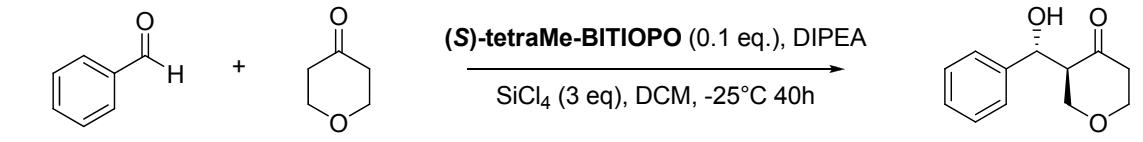

93 41% yield, 91:9 *anti:syn,* 77% ee **G-20**

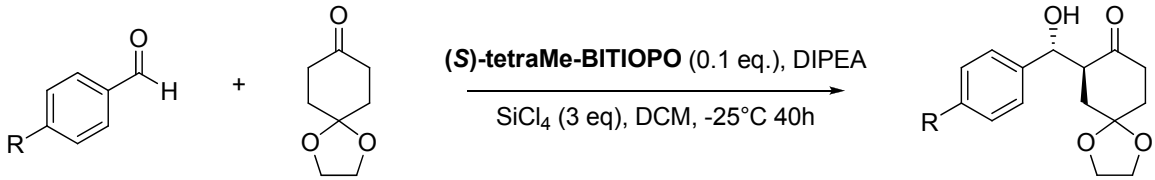

94 R = H, 45% yield, 93:7 *anti/syn,* 86% ee **G-21**
R = Cl, 55% yield, 85:15 *anti/syn,* 66% ee **G-22**

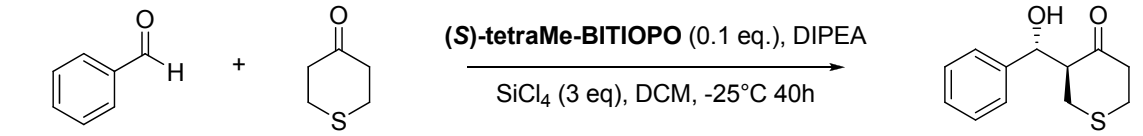

95 90:10 *anti:syn,* 83% ee **G-23**

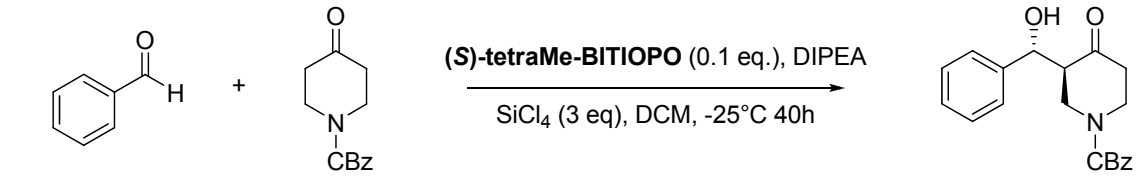

96 86:14 *anti:syn,* 47% ee **G-24**

Scheme 4.9

The products were generally obtained in high *anti:syn* ratios (>80% d.r.) and enantioselectivity up to 86% ee. The best result was reached with ketone **94** that afforded, after condensation with benzaldehyde, the *anti* isomer of compound **G-21** in 93:7 d.r. and 86% ee. The methodology could be applied to ketones containing oxygen, nitrogen or sulphur atoms. Usually a good *anti* selectivity was obtained with all substrates. For example, ketone **95** afforded the aldol product with benzaldehyde with good *anti* selectivity and 83% ee for the major isomer.

A tentative model explaining the stereoselection observed in the reactions promoted by TetraMe-BITIOPO must take into account mechanistic considerations. It is well known that the coordination of a Lewis base to a Lewis acid makes it more electrophilic;[76] the chiral cationic hypervalent silicon species[82] coordinates and activates the aldehyde towards the attack of the *in situ* generated trichlorosilyl enolether. A chairlike six-membered cyclic transition state may be hypothesized and would explain the *anti* selectivity generally observed for these reactions (scheme 4.10). The observed *syn* stereoselectivity for the reaction in toluene might be explained with the preference for a boat-like transition state instead of a chairlike transition state. The steric hindrance of the diphenyl-phosphinoyl group of the Lewis base with cyclohexanone-derived enolether would be responsible for the favourable attack of the enolether onto the *Re* face of the aldehyde, to afford the experimentally observed major (2*S*, 1'*R*)-*anti* stereoisomer.

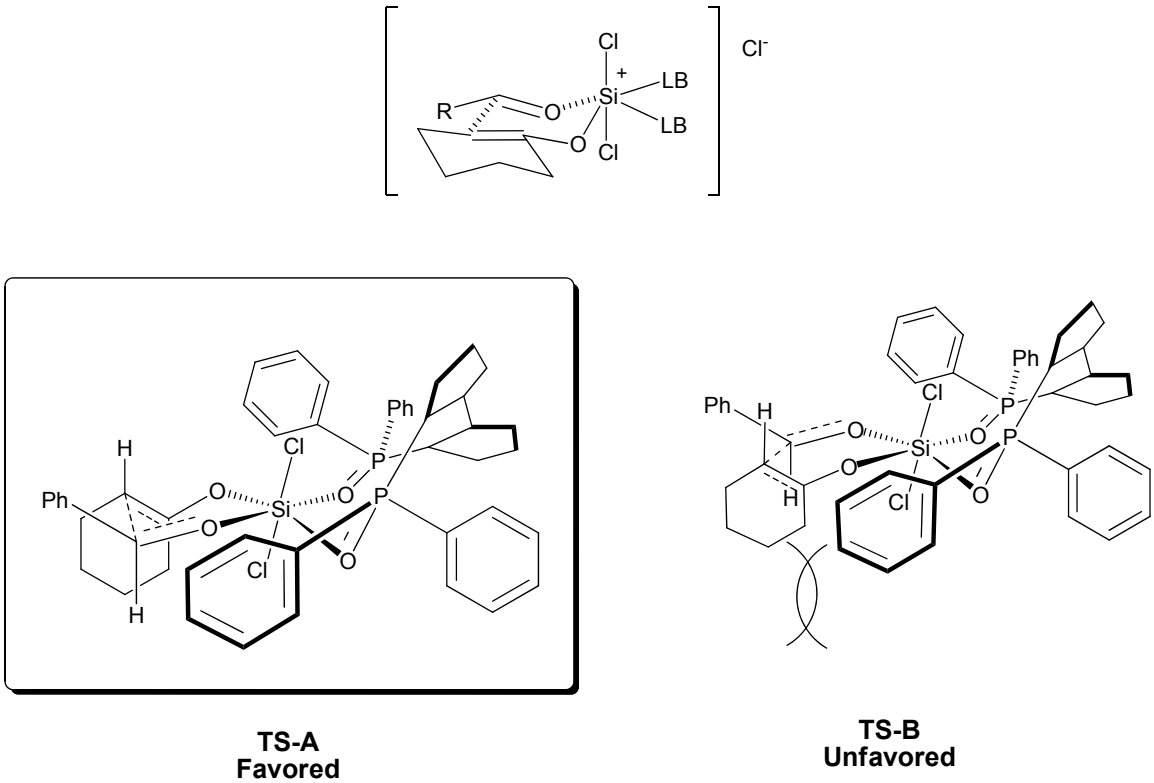

Scheme 4.10: *a tentative chairlike six-membered cyclic transition state; the bisthiophene scaffold was represented simplified for clarity.*

Support to the proposed cyclic transition state was obtained by an additional experiment, where the aldol condensation between benzaldehyde and cyclohexanone was performed at -25°C in the presence of a stoichiometric amount of BF_3, a Lewis acid able

to coordinate the aldehyde. In that case the product was isolated in 65% yield as 60:40 *syn:anti* mixture, both isomers basically as racemic compounds, clearly suggesting the importance of the aldehydes coordination to the chiral cationic silicon species.

NMR preliminary investigations[183] seem to support the proposed mechanism: ^{31}P NMR analysis shows that the coordination of tetraMe-BITIOPO with $SiCl_4$ at 0°C in $CDCl_3$ caused a shift of the P signal from 22.3 ppm to 34.8 ppm (neutral $SiCl_4$/phosphine oxide complex) that is different from the cationic specie obtained with treatment of tetraMe-BITIOPO with HCl (P signal at 31.9 ppm). After addition of DIPEA at the neutral $SiCl_4$/phosphine oxide complex, the chemical shift change from 34.8 to 27.6 ppm. The same cationic silicon species was observed when the ketone was treated with DIPEA in the presence of $SiCl_4$ and TetraMe-BITIOPO (P signal at 28.0 ppm).

A computational investigation about **TS-A** and **TS-B** was also performed. Initial estimates for the geometries of the two hypothesized transition states were obtained by a molecular mechanics program (Merck Molecular Force Field),[184] followed by full optimization of all geometrical variables. A symmetry constraint for the biaryl bond was imposed, in order to prevent the interconversion between the two enantiomeric forms of tetraMe-BITIOPO.

Subsequently, using the semi-empirical AM1 quantum chemical method in the MOPAC 2009 program,[185] the two structures were minimized and used as starting point for a reaction path study. The distance between the two carbon atoms involved in the formation of the new C-C bond was fixed at progressively smaller values (with steps of 0.5 Å), in order to simulate the course of the reaction. For each distance, two structures of complex were minimized, and their heat of formation was reported in table 4.9.

structure	C-C fixed distance (Å)	Favored structure A (kcal/mol)	Unfavored structure B (kcal/mol)
$S_{3.2}$	3.179	-101.66	-105.54
$S_{2.7}$	2.679	-99.95	-105.72
$S_{2.5}$	2.479	-93.75	-105.52
$S_{2.0}$	**1.979**	**-57.93**	**-42.56**

Table 4.9

These results show that when the C-C bond distance is fixed at 1.979 Å, the proposed structure **S-A** (where the enolether attacks onto the *Re* face of the aldehyde) is energetically favored than **S-B.** When the distance is reduced at 1.479 Å, the complex between the hypervalent cationic silicon specie and the product of the reaction, β-hydroxy ketone, was obtained. So, the structures $\mathbf{S_{2.0}}$**-A** and $\mathbf{S_{2.0}}$**-B** were minimized removing the constraint distance between the two carbon atoms, in order to search the TS. While unconstrained $\mathbf{S_{2.0}}$**-A** gave a product similar to constrained $\mathbf{S_{2.0}}$**-A**, in unconstrained $\mathbf{S_{2.0}}$**-B** the C-C distance between enolether and benzaldehyde increases. This distance increment was expected and it is due to the electronic repulsion and to the steric hindrance between the diphenyl-phosphinoyl group of the catalyst with cyclohexanone-derived enolether. The only way to accommodate both these structures near to the silicon atom in a stable system is to decrease the steric hindrance, and this is possible only when their distance is greater.

The unconstrained structure $\mathbf{S_{2.0}}$**-A** was also used as starting point for TS search with TS routine in order to generate the force constants relative to the formation of the new C-C bond. In order to decrease the gradient, a keyword PRECISE was added in the search of the stationary point. However, the gradient value was higher than that accepted for the generation of the force constants, so a keyword LET was added in a FORCE calculation. In this way, a calculation could be done, and a structure with 4 negative frequencies is obtained. The first, about -529.15 cm^{-1}, presents a 99.6% of stretching energy contribution between the two carbon atoms responsible for the formation of the new bond. The other negative frequencies present a very small value and they can be correlated to the torsional motions. Since we did not find a single negative frequency, the structure cannot be considered as a real transition state of the reaction, although it is very close to the stationary point. A picture of this structure was reported in scheme 4.11. Further studies, that involve also *ab initio* approach are under investigation.

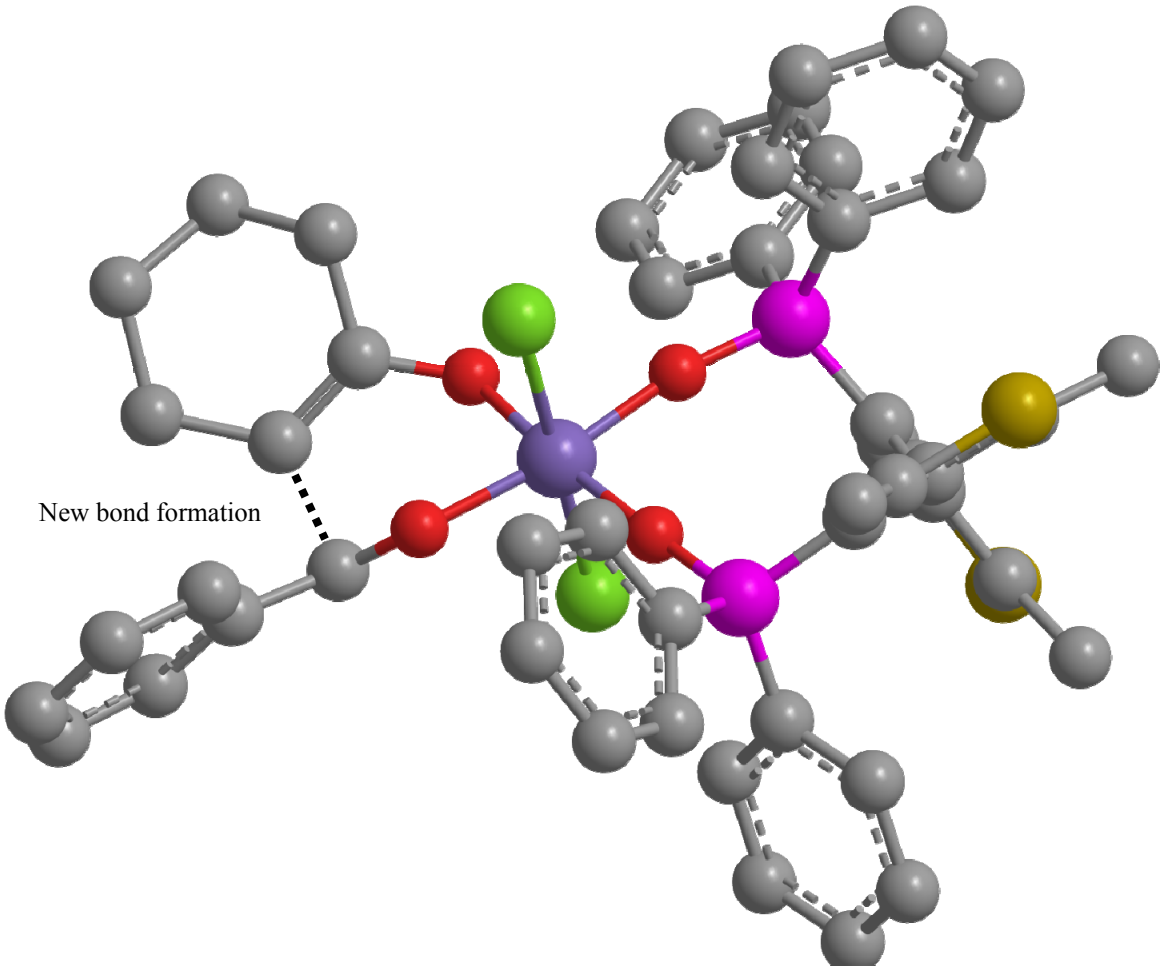

Scheme 4.11: *picture of transition state:*
green = chloro; violet = silicon; red = oxygen; purple = phosphorous, yellow = sulfur.

4.1.2 Cross-aldol reaction between two aldehydes

The direct catalytic asymmetric aldol reaction is a powerful carbon–carbon bond forming reaction and is used for the construction of enantiomerically enriched β -hydroxy carbonyl compounds and their derivatives with an atom-economical approach. The intense demand for stereoselective synthesis of aldol products has been fuelled by its application in producing key synthons in numerous synthetic strategies for natural products synthesis, as well as in medicinal chemistry.

So far, only three types of catalytic direct aldol reactions have been reported in literature: the reactions catalyzed by chiral metal alkoxide complexes reported by Shibasaki;[186] the reactions involving enamine catalysts pioneered by List and

Barbas[23,187] and the reactions involving a hypervalent cationic silicon specie promoted by BINAPO and developed by Nakajima.[177]

In this chapter, it has been demonstrated that TetraMe-BITIOPO performs better than BINAPO in the aldol condensation, even if it presents the same poor reactivity in the condensation of aliphatic aldehydes. This fact, however, is very important in the cross-aldol reaction, because it permits to obtain β -hydroxy carbonyl compounds without any self-condensation of aliphatic aldehyde.

In very preliminary studies, the reaction of isobutyraldehyde with benzaldehyde was attempted in DCM in the presence of 3 equiv. of $SiCl_4$ and 0.1 equiv of TetraMe-BITIOPO, followed by reduction of the carbonyl group by treatment with $NaBH_4$ in order to facilitate the isolation of the product.

By working at 0°C 1-phenyl, 2,2-dimethyl-1,3-propanediol **H-1** was isolated in 55% yield and 48% ee, that was increased up to 70% by running the reaction at -45°C (scheme 4.12).

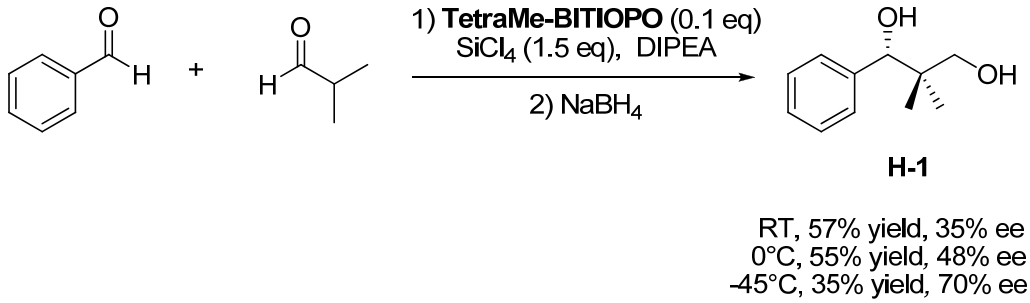

Scheme 4.12

The cross condensation between benzaldehyde and cyclohexane carboxyaldehyde afforded the 1,3-diol **H-2** with lower enantioselectivity. By exploring the use of other aromatic aldehydes in the reaction with isobutyraldehyde different results were observed (scheme 4.13); while 4-chloro benzaldehyde afforded product **H-3** only in 48% ee, 4-nitrobenzaldehyde led to the formation of **H-4** in 93% ee at 0°C. More studies are needed in order to fully investigate the scope of the methodology, but the feasibility of the synthetic approach was surely demonstrated.

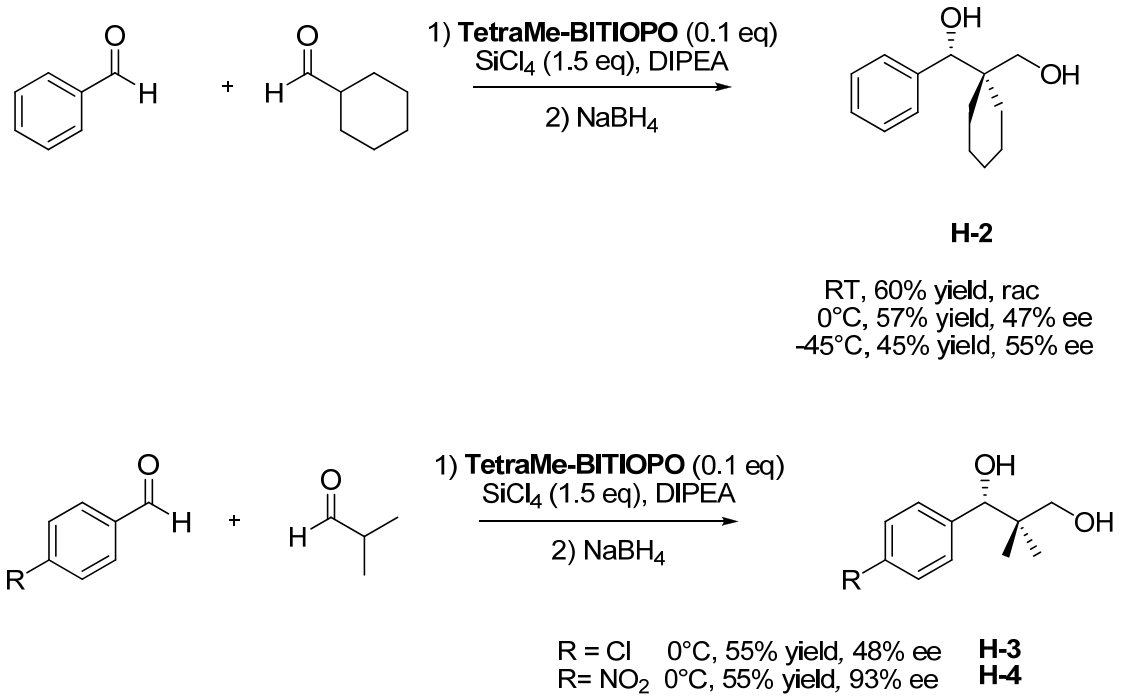

Scheme 4.13

4.1.3 The direct aldol reaction of thioesters with aromatic aldehydes

The development of a direct diastereo- and enantioselective catalytic aldol reaction of esters with carbonyl derivatives is still one of the unsolved challenge in organocatalysis. Numerous examples of catalytic systems that generated *in situ* the nucleophilic species starting from ketones or aldehydes are reported, but systems that involve the use of esters as nucleophiles are extremely rare. The difficulty with this class of potential nucleophiles lies in the relatively inert nature of the proton in the α-position of a simple carboxylic ester compared to those of a ketone or an aldehyde. In the case of ester derivatives, the pKa value is approximately 19 and is significantly higher than the pKa values range of 16-17, necessary to activate a nucleophilic substrate via amine catalysis. [188]

Taking inspiration from nature, where acetyl coenzyme A is involved in many biological cycles, as the synthesis of fatty acids,[189] few groups have recently studied the possibility to perform catalytic stereoselective transformations with activated thioesters, such as malonic acid half thioesters. Catalytic enantioselective reactions based on either metal catalysis or organocatalysis have recently been reported.

In an organometallic approach, our group[190] and Shair[191] have investigated the use of chiral copper (II) complexes in the malonic acid emithioester addition to aldehydes. For the metal-free methodologies, in 2007 Ricci's group has realized a decarboxylative addition to imines catalyzed by a readily available Cinchona-based compound to afford β-amino thioesters (scheme 4.14).[192]

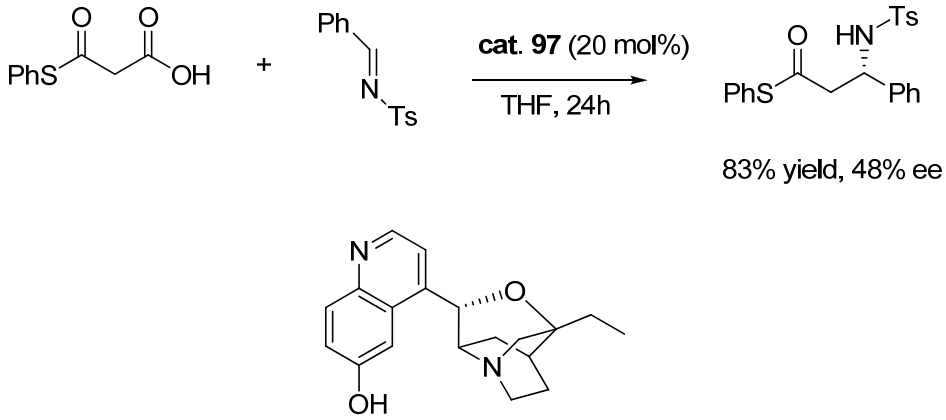

Scheme 4.14*: asymmetric addition of malonic acid half thioesters to imines.*

At the same time Wennemers showed that a bifunctional thiourea derivative of a Cinchona alkaloid could efficiently promote the enantioselective 1,4-addition of malonic acid half-thioesters to nitroolefins under mild conditions and in up to 90% ee. (scheme 4.15).[193]

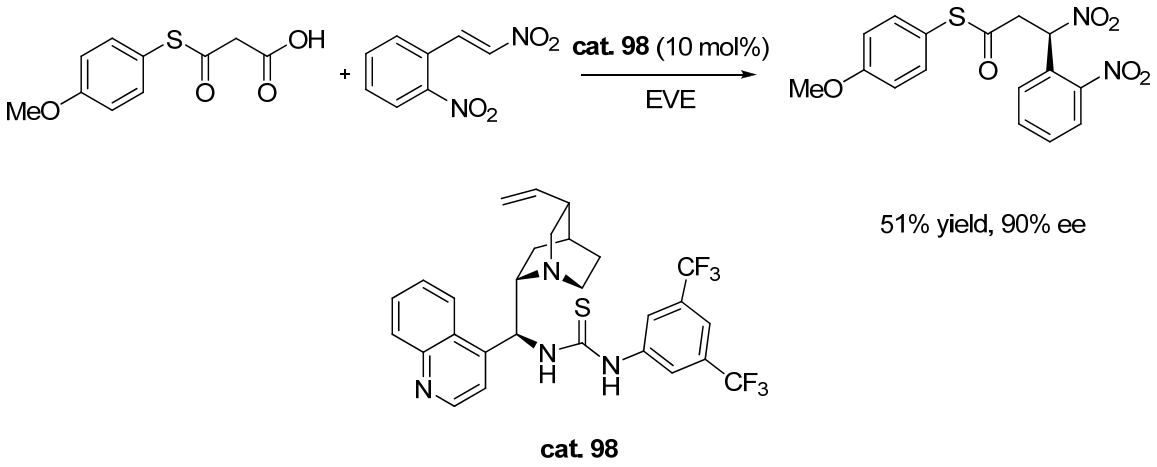

Scheme 4.15*: asymmetric Michael reaction.*

Significantly, each of these reports involves malonic acid half thioesters as enolate precursors, and the decarboxylation of this reagent is used to drive enolate formation. An alternative approach has been recently investigated by Barbas, who introduced the use of trifluoroethylthioester derivatives as activated nucleophilic substrates suitable for organocatalytic amine activation.[194]

In order to have access to a variety of reacting substrates than malonic acid compounds only, the electronic properties of trifluoro-ehtylthioesters were investigated to identify proper substrates suitable for organocatalytic amine activation. Indeed, the change from phenol ester to a thiophenol ester results in a reduction in the pKa value of the α-proton of an ester by approximately 2 units.

Um and Drueckhammer kinetic studied demonstrated that trifluoroethyl thioesters have a α-proton exchange rates in toluene/triethylamine solution that are approximately ten times faster than phenyl thioesters, suggesting that the pKa value of the α-proton of trifluoroethyl thioesters might be close to those of malonate diesters, making them potential ester nucleophiles in catalytic direct asymmetric synthesis (scheme 4.16).[195]

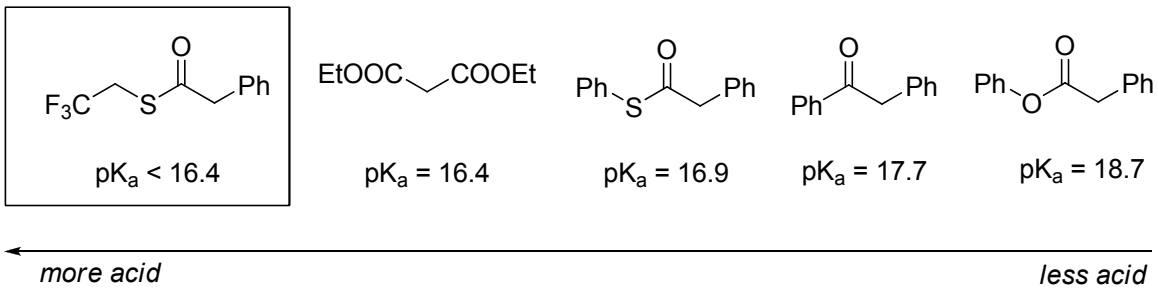

***Scheme 4.16**: pK_a values of the a-protons of potential nucleophiles in DMSO.*

A steoreoselective Michael reaction involving the use of trifluoroethyl thioesters was then successfully accomplished by using catalytic amounts of α,α-diphenyl prolinol ether with modest yield and a good level of enantioselection (scheme 4.17).

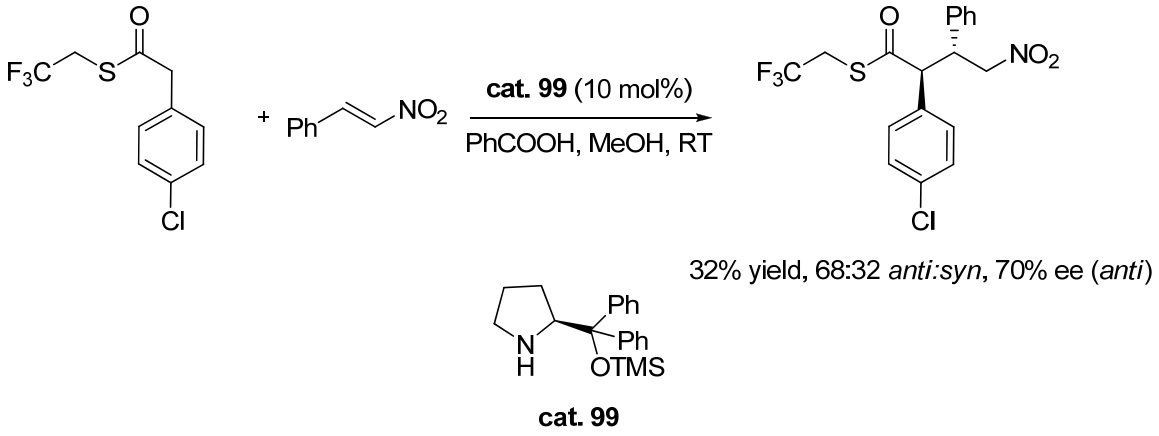

***Scheme 4.17**: asymmetric Michael reaction catalyzed by α,α-diphenyl prolinol ether.*

Later, catalytic Mannich reactions promoted by DBU were also reported, although only with modest level of enantioselection (scheme 4.18).[196]

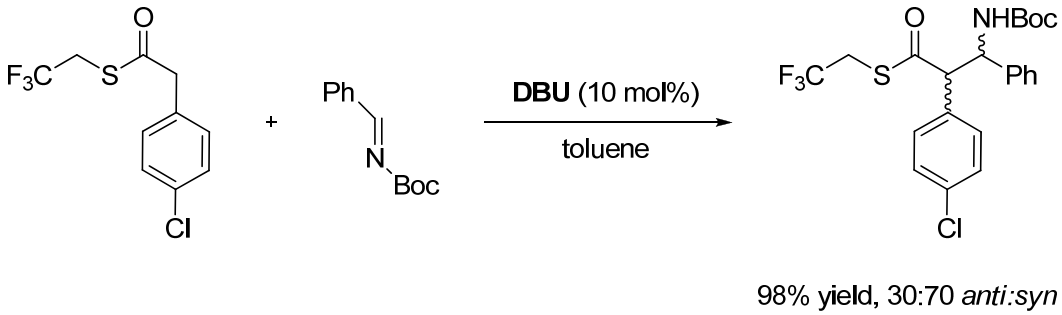

***Scheme 4.18**: asymmetric addition of activated thioesters to imines.*

In both cases, however, trifluoroethyl thioesters required an electronwithdrawing group in α position, such as an aryl group or halogen, as further activating element, necessary to guarantee the required low pK*a* value necessary for the deprotonation by an amine.

As shown above, only a very limited number of examples have been reported describing the stereoselective catalytic reaction of ester derivatives, and no examples for aldol type reactions were realized. For this reason, we decided to study the direct aldol addition of thioesters to aldehydes involving the use of chiral Lewis acids rather than amines. Based on promising results obtained in the direct aldol condensation of ketones to aromatic aldehydes promoted by (S)-TetraMe-BITIOPO in the presence of

tetrachlorosilane, we decided to extend the use of such synthetic methodology to the addition of activated thioesters to carbonyl compounds. As far as we know, this procedure, if successful, would represent the first stereoselective organocatalytic direct aldol addition of thioesters to aldehydes.

First, the activated trifluoroethyl thioester **100** was synthesized in quantitative yield by condensation of 2-phenylacetic acid with 2,2,2-trifluoroethanthiol in the presence of EDC and HOBt (scheme 4.19).

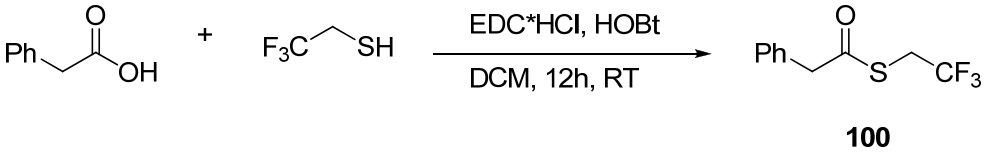

Scheme 4.19: *synthesis of activated trifluoroethyl thioester.*

Subsequently, the addition of trifluoroethyl phenylthioacetate **100** to benzaldehyde was investigated as a model reaction in the presence of stoichiometric amounts of $SiCl_4$, a nitrogen base and a catalytic amount of enantiomerically pure phosphine oxides. Three different enantiomerically pure phosphine oxides were considered: the electron poor bibenzothiophene phosphine oxides (*S*)-BITIANPO and (*S*)-BINAPO, and the more electron rich (*S*)-TetraMe-BITIOPO (scheme 4.20).

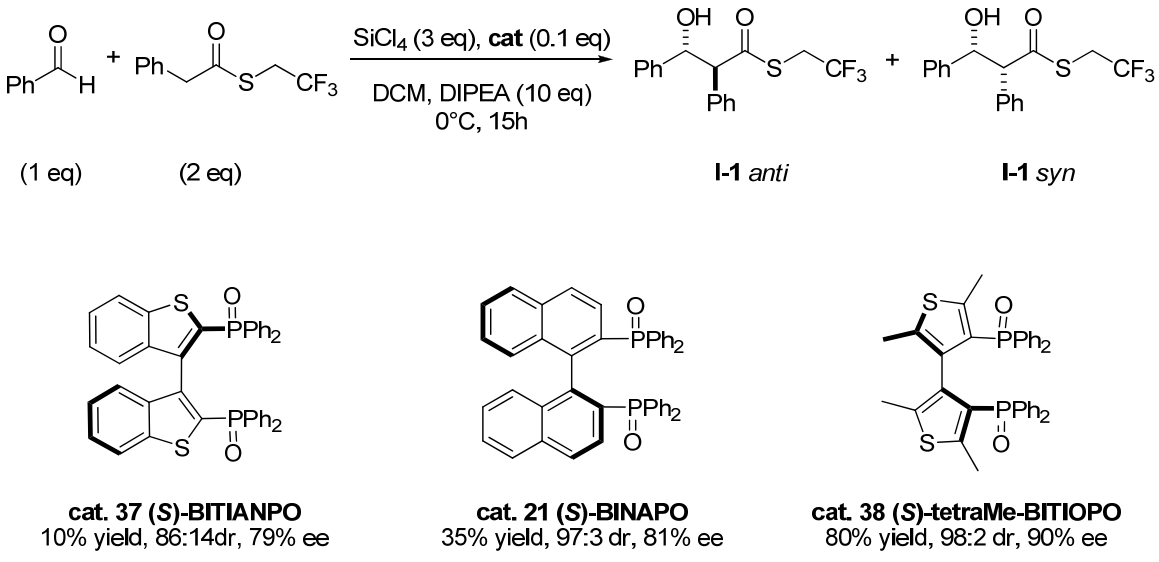

Scheme 4.20

Results showed that the direct condensation of 2 mol equiv of thioester with 1 mol equiv of benzaldehyde in the presence of 3 mol equiv of silicon tetrachloride, 10 mol equiv of DIPEA and 10% mol amount of (*S*)-BITIANPO afforded the corresponding β-hydroxy thioester **I-1** with only 10% yield. However, the use of (S)-BINAPO gave the product with 35% yield, 97:3 diastereoisomeric ratio and 81% ee for the major isomer. Only using (S)-tetraMe-BITIOPO it was possible to obtain the product with high yield (up to 80%), high diastereoselection (92:8 dr) and high enantiomeric excess for the major isomer (90% ee).

These results confirmed a trend already observed in the chiral Lewis base-promoted enantioselective addition of allyltrichlorosilane to aldehydes (see Chapter 1).

On the basis of these preliminary results, (*S*)-TetraMe-BITIOPO was chosen as catalyst in the direct aldol reaction of thioesters with aromatic aldehydes. Different experimental conditions of solvent, temperature and additives were screened in order to optimize the performance of the Lewis base; a few selected results are shown in table 4.10. The reaction was found to proceed better in dichloromethane at 0°C. Further lowering the reaction temperature to -40°C depressed the chemical yield and longer reaction times were required in order to obtain the product in fair yield; however no improvement in the enantioselectivity of the process was observed.

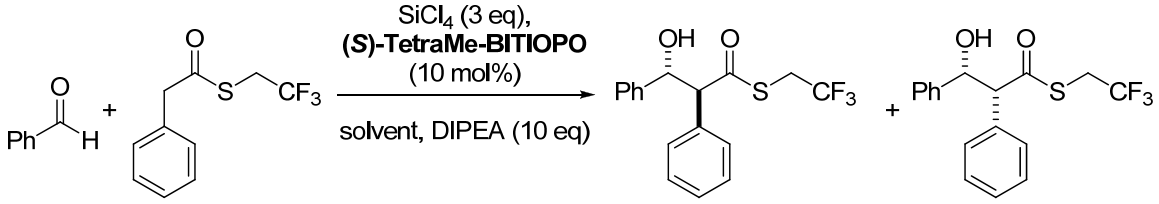

entry	solvent	time (h)	temp (°C)	yield (%)	*dr ratio*	ee *major* (ee *minor*) (%)
1[a]	DCM	15	0	29	> 98:2	79 (n.d.)
2[b]	DCM	15	0	24	83:17	68 (rac)
3	DCM	15	0	80	98:2	90 (n.d.)
4	CH_3CN	15	0	49	82:18	65 (16)
5	THF	15	0	53	98:2	81 (n.d.)
6	DCM	40	-40	55	88:12	83 (55)

[a] 1 mol eq of thioester was used, [b] 2 mol eq of aldehyde for 1 mol eq of thioester

Table 4.10

Different bases were also screened; for example the use of *N*-methylmorpholine instead of DIPEA lead to the hydroxy thioester in comparable stereoselectivity but in lower chemical yield; with other bases a significative decrease in the enantioselection was observed (table 4.11).

entry	solvent	base	temp (°C)	time (h)	yield (%)	*dr ratio*	ee *major* (ee *minor*) (%)
1	DCM	NMM	0	15	41	98:2	83 (n.d)
2	DCM	DIPA	0	15	10	48:52	n.d.
3	DCM	DABCO	0	15	3	-	-

Table 4.11

In order to expand the scope of this synthetic procedure, the use of other aromatic aldehydes with different electron withdrawing or electron donating substituents on the aromatic ring was investigated (table 4.12).

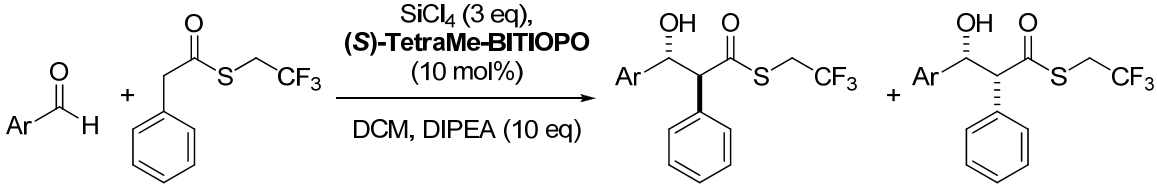

entry	Ar	product	temp (°C)	time (h)	yield (%)	*dr ratio*	ee *major* (%)
1	4-OMePh	**I-2**	0	40	51	>98:2	83
2	4-OMePh	**I-2**	-40	15	35	70:30	80
3	4-ClPh	**I-3**	-40	40	40	88:12	81
4	4-NO_2Ph	**I-4**	0	15	33	80:20	55
5	4-MePh	**I-5**	0	15	51	>98:2	85
6	1-naphth	**I-6**	0	15	41	66:14	63

Table 4.12

A high level of enantioselection was maintained independently of the attracting or donating nature of the substituent: for instance, the products derived from 4-methoxy- or 4-chlorobenzaldehyde present the same enantiomeric excess for the major isomer (table 4.12 entry 2 vs entry 3). Also the diastereoselection is very high, and in some case greater than 98:2.

Heteroaromatic aldehydes also proved to be suitable substrates for the direct aldol condensation. High values of diastereoselection and enantioselection were reached, but only modest yields were observed both with 2-thienyl and 2-furylcarboxyaldehyde (table 4.13, entry 1 and 2).

The aldol condensation was also attempted with non aromatic aldehydes such as cynnamaldehyde; this reacted with the activated thioester to give the product in 55% yield, ≥ 98:2 diastereoisomeric ratio, and 79% enantioselectivity for the major isomer (table 4.13, entry 3).

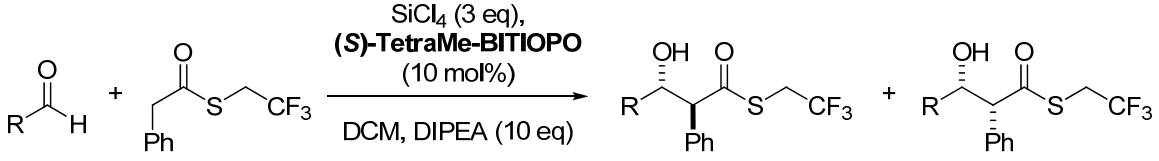

entry	R	product	yield (%)	*dr ratio*	ee *major* (%)
1	2-Thioph	**I-7**	11	> 98:2	93
2	2-Furyl	**I-8**	19	> 98:2	91
3	PhCH=CH	**I-9**	55	> 98:2	79

Table 4.13

Different activated thioesters were also prepared and tested in the direct aldol condensation with benzaldehyde. The results are shown in scheme 4.21.

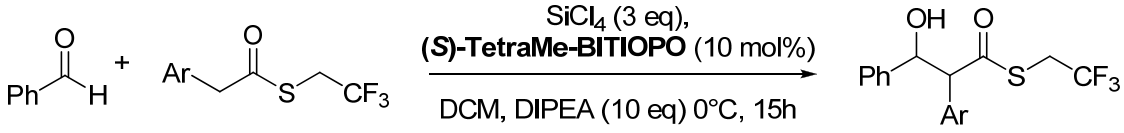

Ar =	4-F-C_6H_4	(**101**)	37% yield, 88:12 *dr*, 71% ee major	**I-10**
	3,4-OMe-C_6H_3	(**102**)	37% yield, 80:20 *dr*, 95% ee major	**I-11**
	4-*i*-Bu-C_6H_4	(**103**)	24% yield, 94:6 *dr*, 79% ee major	**I-12**
	4-OH	(**104**)	59% yield, > 98:2 *dr*, 80% ee major	**I-13**

Scheme 4.21

Thioesters with electron donating or withdrawing substituent in α position are suitable reagents for the condensation with benzaldehyde: with thioester **102** it is possible to obtain the corresponding product **I-11** with good diastereoselection and 95% enantiomeric excess for the major isomer. Using thioesters **105** and **106**, the corresponding β-hydroxy thioesters **I-14** and **I-15** were not isolated, and only the formation of the α,β-unsaturated thioester occurred in good yield (scheme 4.22).

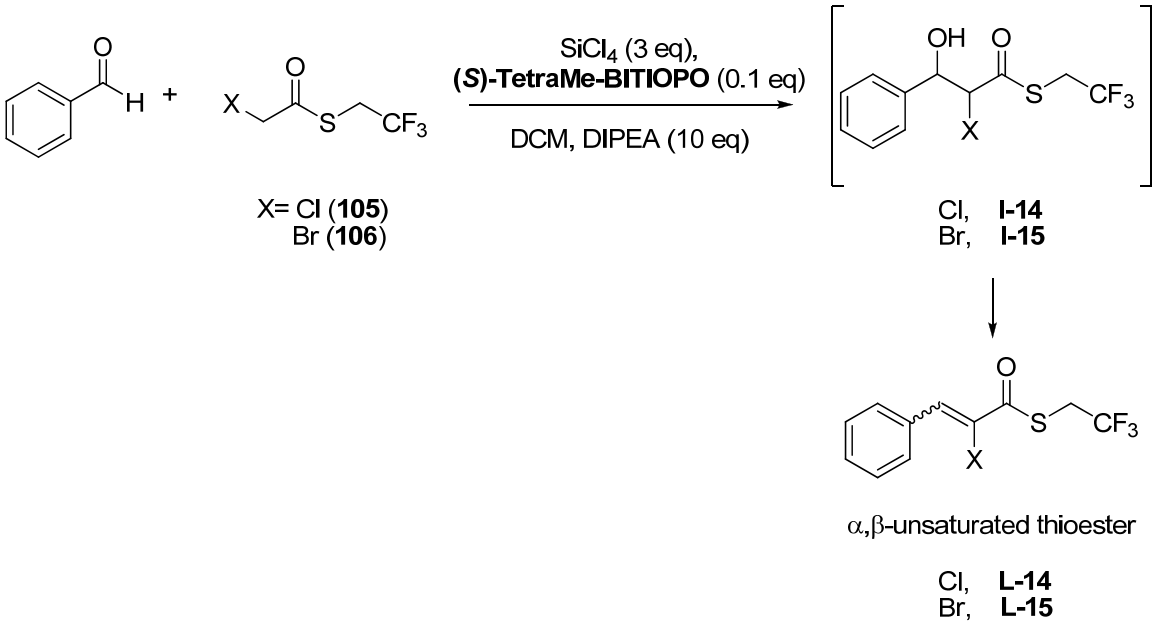

Scheme 4.22

Attempts to determine the absolute and relative configuration of the predominant diastereoisomer of the direct aldol condensation of thioesters with aromatic aldehydes is currently under investigation.

In conclusion, it was shown that the stereoselective direct aldol reaction of activated thioesters with aldehydes catalyzed by phosphine oxides is possible; this strategy represents the first method of stereoselective organocatalytic direct aldol addition of thioesters to aldehydes.

4.1.4 Conjugate reduction and reductive aldol reaction of α,β-unsaturated ketones

Conjugate reduction of α,β-unsaturated carbonyl compounds and subsequent one-pot reactions with electrophiles such as aldehydes are efficient synthetic tactics in organic synthesis. In 2008 Nakajima reported the use of HMPA and BINAPO as Lewis base-catalysts in the presence of trichlorosilane as a reductant to promote this reaction.[118]

The mechanicistic pathway is similar to that shown before; if a suitable Lewis base activates the silane, the 1,4-reduction may proceed selectively via a six-membered transition state, and with the assistance of the same Lewis base, the generated trichlorosilyl enolate should react with coexisting aldehyde electrophile.

Some interesting results, obtained with TetraMe-BITIOPO in our laboratories are showed in scheme 4.23.

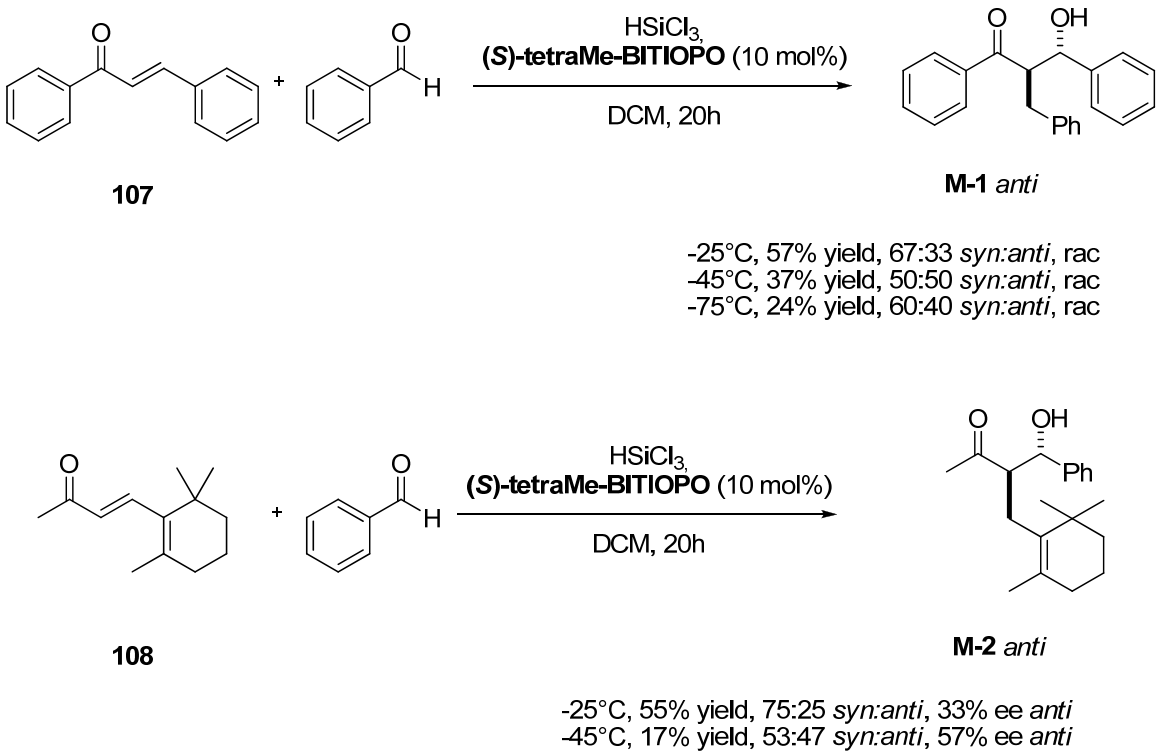

Scheme 4.23

Interesting, acyclic β-monosubstituted enones in the presence of TetraMe-BITIOPO gave the 1,4-reduction products with exclusive 1,4-selectivity; reduction was not observed in the absence of catalyst. In the case of chalcone (**107**) the reductive aldol

reaction gave the product **M-1** with good yield, but without diastereo- and stereoselection. Lowering the temperature had no effect on the stereocontrol of the process. With β-ionone (**108**) however, the conjugate reduction and reductive aldol reaction gave the product **M-2** with good yield and stereocontrol (up to 57%). At the moment, the diastereoselection is not satisfactory, and other experiments using TetraMe-BITIOPO in this type of reaction are under investigations.

4.2 New bisthiophene-based phosphine oxides

The interesting chemical and stereochemical results obtained in the allyltrichlorosilane addition to aldehydes and in the direct aldol condensations promoted by tetraMe-BITIOPO, paved the way to further studies towards the development of new chiral heteroaromatic Lewis bases.

As shown so far, tetraMe-BITIOPO can be employed as efficient metal-free catalyst in many organic reactions with good results, often better that those obtained with its corresponding binaphtyl analogue BINAPO. The ability of tetraMe-BITIOPO to promote a reaction is correlated to the greater Lewis base character that is connected in turn to its electronic properties. From a electronic point of view in fact, tetraMe-BITIOPO is more electron rich than BINAPO because of the presence of two thiophene rings in place of the binaphtyl scaffold.

Recently, our group has investigated the synthesis of new bithiophene-based phosphine oxides bearing modified aryl groups connected to the phosphorus atoms, with the aim of modulating the electronic characteristics of the two P=O double bonds, and consequently, of activation by the silicon species.

Initially, the idea was to improve the sterical hindrance of the four phenyl groups on the P atoms replacing them with naphtyl, anthracenyl or phenantryl groups; simple molecular mechanics analysis with macromodel calculations, though, have shown that these groups were too bulky and would not permit the correct orientation of the two P=O bonds. So, we decided to modify the four phenyl groups introducing electron withdrawing and electron donating substituents directly on the aromatic rings and to synthesize the derivatives shown in scheme 4.24.

CF_3-TetraMe-BITIOPO is the less electron rich bistiophene phosphine oxide, and from a teorical point of view, its performances should be worst than tetraMe-BITIOPO. MPP-tetraMe-BITIOPO presents the same steric hindrance of CF_3-TetraMe-BITIOPO but is more electron rich at both the phosphine oxides. Another electron rich posphine oxides without steric hindrance is PMP-tetraMe-BITIOPO. The most electron rich and sterically hindered BITIOPO derivative is MMP-tetraMe-BITIOPO.

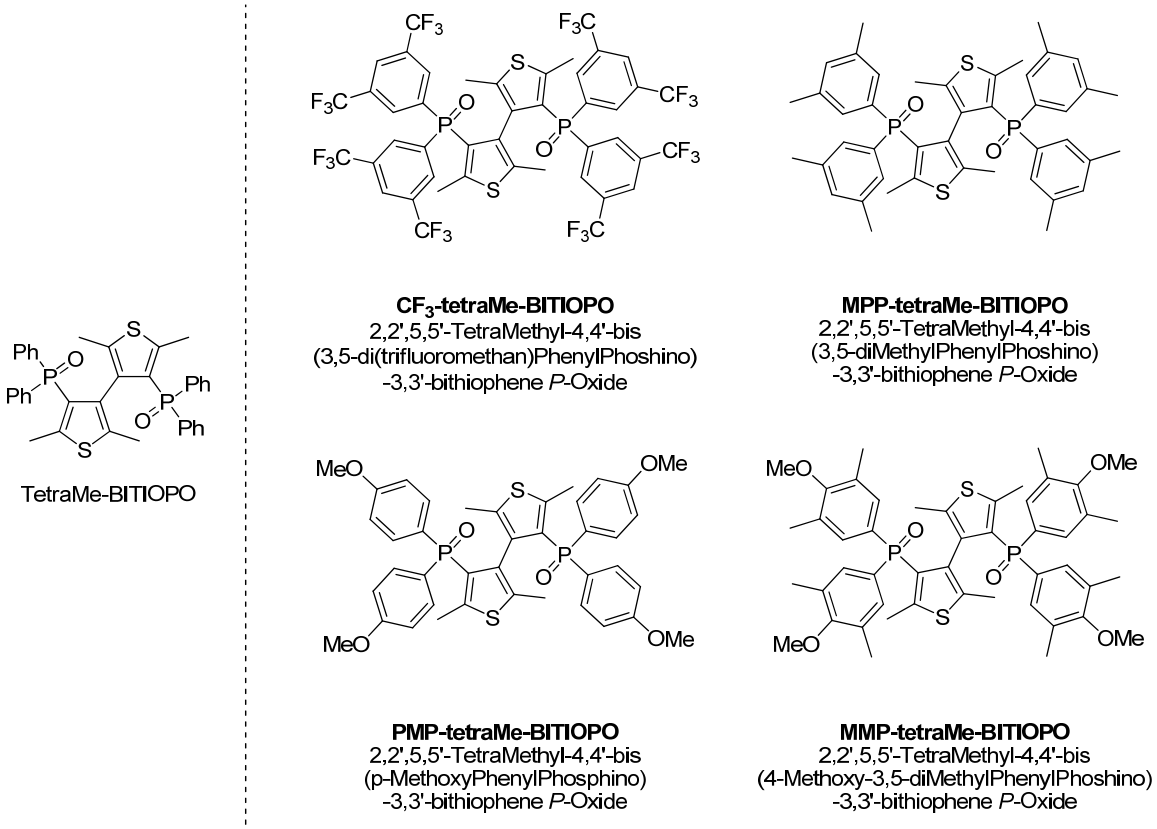

Scheme 4.24

The synthetic approach is similar to that showed in scheme 4.1 for the synthesis of tetraMe-BITIOPO and starts from the inexpensive and commercially available 2,5-dimethylthiophene as a precursor. The synthetic plan is very simple, and two pathways are possible to obtain tetraMe-BITIOPO derivatives (scheme 4.25). The first one (pathway *a*) consists in the reaction of diarylphosphinchloride with lithiated tetramethyl bisthiophene scaffold and a successive oxidation *in situ* with hydrogen peroxide; pathway *b,* instead, consists in the direct introduction of diarylphosphoric chloride without oxidation.

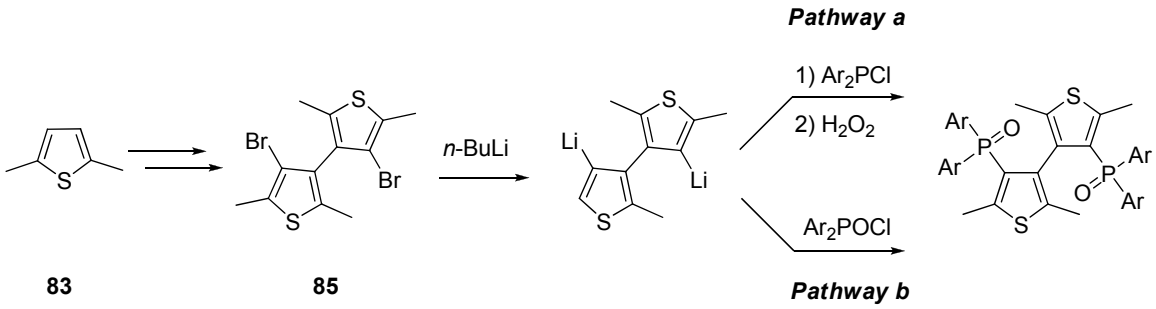

Scheme 4.25

Both these procedures suffer from a common problem that is the preparation of chloride derivatives, products that are not commercially available and are poorly described in literature. The synthesis of dibromo bisthiophene scaffold **85** proceeds without any problem (scheme 4.26).

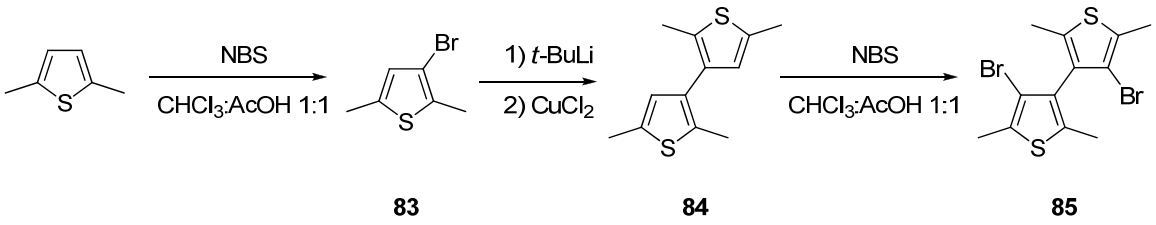

Scheme 4.26

The first step is the bromuration of the thiophene ring with NBS, in a mixture of $CHCl_3$ and CH_3COOH as solvent. Oxidative coupling with $CuCl_2$ of 2,5-dimethyl-3-thienyllithium, obtained by transmetalation of 3-bromo-2,5-dimethylthiophene with tert-butyllithium, gives the 2,2',5,5'-tetramethyl-3,3'-bithiophene **84** in 65% yield. Bisbromination of the latter with NBS, in acetic acid-chloroform solution, in the presence of hydroquinone, affords the known 4,4'-dibromo-2,2',5,5'-tetramethyl-3,3'-bithiophene **85** in a 90% yield.

4.2.1 Pathway a: synthesis and use of diarylphosphin chloride

The first method to obtain the desired diarylphosphin chloride is the direct introduction of two aromatic rings on PCl_3. This procedure starts from an aromatic halogen derivative, that in the presence of BuLi gives the corresponding aryllithium. This

compound should react with phosphorous trichloride to give the desired product. A Grignard reagent can be employed instead of the lithium derivative.

Despite the simplicity of this synthesis, there are some drawbacks correlated to the formation of byproducts. In fact it is not possible to control the selective substitution of one or two chloride atoms, and a mixture of mono- or diarylphosphin chloride is usually obtained. Furthermore, these compounds are very sensitive to oxygen and their preparation requires an inert atmosphere. In our hands, attempts to separate mono and bis derivative of 3,5-dimethylbromobenzene by distillation failed (scheme 4.27).

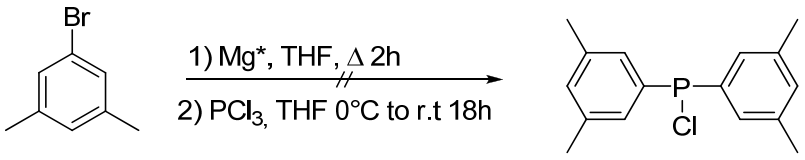

107

Scheme 4.27

Ar_2PCl reagents can also be prepared in two steps by treatment of readily available dialkyl phosphites, such as dibutyl phosphite, $(BuO)_2P(O)H$, with a Grignard reagent, followed by treatment of the resulting $Ar_2P(O)H$ product with $PC1_3$; but also in this case, extensive formation of byproduct is observed.[197]

Alternatively, diarylphosphinchloride reagents can be prepared by treating $(Et_2N)PCl_2$ with 2 equiv of ArMgBr, followed by treatment of the resulting product with HCl (scheme 4.28).[198]

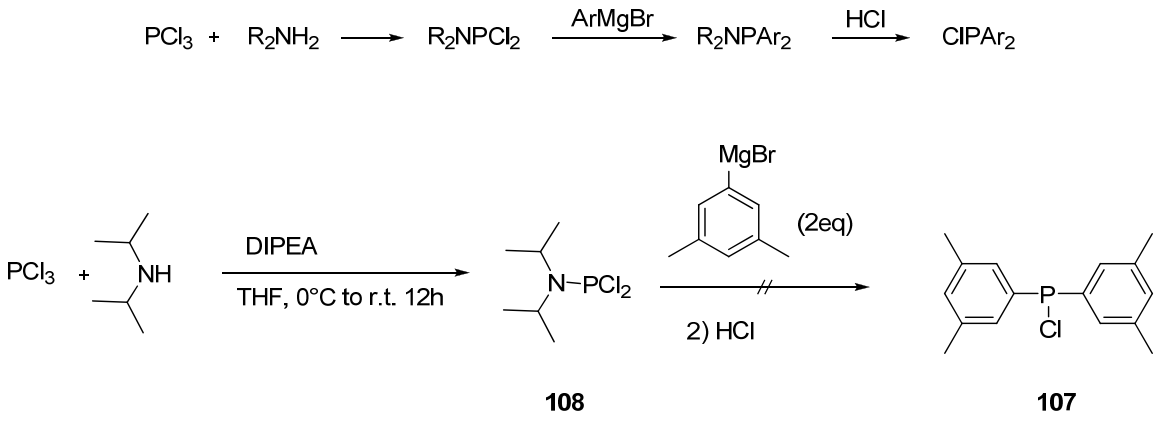

108 **107**

Scheme 4.28

Even if this procedure proves to be more performant that the previous, because it prevents the formation of mono derivatives, it requires the use of gaseous hydrochloric acid, with all the problems related to the use of gas cylinder in a research laboratory. For this reason we tried to substitute the HCl gaseous with a solution of HCl dissolved in dietylether or THF (both commercially available), but no product was obtained. So, we decided to give up the synthesis of diarylphosphin chloride in favor of that of diarylphosphoric chloride.

4.2.2 Pathway b: synthesis and use of diarylphosphoric chloride

The synthetic process of diarylphosphoric chloride is similar to that of diarylphosphin chloride where $POCl_3$ is used instead of PCl_3. The direct introduction of aromatic rings on $POCl_3$ presents the same problems shown before, so the synthesis of diarylphosphinic amide followed by hydrolysis is a necessary step in order to obtain the desired product (scheme 4.29).

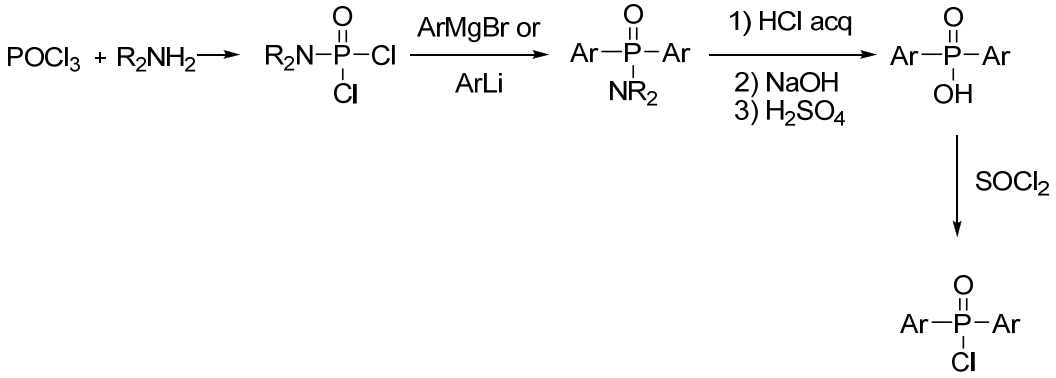

Scheme 4.29

At first, diethylamidophosphoric dichloride was synthesized by reaction of $POCl_3$ and diethylamine in diethylether for three days (scheme 4.30). This reaction gave the products **109** and **110**, that can be easily separated by chromatography. Recently, dimethylamidophosphoric dichloride became commercially available at low cost, so it was directly used in our synthesis.

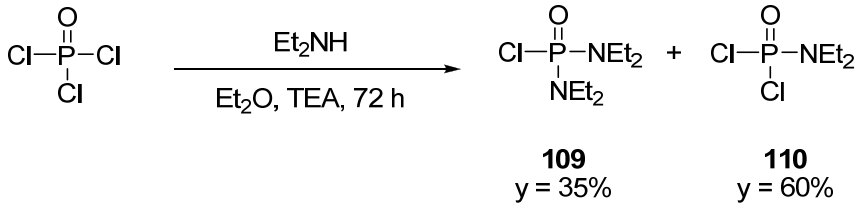

Scheme 4.30

The second step consists in the reaction of the amide with aryl lithium compound, prepared by a lithium-halogen exchange starting from the desired arylbromo derivative with butyllithium; the reaction with $(R_2N)P(O)Cl_2$ and further hydrolysis *in situ* of amino group with aqueous HCl should give the corresponding acid (scheme 4.31). Use of aqueous HCl is an alternative to gaseous HCl, but present some disadvantages. The treatment of bromoaryl derivative with BuLi is carried out in apolar aprotic solvents such as THF or Et_2O. In the presence of HCl and at high temperature tetrahydrofuran can be opened to 4-clorobutanol that can react with H_2O to afford 1,4-butanediol. This product has high boiling point, and can't be eliminated by evaporation without the degradation of the desired product. Moreover, phosphoric chloride obtained from treatment with HCl is insoluble in THF, and can be easily isolated by filtration; if polyols are present in the reaction mixture as byproducts, phosphoric chloride is kept into solution and cannot be separated.

The problem correlated with the use of Et_2O is due to its highly inflammability and volatility, that can't permit to reach the temperature necessary for the hydrolysis process. Use of other ethers with higher boiling point is similarly deleterious for the further operations. However, phosphoric acid can be obtained in THF and can be converted into chloride derivative by treatment with $SOCl_2$ (scheme 4.31).

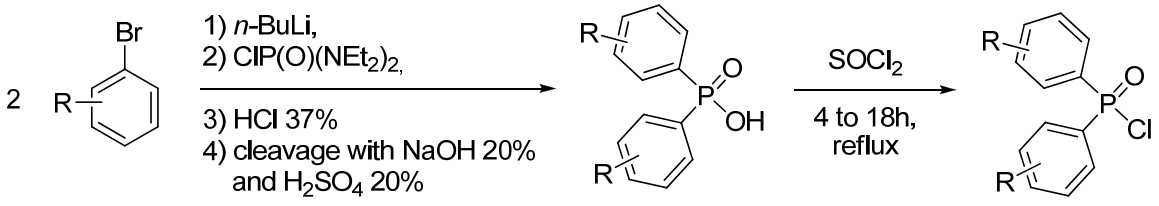

R =			
3,5-diCF$_3$	**111**, not obtained	**115**
3,5-diMe	**112**, y= 60%	**116**
3,5-diMe-4-OMe	**113**, y= 12%	**117**
4-OMe	**114**	**118**

Scheme 4.31

Using this method, phosphoric acids **112** and **113** were synthesized in modest yield and converted into their chloride derivatives, that were directly used in the synthesis of tetraMe-BITIOPO derivatives. Bis(4-methoxyphenyl)phosphinic acid **114** is commercially available, and was used as received.

Acid **111** could not be prepared with this procedure: the debrominated starting material was recovered, along with trace of products containing a butyl chain on the aromatic ring. This is a common problem for these type of derivatives, where the alkyl chain of BuLi replaces one or more chlorine atoms of diethylamidophosphoric dichloride by nuceophilic substitution. Stronger bases as *sec*-BuLi and *tert*-BuLi (that are less nucleophilic) were also tested, leading to product degradation only.

The replacement of aryllithium compounds with the Grignard reagents in the reaction with the diaminophosphoric derivative did not afford the desired products, and dehalogenated starting compounds were partially recovered along with degradation products.

These results highlighted the main problem in the synthesis of diarylphosphoric chloride, that is the substitution of chloride atoms bonded to the phosphorous atom with the aromatic group. The trick to use an amidophosphoric dichloride can provide a solution: the hydrolysis of the amino group, however, requires strong reaction conditions leading to the formation of several byproducts.

In order to avoid these drawbacks, we decided to use a phosphoric ester derivative, since that the hydrolysis of an ester should be easier than the hydrolysis of an amide. Two pathways are possible: the first consists in the isolation of the dialkyl diarylphosphinic amide and in its conversion to a methyl ester by treatment with HCl in MeOH. Different from phosphinic amides, phosphinic esters are more stable and can be isolated by chromatographic purification. The second consists in the use of ethyl dichlorophosphate, that can be usefully converted in the diarylphosphoric chloride using $SOCl_2$ or PCl_5, without any hydrolysis process (scheme 4.32).

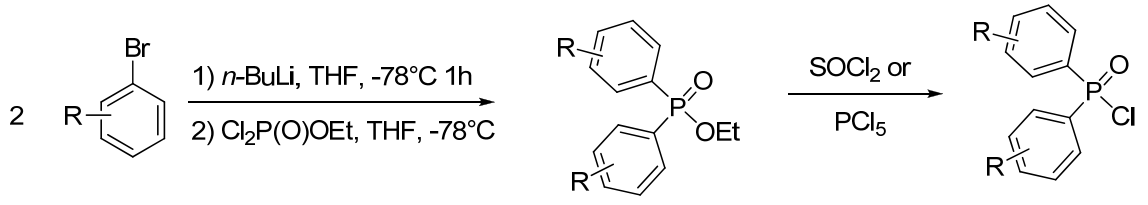

R = 3,5-diMe
3,5-diMe-4-OMe
3,5-diCF$_3$

119, y= 63%
120, y= 60%
121

116
118
115

Scheme 4.32

Products **119** and **120** were successfully prepared in good yield using this methodology. However, when 3,5-di(trifluoromethyl)bromo benzene was employed, the phosphate ester was not recovered, but the corresponding acid **111** was isolated with 80% yield. This is probably due to the electron-withdrowing effect of the two trifluoromethyl substituents, that make the phosphorous atom more electronpoor and amenable to the hydrolysis process.

Independently of the procedures employed to obtain the diarylphosphoric chloride derivatives, the last step required to obtain the modified tetraMe-BITIOPO is common to all the precursors. Different conditions, methods and temperatures for the reaction with the diarylphosphoric chloride were tested, and the best results were obtained when utyllithium was employed in THF at -55°C to generate the bislithium derivative of dibromo bisthiophene **85.** This intermediated was reacted with the diarylphosphoric chloride to give the desired product in a racemic form after chromatographic purification (scheme 4.33).

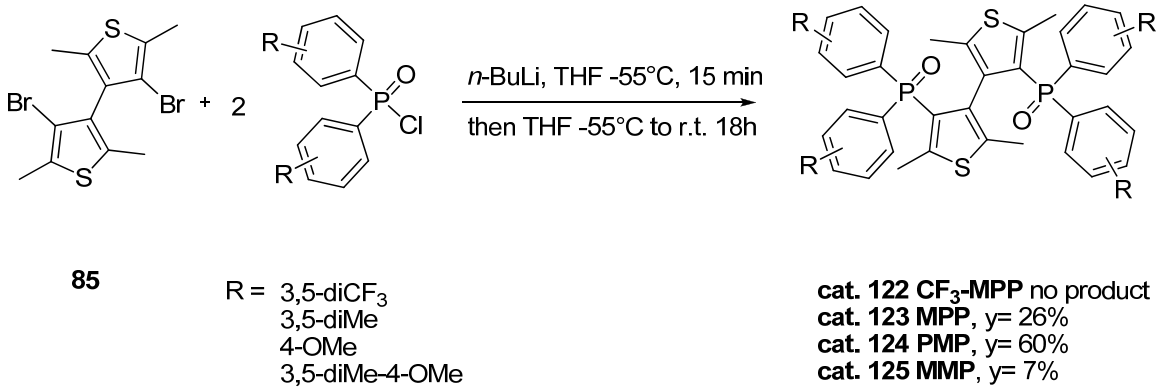

Scheme 4.33: *synthesis of tetraMe-BITIOPO derivatives.*

Only the synthesis of CF_3-tetraMe-BITIOPO did not give the expected result, and a complex mixture of byproducts was obtained. Before attempting the resolution of the racemic mixture of these phosphine oxides, these compound were tested as catalysts in the organic reactions promoted by the activation of the Lewis acid from a Lewis base, to verify if the initial hypothesis of reactivity is correct.

4.3 Reactivity of new bistiophene based phosphine oxides

A reaction where tetraMe-BITIOPO has shown good results was the allylation of benzaldehyde in the presence of allyl trichlorosilane. So, we tested the racemic MPP-tetraMe-BITIOPO in this reaction. The results are collected in table 4.14.

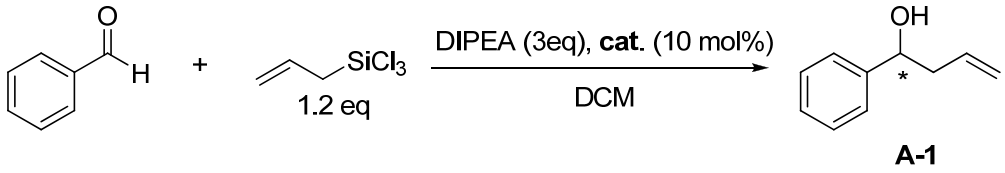

entry	catalyst	temp (°C)	time (h)	yield (%)	ee (%)
1	(*S*)-tetraMe-BITIOPO	0	40	85	93
2	(*rac*)-MPP- tetraMe-BITIOPO	0	40	95	
3	(*S*)-tetraMe-BITIOPO	-20	50	<5	n.d.
4	(*rac*)-MPP-tetraMe-BITIOPO	-20	72	55	

Table 4.14

Under the same conditions (0°C, 40h), MPP-tetraMe-BITIOPO showed a better chemical efficiency than (*S*)-tetraMe-BITIOPO, leading to the allylic alchool in 95% yield rather than of 85% (entry 1 vs 2, table 4.9). When the reaction was conducted at lower temperature, while (S)-TetraMe-BITIOPO was not able to promote the reaction, MPP-tetraMe-BITIOPO gave the product with a good yield (55%, entry 4).

This indicates that the chemical activity of this phosphine oxide is higher than that of tetraMe-BITIOPO, probably because of the enhanced larger steric hindrance generated by the two methyl groups on each phenyl ring. In addition. MPP-TetraMe-BITIOPO is a more electron rich catalyst than TetraMe-BITIOPO. However, despite the best performance in terms of yield, nothing can be said about the stereocontrol.

Another class of reaction where MPP-TetraMe-BITIOPO can be employed as catalyst is the asymmetric synthesis of oxazines by reductive cyclization of *N*-acylated β-amino enones with $HSiCl_3$ (scheme 4.36). In this reaction, however, no appreciable variation in reactivity with respect to TetraMe-BITIOPO was observed.

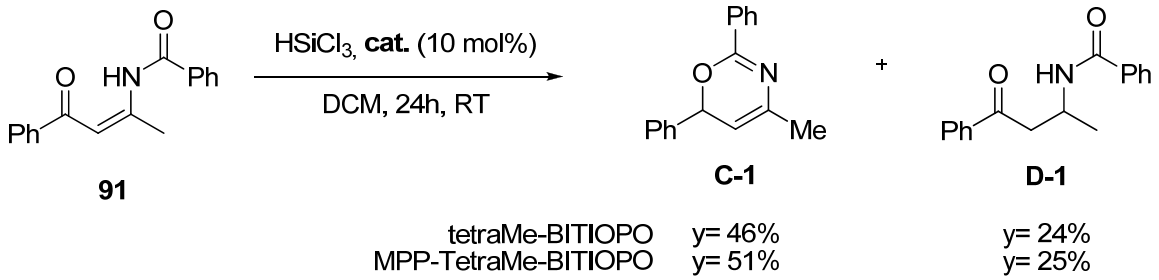

Scheme 4.36

MPP-TetraMe-BITIOPO was also employed in many other reactions to assess its reactivity. One example is the addition of allyl tributyl tin to benzaldehyde in the presence of $SiCl_4$ that afforded the product with 87% yield at -20°C (scheme 4.37) and the addition of silyl ketene acetals to benzaldehyde, mediated by $SiCl_4$ that gave the corresponding aldol adduct with 98% yield (scheme 4.37).

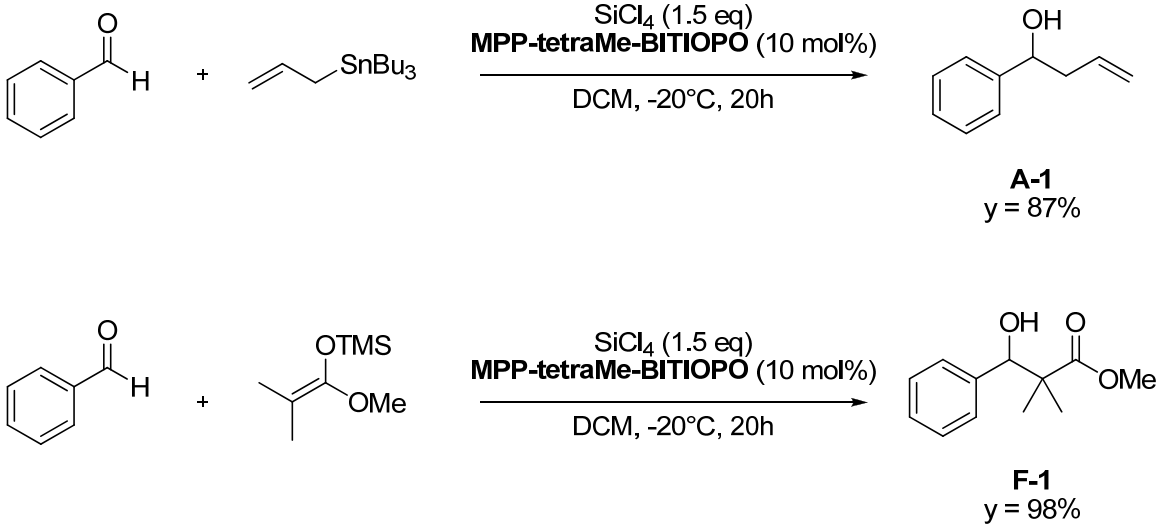

Scheme 4.37

The good results obtained in the aldol condensation of silyl ketene acetals to aldehydes with MPP-tetraMe-BITIOPO opened the way to the studies of the direct aldol condensation between benzaldehyde and cycloexanone.

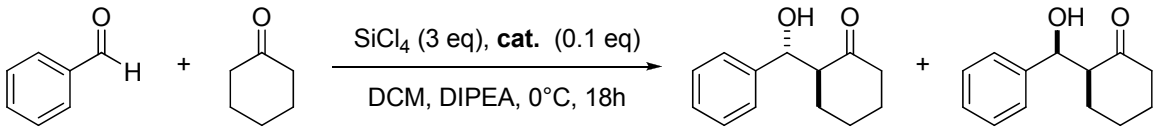

(1 eq) (2 eq) **G-1** *anti* **G-1** *syn*

entry	catalyst	Yield (%)	*Anti:syn*
1	(*S*)-tetraMe-BITIOPO	63	88:12
2	(*rac*)-MPP-tetraMe-BITIOPO	67	88:12
3	*(rac*)-PMP-tetraMe-BITIOPO	70	77:23

Table 4.15

The data in table 4.15, showed that MPP-TetraMe-BITIOPO and TetraMe-BITIOPO are comparable both in chemical efficiency and in diastreoselectivity, leading to the aldol products with 67% yield and 88:12 *anti:syn* ratio. The more electron rich phosphine oxide PMP-TetraMe-BITIOPO gave the aldol adduct in 70% yield, but with a lower diastereoselectivity.

On the basis of these results, it is possible to say that MPP-tetraMe-BITIOPO is potentially a good catalyst in silicate-mediated reactions. In all the organic reactions where it was tested it afforded comparable, and in some case better, yields than those obtained using TetraMe-BITIOPO as a catalyst. The following step consisted of an evaluation of the stereochemical efficiency of this phosphine oxide. To do that, an enantiopure form of MPP-tetraMe-BITIOPO was required, and an adequate process of resolution was then developed.

4.3.1 Resolution of a racemic mixture of new phosphine oxide

In collaboration with the group of Prof. Sannicolò at University of Milan, we have tried to separate racemic MPP-tetraMe-BITIOPO with the same procedure developed in his laboratories for the resolution of TetraMe-BITIOPO.[182] This procedure consists in a fractional crystallization from tetrahydrofuran of the diastereoisomeric adducts obtained by the complexation of phosphine oxide with (+)- and (-)-dibenzoyltartaric acid. Alkaline decomplexation of the adducts affords enantiomerically enriched isomers, which can be obtained in their enantiopure forms by crystallization from a 1:1 benzene:hexane mixture.

When this procedure was applied to MPP- or PMP- tetraMe-BITIOPO, the diastereoisomeric adducts obtained with the two enantiomers of dibenzoyltartaric acid could not be isolated by precipitation. Attempts to use other chiral acids failed. So, we decided to separate these phosphine oxides by HPLC on a chiral stationary phase, in order to obtain small quantities of enantiopure crystals to be used as crystallization seed.

A screening of the most common chiral columns showed that the Chiralcel OD column was able to separate the two enantiomers. Unfortunately only an analytical column was avaiable in our laboratories, so, we separated only 10 mg of BITIOPO derivatives. Attempts to use pure enantiomers as crystallization seed for the resolution of a racemic mixture failed, thwarting efforts made so far. However, a small quantity of pure TetraMe-BITIOPO derivatives were employed as catalyst in the allylation of benzaldehydes and in the direct aldol condensation between benzaldehyde and cyclohexanone.

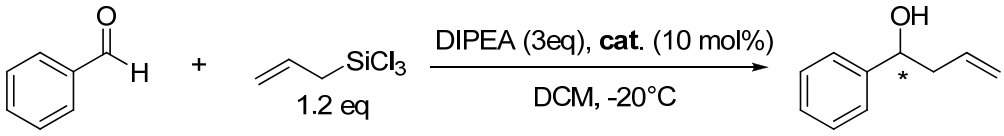

A-1

entry	catalyst	time (h)	yield (%)	ee (%)
1	(*S*)-tetraMe-BITIOPO	50	< 5	n.d.
2	(+)-MPP-TetraMe-BITIOPO	72	60	38
3	(+)-PMP-TetraMe-BITIOPO	72	76	86
4	(+)-MMP-TetraMe-BITIOPO	72	52	27

Table 4.16

The data in table 4.16 confirm that, at lower temperatures, (-20°C) TetraMe-BITIOPO derivatives are more chemically efficient than TetraMe-BITIOPO. Using (+)-PMP-tetraMe-BITIOPO in fact, it is possible to obtain the allylic alcool **A-1** in 76% yield and 86% of enantiomeric excess. (+)-MMP-TetraMe-BITIOPO, instead, affords the product with modest yield and lower enantioselection (entry 4, table 4.16); this is probably due to its steric hindrance.

These catalysts are also employed in the direct aldol condensation between benzaldehyde and cyclohexanone. Results are reported in table 4.17.

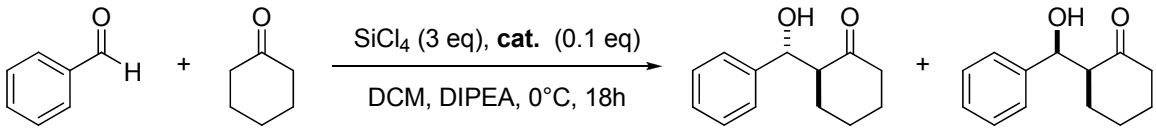

(1 eq) (2 eq) **G-1** *anti* **G-1** *syn*

entry	catalyst	Yield (%)	*Anti:syn*	ee (*anti*)
1	(S)-(-)-TetraMe-BITIOPO	63	88:12	75
2	(-)-MPP-TetraMe-BITIOPO	67	88:12	72
3	(-)-PMP-TetraMe-BITIOPO	70	70:23	34
4	(-)-MMP-TetraMe-BITIOPO	77	88:12	57

Table 4.17

All the TetraMe-BITIOPO derivatives are able to promote the reaction with good yields and high level of diastereoselection. (-)-MPP-TetraMe-BITIOPO presents a comparable level of enantioselection to TetraMe-BITIOPO (table 4.17 entry 2 vs entry 1), while (-)-PMP- and (-)-MMP-TetraMe-BITIOPO give modest result in terms of enantiomeric excess.

These results opened the way to further application of TetraMe-BITIOPO derivatives as catalysts in a novel and unexplored Lewis base catalyzed Lewis acid mediated activation strategy.

4.4 Synthesis of bisthiophene based phosphine oxide: a novel approach

The problems associated with a difficult and cumbersome resolution on a large scale of a racemic mixture of tetraMe-BITIOPO derivatives by analytical HPLC, and those connected to the synthesis of desired diarylphosphoric chlorides, led us to develop a novel synthetic approach for the synthesis of new bisthiophene based phosphine oxides.

In particular we planned a novel strategic synthesis where the resolution step is performed before the functionalization of the phenyl rings connected to the phosphorous atom. The process of resolution is then the same for all the phosphine oxides, because all these TetraMe-BITIOPO derivatives share a common starting precursor. To do that, and inspired by a work of Zhang[199] we decided to synthesize the tetraethyl bistiophen phosphonate **126** (scheme 4.38). This compounds is a bisphosphoric ester, and its resolution is easier than that of a phosphine oxide; moreover it is also possible to convert this product in the corresponding phosphoric acid **127**, that should be resolved with a chiral amine. Furthermore, the substitution of the ethoxy groups of a phosphonate with aromatic rings by Grignard reagents are well documented in literature. [199]

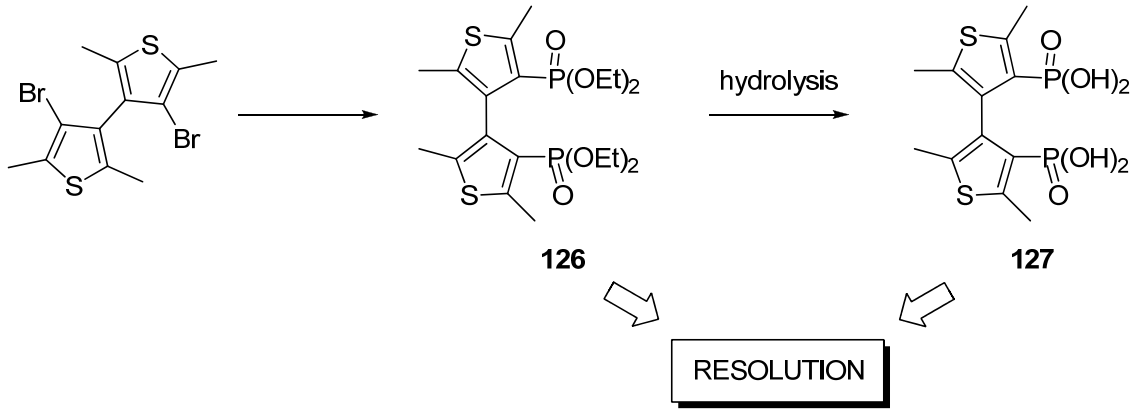

Scheme 4.38

Preliminary investigations were carried out on 3-bromo-2,2-dimethylthiophene, and different methodologies were tested in order to optimize the reaction conditions. A general access to dialkyl arylphosphonates based on the palladium-catalyzed reaction of aryl halides with dialkyl phosphite has been disclosed by Hirao et al.[200] where the use of catalytic amounts of $Pd(PPh_3)_4$ in the presence of triethylamine and under solvent-free conditions promotes this type of reactions. Very recently, a general and efficient method for the microwave-assisted formation of the C-P bond was developed by Stawinski using

$Pd(PPh_3)_4$.[201] With this procedure, a quantitative cross-coupling of various *H*-phosphonate diesters with aryl halides was achieved in less than 10 min. Unfortunately, in our laboratories, operating under these condition with a CEM Discover S-Class microwave oven no product was obtained (scheme 4.39a).

Further studies by Gooßen[202] revealed that the palladium-catalyzed reaction of aryl halides with dialkyl phosphite conducted in a polar solvents as EtOH in the presence of triethylamine gives aryl phosphonates in excellent yields. As we found out, this procedure did not work with etheroaromatic rings (scheme 4.39b).

We decided then to employ a commercially available diethyl chlorophosphate instead of diethyl phosphite; using a procedure similar to that employed in the synthesis of dialkyl diarylphosphinic amide, the thiophenyl phosphonate **128** was synthesized in 58% yield after chromatographic purification (scheme 4.39c). Byproducts derived from the nucleophilic attack of the butyl bromine on the lithiated methyl groups of the thiophene ring were also isolated.

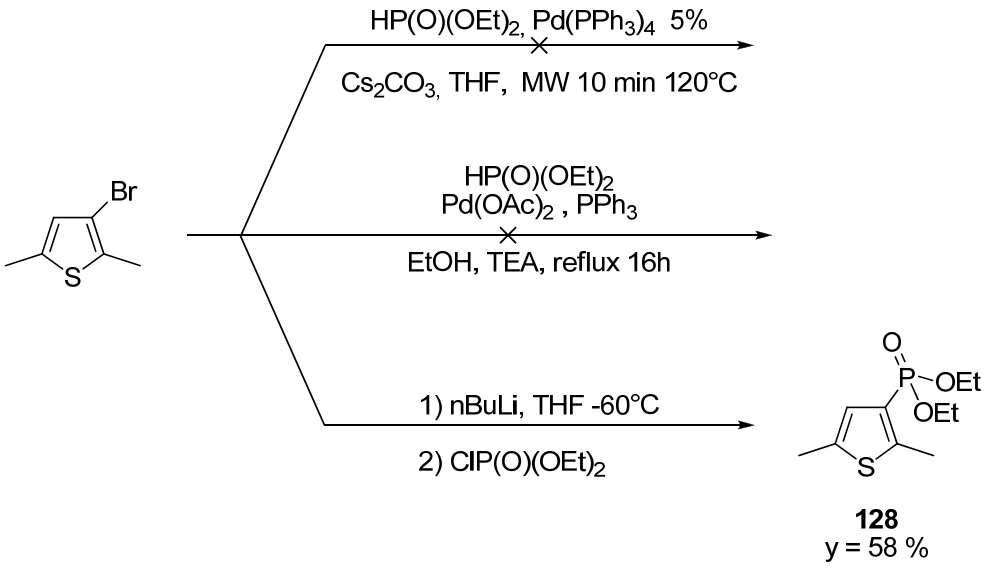

Scheme 4.39

However, when dibromo bisthiophene derivate **85** was used, this procedure failed and no bistiophen phosphonate **126** was obtained. Only the byproduct **129** was recovered in high yield, as determined by NMR and mass spectrometry (scheme 4.40).

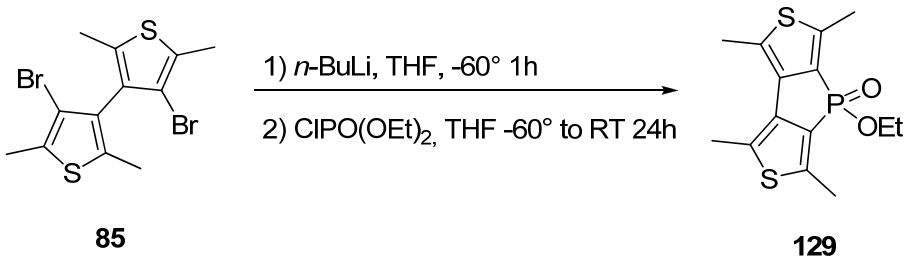

85 **129**

Scheme 4.40

Byproduct **129** could be originated by an intramolecular nucleophilic attack. After a bis lithiation of **85** with butyllithium and introduction of one phosphonate group, the addition of a second diethyl phosphonate does not occur, and a rotation along the interanular bond allows the other thiophene ring to attack the phosphorous atom with the release of an ethoxy group. Also the use of more substituted phosphonates, led to the formation of this byproduct.

On the basis of these results, another strategy to obtain the bistiophen phosphonate **126** was developed. This consists in the construction of the interanular bond with a coupling reaction after the introduction of diethyl phosphonate.

First, phosphonate **128** was brominated with NBS to afford the bromo thiophenyl phosphonate **130**. This was employed in different coupling reactions, such as the copper-mediated oxidative homocoupling in the presence of phenyl lithium, the Stille coupling with the tin thiophene derivative, and the Suzuki coupling with thiophene boronic acid. All these procedures however, did not lead to the desired phosphonate **126**, probably due to steric hindrance of the starting material.

Only by employing the iodothiophenyl phosphonate **138** in a Ullmann reaction, tetraethyl bisthiophen bisphosphonate **126** was obtained with 62% yield (160°C, no solvent, scheme 4.41).

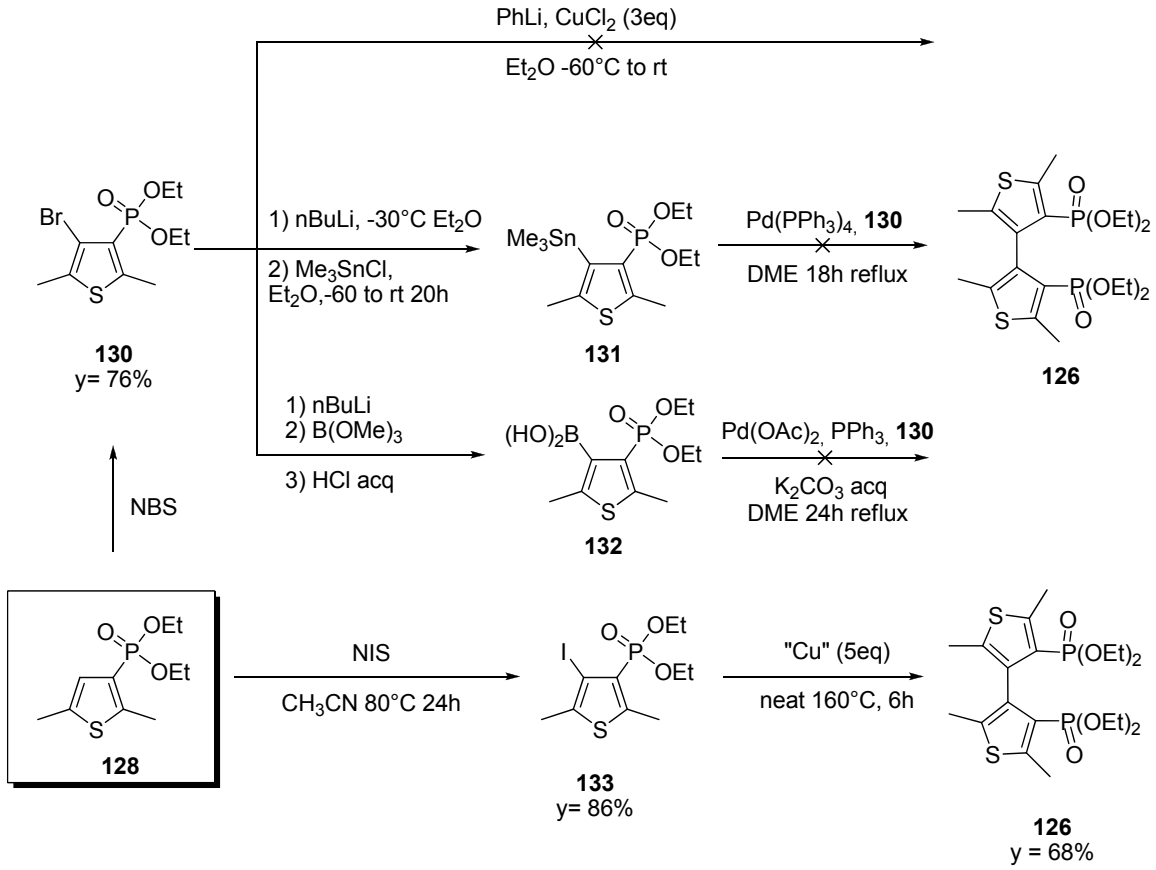

Scheme 4.41: *Coupling reactions.*

Attempts to resolve the racemic mixture of compound **126** are under investigation with the collaboration with Prof. Sannicolò's group.

The next step after the resolution is the conversion of tetraethyl bisphosphonate **126** in the corresponding TetraMe-BITIOPO derivatives. An outline of this process is reported in scheme 4.42.

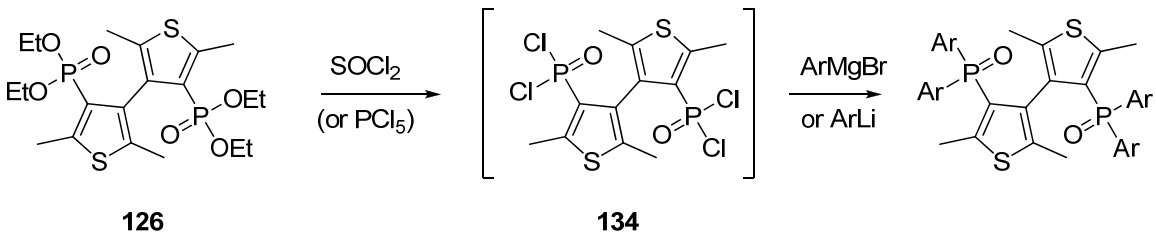

Scheme 4.42

Literature data show that the conversion of **126** in the bisphosphonic tetrachloride **68** can be carried out with thionyl chloride. [202] Also PCl_5 and $(COCl)_2$ after TMSCl/NaI treatment of the ester to give the acid can be employed in this transformation. [203]

After the generation of tetrachloride **134**, the introduction of arillithium compounds (obtained by lithium halogen exchange from halogen derivatives) or Grignard reagents should lead to the formation of the desired product. Attempts to synthesize TetraMe-BITIOPO with this procedure using commercially available PhLi or PhMgBr failed; this can be probably ascribed to the poor concentration of the reactives (2M) and not to a problem in the procedure: in fact, when tetrachloride **134**, generated *in situ* using $SOCl_2$, is quenched with dimethylamine, phosphoramide **135** is obtained in 16% yield (scheme 4.43).

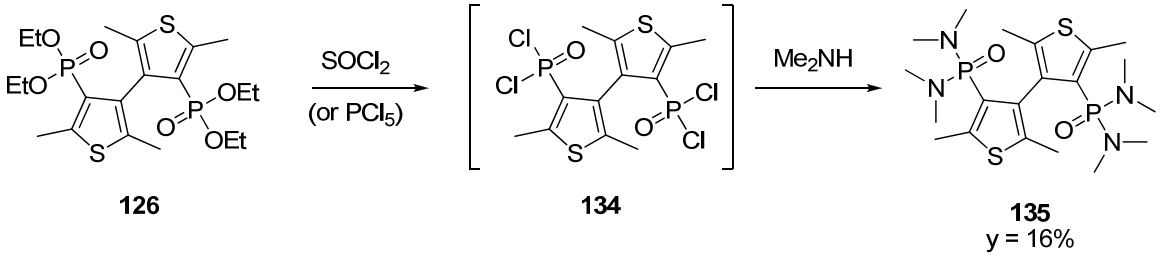

126 **134** **135**
y = 16%

Scheme 4.43

Further studies on the direct conversion of bisphosphonic tetrachloride **134** in the desired tetraMe-BITIOPO derivates are now under way as is the synthesis through bisphosphoric acids **127**.

OUTLOOK AND PERSPECTIVE

Since hypervalent silicon species may work through different activation mechanisms, they have recently attracted much attention for their versatility and for the possibility to develop several, catalytic processes. Indeed tuning the chemistry of penta and/or hexavalent silicon compounds by the design and the synthesis of chiral organocatalytic species is not only feasible, but highly desirable, with the goal to develop always new enantioselective reactions in the presence of cheap, low toxic and environmental friendly species such as silicon-based reagents.

The development of new Lewis base-catalyzed methodologies for increasing molecular diversity and complexity is a field in a rapid expansion. In this context, enantiomerically pure phosphine oxides have found considerable and extensive application, as demonstrated for example by the aldol reactions with different substrates discussed in this thesis.

TetraMe-BITIOPO showed to perform better than other phosphine oxides, for example BINAPO, to afford β-hydroxy ketones with good *anti* stereoselectivity, and enantioselectivity often higher than 85% and up to 95% in the presence of $SiCl_4$. This new and interesting methodology was also successfully extended to structurally different ketones (including compounds containing heteroatoms) and activate thioesters, where β-hydroxy thioesters are obtained with 80% yield and up to 95% of enantiomeric excess for the *anti* isomer.

The process in which a Lewis base activates a Lewis acid was shown to be feasible also for the development of cross-aldol condensation between an aromatic and an aliphatic aldehyde. In this case, the major drawback of the proposed catalytic system seems to be the sometimes low chemical efficiency. However, even if many issues still need to be tackled, the results clearly show that a still unexplored novel class of chiral

biheteroaryl-based phosphine oxides are now available as suitable catalysts, whose electronic and steric properties could be modulated by a proper choice of substituents.

In this context a novel approach to the synthesis of new chiral biheteroaromatic phosphine oxides was developed, and it is clear how many more options and possibilities could be offered by the availability of properly designed multifunctional phosphine oxide-based catalysts.

It is remarkable that the use of phosphine oxides as catalysts is a new approach in Lewis bases-organocatalyzed reactions, and becomes immediately clear that there is a broad area of investigation in this field. There is a large variety of potentially phosphine oxides that could be easily obtained from the oxidation of commercially available enantiopure phosphines.

On the basis of these considerations it is easy to predict that we will see a continously increasing interest in the field of stereoselective reactions promoted by chiral Lewis bases; hopefully this survey will stimulate further research in a very exciting area, where hypervalent silicate species will play a decisive role in the invention of new, highly chemically and stereochemically efficient catalytic systems of low environmental impact.

CHAPTER 5

Molecular Modeling: basic principles

" A model must be wrong, in some respects,
else it would be the thing itself.
The trick is to see where it is right"
Henry A. Bent

Molecular modeling includes all the theoretical methods and computational techniques used in a model to mimic the behavior of molecules. The definition currently accepted of what molecular modeling is, can be stated as this: "molecular modeling is anything that requires the use of a computer to paint, describe or evaluate any aspect of the properties of the structure of a molecule" (Pensak, 1989).[204] The term "Molecular" clearly implies some connection with molecules, instead the term "Model" identifies a simplified or idealized description of a system or process (in mathematical terms), devised to facilitate calculations and predictions.

Today, molecular modeling is invariably associated with computer modeling, and computational techniques have revolutionized molecular modeling to the extent that most calculations could not be performed without the use of a computer. This does not imply that a more sophisticated model is necessarily better than a simple one, but computers, with their power calculations, have certainly extended the range of models that can be considered and the systems to which they can be applied.

A molecular modeling study is generally composed by three steps: in the first step a model is selected to describe the intra- and inter-molecular interactions in the system; the second step is the calculation itself and the third step consists in the analysis not only of the calculate properties but also in the check if the system has been properly performed. There are different methods to define how the calculation can be done: the

two most common methods are **molecular mechanics** and **quantum mechanics** that will be discussed separately in this chapter. These methods allow to calculate the energy of any arrangement of the atoms and molecules in the system with different approach, and are able to show how the energy of the system changes when the positions of the atoms and molecules change.

Molecular modeling methods for the calculation of energy are based on the Born-Oppenheimer approximation,[205] that enables to separate the electronic motions from the nuclear motions. The state of a system is mathematically described in exact way by the Schrödinger equation[206] (that cannot be solved exactly for any molecular systems):

$$H\,\psi = E\,\psi$$

Where H is the Hamiltonian, ψ is the wave function and E is the energy of the system. Under the Born-Oppenheimer approximation the total wave function for the molecule can be split in two independent parts, one nuclear and one electronic that can be consider separately:

$$\psi_{tot} = \psi_{(nuclei)}\,\psi_{(electrons)}$$

and the total energy equals the sum of the nuclear energy (the electrostatic repulsion between the positively charged nuclei) and the electronic energy. The electronic energy comprises the kinetic and potential energy of the electrons moving in the electrostatic field of the nuclei, together with electron-electron repulsion:

$$E_{tot} = E_{(electrons)} + E_{(nuclei)}$$

This approximation is possible because the mass of an electron ($e^- = 9.11 \times 10^{-28}$ g) is less than the mass of a nucleus ($H^+ = 1{,}67 \times 10^{-24}$ g) and the speed of electrons in the molecule is enormously greater than the speed of nuclei. When the motion of electrons is considered (quantum mechanics), it is possible to say that the nuclei are fixed compared to their electrons moving quickly around them, and for this reason it is possible to ignore the existence of nuclei motion. Instead, when the motion of nuclei is considered (molecular mechanics), the electrons can rapidly adjust to any change in the nuclear positions, and it is possible to ignore the existence of electrons; consequently, the energy

of a molecule in its ground electronic state can be considered as a function of the nuclear coordinates only.

The surface that describes the variation of the potential energy of a molecule in function of the relative position of the nuclei is called Potential Energy Surface (PES) and it's a hyper-surface, because it can't be represented in a tridimensional space. The PES is described exactly in the Schrödinger equation, but it is approximated in the calculations. The quality of a calculation method is correlated to the best approximation of the PES; if the calculated PES is similar to the real PES the method is good, on the other hand, the method is not valid.

When starting a molecular modeling study, the first thing to do is to generate a model of the molecule in the computer by defining the relative positions of the atoms in space. Two are the common ways: one of them is to specify the cartesian (x,y,z) coordinates of all the atoms present. The alternative is to use internal coordinates, in which the position of each atom is described relatively to other atoms in the system. Internal coordinates are usually written as a Z-matrix that contains one line for each atom in the system. One example is reported in figure 5.1, where a molecule of methane is described using the two approaches.

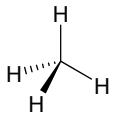

Cartesian coordinates

atom type	x	y	z
C	-0.67400	0.35400	0.00000
H	-0.52400	1.45700	0.00000
H	-1.25500	0.05900	0.90200
H	-1.23300	0.05600	-0.91500
H	0.31600	-0.15400	0.01300

Z-Matrix

atom type		distance		angle		torsion angle
C						
H	1	1.11315				
H	1	1.11274	2	109.45414		
H	1	1.11288	2	109.45197	3	119.96922
H	1	1.11280	2	109.41810	3	239.99186

***Figure 5.1**: Representation of CH_4 molecule in cartesian coordinates and in internal coordinates*

In the first line of the Z-matrix, atom 1, a Carbon atom, is defined. Atom number 2 is hydrogen atom that has a distance of 1.11274 Å from atom 1. Atom 3 is a hydrogen atom that is bonded to atom 1 with a bond length of 1.11274 Å. The angle formed by

atoms 2-1-3 is 109.45°, information that is specified in columns 4 and 5. The fourth atom is a hydrogen, with a distance of 1.11288 Å from atom 2, the angle 4-2-1 is 109.45°, and the torsion angle for atoms 4-2-1-3 is 119.96°, and so on.

However, one coordinate system is usually preferred for a given application. Internal coordinates can usefully describe the relationship between the atoms in a single molecule, but Cartesian coordinates may be more appropriate when describing a collection of discrete molecules. Internal coordinates are commonly used as input to quantum mechanics programs, whereas calculations using molecular mechanics are usually done in Cartesian coordinates. The total number of coordinates that must be specified in the internal coordinate system is six fewer than the number of Cartesian coordinates for a non-linear molecule.

5.1. Molecular mechanics

According to the Born-Oppenheimer approximation, molecular mechanics ignore electrons and compute the energy of a system only as a function of the nuclear positions. It is possible, then to take into account in an implicit way the electronic component of the system by adequate parameterization of the potential energy function. The set of equations and parameters which defines the potential surface of a molecule is called force field.

5.1.1 Force field methods

Generally, a common simplification in molecular mechanics is to consider a molecule as a collection of masses interacting one with each other through harmonic forces. Thus, the atoms in molecules are treated as balls of different sizes and flavors joined together by springs of variable strength and equilibrium distances (bonds). This simplification (harmonic oscillator) allows molecular mechanics to be used as a fast computational model that can be applied to molecules of any size. In the course of a calculation, the total energy is minimized with respect to the atomic coordinates, and consists in a sum of different and independent contributions that compute the deviations from equilibrium of bond lengths, angles and torsions plus non-bonded interactions:

$$E_{tot} = E_{str} + E_{bend} + E_{tors} + E_{elec} + E_{vdw} + \ldots$$

where E_{tot} is the total energy of the molecule, E_{str} is the bond-stretching energy term, E_{bend} is the angle-bending energy term, E_{tors} is the torsional energy term, E_{vdw} is the Van der Waals energy term, and E_{elec} is the electrostatic energy term.

These contributions are present in all the force fields, but every force field uses different equations or parameters to calculate the different energetic terms; in some case it is possible to observe the presence of other supplementary parameters. Moreover, force fields with the same functional form but different parameters, and force fields with different functional forms, may give results of comparable accuracy.

A force field should be considered as a single entity; it is not strictly correct to divide the energy into its individual components, let alone to take some of the parameters from one force field and mix them with parameters from another force field. Nevertheless, some of the terms in a force field are sufficiently independent of the others (particularly the bond and angle terms) to make this an acceptable approximation in certain cases. The force fields used in molecular modeling are primarily designed and parameterized to reproduce structural properties obtained from experimental data (neutron diffraction, X-Ray, NMR). The transferability of the functional form and parameters is an important feature of a force field; infact the same set of parameters should be used to model in a series of related molecules, without defining a new set of parameters for each individual molecule. On the basis of transferability it is possible to catalogue the force field in two classes:

- Class I: force fields have limited transferability, therefore are only parameterized for a limited number of chemical types and are of limited value for screening large numbers of compounds (AMBER[207] (Assisted Model Building and Energy Refinement), MM1[208]);
- Class II: greater transferability, allow for a large number of compounds to be treated, as required for database screening (MMFF[184] (Merck Molecular Force Field), CHARMM[209] (Chemistry at HARvard Molecular Mechanics), MM2[210]).

Note that transferability is relative; the more the extrapolation of a force field, the less the accuracy of the force field, and the force field could fail. This should always be taken into account when analyzing the results. There are also many other force field types, often

exclusive for a particular program or for a particular class of compounds, as UFF,[211] that presents parameters for metallic elements.

The functional forms employed in molecular mechanics force fields are often a compromise between accuracy and computational efficiency; the most accurate functional form may often be unsatisfactory for efficient computation. As the performance of computers increases it becomes possible to incorporate more sophisticated models.
Another concept that is basilar in force fields is that of an atom type. The atom type is more than just the atomic number of an atom; it usually contains information about its hybridization state and sometimes the local environment. For example, in most force fields it is necessary to distinguish between sp^3-hybridised carbon atoms (which adopt a tetrahedral geometry), sp^2-hybridised carbons (which are trigonal) and sp-hybridised carbons (which are linear). Each force field parameter is expressed in terms of these atom types, so that the reference angle for a tetrahedral carbon atom would be near 109.5° and that for a trigonal carbon would be near 120°. The atom types in some force fields reflect the neighbouring environment as well as the hybridization and can be quite extensive for some atoms.

5.1.2 The force fields equations

The interactions between the atoms in a molecule are described by a set of classical-mechanical potential functions. The energy obtained is only a measure of intramolecular strain relative to a hypothetical situation, and has no physical meaning: with different force fields it is possible to obtain different energy values.

Although the exact form of the potential functions depends on the force field, almost all molecular mechanics force fields use relatively simple expressions to describe the energy dependence on bond lengths, bond angles and so on. These can be solved very rapidly with computers thus permitting calculations on large molecules. However, in general, they are appropriate only for small changes from standard values. The results are less reliable for large deviations. Just one typical example of such a function is the equation of the energy of a stretched bond (derived from Hooke role) that is:

$$E_{str} = \frac{1}{2} k_s (r - r_0)^2$$

where k_s is the bond-stretching force constant, r_0 is the unstrained bond length, and r is the actual bond length. In more force fields, a cubic term (MM2),[210] a quartic function (MM3)[212] or a Morse function[213] (AMBER) has been included. The values of k_s and r_0 are derived from experimental or theoretical experiments and improved by comparison with a particular set of molecules.

Also for angle bonding a simple harmonic, spring-like representation is employed. The expression describing the angle-bending term is:

$$E_{bend} = \frac{1}{2} k_\theta (\theta - \theta_0)^2$$

where k_θ is the angle-bending force constant, θ_0 is the equilibrium value for θ, and θ is the actual bond angle (in some force fields other additional terms are present). When a system presents sp^2 hybridized atoms, (with trigonal-geometry), to preserve the planarity of the system, an appropriate term for the bending "out of plane" was introduced. Another problem is due to the angles of small cycles (3 or 4 terms) that were treated separately with a specific term (MM3 is able to study separately since 5-member rings).

A common expression for the dihedral potential energy term is a cosine series about the dihedral angle ω:

$$E_{tors} = \frac{V_1}{2}(1 + \cos\omega) + \frac{V_2}{2}(1 - \cos 2\omega) + \frac{V_3}{2}(1 + \cos 3\omega) + \ \ldots$$

generally, this Fourier expansion is truncated at the third term, and V_1, V_2, and V_3 are a theoretical constants.

To describe the electrostatic potential energy, the Coulomb interaction term is used:

$$E_{elec} = \frac{1}{\varepsilon}\frac{Q_1 Q_2}{r}$$

where ε is the dielectric costant, Q_1 and Q_2 are atomic charges of interacting atoms, and r is the interatomic distance. In force fields the charges are implemented as empirically

derived parameter sets. Molecular mechanics calculations are traditionally carried out in vacuum conditions with ε = 1. The investigation of molecules containing charges and dipoles however requires the consideration of solvent effects[214] and this can be done by employing the corresponding solvent dielectric constant (for example, ε = 80 in water).[215]

The Van der Waals interactions are usually represented by a Lennard-Jones potential, composed by two terms; the first is a repulsive term (for short distances), the second is an attractive term (for long distances):

$$E_{VdW} = \varepsilon\left[\left(\frac{d_0}{d}\right)^{12} - 2\left(\frac{d_0}{d}\right)^{6}\right]$$

where d_0 is the sum of Van der Waals rays, and ε is the value of the potential hole.

These equations, with some variations, are common to all the force fields. Some force fields can also include cross terms (the most commons are E_{st} that is the stretching/torsional term, E_{sb} that is the stretching/bending term), hydrogen bonding terms and more differentiated potential energy functions to describe the system.[216]

The equilibrium values of these bond lengths and bond angles are the corresponding force constants used in the potential energy function defined in the force field and define a set known as force field parameters. Each deviation from these equilibrium values will result in increasing total energy of the molecule. So, the total energy is a measure of intramolecular strain relative to a hypothetical molecule with an ideal geometry of equilibrium. The total energy has no strict physical meaning by itself, but differences in total energy between two different conformations of the same molecule can be compared.

5.1.3 Energy-miminization

In molecular modeling interest is directed at individuating the minimum points on the energy surface. Minimum energy arrangements of the atoms correspond to stable states of the system; any movement away from a minimum gives a configuration with a

higher energy. There may be a very large number of minima on the energy surface. The minimum with the lowest energy is known as the global energy minimum.

There are many methods to calculate the global energy minimum, and these can be divided into three different classes depending on the order of the derivative used for locating a minimum on the energy surface:

- **Zero order methods** are those that use only the energy function to identify regions of low energy through a grid search procedure;
- **First order methods** are those that employ the gradient of the function to identify a region of low energy;
- **Second order methods**, like the Newton-Raphson algorithm, that use the hessian to locate minima.

The zero-order method is the most useful where the initial configuration of the system is very high in energy, because it rarely fails to find a better solution. However, it can be rather expensive in terms of computer time and often is used in combination with a different minimization algorithm.

There are many first order methods, and the most common is the conjugate gradient method. With this procedure the information about the energy function is accumulated by sequential iteration. For each minimization step the gradient is calculated (first order derivatives) and used as additional information for computing the new direction vector of the minimization procedure. Thus, each successive step continually refines the direction towards the minimum.

In the second order methods not only the first derivatives (gradient) are employed, but also the second derivatives that give information about the curvature of the function to facilitate the identification of the search direction. One example is the Newton-Raphson Minimizer[217] and TNCG (Truncated Newton Conjugate Gradient)[218] that was employed in our studies.

For structures far from minimum, the zero order method is often the best choice; subsequently the minimization can be completed to convergence with conjugate gradients or a Newton-Raphson minimizer. To very big and complicated systems, that are too large for storing and calculating numerous second-derivatives, the conjugate gradient minimizer is the only practicable method.

5.1.4 Conformational analysis

The physical, chemical and biological properties of a molecule often depend critically upon the three-dimensional structures, or conformations, that it can adopt. The study of these conformations and their influence on the properties of a molecule is called conformational analysis. The conformations of a molecule are traditionally defined as arrangements of its atoms in space that can be interconverted by rotation about single bonds or for small distortions in bond angles and bond lengths.

Each point on the potential energy surface represents the potential energy of a single conformation. Stable conformations of a molecule correspond to local minima on this energy surface. The relative population of a conformation depends on its statistical weight which is influenced not only by the potential energy but also by the entropy.

A goal of the conformational analysis is the capability to identify the preferred conformations of a molecule. In this field, the methods employed for the minimization of the energy play a crucial role, because they move to the minimum point that is closest to the starting structure. For this reason, it is necessary to have a separate algorithm which generates the initial starting structures for subsequent minimization.

The most general methods for conformational analysis are those that are able to identify all minima on the potential energy surface; for these reasons, the conformational search methods can be divided into five categories (in this study, only the first two method was described):

- systematic search algorithms;
- random approaches;
- distance geometry;
- model-building methods;
- molecular dynamics.

The systematic search algorithm is the most intuitive method that was performed by varying systematically each of the torsion angle of a molecule in order to generate all possible conformations. Every conformation so generated is subjected to energy minimization to derive the associated minimum energy conformation. The search stops when all possible combinations of torsion angles have been generated and minimized. However, in many cases the number of conformations generated may be too large to allow a reasonable treatment, without considering the time for the machine calculations.

It's also possible that the presence of constrain can't permit to generate all the possible conformations with a incomplete analysis of PES. When the structures are generated and minimized, it's possible to remove the duplicates; these eliminations take place by superimposing two structures with the same energy values and comparing the atom positions of molecules. If the atom positions are the same in the two structures, the two molecules are the same conformation, and one of them can be eliminated.

A completely opposite approach from systematic search algorithm are the random approaches, where the generation of conformations implies a casual variation of the initial geometry. This variation could be done in the Cartesian coordinates or in the internal coordinates (torsion angles and rotatable bonds), and can move from one region of the energy surface to a completely unconnected region in a single step. Both types of algorithm use a similar approach with is shown in flow chart form in figure 5.2.

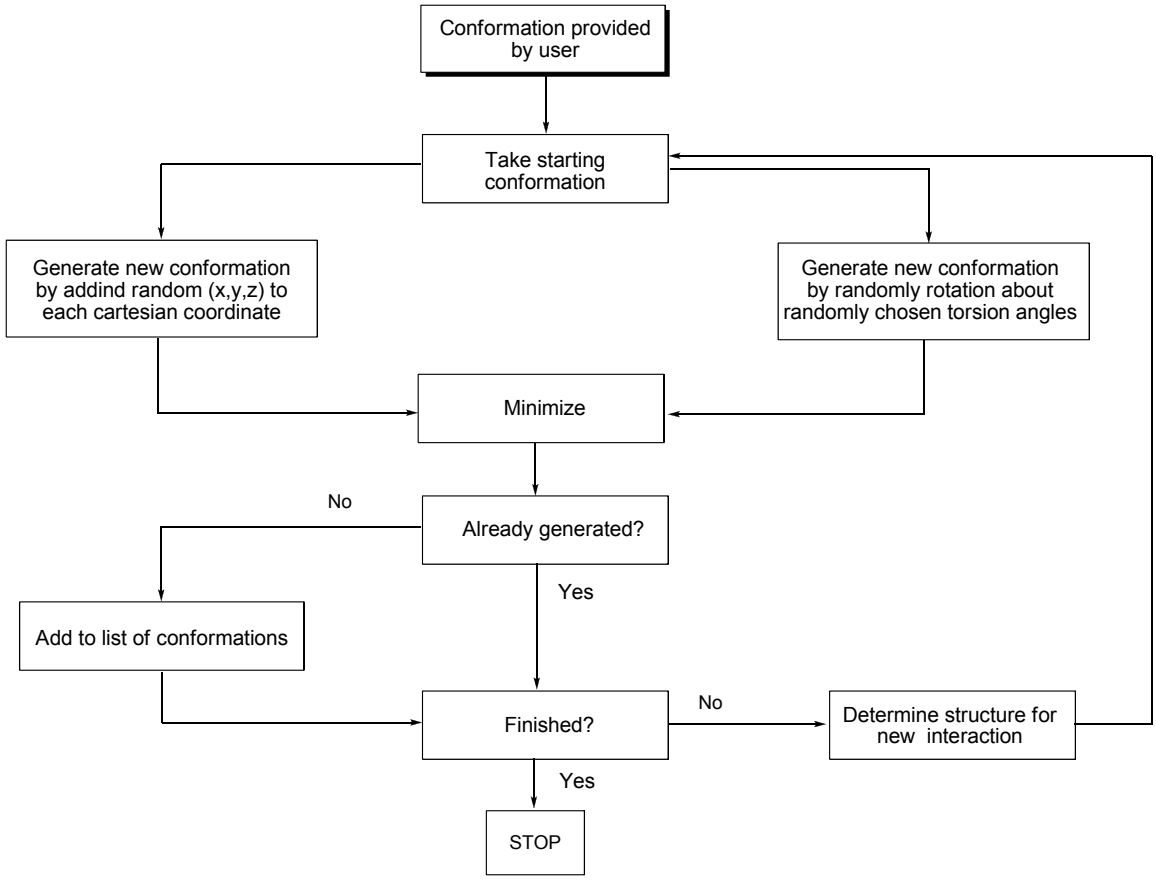

***Figure 5.2**: flow chart steps followed by a random conformational search.*

One example of this procedure is the Monte Carlo (MC) method[219] (the name "Monte Carlo" is a reference to the Monte Carlo Casino in Monaco where Ulam's uncle would borrow money to gamble), that was the first technique used to perform the first computer simulation of a molecular system. A random search starts with an optimized structure, and at each stage of a Monte Carlo search the actual conformation is modified randomly moving a single atom or molecule in order to obtain a new one. In some cases new configurations may also be obtained by moving several atoms or molecules or by rotating about one or more bonds. The new structure generated is then refined using energy minimization. If the energy of the new minimized configuration is lower than the energy of its predecessor then the new configuration is accepted, and stored and used as the starting point for the next iteration in the next cycle. The procedure continues until a given number of iterations have been performed or until it is decided that no new conformations can be found. This random method potentially cover all regions of conformational space, but this is true only if the process is allowed to run for a sufficiently long time, so it is very important to establish when the analysis was completely tested.

This can be efficiently done by performing several runs in a parallel mode, each one starting with a different initial conformation; the numbers produced by a random number generator are not, in fact, truly random because the same sequence of numbers should always be generated when the program is run with the same initial conditions. If the results are identical or nearly identical, then completeness can be assumed. Another empirical way to establish that the analysis was terminated is to analyze the output file: if the structures with a low energies were generated for many time, and for a long time, no new structure was generated and completeness can be reached.

When a Monte Carlo analysis is finished, numerous structures with different energies value were generated, and it's important to calculate the statistical distribution of the system using the Boltzmann equation, that is fundamental to describe the state of molecule in each energy level. The probability that a molecule lives in a given conformation is proportional to the Boltzmann factor:

$$P \div e^{-\frac{\Delta E}{kT}}$$

where P is the probability that the molecule live as a given conformation, ΔE is the energetic difference between two sequential conformations, k is the Boltzmann constant and T is the temperature.

5.2 Quantum mechanics

Differently from molecular mechanics, quantum mechanics explicitly consider the electrons in a calculation, and try to resolve the Schrödinger equation. On the basis of Born-Oppenheimer approximation, it's possible to say that the wave function that describes a molecular system is not influenced by the nuclear motion, because the electron motion is faster than the nuclear motion. Quantum mechanical methods are very valuable tools in computational chemistry, and often are employed when force field parameters for a certain structure are not available. In addition, the calculation of transition states or reaction paths as well as the determination of geometries influenced by polarization or unusual electron distribution in a molecule is the domain of quantum mechanical calculations and such properties often cannot be determined by any other method.

Their disadvantages, in comparison to other methods, are the computational costs and the limitation to rather small molecules So, the use of quantum mechanical methods should be reserved for the treatment of special problems.

There are a lot of quantum mechanical methods, but only two will be simply discussed in this study: *ab initio* methods and semi-empirical methods.

5.2.1 ab initio methods

Unlike molecular mechanics, *ab initio* quantum chemistry methods are capable of reproducing experimental data without employing empirical parameters because they try to solve the Schrödinger equation that defines the state of a molecule.

The Schrödinger equation is exactly solvable only for little systems, as hydrogen atoms and small cationic species: in the other cases, some approximations are required. The first approximation employed in the *ab initio* methods is the Born-Oppenheimer approximation, already discussed at the beginning of this chapter. The second one is the

use of the LCAO approximation (Linear Combination of Atomic Orbitals)[220] to define the wave function. The molecular orbitals are generated as linear combinations of atomic orbitals present in the molecule, and, as for isolated atoms, the electrons of a molecule occupy the molecular orbitals from the minor to the higher energetic state with two electrons for state with anti-parallel spins. With this approximation, the σ molecular orbitals are localized only on two nuclei, while the π molecular orbitals can be localized on multiple nuclei (as for delocalized or coniugated systems).

Another approximation employed in the "*ab initio*" methods permit to consider σ- and π-orbitals separately, without mutual influence, in according with the Hückel theory. The fourth and last approximation is called Self Consistent Field (SCF) or Hartree-Fock theory, where an electron isn't affected by the presence of another one. In this way, the electronic repulsion is considered imaging that every electron is influenced by the electronic field generated by all the other electrons, and the electronic correlation is not considered. When a SCF method is employed, the Hamiltonian is exactly calculated but the wave function is approximated. For this reason, it's possible to obtain more wave functions for the same system, but only the wave function that gives lowest value of energy is the best one.

The quality of an *ab initio* calculation depends on the basis set used for the calculation and the computational method employed to generate orbitals; for these reasons pre-constituted base sets, where each orbital is approximated with an established number of Gaussian function of probability were formed. The STO-3G basis set (Slater Type Orbitals, approximated by three Gaussian functions each) has been frequently used in the past because it is a minimal base set, that considers the smallest number of atomic orbitals necessary to accommodate all electrons of the atoms in their ground state, assuming spherical symmetry of the atoms.

There are also many other base sets that consider the internal and the external orbitals, as 3-21G, 4-31G, and 6-31G that differ only in the number of primitive Gaussians used in expanding the inner shell and first contracted valence function.[221]

Many different computer programs are now available for performing "*ab initio*" calculations; probably the best known is the Gaussian series of programs[222] which originated in the laboratory of John Pople, who has made numerous contributions to the field, recognized by the award of the Nobel Prize in 1998.

5.2.1.1 DFT method

The Density Functional Theory (DFT) method is a particular method that correlates the total electronic energy to the total electronic density, expressing the Schrödinger equation as a function of electron density (and not of wave function). The energy hence is a function of ρ and R

$$E\ f(\rho,R)$$

consequently, the calculated wave function is exact, because derives from electronic density, while the Hamiltonian is approximated.

5.2.2 Semi-empirical methods

The semi-empirical molecular orbital methods are at the cross line between molecular mechanics and the *ab initio* calculations. They are basically quantum mechanical in nature but the main difference to *ab initio* methods is the introduction of empirical parameters in order to reduce the high costs of computer time necessary for explicit evaluation of all integrals.

Another basic idea of the semi-empirical approach is the consideration of the fact that most of the interesting molecular properties are mainly influenced only by the valence electrons of the corresponding atoms; therefore only the valence electrons are considered.

One semi-empirical method differ froms another only for the type of the integrals that are substituted with empirical parameters. The firsts semi-empirical method are CNDO (complete neglect of differential overlap),[223] INDO (intermediate neglect of differential overlap)[224] and NDDO (neglect of diatomic differential overlap),[223] but today they are not used anymore. A more useful derivation of these methods was represented by:

- MINDO: based upon INDO (MINDO stands for modified INDO), but it does differ significantly in the way in which the method was parameterized, making much more use of experimental data.[225]

- MNDO,[226] based on NDDO introduces the Modified Neglect of Diatomic Overlap and has much wider variety of elements such as aluminium, silicon, germanium, tin and bromine.
- AM1 (Austin Model 1) [227] is a re-parameterized MNDO.
- PM3 (Parameterization method 3)[228] is also based on MNDO and presents empirical values different from AM1
- PM6 (Parameterization method 6) [229] that corrects some errors in the previous PM methods.

The advantage of semi-empirical methods over *ab initio* calculations is not only that they are faster, but also that calculations for systems up to 200 atoms are possible with the semi-empirical methods only. However, it is recommended to check one's results carefully; it should be noted that, in general, semi-empirical methods may give erroneous results for the third-row elements.

Nevertheless, it's important to remember that the most recently semi-empirical method isn't always the best one, since this depends on the characteristics of the studied systems.

5.2.2.1 MOPAC®

MOPAC[185] is a general-purpose semiempirical Molecular Orbital PACkage for the study of solid state and molecular structures and reaction, and it was largely written in the group of professor Michael Dewar.[230] The author of MOPAC, James Stewart, released in 2006 a public domain version of MOPAC7 entirely written in Fortran 90 called MOPAC7.1, that was upgraded to MOPAC2009.

The semi-empirical Hamiltonians MNDO, AM1, PM3, PM6, RM1, and MNDO are used in the electronic part of the calculation to obtain molecular orbitals, the heat of formation and its derivative with respect to molecular geometry. Using these results MOPAC is able to calculate the vibrational spectra, thermodynamic quantities, isotopic substitution effects and force constants for molecules, radicals, ions, and polymers.

The input data of this free software is very simple, and for these reasons MOPAC represents a very important research tool, that can be used for educational purpose.

In Chapter 6, some detailed examples of studies carried out with this package are reported.

5.3 Schrödinger® suite

Schrödinger[231] is a suite of molecular modeling packages that include many applications, as CombiGlide, Epik, Glide, Impact, Jaguar, Liaison, LigPrep, MacroModel, Phase, Prime, QikProp, QSite, SiteMap, and Strike. All these features are the same graphical free user interface: Maestro, that presents the most common graphics interface conventions.

In our studies we have worked with MacroModel (v. 8.5), a force-field-based molecular modeling program with applicability to a wide range of chemical systems, since it presents a large selection of force fields and numerous minimization methods. Further information about the use of MacroModel, and some examples are reported in details in chapter 6.

CHAPTER 6

Experimental section

"We ourselves feel that what we are doing is just a drop in the ocean.
But the ocean would be less because of that missing drop."
Mother Teresa

In this chapter the synthetic procedures of all products shown in the previous chapters have been reported. The compounds preserve the numbering established in precedence.

All reactions were carried out in oven-dried glassware with magnetic stirring under nitrogen atmosphere, unless otherwise stated. Dry solvents were purchased by Fluka and stored under nitrogen over molecular sieves (bottles with crown cap). Reactions were monitored by analytical thin-layer chromatography (TLC) using silica gel 60 F_{254} pre-coated glass plates (0.25 mm thickness) and visualized using UV light or phosphomolibdic acid. Purification of the products was performed by column chromatography on silica gel (230-400 mesh ASTM, Merck), unless otherwise stated.

NMR spectra were recorded on a AMX 300 Bruker, a Bruker Avance 500, a Bruker AC 200 or AC 300 spectrometers. ^{1}H-NMR were recorded at 200, 300 or 500 MHz and chemical shifts are reported in ppm (δ), with the solvent reference relative to tetramethylsilane (TMS), employed as the internal standard ($CDCl_3$ δ = 7.26 ppm). The following abbreviations are used to describe spin multiplicity: s = singlet, d = doublet, t = triplet, q = quartet, m = multiplet, br = broad signal, dd = doublet of doublets. ^{13}C-NMR spectra were recorded at 75 and 125 MHz respectively, with complete proton decoupling. Carbon chemical shifts are reported in ppm (δ) relative to TMS with the respective solvent resonance as the internal standard ($CDCl_3$, δ = 77.0 ppm). ^{31}P-NMR

spectra were recorded at 121.4 or 202.4 MHz with complete proton decoupling. Phosphorus chemical shifts are reported in ppm (δ) and were referenced to phosphoric acid (H_3PO_4) at 0.0 ppm.

Optical rotations were obtained on a Perkin-Elmer 241 polarimeter at 589 nm using a 5 mL cell, with a length of 1 dm. IR spectra were obtained on a Jasco FT/IR-4100 type A instrument. Mass spectra were registered on a Thermo Finnigan LCQ Advantage instrument equipped with an ESI ion source. HPLC analysis for ee determination was performed on a Agilent Instrument Series 1100 on chiral stationary phase, under the conditions reported below. Microwave-accelerated reactions were performed with a CEM Discover class S instrument.

6.1 Synthesis of phosphoramides

*Preparation of compound **52***

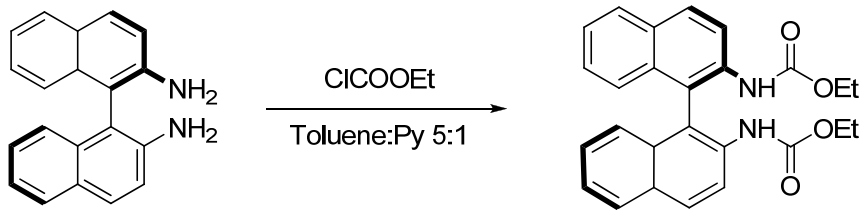

	eq	mmol	MW	mg	d (g/mL)	mL
(*R*)-1,1'-binaphthyl-2,2'-diamine	1.00	1.76	284.13	500.00		
ethyl chloroformate	2.60	4.58	108.52	496.52	1.14	0.44
pyridine	8.70	15.31	79.10	1211.01	0.98	1.23
toluene						6.00

(*R*)-1,1'-binaphthyl-2,2'-diamine was dissolved in a mixture of toluene and pyridine and cooled to 0°C. A solution of ethyl chloroformate in toluene (1 mL) was then added dropwise within 15 min. The mixture was subsequently warmed to room temperature and stirred for 2 h. The reaction, followed by TLC using 8:2 hexane/ethyl acetate as eluent, was then quenched by the addition of 2 N KOH (10 mL); the organic layer was separated, and the aqueous layer was extracted with AcOEt (3 × 20 mL). The organic layers were dried over Na_2SO_4 and the solvent was removed by rotary evaporation. After drying, a pale pink powder was obtained, that was purified by flash chromatography on silica gel.
TLC of the crude product (8:2 hexane/ethyl acetate): the product has a R_f of 0.26.

Flash chromatography (diameter: 3 cm, h: 18 cm, eluent: 8:2 hexane/ethyl acetate). A purification through silica gel gave the desired product with 95% yield.

^{1}H-NMR (300 MHz, $CDCl_3$): δ 8.57 (d, *J* = 9.1 Hz, 2H), 8.08 (d, *J* = 9.1 Hz, 2H), 7.94 (d, *J* = 8.1 Hz, 2H), 7.46-7.41 (m, 2H), 7.30-7.24 (m, 2H), 6.98 (d, *J* = 8.5 Hz, 2H), 6.28 (br, 2H), 4.1 (q, *J* = 7.1 Hz, 4H), 1.18 (t, *J* = 7.1 Hz, 6H).

^{13}C-NMR (75.5 MHz, $CDCl_3$): δ 154.0 (2C), 135.7 (2C), 132.9 (2C), 131.0 (2C), 130.7 (2C), 128.7 (2C), 127.7 (2C), 125.5 (2C), 125.2 (2C), 119.7 (2C), 117.8 (2C), 61.8 (2C), 14.7 (2C).

$[\alpha]_D^{25}$ = + 86.68 (solvent: $CHCl_3$, c = $4.28 \cdot 10^{-3}$ g/100 mL; λ = 589 nm).

Mass (ESI+): *m/z* = 429.48 [M + 1].

*Preparation of compound **53***

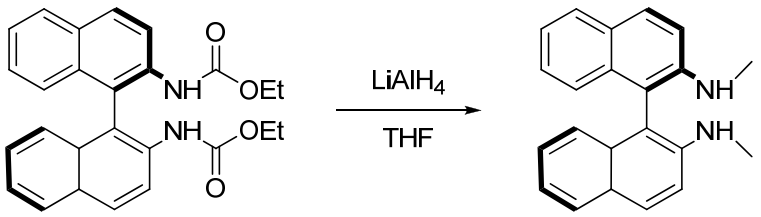

	eq	mmol	MW	mg	d (g/mL)	mL
compound **52**	1.00	1.17	428.27	500.00		
$LiAlH_4$	10.00	11.67	37.95	443.06		
dry THF						10.00

$LiAlH_4$ was suspended in dry THF and cooled to 0°C under nitrogen atmosphere. The dicarbamate **52** dissolved in dry THF (3 mL) was then slowly added *via* a dropping funnel; the mixture was warmed and then refluxed for 24 h. The reaction was followed by TLC using 8:2 hexane/ethyl acetate as eluent. After cooling to room temperature, excess $LiAlH_4$ was quenched with MeOH (1 mL), NaOH 15% (0.5 mL) and finally water (0.5 mL). The resultant gray precipitate was filtered off through a celite pad and washed with diethyl ether. The filtrate and washings were combined and the solvent was removed by rotary evaporation under vacuum, giving a pale yellow solid, with sufficient purity for being employed in the subsequent reaction (quantitative yield).
TLC of the product (8:2 hexane/ethyl acetate): the product has a R_f of 0.65.

^{1}H-NMR (300 MHz, $CDCl_3$): δ 8.57 (d, *J* = 9.1 Hz, 2H), 8.08 (d, *J* = 9.1Hz, 2H), 7.94 (d, *J* = 8.1 Hz, 2H), 7.46-7.41 (m, 2H), 7.30-7.24 (m, 2H), 6.98 (d, *J* = 8.5 Hz, 2H), 6.28 (br, 2H), 4.1 (q, *J* = 7.1 Hz, 4H), 1.18 (t, *J* = 7.1 Hz, 6H).
^{13}C-NMR (75.5 MHz, $CDCl_3$): δ 154.0 (2C), 135.7 (2C), 132.9 (2C), 131.0 (2C), 130.7(2C), 128.7 (2C), 127.7 (2C), 125.5 (2C), 125.2 (2C), 119.7 (2C), 117.8 (2C), 61.8 (2C), 14.7 (2C).
Mass (ESI+): *m/z* = 429.48 [M + 1].

*Preparation of compound **54***

Method a:

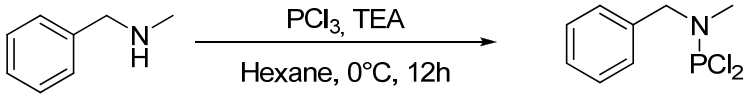

	eq	mmol	MW	mg	d (g/mL)	mL
N-methyl-*N*-benzylamine	1.00	4.95	121.18	600.00	0.939	0.64
PCl_3	6.00	29.71	137.33	4079.78	1.574	2.59
TEA	1.50	7.43	101.00	750.12	0.73	1.03
dry Hexane						40.00

A solution of *N*-methyl-*N*-benzylamine and TEA (20 mL) was added to a solution of phosphorus trichloride in dry hexane (20 mL) at 0°C under nitrogen atmosphere. The mixture was subsequently warmed to room temperature and stirred for 12 h. Then, the generated ammonium salts were filtered off through a celite pad under inert atmosphere, and washed with hexane (10 mL). The solvent and the excess of PCl_3 were removed by rotary evaporation under vacuum, giving a pale yellow oil in 42% yield, that was employed in the next step without further purification.

^{1}H-NMR (300 MHz, $CDCl_3$): δ 7.47-7.36 (m, 3H), 7.36-7.32 (m, 2H), 4.41 (d, J_{PH} = 12.5 Hz, 2H), 2.80 (d, J_{PH} = 9.5 Hz, 3H).
^{13}C-NMR (75.5 MHz, $CDCl_3$): δ 136.04, 128.77, 128.04, 127.97, 55.67, 33.67.
^{31}P-NMR (121.4 MHz, $CDCl_3$): δ 163.66.

Method b: [232]

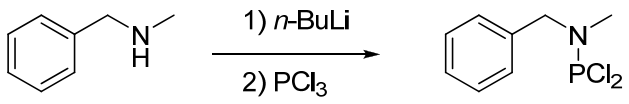

	eq	mmol	MW	mg	d (g/mL)	mL
N-methyl-*N*-benzylamine	1.00	5.78	121.18	700.00	0.939	0.75
PCl_3	2.00	11.55	137.33	1586.58	1.574	1.01
n-BuLi (1.6 M)	1.00	5.78				3.61
dry THF						22.00

A solution of *n*-BuLi was added to a solution of *N*-methyl-*N*-benzylamine in dry THF (20 mL) at -30°C under nitrogen atmosphere. After 30 min of stirring at this temperature, a solution of phosphorus trichloride in THF (2 mL) was added. This reaction mixture was stirred at -30°C for 45 min. Then, the generated LiCl was filtered off through a celite pad under inert atmosphere, and the THF and the excess of PCl_3 were distilled under vacuum. The reaction crude oil thus obtained is dried, and 50 mL of diethyl ether was added. Once the amine chlorohydrate was eliminated by filtration, solvent evaporation in vacuum afforded the desired product (a pale yellow oil) in 40% yield, that was employed in the next step without further purification.

Preparation of phosphoramide catalyst ***51***

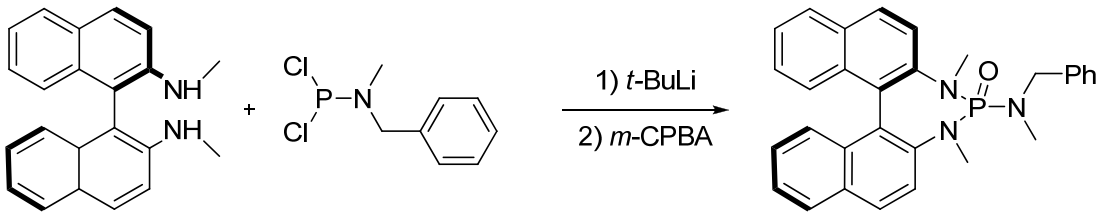

	eq	mmol	MW	mg	d (g/mL)	mL
compound **53**	1.00	0.32	314.12	100.00		
compound **54**	1.10	0.35	221.18	77.45		
t -BuLi (1.3 M)	2.20	0.70				0.54
m -CPBA	1.10	0.35	172.57	60.43		
dry THF						9.00

N,N'-dimethyl-binaphthyl-2,2'-diamine **53** was dissolved in dry THF (3 mL) and cooled to -78°C under nitrogen atmosphere. A solution of *t*-Butyl lithium was then added dropwise and the mixture was subsequently warmed to -30°C. After 30 minutes, the mixture was cooled to -78°C and a solution of dichloride **54** in THF (3 mL) was added in 1 hour using a syringe pump. When the addition is completed, the mixture was warmed to room temperature and stirred for 12 h. After this time, the brown mixture was cooled to 0°C and a solution of *meta*-chloroperbenzoic acid in THF (3 mL) was added, then the mixture was warmed to room temperature and stirred for 18 h.

The reaction, followed by TLC using a 99:1 ethyl acetate/*i*-propanol mixture as eluent, was quenched by the addition of a saturated aqueous solution of $NaHCO_3$ (10 mL). The organic layer was separated, and the aqueous layer was extracted with DCM (5 × 5 mL). The organic layers were then washed with saturated $NaHCO_3$ (10 mL) and NaOH 5% (10 mL), dried over Na_2SO_4 and the solvent was removed by rotary evaporation. After drying, a yellow powder was obtained, that was purified by silica gel flash chromatography.

Flash chromatography (diameter: 1.5 cm, h: 18 cm, eluent: 99:1 ethyl acetate/*i*-propanol). A purification through silica gel gave the desired product with 13% yield.

^{1}H-NMR (200 MHz, $CDCl_3$): δ 8.00-7.73 (m, 5H), 7.40-7.07 (m, 12H), 4.35-4.20 (m, 2H), 3.06 (dd, J = 3.80 Hz, J = 8.9 Hz, 6H), 2.19 (d, J = 8.9 Hz, 3H).

^{31}P-NMR (121.4 MHz, $CDCl_3$): δ 28.58.

Mass (ESI+): m/z = 478.3 [M + 1].

*Preparation of compounds **55** and **56***

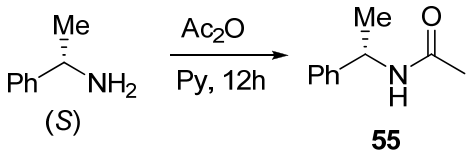

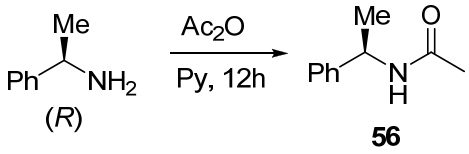

	eq	mmol	MW	mg	d (g/mL)	mL
phenylalanine	1.00	7.76	121.18	940.00	0.940	1.00
acetic anhydride	5.00	38.79	102.00	3956.10	1.080	3.66
DMAP	0.15	1.16	122.19	142.18		
Pyridine						15.00

DMAP was added to a solution of (*S*)-(-)-phenylalanine or (*R*)-(+)-phenylalanine dissolved in pyridine. Acetic anhydride was then added dropwise in 5 min. The mixture was subsequently stirred for 12 h at room temperature, and followed by TLC using 1:1 hexane/ethyl acetate as eluent. When the starting material disappeared, the mixture was diluted with AcOEt (30 mL) and quenched by the addition of 1 M HCl (40 mL) up to pH 3. The organic layer was separated, and the aqueous layer was extracted with AcOEt (2 × 20 mL). The organic layers were then washed with a $NaHCO_3$ solution, dried over Na_2SO_4 and the solvent was removed by rotary evaporation. After drying, a yellow powder was obtained, that was employed in the next step without further purification.

Yield: product **55**: 84% yield;

product **56**: quantitative yield.

^{1}H-NMR (200 MHz, $CDCl_3$): δ 7.32-7.30 (m, 5H), 5.93 (br, 1H), 5.05 (q, J = 12.1 Hz, J = 6.9 Hz, 1H), 1.95 (s, 3H), 1.47 (d, J = 6.9 Hz, 3H).

*Preparation of compounds **57** and **58***

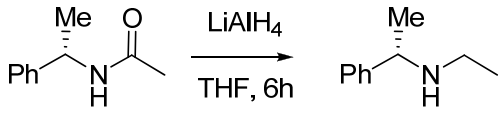

(*S*) **55** **57**

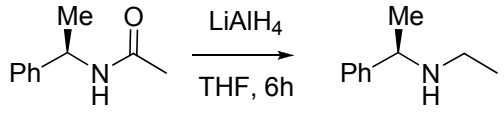

(*R*) **56** **58**

	eq	mmol	MW	mg	d (g/mL)	mL
compound **55** or **56**	1.00	5.82	163.22	950.00		
$LiAlH_4$	5.00	29.14	37.95	1105.86		
dry THF						19.00

$LiAlH_4$ was suspended in dry THF and cooled to 0°C under nitrogen atmosphere. The compound **55** or **56** dissolved in dry THF (5 mL) was then slowly added via dropping funnel, and the mixture was warmed and then refluxed for 6 h. The reaction was followed by TLC using 8:2 hexane/ethyl acetate as eluent. After cooling to room temperature, excess $LiAlH_4$ was quenched with MeOH (1 mL), NaOH 15% (0.5 mL) and finally water (0.5 mL). The resultant precipitate was filtered off through a celite pad and washed with DCM. The filtrate and washings were combined and the solvent was removed by rotary evaporation under vacuum, giving a pale yellow oil, with sufficient purity for being employed in the subsequent reaction.

Yield: product **57**: 83% yield;

product **58**: 96% yield.

^{1}H-NMR (200 MHz, $CDCl_3$): δ 7.32-7.23 (m, 5H), 3.76 (q, J = 12.0 Hz, J = 6.6 Hz, 1H), 2.52 (m, 2H), 1.35 (d, J = 6.6 Hz, 3H), 1.07 (t, J = 7.1 Hz, 3H).

*Preparation of compounds **59** and **60***

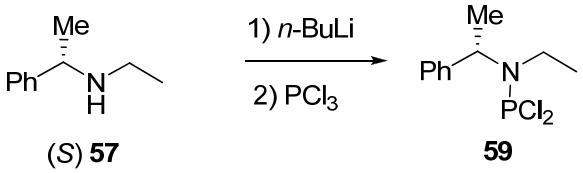

(*S*) **57** **59**

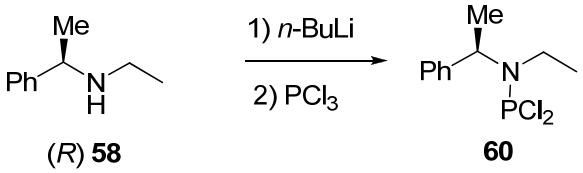

(*R*) **58** **60**

	eq	mmol	MW	mg	d (g/mL)	mL
compound **57** or **58**	1.00	4.69	149.23	700.00		
PCl_3	2.00	9.38	137.33	1288.36	1.574	0.82
n -BuLi (1.4 M)	1.00	4.69				3.35
dry THF						22.00

A solution of *n*-BuLi was added to a stirred solution of compound **57** or **58** in dry THF (20 mL) at -30°C under nitrogen atmosphere. After 30 min at this temperature, a solution of phosphorus trichloride in THF (2 mL) was added. This reaction mixture was stirred at -30°C for 2 h. Then, the generated LiCl was filtered through a celite pad under inert atmosphere, and the THF and the excess of PCl_3 were distilled under vacuum to give the desired product (a yellow oil) that was employed in the next step without further purification.

Yield: product **59**: 95% yield;

product **60**: 78% yield.

^{1}H-NMR (200 MHz, $CDCl_3$): δ 7.43-7.25 (m, 5H), 4.85-4.70 (m, 1H), 3.45-3.25 (m, 1H), 3.25-3.00 (m, 1H), 1.67 (dd, J = 7.2 Hz, J = 2.6 Hz, 3H), 1.05 (t, J = 7.2 Hz, 3H).

^{31}P-NMR (121.4 MHz, $CDCl_3$): δ 165.33.

*Preparation of phosphoramide catalyst **61***

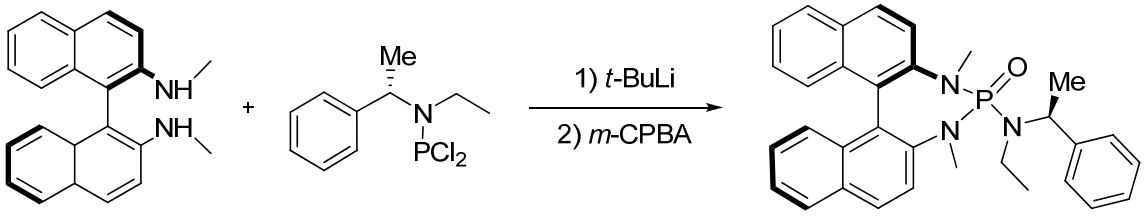

	eq	mmol	MW	mg	d (g/mL)	mL
compound **53**	1.00	0.48	314.42	150.00		
compound **59**	1.10	0.52	250.10	131.25		
t -BuLi (1.7 M)	2.20	1.05				0.62
m -CPBA	1.10	0.52	172.57	90.56		
dry THF						13.00

N,N'-dimethyl-binaphthyl-2,2'-diamine **53** was dissolved in dry THF (5 mL) and cooled to -78°C under nitrogen atmosphere. A solution of *t*-Butyl lithium was then added dropwise and the mixture was subsequently warmed to -30°C. After 2 h, the mixture was cooled to -78°C and a solution of dichloride **59** in THF (5 mL) was added in 30 minutes using a syringe pump. When the addition is completed, the mixture was warmed to room temperature and stirred for 72 h. After this time, the mixture was cooled to 0°C and a solution of *meta*-chloroperbenzoic acid in THF (3 mL) was added. Then the reaction was warmed to room temperature and stirred for 18 h.

The reaction, followed by TLC using 99:1 ethyl acetate/*i*-propanol as eluent, was then quenched by the addition of a saturated aqueous solution of $NaHCO_3$ (10 mL). The organic layer was separated, and the aqueous layer was extracted with DCM (5 × 5 mL). The organic layers were then washed with a saturated aqueous solution of $NaHCO_3$ (10 mL), NaOH 5% (10 mL), dried over Na_2SO_4 and the solvent was removed by rotary evaporation. After drying, a brown powder was obtained, that was purified by flash chromatography on silica gel.

Flash chromatography (diameter: 2.5 cm, h: 18 cm, eluent: 99:1 ethyl acetate/*i*-propanol). A purification through silica gel only allowed to recover a partial amount of compound **53** unreacted and byproducts.

Preparation of phosphoramide catalyst ***62***

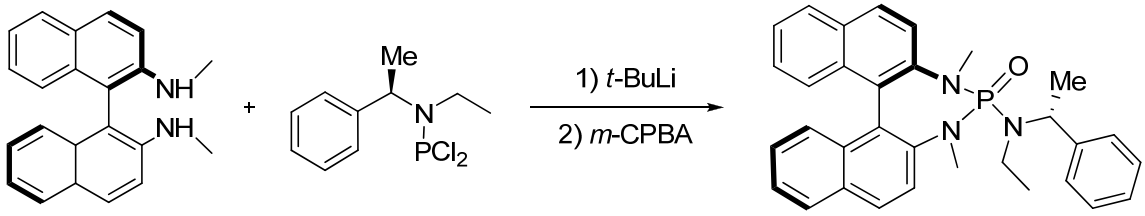

	eq	mmol	MW	mg	d (g/mL)	mL
compound **53**	1.00	0.48	314.42	150.00		
compound **60**	1.10	0.52	250.10	131.25		
t -BuLi (1.7 M)	2.20	1.05				0.62
m -CPBA	1.10	0.52	172.57	90.56		
dry THF						13.00

The synthetic procedure is identical to that reported for phosphoramide **61**.

A purification through silica gel only allowed to recover a partial amount of compound **53** unreacted and some byproducts.

*Preparation of compound **63*** [233]

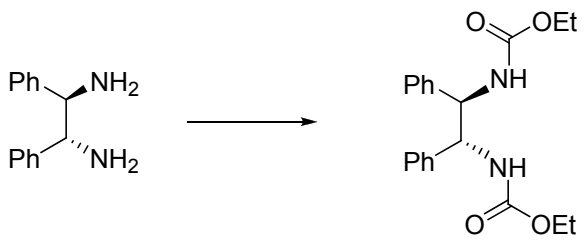

	eq	mmol	MW	mg	d (g/mL)	mL
(1*R*, 2*R*)-1,2-diphenyl ethane-1,2-diamine	1.00	0.94	212.13	200.00		
ethyl chloroformate	6.00	5.66	108.52	613.89	1.14	0.54
K_2CO_3	2.50	2.36	138.21	325.77		
toluene						8.00

(1*R*,2*R*)-1,2-diphenylethane-1,2-diamine was dissolved in THF, cooled to 0°C and treated with K_2CO_3 in water (818 µl) and then with ClCOOEt. The resulting biphasic mixture was stirred at ambient temperature for 4 h. The upper layer was separated and evaporated to dryness. The residue was dissolved in DCM (about 10 mL), and the solution was dried over Na_2SO_4, filtered, evaporated, and dried under vacuum at 100°C to give the desired product in quantitative yield.

^{1}H-NMR (300 MHz, $CDCl_3$): δ 7.2-7.1 (m, 10H), 5.9 (br, 2H), 5.0 (br, 2H), 4.1 (q, 4H), 1.2 (t, 6H).
Mass (ESI+): m/z = 357.3 [M + 1].

*Preparation of compound **64***

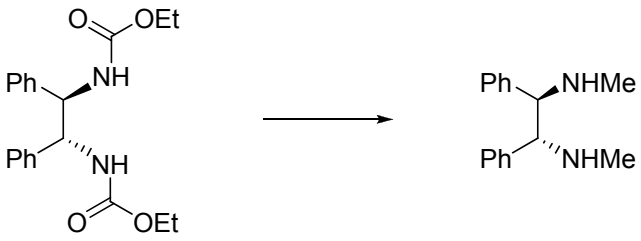

	eq	mmol	MW	mg	d (g/mL)	mL
compound **63**	1.00	0.84	356.42	300.00		
$LiAlH_4$	6.30	5.30	37.95	201.24		
dry THF						10.00

Compound **63** was added to a stirred suspension of $LiAlH_4$ in dry THF at 0°C under nitrogen atmosphere. The mixture was stirred at room temperature for 1 h and then heated to reflux overnight, cooled to 0°C, and treated subsequently with water (1 mL) and 15% NaOH (1 mL). The resulting suspension was stirred at room temperature for 1 h, heated to reflux, and filtered while hot. The white precipitate on the filter was washed with THF (3 × 10 mL), and the combined filtrates were evaporated to dryness.
TLC of the crude product (9:1 DCM/MeOH): the product has a R_f of 0.49.

Flash chromatography (diameter: 2.5 cm, h: 15 cm, eluent: 300 mL of 95:5 DCM/MeOH, 300 mL of 9:1 DCM/MeOH, then 300 mL of 7:3 DCM/MeOH). A purification through silica gel gave the desired product with 87% yield.

^{1}H-NMR (300 MHz, $CDCl_3$): δ 7.20-7.05 (m, 10H), 3.4 (s, 2H), 2.3 (s, 6H).
Mass (ESI+): m/z = 241.3 [M + 1].

Preparation of phosphoramide catalyst ***65***

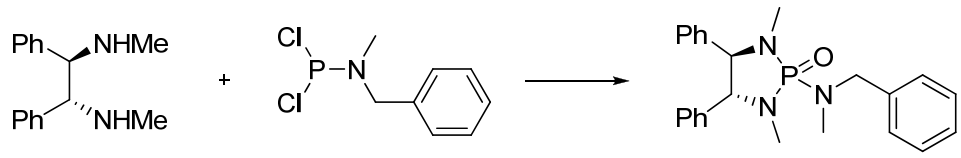

	eq	mmol	MW	mg	d (g/mL)	mL
compound **64**	1.00	0.42	240.34	100.00		
compound **54**	1.10	0.46	221.18	101.23		
t -BuLi (1.3 M)	2.20	0.92				0.70
m -CPBA	1.10	0.46	172.57	78.98		
dry THF						10.00

The synthetic procedure is identical to that reported for phosphoramide **51**.

TLC of the crude product (98:2 AcOEt/*i*-PrOH stained with ninhydrin): the product has a R_f of 0.30.

Flash chromatography (diameter: 1.5 cm, h: 20 cm, eluent: 98:2 AcOEt/*i*-PrOH).

A purification through silica gel gave the desired product with 30% yield.

^{1}H-NMR (200 MHz, $CDCl_3$): δ 7.45-7.20 (m, 6H), 7.20-7.05 (m, 2H), 7.05-6.95 (m, 2H), 4.55-4.25 (m, 2H), 3.94 (d, J = 4.0 Hz, 2H), 2.70 (d, J = 9.8 Hz, 3H), 2.40 (dd, J = 10.3 Hz, J = 5.0 Hz, 6H).

^{31}P-NMR (121.4 MHz, $CDCl_3$): δ 29.48.

Mass (ESI+): m/z = 406.4 [M + Na].

6.2 Synthesis of phosphoramidates

*Preparation of phosphoramidate catalyst **67***

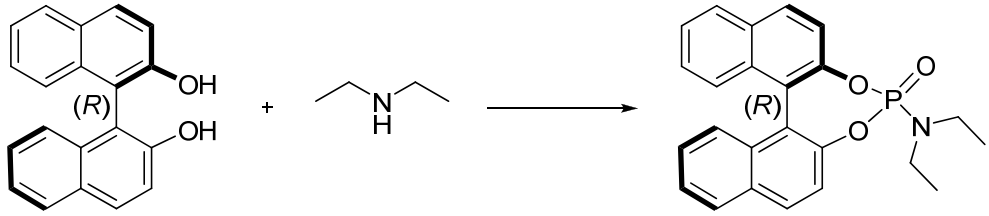

	eq	mmol	MW	mg	d (g/mL)	mL
(*R*)-BINOL	1.00	0.63	286.32	180.00		
$POCl_3$	1.10	0.69	153.50	106.15	1.65	0.065
DEA	1.00	0.63	73.00	45.89	0.71	0.065
TEA	5.00	3.14	101.00	317.48	0.73	0.44
dry DCM						10.00

(*R*)-BINOL was dissolved in dry DCM and cooled to 0°C under nitrogen atmosphere, then phosphoric trichloride and TEA were added. After 30 min, a solution of DEA in DCM (3 mL) was added dropwise and the mixture was stirred at 0°C for 1 h. After this time, the mixture was subsequently warmed at room temperature and stirred for 18h. The reaction, followed by TLC using 8:2 hexane/ethyl acetate as eluent, was then quenched by the addition of H_2O (10 mL). The organic layer was separated, and the aqueous layer was extracted with AcOEt (2 × 10 mL). The organic layers were then washed with brine, dried over Na_2SO_4 and the solvent was removed by rotary evaporation. After drying, a powder was obtained, that was purified by flash chromatography on silica gel.

TLC of the crude product (8:2 hexane/ethyl acetate): the product has a R_f of 0.62.

Flash chromatography (diameter: 2 cm, h: 18 cm, eluent: 8:2 hexane/ethyl acetate). A purification through silica gel gave the desired product with 54% yield.

^{1}H-NMR (300 MHz, $CDCl_3$): δ 8.10-7.90 (m, 5H), 7.65-7.45 (m, 4H), 7.45-30 (m, 3H), 3.30 (m, 4H), 1.15 (m, 6H).

^{31}P-NMR (121.4 MHz, $CDCl_3$): δ 12.72.

$[\alpha]_D^{25}$ = - 11.51 (solvent: $CHCl_3$, c = 0.1 g/100 mL; λ = 589 nm).

Mass (ESI+): *m/z* = 404.3 [M + 1].

Preparation of phosphoramidate catalyst ***68***

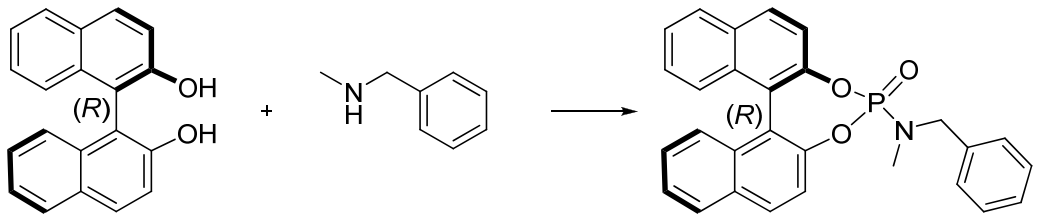

	eq	mmol	MW	mg	d (g/mL)	mL
(*R*)-BINOL	1.00	0.63	286.32	180.00		
$POCl_3$	1.10	0.69	153.50	106.15	1.65	0.065
N-benzyl-*N*-methylamine	1	0.629	121.18	76.18		
triethylamine (TEA)	5.00	3.14	101.00	317.48	0.73	0.44
dry DCM						10.00

The synthetic procedure is identical to that reported for phosphoramidate **67**.

Flash chromatography (diameter: 2 cm, h: 18 cm, eluent: 95:5 DCM/MeOH).
A purification through silica gel gave the desired product with 36% yield.

^{1}H-NMR Two sets of signals indicating the presence of two rotamers were detected. (300 MHz, $CDCl_3$): δ 8.10-7.90 (m, 5H), 4.35-4.15 (dd, *J* = 15 Hz, *J* = 12 Hz, 2H, *major*), 4.05 (dd, *J* = 18 Hz, *J* = 15 Hz, 2H, *minor*), 2.65 (d, *J* = 15 Hz, 3H, *minor*), 2.45 (d, *J* = 12 Hz, *major*).
^{31}P-NMR (121.4 MHz, $CDCl_3$): δ 14.61.
Mass (ESI+): *m/z* = 452.3 [M + 1].

Preparation of phosphoramidate catalyst ***69***

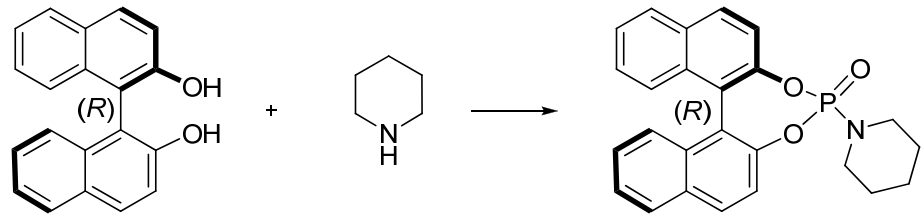

	eq	mmol	MW	mg	d (g/mL)	mL
(*R*)-BINOL	1.00	0.63	286.32	180.00		
$POCl_3$	1.10	0.69	153.50	106.15	1.65	0.065
piperidine	1	0.629	85.15	53.53	0.861	0.062
triethylamine (TEA)	5.00	3.14	101.00	317.48	0.73	0.44
dry DCM						10.00

The synthetic procedure is identical to that reported for phosphoramidate **67**.

Flash chromatography (diameter: 2 cm, h: 18 cm, eluent: 98:2 DCM/MeOH).
A purification through silica gel gave the desired product with 20% yield.

^{1}H-NMR (200 MHz, $CDCl_3$): δ 8.10-7.90 (m, 4H), 7.65 (d, 1H), 7.60-7.35 (m, 4H), 7.35-7.20 (m, 3H) 3.10-2.90 (m, 4H), 1.60-1.40 (m, 6H).
^{31}P-NMR (121.4 MHz, $CDCl_3$): δ 13.94.

*Preparation of phosphoramidate catalyst **70***

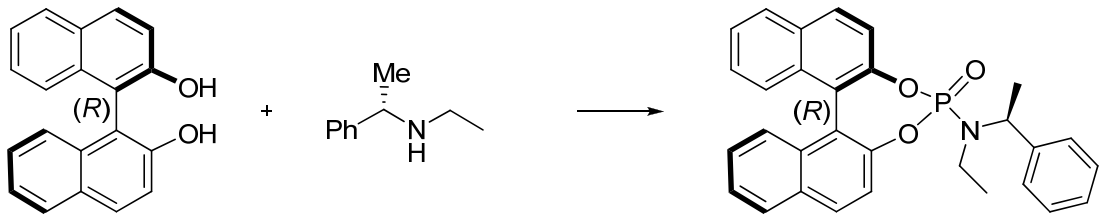

	eq	mmol	MW	mg	d (g/mL)	mL
(*R*)-BINOL	1.00	0.63	286.32	180.00		
$POCl_3$	1.10	0.69	153.50	106.15	1.65	0.065
amine **57**	1	0.629	149.23	93.82		
triethylamine (TEA)	5.00	3.14	101.00	317.48	0.73	0.44
dry DCM						10.00

The synthetic procedure is identical to that reported for phosphoramidate **67**.

Flash chromatography (diameter: 2 cm, h: 18 cm, eluent: 2:8 hexane/ethyl acetate).
A purification through silica gel gave the desired product with 65% yield.

^{1}H-NMR (200 MHz, $CDCl_3$): δ 8.10-7.90 (m, 5H), 7.65 (d, 1H), 7.60-7.30 (m, 10H), 5.30-5.15 (m, 1H), 3.30-3.00 (m, 2H), 1.70 (d, 3H), 1.00 (t, 3H).
^{31}P-NMR (121.4 MHz, $CDCl_3$): δ 14.18.
$[\alpha]_D^{25}$ = - 257.7 (solvent: $CHCl_3$, c = 0.3 g/100 mL; λ = 589 nm).

*Preparation of phosphoramidate catalyst **71***

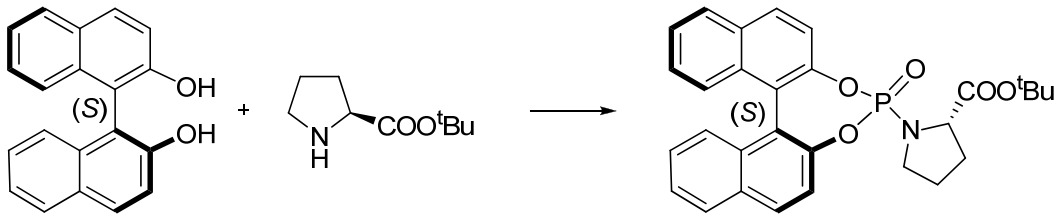

	eq	mmol	MW	mg	d (g/mL)	mL
(*S*)-BINOL	1.00	0.63	286.32	180.00		
$POCl_3$	1.10	0.69	153.50	106.15	1.65	0.065
(*S*)-proline *t*-butyl ester	1	0.629	171.24	107.65		
triethylamine (TEA)	5.00	3.14	101.00	317.48	0.73	0.44
dry DCM						10.00

The synthetic procedure is identical to that reported for phosphoramidate **67**.

Flash chromatography (diameter: 2 cm, h: 18 cm, eluent: 150 ml 95:5 DCM/MeOH, 150 ml 9:1 DCM/MeOH). A purification through silica gel gave the desired product with 86% yield.

^{1}H-NMR (300 MHz, $CDCl_3$): δ 8.05-7.85 (m, 4H), 7.65 (d, 1H), 7.50-7.35 (m, 4H), 7.35-7.20 (m, 3H), 4.40-4.20 (m, 1H), 3.50-3.35 (m, 1H), 3.20-3.05 (m, 1H), 2.30-1.60 (m, 4H), 1.90 (s, 9H).
^{31}P-NMR (121.4 MHz, $CDCl_3$): δ 11.14.

*Preparation of phosphoramidate catalyst **72***

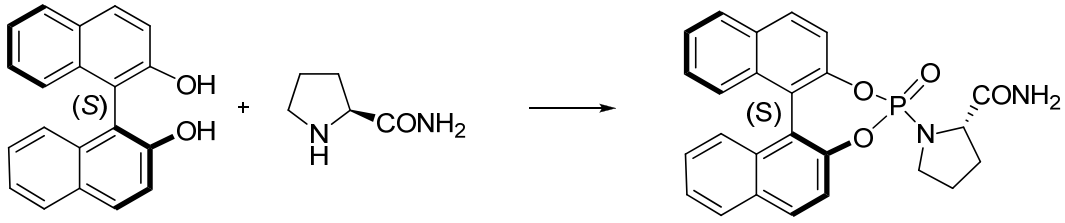

	eq	mmol	MW	mg	d (g/mL)	mL
(*S*)-BINOL	1.00	0.63	286.32	180.00		
$POCl_3$	1.10	0.69	153.50	106.15	1.65	0.065
(*S*)-proline amide	1	0.629	114.15	71.76		
triethylamine (TEA)	5.00	3.14	101.00	317.48	0.73	0.44
dry DCM						10.00

The synthetic procedure is identical to that reported for phosphoramidate **67**.

Flash chromatography (diameter: 2 cm, h: 18 cm, eluent: 95:5 DCM/MeOH).
A purification through silica gel gave the desired product with 16% yield.

^{1}H-NMR (300 MHz, $CDCl_3$): δ 8.00-7.90 (m, 2H), 7.50-7.25 (m, 9H), 7.15-7.05 (br, 1H), 5.50 (br, 1H), 4.45-4.35 (m, 1H), 3.25-3.15 (m, 1H), 2.75-2.65 (m, 1H), 2.45-2.35 (m, 1H), 2.05-1.95 (m, 1H), 1.85-1.70 (m, 1H), 1.60-1.40 (m, 1H).
^{31}P-NMR (121.4 MHz, $CDCl_3$): δ 12.84.
Mass (ESI+): *m/z* = 467.3 [M + Na].

*Preparation of phosphoramidate catalyst **73***

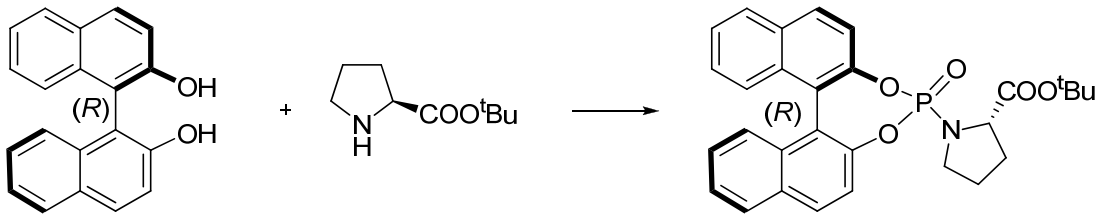

	eq	mmol	MW	mg	d (g/mL)	mL
(*R*)-BINOL	1.00	0.63	286.32	180.00		
$POCl_3$	1.10	0.69	153.50	106.15	1.65	0.065
(*S*)-proline *t*-butyl ester	1	0.629	171.24	107.65		
triethylamine (TEA)	5.00	3.14	101.00	317.48	0.73	0.44
dry DCM						10.00

The synthetic procedure is identical to that reported for phosphoramidate **67**.

Flash chromatography (diameter: 2 cm, h: 18 cm, eluent: 150 ml 95:5 DCM/MeOH, 150 ml 9:1 DCM/MeOH). A purification through silica gel gave the desired product with 25% yield.

^{1}H-NMR (300 MHz, $CDCl_3$): δ 8.10-7.90 (m, 4H), 7.65-7.40 (m, 5H), 7.40-7.20 (m, 3H), 4.45 (m, 1H), 3.60-3.35 (m, 2H), 2.25-1.95 (m, 3H), 1.45 (s, 9H).
^{31}P-NMR (121.4 MHz, $CDCl_3$): δ 12.17.

*Preparation of phosphoramidate catalyst **74***

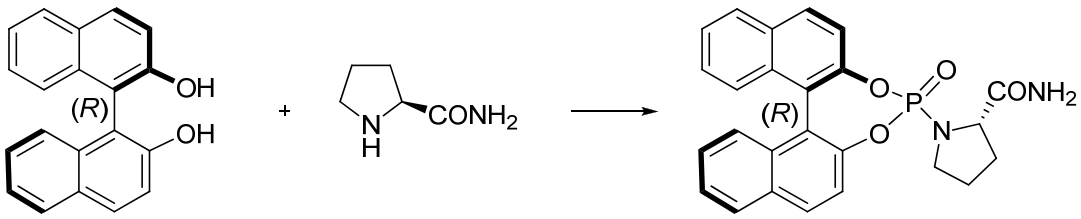

	eq	mmol	MW	mg	d (g/mL)	mL
(*R*)-BINOL	1.00	0.63	286.32	180.00		
$POCl_3$	1.10	0.69	153.50	106.15	1.65	0.065
(*S*)-proline amide	1	0.629	114.15	71.76		
triethylamine (TEA)	5.00	3.14	101.00	317.48	0.73	0.44
dry DCM						10.00

The synthetic procedure is identical to that reported for phosphoramidate **67**.

Flash chromatography (diameter: 2 cm, h: 18 cm, eluent: 9:1 DCM/MeOH).
A purification through silica gel gave the desired product with 14% yield.

^{1}H-NMR (300 MHz, $CDCl_3$): δ 8.00-7.90 (m, 4H), 7.60-7.40 (m, 4H), 7.40-7.25 (m, 4H), 6.80-6.70 (br, 1H), 5.50 (br, 1H), 4.15-4.05 (m, 1H), 3.20-3.05 (m, 1H), 3.05-2.95 (m, 1H), 2.30-2.15 (m, 1H), 2.05-1.75 (m, 2H), 1.75-1.55 (m, 1H).
^{31}P-NMR (121.4 MHz, $CDCl_3$): δ 12.19.
Mass (ESI+): *m/z* = 445.3 (M+1) and 467.3 [M + Na].

6.3 Synthesis of phosphine oxide: TetraMe-BITIOPO[182]

*Preparation of compound **83***

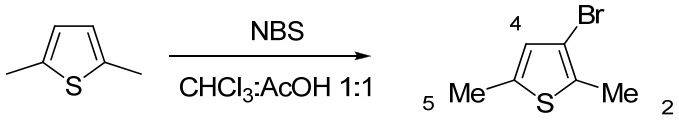

	eq	mmol	MW	mg	d (g/mL)	mL
2,5-dimethylthiophene	1.00	17.84	112.11	2000.00	0.98	2.03
NBS	1.00	17.84	177.98	3175.10		
Hydroquinone	0	0.036	110.11	3.93		
$CHCl_3$:AcOH						35.00

2,5-dimethylthiophene was dissolved in a 1:1 mixture of $CHCl_3$:AcOH and cooled to 0°C, then hydroquinone and a recent crystallized NBS were added. The mixture was stirred at 0°C for 1 h, then was warmed to room temperature and stirred for 2 h. The reaction, followed by TLC using 9:1 hexane/ethyl acetate as eluent, was quenched by the addition of H_2O (10 mL) and diluted with DCM (15 mL).

The organic layer was separated, and washed with a saturated solution of $NaHCO_3$ (10 mL) and water (10 mL), dried over Na_2SO_4 and the solvent was removed by rotary evaporation. After drying, a brown oil was obtained in 96% yield, that was employed in the next step without further purification.

TLC of the product (9:1 hexane/ethyl acetate): the product has a R_f of 0.65.

^{1}H-NMR (200 MHz, $CDCl_3$): δ 6.53 (s, 1H, **4**), 2.40 (s, 3H, **2**), 2.29 (s, 3H, **5**).

*Preparation of compound **84***

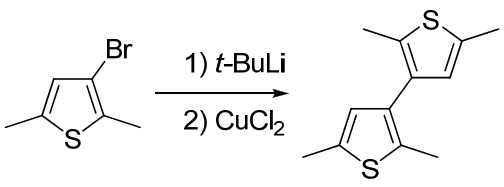

	eq	mmol	MW	mg	d (g/mL)	mL
compound **83**	1.00	10.47	191.09	2000		
t -BuLi 1.5 M	2.10	21.98				14.653
$CuCl_2$	1	10.47	134.45	1407.19		
dry Et_2O						10.00

A solution of compound **83** in dry Et_2O (10 ml) was added dropwise to a solution of *t*-butyl lithium cooled to -30°C under nitrogen atmosphere. After 30 min, the mixture was cooled to -60°C and $CuCl_2$ was added. The mixture was stirred for 4 h at -60°C then it was allowed to warm to room temperature.

After this time, a solution of 5% HCl was added (20 mL). The organic layer was separated and the aqueous layer was extracted with DCM (2 × 15 mL). The organic layers were then washed with H_2O (10 mL), a saturated solution of $NaHCO_3$ (10 mL) and H_2O (10 mL), dried over Na_2SO_4 and the solvent was removed by rotary evaporation. The crude product was purified by flash chromatography on silica gel.

TLC of the crude product (hexane): the product has a R_f of 0.73.

Flash chromatography using VersaFlash Station and VersaPak cartridge (40x75 mm, Supelco, eluent: hexane). A purification through silica gel gave the desired product with 77% yield.

^{1}H-NMR (200 MHz, $CDCl_3$): δ 6.52 (s, 2H), 2.41 (s, 6H), 2.27 (s, 6H).

*Preparation of compound **85***

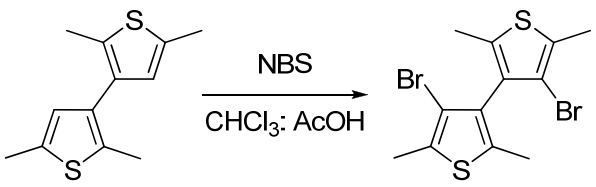

	eq	mmol	MW	mg	d (g/mL)	mL
compound **84**	1.00	2.25	222.37	500.00		
NBS	1.00	2.25	177.98	400.19		
Hydroquinone	0	0.004	110.11	0.50		
$CHCl_3$:AcOH						20.00

The synthetic procedure is identical to that reported for compound **83**.

^{1}H-NMR (300 MHz, $CDCl_3$): δ 2.40 (s, 6H), 2.15 (s, 6H).

mp = 93-95°C

*Preparation of TetraMeBITIOPO (catalyst **87**)*

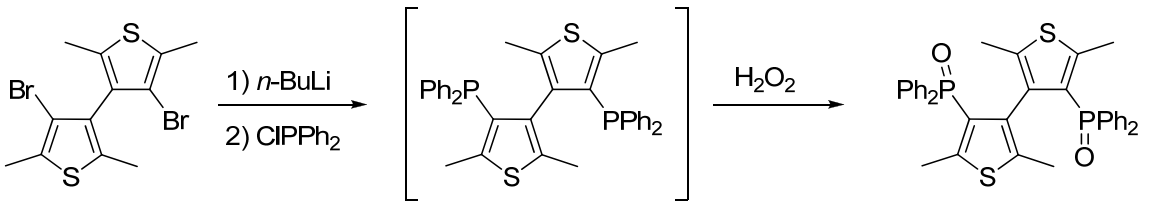

(rac)-TetraMe-BITIOPO
cat. 87

	eq	mmol	MW	mg	d (g/mL)	mL
compound **85**	1.00	3.03	380.16	1150		
Ph_2PCl	2.00	6.05	220.64	1334.89	1.23	1.086
n -BuLi 1.6 M	2	6.05				3.78
dry THF						30.00

A solution of compound **85** in dry THF (15 mL) at -60°C under nitrogen atmosphere was dropped into a solution of *n*-BuLi in dry THF (10 mL). The mixture was allowed to warm to -30°C then, after 20 min of stirring, a solution of diphenylphosphin chloride in THF (5 mL) was added dropwise in 15 min using a syringe pump. After 1 h, the mixture was warmed to room temperature and stirred for an additional of 18 h. After this time, the mixture was concentrated under reduced pressure and the residue was treated with water (20 mL) and extracted with DCM (10 mL). The organic layer was treated with H_2O_2 (10 mL, 35%) at 0°C. The mixture was stirred for 1 h at 0°C and for 1 h at RT and then diluted with water. The organic layer was separated, dried over Na_2SO_4 and the solvent was removed by rotary evaporation. The crude product was purified by flash chromatography on silica gel.

TLC of the crude product (AcOEt: *i*PA 95:5): the product has a R_f of 0.75.

Flash chromatography (diameter: 3 cm, h: 18 cm, eluent: AcOEt/DCM/TEA 3:7:0.1).
A purification through silica gel gave the desired product with 85% yield.

^{1}H-NMR (300 MHz, $CDCl_3$): δ 7.60 (m, 20H), 1.95 (d, 6H), 1.65 (s, 6H).
^{31}P-NMR (121.4 MHz, $CDCl_3$): δ 21.19.

*Resolution of TetraMe-BITIOPO (cat. **87**) to give catalyst **38** and **88***

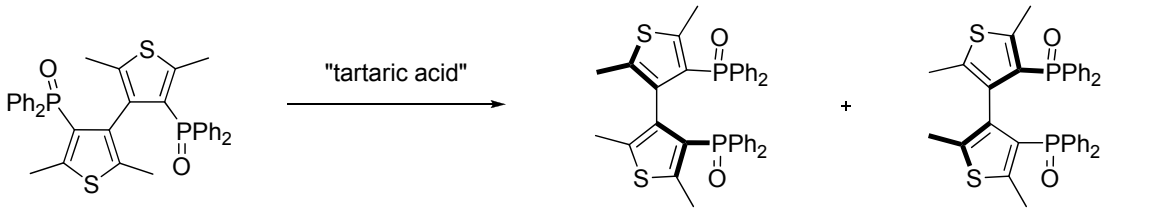

(-)-(*S*)-TetraMe-BITIOPO cat. 38 + **(+)-(*R*)-TetraMe-BITIOPO cat. 88**

	eq	mmol	MW	mg	d (g/mL)	mL
compound **85**	1.00	3.21	622.72	2000		
2,3-O,O'-Dibenzoyl tartaric acid	1.05	3.37	376.31	1269.03		
THF						15.00

A racemic mixture of compound **87** and monohydrate (-)-DBTA was dissolved in THF, refluxed for a few minutes, and allowed to stand at room temperature for 24 h.
An adduct between (+)-TetraMe-BITIOPO and (-)-DBTA was collected, and the filtrate was stored for recovery of (-)-TetraMe-BITIOPO. The adduct was dissolved into warm THF (30 mL), and a pure adduct was collected after standing for 10 days. The adduct was treated with NaOH solution, and the mixture was extracted exhaustively with DCM. The combined organic layers were dried over Na_2SO_4 and concentrated *in vacuo* to give a solid that was recrystallized from a hexane/benzene 1:1 mixture to give (+)-TetraMe-BITIOPO (cat. **88**). The mother liquors from the first resolution step were concentrated to dryness to give a solid that was treated with a 0.75 N NaOH solution and extracted with DCM. The organic layer was washed with water, dried over Na_2SO_4 and concentrated *in vacuo* to give (-)-TetraMe-BITIOPO (cat. **38**), which was recrystallized from a mixture of hexane/benzene 1:1.

(+)-TetraMe-BITIOPO: $[\alpha]_D^{25}$ = +62 (solvent: benzene, c = 0.49 g/100 mL; λ = 589 nm).
(-)-TetraMe-BITIOPO: $[\alpha]_D^{25}$ = -62 (solvent: benzene, c = 0.49 g/100 mL; λ = 589 nm).

6.4 Synthesis of *N*-acylated β-amino enones

Preparation of compound ***89*** [234]

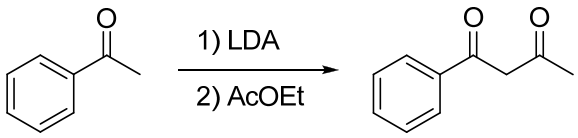

	eq	mmol	MW	mg	d (g/mL)	mL
Acetophenone	1.00	34.17	120.00	4100	1.03	4.00
DIPA	1.10	37.58	101.19	3803	0.72	5.31
n -BuLi (1.6M)	1.10	37.58				23.49
dry AcOEt	1.00	34.17	88.11	3010.43	0.98	3.07
dry THF						10.00

Dry THF and dry AcOEt were previously degassed under a steam of nitrogen for nearly half an hour. A solution of DIPA in degassed THF (6 mL) was cooled to -78°C, then *n*-BuLi was added dropwise *via* dropping funnel. After 15 min, the solution was warmed to 0°C, then a solution of acetophenone (4 mL) was added. After 10 min degassed dry AcOEt was added. The mixture was warmed to room temperature and stirred for 18h. After this time, Et_2O (60 mL) was added into the reaction mixture and stirred for 20 min. The resulting precipitate was filtered and washed with ether (2 x 30 mL). The precipitate was treated with ether (30 ml) and 0.3 M HCl (40 mL) was dropped while stirring until a pH lower than 4 was reached.

After 1 h, the product was extracted with ether (2 x 50 ml). The combined ether extracts were dried over anhydrous Na_2SO_4 and the solvent was removed by rotary evaporation. A pale yellow solid was obtained, with sufficient purity for being employed in the subsequent reaction (yield 25%).

^{1}H-NMR (300 MHz, $CDCl_3$): δ 7.85 (m, 2H), 7.55-7.45 (m, 3H), 6.15 (s, 1H enol C*H*), 4.15 (s, 2H, keto CH_2), 2.3 (s, 3H, keto CH_3), 2.2 (s, 3H, enol CH_3).

*Preparation of compound **90***

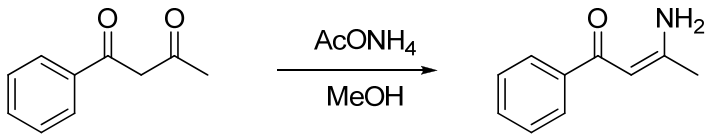

	eq	mmol	MW	mg	d (g/mL)	mL
compound **89**	1.00	8.02	162.19	1300		
NH_4OAc	5.00	40.08	77.08	3089		
dry MeOH						13.00

A solution of 1-phenylbutane-1,3-dione (compound **89**) and ammonium acetate in dry methanol was refluxed for 2.5 h. After cooling to room temperature, water (15 mL) was added and the mixture was stirred well. Precipitated colorless crystals were collected by filtration and dried at 50°C under vacuum to give the desired product in 85% yield.

^{1}H-NMR (300 MHz, $CDCl_3$): δ 10.20 (br, 1H), 7.90 (m, 2H), 7.45-7.35 (m, 3H), 5.70 (s, 1H), 5.15 (s, 1H), 2.05 (s, 3H).
^{13}C-NMR (200 MHz, $CDCl_3$): δ 189.5, 162.8, 140.2, 130.8, 128.2, 127.1, 92.3, 22.9.

*Preparation of compound **91***

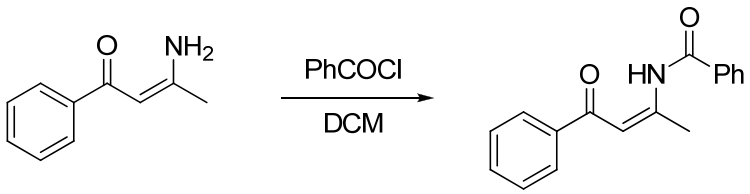

	eq	mmol	MW	mg	d (g/mL)	mL
compound **90**	1.00	6.20	161.20	1000		
benzoyl chloride	1.20	7.4	140.57	1046.4	1.21	0.86
pyridine	1.20	7.4	79.10	588.8	0.98	0.60
dry DCM						12.00

Pyridine and benzoyl chloride were added successively to a solution of compound **90** in dry DCM at room temperature. After being stirred for 1 h, water (10 mL) was added and the mixture was extracted with AcOEt (2 x 10 mL). The combined organic layers were dried over anhydrous $NaSO_4$, filtered, and concentrated under vacuum to give crude crystals which were purified by recrystallization from ethanol/water (4/1) to afford **91** as yellowish needles (yield 48%).

^{1}H-NMR (200 MHz, $CDCl_3$): δ 13.84 (br, 1H), 8.13-8.09 (d, J = 9.5 Hz, 2H), 7.98-7.90 (d, J = 7.7 Hz, 2H), 7.59-7.43 (m, 6H), 6.18 (s, 1H), 2.68 (s, 3H).
^{13}C-NMR (200 MHz, $CDCl_3$): δ 191.9, 166.2, 158.2, 138.7, 133.7, 132.7, 132.4, 128.9, 128.6, 128.0, 127.7, 102.5, 22.8.
mp 108-110°C

6.5 Synthesis of diarylphosphin chloride

*Preparation of compound **108***

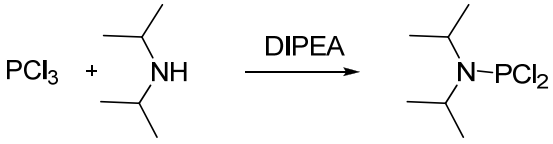

	eq	mmol	MW	mg	d (g/mL)	mL
DIPA	1.00	8.0	101.19	809.5	0.722	1.12
PCl_3	1.00	8.0	137.50	1100.0	2.57	0.43
DIPEA	1.00	8.0	129.25	1034.0	0.76	1.37
dry THF						20.00

A solution of DIPEA and PCl_3 in dry THF was cooled to 0°C, then diisopropylamine was added dropwise by means of syringe. The mixture was warmed to room temperature and stirred for 12 h. After this time, the generated ammonium salts were filtered through a celite pad under inert atmosphere, and washed with hexane (3 x10 mL). The solvent was removed by nitrogen flux, to give a pale yellow oil, that was employed in the next step without further purification.

^{1}H-NMR (200 MHz, $CDCl_3$): δ 3.40 (m, 1H), 3.20 (m, 1H), 1.45 (m, 9H).
^{31}P-NMR (300 MHz, $CDCl_3$): δ 4.95.

*Preparation of compound **107***

Method a:

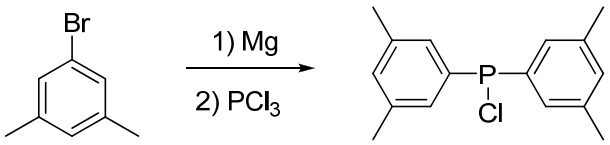

	eq	mmol	MW	mg	d (g/mL)	mL
1-bromo-3,5-dimethylbenzene	1	10	185.07	1850.7	1.362	1.36
PCl_3	2.00	20.0	137.50	2750.0	2.57	1.07
Mg turnings	1.00	10.0	24.30	243.0		
dry THF						15.00

In a three-necked round-bottom flask equipped with a reflux condenser and a dropping funnel, magnesium turnings were suspended in dry THF (2.5 mL). A solution of bromo-3,5-dimethylbenzene in dry THF (2.5 mL) was slowly added by the dropping funnel so that the reaction warmed up. An oil bath was used in order to keep the temperature constant (65°C) until the magnesium disappeared; then, the reaction was allowed to cool to room temperature.

To a stirred solution of PCl_3 in dry THF (10 mL) cooled to 0°C, the Grignard reagent was added dropwise *via* a syringe. The dark solution was allowed to stir at room temperature overnight. Then, the generated magnesium salts were filtered off through a celite pad under inert atmosphere, and washed with hexane (3 x10 mL). The solvent and the excess of PCl_3 were removed by rotary evaporation under vacuum, giving a pale yellow solid that was stored under nitrogen atmosphere (this compound is very sensible to the oxygen!).

^{31}P-NMR of the crude product showed the presence of two species at 39.6 ppm and 30 ppm (PCl_3 signal is at 220 ppm). Attempts to purify the product by distillation in order to separate mono and bis derivatives failed, giving only extensive degradation of the products.

Method b:

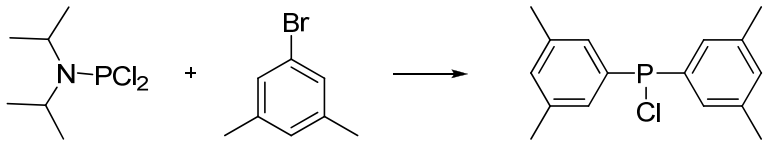

	eq	mmol	MW	mg	d (g/mL)	mL
1-bromo-3,5-dimethylbenzene	2.00	14.72	185.07	2724	1.362	2.00
compound **108**	1.00	7.36	202.60	1491.0		
Mg turnings	2.00	14.72	24.30	357.7		
HCl 2M (Et_2O)	2.00	14.72				7.36
dry THF						10.00

In a three-necked round-bottom flask equipped with a reflux condenser and a dropping funnel, magnesium turnings were suspended in dry THF (2.5 mL). A solution of bromo-3,5-dimethylbenzene in dry THF (2.5 mL) was slowly added by means of a dropping funnel so that the reaction warmed up. An oil bath was used in order to keep the temperature constant (65°C) until the magnesium disappeared; then, the reaction was allowed to cool to room temperature.

To a stirred solution of compound **108** in dry THF (5 mL) cooled to 0°C, the Grignard reagent was added dropwise *via* a syringe. The dark solution was allowed to warm at room temperature and stirred for 2 h, then, the solvent was removed by rotary evaporation under vacuum. The slurry obtained was washed with cyclohexane (5 x 10 mL) under inert atmosphere.

^{31}P-NMR and ^{1}H-NMR of the crude product showed only the presence of degraded by-products.

Method c:

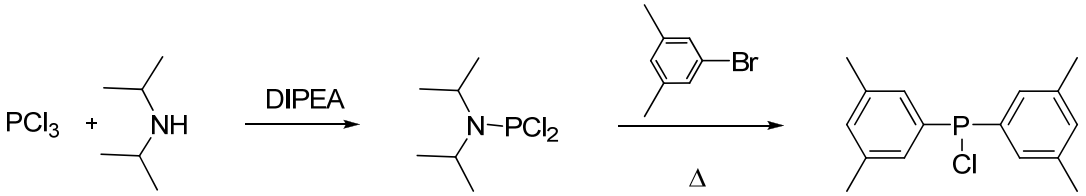

	eq	mmol	MW	mg	d (g/mL)	mL
1-bromo-3,5-dimethylbenzene	3.00	30.00	185.07	5552.1	1.362	4.08
PCl_3	1.00	10.00	135.70	1357.0	2.57	0.53
DIPA	1.00	10.00	101.19	1011.9	0.72	1.40
TEA	5.00	50.00	101.00	5050.0	0.73	6.96
Mg turnings	3.00	30.00	24.30	729.0		
HCl 2M (Et_2O)	2.00	20.00				10.00
dry THF						75.00

A solution of TEA and PCl_3 in dry THF (35 mL) was cooled to 0°C, then a solution of DIPA in dry THF (35 mL) was added dropwise by means of syringe over a period of 1 h. The mixture was warmed to room temperature and stirred for 12 h.

In a three-necked round-bottom flask equipped with a reflux condenser and a dropping funnel, magnesium turnings were suspended in dry THF (2.5 mL). A solution of bromo-3,5-dimethylbenzene in THF (2.5 mL) was slowly added by means of a dropping funnel so that the reaction warmed up. An oil bath was used in order to keep the temperature constant (65°C) until the magnesium disappeared; then the reaction was allowed to cool to room temperature.

After this time, the mixture previously prepared was cooled to -30°C and the Grignard reagent was added dropwise *via* syringe. The dark solution was allowed to warm to room temperature and stirred for 30 min, then was refluxed for 18 h. Subsequently, the mixture was concentrated under reduced pressure (about 10 mL) and 10 mL of cyclohexane were added. This solution was filtered through a celite pad and concentrated under reduced pressure (to about 15 mL).

Preliminary ^{1}H-NMR and ^{31}P-NMR investigations confirm the presence of *N,N*-diisopropyl-1,1-(3,5dimethyl)phenylphosphin amine (P signal at 86.22 ppm), according to literature data.[235]

HCl 2M in Et_2O was added to this solution cooled to 0°C, then the reaction was warmed at room temperature and stirred for an additional 72 h. After this time, the mixture was filtered through a celite pad and concentrated under reduced pressure.

^{31}P-NMR and ^{1}H-NMR of the crude product showed only the presence of degraded by-products.

6.6 Synthesis of diarylphosphoric chloride

*Preparation of compounds **109** and **110***

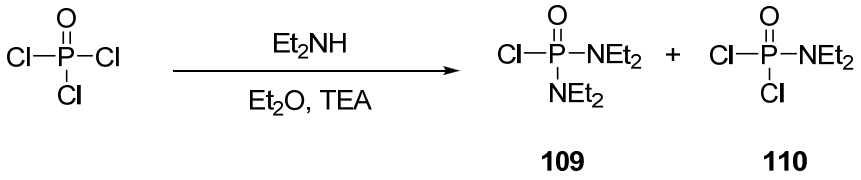

	eq	mmol	MW	mg	d (g/mL)	mL
DEA	2.00	48.10	73.14	3518	0.707	4.98
TEA	2.00	48.10	101.00	4858.1	0.73	6.69
$POCl_3$	0.90	21.64	152.00	3290.0	1.65	2.00
dry Et_2O						60.00

A solution of freshly distilled $POCl_3$ in dry Et_2O (40 mL) was cooled to 0°C under nitrogen atmosphere, then a solution of DEA and TEA in dry Et_2O (20 mL) was added by dropping funnel.

The mixture was subsequently warmed to room temperature and stirred for 72 h. After this time, the generated ammonium salts were filtered off through a celite pad under inert atmosphere, and washed with hexane (3 x10 mL).

The mixture was treated with a saturated aqueous solution of $NaHCO_3$ (10 mL) and brine (10 mL), dried over Na_2SO_4 and the solvent was removed by rotary evaporation. The crude product (pale yellow oil) was purified by flash chromatography on silica gel.

TLC of the crude product (1:1 hexane/ethyl acetate stained with permanganate):

compound **109** present a R_f of 0.30;

compound **110** present a R_f of 0.86.

Flash chromatography (diameter: 5 cm, h: 12 cm, eluent: 1:1 hexane/ethyl acetate).

A purification through silica gel gave compound **109** with 20% yield and compound **110** with 60% yield.

^{1}H-NMR (300 MHz, $CDCl_3$):

Compound **109**: δ 3.15 (q, *J* = 8 Hz, *J* = 5.3 Hz, 8H), 1.15 (t, *J* = 5.3 Hz, 12H).

Compound **110**: δ 3.30 (q, *J* = 7.9 Hz, *J* = 5.2 Hz, 4H), 1.20 (t, *J* = 5.2 Hz, 6H).

Mass (ESI+):

Compound **109**: *m/z* = 227.1 [M + 1].

Compound **110**: *m/z* = 190.2 [M + 1].

6.7 Synthesis of diarylphosphoric acids and esters [236]

*Preparation of compound **111***

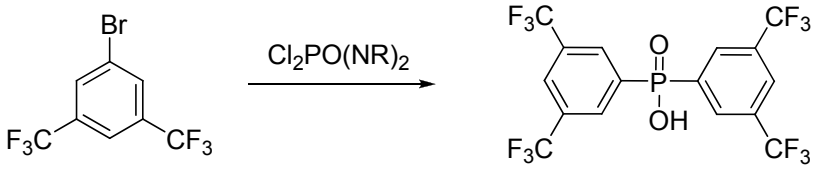

	eq	mmol	MW	mg	d (g/mL)	mL
1-bromo-3,5-bis(trifluoromethyl)benzene	1.00	10.24	293.00	3000	1.699	1.77
n-BuLi 1.6 M	1.10	11.26				7.04
$Me_2NP(O)Cl_2$	0.50	5.12	161.96	829.1	1.36	0.61
dry THF						25.00

A solution of 1-bromo-3,5-bis(trifluoromethyl)benzene in dry THF was cooled to -78°C in a three-necked round-bottom flask equipped with a reflux condenser and a dropping funnel under nitrogen atmosphere. Subsequently, a solution of *n*-BuLi was added dropwise over a period of 1 h, then $Me_2NP(O)Cl_2$ (neat) was added. The mixture was warmed to room temperature and stirred for 2 h and then refluxed for an additional 2 h.
After this time, the reaction was diluted with water (20 mL), then washed with saturated aq NH_4Cl (20 mL). The organic layer was separated, concentrated aq HCl (20 mL) was added and the mixture was heated at 80°C for 4 h.
The resulting precipitate was isolated by filtration and added to 0.5 M aq NaOH (60 mL). The slurry was then filtered to remove insoluble matter and the resulting solution was acidified with 20% aq H_2SO_4. The resulting precipitate was isolated as a white solid by filtration.

^{31}P-NMR and ^{1}H-NMR of the crude product showed only the presence of debrominated starting material with trace of products containing a butyl chain on the aromatic ring.

*Preparation of compound **112***

	eq	mmol	MW	mg	d (g/mL)	mL
1-bromo-3,5-dimethylbenzene	1.00	14.72	185.07	2724	1.362	2.00
n- BuLi 1.6 M	1.10	16.19				10.12
$Me_2NP(O)Cl_2$	0.50	7.36	161.96	1191.9	1.36	0.88
dry THF						20.00

The synthetic procedure is identical to that reported for compound **111.**

A white solid is obtained in 60% yield.

^{1}H-NMR (200 MHz, $CDCl_3$): δ 7.36 (d, J = 12.9, 4H), 7.07 (s, 2H), 6.23 (s, 1H), 2.26 (s, 12H).

^{31}P-NMR (121.4 MHz, $CDCl_3$): δ 36.0.

*Preparation of compound **113***

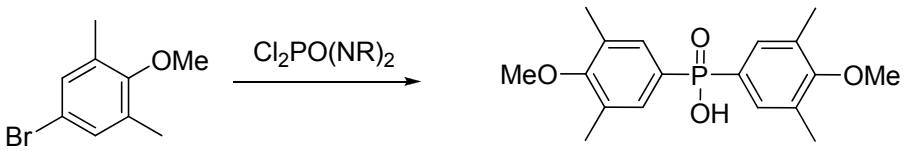

	eq	mmol	MW	mg	d (g/mL)	mL
4-Bromo-2,6-dimethylanisole	1.00	12.66	215.09	2724	1.347	2.02
n- BuLi 1.6 M	1.10	13.93				8.71
$Me_2NP(O)Cl_2$	0.50	6.33	161.96	1025.6	1.36	0.75
dry THF						20.00

The synthetic procedure is identical to that reported for compound **111.**
A white solid is obtained in 12% yield.

^{1}H-NMR (200 MHz, $CDCl_3$): 7.51 (d, J = 9.4 Hz, 4H), 3.78 (s, 6H),2.30 (s, 12H).
^{31}P-NMR (121.4 MHz, $CDCl_3$): 45.2.

The intermediate of the reaction was isolated: [237]

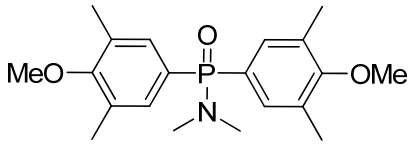

^{1}H-NMR (300 MHz, $CDCl_3$): δ 7.47 (d, J = 11.6 Hz, 4H), 3.69 (s, 6H), 2.61 (dd, J = 10.86 Hz, J = 1.78 Hz, 6H), 2.25 (s, 12H).
^{31}P-NMR (121.4 MHz, $CDCl_3$): δ 23.62.

*Preparation of compound **116***

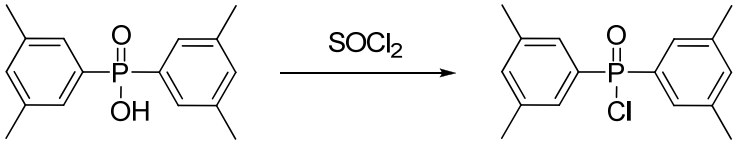

	eq	mmol	MW	mg	d (g/mL)	mL
compound **112**	1.00	5.47	274.1	1500		
$SOCl_2$						10.00

A solution of phosphinic acid **112** in thionyl chloride (10 mL) was heated at 60°C for 5 h. The reaction mixture was filtered and then diluted with hexanes (20 mL). The resulting precipitate was filtered to give phosphonyl chloride in 60% yield as a white solid, that was used immediately in the next step.

^{1}H-NMR (300 MHz, $CDCl_3$): δ 7.39 (m, 4H), 7.09 (s, 2H), 2.27 (s, 12H).
^{31}P-NMR (121.4 MHz, $CDCl_3$): δ 27.5.

*Preparation of compound **119***

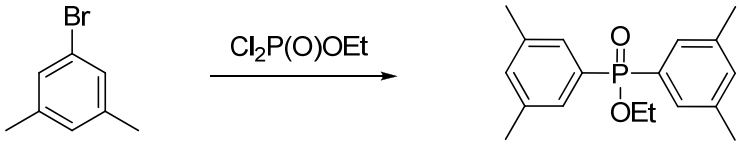

	eq	mmol	MW	mg	d (g/mL)	mL
1-bromo-3,5-dimethylbenzene	2.00	14.72	185.07	2724	1.362	2.00
n- BuLi 1.6 M	2.20	16.19				10.12
$Cl_2P(O)OEt$	1.00	7.36	163.00	1199.6	1.37	0.87
dry THF						20.00

A solution of 1-bromo-3,5-bis(trifluoromethyl)benzene in dry THF was cooled to -78°C under nitrogen atmosphere, then a solution of *n*-BuLi was added dropwise. The mixture was stirred for 40 min at -78°C, then $Cl_2P(O)OEt$ (neat) was added. Subsequently, the mixture was stirred for 6 h at -78°C and then warmed to room temperature and stirred for an additional 12 h.

The reaction, followed by TLC using 6:4 hexane/ethyl acetate as eluent, was then quenched by the addition of water (10 mL) and diluted with AcOEt (30 mL). The organic layer was separated, and the aqueous layer was extracted with AcOEt (10 mL). The organic layers were dried over Na_2SO_4 and the solvent was removed by rotary evaporation to give a white oil that was purified by flash chromatography on silica gel.

TLC of the crude product (8:2 hexane/ethyl acetate): the product has a R_f of 0.14.

Flash chromatography (diameter: 3 cm, h: 18 cm, eluent: 8:2 hexane/ethyl acetate).

A purification through silica gel gave the desired product with 63% yield.

^{1}H-NMR (200 MHz, $CDCl_3$): δ 7.42 (d, *J* = 13.0 Hz, 2H), 7.27 (d, *J* = 13.0 Hz, 2H), 7.14 (m, 2H), 4.10 (m, 2H), 2.32 (d, *J* = 4.1 Hz, 12H), 1.35 (m, 3H).

^{31}P-NMR (121.4 MHz, $CDCl_3$) δ 30.48.

*Preparation of compound **120***

	eq	mmol	MW	mg	d (g/mL)	mL
4-Bromo-2,6-dimethylanisole	2.00	12.66	215.09	2724	1.347	2.02
n- BuLi 1.6 M	2.20	13.93				8.71
$Cl_2P(O)OEt$	1.00	6.33	163.00	1032.2	1.37	0.75
dry THF						20.00

The synthetic procedure is identical to that reported for compound **119.**

A white solid is obtained in 60% yield.

^{1}H-NMR (200 MHz, $CDCl_3$): 7.45 (d, J = 12.14 Hz, 4H), 4.05 (m, 2H), 3.72 (s, 6H), 2.28 (s, 12H), 1.35 (m, 3H).

^{31}P-NMR (121.4 MHz, $CDCl_3$): 33.18.

*Preparation of compound **121***

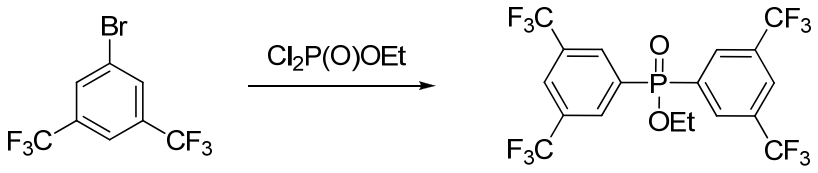

	eq	mmol	MW	mg	d (g/mL)	mL
1-bromo-3,5-bis(trifluoromethyl)benzene	2.00	6.83	293.00	2000	1.699	1.18
n- BuLi 1.6 M	2.20	7.51				4.69
$Cl_2NP(O)OEt$	1.00	3.41	163.00	556.3	1.37	0.41
dry THF						25.00

The synthetic procedure is identical to that reported for compound **119**, but compound **121** was not isolated because of the hydrolysis process that give the corresponding **111** product as a white solid in 80% yield.

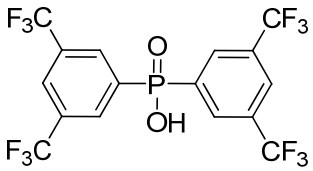

^{1}H-NMR (300 MHz, $CDCl_3$): δ 8.15-8.05 (m, 4 H), 8.00-7.90 (m, 4 H).

^{31}P-NMR (121.4 MHz, $CDCl_3$): 17.8.

6.8 Synthesis of TetraMe-BITIOPO derivatives

General procedures

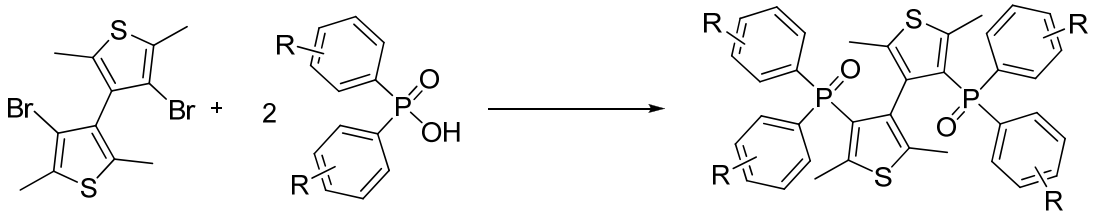

85

A solution of diarylphosphoric acid or ester (2.5 eq) in thionyl chloride (2 mL/mmol substrate) was heated at 60°C for 5 h, then thionyl chloride was removed by rotary evaporation and gentle hating under nitrogen flux.

A solution of *n*-BuLi (2.2 eq, 4.81 mmol) was added to a solution of compound **85** (1 eq, 2.19 mmol) in dry THF (20 mL) at -55°C under nitrogen atmosphere. After 15 min of stirring at this temperature, the solution of phosphoric chloride in THF (5 mL) previously prepared was added dropwise *via* syringe. This reaction mixture was stirred at -55°C for 12 h, then was warmed to room temperature and stirred for an additional 12 h.

After this time, a solution of 5% HCl (15 mL) and AcOEt (20 mL) were added. The organic layer was separated, and the aqueous layer was extracted with AcOEt (2 × 20 mL). The organic layers were then dried over Na_2SO_4 filtered and concentrated under vacuum to give the crude product that was purified by column chromatography on silica gel.

CF_3-MPP-TetraMe-BITIOPO (catalyst 122)

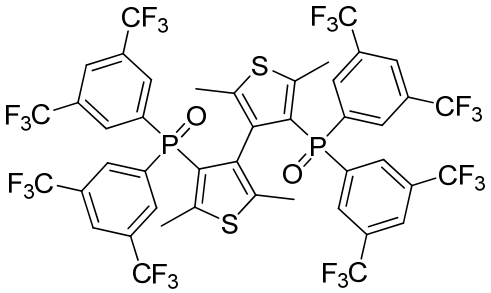

Flash chromatography (diameter: 2 cm, h: 18 cm, eluent: DCM/MeOH 98:2).

A purification through silica gel allowed to recover a partial amount of phosphoric acid and byproducts.

MPP-tetraMe-BITIOPO (catalyst 123)

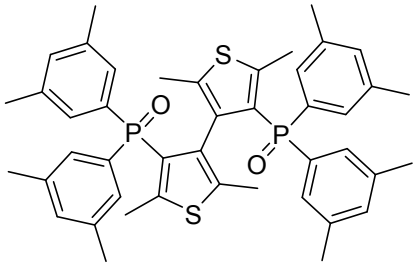

Flash chromatography (diameter: 2 cm, h: 18 cm, eluent: DCM/MeOH 98:2). R_f = 0.18

A purification through silica gel gave the desired product with 26% yield.

^{1}H-NMR (200 MHz, $CDCl_3$): δ 7.35 (d, *J* = 12.8 Hz, 4H), 7.08 (t, *J* = 15.3 Hz, 8H), 2.30 (s, 12H), 2.13 (s, 18H), 1.69 (s, 6H).

^{31}P-NMR (121.4 MHz, $CDCl_3$): δ 25.06.

HPLC: Chiralcel OD column [eluent: Hex:iPA:DEA 95:5:0.1, flux: 0.8 ml/min, detection: 280 nm; t_1= 8.4 min ((-)-*enantiomer*) t_2= 10.8 min ((+)-*enantiomer*).

Racemic mixture:

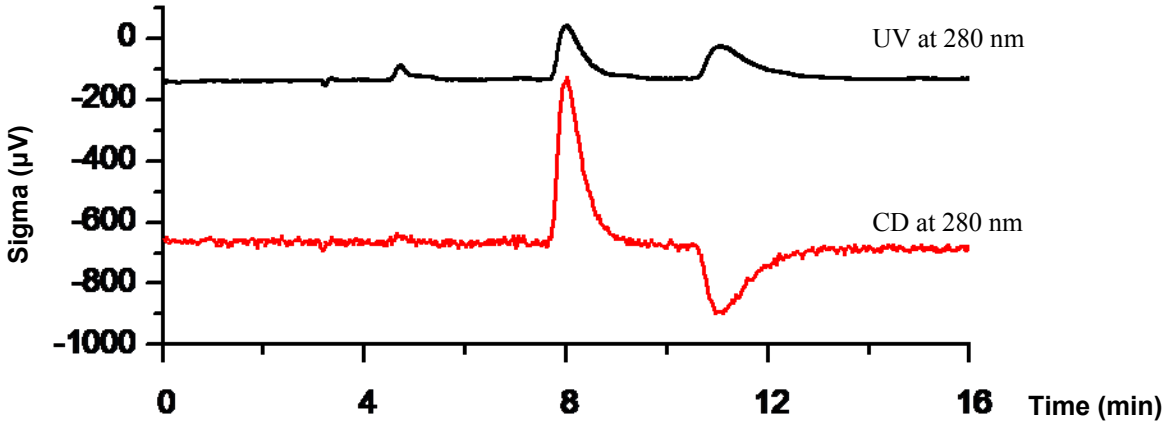

First eluted enantiomer:

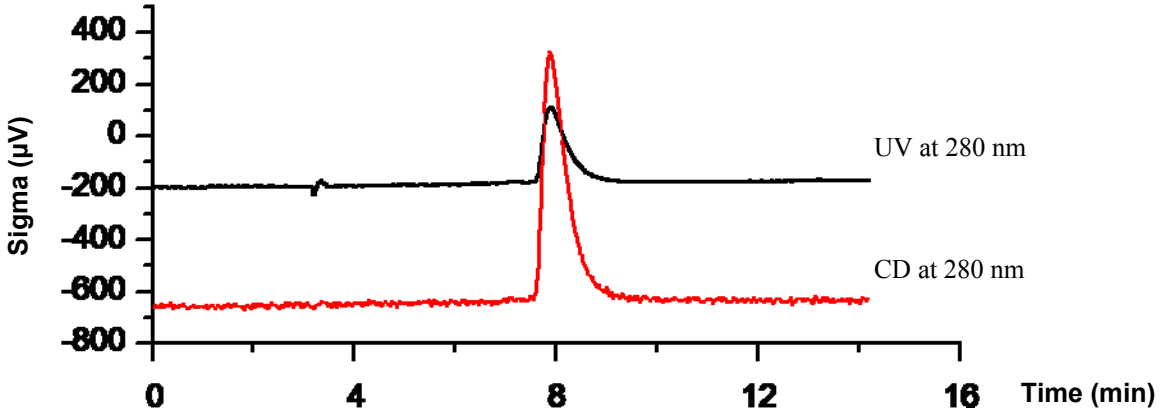

$[\alpha]_D^{25}$ = - 56 (c 0.1, EtOH, λ = 589 nm); ee > 99%.

Second eluted enantiomer:

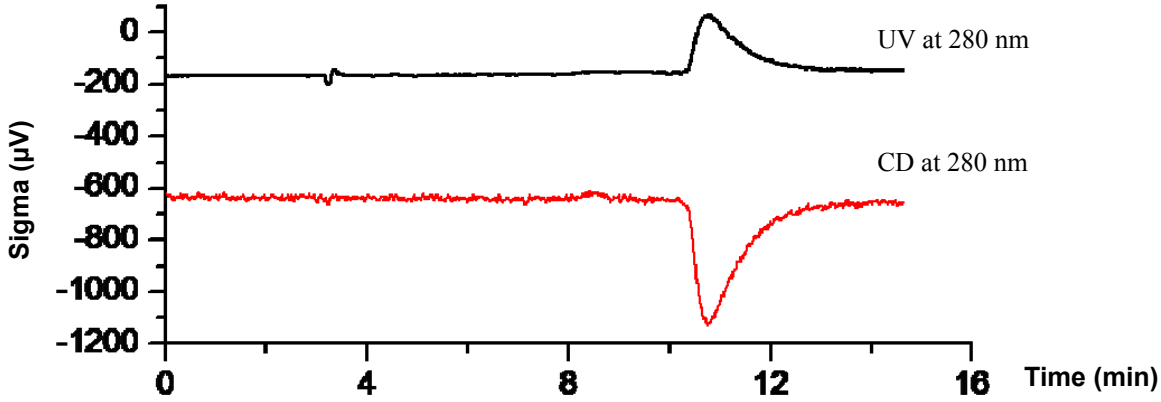

$[\alpha]_D^{25}$ = + 54 (c 0.1, EtOH, λ = 589 nm); ee > 99%.

CD: Circular dichroism spectra of the first eluted ((-), grey) and second eluted ((+), black) of MPP-tetraMe-BITIOPO [solvent: ethanol, concentration: 0.3 mg/ml].

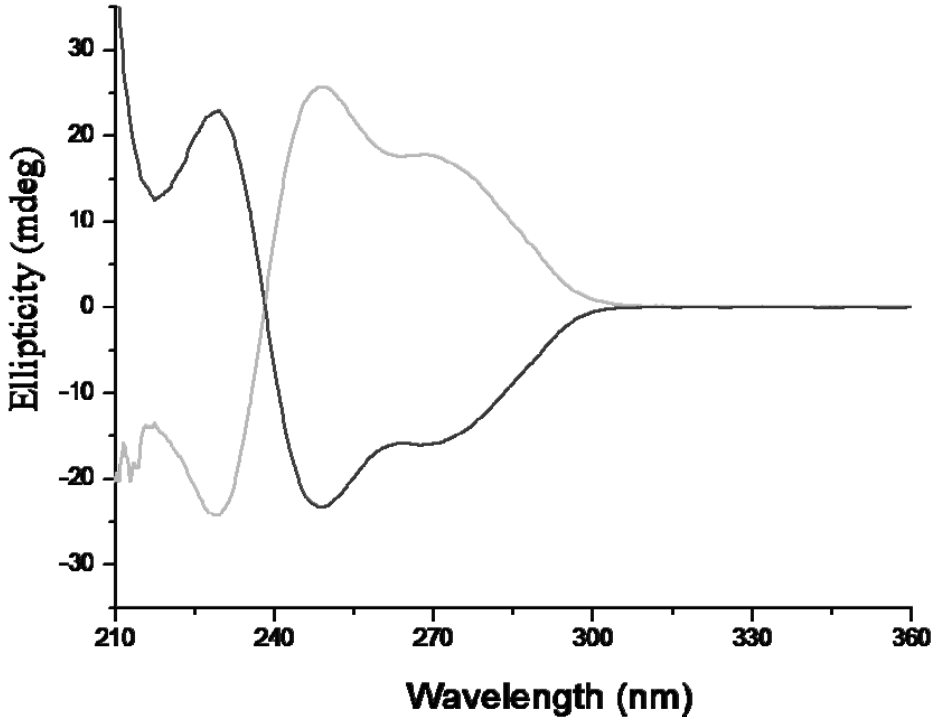

ORD: optical rotary dispersion curves of the first (grey) and second (black) eluted enantiomer of MPP-tetraMe-BITIOPO in ethanol.

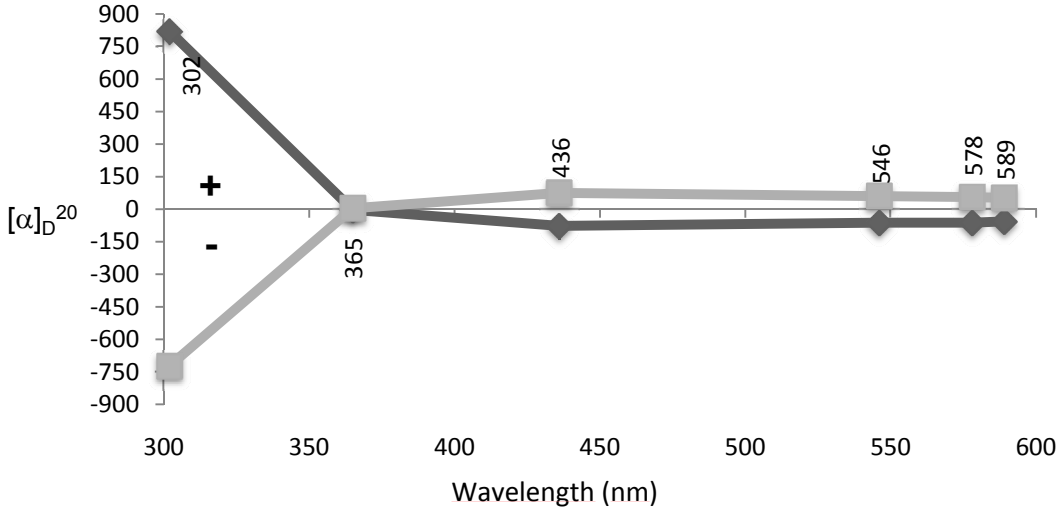

PMP-tetraMe-BITIOPO (catalyst 124)

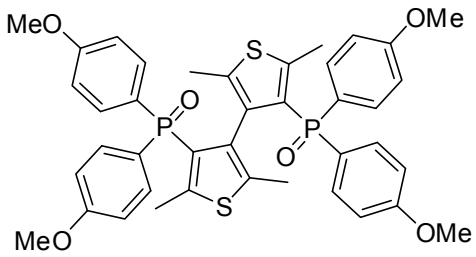

Flash chromatography (diameter: 2 cm, h: 18 cm, eluent: DCM/MeOH 98:2). R_f = 0.23

A purification through silica gel gave the desired product with 60% yield.

^{1}H-NMR (200 MHz, $CDCl_3$): δ 7.44 (dt, *J* = 11.0 Hz, *J* = 24 Hz, 8H), 6.83 (dd, *J* = 18 Hz, *J* = 8.4 Hz, 8H), 3.81 (s, 6H), 3.78 (s, 6H), 2.03 (s, 6H), 1.67 (s, 2H).

^{31}P-NMR (121.4 MHz, $CDCl_3$): δ 21.69.

Mass (ESI+): *m/z* = 473.3 [M + 1] and 765.3 [M + Na].

HPLC: Chiralcel OD-H column [eluent: Hex:*i*PA 8:2, detection: 230 nm; t_1= 8.7 min ((-)-*enantiomer*) t_2= 27.8 min ((+)-*enantiomer*)].

First eluted $[\alpha]_D^{25}$ = - 12.87 (c 0.22, C_6H_6, λ = 589 nm); ee > 99%.

Second eluted $[\alpha]_D^{25}$ = + 14.45 (c 0.28, C_6H_6, λ = 589 nm); ee > 99%.

MMP-tetraMe-BITIOPO (catalyst 125)

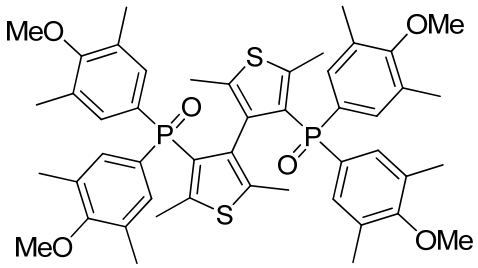

Flash chromatography (diameter: 2 cm, h: 18 cm, eluent: DCM/MeOH 98:2). R_f = 0.20

A purification through silica gel gave the desired product with 7% yield.

^{1}H-NMR (200 MHz, $CDCl_3$): δ 7.77-7.46 (m, 4H), 6.86 (dd, *J* = 15.0 Hz, *J* = 7.4 Hz, 4H), 3.81 (s, 6H), 3.78 (s, 6H), 2.02 (s, 6H), 1.57 (s, 6H).

^{31}P-NMR (121.4 MHz, $CDCl_3$): δ 22.94

HPLC: Chiralcel OD column [eluent: Hex:*i*PA 7:3, detection: 230 nm; t_1= 10.7 min ((-)-*enantiomer*), t_2= 17.0 min ((+)-*enantiomer*)].

6.9 Synthesis of TetraMe-BITIOPO derivatives: a novel approach

*Preparation of compound **128***

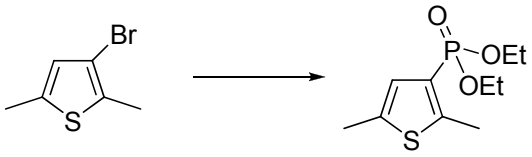

Method a: [201]

$Pd(PPh_3)_4$ (0.05 eq, 0.05 mmol), Cs_2CO_3 (1.2 eq, 1.2 mmol) and 3-bromo-2,5-dimethyl thiophene (1 eq, 1 mmol), and *H*-diethyl phosphonate (2 eq, 2 mmol) were dissolved in THF (4 mL) and reacted in a microwave reactor (PW = 200 W; T = 120°C; time: 20 min).

After cooling down, the mixture was washed with water (10 mL) and extracted with AcOEt (2 x 10 mL). The organic layers were then dried over Na_2SO_4 filtered and concentrated under vacuum to give an oil that was purified by column chromatography on silica gel.

A purification through silica gel (eluent hexane:ethyl acetate 9:1) only allowed to recover the starting compounds unreacted.

Method b: [202]

Dry EtOH (5 mL) was previously degassed under a steam of nitrogen for nearly half an hour. A round bottom flask equipped with a reflux condenser and a magnetic stirring bar was charged with $Pd(OAc)_2$ (0.05 eq, 0.05 mmol), TEA (1.5 eq, 1.5 mmol) and BINAP (0.08 eq, 0.08 mmol) dissolved in THF (5 mL). Subsequently, 3-bromo-2,5-dimethyl thiophene (1 eq, 1 mmol) was added, and after 10 min the *H*-diethyl phosphonate (1.2 eq, 1.2 mmol) was introduced. The reaction mixture was stirred at reflux for 16 h, and the resulting yellow solution was diluted with AcOEt (10 mL) and washed with 1 N HCl (10 mL), sat. aq $NaHCO_3$ (10 mL) and brine (10 mL). The organic layer was dried over Na_2SO_4, filtered and concentrated under vacuum to give a oil that was purified by column chromatography on silica gel.

A purification through silica gel (eluent hexane:AcOEt 9:1) only allowed to partially recover starting compounds unreacted and debrominated 2,5-dimethyl thiophene.

Method c:

A solution of 3-bromo-2,5-dimethyl thiophene (1 eq, 1 mmol) in dry THF (10 mL) was cooled to -60°C under nitrogen atmosphere, then a solution of *n*-BuLi (1.1 eq, 1.1 mmol) was added dropwise. The mixture was stirred for 40 min at -60°C, then a solution of $ClPO(OEt)_2$ (2 eq, 2 mmol) in dry THF (2 mL) was added. Subsequently the mixture was warmed to room temperature and stirred for 16 h.

The reaction was then quenched by the addition of water (10 mL) and diluted with DCM (10 mL). The organic layer was separated, and the aqueous layer was extracted with DCM (2 x 10 mL). The organic layers were dried over Na_2SO_4 and the solvent was removed by rotary evaporation to give a brown oil that was purified by flash chromatography on silica gel.

Flash chromatography (diameter: 1.5 cm, h: 15 cm, eluent: 6:7 hexane/ethyl acetate), $R_f = 0.35$. A purification through silica gel gave the desired product with 58% yield.

^{1}H-NMR (300 MHz, $CDCl_3$): δ 6.75 (s, 1H), 4.10-3.90 (m, 4H), 2.55 (s, 3H), 2.30 (s, 3H), 1.35-1.20 (m, 6H).

^{31}P-NMR (121.4 MHz, $CDCl_3$) δ 14.60.

Mass (ESI+): m/z = 249.2 [M + 1].

*Preparation of compound **129***

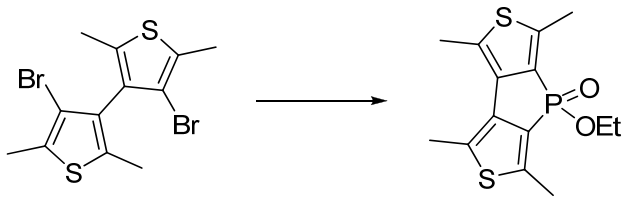

	eq	mmol	MW	mg	d (g/mL)	mL
compound **85**	1.00	0.79	380.16	300		
n- BuLi 1.6 M	2.10	1.66				1.04
$ClPO(OEt)_2$	3.50	2.76	172.55	476.6	1.19	0.40
dry THF						10.00

The synthetic procedure is identical to that reported for compound **128**, method c**.**

Flash chromatography (diameter: 1.5 cm, h: 15 cm, eluent: 1:1 hexane/ethyl acetate), R_f = 0.15

A purification through silica gel gave the desired product with 55% yield.

^{1}H-NMR (200 MHz, $CDCl_3$): δ 3.85 (m, 2H), 2.55 (s, 6H), 2.48 (s, 6H), 1.37-1.20 (m, 3H).

^{31}P-NMR (121.4 MHz, $CDCl_3$): δ 20.34.

Mass (ESI+): m/z = 312.9 [M + 1].

*Preparation of compound **130***

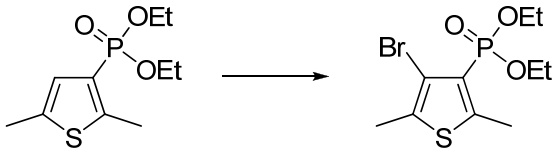

	eq	mmol	MW	mg	d (g/mL)	mL
compound **129**	1.00	6.04	248.28	1500.00		
NBS	1.00	6.04	177.98	1075.28		
Hydroquinone	0.002	0.012	110.11	1.33		
$CHCl_3$:AcOH						10.00

The synthetic procedure is identical to that reported for compound **83**.

Flash chromatography (diameter: 1.5 cm, h: 15 cm, eluent: ethyl acetate), $R_f = 0.45$
A purification through silica gel gave the desired product with 55% yield.

^{1}H-NMR (200 MHz, $CDCl_3$): δ 4.17-4.01 (m, 4H), 2.72 (d, J = 2.2 Hz, 3H), 2.33 (s, 3H), 1.27-1.07 (m, 6H).

*Preparation of compound **131*** [238]

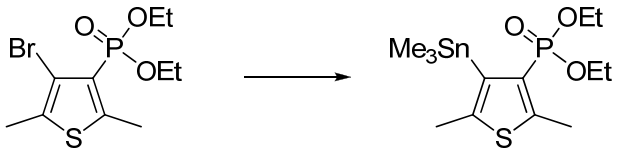

	eq	mmol	MW	mg	d (g/mL)	mL
compound **130**	1.00	1.22	327.05	400.00		
n- BuLi 1.6 M	1.50	1.83				1.144
Me_3SnCl 1M (Et_2O)	1.50	1.83				1.835
dry Et_2O						5.00

A solution of compound **130** in dry Et_2O was cooled to -78°C and treated dropwise with a 1.6 M solution of *n*-BuLi in hexane. The reaction mixture was stirred at that temperature for 30 min, and then a solution of Me_3SnCl in dry Et_2O was added dropwise within 10 min. The mixture was allowed to stand at -78°C for 1 h and then was slowly warmed to room temperature and stirred for an additional 18 h.

After this time, the solvent was removed under reduced pressure and the crude oil was diluted with cool Et_2O (10 mL). This solution was filtered and concentrated under vacuum to give the desired product as an oil in 40% yield. It was employed in the next step without further purification.

^{1}H-NMR (200 MHz, $CDCl_3$): δ 4.17-3.95 (m, 4H), 2.57 (m, 3H), 2.37 (m, 3H), 1.32-1.24 (m, 6H), 0.52 (t, J = 43.6 Hz, 9H).

*Preparation of compound **132*** [239]

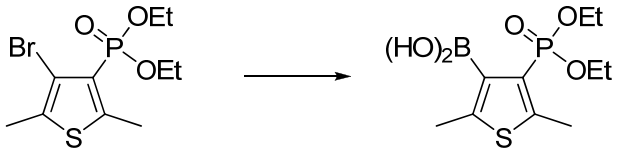

	eq	mmol	MW	mg	d (g/mL)	mL
compound **130**	1.00	0.92	327.05	300.00		
n- BuLi 1.6 M	1.00	0.92				1.144
$(MeO)_3B$	2.00	1.83	103.91	190.63	0.932	0.205
dry THF						2.00

A solution of compound **130** in dry THF was cooled to -60°C and treated dropwise with a 1.6 M solution of *n*-BuLi in hexane. The reaction mixture was stirred at that temperature for 1 h, and then triethyl borate was added dropwise within 10 min. The mixture was allowed to stand at -78°C for 1 h and then was slowly warmed to room temperature and stirred for an additional 18 h.

After this time, a solution of 10% HCl (1 mL) was added The resulting solution was stirred for 2 h at room temperature and extracted with ether. The combined organic layers were washed with brine, dried over Na_2SO_4 and concentrated *in vacuo*. The resulting solid was employed in the next step without further purification.

^{1}H-NMR (200 MHz, $CDCl_3$): δ 4.15-4.05 (m, 4H), 2.45 (s, 6), 1.48-1.32 (m, 6H).

*Preparation of compound **133***

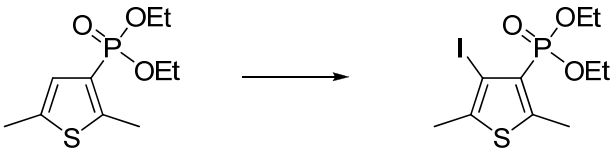

	eq	mmol	MW	mg	d (g/mL)	mL
compound **128**	1.00	2.83	247.74	700.00		
NIS	1.10	3.11	274.99	854.70		
CF_3COOH	0.3	0.85	45	38.14	1.48	0.026
dry CH_3CN						10.00

Compound **128** and trifluoroacetic acid were dissolved in dry CH_3CN (10 mL), then NIS was added and the mixture was refluxed for 24 h. The reaction was followed by TLC using 1:1 hexane/ethyl acetate as eluent. After cooling to room temperature, water (10 mL) and AcOEt (20 mL) were added. The organic layers was separated, dried over Na_2SO_4 and the solvent was removed by rotary evaporation to give a brown oil that was purified by flash chromatography on silica gel.

Flash chromatography (diameter: 2.5 cm, h: 20 cm, eluent: 1:1 hexane/ethyl acetate), $R_f = 0.43$. A purification through silica gel gave the desired product with 86% yield.

^{1}H-NMR (200 MHz, $CDCl_3$): δ 4.16-4.03 (m, 4H), 2.75 (d, J = 2.29 Hz, 3H), 2.36 (s, 3H), 1.34 (t, J = 7.0 Hz, 6H).
^{31}P-NMR (121.4 MHz, $CDCl_3$): δ 11.19.

*Preparation of compound **126***

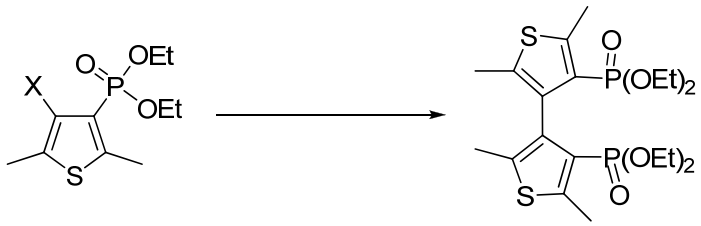

Method a:

A solution of compound **130** (1 eq, 1.22 mmol) in dry Et_2O (2 mL) was added dropwise to a solution of PhLi (1.1 eq, 1.34 mol) in dry Et_2O (4 ml) at -40°C in a spoon box system. After 30 min, the mixture was cooled to -60°C and $CuCl_2$ (1.1 eq, 1.34 mmol) was added; the mixture was allowed to warm to room temperature and stirred for 20h.

After this time, water (10 mL) and DCM (20 mL) were added. The organic layer was separated and the aqueous layer was extracted with DCM (2 × 15 mL). The organic layers were then dried over Na_2SO_4 and the solvent was removed by rotary evaporation.

The crude product was purified by flash chromatography on silica gel (8:2 hexane/ethyl acetate), but only unreacted compound **130** and debrominated compound **130** were obtained.

Method b:

Dry DME was previously degassed under a steam of nitrogen for nearly half an hour. A mixture of compound **130** (1 eq, 0.61 mmol), compound **131** (2 eq, 1.22 mmol), and $Pd(PPh_3)_4$ (0.1 eq, 0.061 mmol) was refluxed until complete consumption of the starting materials as judged by TLC. After that, the mixture was filtered, evaporated and the residue was purified by flash chromatography (8:2 hexane/ethyl acetate) but only unreacted compound **130** and debrominated compound **130** were recovered.

Method c:

Dry DME was previously degassed under a steam of nitrogen for nearly half an hour. Then, the degassed solvent (10 mL) was added *via* a cannula to a reaction vessel containing $Pd(OAc)_2$ (0.1 eq, 0.092 mmol) and PPh_3 (0.3 eq, 0.276 mmol). To this stirred solution, compound **130** (1 eq, 0.92 mmol) was added in one portion and the resulting mixture was stirred for 10 min. Then, compound **132** (1 eq, 0.92 mmol) and the

potassium carbonate solution (6 eq, 5.52 mmol in 2 mL H_2O) were added. The reaction was heated at reflux for 16 h. After cooling down, the mixture was diluted with DCM (10 mL) and the layers were separated. The organic phase was washed with a saturated solution of NH_4Cl (1 × 5 mL), dried over Na_2SO_4, filtered and evaporated in vacuum.
The residue was purified by flash chromatography (8:2 hexane/ethyl acetate) but only unreacted compound **130** and byproducts were obtained.

Method d:
A mixture of compound **133** (1 eq, 1.60 mmol) and Cu (5 eq, 8 mmol) was stirred and refluxed for 6 h without solvent, then the crude product was filtered off through a celite pad and washed with diethyl ether (20 mL), hexane (20 mL) and acetone (20 mL). The filtrate and washings were combined and the solvent was removed by rotary evaporation under vacuum, giving a pale brown solid, that was purified by flash chromatography on silica gel.

Flash chromatography (diameter: 2 cm, h: 20 cm, eluent: 1:1 hexane/ethyl acetate),
R_f = 0.45. A purification through silica gel gave the desired product with 68% yield.

^{1}H-NMR (200 MHz, $CDCl_3$): δ 3.95-3.78 (m, 8H), 2.63 (d, *J* = 2.29 Hz, 6H), 2.01 (d, *J* = 4.51 Hz, 6H), 1.22-1.08 (m, 12H).
^{31}P-NMR (121.4 MHz, $CDCl_3$): δ 13.70.
Mass (ESI+): *m/z* = 495.3 [M + 1] and 517.3 [M + Na].

*Preparation of compound **135***

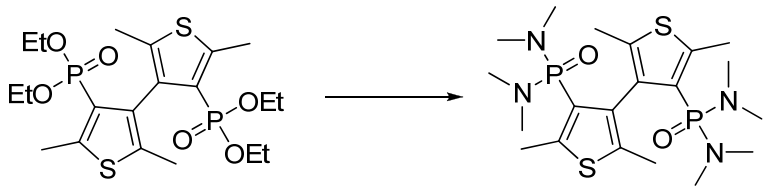

	eq	mmol	MW	mg	d (g/mL)	mL
compound **126**	1.00	0.44	494.54	218.00		
$NHMe_2$ 2M in THF	20.00	8.82				4.408
$SOCl_2$						2.00
dry THF						1.00

A solution of compound **126** in thionyl chloride (2 mL) was heated at 60°C for 72 h, then excess of solvent was removed by nitrogen flux and the crude product was diluted in dry THF (1 mL). The mixture was cooled to 0°C and dimethylamine was added dropwise; then, the reaction, was warmed to room temperature and stirred for 18h. The reaction was the diluted with dry DCM (15 mL) and dried over Na_2SO_4. The solvent was removed by rotary evaporation. After drying, a brown powder was obtained, that was purified by flash chromatography on silica gel.

Flash chromatography (diameter: 1 cm, h: 18 cm, eluent: 9:1 DCM/MeOH). R_f = 0.18.
A purification through silica gel gave the desired product with 16% yield.

^{1}H-NMR (300 MHz, $CDCl_3$): δ 2.68 (s, 6H), 2.60-2.30 (m, 24H), 1.95 (s, 6H).
^{31}P-NMR (121.4 MHz, $CDCl_3$): δ 23.51
Mass (ESI+): *m/z* = 491.1 [M + 1] and 513.3 [M + Na].

6.10 Catalysis reactions

6.10.1 General procedure for allylation of aldehydes with allyl trichlorosilane[142]

To a stirred solution of catalyst (0.1 eq, 0.03 mmol) in dichloromethane (2 mL) kept under nitrogen, a freshly distilled aldehyde (1 eq, 0.3 mmol) and DIPEA (3 eq, 0.154 mL, 0.9 mmol) were added in this order. The mixture was then cooled to the chosen temperature and allyl trichlorosilane (1.2 eq, 0.054 mL, 0.36 mmol) was added dropwise by means of a syringe. After 12 h stirring at 0°C (or 48 h if the temperature is -20°C) the reaction was quenched by the addition of a saturated aqueous solution of $NaHCO_3$ (1 mL). The mixture was allowed to warm up to room temperature and water (2 mL) and AcOEt (5 mL) were added. The organic phase was separated and dried over Na_2SO_4, filtered, and concentrated under vacuum at room temperature to afford the crude products. These were purified by flash chromatography with different hexane:AcOEt mixtures as eluant. Yield and ee for each reaction are indicated in the tables of previous chapters.

6.10.2 General procedure for allylation of aldehydes with allyltributylstannane[174]

To a stirred solution of catalyst (0.1 eq, 0.05 mmol) in dichloromethane (1 mL) kept under nitrogen, allyltributylstannane (1 eq, 0.5 mmol) was added. The mixture was then cooled to 0°C and after 20 min, freshly distilled $SiCl_4$ (2 eq, 1 mmol) and aldehyde (1 eq, 0.5 mmol) were added dropwise by means of a syringe. The resulting mixture was allowed to stir at 0°C for 16 h, whereupon the cold reaction mixture was poured into a rapidly stirring solution of 1/1 sat. aq. KF/1M KH_2PO_4 (5 mL). This biphasic mixture was stirred vigorously for 2 h after which the mixture was filtered and the aqueous layer was

washed with DCM (2 x 10 mL). The combined organic extracts were dried over Na_2SO_4, filtered and the filtrate was concentrated *in vacuo.*

These crude products were purified by flash chromatography with different hexane:ethyl acetate mixtures as eluent. Yield and ee for each reaction are indicated in the tables of previous chapters.

6.10.3 Characterization of allylation products

A-1: *1-Phenylbut-3-en-1-ol*[240]

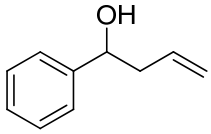

TLC of the product (9:1 hexane/ethyl acetate): the product has a R_f of 0.31.

^{1}H-NMR (300 MHz, $CDCl_3$): δ 7.29-7.17 (m, 5H), 5.79-5.68 (m, 1H), 5.12-5.06 (m, 2H), 4.65 (dd, *J* = 7.6 Hz, *J* = 5.6 Hz, 1H), 2.47-2.39 (m, 2H), 1.93 (br s, 1H).

^{13}C-NMR (300 MHz, $CDCl_3$): δ 143.8, 134.4, 128.3, 127.5, 125.7, 118.4, 73.2, 43.8.

The enantiomeric excess was determined by chiral HPLC with Chiralcel OD-H column [eluent: 95:5 Hex/IPA; 0.5 mL/min flow rate, detection: 210 nm; t_R 14.4 min, t_R 17.2 min].

A-2: *1-(4-Nitrophenyl)but-3-en-1-ol*[241]

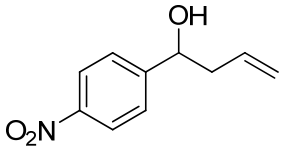

TLC of the product (8:2 hexane/ethyl acetate): the product has a R_f of 0.26.

^{1}H-NMR (300 MHz, $CDCl_3$): δ 8.18 (d, *J* = 8.8 Hz, 2H), 7.52 (d, *J* = 8.8 Hz, 2H), 5.83-5.72 (m, 1H), 5.21-5.14 (m, 2H), 4.85 (dd, *J* = 8.0, *J* = 4.8 Hz, 1H), 2.59-2.52 (m, 1H), 2.49-2.40 (m, 1H), 2.32 (br s, 1H).

^{13}C- NMR (300 MHz, $CDCl_3$): δ 151.3, 147.4, 133.4, 126.7, 123.8, 119.9, 72.3, 44.1.

The enantiomeric excess was determined by chiral HPLC with Chiralcel AD column [eluent: 97:3 Hex/IPA; 0.8 mL/min flow rate, detection: 210 nm; t_R 31.4 min, t_R 33.1 min].

6.10.4 General procedure for the synthesis of keto-imines

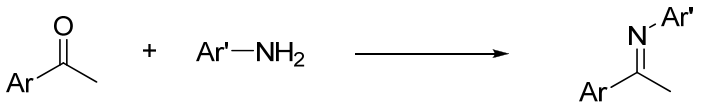

Method a: [242]

In a typical experiment: amine (1 eq) was reacted in toluene (2.5 mL for 5 mmol of reagent) with ketone (1 eq) in the presence of montmorillonite (250 mg for 5 mmol of reagent) in a microwave reactor (PW = 200 W; T = 130°C; time: 4 h and 30 min). The product was purified by fractional distillation at reduced pressure.

Method b:

In a typical experiment: amine (3 eq, 16.8 mmol) was reacted in benzene (7 mL) with β-ketoester (1 eq, 5.6 mmol) under inert atmosphere. The mixture was refluxed for 24h with a Dean Stark system, then the solvent was removed by rotary evaporation under vacuum. The product was purified by chromatographic column.

Keto-imine 67*: N-phenyl-(1-phenylethylidene) amine (method a)*

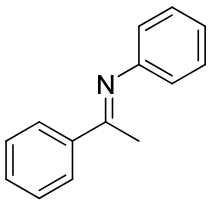

Yield after distillation: 70%.

^{1}H-NMR (300 MHz, $CDCl_3$): δ 8.00-7.95 (m, 2H), 7.49-7.41 (m, 3H), 7.39-7.32 (m, 2H), 7.12-7.06 (m, 1H), 6.83-6.77 (m, 2 H), 2.24 (s, 3H).

Keto-imine 92*: methyl-3-(N-benzylamino)-3-phenylpropenoate (method b)*

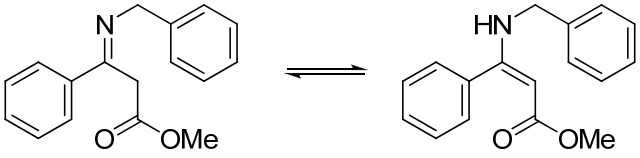

Yield after chromatographic purification: 45%.

^{1}H-NMR (300 MHz, $CDCl_3$): δ 8.91 (br, 1H), 7.38-7.15 (m, 10H), 4.69 (s 1H), 4.27 (d, J = 6.0 Hz, 2H), 3.69 (s, 3H).

6.10.5 General procedure for reduction of keto-imines with trichlorosilane

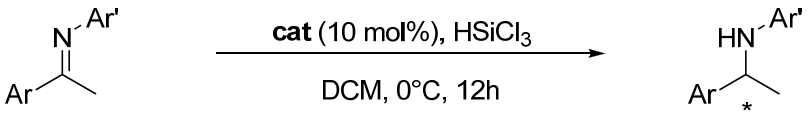

B

To a stirred solution of catalyst (0.1 eq, 0.015 mmol) in DCM (2 mL), the imine (1 eq, 0.15 mmol) was added. The mixture was then cooled to 0°C and trichlorosilane (3.5 eq, 0.525 mmol) was added dropwise by means of a syringe. After stirring at 0°C for 12 h, the reaction was quenched by the addition of a saturated aqueous solution of $NaHCO_3$ (1 mL). The mixture was allowed to warm up to room temperature and water (2 mL) and dichloromethane (5 mL) were added. The organic phase was separated, dried over Na_2SO_4, filtered and concentrated under vacuum at room temperature to afford the crude product. When it was necessary, the amine was purified by flash chromatography. Yield and ee for each reaction are indicated in the tables of previous chapters.

B-1: *N-(1-phenylethyl)aniline*[242]

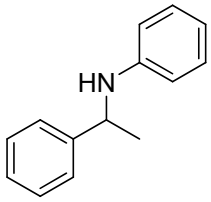

TLC of the product (98:2 hexane/ethyl acetate): the product has a R_f of 0.58 stained blue with phosphomolibdic acid.

^{1}H-NMR (300 MHz, $CDCl_3$): δ 7.30 (d, 2H), 7.27 (t, 2H), 7.13 (t, 1H), 7.01 (t, 2H), 6.57 (t, 1H), 6.44 (d, 2H), 4.41 (q, 1H), 3.94 (br s, 1H), 1.41 (d, 3H).

^{13}C- NMR (300 MHz, $CDCl_3$): δ 151.3, 147.4, 133.4, 126.7, 123.8, 119.9, 72.3, 44.1.

The enantiomeric excess was determined by chiral HPLC with Chiralpak IB column [eluent: 99:1 Hex/IPA; 0.8 mL/min flow rate, detection: 254 nm; t_R 10.6 min (*S*-enantiomer), t_R 12.1 min (*R*-enantiomer)].

B-2: *methyl 3-(N-benzylamino)-3-phenylpropanoate*[243]

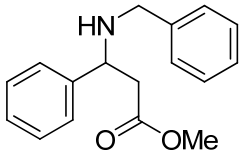

TLC of the product (8:2 hexane/ethyl acetate): the product has a R_f of 0.56.

^{1}H-NMR (300 MHz, $CDCl_3$): δ 7.36–7.18 (m, 10 H), 4.11 (dd, *J* = 8.6 Hz, *J* = 5.4 Hz, 1H), 3.66 (d, *J* = 13.2 Hz, 1H), 3.63 (s, 3H), 3.54 (d, *J* = 13.2 Hz, 1H), 2.73 (dd, *J* = 15.5 Hz, *J* = 8.6 Hz, 1H), 2.62 (dd, *J* = 15.5, J = 5.4 Hz, 1H), 1.95 (br, 1H).

^{13}C- NMR (300 MHz, $CDCl_3$): δ 142.6, 140.3, 128.6, 128.3, 128.1, 127.5, 127.1, 126.8, 58.8, 51.5, 51.3, 42.9.

The enantiomeric excess was determined by chiral HPLC with Chiralcel OD-H column [eluent: 98:2 Hex/IPA; 0.5 mL/min flow rate, detection: 254 nm; t_R 18.0 min (*R*-enantiomer), t_R 30.1 min (*S*-enantiomer)].

6.10.6 *Synthesis of oxazines by reductive cyclization of N-acylated β-amino enones with $HSiCl_3$*[119]

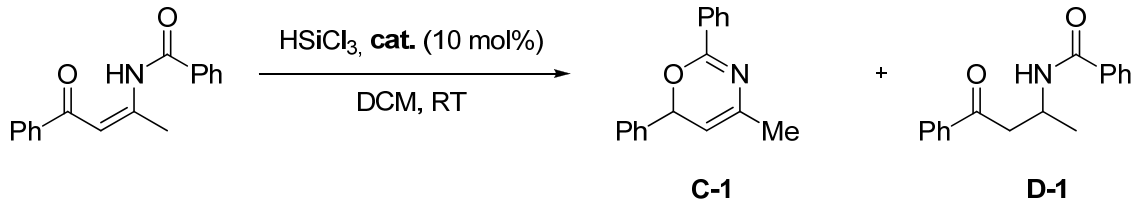

To a solution of catalyst (0.1 eq, 0.025 mmol) and *N*-acylated β-amino enone (1 eq, 0.25 mmol) in dry DCM (1 mL) was added dropwise trichlorosilane (3 eq, 0.75 mmol, 1M DCM solution) at 0°C. The reaction was stirred at room temperature for the desired time (24 or 72 h) and quenched with water (3 mL). The mixture was diluted with DCM (5 mL) and was stirred for 1 h, filtered through a celite pad and extracted with DCM (2 x 10 mL). The combined organic layers were dried over anhydrous Na_2SO_4, filtered, evaporated, and purified by silica gel column chromatography. Yield and ee for each reaction are indicated in the tables of previous chapters.

C-1: *4-Methyl-2,6-diphenyl-4H-1,3-oxazine*

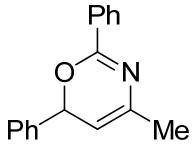

TLC of the product (98:2 hexane/ethyl acetate): the product has a R_f of 0.28.

^{1}H-NMR (300 MHz, $CDCl_3$): δ 8.12-8.05 (m, 2H), 7.70-7.64 (m, 2H), 7.51-7.33 (m, 6H), 5.52 (d, J = 3.2 Hz, 1H), 4.38 (dq, J = 6.9, J = 3.2 Hz, 1H), 1.45 (d, J = 6.9 Hz, 3H).

^{13}C- NMR (300 MHz, $CDCl_3$): δ 152.0, 146.7, 133.0, 132.5, 130.8, 128.7, 128.5, 128.2, 127.3, 124.1, 102.3, 48.1, 25.0.

The enantiomeric excess was determined by chiral HPLC with Chiralcel AD column [eluent: 95:5 Hex/IPA; 1 mL/min flow rate, detection: 210 nm; t_R 4.3 min (minor), t_R 6.0 min (major)].

D-1: *N-(4-Oxo-4-phenylbutan-2-yl)benzamide*

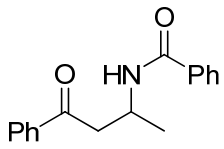

D-1

TLC of the product (98:2 hexane/ethyl acetate): the product has a R_f of 0.20.

^{1}H-NMR (300 MHz, $CDCl_3$): δ 7.99 (d, *J* = 7.8 Hz, 2H), 7.78 (d, *J* = 7.8 Hz, 2H), 7.60 (t, *J* = 7.8 Hz, 1H), 7.55-7.41 (m, 5H), 7.06 (br, 1H), 4.70 (dddq, *J* = 7.8, *J* = 5.9, *J* = 4.1, *J* = 6.9 Hz, 1H), 3.48 (dd, *J* = 17.0, *J* = 4.1 Hz, 1H), 3.21 (dd, *J* = 17.0, 5.9 Hz, 1H), 1.42 (d, *J* = 6.9 Hz, 3H).

The enantiomeric excess was determined by chiral HPLC with Chiralcel AD column [eluent: 95:5 Hex/IPA; 1 mL/min flow rate, detection: 210 nm; t_R 27.9 min (major), t_R 31.1 min (minor)].

6.10.7 General procedure for phosphonylation of aldehydes catalyzed by phosphine oxides

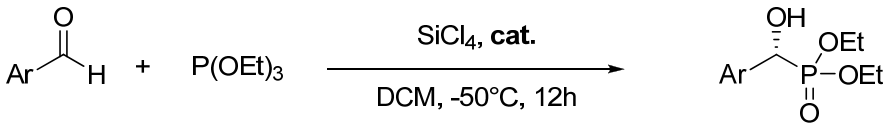

E

A phosphite (1.5 eq, 0.45 mmol) was added to a solution of an aldehyde (1 eq, 0.3 mmol), DIPEA (1.5 eq, 0.45 mmol), and phosphine oxide (0.1 eq, 0.03 mmol) in DCM (1 mL) at -50°C, then frresh distilled silicon tetrachloride (1.5 eq, 0.45 mmol, 0.75 M solution) was introduced in 6 portions, every 15 min. After the last addition, the mixture was stirred for 12 h at -50°C, then water (2 mL), saturated aq $NaHCO_3$ (5 mL), and ethyl acetate (5 mL) were added in turn to the reaction mixture. After being stirred for 1 h, the mixture was filtered *via* a celite pad and extracted with ethyl acetate (3 x5 mL). The combined organic layers were washed with brine, dried over anhydrous $NaSO_4$, filtered, and evaporated under reduced pressure. The residue was purified by silica gel column chromatography. Yield and ee for each reaction are indicated in the tables of previous chapters.

After separation of the product, phosphine oxide could be recovered quantitatively by eluting with ethyl acetate/ethanol (95:5) without loss of the optical activity.

E-1: *Diethyl 1-hydroxy-1-phenylmethylphosphonate*[170]

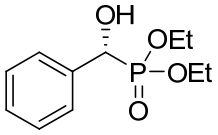

TLC of the product (95:5 DCM:MeOH): the product has a R_f of 0.52 stained blue with phosphomolybdic acid.

^{1}H-NMR (200 MHz, $CDCl_3$): δ 7.50–7.45 (m, 2H), 7.40-7.25 (m, 3H), 5.03 (d, J = 10.5 Hz, 1H), 4.15-3.80 (m, 4H), 2.70 (br, 1H), 1.27 (t, J = 7.3 Hz, 3H), 1.22 (t, J = 7.3 Hz, 3H).

^{31}P-NMR (300 MHz, $CDCl_3$): δ 21.4.

The enantiomeric excess was determined by chiral HPLC with Chiralcel AS-H column [eluent: 95:5 Hex/IPA; 1 mL/min flow rate, detection: 254 nm; t_R 17.6 min (*R*-enantiomer), t_R 22.8 min (*S*-enantiomer)].

6.10.8 Addition of silyl ketene acetals to aldehydes catalyzed by phosphine oxides

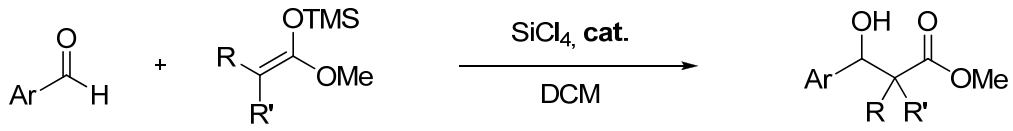

A solution of phosphine oxide (0.1 eq, 0.01 mmol) in DCM (2 mL) was cooled to the desired temperature and then freshly distilled benzaldehyde (1 eq, 0.5 mmol) and freshly distilled $SiCl_4$ (1.1 eq, 0.55 mmol) were added. After 15 min, silyl ketene acetal (1.2 eq, 0.6 mmol) was added dropwise (over 5 min) to the reaction mixture. The reaction mixture was allowed to stir at the desired temperature for 20 h, whereupon the cold reaction mixture was poured into a rapidly stirring solution of 1/1 sat. aq. KF/1M KH_2PO_4 (5 mL). This biphasic mixture was stirred vigorously for 2 h after which the aqueous layer was washed with DCM (3 x 50 mL). The combined organic extracts were dried over Na_2SO_4, filtered and the filtrate was concentrated *in vacuo*. The residue was purified by silica gel column chromatography. Yield and ee for each reaction are indicated in the tables of previous chapters.

F-1: *methyl 3-hydroxy-2,2-dimethyl-3-phenylpropanoate*

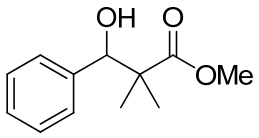

TLC of the product (8:2 hexane:ethyl acetate): the product has a R_f of 0.46

^{1}H-NMR (200 MHz, $CDCl_3$): δ 7.28 (s, 5H), 4.87 (s, 1H), 3.69 (s, 3H), 1.10 (d, J = 8 Hz, 6H).

The enantiomeric excess was determined by chiral HPLC with Chiralcel OJ-H column [eluent: 9:1 Hex/IPA; 0.5 mL/min flow rate, detection: 210 nm; t_R 26.3 min, t_R 32.4 min].

6.10.9 General procedure for the direct aldol condensation of ketones with aldehydes

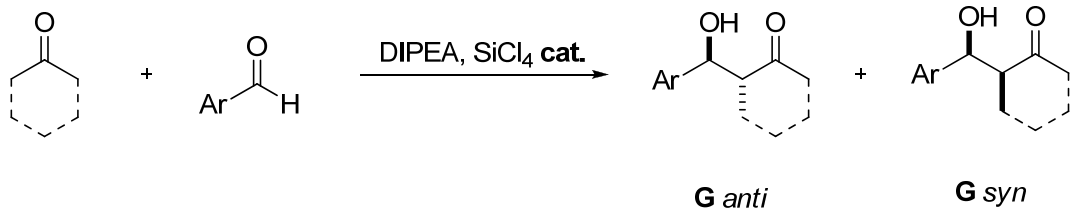

G *anti* **G** *syn*

To a stirred solution of phosphine oxide (0.1 eq, 0.03 mmol or 0.2 eq, 0.06 mmol) in the chosen solvent (2 mL), the ketone (2 eq, 0.60 mmol) and DIPEA (10 eq, 3 mmol) were added. The mixture was then cooled to the chosen temperature and freshly distilled tetrachlorosilane (1.5 eq, 0.45 mmol) was added dropwise *via* a syringe. After 15 min, freshly distilled aldehyde (1 eq, 0.30 mmol) was added. The mixture was stirred for 5 h (if the operating temperature is 0°C) or 12 h (if the operating temperature is -25°C), then the same amount of tetrachlorosilane (1.5 eq, 0.45 mmol) was added. After a proper time (see tables of previous chapters), the reaction was quenched by the addition of a saturated aqueous solution of $NaHCO_3$ (3 mL). The mixture was allowed to warm up to room temperature and stirred for 30 min, then water (5 ml) and ethyl acetate (15 mL) were added. The two-layers mixture was separated and the aqueous layer was extracted with ethyl acetate (15 mL). The combined organic layers were washed with 10% HCl (20 mL), saturated $NaHCO_3$ (20 mL) and brine (20 mL), dried over Na_2SO_4, filtered and concentrated under vacuum at room temperature. The crude product was purified by column chromatography with different hexane:ethyl acetate mixtures as eluent to afford the pure aldol adducts.

Yield and ee for each reaction are indicated in the tables of previous chapters. The *syn:anti* ratio was calculated by ^{1}H-NMR spectroscopy. Phosphine oxides were quantitatively recovered by further elution with 10% MeOH in DCM without any loss of optical purity.

G-1*: 2-(hydroxyphenylmethyl)cyclohexan-1-one*

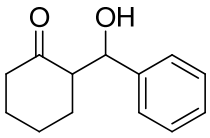

This product was purified by flash column chromatography on silica gel with a 9:1 hexane/ethyl acetate mixture as eluent. The purification afforded a mixture of *anti* and *syn* aldol adducts.

Data for *anti* isomer:

R_f= 0.21 (Hex/AcOEt 9:1 stained blue with phosphomolibdic acid)

^{1}H-NMR (200 MHz, $CDCl_3$): δ 7.31-7.24 (m, 5H), 4.79 (d, 1H, *J* = 8.6 Hz), 3.95 (br, 1H), 2.72-2.35 (m, 3H), 2.12-2.05 (m, 1H), 1.71-1.52 (m, 4H), 1.31-1.26 (m, 1H).

Data for *syn* isomer:

R_f= 0.32 (Hex/AcOEt 9:1 stained blue with phosphomolibdic acid)

^{1}H-NMR (200 MHz, $CDCl_3$): δ 7.38-7.25 (m, 5H), 5.39 (d, 1H), 2.60 (m, 1H), 2.60-2.32 (m, 2H), 2.08-2.01 (m, 1H), 1.87-1.29 (m, 5H).

The enantiomeric excess was determined by chiral HPLC with Daicel Chiralcel OD-H column [eluent: 98:2 Hex/IPA; 0.8 mL/min flow rate, detection: 210 nm; t_R 19.7 min (*syn*-minor), t_R 21.8 min (*syn*-major), t_R 27.8 min (*anti*-major (1'*R*, 2*S*)), t_R 44.9 min (*anti*-minor (1'*S*, 2*R*))].

G-2: *2-(hydroxy-(4-nitrophenyl)methyl)cyclohexan-1-one*

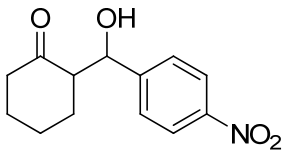

This product was purified by flash column chromatography on silica gel with a 7:3 hexane/ethyl acetate mixture as eluent. The purification afforded a mixture of *anti* and *syn* aldol adducts. Data for *anti* isomer:

R_f= 0.11 (Hex/AcOEt 7:3, stained blue with phosphomolibdic acid)

$[\alpha]_D^{25}$ = +12.3 (c= 0.26, $CHCl_3$), 95% ee,

$[\alpha]_{D\,theoretic}^{25}$ = +12.8 (c= 0.26, $CHCl_3$), > 99% ee.

^{1}H-NMR (200 MHz, $CDCl_3$): δ 8.20 (d, 2H, *J* = 8.5 Hz), 7.51 (d, 2H, *J* = 8.5 Hz), 4.90 (d, 1H), 2.65-2.55 (m, 1H), 2.55-2.25 (m, 1H), 2.20-1.95 (m, 1H), 1.95-1.70 (m, 1H), 1.65-1.15 (m, 5H).

Data for *syn* isomer:

R_f= 0.15 (Hex/AcOEt 7:3, stained blue with phosphomolibdic acid)

^{1}H-NMR (200 MHz, $CDCl_3$): δ 8.23 (d, 2H, *J* = 8.8 Hz), 7.51 (d, 2H, *J* = 8.8 Hz), 5.48 (s, 1H), 2.70-2.65 (m, 1H), 2.65-2.30 (m, 2H), 2.20-2.05 (m, 1H), 1.95-1.35 (m, 4H), 1.30-1.20 (m, 1H).

The enantiomeric excess was determined by chiral HPLC with Daicel Chiralcel OJ-H column [eluent: 7:3 Hex/IPA; 0.8 mL/min flow rate, detection: 210 nm; t_R 14.3 min (*syn*-major), t_R 23.4 min (*syn*-minor), t_R 12.9 min (*anti*-major (1'*R*, 2*S)*), t_R 15.6 min (*anti*-minor (1'*S*, 2*R*))]

G-3: *2-(hydroxy-(4-chlorophenyl)methyl)cyclohexan-1-one*

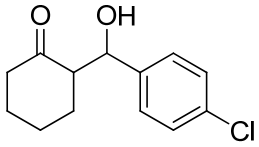

This product was purified by flash column chromatography on silica gel with a 9:1 hexane/ethyl acetate mixture as eluent. The purification afforded a mixture of *anti* and *syn* aldol adducts. Data for a mixture of *syn*:*anti* isomer:

R_f= 0.25 (Hex/AcOEt 9:1, stained blue with phosphomolibdic acid)

^{1}H-NMR (200 MHz, $CDCl_3$): δ 7.33-7.22 (m, 4H), 5.35 (s, 1H ***syn***), 4.78 (d, 1H, *J* = 8.7 Hz, ***anti***), 3.04-2.20 (m, 3H), 2.20-1.95 (m, 1H), 1.95-1.40 (m, 3H), 1.40-1.05 (m, 1H), 1.05-0.85 (m, 1H).

The enantiomeric excess was determined by chiral HPLC with Daicel Chiralcel OD column [eluent: 95:5 Hex/IPA; 0.8 mL/min flow rate, detection: 210 nm; t_R 11.06 min (*syn*-major), t_R 11.82 min (*syn*-minor), t_R 15.7 min (*anti*-major), t_R 25.5 min (*anti*-minor)].

G-4: *2-(hydroxy-(2-chlorophenyl)methyl)cyclohexan-1-one*

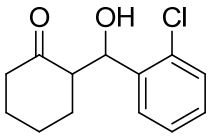

This product was purified by flash column chromatography on silica gel with a 9:1 hexane/ethyl acetate mixture as eluent. The purification afforded a mixture of *anti* and *syn* aldol adducts. Data for a mixture of *syn*:*anti* isomer:

R_f = 0.10 (Hex/AcOEt = 9:1, stained stained blue with phosphomolibdic acid);

^{1}H-NMR (300 MHz, $CDCl_3$): δ 7.55 (d, 1H, *J* = 8.4 Hz), 7.35-7.20 (m, 3H), 5.75 (s, 1H ***syn***), 5.35 (d, 1H, *J* = 8.0 Hz, ***anti***), 4.10-3.85 (br, 1H), 2.71-2.65 (m, 1H), 2.59-2.46 (m, 1H), 2.45-2.25 (m, 1H), 2.15-2.00 (m, 1H), 1.90-1.50 (m, 5H).

The enantiomeric excess was determined by chiral HPLC with Daicel Chiralcel AD column [eluent: 8:2 Hex/IPA; flow rate: 0.8 mL/min; detection: 210 nm; t_R: 6.4 min (*syn*-major), t_R: 6.9 (*syn*-minor), t_R: 9.0 min (*anti*-major), t_R: 10.2 min (*anti*-minor)].

G-5: *2-(hydroxy(4-trifluoromethylphenyl)methyl)cyclohexan-1-one*

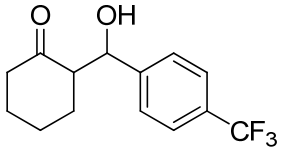

This product was purified by flash column chromatography on silica gel with a 9:1 hexane/ethyl acetate mixture as eluent. The purification afforded a mixture of *anti* and *syn* aldol adducts. Data for a mixture of *syn*:*anti* isomer:

R_f= 0.13 (Hex/AcOEt 9:1 stained blue with phosphomolibdic acid)

^{1}H-NMR (200 MHz, $CDCl_3$): δ 7.70-7.60 (m, 2H), 7.57-7.33 (m, 2H), 5.44 (m, 1H, ***syn***), 4.86-4.88 (d, 1H, J= 8.55 Hz, ***anti***), 4.04 (s, 1H), 2.70-2.20 (m, 3H), 2.15-2.05 (m, 1H), 1.85-1.25 (m, 5H).

The enantiomeric excess was determined by chiral HPLC with Daicel Chiralpak IB column [eluent: 99:1 Hex/IPA; 0.8 mL/min flow rate, detection: 213 nm; t_R 13.5 min (*syn*-major), t_R 14.5 min (*syn*-minor), t_R 18.7 min (*anti*-major), t_R 21.2 min (*anti*-minor)].

G-6: *2-(hydroxy-(3,5--bis(trifluoromethyl)phenyl)methyl)cyclohexan-1-one*

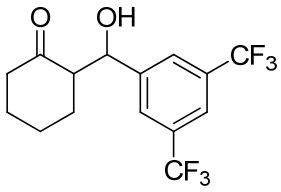

This product was purified by flash column chromatography on silica gel with a 95:5 hexane/ethyl acetate mixture as eluent afforded a mixture of *anti* and *syn* aldol adducts.

Data for a mixture of *syn*:*anti* isomer:

R_f= 0.14 (Hex/AcOEt 95:5, stained blue with phosphomolibdic acid)

^{1}H-NMR (300 MHz, $CDCl_3$): δ 7.80 (m, 3H), 5.50 (s, 1H, ***syn***), 4.92 (d, 1H, *J* = 8.4 Hz, ***anti***,), 4.16 (s, 1H), 2.75-2.25 (m, 2H), 2.25-2.00 (m, 1H), 2.00-1.80 (m, 1H), 1.75-1.40 (m, 3H), 1.40-1.05 (m, 2H).

^{13}C-NMR (300 MHz, $CDCl_3$): δ 214.53 (s), 143.79 (s), 131.56 (q), 127.24 (s), 123.14 (q), 73.97 (s), 42.64 (s), 30.67 (s), 27.58 (s), 24.66 (s).

The enantiomeric excess was determined by chiral HPLC with Daicel Chiralcel OD-H column [eluent: 95:5 Hex/IPA; 0.8 mL/min flow rate, detection: 254 nm; t_R 9.0 min (*anti*-major), t_R 10.2 min (*anti*-minor)].

G-7: *2-(hydroxy(2-methylphenyl)methyl)cyclohexan-1-one*

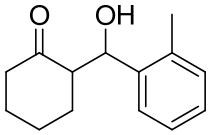

This product was purified by flash column chromatography on silica gel with a 9:1 hexane/ethyl acetate mixture as eluent. Data for a mixture of *syn*:*anti* isomer:

R_f= 0.22 (Hex/AcOEt 9:1 stained blue with phosphomolibdic acid)

^{1}H-NMR (200 MHz, $CDCl_3$): δ 7.42-7.15 (m, 4H), 5.60 (m, 1H, ***syn***) 5.15 (d, *J* = 8.6 Hz, ***anti***), 3.93 (br, 1H), 2.60-2.55 (m, 1H), 2.55-1.95 (m, 3H), 1.90-1.00 (m, 8H).

The enantiomeric excess was determined by chiral HPLC with Daicel Chiralpak IB column [eluent: 99:1 Hex/IPA; 0.8 mL/min flow rate, detection: 210 nm; t_R 11.4 min (*syn*-minor), t_R 12.5 min (*syn*-major), t_R 18.1 min (*anti*-major), t_R 20.6 min (*anti*-minor)].

G-8: *2-(hydroxy(3-methylphenyl)methyl)cyclohexan-1-one*

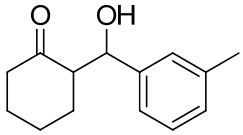

This product was purified by flash column chromatography on silica gel with a 9:1 hexane/ethyl acetate mixture as eluent. Data of *anti* isomer:

R_f= 0.25 (Hex/AcOEt 9:1 stained blue with phosphomolibdic acid)

^{1}H-NMR (300 MHz, $CDCl_3$): δ 7.35-7.10 (m, 4H), 4.74 (d, *J* = 8.4 Hz, ***anti***), 3.93 (br, 1H), 2.70-2.60 (m, 1H), 2.41 (m, 3H), 1.90-1.00 (m, 8H).

The enantiomeric excess was determined by chiral HPLC with Daicel Chiralpak IB column [eluent: 99:1 Hex/IPA; 0.8 mL/min flow rate, detection: 210 nm; t_R 17.8 min (*anti*-major), t_R 19.9 min (*anti*-minor)].

G-9: *2-(hydroxy(4-methylphenyl)methyl)cyclohexan-1-one*

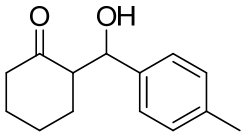

This product was purified by flash column chromatography on silica gel with a 9:1 hexane/ethyl acetate mixture as eluent. The purification afforded a mixture of *anti* and *syn* aldol adducts. Data for a mixture of *syn*:*anti* isomer:

R_f= 0.18 (Hex/AcOEt 9:1 stained blue with phosphomolibdic acid)

^{1}H-NMR (300 MHz, $CDCl_3$): δ 7.13-7.21 (m, 4H), 5.38 (m, 1H, ***syn***) 4.73-4.75 (d, *J* = 8.6 Hz, ***anti***), 3.87 (br, 1H), 2.59-2.48 (m, 1H), 2.44-2.20 (m, 2H), 2.18-2.09 (m, 1H), 1.78-1.42 (m, 4H), 1.30-1.12 (m, 4H).

The enantiomeric excess was determined by chiral HPLC with Daicel Chiralpak IB column [eluent: 99:1 Hex/IPA; 0.8 mL/min flow rate, detection: 213 nm; t_R 19.0 min (*anti*-major), t_R 21.2 min (*anti*-minor)].

G-10: *2-(hydroxy-(4-nitrophenyl)methyl)cyclohexan-1-one*

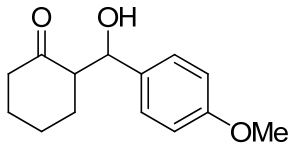

This product was purified by flash column chromatography on silica gel with a 9:1 hexane/ethyl acetate mixture as eluent. The purification afforded a mixture of *anti* and *syn* aldol adducts. Data for a mixture of *syn*:*anti* isomer:

R_f= 0.10 (Hex/AcOEt 9:1, stained blue with phosphomolibdic acid)

^{1}H-NMR (200 MHz, $CDCl_3$): δ 7.25 (dd, 2H, *J* = 8.4 Hz, *J* = 14.6 Hz), 6.89 (d, 2H, *J* = 8.4 Hz, *J* = 14.6 Hz), 5.30 (s, 1H, ***syn***), 4.76 (d, 1H, *J* = 8.8 Hz, ***anti***), 3.82 (s, 3H), 2.65-2.45 (m, 1H), 2.45-2.25 (m, 2H), 2.20-2.00 (m, 1H), 1.85-1.65 (m, 2H), 1.65-1.45 (m, 2H), 1.35-1.10 (m, 1H).

The enantiomeric excess was determined by chiral HPLC with Daicel Chiralcel AD column [eluent: 97:3 Hex/IPA; 0.8 mL/min flow rate, detection: 225 nm; t_R 37.9 min (*syn*-major), t_R 46.4 min (*syn*-minor), t_R 74.0 min (*anti*-minor), t_R 80.1 min (*anti*-major)].

G-11: *2-(hydroxyl-1-napthylmethyl)cyclohexan-1-one*

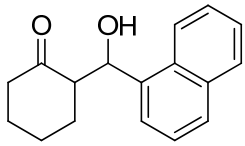

This product was purified by flash column chromatography on silica gel with a 9:1 hexane/ethyl acetate mixture as eluent. The purification afforded a mixture of *anti* and *syn* aldol adducts. Data for a mixture of *syn*:*anti* isomer:

R_f= 0.18 (Hex/AcOEt 9:1 stained blue with phosphomolibdic acid)

^{1}H-NMR (200 MHz, $CDCl_3$): δ 8.24-8.27 (m, 1H), 7.80-7.89 (m, 2H), 7.45-7.56 (m, 4H), 6.25 (br, 1H, ***syn***), 5.60 (d, *J* = 9.0 Hz, ***anti***), 4.16 (br, 1H), 3.05 (m, 1H), 2.35-2.51 (m, 2H), 2.06-2.12 (m, 2H), 1.65-1.75 (m, 2H), 1.36-1.52 (m, 2H).

The enantiomeric excess was determined by chiral HPLC with Daicel Chiralcel AD column [eluent: 9:1 Hex/IPA; 0.8 mL/min flow rate, detection: 210 nm; t_R 23.9 min (*anti*-minor), t_R 28.8 min (*anti*-major)].

G-12: *2-(hydroxy(thiophen-2-yl)methyl)cyclohexan-1-one*

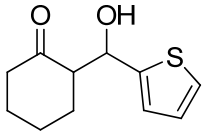

This product was purified by flash column chromatography on silica gel with a 9:1 hexane/ethyl acetate mixture as eluent. The purification afforded a mixture of *anti* and *syn* aldol adducts. Data for a mixture of *syn*:*anti* isomer:

R_f= 0.16 (Hex/AcOEt 9:1 stained blue with phosphomolibdic acid)

^{1}H-NMR (200 MHz, $CDCl_3$): δ 7.30 (m, 1H), 6.93-6.95 (m, 2H), 5.52 (m, 1H, ***syn***), 5.05-5.08 (d, *J* = 8.37 Hz, ***anti***), 4.05 (br, 1H), 2.80-2.60 (m, 1H), 2.60-2.20 (m, 2H), 2.20-2.05 (m, 1H), 1.90-1.50 (m, 4H), 1.40-1.20 (m, 1H).

The enantiomeric excess was determined by chiral HPLC with Daicel Chiralcel OD-H column [eluent: 9:1 Hex/IPA; 0.8 mL/min flow rate, detection: 230 nm; t_R 8.93 min (*anti*-major), t_R 12.7 min (*anti*-minor)].

G-13: *2-(hydroxy(furan-2-yl)methyl)cyclohexan-1-one*

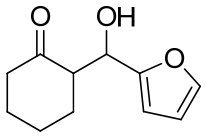

This product was purified by flash column chromatography on silica gel with a 9:1 hexane/ethyl acetate mixture as eluent. The purification afforded a mixture of *anti* aldol adduct. Data for a mixture of *syn*:*anti* isomer:

R_f= 0.21 (Hex/AcOEt 9:1 stained blue with phosphomolibdic acid)

^{1}H-NMR (200 MHz, $CDCl_3$): δ 7.40 (s, 1H), 6.27-6.33 (m, 2H), 4.81-4.84 (dd, *J* = 8.22 Hz), 3.85 (d, 1H, *J* = 3.68 Hz), 2.97-2.83 (m, 1H), 2.50-2.30 (m, 2H), 2.20-2.05 (m, 1H), 1.95-1.45 (m, 4H), 1.40-1.25 (m, 1H).

The enantiomeric excess was determined by chiral HPLC with Daicel Chiralpak IB column [eluent: 99:1 Hex/IPA; 0.8 mL/min flow rate, detection: 213 nm; t_R 23.2 min (*anti*-major), t_R 26.3 min (*anti*-minor)].

G-14: *2-(1-Hydroxy-3-phenyl-2-propenyl)cyclohexanone*

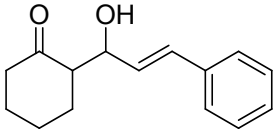

This product was purified by flash column chromatography on silica gel with a 9:1 hexane/ethyl acetate mixture as eluent.

R_f = 0.27 (Hex/AcOEt = 9:1, stained blue with phosphomolybdic acid);

^{1}H-NMR (300 MHz, $CDCl_3$): δ 7.40-7.10 (m, 10H), 6.70-6.50 (m, 2H), 4.77 (br, 1H, ***syn***), 4.43 (t, 1H, ***anti***), 3.60 (br, 1H), 2.60-2.30 (m, 6H), 2.20-2.00 (m, 2H), 1.90-1.80 (m, 2H), 1.80-1.30 (m, 8H).

The enantiomeric excess was determined by chiral HPLC with Daicel Chiralcel AD column [eluent 97:3 Hex/IPA; flow rate: 0.5 mL/min; detection: 254 nm; t_R: 47.7 min (*syn*-major), t_R: 52.2 min (*syn*-minor), t_R: 56.7 min (*anti*-major), t_R: 66.9 min (*anti*-minor)].

G-17: *2-(hydroxyphenylmethyl)cyclopentan-1-one*

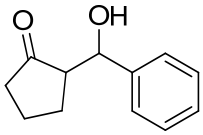

This product was purified by flash column chromatography on silica gel with a 9:1 hexane/ethyl acetate mixture as eluent. The purification afforded a mixture of *anti* and *syn* aldol adducts. Data for a mixture of *syn*:*anti* isomer:

R_f = 0.27 (Hex/AcOEt 8:2, stained blue with phosphomolibdic acid)

^{1}H-NMR (200 MHz, $CDCl_3$): δ 7.25-7.35 (m, 5H), 5.29 (br, 1H ***syn***), 4.72 (d, 1H, J = 9.1 Hz, ***anti***), 2.49-2.25 (m, 3H), 2.25-1.85 (m, 1H), 1.85-1.30 (m, 3H).

The enantiomeric excess was determined by chiral HPLC with Daicel Chiralcel OD-H column [eluent: 9:1 Hex/IPA; 0.5 mL/min flow rate, detection: 210 nm; t_R 14.1 min (*syn*-minor), t_R 16.6 min (*syn*-major) t_R 21.1 (*anti*-major (2*S*, 1'*R*)), t_R 25.7 min (*anti*-minor (2*R*, 1'*S*))].

G-18: *2-(hydroxyl-(4-nitrophenyl)methyl)cyclopentan-1-one*

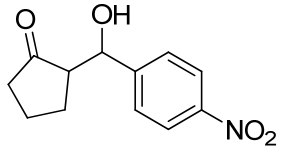

This product was purified by flash column chromatography on silica gel with a 9:1 then 8:2 hexane/ethyl acetate mixture as eluent. The purification afforded a mixture of *anti* and *syn* aldol adducts. Data for a mixture of *syn*:*anti* isomer:

R_f= 0.12 (Hex/AcOEt 9:1 then 8:2, stained blue with phosphomolibdic acid)

^{1}H-NMR (300 MHz, $CDCl_3$): δ 8.22 (d, 2H, *J* = 8.6), 7.54 (d, 2H, *J* = 8.6), 5.41 (d, 1H, *J* = 2.8, ***syn***), 4.86 (d, 1H, *J* = 9 Hz, ***anti***), 2.50-2.10 (m, 2H), 2.10-1.85 (m, 2H), 1.85-1.60 (m, 2H), 1.60-1.40 (m, 1H).

The enantiomeric excess was determined by chiral HPLC with Daicel Chiralcel AD column [eluent: 95:5 Hex/IPA; 0.8 flow rate, detection: 254 nm; t_R 24.6 min (*syn*-minor), t_R 31.5 min (*syn*-major) t_R 160.8 min (*anti*-minor (1'*R*, 2*S*)), t_R 171.3 min (*anti*-major (1'*S*, 2*R*))].

G-19: *2-(hydroxyl-(4-nitrophenyl)methyl)cycloheptan-1-one*

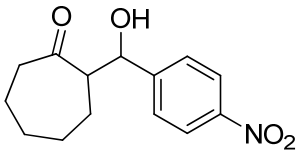

This product was purified by flash column chromatography on silica gel with a 9:1 hexane/ethyl acetate mixture as eluent. The purification afforded a mixture of *anti* and *syn* aldol adducts. Data for a mixture of *syn*:*anti* isomer:

R_f= 0.19 (Hex/AcOEt 9:1 then 8:2, stained blue with phosphomolibdic acid)

^{1}H-NMR (300 MHz, $CDCl_3$): δ = 8.20 (d, *J* = 8.8 Hz, 2H), 7.55 (d, *J* = 8.8 Hz, 2H), 5.50 (br, 1H, ***syn***), 4.93 (dd, *J* = 7.4, *J* = 4.7 Hz, 1H, ***anti***), 2.95-2.85 (m, 1H), 2.70-2.35 (m, 2H), 2.00-1.15 (m, 8H).

The enantiomeric excess was determined by chiral HPLC with Daicel Chiralcel AD column [eluent: 8:2 Hex/IPA; 0.8 flow rate, detection: 270 nm; t_R 8.9 min (*anti*-minor), t_R 17.6 min (*anti*-major)].

G-20: *Tetrahydro-3-(hydroxyphenylmethyl)-4H-pyran-4-one*

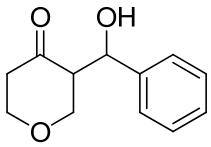

This product was purified by flash column chromatography on silica gel with a 9:1 hexane/ethyl acetate mixture as eluent. The purification afforded a mixture of *anti* and *syn* aldol adducts. Data for a mixture of *syn*:*anti* isomer:

R_f = 0.12 (Hex/AcOEt = 9:1, stained stained blue with phosphomolibdic acid);

^{1}H-NMR (300 MHz, $CDCl_3$): δ 7.52-7.47 (m, 5H), 5.75 (s, 1H, ***syn***), 4.91 (m, 1H, J = 8.2 Hz, ***anti***), 4.20-3.75 (m, 4H), 3.05 (m, 1H), 2.70-2.45 (m, 2H).

The enantiomeric excess was determined by chiral HPLC with Daicel Chiralcel AD column [eluent: 9:1 Hex/IPA; flow rate: 0.8 mL/min; detection: 270 nm; t_R: 19.5 min (*anti*-major), t_R 23.5 min (*anti*-minor)].

G-21: *4,4-(Ethylenedioxy)-2-(hydroxyphenylmethyl)cyclohexan-1-one*

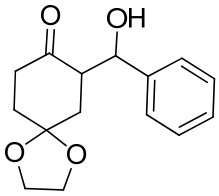

This product was purified by flash column chromatography on silica gel with a 9:1 hexane/ethyl acetate mixture as eluent. The purification afforded a mixture of *anti* and *syn* aldol adducts. Data for a mixture of *syn*:*anti* isomer:

R_f = 0.10 (Hex/AcOEt = 8:2, stained stained blue with phosphomolibdic acid);

^{1}H-NMR (300 MHz, $CDCl_3$): δ 7.32-7.26 (m, 5H), 5.43 (m, 1H, ***syn***), 4.83 (d, 1H, J = 8.5 Hz, ***anti***), 3.88-3.82 (m, 5H), 3.05-2.95 (m, 1H), 2.80-2.65 (m, 1H), 2.55-2.40 (m, 1H), 2.10-1.90 (m, 2H), 1.60-1.45 (m, 2H).

The enantiomeric excess was determined by chiral HPLC with Daicel Chiralcel OD-H column [eluent: 95:5 Hex/IPA; 0.8 mL/min flow rate; detection: 210 nm; t_R: 20.8 min (*anti*-major), t_R 29.0 min (*anti*-minor)].

G-22: *4,4-(Ethylenedioxy)-2-(hydroxy-4-chlorophenylmethyl)cyclohexan-1-one*

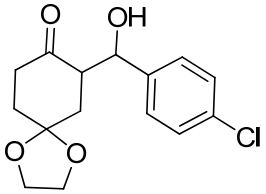

This product was purified by flash column chromatography on silica gel with a 9:1 hexane/ethyl acetate mixture as eluent. The purification afforded a mixture of *anti* and *syn* aldol adducts. Data for a mixture of *syn*:*anti* isomer:

R_f = 0.18 (Hex/EtOAc = 8:2, stained stained blue with phosphomolibdic acid);

^{1}H-NMR (300 MHz, $CDCl_3$): δ 7.40-7.25 (m, 4H), 5.40 (m, 1H, ***syn***), 4.70 (d, 1H, J = 8 Hz, ***anti***), 3.88-3.82 (m, 5H), 3.00-2.80 (m, 1H), 2.80-2.60 (m, 1H), 2.55-2.40 (m, 1H), 2.10-1.90 (m, 2H), 1.60-1.45 (m, 2H).

The enantiomeric excess was determined by chiral HPLC with Daicel Chiralcel OD-H column [eluent: 8:2 Hex/IPA; 0.8 mL/min flow rate; detection: 225 nm; t_R: 8.2 min (*anti*-minor), t_R 9.1 min (*anti*-major)].

G-23: *Tetrahydro-3-(hydroxyphenylmethyl)-4H-thiopyran-4-one*

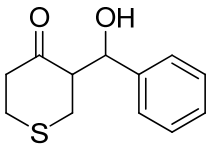

This product was purified by flash column chromatography on silica gel with a 9:1 hexane/ethyl acetate mixture as eluent. The purification afforded a mixture of *anti* and *syn* aldol adducts.

R_f = 0.21 (Hex/EtOAc 9:1 stained blue with phosphomolibdic acid)

^{1}H-NMR (300 MHz, $CDCl_3$): δ 7.36-7.24 (m, 5H), 5.38 (s, 1H ***syn***), 4.97 (dd, 1H, J = 3.2 Hz, J = 8.7 Hz, ***anti***), 3.37 (d, 1H, J = 3.2 Hz), 3.01-2.85 (m, 3H), 2.85-2.65 (m, 2H), 2.65-2.55 (m, 2H).

The enantiomeric excess was determined by chiral HPLC with Daicel Chiralcel OD column [eluent: 97:3 hex/IPA; 1 mL/min flow rate, detection: 210 nm; t_R: 28.3 min (anti-major), t_R: 39.5 min (anti-minor)].

G-24: *3-(hydroxy(phenyl)methyl)-4-oxopiperidine-1-benzylcarboxylate*

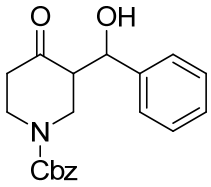

This product was purified by flash column chromatography on silica gel with a 9:1 hexane/ethyl acetate mixture as eluent afforded a mixture of *anti* and *syn* aldol adducts.

Data for a mixture of *syn*:*anti* isomer:

R_f= 0.14 (Hex/EtOAc 9:1, stained blue with phosphomolibdic acid)

^{1}H-NMR (300 MHz, $CDCl_3$): δ 7.40-7.20 (m, 10H), 5.35 (m, 1H, ***syn***), 5.20-5.00 (m, 2H), 4.85 (d, 1H, J= 4 Hz, ***anti***), 4.25-4.15 (m, 1H, ***anti***), 4.05-3.95 (m, 1H, ***syn***), 3.85-3.65 (m, 2H), 3.60-3.30 (m, 2H), 3.10-2.40 (m, 1H), 2.60-2.40 (m, 2H), 1.75-1.50 (m, 1H).

^{13}C-NMR (300 MHz, $CDCl_3$): δ 213.2 (s), 155.0 (s), 141.4 (s), 128.6 (m), 126.8 (s), 72.7 (s), 67.6 (s), 56.6 (s), 45.9 (s), 43.8 (s), 41.3 (s), 40.8 (s).

The enantiomeric excess was determined by chiral HPLC with Daicel Chiralpak OD column [eluent: 97:3 Hex/IPA; 1 mL/min flow rate, detection: 210 nm; t_R 37.4 min (*anti*-minor), t_R 41.0 min (*anti*-major)].

6.10.10 General procedure for the direct aldol-type reactions between aldehydes

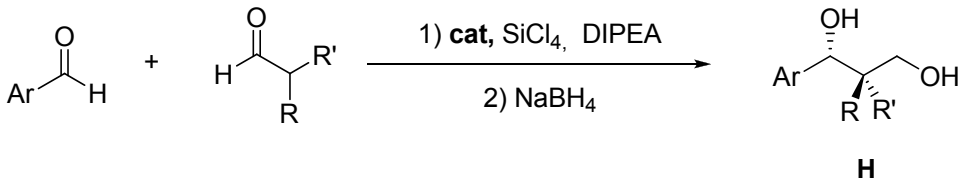

H

Tetrachlorosilane (1.5 eq, 0.45 mmol) was added to a solution of aliphatic aldehyde (1.5 eq, 0.45 mmol), an aromatic aldehyde (1.0 eq, 0.30 mmol), DIPEA (5 eq, 1.50 mmol) and phosphine oxide (0.1 eq, 0.03 mmol) in DCM (2 mL) at the chosen temperature. After being stirred for 12 h, the reaction was quenched with sat. $NaHCO_3$ (3 mL) and the slurry was stirred for 30 min at room temperature. The mixture was extracted with EtOAc (2 x 15 mL). The combined organic layers were washed with brine (2 x 15 mL), dried over Na_2SO_4, filtered and concentrated. The crude product was used for the next step without further purification. $NaBH_4$ (1.5 eq, 0.45 mmol) was added to the solution of the obtained crude product in MeOH (5 mL), and the reaction mixture was stirred for 30 min at room temperature. The reaction was quenched with saturated NH_4Cl (5 mL), and extracted with DCM (3 x 10 mL). The combined organic layers were washed with brine (10 mL) and dried over Na_2SO_4. Evaporation of the solvent furnished the crude product, which was purified by column chromatography to give the desired diol. Yield and ee for each reaction are indicated in the tables of previous chapters.

H-1: *2,2-Dimethyl-1-phenyl-1,3-propanediol*

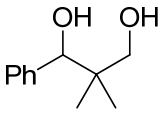

This product was purified by flash column chromatography on silica gel with a 7:3 hexane/ethyl acetate mixture as eluent.

R_f 0.25 (Hex/EtOAc = 7:3, stained blue with phosphomolybdic acid/EtOH);

^{1}H-NMR (300 MHz, $CDCl_3$): δ 7.34-7.31 (m, 5H), 4.66 (m, 1H), 3.56 (d, 1H, J = 10.5 Hz), 3.48 (d, 1H, J = 10.5 Hz), 2.70 (s, 2H), 0.88 (s, 3H), 0.84 (s, 3H).

The enantiomeric excess was determined by chiral HPLC with Daicel Chiralcel AD column [eluent 98:2 Hex/IPA; flow rate: 0.8 mL/min; detection: 220 nm; t_R: 54.6 min (*S*-major), t_R: 60.0 min (*R*-minor)].

H-2: *2-cyclohexyl-1-(4-phenyl)-1,3-propanediol*

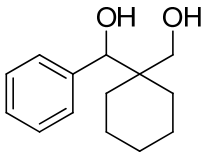

This product was purified by flash column chromatography on silica gel with a 7:3 hexane/ethyl acetate mixture as eluent.

R_f = 0.22 (Hex/EtOAc = 7:3, stained blue with phosphomolybdic acid);

^{1}H-NMR (300 MHz, $CDCl_3$): δ 7.35-7.25 (m, 5H), 4.73 (s, 1H), 3.80-3.60 (dd, 2H), 2.80 (br, 1H), 1.95-1.80 (m, 1H), 1.65-1.50 (m, 5H), 1.40-1.00 (m, 4H).

The enantiomeric excess was determined by chiral HPLC with Daicel Chiralcel AD column [eluent 98:2 Hex/IPA; flow rate: 0.8 mL/min; detection: 210 nm; t_R: 61.6 min (minor), t_R: 80.2 min (major)].

H-3: *2,2-Dimethyl-1-(4-chlorophenyl)-1,3-propanediol*

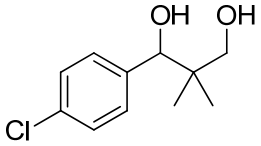

This product was purified by flash column chromatography on silica gel with a 7:3 hexane/ethyl acetate mixture as eluent.

R_f = 0.25 (Hex/AcOEt = 7:3 stained blue with phosphomolybdic acid);

^{1}H-NMR (300 MHz, $CDCl_3$): δ 7.40-7.20 (m, 4H), 4.60 (s, 1H), 3.45 (q, 2H), 0.85 (s, 3H), 0.80 (s, 3H).

The enantiomeric excess was determined by chiral HPLC with Daicel Chiralcel AD column [eluent 98:2 Hex/IPA; flow rate: 0.8 mL/min; detection: 210 nm; t_R: 46.2 min (minor), t_R: 48.2 min (major)].

H-4: *2,2-Dimethyl-1-(4-nitrophenyl)-1,3-propanediol*

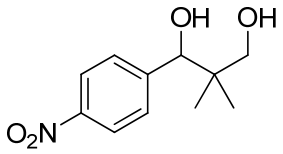

This product was purified by flash column chromatography on silica gel with a 7:3 hexane/ethyl acetate mixture as eluent.

R_f = 0.19 (Hex/AcOEt = 7:3, stained blue with phosphomolybdic acid);

^{1}H-NMR (300 MHz, $CDCl_3$): δ 8.25 (d, 2H), 7.55 (d, 2H), 4.78 (m, 1H), 3.59 (br, 1H), 3.57 (d, 2H), 2.40 (br, 1H), 0.86 (s, 6H).

The enantiomeric excess was determined by chiral HPLC with Daicel Chiralcel AD column [eluent 95:5 Hex/IPA; flow rate: 0.8 mL/min; detection: 270 nm; t_R: 28.1 min (minor), t_R: 43.8 min (major)].

6.10.11 General procedure for the synthesis of thioesters

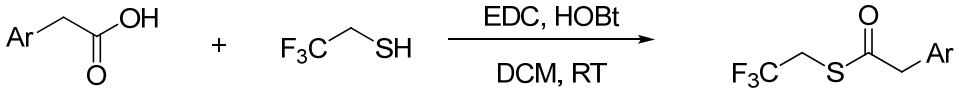

To a solution of carboxylic acid (1 eq, 5 mmol) in DCM (25 mL) was added HOBt (1.05 eq, 5.25 mmol) at 0°C, and the resulting solution was stirred for 10 min at the same temperature. EDC·HCl (1.05 eq, 5.25 mmol) was added and the mixture was stirred for 30 min at that temperature. Finally, 2,2,2-trifluoroethanethiol (1 eq, 5 mmol) was added at 0°C, and the mixture was allowed to warm to room temperature. After being stirred overnight, the reaction mixture was diluted with DCM (10 mL) and water was added (10 mL). Aqueous layer was extracted with DCM, and the extract was washed with water and brine, dried over Na_2SO_4, and concentrated in vacuum at room temperature to afford the crude product, that was purified by column chromatography to give the desired thioester.

Compound 100: *S-2,2,2-Trifluoroethyl phenylthioacetate*

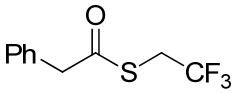

This product was purified by flash column chromatography on silica gel with a 9:1 hexane/ethyl acetate mixture as eluent. Yield: 80%.

TLC of the product (9:1 hexane/ethyl acetate): the product has a R_f of 0.77.

^{1}H-NMR (300 MHz, $CDCl_3$): δ 7.45-7.25 (m, 5H), 3.90 (s, 1H), 3.45 (q, J = 19.5 Hz, J = 9.9 Hz, 2H).

^{13}C-NMR (75 MHz, $CDCl_3$): δ 193.7, 132.4, 129.6, 128.8, 127.8, 124.6 (t, J = 275.8 Hz), 50.0, 30.8 (q, J = 34.1 Hz).

Compound 101*: S-2,2,2-Trifluoroethyl 4-fluorophenylthioacetate*

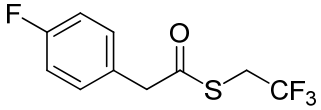

This product was purified by flash column chromatography on silica gel with a 9:1 hexane/ethyl acetate mixture as eluent. Yield: 62%.

TLC of the product (9:1 hexane/ethyl acetate): the product has a R_f of 0.75.

^{1}H-NMR (200 MHz, $CDCl_3$): δ 7.30-7.22 (m, 2H), 7.09-7.00 (m, 2H), 3.88 (s, 2H), 3.55 (q, J = 19.7 Hz, J = 9.8 Hz, 2H).

^{13}C-NMR (75 MHz, $CDCl_3$): δ 193.58 (1C), 164.09 (1C), 160.82 (1C), 131.33 (2C), 126.4 (t, J = 274.2 Hz, 1C), 115.32 (2C), 49.56 (1C), 30.15 (q, J = 34.1 Hz, 1C).

Compound 102: *S-2,2,2-trifluoroethyl 3,4-dimethoxyphenylthioacetate*

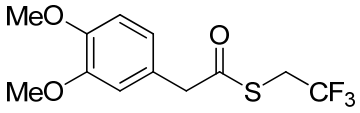

This product was purified by flash column chromatography on silica gel with a 9:1 hexane/ethyl acetate mixture as eluent. Yield: 84%.

TLC of the product (9:1 hexane/ethyl acetate): the product has a R_f of 0.31.

^{1}H-NMR (200 MHz, $CDCl_3$): δ 6.84 (s, 2H), 6.75 (s, 1H), 3.88 (s, 6H), 3.84 (s, 2H), 3.55 (q, J = 19.7 Hz, J = 9.8 Hz, 2H).

^{13}C-NMR (75 MHz, $CDCl_3$): δ 192.14 (1C), 124.78 (t, J = 274.4 Hz, 1C), 122.17 (1C), 112.86 (1C), 111.53 (1C), 55.95 (2C), 49.65 (1C), 30.72 (q, J = 33.7 Hz, 1C).

Compound 103: *S-2,2,2-trifluoroethyl 4-isoprobutylphenylthioacetate*

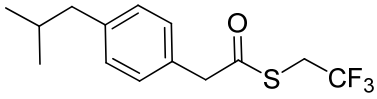

This product was purified by flash column chromatography on silica gel with a 9:1 hexane/ethyl acetate mixture as eluent. Yield: 63%.

TLC of the product (9:1 hexane/ethyl acetate): the product has a R_f of 0.31.

^{1}H-NMR (300 MHz, $CDCl_3$): δ 7.20 (d, 2H), 7.12 (d, 2H), 3.88 (s, 2H), 3.55 (q, J = 19.6 Hz, J = 9.7 Hz, 2H), 2.45 (d, J = 6.2 Hz, 2H), 1.85 (m, 1H), 1.88 (d, J = 6.2 Hz, 6H).

^{13}C-NMR (75 MHz, $CDCl_3$): δ 193.9 (1C), 141.5 (1C), 130.6 (1C), 129.4 (4C), 126.6 (t, J = 274.2 Hz, 1C), 49.7 (1C), 45.1 (1C), 30.7 (q, J = 33.7 Hz, 1C), 22.3 (2C).

Compound 104: *S-2,2,2-trifluoroethyl 4-hydroxyphenylthioacetate*

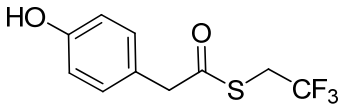

This product was purified by flash column chromatography on silica gel with a 9:1 hexane/ethyl acetate mixture as eluent. Yield: 57%.

TLC of the product (9:1 hexane/ethyl acetate): the product has a R_f of 0.48.

^{1}H-NMR (300 MHz, $CDCl_3$): δ 7.12 (d, 2H), 6.82 (d, 2H), 5.8 (br, 1H), 3.88 (s, 2H), 3.55 (q, J = 19.6 Hz, J = 9.7 Hz, 2H).

^{13}C-NMR (75 MHz, $CDCl_3$): δ 195.2 (1C), 132.7 (1C), 131.1 (2C), 124.1 (t, J = 275.0 Hz, 1C), 115.8 (1C), 49.6 (1C), 30.9 (q, J = 33.5 Hz, 1C).

Compound 105: *S-2,2,2-trifluoroethyl 2-chlorothioacetate*

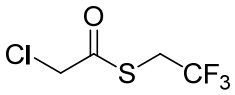

This product was purified by flash column chromatography on silica gel with a 98:2 pentane/diethyl ether mixture as eluent. Yield: 31%

TLC of the product (98:2 pentane/Et_2O): the product has a R_f of 0.63.

^{1}H-NMR (300 MHz, $CDCl_3$): δ 4.26 (s, 2H), 3.64 (q, J = 19.8 Hz, J = 9.9 Hz, 2H).

Compound 106: *S-2,2,2-trifluoroethyl 2-bromothioacetate*

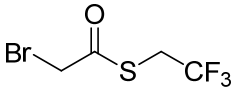

This product was purified by flash column chromatography on silica gel with a 98:2 pentane/diethyl ether mixture as eluent. Yield: 32%

TLC of the product (98:2 pentane/Et_2O): the product has a R_f of 0.68.

^{1}H-NMR (300 MHz, $CDCl_3$): δ 4.09 (s, 2H), 3.64 (q, J = 19.5 Hz, J = 9.6 Hz, 2H).

^{13}C-NMR (75 MHz, $CDCl_3$): δ 189.6 (1C), 127.2 (t, J = 274.9 Hz, 1C), 77.0 (t, J = 32 Hz, 1C), 31.6 (q, J = 34.6 Hz, 1C).

6.10.12 General procedure of direct aldol condensation of thioesters with aldehydes

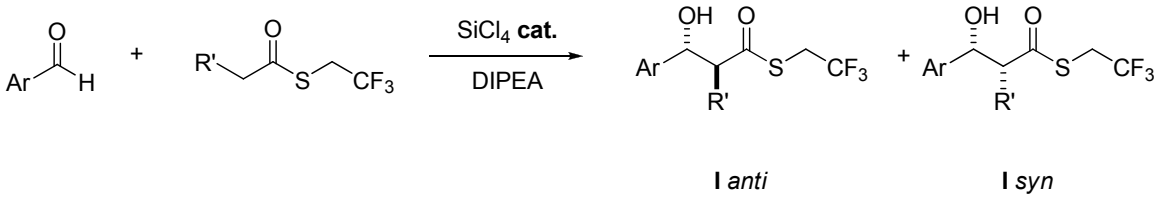

I *anti* **I** *syn*

To a stirred solution of phosphine oxide (0.1 eq, 0.03 mmol) in the chosen solvent (2 mL), the thioester (2 eq, 0.60 mmol) and DIPEA (10 eq, 3 mmol) were added. The mixture was then cooled to the chosen temperature and freshly distilled tetrachlorosilane (1.5 eq, 0.45 mmol) was added dropwise *via* syringe. After 15 min, freshly distilled aldehyde (1 eq, 0.30 mmol) was added. The mixture was stirred for 5 h (if the operating temperature is 0°C) or 12 h (if the operating temperature is -25°C), then the same amount of tetrachlorosilane (1.5 eq, 0.45 mmol) was added. After a proper time (see tables of previous chapters) the reaction was quenched by the addition of a saturated aqueous solution of $NaHCO_3$ (3 mL). The mixture was allowed to warm up to room temperature and stirred for 30 min, then water (5 ml) and ethyl acetate (15 mL) were added. The two-layers mixture was separated and the aqueous layer was extracted with ethyl acetate (15 mL). The combined organic layers were washed with saturated NH_4Cl (20 mL) and brine (20 mL), dried over Na_2SO_4, filtered, and concentrated under vacuum at room temperature. The crude product was purified by column chromatography with different hexane:ethyl acetate mixtures as eluent to afford the pure aldol adducts.

Yield and ee for each reaction are indicated in the tables of previous chapters. The *syn:anti* ratio was calculated by ^{1}H-NMR spectroscopy. Phosphine oxides were quantitatively recovered by further elution with 10% MeOH in DCM without any loss of optical purity.

I-1: *S-2,2,2-trifluoroethyl 3-hydroxy-2,3-diphenylpropanthioate*

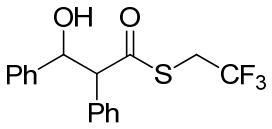

This product was purified by flash column chromatography on silica gel with a 8:2 hexane/ethyl acetate mixture as eluent.

Data for the *major* diastereoisomer

R_f= 0.62 (Hex/AcOEt 8:1 stained blue with phosphomolibdic acid)

^{1}H-NMR (200 MHz, $CDCl_3$): δ 7.37 (s, 5H), 7.31 (s, 5H), 5.35 (d, *J* = 9.0 Hz, 1H), 4.10 (d, *J* = 7.5 Hz, 1H), 3.42-2.24 (m, 2H), 2.37 (br, 1H).

^{13}C-NMR (75 MHz, $CDCl_3$): δ 195.42 (1C), 140.27 (1C), 133.58 (1C), 129.43 (2C), 128.89 (2C), 128.52 (2C), 128.39 (2C), 126.64 (2C), 126.23 (t, *J* = 281.2 Hz, 1C), 75.01 (1C), 68.21 (1C), 30.50 (q, *J* = 33.75, 1C).

HRMS Mass (ESI+): m/z = calc for $C_{17}H_{15}F_3O_2S$ 363.06425, found 363.0632 [M+ Na].

Data for the *minor* diastereoisomer

R_f= 0.58 (Hex/AcOEt 8:2 stained blue with phosphomolibdic acid)

^{1}H-NMR (200 MHz, $CDCl_3$): δ 7.36 (s, 5H), 7.30 (s, 5H), 5.20 (d, *J* = 10.0 Hz, 1H), 4.15-3.90 (m, 2H), 3.6 (d, *J* = 4.8 Hz, 1H), 1.73 (br, 1H).

The enantiomeric excess was determined by chiral HPLC with Daicel Chiralcel AD column [eluent: 9:1 hex/IPA; 0.8 mL/min flow rate, detection: 230 nm; t_R: 13.8 min (major-diast major), t_R: 15.1 min (minor-diast minor), t_R: 18.9 min (minor-diast major), t_R: 23.5 min (major-diast minor)].

I-2: *S-2,2,2-trifluoroethyl 3-hydroxy-3-(4-methoxyphenyl)-2-phenylpropanthioate*

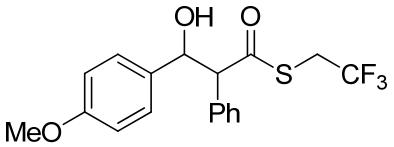

This product was purified by flash column chromatography on silica gel with a 9:1 hexane/ethyl acetate mixture as eluent afforded a mixture of *anti* and *syn* aldol adducts.

Data for a *syn*:*anti* mixture:

R_f= 0.48 (Hex/AcOEt 9:1 stained blue with phosphomolibdic acid)

^{1}H-NMR (300 MHz, $CDCl_3$): δ 7.45 (s, 5H), 7.25-7.15 (m, 3H), 6.90-6.80 (m, 2H), 5.33 (dd, *J* = 14.6 Hz, *J* = 8.1 Hz, 1H, ***minor***), 5.14 (dd, *J* = 6.2 *J* = 3.3 Hz, 1H, ***major***), 4.10-4.00 (m, 2H), 3.80 (s, 3H), 3.45-3.25 (m, 2H).

The enantiomeric excess was determined by chiral HPLC with Daicel Chiralcel AD column [eluent: 9:1 hex/IPA; 0.8 mL/min flow rate, detection: 230 nm; t_R: 23.2 min (major-diast major), t_R: 28.7 min (minor-diast major), t_R: 32.6 min (minor-diast minor), t_R: 39.1 min (major-diast minor)].

I-3: *S-2,2,2-trifluoroethyl 3-hydroxy-3-(4-chlorophenyl)-2-phenylpropanthioate*

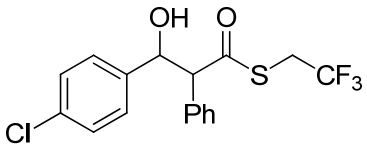

This product was purified by flash column chromatography on silica gel with a 9:1 hexane/ethyl acetate mixture as eluent afforded a mixture of *anti* and *syn* aldol adducts.

Data for a *syn*:*anti* mixture:

R_f= 0.44 (Hex/AcOEt 9:1 stained blue with phosphomolibdic acid)

^{1}H-NMR (300 MHz, $CDCl_3$): δ 7.36-6.85 (m, 9H), 5.36 (d, *J* = 6.9 Hz, 1H, ***minor***), 5.13 (d, *J* = 8.1 Hz, 1H, ***major***), 4.05-3.95 (m, 2H), 3.65-3.45 (m, 2H), 2.80 (br, 1H).

The enantiomeric excess was determined by chiral HPLC with Daicel Chiralcel AD column [eluent: 9:1 hex/IPA; 0.8 mL/min flow rate, detection: 220 nm; t_R: 17.1 min (major-diast major), t_R: 20.0 min (minor-diast), t_R: 22.4 min (minor-diast), t_R 24.4 min (major-diast minor)].

I-4: *S-2,2,2-trifluoroethyl 3-hydroxy-3-(4-nitrophenyl)-2-phenylpropanthioate*

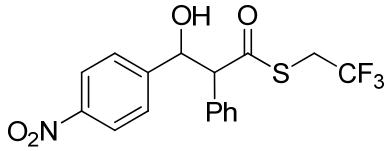

This product was purified by flash column chromatography on silica gel with a 9:1 hexane/ethyl acetate mixture as eluent afforded a mixture of *anti* and *syn* aldol adducts.

Data for a *syn*:*anti* mixture:

R_f= 0.52 (Hex/AcOEt 9:1 stained blue with phosphomolibdic acid)

^{1}H-NMR (200 MHz, $CDCl_3$): δ 8.14 (d, *J* = 7.3 Hz, 2H ***major***), 8.00 (d, 5.36 (d, *J* = 17.7 Hz, 2H, ***minor***), 7.41 (d, *J* = 7.3 Hz, 2H ***major***), 7.39-7.23 (m, 5H), 5.52 (d, *J* = 6.5 Hz, 1H, ***major***), 5.41 (d, *J* = 8.7 Hz, 1H, ***minor***) 4.01 (d, *J* = 6.5 Hz, 1H), 3.70-3.47 (m, 2H), 2.65 (br, 1H).

^{13}C-NMR (75 MHz, $CDCl_3$): δ 196.7 (1C), 147.68 (1C), 133.06 (1C), 129.88 (1C), 129.58 (2C), 129.11 (2C), 127.48 (3C), 126.30 (t, *J* = 286.5 Hz, 1C), 123.24 (2C), 73.78 (1C), 67.48 (1C), 30.36 (q, *J* = 35.2 Hz, 1C).

The enantiomeric excess was determined by chiral HPLC with Daicel Chiralcel AD column [eluent: 9:1 hex/IPA; 0.8 mL/min flow rate, detection: 230 nm; t_R: 19.3 min (major-diast major), t_R: 23.2 min (minor-diast), t_R: 28.5 min (minor-diast), t_R 35.4 min (major-diast minor)].

I-5: *S-2,2,2-trifluoroethyl 3-hydroxy-3-(4-methylphenyl)-2-phenylpropanthioate*

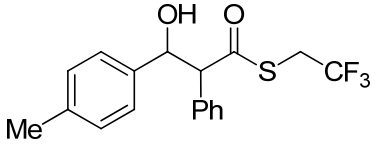

This product was purified by flash column chromatography on silica gel with a 9:1 hexane/ethyl acetate mixture as eluent afforded a mixture of *anti* and *syn* aldol adducts.

Data for a *syn*:*anti* mixture:

R_f= 0.21 (Hex/AcOEt 9:1 stained blue with phosphomolibdic acid)

^{1}H-NMR (300 MHz, $CDCl_3$): δ 7.26 (s, 5H), 7.16-7.13 (m, 4H), 5.37 (d, 1H, ***major***), 5.32 (d, 1H, ***minor***), 4.15 (d, 1H), 3.45-3.27 (m, 2H), 2.17 (br, 1H), 1.52 (s, 3H).

The enantiomeric excess was determined by chiral HPLC with Daicel Chiralcel AD column [eluent: 9:1 hex/IPA; 0.8 mL/min flow rate, detection: 220 nm; t_R: 21.0 min (major-diast major), t_R: 25.5 min (minor-diast), t_R: 29.5 min (minor-diast), t_R 33.0 min (major-diast minor)].

I-6: *S-2,2,2-trifluoroethyl 3-hydroxy-3-(1-naphthyl)-2-phenylpropanthioate*

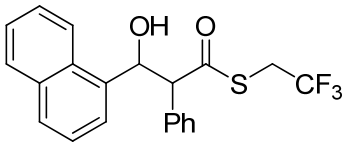

This product was purified by flash column chromatography on silica gel with a 9:1 hexane/ethyl acetate mixture as eluent afforded a mixture of *anti* and *syn* aldol adducts.

Data for a *syn*:*anti* mixture:

R_f= 0.18 (Hex/AcOEt 9:1 stained blue with phosphomolibdic acid)

^{1}H-NMR (300 MHz, $CDCl_3$): δ 8.16 (d, J = 8.4 Hz, 1H), 7.87 (d, J = 8.1 Hz, 1H), 7.76 (d, J = 7.5 Hz, 1H), 7.59-7.51 (m, 2H), 7.31-7.23 (m, 5H), 7.20-7.17 (m, 2H), 6.24 (d, J = 3 Hz, 1H, ***major***), 6.22 (d, J = 3Hz, 1H, ***minor***), 4.41 (d, J = 6 Hz, 1H), 3.48-3.44 (m, 2H), 2.65 (br, 1H).

The enantiomeric excess was determined by chiral HPLC with Daicel Chiralcel AD column [eluent: 9:1 hex/IPA; 0.8 mL/min flow rate, detection: 220 nm; t_R: 20.1 min (major-diast major), t_R: 24.6 min (minor-diast), t_R: 28.3 min (minor-diast), t_R 33.8 min (major-diast minor)].

I-7: *S-2,2,2-trifluoroethyl 3-hydroxy-2-phenyl-3-(thiophen-2-yl)propanethioate*

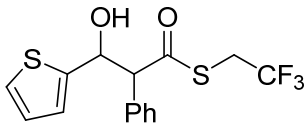

This product was purified by flash column chromatography on silica gel with a 9:1 hexane/ethyl acetate mixture as eluent afforded only one diastereoisomer.

R_f= 0.38 (Hex/AcOEt 9:1 stained blue with phosphomolibdic acid)

^{1}H-NMR (200 MHz, $CDCl_3$): δ 7.40-7.37 (m, 4H), 2.26-1.24 (m, 2H), 6.96-6.93 (m, 2H), 5.65 (d, *J* = 7.8 Hz, 1H), 4.14 (d, *J* = 7.8 Hz, 1H), 3.51-3.42 (m, 2H), 2.31-2.29 (br, 1H).

The enantiomeric excess was determined by chiral HPLC with Daicel Chiralcel AD column [eluent: 9:1 hex/IPA; 0.6 mL/min flow rate, detection: 230 nm; t_R: 26.7 min (major), t_R: 38.5 min (minor)].

I-8: *S-2,2,2-trifluoroethyl 3-hydroxy-2-phenyl-3-(furan-2-yl)propanethioate*

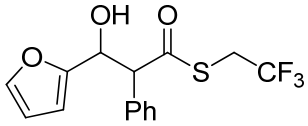

This product was purified by flash column chromatography on silica gel with a 9:1 hexane/ethyl acetate mixture as eluent afforded of *anti* and *syn* aldol adducts.

Data for a *syn*:*anti* mixture:

R_f= 0.41 (Hex/AcOEt 9:1 stained blue with phosphomolibdic acid)

^{1}H-NMR (300 MHz, $CDCl_3$): δ 7.38 (s, 6H), 7.25 (s, 2H), 6.3 (dd, *J* = 3.3 Hz, *J* = 1.8 Hz, 1H, ***major***), 6.2 (d, *J* = 3.3 Hz, 1H, ***minor***), 5.39 (d, *J* = 3.3 Hz, 1H, ***major***), 4.41 (m, 1H, ***minor***), 3.65-3.30 (m, 2H).

The enantiomeric excess was determined by chiral HPLC with Daicel Chiralcel AD column [eluent: 9:1 hex/IPA; 0.8 mL/min flow rate, detection: 225 nm; t_R: 23.2 min (major-diast major), t_R: 32.4 min (minor-diast), t_R: 38.1 min (minor-diast), t_R 62.2 min (major-diast minor)].

I-9: *S-2,2,2-trifluoroethyl 3-hydroxy-2,5-diphenylpent-4-enethioate*

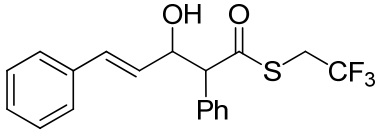

This product was purified by flash column chromatography on silica gel with a 9:1 hexane/ethyl acetate mixture as eluent afforded only one diastereoisomer.

R_f= 0.35 (Hex/AcOEt 9:1 stained blue with phosphomolibdic acid)

^{1}H-NMR (300 MHz, $CDCl_3$): δ 7.45-7.25 (m, 10H), 6.65 (d, *J* = 12 Hz, 1H), 6.28 (dd, *J* = 12 Hz, *J* = 6 Hz, 1H), 4.95 (t, *J* = 3.6 Hz, 1H), 3.97 (d, *J* = 6 Hz, 1H), 3.70-3.40 (m, 2H).

The enantiomeric excess was determined by chiral HPLC with Daicel Chiralcel AD column [eluent: 9:1 hex/IPA; 0.8 mL/min flow rate, detection: 230 nm; t_R: 26.6 min (major), t_R: 57.9 min (minor)].

I-10: *S-2,2,2-trifluoroethyl 2-(4-fluorophenyl)-3-hydroxy-3-phenylpropanethioate*

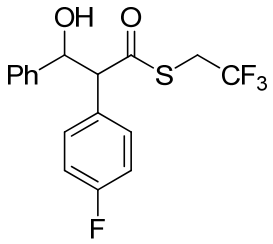

This product was purified by flash column chromatography on silica gel with a 9:1 hexane/ethyl acetate mixture as eluent afforded of *anti* and *syn* aldol adducts.

Data for a *syn*:*anti* mixture:

R_f= 0.47 (Hex/AcOEt 9:1 stained blue with phosphomolibdic acid)

^{1}H-NMR (300 MHz, $CDCl_3$): δ 7.38-7.12 (m, 7H), 7.11-7.7.02 (m, 2H), 5.37 (d, *J* = 6.9 Hz, 1H, ***major***), 5.25 (d, *J* = 9.3 Hz, 1H, ***minor***), 4.10-4.02 (m, 1H), 3.65-3.29 (m, 2H), 2.36 (br, 1H).

The enantiomeric excess was determined by chiral HPLC with Daicel Chiralcel AD column [eluent: 9:1 hex/IPA; 0.8 mL/min flow rate, detection: 225 nm; t_R: 18.9 min (major-diast major), t_R: 25.9 min (minor-diast), t_R: 32.4 min (minor-diast), t_R 49.9 min (major-diast minor)].

I-11: *S-2,2,2-trifluoroethyl 2-(3,4-dimethoxyphenyl)-3-hydroxy-3-phenylpropanethioate*

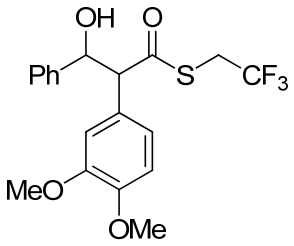

This product was purified by flash column chromatography on silica gel with a 9:1 hexane/ethyl acetate mixture as eluent afforded of *anti* and *syn* aldol adducts.

Data for a *syn*:*anti* mixture:

R_f= 0.31 (Hex/AcOEt 9:1 stained blue with phosphomolibdic acid)

^{1}H-NMR (300 MHz, $CDCl_3$): δ 7.45-7.25 (m, 5H), 6.92-6.80 (m, 3H), 5.33 (d, *J* = 7.4 Hz, 1H, ***major***), 5.25 (d, *J* = 9.6 Hz, 1H, ***minor***), 4.0 (d, *J* = 7.5 Hz, 1H), 3.88 (s, 3H), 3.85 (s, 3H), 3.55-3.35 (m, 2H), 2.30 (br, 1H).

The enantiomeric excess was determined by chiral HPLC with Daicel Chiralcel AD column [eluent: 9:1 hex/IPA; 0.8 mL/min flow rate, detection: 225 nm; t_R: 33.1 min (major-diast major), t_R: 36.1 min (minor-diast), t_R: 51.9 min (minor-diast), t_R 58.9 min (major-diast minor)].

I-12: *S-2,2,2-trifluoroethyl 3-hydroxy-2-(4-isobutylphenyl)-3-phenylpropanethioate*

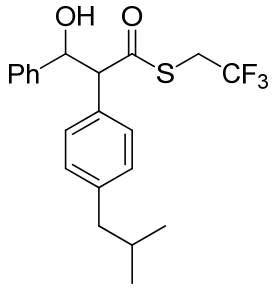

This product was purified by flash column chromatography on silica gel with a 9:1 hexane/ethyl acetate mixture as eluent afforded of *anti* and *syn* aldol adducts.

Data for the *major* diastereoisomer:

R_f= 0.35 (Hex/AcOEt 9:1 stained blue with phosphomolibdic acid)

^{1}H-NMR (300 MHz, $CDCl_3$): δ 7.35-7.22 (m, 7H), 7.21-7.11 (m, 2H), 5.35 (d, *J* = 7 Hz, 1H), 4.02 (d, *J* = 7 Hz, 1H), 3.65-3.30 (m, 2H), 2.45 (d, *J* = 7 Hz, 2H), 1.95-1.71 (m, 1H), 0.98-0.89 (m, 6H).

Data for the *minor* diastereoisomer:

R_f= 0.32 (Hex/AcOEt 9:1 stained blue with phosphomolibdic acid)

^{1}H-NMR (300 MHz, $CDCl_3$): δ 7.35-7.22 (m, 7H), 7.21-7.11 (m, 2H), 5.28 (d, *J* = 10 Hz, 1H), 4.00 (d, *J* = 7 Hz, 1H), 3.65-3.30 (m, 2H), 2.35 (d, *J* = 10 Hz, 2H), 1.95-1.71 (m, 1H), 0.89-0.80 (m, 6H).

The enantiomeric excess was determined by chiral HPLC with Daicel Chiralcel AD column [eluent: 9:1 hex/IPA; 0.8 mL/min flow rate, detection: 225 nm; t_R: 12.2 min (major-diast major), t_R: 13.5 min (minor-diast), t_R: 18.1 min (minor-diast), t_R 26.9 min (major-diast minor)].

I-13: *S-2,2,2-trifluoroethyl 3-hydroxy-2-(4-hydroxyphenyl)-3-phenylpropanethioate*

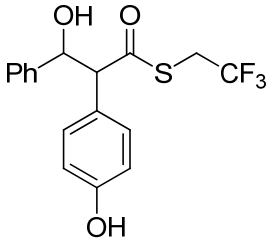

This product was purified by flash column chromatography on silica gel with a 9:1 hexane/ethyl acetate mixture as eluent afforded only one diastereoisomer.

R_f = 0.39 (Hex/AcOEt 9:1 stained blue with phosphomolibdic acid)

^{1}H-NMR (300 MHz, $CDCl_3$): δ 7.32-7.28 (m, 5H), 7.25 (d, *J* = 12 Hz, 1H), 6.82 (d, *J* = 12 Hz, 1H), 5.35 (d, *J* = 10 Hz, 1H), 4.00 (d, *J* = 10 Hz, 1H), 3.58-3.50 (m, 2H).

The enantiomeric excess was determined by chiral HPLC with Daicel Chiralcel AD column [eluent: 9:1 hex/IPA; 0.8 mL/min flow rate, detection: 230 nm; t_R: 14.3 min (minor), t_R: 33.4 min (major)].

L-14:

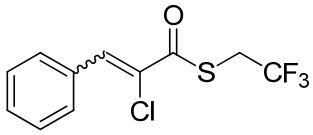

This byproduct was purified by flash column chromatography on silica gel with a 9:1 hexane/ethyl acetate mixture as eluent.

^{1}H-NMR (300 MHz, $CDCl_3$): δ 7.88-7.84 (m, 3H), 7.46-7.44 (m, 3H), 3.72 (q, *J* = 19.0 Hz, *J* = 6.6 Hz, 2H).

L-15:

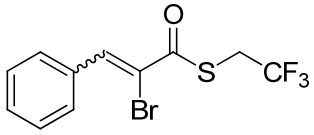

This byproduct was purified by flash column chromatography on silica gel with a 9:1 hexane/ethyl acetate mixture as eluent.

^{1}H-NMR (300 MHz, $CDCl_3$): δ 7.92-7.82 (m, 3H), 7.50-7.41 (m, 3H), 3.65 (m 2H).

6.10.13 Conjugate reduction and reductive aldol reaction of α,β-unsaturated ketones [118]

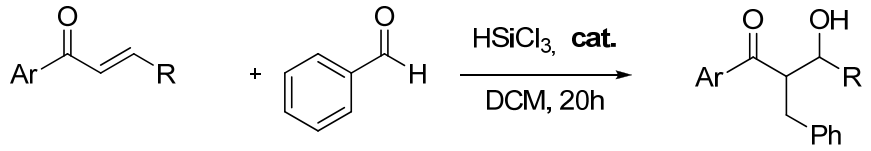

M

A solution of a phosphine oxide (0.1 eq, 0.05 mmol) and an enone (1.0 eq, 0.50 mmol) in dry DCM (2 mL) was cooled to the desired temperature, then a freshly distilled aldehyde (1.2 eq, 0.60 mmol) was added dropwise by means of a syringe. After 10 min, a freshly distilled trichlorosilane (2 eq, 1 mmol) was added.

After a proper time (see tables of previous chapters) the reaction was quenched by the addition of a saturated aqueous $NaHCO_3$ (3 mL). After addition of ethyl acetate (10 mL), the mixture was stirred for 1 h, filtered through a celite pad with ethyl acetate and extracted with ethyl acetate (3 × 5 mL). The combined organic layers were washed with brine, dried over anhydrous $NaSO_4$ filtered, evaporated and purified by silica gel column chromatography with different hexane:ethyl acetate mixtures as eluant. Yield and ee for each reaction are indicated in the tables of previous chapters.

M-1: *2-Benzyl-1,3-diphenyl-3-hydrodxy-1-propanone*

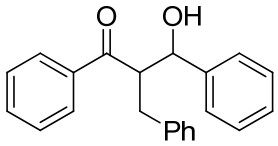

This product was purified by flash column chromatography on silica gel with a 9:1 hexane/ethyl acetate mixture as eluent. The purification afforded a mixture of *anti* and *syn* aldol adducts.

^{1}H-NMR (200 MHz, $CDCl_3$): δ 7.68-7.63 (m, 2H), 7.48-7.42 (m, 1H), 7.37-7.07 (m, 12H), 5.12 (d, 1H, J = 4.6 Hz, ***sin***), 4.97 (d, 1H, J = 6.0 Hz, ***anti***), 4.09 (m, 1H), 4.15-4.05 (m, 1H), 3.05 (dd, 1H, J = 6.0, J = 12 Hz), 2.91 (dd, 1H, J = 6.0, J = 12 Hz).

The enantiomeric excess was determined by chiral HPLC with Daicel Chiralcel OD-H column [eluent 95:5 Hex/IPA; flow rate: 0.8 mL/min; detection: 254 nm; t_R: 19.9 min (*syn*-minor), t_R: 22.4 min (*anti*-minor), t_R: 25.9 min (*anti*-major), t_R: 28.9 min (*syn*-major)].

M-2: *4-Hydroxy-3-(2,6,6-trimethyl-1-cyclohexen-1-yl)methyl-4-phenylbutan-2-one*

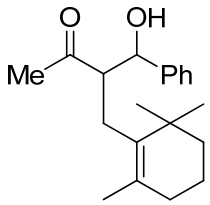

This product was purified by flash column chromatography on silica gel with a 9:1 hexane/ethyl acetate mixture as eluent. The purification afforded a mixture of *anti* and *syn* aldol adducts.

Data for the *anti* isomer:

R_f= 0.31 (Hex/AcOEt 9:1 stained blue with phosphomolibdic acid)

^{1}H-NMR (300 MHz, $CDCl_3$): 7.27-7.36 (m, 5H), 4.80 (d, 1H J = 6 Hz), 3.43 (br, 1H), 3.20 (m, 1H), 2.62 (m, 1H), 2.28 (m, 1H), 2.05 (s 3H), 1.90 (m, 2H), 1.60 (m, 2H), 1.55 (s, 3H), 1.38 (m, 2H), 0.99 (s, 3H), 0.83 (s, 3H).

Data for the *syn* isomer:

R_f= 0.28 (Hex/AcOEt 9:1 stained blue with phosphomolibdic acid)

^{1}H-NMR (300 MHz, $CDCl_3$): δ 7.30 (m, 5 H), 4.97 (d, 1H, J = 4.6 Hz), 3.55 (s, 1H), 3.15 (m, 1H), 2.60 (m, 1H), 2.30 (m, 1H), 2.05 (s 3H), 1.90 (m, 2H), 1.55 (m, 2H), 1.45 (s, 3H), 1.40 (m, 2H), 0.90 (s, 3H), 0.80 (s, 3H).

The enantiomeric excess was determined by chiral HPLC with Daicel Chiralcel OD-H column [eluent 95:5 Hex/IPA; flow rate: 0.8 mL/min; detection: 210 nm; t_R: 27.3 min (*syn*-minor), t_R: 29.2 min (*syn*-major), t_R: 36.9 min (*anti*-minor), t_R: 40.6 min (*anti*-major)].

6.11 Molecular Modeling: computational data

In this section, a computational description of the command files for molecular modeling calculations has been reported. All calculations were done using commercially available software from Schrödinger (2007 Suite) with MacroModel (v.8.5) module, and MOPAC 2009 on an Asus workstation (Intel(R) Core (TM) 2 CPU 6400@2.13 GH with 2.5 GB RAM).

6.11.1 MacroModel syntax

To run a MacroModel job, a command file (the *.com* file) and a molecular structure file are required. The *.com* file is so called because it generally has the name *filename.com*, where *filename* is a valid filename prefix. The *.com* file contains the name of the input structure file, the intended name of the output structure file, and a list of operation codes ("opcodes") telling Macromodel which operations are to be performed and in which order they are to be performed. The first line of the instruction file is the name of the input structure file written with MacroModel language (*filename.mae*). The resulting output structure file will be given the name listed on the second line of the instruction file (*filename-out.mae*). The input structure file contains the molecular structure(s) of the molecules to be processed (written in MacroModel language), and the output file will contain the structures after processing. The remaining lines in the *.com* file provide the instructions to MacroModel about the type and order of calculations to be performed with a precise sintax. For detailed informations about opcodes, see MacroModel Reference Manual. Each calculation job generated also a *filename.log* file, where numerous informations about the calculation process were collected.

6.11.2 Validation of MMFFs force field method

In order to validate MMFFs force field employed in calculations, a structure of BINAPO has been reproduced and minimized. The global minimum of this structure was obtained after a conformational analysis using a Monte Carlo method. Our results are compared with that obtained by Ogretir et al. in their quantum chemical studies[244] and with the real values obtained by experimental studies and X-ray analysis.[245] These values are in agree with the data reported in literature. For example, the real dihedral angle between the two naphthyl rings in (*S*)-BINAPO is 88.74°; [246] in our calculations,

this value was found to be 84.5°. The input command of this calculation was generated with Maestro (the graphical user interface (GUI) for MacroModel). A symmetry constraint for the torsion about binaphthyl bond was imposed (FXTA), in order to prevent the interconversion between the two enantiomeric forms of BINAPO. Only in this case, the command file for the minimization of the structure (*binapo_min.com*) with corresponding log file (*binapo_min.log*) and the command file for the MonteCarlo conformational analysis (*binapo_mc.com*) with corresponding log file (*binapo_mc.log*) has been reported.

The output geometry was reported instead as *.pdb* file (*protein data bank*) because PDB is a standard representation for macromolecular structure data and is compatible with a large amount of graphical molecular modeling software.

___binapo_min.com_____

```
binapo_min.mae
binapo_min-out.mae
 MMOD       0      1      0      0     0.0000     0.0000     0.0000     0.0000
 FFLD      10      1      0      1     1.0000     0.0000     0.0000     0.0000
 BDCO       0      0      0      0    41.5692 99999.0000     0.0000     0.0000
 READ       0      0      0      0     0.0000     0.0000     0.0000     0.0000
 FXTA      13     14     19     18   100.0000     0.0000    30.0000     0.0000
 CONV       2      0      0      0     0.0500     0.0000     0.0000     0.0000
 MINI       9      1    500      0     0.0000     0.0000     0.0000     0.0000
```

___binapo_min.log_____

```
[…]
 Input filename:  binapo_min.mae
 Output filename: binapo_min-out.mae
[…]
 *** This calculation will use the MMFF94S force field ***
    (promotes planarity at delocalized trigonal nitrogens)
    (preferred for comparison with crystal structures)
[…]
Quality of Force Field Parameters in Use:
   Numbers of high, medium and low quality stretch parameters =   78    2    7
   Numbers of high, medium and low quality bend parameters    =  116    0   28
   Numbers of high, medium and low quality torsion parameters =  160    0   64
   Interactions examined:  455 of        455 total, including unused params.
[…]
Iter=     1  Move(A)=  0.053144 E(kJ/mol)=   2176.797     Grad=   403.1112
Iter=     2  Move(A)=  0.055902 E(kJ/mol)=   1846.279     Grad=   166.9167
Iter=     3  Move(A)=  0.220867 E(kJ/mol)=   1514.102     Grad=   78.93822
[…]
Iter=    49  Move(A)=  0.007617 E(kJ/mol)=   1134.978     Grad=  0.4904662E-01
 Minimization converged; gradient = 0.490E-01 .LT.  0.500E-01
         Constraint E (included in E shown)=          21.97kJ/mol
                  Total Energy =     1134.9870 kJ/mol
                       Stretch =       96.4940 kJ/mol
                          Bend =       62.8353 kJ/mol
                       Torsion =       36.8755 kJ/mol
               Improper Torsion =        0.9180 kJ/mol
```

```
                          VDW =      426.1219 kJ/mol
                Electrostatic =      506.3807 kJ/mol
       Explicit Hydrogen Bonds =        0.0000 kJ/mol
                   Cross Terms =      -16.6079 kJ/mol

 T.E. for cross-checking:      1134.9870 kJ/mol
 Iterations =  49  out of   500
 Conf    1 E =  1134.987 (  0.049) kJ/mol
 Total number of structures processed =  1

BatchMin: normal termination

real   0m1.482s user 0m1.200s sys  0m0.016s
```

___binapo_mc.com _____

```
binapo_min-out.mae
binapo_mc-out.mae
 MMOD       0      1      0      0     0.0000     0.0000     0.0000     0.0000
 FFLD      10      1      0      1     1.0000     0.0000     0.0000     0.0000
 BDCO       0      0      0      0    41.5692 99999.0000     0.0000     0.0000
 READ       0      0      0      0     0.0000     0.0000     0.0000     0.0000
 FXTA      13     14     19     18   100.0000     0.0000    30.0000     0.0000
 CRMS       0      0      0      0     0.0000     0.5000     0.0000     0.0000
 MCMM   10000      0      0      0     0.0000     0.0000     0.0000     0.0000
 NANT       0      0      0      0     0.0000     0.0000     0.0000     0.0000
 MCNV       1      6      0      0     0.0000     0.0000     0.0000     0.0000
 MCSS       2      0      0      0    21.0000     0.0000     0.0000     0.0000
 MCOP     500      0      0      0     0.0000     0.0000     0.0000     0.0000
 DEMX       0    166      0      0    21.0000    42.0000     0.0000     0.0000
 COMP       9     10     11     12     0.0000     0.0000     0.0000     0.0000
 COMP      13     14     17     18     0.0000     0.0000     0.0000     0.0000
 COMP      19     20     21     22     0.0000     0.0000     0.0000     0.0000
 COMP      25     26     35     36     0.0000     0.0000     0.0000     0.0000
 COMP      39     40     41     50     0.0000     0.0000     0.0000     0.0000
 COMP      51     52     61     62     0.0000     0.0000     0.0000     0.0000
 COMP      63     72     73     74     0.0000     0.0000     0.0000     0.0000
 MSYM       0      0      0      0     0.0000     0.0000     0.0000     0.0000
 AUOP       0      0      0      0   100.0000     0.0000     0.0000     0.0000
 TORS      13     17      0      0     0.0000   180.0000     0.0000     0.0000
 TORS      17     40      0      0     0.0000   180.0000     0.0000     0.0000
 TORS      17     73      0      0     0.0000   180.0000     0.0000     0.0000
 TORS      18     22      0      0     0.0000   180.0000     0.0000     0.0000
 TORS      22     51      0      0     0.0000   180.0000     0.0000     0.0000
 TORS      22     62      0      0     0.0000   180.0000     0.0000     0.0000
 CONV       2      0      0      0     0.0500     0.0000     0.0000     0.0000
 MINI       9      1    500      0     0.0000     0.0000     0.0000     0.0000
```

___binapo_mc.log _____

```
[…]
 Input filename:  binapo_min-out.mae
 Output filename: binapo_mc-out.mae
[…]
 *** This calculation will use the MMFF94S force field ***
    (promotes planarity at delocalized trigonal nitrogens)
    (preferred for comparison with crystal structures)
[…]
 Quality of Force Field Parameters in Use:
   Numbers of high, medium and low quality stretch parameters =   78    2    7
   Numbers of high, medium and low quality bend parameters    =  116    0   28
   Numbers of high, medium and low quality torsion parameters =  160    0   64
```

```
   Interactions examined:  455 of        455 total, including unused params.
 […]
 Starting truncated Newton minimization.
          Step     1 New global minimum.  E (kJ/mol) =     1134.99
          Step     2 New global minimum.  E (kJ/mol) =     1095.80
          Step     3 New global minimum.  E (kJ/mol) =     1095.78
          Step    19 New global minimum.  E (kJ/mol) =     1095.78
          Step    39 New global minimum.  E (kJ/mol) =     1095.77
          Step    77 New global minimum.  E (kJ/mol) =     1095.76
          Step   211 New global minimum.  E (kJ/mol) =     1095.76
[…]
          Step   549 New global minimum.  E (kJ/mol) =     1095.75
          Step   735 New global minimum.  E (kJ/mol) =     1095.74
[…]
          Step  1538 New global minimum.  E (kJ/mol) =     1095.74
[…]

Final report:
    2 unique conformations found
    2 minimized with good convergence
Found     1 confs within  1.00 kcal/mol ( 4.18 kJ/mol) of glob. min.
Found     2 confs within  5.00 kcal/mol (20.92 kJ/mol) of glob. min.
Global minimum E =   1095.74 found  2455 times.

 Total number of structures processed =  10000
 Conformations with poor convergence marked with a *
 Conformation       1 (    1095.742     kJ/mol) was found  2455 times
 Conformation       2 (    1115.406     kJ/mol) was found    25 times
          *** MC Statistics ***
 Percent of minimized structures within energetic window:  24.8000
 Average number of duplicates:    1240.00
 Duplication standard deviation:  1718.27
   16130  structures generated
   0  rejected by ring closure
   6131  rejected by van der Waals
   2478  duplicate minimised structures
              Time in Monte Carlo generation loop:       1.5 CPU sec
                    Time in energy minimizations:    4955.2 CPU sec
                   Time in geometry optimisation:       0.0 CPU sec

BatchMin: normal termination
real   84m6.737s   user 84m1.591s   sys 0m4.168s
```

___ binapo_mc-out.PDB_____

```
REMARK 888
REMARK 888 WRITTEN BY MAESTRO (A PRODUCT OF SCHRODINGER, LLC)
TITLE     binapo_mc-out
MODEL        1
HETATM    1  C1  UNK     1      -2.131  -0.932  -2.828  1.00  0.00           C
HETATM    2  C2  UNK     1      -1.664  -0.069  -1.839  1.00  0.00           C
HETATM    3  C3  UNK     1      -1.279  -0.582  -0.610  1.00  0.00           C
HETATM    4  C4  UNK     1      -1.367  -1.956  -0.372  1.00  0.00           C
HETATM    5  C5  UNK     1      -1.840  -2.866  -1.352  1.00  0.00           C
HETATM    6  C6  UNK     1      -2.220  -2.316  -2.600  1.00  0.00           C
HETATM    7  C7  UNK     1      -2.674  -3.154  -3.618  1.00  0.00           C
HETATM    8  C8  UNK     1      -2.761  -4.530  -3.425  1.00  0.00           C
HETATM    9  C9  UNK     1      -2.387  -5.121  -2.206  1.00  0.00           C
HETATM   10  C10 UNK     1      -1.936  -4.287  -1.147  1.00  0.00           C
HETATM   11  P1  UNK     1      -2.654  -6.916  -1.981  1.00  0.00           P
HETATM   12  C11 UNK     1      -1.833  -5.554   2.453  1.00  0.00           C
HETATM   13  C12 UNK     1      -2.272  -4.892   1.280  1.00  0.00           C
HETATM   14  C13 UNK     1      -3.556  -4.291   1.331  1.00  0.00           C
HETATM   15  C14 UNK     1      -4.356  -4.336   2.475  1.00  0.00           C
HETATM   16  C15 UNK     1      -3.899  -4.984   3.612  1.00  0.00           C
```

```
HETATM   17  C16 UNK     1      -2.645  -5.590   3.600  1.00  0.00           C
HETATM   18  O1  UNK     1      -1.533  -7.642  -1.256  1.00  0.00           O
HETATM   19  O2  UNK     1       0.408  -5.677  -2.608  1.00  0.00           O
HETATM   20  C17 UNK     1      -6.583  -7.260   0.423  1.00  0.00           C
HETATM   21  C18 UNK     1      -5.478  -8.039   0.758  1.00  0.00           C
HETATM   22  C19 UNK     1      -4.299  -7.931   0.021  1.00  0.00           C
HETATM   23  C20 UNK     1      -4.210  -7.041  -1.059  1.00  0.00           C
HETATM   24  C21 UNK     1      -5.329  -6.257  -1.382  1.00  0.00           C
HETATM   25  C22 UNK     1      -6.509  -6.369  -0.645  1.00  0.00           C
HETATM   26  C23 UNK     1      -3.140  -8.861  -6.147  1.00  0.00           C
HETATM   27  C24 UNK     1      -4.233  -8.829  -5.283  1.00  0.00           C
HETATM   28  C25 UNK     1      -4.111  -8.249  -4.017  1.00  0.00           C
HETATM   29  C26 UNK     1      -2.896  -7.685  -3.605  1.00  0.00           C
HETATM   30  C27 UNK     1      -1.799  -7.743  -4.482  1.00  0.00           C
HETATM   31  C28 UNK     1      -1.921  -8.321  -5.746  1.00  0.00           C
HETATM   32  H1  UNK     1      -2.421  -0.513  -3.789  1.00  0.00           H
HETATM   33  H2  UNK     1      -1.595   0.997  -2.033  1.00  0.00           H
HETATM   34  H3  UNK     1      -0.904   0.078   0.166  1.00  0.00           H
HETATM   35  H4  UNK     1      -1.046  -2.313   0.605  1.00  0.00           H
HETATM   36  H5  UNK     1      -2.964  -2.745  -4.584  1.00  0.00           H
HETATM   37  H6  UNK     1      -3.130  -5.136  -4.249  1.00  0.00           H
HETATM   38  H7  UNK     1      -3.960  -3.777   0.461  1.00  0.00           H
HETATM   39  H8  UNK     1      -5.337  -3.868   2.468  1.00  0.00           H
HETATM   40  H9  UNK     1      -4.517  -5.026   4.504  1.00  0.00           H
HETATM   41  H10 UNK     1      -2.306  -6.102   4.498  1.00  0.00           H
HETATM   42  H11 UNK     1      -7.500  -7.342   1.001  1.00  0.00           H
HETATM   43  H12 UNK     1      -5.529  -8.726   1.598  1.00  0.00           H
HETATM   44  H13 UNK     1      -3.434  -8.532   0.297  1.00  0.00           H
HETATM   45  H14 UNK     1      -5.288  -5.553  -2.209  1.00  0.00           H
HETATM   46  H15 UNK     1      -7.370  -5.757  -0.901  1.00  0.00           H
HETATM   47  H16 UNK     1      -3.235  -9.317  -7.129  1.00  0.00           H
HETATM   48  H17 UNK     1      -5.180  -9.265  -5.591  1.00  0.00           H
HETATM   49  H18 UNK     1      -4.975  -8.260  -3.359  1.00  0.00           H
HETATM   50  H19 UNK     1      -0.838  -7.333  -4.171  1.00  0.00           H
HETATM   51  H20 UNK     1      -1.061  -8.354  -6.410  1.00  0.00           H
HETATM   52  C1  UNK     2      -0.167  -5.541   0.156  1.00  0.00           C
HETATM   53  C2  UNK     2      -1.423  -4.876   0.119  1.00  0.00           C
HETATM   54  C3  UNK     2      -0.590  -6.187   2.469  1.00  0.00           C
HETATM   55  C4  UNK     2       0.230  -6.178   1.344  1.00  0.00           C
HETATM   56  P1  UNK     2       1.017  -5.454  -1.233  1.00  0.00           P
HETATM   57  C5  UNK     2       2.855  -1.224  -0.981  1.00  0.00           C
HETATM   58  C6  UNK     2       2.709  -1.977   0.181  1.00  0.00           C
HETATM   59  C7  UNK     2       2.158  -3.259   0.119  1.00  0.00           C
HETATM   60  C8  UNK     2       1.753  -3.801  -1.111  1.00  0.00           C
HETATM   61  C9  UNK     2       1.905  -3.029  -2.272  1.00  0.00           C
HETATM   62  C10 UNK     2       2.453  -1.748  -2.208  1.00  0.00           C
HETATM   63  C11 UNK     2       4.273  -8.673  -0.588  1.00  0.00           C
HETATM   64  C12 UNK     2       2.958  -9.030  -0.874  1.00  0.00           C
HETATM   65  C13 UNK     2       1.995  -8.040  -1.068  1.00  0.00           C
HETATM   66  C14 UNK     2       2.328  -6.678  -0.968  1.00  0.00           C
HETATM   67  C15 UNK     2       3.660  -6.335  -0.698  1.00  0.00           C
HETATM   68  C16 UNK     2       4.625  -7.327  -0.505  1.00  0.00           C
HETATM   69  H1  UNK     2      -0.244  -6.704   3.362  1.00  0.00           H
HETATM   70  H2  UNK     2       1.192  -6.679   1.413  1.00  0.00           H
HETATM   71  H3  UNK     2       3.278  -0.224  -0.932  1.00  0.00           H
HETATM   72  H4  UNK     2       3.017  -1.565   1.138  1.00  0.00           H
HETATM   73  H5  UNK     2       2.046  -3.830   1.037  1.00  0.00           H
HETATM   74  H6  UNK     2       1.578  -3.428  -3.231  1.00  0.00           H
HETATM   75  H7  UNK     2       2.555  -1.158  -3.114  1.00  0.00           H
HETATM   76  H8  UNK     2       5.026  -9.443  -0.442  1.00  0.00           H
HETATM   77  H9  UNK     2       2.680 -10.078  -0.953  1.00  0.00           H
HETATM   78  H10 UNK     2       0.970  -8.327  -1.302  1.00  0.00           H
HETATM   79  H11 UNK     2       3.972  -5.295  -0.648  1.00  0.00           H
HETATM   80  H12 UNK     2       5.655  -7.048  -0.297  1.00  0.00           H
CONECT    1    2   32    6
CONECT    1    6
CONECT    2    1    3   33
CONECT    2    3
```

```
CONECT    3    2    4   34
CONECT    3    2
CONECT    4    3   35    5
CONECT    4    5
CONECT   32    1
CONECT   33    2
CONECT   34    3
CONECT   35    4
CONECT    5    4    6   10
CONECT    5    4
CONECT    6    1    5    7
CONECT    6    1
CONECT    7    6    8   36
CONECT    7    8
CONECT    8    7    9   37
CONECT    8    7
CONECT    9    8   10   11
CONECT    9   10
CONECT   10    5    9   53
CONECT   10    9
CONECT   36    7
CONECT   37    8
CONECT   11    9   18   23   29
CONECT   11   18
CONECT   52   53   55   56
CONECT   52   53
CONECT   53   10   52   13
CONECT   53   52
CONECT   54   55   69   12
CONECT   54   55
CONECT   55   52   54   70
CONECT   55   54
CONECT   56   52   19   60   66
CONECT   56   19
CONECT   69   54
CONECT   70   55
CONECT   12   54   13   17
CONECT   12   13
CONECT   13   53   12   14
CONECT   13   12
CONECT   14   13   15   38
CONECT   14   15
CONECT   15   14   16   39
CONECT   15   14
CONECT   16   15   17   40
CONECT   16   17
CONECT   17   12   16   41
CONECT   17   16
CONECT   38   14
CONECT   39   15
CONECT   40   16
CONECT   41   17
CONECT   18   11
CONECT   18   11
CONECT   19   56
CONECT   19   56
CONECT   20   21   25   42
CONECT   20   21
CONECT   21   20   22   43
CONECT   21   20
CONECT   22   21   23   44
CONECT   22   23
CONECT   23   11   22   24
CONECT   23   22
CONECT   24   23   25   45
CONECT   24   25
CONECT   25   20   24   46
CONECT   25   24
```

```
CONECT   42   20
CONECT   43   21
CONECT   44   22
CONECT   45   24
CONECT   46   25
CONECT   57   58   62   71
CONECT   57   58
CONECT   58   57   59   72
CONECT   58   57
CONECT   59   58   60   73
CONECT   59   60
CONECT   60   56   59   61
CONECT   60   59
CONECT   61   60   62   74
CONECT   61   62
CONECT   62   57   61   75
CONECT   62   61
CONECT   71   57
CONECT   72   58
CONECT   73   59
CONECT   74   61
CONECT   75   62
CONECT   63   64   68   76
CONECT   63   64
CONECT   64   63   65   77
CONECT   64   63
CONECT   65   64   66   78
CONECT   65   66
CONECT   66   56   65   67
CONECT   66   65
CONECT   67   66   68   79
CONECT   67   68
CONECT   68   63   67   80
CONECT   68   67
CONECT   76   63
CONECT   77   64
CONECT   78   65
CONECT   79   67
CONECT   80   68
CONECT   26   27   31   47
CONECT   26   27
CONECT   27   26   28   48
CONECT   27   26
CONECT   28   27   29   49
CONECT   28   29
CONECT   29   11   28   30
CONECT   29   28
CONECT   30   29   31   50
CONECT   30   31
CONECT   31   26   30   51
CONECT   31   30
CONECT   47   26
CONECT   48   27
CONECT   49   28
CONECT   50   30
CONECT   51   31
ENDMDL
END
```

6.11.3 TetraMe-BITIOPO calculations with MacroModel

The structure of (*S*)-tetraMe-BITIOPO has been minimized in vacuo with MMFFS force field and the conformational analysis has been performed with Monte Carlo method; a symmetry constraint for the torsion about biaryl bond was imposed (FXTA), in order to prevent the interconversion between the two enantiomeric forms of tetraMe-BITIOPO. Only the job file and the global minimum of the final structure has been reported. This geometry has employed in all next calculations.

```
___ TetraMe-BITIOPO.com_____________________________________________________
ph_bistiofene_mc.mae
ph_bistiofene_mc-out.mae
 MMOD       0      1      0      0     0.0000     0.0000     0.0000     0.0000
 DEBG      17      0      0      0     0.0000     0.0000     0.0000     0.0000
 FFLD      10      1      0      1     1.0000     0.0000     0.0000     0.0000
 BDCO       0      0      0      0    41.5692 99999.0000     0.0000     0.0000
 READ       0      0      0      0     0.0000     0.0000     0.0000     0.0000
 FXTA       7      8      3      4   100.0000    86.2243    30.0000     0.0000
 CRMS       0      0      0      0     0.0000     0.5000     0.0000     0.0000
 MCMM   20000      0      0      0     0.0000     0.0000     0.0000     0.0000
 NANT       0      0      0      0     0.0000     0.0000     0.0000     0.0000
 MCNV       2      7      0      0     0.0000     0.0000     0.0000     0.0000
 MCSS       2      0      0      0    21.0000     0.0000     0.0000     0.0000
 MCOP    1000      0      0      0     0.0000     0.0000     0.0000     0.0000
 DEMX       0    166      0      0    21.0000    42.0000     0.0000     0.0000
 COMP       1      2      3      4     0.0000     0.0000     0.0000     0.0000
 COMP       5      6      7      8     0.0000     0.0000     0.0000     0.0000
 COMP       9     10     11     12     0.0000     0.0000     0.0000     0.0000
 COMP      13     14     15     16     0.0000     0.0000     0.0000     0.0000
 COMP      17     18     21     22     0.0000     0.0000     0.0000     0.0000
 COMP      23     30     31     32     0.0000     0.0000     0.0000     0.0000
 COMP      39     40     41     48     0.0000     0.0000     0.0000     0.0000
 COMP      49     50      0      0     0.0000     0.0000     0.0000     0.0000
 MSYM       0      0      0      0     0.0000     0.0000     0.0000     0.0000
 AUOP       0      0      0      0   100.0000     0.0000     0.0000     0.0000
 TORS       2      6      0      0     0.0000   180.0000     0.0000     0.0000
 TORS       3      8      0      0     0.0000   180.0000     0.0000     0.0000
 TORS       6     40      0      0     0.0000   180.0000     0.0000     0.0000
 TORS       6     49      0      0     0.0000   180.0000     0.0000     0.0000
 TORS       9     12      0      0     0.0000   180.0000     0.0000     0.0000
 TORS      12     22      0      0     0.0000   180.0000     0.0000     0.0000
 TORS      12     31      0      0     0.0000   180.0000     0.0000     0.0000
 CONV       2      0      0      0     0.0500     0.0000     0.0000     0.0000
 MINI       9      1    500      0     0.0000     0.0000     0.0000     0.0000
_____________________________________________________________________________
```

```
___ TetraMe-BITIOPO.PDB_____________________________________________________
REMARK 888
REMARK 888 WRITTEN BY MAESTRO (A PRODUCT OF SCHRODINGER, LLC)
TITLE     s-tetraMe-BITIOPO
MODEL        1
HETATM    1  C1  UNK     1       0.537  -2.984  -2.002  1.00  0.00           C
HETATM    2  C2  UNK     1      -0.765  -2.601  -2.319  1.00  0.00           C
HETATM    3  C3  UNK     1      -1.572  -2.489  -1.134  1.00  0.00           C
HETATM    4  C4  UNK     1      -0.834  -2.702   0.021  1.00  0.00           C
HETATM    5  S1  UNK     1       0.743  -3.242  -0.327  1.00  0.00           S
HETATM    6  P1  UNK     1      -1.198  -2.187  -4.026  1.00  0.00           P
```

```
HETATM    7  C5  UNK     1      -1.204  -2.493   1.453  1.00  0.00           C
HETATM    8  C6  UNK     1       1.730  -3.172  -2.886  1.00  0.00           C
HETATM    9  C7  UNK     1      -2.422   0.496  -1.021  1.00  0.00           C
HETATM   10  C8  UNK     1      -6.718  -2.621  -0.757  1.00  0.00           C
HETATM   11  O1  UNK     1      -0.340  -0.946  -4.192  1.00  0.00           O
HETATM   12  O2  UNK     1      -2.962  -4.975  -2.042  1.00  0.00           O
HETATM   13  C9  UNK     1      -5.611  -1.281  -4.880  1.00  0.00           C
HETATM   14  C10 UNK     1      -4.698  -0.248  -4.698  1.00  0.00           C
HETATM   15  C11 UNK     1      -3.364  -0.543  -4.412  1.00  0.00           C
HETATM   16  C12 UNK     1      -2.921  -1.871  -4.286  1.00  0.00           C
HETATM   17  C13 UNK     1      -3.852  -2.896  -4.493  1.00  0.00           C
HETATM   18  C14 UNK     1      -5.188  -2.604  -4.785  1.00  0.00           C
HETATM   19  C15 UNK     1       0.157  -5.616  -6.772  1.00  0.00           C
HETATM   20  C16 UNK     1       0.284  -4.288  -7.172  1.00  0.00           C
HETATM   21  C17 UNK     1      -0.130  -3.263  -6.321  1.00  0.00           C
HETATM   22  C18 UNK     1      -0.674  -3.548  -5.057  1.00  0.00           C
HETATM   23  C19 UNK     1      -0.793  -4.890  -4.673  1.00  0.00           C
HETATM   24  C20 UNK     1      -0.380  -5.917  -5.523  1.00  0.00           C
HETATM   25  H1  UNK     1      -6.650  -1.055  -5.104  1.00  0.00           H
HETATM   26  H2  UNK     1      -2.653   0.273  -4.289  1.00  0.00           H
HETATM   27  H3  UNK     1      -3.537  -3.935  -4.439  1.00  0.00           H
HETATM   28  H4  UNK     1       0.480  -6.417  -7.433  1.00  0.00           H
HETATM   29  H5  UNK     1      -0.023  -2.226  -6.638  1.00  0.00           H
HETATM   30  H6  UNK     1      -1.201  -5.147  -3.698  1.00  0.00           H
HETATM   31  H7  UNK     1      -0.635  -1.653   1.868  1.00  0.00           H
HETATM   32  H8  UNK     1      -2.263  -2.255   1.577  1.00  0.00           H
HETATM   33  H9  UNK     1      -0.981  -3.381   2.053  1.00  0.00           H
HETATM   34  H10 UNK     1       1.772  -4.201  -3.254  1.00  0.00           H
HETATM   35  H11 UNK     1       1.712  -2.494  -3.743  1.00  0.00           H
HETATM   36  H12 UNK     1       2.665  -2.970  -2.351  1.00  0.00           H
HETATM   37  H13 UNK     1      -2.959   1.406  -1.308  1.00  0.00           H
HETATM   38  H14 UNK     1      -1.995   0.652  -0.025  1.00  0.00           H
HETATM   39  H15 UNK     1      -1.598   0.369  -1.730  1.00  0.00           H
HETATM   40  H16 UNK     1      -7.402  -1.776  -0.617  1.00  0.00           H
HETATM   41  H17 UNK     1      -7.042  -3.139  -1.664  1.00  0.00           H
HETATM   42  H18 UNK     1      -6.847  -3.273   0.111  1.00  0.00           H
HETATM   43  H19 UNK     1      -5.019   0.786  -4.779  1.00  0.00           H
HETATM   44  H20 UNK     1      -1.190  -7.164   2.265  1.00  0.00           H
HETATM   45  H21 UNK     1      -4.063  -4.480   3.996  1.00  0.00           H
HETATM   46  H22 UNK     1      -7.396  -6.427  -4.033  1.00  0.00           H
HETATM   47  H23 UNK     1      -8.274  -6.968   0.133  1.00  0.00           H
HETATM   48  H24 UNK     1       0.705  -4.049  -8.145  1.00  0.00           H
HETATM   49  H25 UNK     1      -0.477  -6.953  -5.206  1.00  0.00           H
HETATM   50  H26 UNK     1      -5.899  -3.410  -4.945  1.00  0.00           H
HETATM   51  C1  UNK     2      -3.315  -0.703  -1.012  1.00  0.00           C
HETATM   52  C2  UNK     2      -2.973  -2.040  -1.089  1.00  0.00           C
HETATM   53  C3  UNK     2      -4.119  -2.918  -0.987  1.00  0.00           C
HETATM   54  C4  UNK     2      -5.295  -2.187  -0.877  1.00  0.00           C
HETATM   55  S1  UNK     2      -4.996  -0.498  -0.858  1.00  0.00           S
HETATM   56  P1  UNK     2      -3.977  -4.730  -0.949  1.00  0.00           P
HETATM   57  C5  UNK     2      -2.587  -5.869   3.271  1.00  0.00           C
HETATM   58  C6  UNK     2      -3.602  -4.928   3.119  1.00  0.00           C
HETATM   59  C7  UNK     2      -4.024  -4.555   1.841  1.00  0.00           C
HETATM   60  C8  UNK     2      -3.438  -5.124   0.699  1.00  0.00           C
HETATM   61  C9  UNK     2      -2.413  -6.067   0.871  1.00  0.00           C
HETATM   62  C10 UNK     2      -1.989  -6.436   2.148  1.00  0.00           C
HETATM   63  C11 UNK     2      -7.981  -6.746  -1.986  1.00  0.00           C
HETATM   64  C12 UNK     2      -7.618  -6.597  -0.651  1.00  0.00           C
HETATM   65  C13 UNK     2      -6.407  -5.984  -0.316  1.00  0.00           C
HETATM   66  C14 UNK     2      -5.547  -5.491  -1.310  1.00  0.00           C
HETATM   67  C15 UNK     2      -5.920  -5.681  -2.650  1.00  0.00           C
HETATM   68  C16 UNK     2      -7.128  -6.293  -2.988  1.00  0.00           C
HETATM   69  H1  UNK     2      -2.255  -6.156   4.266  1.00  0.00           H
HETATM   70  H2  UNK     2      -4.814  -3.814   1.743  1.00  0.00           H
HETATM   71  H3  UNK     2      -1.935  -6.511  -0.001  1.00  0.00           H
HETATM   72  H4  UNK     2      -8.920  -7.228  -2.246  1.00  0.00           H
HETATM   73  H5  UNK     2      -6.150  -5.904   0.736  1.00  0.00           H
HETATM   74  H6  UNK     2      -5.249  -5.362  -3.444  1.00  0.00           H
```

```
CONECT    1    2    5    8
CONECT    1    2
CONECT    2    1    3    6
CONECT    2    1
CONECT    3    2    4   52
CONECT    3    4
CONECT    4    3    5    7
CONECT    4    3
CONECT    5    1    4
CONECT    6    2   11   16   22
CONECT    6   11
CONECT   51   52   55    9
CONECT   51   52
CONECT   52    3   51   53
CONECT   52   51
CONECT   53   52   54   56
CONECT   53   54
CONECT   54   53   55   10
CONECT   54   53
CONECT   55   51   54
CONECT   56   53   12   60   66
CONECT   56   12
CONECT    7    4   31   32   33
CONECT    8    1   34   35   36
CONECT    9   51   37   38   39
CONECT   10   54   40   41   42
CONECT   11    6
CONECT   11    6
CONECT   12   56
CONECT   12   56
CONECT   57   58   62   69
CONECT   57   58
CONECT   58   57   59   45
CONECT   58   57
CONECT   59   58   60   70
CONECT   59   60
CONECT   60   56   59   61
CONECT   60   59
CONECT   61   60   62   71
CONECT   61   62
CONECT   62   57   61   44
CONECT   62   61
CONECT   69   57
CONECT   70   59
CONECT   71   61
CONECT   63   64   68   72
CONECT   63   64
CONECT   64   63   65   47
CONECT   64   63
CONECT   65   64   66   73
CONECT   65   66
CONECT   66   56   65   67
CONECT   66   65
CONECT   67   66   68   74
CONECT   67   68
CONECT   68   63   67   46
CONECT   68   67
CONECT   72   63
CONECT   73   65
CONECT   74   67
CONECT   13   14   18   25
CONECT   13   14
CONECT   14   13   15   43
CONECT   14   13
CONECT   15   14   16   26
CONECT   15   16
CONECT   16    6   15   17
CONECT   16   15
```

```
CONECT   17   16   18   27
CONECT   17   18
CONECT   18   13   17   50
CONECT   18   17
CONECT   25   13
CONECT   26   15
CONECT   27   17
CONECT   19   20   24   28
CONECT   19   20
CONECT   20   19   21   48
CONECT   20   19
CONECT   21   20   22   29
CONECT   21   22
CONECT   22    6   21   23
CONECT   22   21
CONECT   23   22   24   30
CONECT   23   24
CONECT   24   19   23   49
CONECT   24   23
CONECT   28   19
CONECT   29   21
CONECT   30   23
CONECT   31    7
CONECT   32    7
CONECT   33    7
CONECT   34    8
CONECT   35    8
CONECT   36    8
CONECT   37    9
CONECT   38    9
CONECT   39    9
CONECT   40   10
CONECT   41   10
CONECT   42   10
CONECT   43   14
CONECT   44   62
CONECT   45   58
CONECT   46   68
CONECT   47   64
CONECT   48   20
CONECT   49   24
CONECT   50   18
ENDMDL
END
```

These calculations confirm that (S)-TetraMe-BITIOPO structure is highly hindered and for this reason, in the global minimum, the two P=O double bonds are oriented in opposite direction, a difference of BINAPO, where the two P=O double bonds are oriented in the same direction. For this reason, the energy barrier required to the correct orientation of these bonds was calculated. A variation of the energy in function of the dihedral angle has been reported in the graphic (Figure 6.10.1). At the global minimum, the dihedral angle is about 110 degree, instead, when the two P=O double bond are oriented in the same direction is about 230 degree. The calculated barrier energy is 12.02 kcal/mol.

```
___rotation.com_____________________________________________________________
s-tetraMe-BITIOPO.mae
s-tetraMe-BITIOPO-out.mae
 MMOD        0       1       0       0      0.0000      0.0000      0.0000      0.0000
 FFLD       10       1       0       1      1.0000      0.0000      0.0000      0.0000
 BDCO        0       0       0       0     41.5692  99999.0000      0.0000      0.0000
 READ        0       0       0       0      0.0000      0.0000      0.0000      0.0000
 FXTA        7       8       3       4    100.0000     86.2159     20.0000      0.0000
 BGIN        0       0       0       0      0.0000      0.0000      0.0000      0.0000
 DRIV       17       6       2       3      0.0000    360.0000     10.0000      0.0000
 CONV        2       0       0       0      0.0500      0.0000      0.0000      0.0000
 MINI        9       1     500       0      0.0000      0.0000      0.0000      0.0000
 END         0       0       0       0      0.0000      0.0000      0.0000      0.0000
____________________________________________________________________________________
```

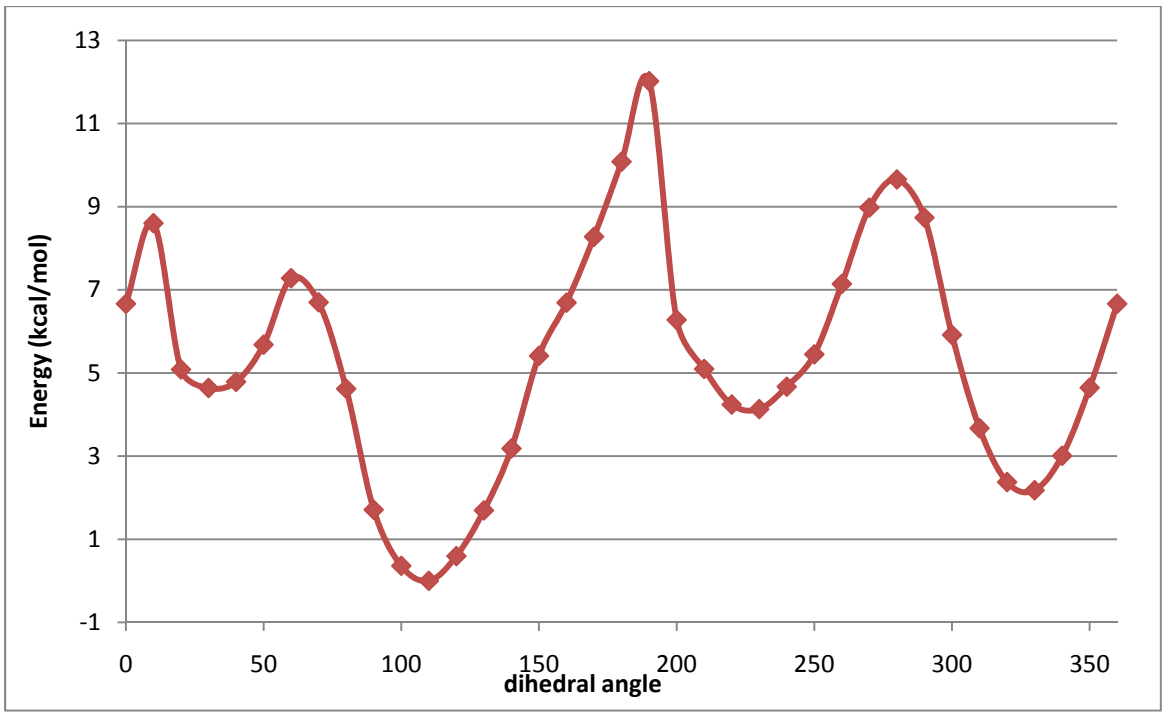

Figure 6.10.1

When a positively charged Li atom is introduced to mimic the presence of a cationic silicon atom, the two P=O double bonds of (*S*)-TetraMeBITIOPO are both oriented towards the lithium atom, and the energy barrier required to realize the correct orientation of these bonds is compensated by the stabilization of the complexation (figure 6.10.2).

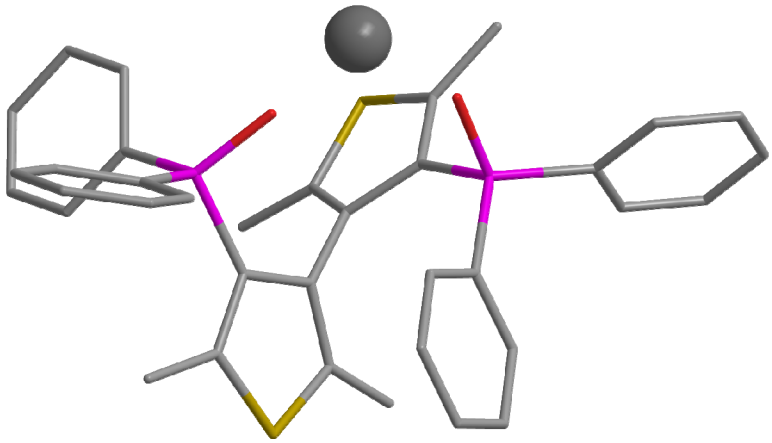

Figure 6.10.2: *MacroModel calculation of (S)-TetraMe-BITIOPO/Li^+ complex. The dimension of lithium atom was increased to improve the graphical picture.*

```
___complesso-Li.com_____________________________________________________________
complesso_Li_mc.mae
complesso_Li_mc-out.mae
 MMOD       0       1       0       0     0.0000     0.0000     0.0000     0.0000
 FFLD      10       1       0       1     1.0000     0.0000     0.0000     0.0000
 BDCO       0       0       0       0    41.5692 99999.0000     0.0000     0.0000
 READ       0       0       0       0     0.0000     0.0000     0.0000     0.0000
 FXTA       7       8       3       4   100.0000    77.9044    30.0000     0.0000
 CRMS       0       0       0       0     0.0000     0.5000     0.0000     0.0000
 MCMM   20000       0       0       0     0.0000     0.0000     0.0000     0.0000
 NANT       0       0       0       0     0.0000     0.0000     0.0000     0.0000
 MCNV       2       6       0       0     0.0000     0.0000     0.0000     0.0000
 MCSS       2       0       0       0    21.0000     0.0000     0.0000     0.0000
 MCOP     500       0       0       0     0.0000     0.0000     0.0000     0.0000
 DEMX       0     166       0       0    21.0000    42.0000     0.0000     0.0000
 COMP       1       2       3       4     0.0000     0.0000     0.0000     0.0000
 COMP       5       6       7       8     0.0000     0.0000     0.0000     0.0000
 COMP       9      10      11      12     0.0000     0.0000     0.0000     0.0000
 COMP      13      14      15      16     0.0000     0.0000     0.0000     0.0000
 COMP      17      18      21      22     0.0000     0.0000     0.0000     0.0000
 COMP      23      30      31      32     0.0000     0.0000     0.0000     0.0000
 COMP      39      40      41      48     0.0000     0.0000     0.0000     0.0000
 COMP      49      50      75       0     0.0000     0.0000     0.0000     0.0000
 MSYM       0       0       0       0     0.0000     0.0000     0.0000     0.0000
 AUOP       0       0       0       0   100.0000     0.0000     0.0000     0.0000
 TORS       2       6       0       0     0.0000   180.0000     0.0000     0.0000
 TORS       6      40       0       0     0.0000   180.0000     0.0000     0.0000
 TORS       6      49       0       0     0.0000   180.0000     0.0000     0.0000
 TORS       9      12       0       0     0.0000   180.0000     0.0000     0.0000
 TORS      12      22       0       0     0.0000   180.0000     0.0000     0.0000
 TORS      12      31       0       0     0.0000   180.0000     0.0000     0.0000
 MOLS      75       0       0       0     0.0000   180.0000     0.0000     1.0000
 TORC       4       3       8       7     0.0000   180.0000     0.0000     0.0000
 CONV       2       0       0       0     0.0500     0.0000     0.0000     0.0000
 MINI       9       1     500       0     0.0000     0.0000     0.0000     0.0000
_____________________________________________________________________________
```

___complesso-Li-BITIOPO.PDB_____

```
REMARK 888
REMARK 888 WRITTEN BY MAESTRO (A PRODUCT OF SCHRODINGER, LLC)
TITLE     Complesso-Li-s-Tetra-MeBITIOPO
MODEL        1
HETATM    1  C1  UNK     1      -5.547  -2.469  -1.737  1.00  0.00           C
HETATM    2  C2  UNK     1      -4.466  -3.246  -1.319  1.00  0.00           C
HETATM    3  C3  UNK     1      -3.246  -2.787  -1.923  1.00  0.00           C
HETATM    4  C4  UNK     1      -3.413  -1.592  -2.605  1.00  0.00           C
HETATM    5  S1  UNK     1      -5.050  -1.131  -2.674  1.00  0.00           S
HETATM    6  P1  UNK     1      -4.729  -4.689  -0.254  1.00  0.00           P
HETATM    7  C5  UNK     1      -2.398  -0.695  -3.241  1.00  0.00           C
HETATM    8  C6  UNK     1      -7.015  -2.608  -1.467  1.00  0.00           C
HETATM    9  C7  UNK     1      -1.121  -1.979   0.217  1.00  0.00           C
HETATM   10  C8  UNK     1       0.941  -5.564  -3.099  1.00  0.00           C
HETATM   11  O1  UNK     1      -5.417  -5.546  -1.320  1.00  0.00           O
HETATM   12  O2  UNK     1      -3.680  -5.190  -3.682  1.00  0.00           O
HETATM   13  C9  UNK     1      -7.456  -3.386   3.192  1.00  0.00           C
HETATM   14  C10 UNK     1      -6.438  -2.536   2.768  1.00  0.00           C
HETATM   15  C11 UNK     1      -5.601  -2.918   1.718  1.00  0.00           C
HETATM   16  C12 UNK     1      -5.776  -4.155   1.076  1.00  0.00           C
HETATM   17  C13 UNK     1      -6.803  -5.002   1.521  1.00  0.00           C
HETATM   18  C14 UNK     1      -7.639  -4.619   2.571  1.00  0.00           C
HETATM   19  C15 UNK     1      -0.941  -6.626   1.436  1.00  0.00           C
HETATM   20  C16 UNK     1      -1.586  -7.179   0.335  1.00  0.00           C
HETATM   21  C17 UNK     1      -2.729  -6.566  -0.181  1.00  0.00           C
HETATM   22  C18 UNK     1      -3.236  -5.382   0.379  1.00  0.00           C
HETATM   23  C19 UNK     1      -2.584  -4.854   1.502  1.00  0.00           C
HETATM   24  C20 UNK     1      -1.442  -5.468   2.024  1.00  0.00           C
HETATM   25  H1  UNK     1      -8.106  -3.088   4.012  1.00  0.00           H
HETATM   26  H2  UNK     1      -4.814  -2.235   1.405  1.00  0.00           H
HETATM   27  H3  UNK     1      -6.956  -5.972   1.052  1.00  0.00           H
HETATM   28  H4  UNK     1      -0.051  -7.100   1.845  1.00  0.00           H
HETATM   29  H5  UNK     1      -3.240  -7.034  -1.018  1.00  0.00           H
HETATM   30  H6  UNK     1      -2.954  -3.960   1.996  1.00  0.00           H
HETATM   31  H7  UNK     1      -2.272   0.213  -2.641  1.00  0.00           H
HETATM   32  H8  UNK     1      -1.418  -1.173  -3.321  1.00  0.00           H
HETATM   33  H9  UNK     1      -2.707  -0.399  -4.249  1.00  0.00           H
HETATM   34  H10 UNK     1      -7.299  -3.653  -1.317  1.00  0.00           H
HETATM   35  H11 UNK     1      -7.299  -2.034  -0.581  1.00  0.00           H
HETATM   36  H12 UNK     1      -7.612  -2.243  -2.310  1.00  0.00           H
HETATM   37  H13 UNK     1      -0.547  -2.245   1.112  1.00  0.00           H
HETATM   38  H14 UNK     1      -0.748  -1.021  -0.158  1.00  0.00           H
HETATM   39  H15 UNK     1      -2.161  -1.839   0.528  1.00  0.00           H
HETATM   40  H16 UNK     1       1.965  -5.333  -2.786  1.00  0.00           H
HETATM   41  H17 UNK     1       0.760  -6.616  -2.860  1.00  0.00           H
HETATM   42  H18 UNK     1       0.916  -5.424  -4.182  1.00  0.00           H
HETATM   43  H19 UNK     1      -6.297  -1.575   3.257  1.00  0.00           H
HETATM   44  H20 UNK     1       0.178  -1.517  -6.795  1.00  0.00           H
HETATM   45  H21 UNK     1      -4.040  -1.796  -7.533  1.00  0.00           H
HETATM   46  H22 UNK     1      -0.024  -7.863  -7.524  1.00  0.00           H
HETATM   47  H23 UNK     1      -1.133  -9.721  -3.819  1.00  0.00           H
HETATM   48  H24 UNK     1      -1.202  -8.094  -0.110  1.00  0.00           H
HETATM   49  H25 UNK     1      -0.943  -5.043   2.892  1.00  0.00           H
HETATM   50  H26 UNK     1      -8.431  -5.283   2.910  1.00  0.00           H
HETATM   51  C1  UNK     2      -1.004  -3.025  -0.845  1.00  0.00           C
HETATM   52  C2  UNK     2      -1.927  -3.424  -1.794  1.00  0.00           C
HETATM   53  C3  UNK     2      -1.384  -4.381  -2.734  1.00  0.00           C
HETATM   54  C4  UNK     2      -0.066  -4.691  -2.419  1.00  0.00           C
HETATM   55  S1  UNK     2       0.464  -3.867  -1.012  1.00  0.00           S
HETATM   56  P1  UNK     2      -2.266  -4.954  -4.215  1.00  0.00           P
HETATM   57  C5  UNK     2      -1.922  -1.547  -7.264  1.00  0.00           C
HETATM   58  C6  UNK     2      -3.154  -2.139  -7.004  1.00  0.00           C
HETATM   59  C7  UNK     2      -3.248  -3.170  -6.068  1.00  0.00           C
HETATM   60  C8  UNK     2      -2.113  -3.621  -5.376  1.00  0.00           C
HETATM   61  C9  UNK     2      -0.879  -3.012  -5.652  1.00  0.00           C
HETATM   62  C10 UNK     2      -0.785  -1.982  -6.589  1.00  0.00           C
HETATM   63  C11 UNK     2      -0.517  -8.921  -5.717  1.00  0.00           C
```

```
HETATM   64  C12 UNK     2      -1.093  -8.838  -4.453  1.00  0.00           C
HETATM   65  C13 UNK     2      -1.613  -7.623  -4.003  1.00  0.00           C
HETATM   66  C14 UNK     2      -1.553  -6.468  -4.802  1.00  0.00           C
HETATM   67  C15 UNK     2      -0.987  -6.578  -6.081  1.00  0.00           C
HETATM   68  C16 UNK     2      -0.467  -7.794  -6.532  1.00  0.00           C
HETATM   69  H1  UNK     2      -1.847  -0.744  -7.995  1.00  0.00           H
HETATM   70  H2  UNK     2      -4.221  -3.620  -5.881  1.00  0.00           H
HETATM   71  H3  UNK     2       0.027  -3.330  -5.141  1.00  0.00           H
HETATM   72  H4  UNK     2      -0.110  -9.866  -6.070  1.00  0.00           H
HETATM   73  H5  UNK     2      -2.054  -7.580  -3.012  1.00  0.00           H
HETATM   74  H6  UNK     2      -0.942  -5.724  -6.753  1.00  0.00           H
HETATM   75 LI1  UNK     1      -5.372  -5.601  -3.136  1.00  0.00          Li1+
CONECT    1    2    5    8
CONECT    1    2
CONECT    2    1    3    6
CONECT    2    1
CONECT    3    2    4   52
CONECT    3    4
CONECT    4    3    5    7
CONECT    4    3
CONECT    5    1    4
CONECT    6    2   11   16   22
CONECT    6   11
CONECT   51   52   55    9
CONECT   51   52
CONECT   52    3   51   53
CONECT   52   51
CONECT   53   52   54   56
CONECT   53   54
CONECT   54   53   55   10
CONECT   54   53
CONECT   55   51   54
CONECT   56   53   12   60   66
CONECT   56   12
CONECT    7    4   31   32   33
CONECT    8    1   34   35   36
CONECT    9   51   37   38   39
CONECT   10   54   40   41   42
CONECT   11    6
CONECT   11    6
CONECT   12   56
CONECT   12   56
CONECT   57   58   62   69
CONECT   57   58
CONECT   58   57   59   45
CONECT   58   57
CONECT   59   58   60   70
CONECT   59   60
CONECT   60   56   59   61
CONECT   60   59
CONECT   61   60   62   71
CONECT   61   62
CONECT   62   57   61   44
CONECT   62   61
CONECT   69   57
CONECT   70   59
CONECT   71   61
CONECT   63   64   68   72
CONECT   63   64
CONECT   64   63   65   47
CONECT   64   63
CONECT   65   64   66   73
CONECT   65   66
CONECT   66   56   65   67
CONECT   66   65
CONECT   67   66   68   74
CONECT   67   68
CONECT   68   63   67   46
```

```
CONECT   68   67
CONECT   72   63
CONECT   73   65
CONECT   74   67
CONECT   13   14   18   25
CONECT   13   14
CONECT   14   13   15   43
CONECT   14   13
CONECT   15   14   16   26
CONECT   15   16
CONECT   16    6   15   17
CONECT   16   15
CONECT   17   16   18   27
CONECT   17   18
CONECT   18   13   17   50
CONECT   18   17
CONECT   25   13
CONECT   26   15
CONECT   27   17
CONECT   19   20   24   28
CONECT   19   20
CONECT   20   19   21   48
CONECT   20   19
CONECT   21   20   22   29
CONECT   21   22
CONECT   22    6   21   23
CONECT   22   21
CONECT   23   22   24   30
CONECT   23   24
CONECT   24   19   23   49
CONECT   24   23
CONECT   28   19
CONECT   29   21
CONECT   30   23
CONECT   31    7
CONECT   32    7
CONECT   33    7
CONECT   34    8
CONECT   35    8
CONECT   36    8
CONECT   37    9
CONECT   38    9
CONECT   39    9
CONECT   40   10
CONECT   41   10
CONECT   42   10
CONECT   43   14
CONECT   44   62
CONECT   45   58
CONECT   46   68
CONECT   47   64
CONECT   48   20
CONECT   49   24
CONECT   50   18
ENDMDL
END
```

The geometry of (S)-MPP-TetraMeBITIOPO is calculated with the same procedure. The global minimum of catalyst (S)-MPP-tetraMe-BITIOPO is reported in figure 6.10.3a while the coordination with a positively charged Lithium atom is shown in figure 6.10.3b.

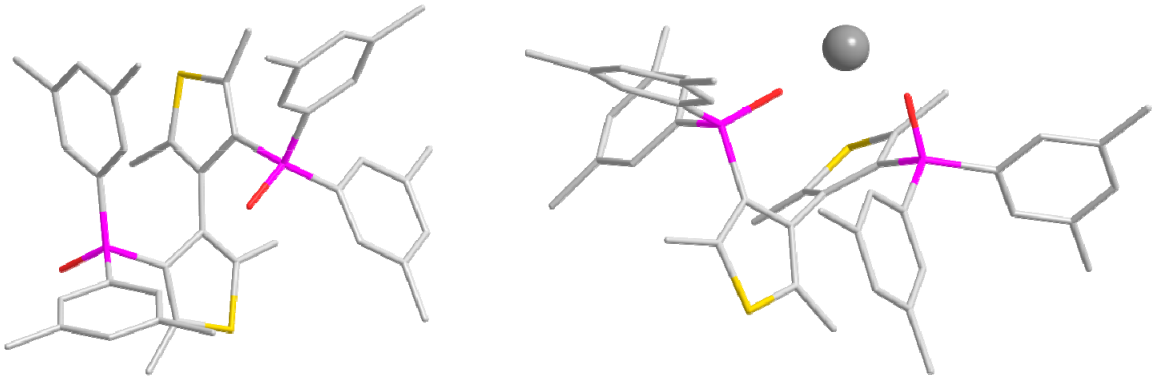

(a) (b)

Scheme 6.10.3: *MacroModel calculation of MPP-TetraMe-BITIOPO. The dimension of lithium atom was increased to improve the graphical picture.*

```
___S-MPP-TetraMe-BITIOPO.PDB_____________________________________________________
REMARK 888
REMARK 888 WRITTEN BY MAESTRO (A PRODUCT OF SCHRODINGER, LLC)
TITLE     arilbistiofene_min-out
MODEL        1
HETATM    1  C1  UNK     1      -6.055  -1.650  -2.043  1.00  0.00           C
HETATM    2  C2  UNK     1      -4.997  -2.491  -1.726  1.00  0.00           C
HETATM    3  C3  UNK     1      -3.732  -1.898  -2.106  1.00  0.00           C
HETATM    4  C4  UNK     1      -3.873  -0.619  -2.610  1.00  0.00           C
HETATM    5  S1  UNK     1      -5.507  -0.152  -2.677  1.00  0.00           S
HETATM    6  P1  UNK     1      -5.109  -4.106  -0.904  1.00  0.00           P
HETATM    7  C5  UNK     1      -2.814   0.339  -3.050  1.00  0.00           C
HETATM    8  C6  UNK     1      -7.530  -1.823  -1.901  1.00  0.00           C
HETATM    9  C7  UNK     1      -1.991  -1.380   0.445  1.00  0.00           C
HETATM   10  C8  UNK     1       0.683  -4.445  -2.926  1.00  0.00           C
HETATM   11  O1  UNK     1      -4.189  -4.937  -1.769  1.00  0.00           O
HETATM   12  O2  UNK     1      -0.960  -2.742  -5.204  1.00  0.00           O
HETATM   13  C9  UNK     1      -9.364  -5.842  -0.967  1.00  0.00           C
HETATM   14  C10 UNK     1      -8.991  -5.011   0.093  1.00  0.00           C
HETATM   15  C11 UNK     1      -7.693  -4.483   0.126  1.00  0.00           C
HETATM   16  C12 UNK     1      -6.777  -4.727  -0.909  1.00  0.00           C
HETATM   17  C13 UNK     1      -7.179  -5.575  -1.954  1.00  0.00           C
HETATM   18  C14 UNK     1      -8.459  -6.143  -1.989  1.00  0.00           C
HETATM   19  C15 UNK     1      -9.946  -4.743   1.219  1.00  0.00           C
HETATM   20  C16 UNK     1      -8.870  -7.030  -3.127  1.00  0.00           C
HETATM   21  C17 UNK     1      -3.671  -3.493   3.406  1.00  0.00           C
HETATM   22  C18 UNK     1      -4.579  -2.578   2.858  1.00  0.00           C
HETATM   23  C19 UNK     1      -5.000  -2.746   1.533  1.00  0.00           C
HETATM   24  C20 UNK     1      -4.550  -3.828   0.761  1.00  0.00           C
HETATM   25  C21 UNK     1      -3.649  -4.735   1.336  1.00  0.00           C
HETATM   26  C22 UNK     1      -3.210  -4.581   2.656  1.00  0.00           C
HETATM   27  C23 UNK     1      -5.034  -1.391   3.655  1.00  0.00           C
HETATM   28  C24 UNK     1      -2.201  -5.531   3.233  1.00  0.00           C
HETATM   29  H1  UNK     1     -10.364  -6.272  -0.991  1.00  0.00           H
HETATM   30  H2  UNK     1      -7.406  -3.870   0.976  1.00  0.00           H
HETATM   31  H3  UNK     1      -6.465  -5.808  -2.743  1.00  0.00           H
HETATM   32  H4  UNK     1      -3.313  -3.352   4.424  1.00  0.00           H
```

```
HETATM   33  H5  UNK     1      -5.682  -2.019   1.095  1.00  0.00           H
HETATM   34  H6  UNK     1      -3.278  -5.565   0.735  1.00  0.00           H
HETATM   35  H7  UNK     1      -2.422   0.887  -2.187  1.00  0.00           H
HETATM   36  H8  UNK     1      -1.981  -0.184  -3.530  1.00  0.00           H
HETATM   37  H9  UNK     1      -3.197   1.068  -3.773  1.00  0.00           H
HETATM   38  H10 UNK     1      -7.870  -2.710  -2.440  1.00  0.00           H
HETATM   39  H11 UNK     1      -7.805  -1.898  -0.846  1.00  0.00           H
HETATM   40  H12 UNK     1      -8.091  -0.977  -2.314  1.00  0.00           H
HETATM   41  H13 UNK     1      -1.860  -1.901   1.398  1.00  0.00           H
HETATM   42  H14 UNK     1      -1.310  -0.521   0.433  1.00  0.00           H
HETATM   43  H15 UNK     1      -3.008  -0.984   0.410  1.00  0.00           H
HETATM   44  H16 UNK     1       1.653  -4.164  -2.500  1.00  0.00           H
HETATM   45  H17 UNK     1       0.545  -5.518  -2.763  1.00  0.00           H
HETATM   46  H18 UNK     1       0.754  -4.262  -4.001  1.00  0.00           H
HETATM   47  H19 UNK     1      -9.819  -5.494   2.005  1.00  0.00           H
HETATM   48  H20 UNK     1      -9.775  -3.749   1.647  1.00  0.00           H
HETATM   49  H21 UNK     1     -10.983  -4.770   0.867  1.00  0.00           H
HETATM   50  H22 UNK     1      -8.000  -7.503  -3.593  1.00  0.00           H
HETATM   51  H23 UNK     1      -9.526  -7.833  -2.775  1.00  0.00           H
HETATM   52  H24 UNK     1      -9.400  -6.445  -3.885  1.00  0.00           H
HETATM   53  H25 UNK     1      -4.354  -0.549   3.492  1.00  0.00           H
HETATM   54  H26 UNK     1      -6.046  -1.092   3.363  1.00  0.00           H
HETATM   55  H27 UNK     1      -5.060  -1.625   4.724  1.00  0.00           H
HETATM   56  H28 UNK     1      -2.326  -6.535   2.814  1.00  0.00           H
HETATM   57  H29 UNK     1      -1.189  -5.178   3.013  1.00  0.00           H
HETATM   58  H30 UNK     1      -2.320  -5.615   4.318  1.00  0.00           H
HETATM   59  C1  UNK     2      -1.694  -2.280  -0.710  1.00  0.00           C
HETATM   60  C2  UNK     2      -2.415  -2.512  -1.871  1.00  0.00           C
HETATM   61  C3  UNK     2      -1.659  -3.272  -2.831  1.00  0.00           C
HETATM   62  C4  UNK     2      -0.437  -3.676  -2.298  1.00  0.00           C
HETATM   63  S1  UNK     2      -0.237  -3.163  -0.682  1.00  0.00           S
HETATM   64  P1  UNK     2      -2.041  -3.601  -4.568  1.00  0.00           P
HETATM   65  C5  UNK     2      -1.402  -8.060  -5.474  1.00  0.00           C
HETATM   66  C6  UNK     2      -1.109  -7.089  -6.437  1.00  0.00           C
HETATM   67  C7  UNK     2      -1.304  -5.739  -6.124  1.00  0.00           C
HETATM   68  C8  UNK     2      -1.804  -5.344  -4.873  1.00  0.00           C
HETATM   69  C9  UNK     2      -2.100  -6.337  -3.932  1.00  0.00           C
HETATM   70  C10 UNK     2      -1.914  -7.694  -4.224  1.00  0.00           C
HETATM   71  C11 UNK     2      -0.532  -7.483  -7.764  1.00  0.00           C
HETATM   72  C12 UNK     2      -2.199  -8.735  -3.182  1.00  0.00           C
HETATM   73  C13 UNK     2      -6.165  -2.340  -6.114  1.00  0.00           C
HETATM   74  C14 UNK     2      -6.024  -3.591  -5.501  1.00  0.00           C
HETATM   75  C15 UNK     2      -4.781  -3.960  -4.963  1.00  0.00           C
HETATM   76  C16 UNK     2      -3.669  -3.114  -5.070  1.00  0.00           C
HETATM   77  C17 UNK     2      -3.833  -1.883  -5.729  1.00  0.00           C
HETATM   78  C18 UNK     2      -5.076  -1.474  -6.225  1.00  0.00           C
HETATM   79  C19 UNK     2      -7.207  -4.508  -5.415  1.00  0.00           C
HETATM   80  C20 UNK     2      -5.217  -0.154  -6.921  1.00  0.00           C
HETATM   81  H1  UNK     2      -1.228  -9.111  -5.697  1.00  0.00           H
HETATM   82  H2  UNK     2      -1.058  -4.971  -6.858  1.00  0.00           H
HETATM   83  H3  UNK     2      -2.469  -6.053  -2.951  1.00  0.00           H
HETATM   84  H4  UNK     2      -7.131  -2.045  -6.518  1.00  0.00           H
HETATM   85  H5  UNK     2      -4.671  -4.929  -4.482  1.00  0.00           H
HETATM   86  H6  UNK     2      -2.966  -1.234  -5.855  1.00  0.00           H
HETATM   87  H7  UNK     2       0.560  -7.504  -7.705  1.00  0.00           H
HETATM   88  H8  UNK     2      -0.889  -8.473  -8.067  1.00  0.00           H
HETATM   89  H9  UNK     2      -0.831  -6.777  -8.545  1.00  0.00           H
HETATM   90  H10 UNK     2      -1.313  -8.894  -2.561  1.00  0.00           H
HETATM   91  H11 UNK     2      -3.031  -8.426  -2.542  1.00  0.00           H
HETATM   92  H12 UNK     2      -2.482  -9.685  -3.645  1.00  0.00           H
HETATM   93  H13 UNK     2      -7.882  -4.175  -4.623  1.00  0.00           H
HETATM   94  H14 UNK     2      -7.752  -4.520  -6.364  1.00  0.00           H
HETATM   95  H15 UNK     2      -6.897  -5.537  -5.209  1.00  0.00           H
HETATM   96  H16 UNK     2      -4.527   0.585  -6.500  1.00  0.00           H
HETATM   97  H17 UNK     2      -5.005  -0.268  -7.989  1.00  0.00           H
HETATM   98  H18 UNK     2      -6.230   0.245  -6.802  1.00  0.00           H
CONECT    1    2    5    8
CONECT    1    2
```

```
CONECT    2    1    3    6
CONECT    2    1
CONECT    3    2    4   60
CONECT    3    4
CONECT    4    3    5    7
CONECT    4    3
CONECT    5    1    4
CONECT    6    2   11   16   24
CONECT    6   11
CONECT   59   60   63    9
CONECT   59   60
CONECT   60    3   59   61
CONECT   60   59
CONECT   61   60   62   64
CONECT   61   62
CONECT   62   61   63   10
CONECT   62   61
CONECT   63   59   62
CONECT   64   61   12   68   76
CONECT   64   12
CONECT    7    4   35   36   37
CONECT    8    1   38   39   40
CONECT    9   59   41   42   43
CONECT   10   62   44   45   46
CONECT   11    6
CONECT   11    6
CONECT   12   64
CONECT   12   64
CONECT   65   66   70   81
CONECT   65   66
CONECT   66   65   67   71
CONECT   66   65
CONECT   67   66   68   82
CONECT   67   68
CONECT   68   64   67   69
CONECT   68   67
CONECT   69   68   70   83
CONECT   69   70
CONECT   70   65   69   72
CONECT   70   69
CONECT   81   65
CONECT   71   66   87   88   89
CONECT   82   67
CONECT   83   69
CONECT   72   70   90   91   92
CONECT   73   74   78   84
CONECT   73   74
CONECT   74   73   75   79
CONECT   74   73
CONECT   75   74   76   85
CONECT   75   76
CONECT   76   64   75   77
CONECT   76   75
CONECT   77   76   78   86
CONECT   77   78
CONECT   78   73   77   80
CONECT   78   77
CONECT   84   73
CONECT   79   74   93   94   95
CONECT   85   75
CONECT   86   77
CONECT   80   78   96   97   98
CONECT   13   14   18   29
CONECT   13   14
CONECT   14   13   15   19
CONECT   14   13
CONECT   15   14   16   30
CONECT   15   16
```

```
CONECT   16    6   15   17
CONECT   16   15
CONECT   17   16   18   31
CONECT   17   18
CONECT   18   13   17   20
CONECT   18   17
CONECT   29   13
CONECT   19   14   47   48   49
CONECT   30   15
CONECT   31   17
CONECT   20   18   50   51   52
CONECT   21   22   26   32
CONECT   21   22
CONECT   22   21   23   27
CONECT   22   21
CONECT   23   22   24   33
CONECT   23   24
CONECT   24    6   23   25
CONECT   24   23
CONECT   25   24   26   34
CONECT   25   26
CONECT   26   21   25   28
CONECT   26   25
CONECT   32   21
CONECT   27   22   53   54   55
CONECT   33   23
CONECT   34   25
CONECT   28   26   56   57   58
CONECT   35    7
CONECT   36    7
CONECT   37    7
CONECT   38    8
CONECT   39    8
CONECT   40    8
CONECT   41    9
CONECT   42    9
CONECT   43    9
CONECT   44   10
CONECT   45   10
CONECT   46   10
CONECT   87   71
CONECT   88   71
CONECT   89   71
CONECT   90   72
CONECT   91   72
CONECT   92   72
CONECT   93   79
CONECT   94   79
CONECT   95   79
CONECT   96   80
CONECT   97   80
CONECT   98   80
CONECT   47   19
CONECT   48   19
CONECT   49   19
CONECT   50   20
CONECT   51   20
CONECT   52   20
CONECT   53   27
CONECT   54   27
CONECT   55   27
CONECT   56   28
CONECT   57   28
CONECT   58   28
ENDMDL
END
```

___complesso-Li-MPP-BITIOPO.PDB_____

```
REMARK   This PDB file is created by CS Chem3D.
SEQRES   1       1  UNK
HETATM    1  C1  UNK     1      -4.792  -2.372  -2.104                          C
HETATM    2  C2  UNK     1      -4.205  -3.431  -1.421                          C
HETATM    3  C3  UNK     1      -2.834  -3.125  -1.073                          C
HETATM    4  C4  UNK     1      -2.459  -1.851  -1.457                          C
HETATM    5  S1  UNK     1      -3.695  -1.073  -2.328                          S
HETATM    6  P1  UNK     1      -5.074  -4.929  -0.873                          P
HETATM    7  C5  UNK     1      -1.190  -1.108  -1.181                          C
HETATM    8  C6  UNK     1      -6.182  -2.170  -2.621                          C
HETATM    9  C7  UNK     1      -2.564  -2.818   2.027                          C
HETATM   10  C8  UNK     1       0.401  -6.884   0.353                          C
HETATM   11  O1  UNK     1      -4.024  -6.016  -1.107                          O
HETATM   12  O2  UNK     1      -1.496  -6.754  -2.419                          O
HETATM   13  C9  UNK     1      -8.727  -5.747  -3.518                          C
HETATM   14  C10 UNK     1      -8.920  -5.425  -2.170                          C
HETATM   15  C11 UNK     1      -7.805  -5.182  -1.358                          C
HETATM   16  C12 UNK     1      -6.504  -5.209  -1.883                          C
HETATM   17  C13 UNK     1      -6.340  -5.542  -3.238                          C
HETATM   18  C14 UNK     1      -7.440  -5.819  -4.059                          C
HETATM   19  C15 UNK     1     -10.304  -5.401  -1.588                          C
HETATM   20  C16 UNK     1      -7.249  -6.132  -5.515                          C
HETATM   21  C17 UNK     1      -6.099  -4.195   3.531                          C
HETATM   22  C18 UNK     1      -6.411  -3.213   2.586                          C
HETATM   23  C19 UNK     1      -6.086  -3.430   1.242                          C
HETATM   24  C20 UNK     1      -5.472  -4.622   0.827                          C
HETATM   25  C21 UNK     1      -5.185  -5.599   1.794                          C
HETATM   26  C22 UNK     1      -5.500  -5.398   3.143                          C
HETATM   27  C23 UNK     1      -7.026  -1.914   3.020                          C
HETATM   28  C24 UNK     1      -5.140  -6.429   4.172                          C
HETATM   29  H1  UNK     1      -9.591  -5.947  -4.151                          H
HETATM   30  H2  UNK     1      -7.971  -4.968  -0.303                          H
HETATM   31  H3  UNK     1      -5.340  -5.577  -3.663                          H
HETATM   32  H4  UNK     1      -6.324  -4.021   4.583                          H
HETATM   33  H5  UNK     1      -6.313  -2.653   0.516                          H
HETATM   34  H6  UNK     1      -4.702  -6.526   1.495                          H
HETATM   35  H7  UNK     1      -1.286  -0.538  -0.251                          H
HETATM   36  H8  UNK     1      -0.343  -1.792  -1.072                          H
HETATM   37  H9  UNK     1      -0.944  -0.409  -1.987                          H
HETATM   38  H10 UNK     1      -6.387  -1.120  -2.858                          H
HETATM   39  H11 UNK     1      -6.336  -2.741  -3.540                          H
HETATM   40  H12 UNK     1      -6.923  -2.465  -1.875                          H
HETATM   41  H13 UNK     1      -1.814  -2.105   2.385                          H
HETATM   42  H14 UNK     1      -3.338  -2.247   1.507                          H
HETATM   43  H15 UNK     1      -3.028  -3.292   2.897                          H
HETATM   44  H16 UNK     1       1.449  -6.570   0.384                          H
HETATM   45  H17 UNK     1       0.215  -7.519   1.226                          H
HETATM   46  H18 UNK     1       0.248  -7.515  -0.526                          H
HETATM   47  H19 UNK     1     -10.373  -4.669  -0.776                          H
HETATM   48  H20 UNK     1     -11.043  -5.116  -2.344                          H
HETATM   49  H21 UNK     1     -10.562  -6.390  -1.196                          H
HETATM   50  H22 UNK     1      -7.237  -5.206  -6.098                          H
HETATM   51  H23 UNK     1      -6.307  -6.666  -5.677                          H
HETATM   52  H24 UNK     1      -8.054  -6.774  -5.887                          H
HETATM   53  H25 UNK     1      -7.655  -1.497   2.227                          H
HETATM   54  H26 UNK     1      -7.664  -2.057   3.898                          H
HETATM   55  H27 UNK     1      -6.241  -1.193   3.265                          H
HETATM   56  H28 UNK     1      -5.173  -7.436   3.743                          H
HETATM   57  H29 UNK     1      -4.132  -6.240   4.553                          H
HETATM   58  H30 UNK     1      -5.845  -6.409   5.009                          H
HETATM   59  C1  UNK     1      -1.918  -3.834   1.136                          C
HETATM   60  C2  UNK     1      -1.977  -3.981  -0.240                          C
HETATM   61  C3  UNK     1      -1.065  -4.982  -0.721                          C
HETATM   62  C4  UNK     1      -0.507  -5.692   0.341                          C
HETATM   63  S1  UNK     1      -0.930  -5.020   1.854                          S
HETATM   64  P1  UNK     1      -0.700  -5.447  -2.435                          P
```

```
HETATM   65  C5  UNK     1      -2.108  -2.491  -5.630                       C
HETATM   66  C6  UNK     1      -0.946  -2.211  -4.906                       C
HETATM   67  C7  UNK     1      -0.519  -3.112  -3.922                       C
HETATM   68  C8  UNK     1      -1.257  -4.266  -3.620                       C
HETATM   69  C9  UNK     1      -2.415  -4.526  -4.371                       C
HETATM   70  C10 UNK     1      -2.843  -3.653  -5.379                       C
HETATM   71  C11 UNK     1      -0.137  -0.986  -5.222                       C
HETATM   72  C12 UNK     1      -4.098  -3.931  -6.153                       C
HETATM   73  C13 UNK     1       3.836  -5.989  -2.789                       C
HETATM   74  C14 UNK     1       2.969  -6.891  -3.415                       C
HETATM   75  C15 UNK     1       1.587  -6.704  -3.297                       C
HETATM   76  C16 UNK     1       1.062  -5.643  -2.542                       C
HETATM   77  C17 UNK     1       1.953  -4.754  -1.918                       C
HETATM   78  C18 UNK     1       3.338  -4.927  -2.025                       C
HETATM   79  C19 UNK     1       3.518  -8.004  -4.261                       C
HETATM   80  C20 UNK     1       4.280  -3.951  -1.382                       C
HETATM   81  H1  UNK     1      -2.438  -1.799  -6.404                       H
HETATM   82  H2  UNK     1       0.404  -2.897  -3.389                       H
HETATM   83  H3  UNK     1      -2.979  -5.435  -4.183                       H
HETATM   84  H4  UNK     1       4.913  -6.112  -2.900                       H
HETATM   85  H5  UNK     1       0.909  -7.389  -3.804                       H
HETATM   86  H6  UNK     1       1.570  -3.917  -1.337                       H
HETATM   87  H7  UNK     1      -0.789  -0.154  -5.511                       H
HETATM   88  H8  UNK     1       0.438  -0.659  -4.350                       H
HETATM   89  H9  UNK     1       0.556  -1.197  -6.043                       H
HETATM   90  H10 UNK     1      -4.031  -3.524  -7.167                       H
HETATM   91  H11 UNK     1      -4.266  -5.009  -6.248                       H
HETATM   92  H12 UNK     1      -4.957  -3.481  -5.647                       H
HETATM   93  H13 UNK     1       3.655  -7.658  -5.290                       H
HETATM   94  H14 UNK     1       4.481  -8.351  -3.871                       H
HETATM   95  H15 UNK     1       2.840  -8.864  -4.263                       H
HETATM   96  H16 UNK     1       5.218  -4.441  -1.100                       H
HETATM   97  H17 UNK     1       4.501  -3.133  -2.075                       H
HETATM   98  H18 UNK     1       3.844  -3.533  -0.468                       H
HETATM   99 LI1  UNK     1      -2.894  -7.399  -1.459                      LI
TER
CONECT    1    2    5    8
CONECT    2    1    3    6
CONECT    3    2    4   60
CONECT    4    3    5    7
CONECT    5    1    4
CONECT    6    2   11   16   24
CONECT    7    4   35   36   37
CONECT    8    1   38   39   40
CONECT    9   41   42   43   59
CONECT   10   44   45   46   62
CONECT   11    6
CONECT   12   64
CONECT   13   14   18   29
CONECT   14   13   15   19
CONECT   15   14   16   30
CONECT   16    6   15   17
CONECT   17   16   18   31
CONECT   18   13   17   20
CONECT   19   14   47   48   49
CONECT   20   18   50   51   52
CONECT   21   22   26   32
CONECT   22   21   23   27
CONECT   23   22   24   33
CONECT   24    6   23   25
CONECT   25   24   26   34
CONECT   26   21   25   28
CONECT   27   22   53   54   55
CONECT   28   26   56   57   58
CONECT   29   13
CONECT   30   15
CONECT   31   17
CONECT   32   21
```

```
CONECT   33   23
CONECT   34   25
CONECT   35    7
CONECT   36    7
CONECT   37    7
CONECT   38    8
CONECT   39    8
CONECT   40    8
CONECT   41    9
CONECT   42    9
CONECT   43    9
CONECT   44   10
CONECT   45   10
CONECT   46   10
CONECT   47   19
CONECT   48   19
CONECT   49   19
CONECT   50   20
CONECT   51   20
CONECT   52   20
CONECT   53   27
CONECT   54   27
CONECT   55   27
CONECT   56   28
CONECT   57   28
CONECT   58   28
CONECT   59    9   60   63
CONECT   60    3   59   61
CONECT   61   60   62   64
CONECT   62   10   61   63
CONECT   63   59   62
CONECT   64   12   61   68   76
CONECT   65   66   70   81
CONECT   66   65   67   71
CONECT   67   66   68   82
CONECT   68   64   67   69
CONECT   69   68   70   83
CONECT   70   65   69   72
CONECT   71   66   87   88   89
CONECT   72   70   90   91   92
CONECT   73   74   78   84
CONECT   74   73   75   79
CONECT   75   74   76   85
CONECT   76   64   75   77
CONECT   77   76   78   86
CONECT   78   73   77   80
CONECT   79   74   93   94   95
CONECT   80   78   96   97   98
CONECT   81   65
CONECT   82   67
CONECT   83   69
CONECT   84   73
CONECT   85   75
CONECT   86   77
CONECT   87   71
CONECT   88   71
CONECT   89   71
CONECT   90   72
CONECT   91   72
CONECT   92   72
CONECT   93   79
CONECT   94   79
CONECT   95   79
CONECT   96   80
CONECT   97   80
CONECT   98   80
END
```

6.11.4 MOPAC syntax

To run a MOPAC job, a file *filename.mop* is required. The *filename.mop* file contain both the input geometry of the structure under investigation that the list of operations ("keywords") telling MOPAC which operations are to be performed.

The first three lines are textual and obligatory. The first line consist of keywords that control the calculation, instead the next two lines are comments or titles. If no name or comment is wanted, blank lines are required. The next set of lines defines instead the geometry. All control data are entered in the form of keywords; the order in which keywords appear is not important although they must be separated by a space. There are three classes of keywords:

- those which CONTROL substantial aspects of the calculation,
- those which determine which OUTPUT will be calculated and printed,
- those which dictate the WORKING of the calculation.

A description of what each keyword does is given in MOPAC manual.

The geometry can be defined in terms of either internal or cartesian coordinates. In both case, each coordinate is followed by an integer number, to indicate the action to be taken. Integer Action "1" optimize the internal coordinate, instead action "0" do not optimize the internal coordinate. Using internal coordinates, the first atom has three unoptimizable coordinates, the second atom two, (the bond-length can be optimized) and the third atom has one unoptimizable coordinate. None of these six unoptimizable coordinates at the start of the geometry should be marked for optimization. If any are so marked, a warning is given, but the calculation will continue. In cartesian coordinates all parameters can be optimized.

When a job is terminated correctly a *filename.out* and *filename.arc* were generated. The first contain the results, the second is a summary of calculation. When, for some reason, the job was interrupted, a *filename.res* was generated, and a restart could be performed.

6.11.5 TetraMe-BITIOPO calculations with MOPAC

A computational investigation about the model that explain the stereoselection observed in the reactions promoted by tetra-Me-BITIOPO was performed with MOPAC.

Initial estimates for the geometries of the two hypothesized transition states (**TS-A** and **TS-B**, chapter 4) were obtained by a MacroModel. Also in this case, a symmetry constraint for the biaryl bond was imposed, in order to prevent the interconversion

between the two enantiomeric forms of tetraMe-BITIOPO. Subsequently, by using the semi-empirical AM1 quantum chemical method in the MOPAC 2009 program, the two structures were minimized and used as starting point for a reaction path study. The distance between the two carbon atoms involved in the formation of the new C-C bond was fixed at progressively smaller values (with steps of 0.5 Å), in order to simulate the course of the reaction. For each distance, two structures of complex were minimized.
Only the *file.mop* and *file.arc* of structures $\mathbf{S_{2.0}}$ with C-C fixed distance 1.979 Å for the favored transition state **TS-A** and for the unfavored transition state **TS-B** were reported (note the presence of the integer value "0" at the line 97 in the fix distance input file).

___TS-A-1.979.mop_____

```
 AM1 CHARGE=1 EF
 distanza C-aledide C-enolato vincolata a 1.979 (re face)

  C     0.00000000 +0    0.0000000 +0    0.0000000 +0                          -0.1528
  C     1.51960260 +1    0.0000000 +0    0.0000000 +0     1     0     0      -0.1458
  C     1.50469844 +1  107.6451499 +1    0.0000000 +0     2     1     0       0.1477
  C     1.35100000 +0  121.5092967 +1  -29.6097888 +1     3     2     1      -0.3172
  C     1.48499405 +1  122.8705197 +1   -5.1642503 +1     4     3     2      -0.1050
  C     1.51407806 +1  109.6396636 +1   60.3166470 +1     1     2     3      -0.1567
  O     1.34780027 +1  116.6396758 +1  139.2668854 +1     3     2     1      -0.5857
 Cl     4.90189823 +1   12.2441042 +1   85.6557838 +1     1     2     3      -0.5499
  C     9.90374304 +1    4.3203835 +1   21.4776300 +1     1     2     3      -0.2871
  C     1.40101098 +1   47.9894809 +1 -120.8774906 +1     9     1     2      -0.9169
  C     1.44962222 +1  109.4095315 +1  107.6422303 +1    10     9     1       0.0251
  C     1.39517622 +1  111.7698543 +1    0.9155274 +1    11    10     9      -0.3990
  S     1.65677272 +1  112.5692298 +1    0.2810964 +1     9    10    11       0.6929
  P     1.62142453 +1  124.0478398 +1  177.2426317 +1    10     9    13       3.2995
  C    10.00788007 +1   27.1798257 +1  -52.3437419 +1     1     2     3      -0.3966
  C     1.47280729 +1  131.1645191 +1  173.2654976 +1    11    10     9       0.0105
  C     1.44772303 +1  131.4730171 +1   92.8097936 +1    16    11    10      -0.9355
  C     1.40047255 +1  109.6325854 +1  176.7219497 +1    17    16    11      -0.2572
  S     1.65168460 +1  111.5562543 +1 -178.0651641 +1    15    16    11       0.7033
  P     1.60910800 +1  125.5579813 +1   -8.0466452 +1    17    16    11       3.3053
  C     1.46952580 +1  127.4183463 +1  175.7989690 +1    12    11    10      -0.1653
  C     1.47767413 +1  134.8043099 +1  179.9004197 +1     9    10    11      -0.1873
  C     1.46789810 +1  127.0120021 +1   -1.0624227 +1    15    16    11      -0.1626
  C     1.47716774 +1  134.3023693 +1  177.1680060 +1    18    17    16      -0.1903
  O     1.54275491 +1  111.3636939 +1  126.8696867 +1    14    10     9      -1.1833
  O     1.54326892 +1  107.8451328 +1  -66.0118293 +1    20    17    16      -1.1704
  C     8.85989342 +1   30.2765706 +1 -145.9986293 +1     1     2     3      -0.0555
  C     1.39400974 +1   26.0643426 +1  -50.9002461 +1    27     1     2      -0.1479
  C     1.39396268 +1  119.8021074 +1   55.3701921 +1    28    27     1      -0.0135
  C     1.59962069 +1  112.5121270 +1   54.2303796 +1    20    17    16      -0.9509
  C     1.39766406 +1  121.9675599 +1   43.6882371 +1    30    20    17      -0.0388
  C     1.39844778 +1  119.9954740 +1   -0.8955064 +1    27    28    29      -0.1588
  C     6.36104738 +1   66.4613637 +1  -92.8393094 +1     1     2     3      -0.0524
  C     1.39376854 +1   38.6934348 +1   66.2221523 +1    33     1     2      -0.1500
  C     1.39409705 +1  119.8448114 +1 -105.1960736 +1    34    33     1      -0.0129
  C     1.60124490 +1  111.7535169 +1  175.3745037 +1    20    17    16      -0.9662
  C     1.39888532 +1  122.5750517 +1  -84.3757020 +1    36    20    17      -0.0346
  C     1.39864490 +1  119.8682538 +1    0.1210001 +1    33    34    35      -0.1559
  C     9.68519692 +1   32.8686394 +1   64.6080843 +1     1     2     3      -0.0553
  C     1.39673032 +1  110.3079998 +1  -68.6555540 +1    39     1     2      -0.1588
  C     1.39185395 +1  119.9011978 +1   34.8662412 +1    40    39     1      -0.0326
  C     1.60710034 +1  110.8426043 +1    9.7092945 +1    14    10     9      -0.9563
  C     1.40230873 +1  118.3340633 +1   78.4400107 +1    42    14    10      -0.0283
  C     1.39486134 +1  119.6696074 +1    0.1097437 +1    39    40    41      -0.1516
  C    11.38119524 +1   35.6058744 +1   -7.3333061 +1     1     2     3      -0.0565
  C     1.39206108 +1   22.4261658 +1 -166.4419751 +1    45     1     2      -0.1492
  C     1.39667824 +1  119.9766993 +1    0.6628563 +1    46    45     1      -0.0170
  C     1.59927162 +1  107.7069106 +1 -109.0639518 +1    14    10     9      -0.9598
```

C	1.40333964 +1	120.0380189 +1	49.2979206 +1	48	14	10	-0.0480
C	1.40071665 +1	119.8755525 +1	-0.6535746 +1	45	46	47	-0.1578
Si	1.77969948 +1	129.9055758 +1	93.5738703 +1	7	3	2	1.8430
H	1.12029124 +1	109.9061491 +1	-60.8983831 +1	1	2	3	0.0854
H	1.12065205 +1	109.5390163 +1	-179.0733328 +1	1	2	3	0.0830
H	1.12137427 +1	110.9837160 +1	-59.9438718 +1	2	1	6	0.1143
H	1.11995304 +1	110.6133035 +1	-179.7496767 +1	2	1	6	0.0961
H	1.09396674 +1	124.2511161 +1	-100.1080400 +1	4	3	2	0.1206
H	1.12535402 +1	108.0267819 +1	130.3763778 +1	5	4	3	0.0778
H	1.12416367 +1	109.0655555 +1	-114.0430277 +1	5	4	3	0.0816
H	1.12239966 +1	108.9422838 +1	62.5122499 +1	6	1	2	0.0812
H	1.12091831 +1	109.6443295 +1	179.4826859 +1	6	1	2	0.0836
H	1.11943574 +1	111.1501806 +1	-10.0099757 +1	21	12	11	0.0993
H	1.12136299 +1	110.6721503 +1	110.1748966 +1	21	12	11	0.0978
H	1.12006269 +1	110.5295466 +1	-129.8329078 +1	21	12	11	0.0954
H	1.12148221 +1	111.3188171 +1	-64.1658652 +1	22	9	10	0.1210
H	1.12038937 +1	112.0034617 +1	57.1340485 +1	22	9	10	0.1098
H	1.12232394 +1	109.8953911 +1	176.6396533 +1	22	9	10	0.1007
H	1.11923434 +1	111.0045616 +1	-172.2987675 +1	23	15	16	0.0909
H	1.12128282 +1	109.9932369 +1	-52.2975605 +1	23	15	16	0.0966
H	1.12057935 +1	111.0520629 +1	67.3953227 +1	23	15	16	0.1033
H	1.12194194 +1	109.9239309 +1	179.3449777 +1	24	18	17	0.1001
H	1.12243471 +1	111.0840159 +1	-61.6352364 +1	24	18	17	0.1302
H	1.12037659 +1	111.8834264 +1	59.6534333 +1	24	18	17	0.1099
H	1.10180504 +1	120.1545461 +1	179.0652223 +1	27	28	29	0.1481
H	1.10121143 +1	120.2977347 +1	179.6313841 +1	28	27	32	0.1562
H	1.10787452 +1	120.1846035 +1	-179.9590591 +1	29	28	27	0.1851
H	1.10296716 +1	118.7126411 +1	-5.4719994 +1	31	30	20	0.1326
H	1.10058569 +1	120.0314547 +1	-179.8101878 +1	32	27	28	0.1469
H	1.10175389 +1	120.2308720 +1	-179.6378295 +1	33	34	35	0.1484
H	1.10128284 +1	120.3489876 +1	179.6002349 +1	34	33	38	0.1568
H	1.11036453 +1	119.9460587 +1	179.0618328 +1	35	34	33	0.1929
H	1.10176380 +1	119.2108117 +1	2.2661022 +1	37	36	20	0.1312
H	1.10058457 +1	120.0258822 +1	-179.6141326 +1	38	33	34	0.1490
H	1.10159328 +1	120.0839685 +1	179.7131485 +1	39	40	41	0.1477
H	1.10073039 +1	120.0508690 +1	-179.3648914 +1	40	39	44	0.1486
H	1.10240203 +1	118.7151283 +1	-178.5907704 +1	41	40	39	0.1421
H	1.10980316 +1	119.0406516 +1	-1.5166996 +1	43	42	14	0.1846
H	1.10121535 +1	120.3710476 +1	179.0545237 +1	44	39	40	0.1562
H	1.10174780 +1	120.3072266 +1	179.5839060 +1	45	46	47	0.1479
H	1.10118500 +1	120.3843055 +1	179.1244411 +1	46	45	50	0.1551
H	1.11403528 +1	119.8994299 +1	177.4079360 +1	47	46	45	0.1995
H	1.10283145 +1	118.3655278 +1	-2.8020967 +1	49	48	14	0.1312
H	1.10041789 +1	120.0207750 +1	-179.4263076 +1	50	45	46	0.1483
Cl	6.32859594 +1	40.5789384 +1	-26.2471880 +1	1	2	3	-0.6371
C	1.97900000 +0	91.0914904 +1	-155.4282592 +1	4	3	2	0.3189
O	1.94598967 +1	86.9803951 +1	-161.3565121 +1	51	25	14	-0.3849
C	4.24948382 +1	121.4462379 +1	-109.3879612 +1	94	95	8	-0.0716
C	3.74376005 +1	139.9762714 +1	-113.6214904 +1	94	95	8	-0.1443
C	2.46563702 +1	150.0954876 +1	122.8429405 +1	94	95	25	-0.0698
C	1.45971006 +1	120.6565296 +1	-108.2732608 +1	94	95	1	-0.1825
C	1.40240586 +1	121.2952703 +1	7.8872646 +1	99	94	95	-0.0474
C	1.39505649 +1	120.2508769 +1	-0.0222642 +1	96	97	98	-0.1493
H	1.12046073 +1	119.6673560 +1	-172.5783299 +1	94	95	99	0.1765
H	1.10158428 +1	119.8091761 +1	179.7465464 +1	96	97	98	0.1477
H	1.10088518 +1	119.9450351 +1	-179.7283998 +1	97	96	101	0.1500
H	1.10177221 +1	120.1848986 +1	-179.4796666 +1	98	97	96	0.1450
H	1.10258192 +1	119.2892909 +1	0.7188257 +1	100	99	94	0.1600
H	1.10066804 +1	120.0491010 +1	179.5856109 +1	101	96	97	0.1481

___ TS-A-1.979.arc_____

SUMMARY OF AM1 CALCULATION, Site No: 4228
Empirical Formula: C49 H47 O4 Cl2 S2 P2 Si = 107 atoms

AM1 CHARGE=1 EF
distanza C-aledide C-enolato vincolata a 1.979

GEOMETRY OPTIMISED USING EIGENVECTOR FOLLOWING (EF).
SCF FIELD WAS ACHIEVED

HEAT OF FORMATION = -57.93892 KCAL = -242.41645 KJ
TOTAL ENERGY = -9677.41563 EV

```
          ELECTRONIC ENERGY       =    -132846.51533 EV
          CORE-CORE REPULSION     =     123169.09970 EV
          GRADIENT NORM           =       3768.47687
          DIPOLE                  =          8.31663 DEBYE    POINT GROUP:       C1
          NO. OF FILLED LEVELS    =        153
          CHARGE ON SYSTEM        =        1
          IONIZATION POTENTIAL    =         10.468787 EV
          HOMO LUMO ENERGIES (EV) =        -10.469 -2.949
          MOLECULAR WEIGHT        =        924.967
          COSMO AREA              =        654.77 SQUARE ANGSTROMS
          COSMO VOLUME            =       1024.59 CUBIC ANGSTROMS

          MOLECULAR DIMENSIONS (Angstroms)

            Atom       Atom       Distance
            H   103    H    77    15.68240
            H   104    H    73    14.88927
            H    83    H    78    10.97272
          SCF CALCULATIONS        =        106

          FINAL GEOMETRY OBTAINED                                        CHARGE
    AM1 CHARGE=1 EF
    distanza C-aledide C-enolato vincolata a 1.979

   C     0.00000000 +0    0.0000000 +0    0.0000000 +0                          -0.1490
   C     1.50842150 +1    0.0000000 +0    0.0000000 +0     1     0     0      -0.2055
   C     1.47955375 +1  111.9059942 +1    0.0000000 +0     2     1     0       0.3856
   C     1.35100000 +0  121.0351353 +1  -45.6541345 +1     3     2     1      -0.4722
   C     1.51047243 +1  119.3781696 +1   18.6246054 +1     4     3     2      -0.1041
   C     1.51517457 +1  107.7642719 +1   58.8054363 +1     1     2     3      -0.1653
   O     1.30955689 +1  116.7883366 +1  134.4098843 +1     3     2     1      -0.5412
  Cl     4.89752322 +1   13.4082995 +1   77.4407209 +1     1     2     3      -0.5971
   C     9.89398061 +1    5.1269950 +1   22.4061960 +1     1     2     3      -0.2929
   C     1.40166048 +1   48.6674631 +1 -119.5949760 +1     9     1     2      -0.9213
   C     1.45058511 +1  109.0278318 +1  106.8654391 +1    10     9     1       0.0285
   C     1.39569057 +1  111.6631709 +1    1.2450416 +1    11    10     9      -0.4133
   S     1.65555886 +1  112.6333987 +1   -0.1893440 +1     9    10    11       0.7138
   P     1.62048542 +1  124.2961253 +1  177.4568925 +1    10     9    13       3.3137
   C     9.99743275 +1   27.3770880 +1  -51.5018134 +1     1     2     3      -0.3985
   C     1.47413347 +1  131.3916283 +1  174.4885090 +1    11    10     9       0.0101
   C     1.45007692 +1  131.3151216 +1   93.0734558 +1    16    11    10      -0.9356
   C     1.40088358 +1  109.4793099 +1  176.9109628 +1    17    16    11      -0.2543
   S     1.65183739 +1  111.5602344 +1 -178.2365509 +1    15    16    11       0.7063
   P     1.60830417 +1  125.8937651 +1   -8.0833444 +1    17    16    11       3.2966
   C     1.46927041 +1  127.4757751 +1  175.6711576 +1    12    11    10      -0.1653
   C     1.47816623 +1  134.5821825 +1  179.9122940 +1     9    10    11      -0.1879
   C     1.46796129 +1  127.0271917 +1   -1.1113559 +1    15    16    11      -0.1621
   C     1.47712364 +1  134.3405275 +1  176.8701647 +1    18    17    16      -0.1910
   O     1.54323338 +1  110.4709578 +1  128.5615637 +1    14    10     9      -1.1738
   O     1.54613867 +1  107.7449994 +1  -65.6405341 +1    20    17    16      -1.1714
   C     8.87602988 +1   29.6565935 +1 -146.8586700 +1     1     2     3      -0.0565
   C     1.39443656 +1   26.1608365 +1  -50.8889687 +1    27     1     2      -0.1490
   C     1.39397765 +1  119.7068565 +1   55.7873033 +1    28    27     1      -0.0125
   C     1.59768813 +1  113.0207551 +1   54.7923621 +1    20    17    16      -0.9470
   C     1.39657000 +1  121.9436018 +1   43.8261244 +1    30    20    17      -0.0407
   C     1.39766759 +1  120.1357568 +1   -0.9526505 +1    27    28    29      -0.1580
   C     6.36819758 +1   65.9683988 +1  -94.0780826 +1     1     2     3      -0.0531
   C     1.39280556 +1   38.8899593 +1   66.8268395 +1    33     1     2      -0.1536
   C     1.39287322 +1  119.8501522 +1 -105.3492057 +1    34    33     1      -0.0111
   C     1.60317479 +1  111.6524597 +1  176.0259023 +1    20    17    16      -0.9560
   C     1.39868711 +1  122.8360861 +1  -85.1405759 +1    36    20    17      -0.0362
   C     1.39905264 +1  119.7271602 +1    0.1326703 +1    33    34    35      -0.1550
   C     9.67893442 +1   33.3601289 +1   63.3054193 +1     1     2     3      -0.0545
   C     1.39726241 +1  110.4756335 +1  -68.7987223 +1    39     1     2      -0.1559
   C     1.39155399 +1  119.8697586 +1   34.3484162 +1    40    39     1      -0.0387
   C     1.60314724 +1  110.8453703 +1   10.4377287 +1    14    10     9      -0.9652
   C     1.40159692 +1  118.6454178 +1   78.3132964 +1    42    14    10      -0.0282
   C     1.39466416 +1  119.6602985 +1    0.3165877 +1    39    40    41      -0.1494
   C    11.37912654 +1   36.5050976 +1   -7.2022660 +1     1     2     3      -0.0530
   C     1.39227325 +1   22.3348738 +1 -166.6040211 +1    45     1     2      -0.1483
   C     1.39582258 +1  119.9573042 +1    0.4361915 +1    46    45     1       0.0006
   C     1.59826924 +1  108.7425858 +1 -109.5983744 +1    14    10     9      -0.9685
   C     1.40212922 +1  120.5363709 +1   49.1709511 +1    48    14    10      -0.0459
   C     1.40107606 +1  119.9690060 +1   -0.6724492 +1    45    46    47      -0.1588
  Si     1.81613607 +1  128.5038310 +1  111.9740914 +1     7     3     2       1.8970
   H     1.12125464 +1  109.9635440 +1  -61.7028774 +1     1     2     3       0.0889
```

```
 H     1.11926505 +1  110.1844994 +1  179.7857642 +1     1     2     3       0.0969
 H     1.12796788 +1  111.1863995 +1  -59.5229139 +1     2     1     6       0.1444
 H     1.12406589 +1  110.1281527 +1 -178.1951987 +1     2     1     6       0.1095
 H     1.13895462 +1  113.5460074 +1 -100.5013778 +1     4     3     2       0.2190
 H     1.11816641 +1  109.0138487 +1  124.1377098 +1     5     4     3       0.0967
 H     1.13043283 +1  107.6578390 +1 -121.4664015 +1     5     4     3       0.0710
 H     1.12874723 +1  106.9527469 +1   67.4273619 +1     6     1     2       0.0783
 H     1.11748814 +1  110.4831269 +1 -176.7434610 +1     6     1     2       0.0961
 H     1.11940030 +1  111.1801845 +1  -10.0100040 +1    21    12    11       0.0999
 H     1.12125890 +1  110.6883850 +1  110.2849191 +1    21    12    11       0.0972
 H     1.12013388 +1  110.5094909 +1 -129.8006740 +1    21    12    11       0.0953
 H     1.12152275 +1  111.3086184 +1  -64.1417735 +1    22     9    10       0.1215
 H     1.12035800 +1  112.0168575 +1   57.1441789 +1    22     9    10       0.1096
 H     1.12231371 +1  109.9062672 +1  176.6628635 +1    22     9    10       0.1006
 H     1.11922499 +1  111.0186434 +1 -172.2761113 +1    23    15    16       0.0913
 H     1.12122471 +1  109.9722891 +1  -52.2759807 +1    23    15    16       0.0958
 H     1.12039283 +1  111.0649641 +1   67.4217965 +1    23    15    16       0.1025
 H     1.12199276 +1  109.9157132 +1  179.3818552 +1    24    18    17       0.1000
 H     1.12288554 +1  110.9509777 +1  -61.7157950 +1    24    18    17       0.1327
 H     1.12019579 +1  111.9204395 +1   59.6743784 +1    24    18    17       0.1081
 H     1.10187926 +1  120.1244248 +1  179.0351399 +1    27    28    29       0.1477
 H     1.10108704 +1  120.3067221 +1  179.5669859 +1    28    27    32       0.1557
 H     1.10814377 +1  120.2547157 +1  179.9389475 +1    29    28    27       0.1850
 H     1.10315317 +1  118.7278337 +1   -5.7049056 +1    31    30    20       0.1323
 H     1.10065974 +1  120.0502976 +1 -179.7321337 +1    32    27    28       0.1484
 H     1.10162621 +1  120.2619012 +1 -179.6094492 +1    33    34    35       0.1483
 H     1.10110916 +1  120.2931328 +1  179.8336989 +1    34    33    38       0.1536
 H     1.10877313 +1  119.9524718 +1  179.4900973 +1    35    34    33       0.1860
 H     1.10164250 +1  119.2765192 +1    2.1873386 +1    37    36    20       0.1301
 H     1.10067982 +1  120.0200542 +1 -179.7185199 +1    38    33    34       0.1503
 H     1.10153195 +1  120.1201823 +1  179.7122491 +1    39    40    41       0.1486
 H     1.10084796 +1  120.0365711 +1 -179.2855951 +1    40    39    44       0.1486
 H     1.10239398 +1  118.7364364 +1 -178.6008212 +1    41    40    39       0.1428
 H     1.11105916 +1  119.0877782 +1   -1.4556712 +1    43    42    14       0.1928
 H     1.10123633 +1  120.3391606 +1  179.0073804 +1    44    39    40       0.1558
 H     1.10191711 +1  120.2677425 +1  179.5516225 +1    45    46    47       0.1489
 H     1.10135701 +1  120.4203252 +1  179.2039841 +1    46    45    50       0.1588
 H     1.10887216 +1  119.9364843 +1  178.0200695 +1    47    46    45       0.1921
 H     1.10256325 +1  118.3958278 +1   -2.9999520 +1    49    48    14       0.1296
 H     1.10044563 +1  120.0098119 +1 -179.4328384 +1    50    45    46       0.1492
Cl     6.33088306 +1   41.5611438 +1  -30.1914516 +1     1     2     3      -0.6292
 C     1.97900000 +0  100.9755601 +1 -177.8304134 +1     4     3     2       0.3381
 O     1.87123109 +1   97.6761542 +1 -161.2574352 +1    51    25    14      -0.5808
 C     4.26875474 +1  120.1485840 +1 -114.5503369 +1    94    95     8      -0.1030
 C     3.76058938 +1  138.7425949 +1 -116.4940169 +1    94    95     8      -0.1345
 C     2.47935987 +1  148.0220332 +1  122.2194879 +1    94    95    25      -0.0937
 C     1.47501598 +1  119.1073675 +1 -122.2293960 +1    94    95     1      -0.1297
 C     1.40100324 +1  121.5989776 +1    5.5788767 +1    99    94    95      -0.0948
 C     1.39574646 +1  119.7549138 +1   -0.0601594 +1    96    97    98      -0.1396
 H     1.11166739 +1  119.5273702 +1 -158.5904159 +1    94    95    99       0.1446
 H     1.10048048 +1  119.8987042 +1  179.8166602 +1    96    97    98       0.1410
 H     1.10039490 +1  120.0365334 +1  179.9677846 +1    97    96   101       0.1441
 H     1.10042044 +1  120.2113485 +1 -179.7463211 +1    98    97    96       0.1359
 H     1.10159870 +1  119.1818776 +1   -1.4596051 +1   100    99    94       0.1496
 H     1.10012010 +1  120.0443170 +1 -179.9587126 +1   101    96    97       0.1375
```

___TS-B-1.979.mop_____

```
 AM1 CHARGE=1 EF
 distanza C-aledide C-enolato vincolata a 1.979A (si face)

 C     0.00000000 +0    0.0000000 +0    0.0000000 +0                          -0.1571
 C     1.51190704 +1    0.0000000 +0    0.0000000 +0     1     0     0      -0.1983
 C     1.50435593 +1  113.0792654 +1    0.0000000 +0     2     1     0       0.3224
 C     1.35100000 +0  123.1090786 +1  -20.9742959 +1     3     2     1      -0.3540
 C     1.49752688 +1  120.4496458 +1   11.6989940 +1     4     3     2      -0.1298
 C     1.51306028 +1  110.9176924 +1   44.1778209 +1     1     2     3      -0.1638
 O     1.30923918 +1  114.4841175 +1  162.1017696 +1     3     2     1      -0.5090
Cl     4.78464404 +1   26.1536056 +1   86.9215391 +1     1     2     3      -0.6346
 C     9.58095324 +1   22.6152508 +1   81.2096114 +1     1     2     3      -0.2758
 C     1.39929690 +1   58.2327620 +1  -55.7884296 +1     9     1     2      -0.9211
 C     1.45011114 +1  109.4578437 +1  111.0555116 +1    10     9     1       0.0223
 C     1.39443934 +1  111.7661627 +1    2.7506165 +1    11    10     9      -0.3973
```

S	1.65725058 +1	112.5599453 +1	-1.4237780 +1	9	10	11	0.6887
P	1.61800915 +1	124.6136843 +1	177.1016590 +1	10	9	13	3.3036
C	10.40250731 +1	14.3508036 +1	-6.3054120 +1	1	2	3	-0.3958
C	1.47271742 +1	130.9696483 +1	177.2770496 +1	11	10	9	0.0122
C	1.44845183 +1	130.9792116 +1	88.8513676 +1	16	11	10	-0.9328
C	1.40004427 +1	109.6053723 +1	179.4128287 +1	17	16	11	-0.2628
S	1.65287053 +1	111.5253466 +1	179.9797143 +1	15	16	11	0.6979
P	1.61203137 +1	125.7426773 +1	-3.4593726 +1	17	16	11	3.3035
C	1.46950798 +1	127.4434962 +1	175.0688756 +1	12	11	10	-0.1654
C	1.47723189 +1	134.6318228 +1	178.1336014 +1	9	10	11	-0.1888
C	1.46800577 +1	127.2616049 +1	-2.7879655 +1	15	16	11	-0.1643
C	1.47718023 +1	134.3127019 +1	175.6093891 +1	18	17	16	-0.1914
O	1.54093543 +1	109.9593436 +1	122.7987473 +1	14	10	9	-1.1778
O	1.54324987 +1	107.7751102 +1	-69.2976637 +1	20	17	16	-1.1705
C	8.84912339 +1	25.1084247 +1	177.1148849 +1	1	2	3	-0.0560
C	1.39378308 +1	19.3719415 +1	-86.5134587 +1	27	1	2	-0.1487
C	1.39456613 +1	119.8807719 +1	64.4522946 +1	28	27	1	-0.0134
C	1.59915274 +1	112.2356816 +1	51.9823089 +1	20	17	16	-0.9532
C	1.39852476 +1	121.9516157 +1	44.0137154 +1	30	20	17	-0.0393
C	1.39868456 +1	119.9063046 +1	-0.9991052 +1	27	28	29	-0.1604
C	7.35561291 +1	44.4040333 +1	-92.2276405 +1	1	2	3	-0.0529
C	1.39412309 +1	39.1527808 +1	72.0542400 +1	33	1	2	-0.1522
C	1.39386816 +1	119.8663643 +1	-94.7803457 +1	34	33	1	-0.0125
C	1.60366000 +1	111.2724766 +1	172.2749689 +1	20	17	16	-0.9599
C	1.39895382 +1	122.5784811 +1	-83.0190770 +1	36	20	17	-0.0341
C	1.39812160 +1	119.7953730 +1	0.0910831 +1	33	34	35	-0.1560
C	9.17382098 +1	52.8956252 +1	68.1055276 +1	1	2	3	-0.0524
C	1.39720813 +1	118.2438474 +1	-48.5625656 +1	39	1	2	-0.1577
C	1.39106302 +1	119.8313587 +1	30.4559578 +1	40	39	1	-0.0313
C	1.60392219 +1	110.9498400 +1	3.8570413 +1	14	10	9	-0.9613
C	1.40143525 +1	118.8401569 +1	82.7629641 +1	42	14	10	-0.0369
C	1.39449141 +1	119.6803850 +1	-0.2046284 +1	39	40	41	-0.1536
C	11.48931235 +1	36.4125837 +1	17.5241432 +1	1	2	3	-0.0566
C	1.39295031 +1	25.0986400 +1	-129.0506488 +1	45	1	2	-0.1479
C	1.39581980 +1	119.9178860 +1	3.3483247 +1	46	45	1	-0.0079
C	1.60019782 +1	109.3742799 +1	-115.5990672 +1	14	10	9	-0.9567
C	1.40077714 +1	120.9784613 +1	45.6546146 +1	48	14	10	-0.0459
C	1.39978382 +1	119.9259553 +1	-0.5534598 +1	45	46	47	-0.1585
Si	1.86988840 +1	125.3799808 +1	114.7729078 +1	7	3	2	1.8620
H	1.12194308 +1	109.8339703 +1	-76.9815492 +1	1	2	3	0.0899
H	1.12128876 +1	109.1508009 +1	165.5413608 +1	1	2	3	0.0954
H	1.12781605 +1	110.3262758 +1	-75.5934247 +1	2	1	6	0.1400
H	1.12271516 +1	110.3914380 +1	166.4312057 +1	2	1	6	0.1217
H	1.11715295 +1	117.9822916 +1	155.6597116 +1	4	3	2	0.1716
H	1.12459325 +1	108.4554690 +1	-95.3681216 +1	5	4	3	0.0918
H	1.12351850 +1	109.4575560 +1	-148.2858796 +1	5	4	3	0.1010
H	1.12205330 +1	109.6333723 +1	61.6767286 +1	6	1	2	0.0793
H	1.12095653 +1	109.7853181 +1	179.5169084 +1	6	1	2	0.0959
H	1.11943674 +1	111.1866811 +1	-6.9743133 +1	21	12	11	0.0984
H	1.12123860 +1	110.7341715 +1	113.2249143 +1	21	12	11	0.0982
H	1.12018024 +1	110.4569288 +1	-126.7587480 +1	21	12	11	0.0955
H	1.12175648 +1	111.1667960 +1	-63.2241923 +1	22	9	10	0.1229
H	1.12038260 +1	112.0727640 +1	58.0084441 +1	22	9	10	0.1121
H	1.12222503 +1	109.9203427 +1	177.6346557 +1	22	9	10	0.1000
H	1.11946069 +1	110.9016666 +1	-165.1943038 +1	23	15	16	0.0914
H	1.12105502 +1	110.1630538 +1	-45.2369388 +1	23	15	16	0.0981
H	1.12036851 +1	111.1030100 +1	74.6535805 +1	23	15	16	0.1030
H	1.12199896 +1	109.9190837 +1	-178.5874132 +1	24	18	17	0.1004
H	1.12232382 +1	111.1524855 +1	-59.5190115 +1	24	18	17	0.1298
H	1.12058308 +1	111.8622641 +1	61.7843335 +1	24	18	17	0.1114
H	1.10170116 +1	120.2019552 +1	179.0247624 +1	27	28	29	0.1474
H	1.10115189 +1	120.3373760 +1	179.3331755 +1	28	27	32	0.1556
H	1.10957378 +1	120.1090027 +1	179.5554820 +1	29	28	27	0.1928
H	1.10296380 +1	118.7262846 +1	-6.1427905 +1	31	30	20	0.1314
H	1.10051665 +1	120.0278295 +1	-179.6637836 +1	32	27	28	0.1462
H	1.10170574 +1	120.2308389 +1	-179.6824145 +1	33	34	35	0.1486
H	1.10110776 +1	120.3029089 +1	179.8385498 +1	34	33	38	0.1545
H	1.10906593 +1	119.9993293 +1	179.1721829 +1	35	34	33	0.1868
H	1.10166135 +1	119.3250453 +1	2.1412554 +1	37	36	20	0.1325
H	1.10062821 +1	120.0362786 +1	-179.6634403 +1	38	33	34	0.1491
H	1.10156160 +1	120.0408399 +1	179.4794001 +1	39	40	41	0.1472
H	1.10066316 +1	120.0481004 +1	-179.5848969 +1	40	39	44	0.1487
H	1.10223958 +1	118.8765743 +1	-178.7608826 +1	41	40	39	0.1397
H	1.11470601 +1	119.0734175 +1	-2.3154621 +1	43	42	14	0.1952
H	1.10093031 +1	120.3031547 +1	179.6025193 +1	44	39	40	0.1525
H	1.10177239 +1	120.2383715 +1	179.4300920 +1	45	46	47	0.1480

H	1.10132655 +1	120.3758858 +1	179.5959718 +1	46	45	50	0.1567
H	1.10912883 +1	120.0017859 +1	179.4381414 +1	47	46	45	0.1920
H	1.10261546 +1	118.5046708 +1	-3.4182305 +1	49	48	14	0.1318
H	1.10040057 +1	120.0398608 +1	-179.8272506 +1	50	45	46	0.1478
Cl	6.41787333 +1	35.8945903 +1	-9.8907111 +1	1	2	3	-0.5663
C	1.97900000 +0	97.1022779 +1	-108.2106975 +1	4	3	2	0.2812
O	1.82755482 +1	91.4908914 +1	-107.9248631 +1	51	25	14	-0.5361
C	4.27134210 +1	114.8835548 +1	-154.2277667 +1	94	95	8	-0.1008
C	3.76683751 +1	130.7169377 +1	-142.3654493 +1	94	95	8	-0.1379
C	2.48616566 +1	138.9407758 +1	-105.3251215 +1	94	95	25	-0.1040
C	1.47805464 +1	114.8689553 +1	145.8996181 +1	94	95	1	-0.1260
C	1.40121545 +1	120.8465874 +1	-28.0523907 +1	99	94	95	-0.0808
C	1.39535931 +1	120.0490074 +1	0.1286046 +1	96	97	98	-0.1389
H	1.11544706 +1	117.9241773 +1	143.1016275 +1	94	95	99	0.1203
H	1.10069444 +1	119.9233060 +1	-179.8498117 +1	96	97	98	0.1419
H	1.10035565 +1	120.0077395 +1	-179.9237330 +1	97	96	101	0.1421
H	1.10085026 +1	120.0543765 +1	179.9808820 +1	98	97	96	0.1360
H	1.10248731 +1	119.1786241 +1	-1.1236633 +1	100	99	94	0.1582
H	1.10039064 +1	120.0368819 +1	179.9975017 +1	101	96	97	0.1420

TS-B-1.979.arc

SUMMARY OF AM1 CALCULATION, Site No: 4228

Empirical Formula: C49 H47 O4 Cl2 S2 P2 Si = 107 atoms

AM1 CHARGE=1 EF
distanza C-aledide C-enolato vincolata a 1.979A (si face)

GEOMETRY OPTIMISED USING EIGENVECTOR FOLLOWING (EF).
SCF FIELD WAS ACHIEVED

HEAT OF FORMATION = -42.56363 KCAL = -178.08623 KJ
TOTAL ENERGY = -9676.74889 EV
ELECTRONIC ENERGY = -133521.81112 EV
CORE-CORE REPULSION = 123845.06223 EV
GRADIENT NORM = 4391.87788
DIPOLE = 7.83837 DEBYE POINT GROUP: C1
NO. OF FILLED LEVELS = 153
CHARGE ON SYSTEM = 1
IONIZATION POTENTIAL = 10.681054 EV
HOMO LUMO ENERGIES (EV) = -10.681 -2.889
MOLECULAR WEIGHT = 924.967
COSMO AREA = 637.07 SQUARE ANGSTROMS
COSMO VOLUME = 1016.63 CUBIC ANGSTROMS

MOLECULAR DIMENSIONS (Angstroms)

Atom		Atom		Distance
H	84	H	78	14.29305
H	103	H	63	14.10776
H	53	H	88	10.78733

SCF CALCULATIONS = 119

FINAL GEOMETRY OBTAINED CHARGE
AM1 CHARGE=1 EF
distanza C-aledide C-enolato vincolata a 1.979A (si face)

C	0.00000000 +0	0.0000000 +0	0.0000000 +0				-0.1557
C	1.52179873 +1	0.0000000 +0	0.0000000 +0	1	0	0	-0.1936
C	1.51395623 +1	111.9203175 +1	0.0000000 +0	2	1	0	0.3247
C	1.35100000 +0	123.0714322 +1	-25.7987582 +1	3	2	1	-0.3294
C	1.48166129 +1	120.5289615 +1	-0.5303921 +1	4	3	2	-0.1910
C	1.49631630 +1	114.4472450 +1	46.1533481 +1	1	2	3	-0.1153
O	1.31135977 +1	113.5250232 +1	160.8998375 +1	3	2	1	-0.5142
Cl	4.78110662 +1	25.7871214 +1	86.2380096 +1	1	2	3	-0.6401
C	9.58377149 +1	22.1445970 +1	81.3617349 +1	1	2	3	-0.2767
C	1.39856945 +1	58.2728016 +1	-55.7123811 +1	9	1	2	-0.9216
C	1.44854323 +1	109.4296145 +1	111.0605879 +1	10	9	1	0.0221
C	1.39485966 +1	111.7996916 +1	2.8340926 +1	11	10	9	-0.3976
S	1.65708384 +1	112.5645235 +1	-1.5897634 +1	9	10	11	0.6921
P	1.61522887 +1	124.6483041 +1	177.4645442 +1	10	9	13	3.3044
C	10.40396375 +1	14.6538611 +1	-7.5905101 +1	1	2	3	-0.4007

C	1.47125417 +1	130.9324991 +1	177.0849530 +1	11	10	9	0.0095
C	1.44847599 +1	131.0029358 +1	89.0249726 +1	16	11	10	-0.9265
C	1.39976770 +1	109.5381957 +1	179.4006523 +1	17	16	11	-0.2738
S	1.65348772 +1	111.4197039 +1	-179.9872830 +1	15	16	11	0.7099
P	1.61348202 +1	125.7730193 +1	-3.5190718 +1	17	16	11	3.3031
C	1.46947075 +1	127.4418897 +1	175.0160142 +1	12	11	10	-0.1651
C	1.47728033 +1	134.6239055 +1	178.1728305 +1	9	10	11	-0.1889
C	1.46800600 +1	127.2566421 +1	-2.8094107 +1	15	16	11	-0.1657
C	1.47687256 +1	134.2868579 +1	175.4995519 +1	18	17	16	-0.1919
O	1.54164758 +1	109.5637712 +1	122.1176897 +1	14	10	9	-1.1793
O	1.54335062 +1	107.7830368 +1	-69.4973291 +1	20	17	16	-1.1690
C	8.85092278 +1	25.1270394 +1	177.5891530 +1	1	2	3	-0.0556
C	1.39417393 +1	19.1168184 +1	-86.1175756 +1	27	1	2	-0.1487
C	1.39458533 +1	119.7390501 +1	64.2231955 +1	28	27	1	-0.0128
C	1.59906708 +1	112.2937044 +1	51.7925980 +1	20	17	16	-0.9547
C	1.39755063 +1	121.9347115 +1	44.0928726 +1	30	20	17	-0.0365
C	1.39765282 +1	120.0217623 +1	-0.8651672 +1	27	28	29	-0.1623
C	7.35870981 +1	44.6806199 +1	-92.3013812 +1	1	2	3	-0.0526
C	1.39268226 +1	39.0869205 +1	72.0461364 +1	33	1	2	-0.1525
C	1.39521397 +1	119.7750882 +1	-94.6778901 +1	34	33	1	-0.0098
C	1.60305020 +1	111.3320275 +1	172.2701611 +1	20	17	16	-0.9611
C	1.39978078 +1	122.4851434 +1	-83.0978312 +1	36	20	17	-0.0379
C	1.39932743 +1	119.8897677 +1	0.1456072 +1	33	34	35	-0.1532
C	9.17191272 +1	52.4441662 +1	68.0957827 +1	1	2	3	-0.0528
C	1.39768440 +1	118.1212275 +1	-48.6088082 +1	39	1	2	-0.1569
C	1.39048321 +1	119.8233871 +1	30.6548516 +1	40	39	1	-0.0345
C	1.60457328 +1	111.1160559 +1	3.5095608 +1	14	10	9	-0.9623
C	1.40059606 +1	118.8730378 +1	82.7473886 +1	42	14	10	-0.0356
C	1.39391039 +1	119.6492725 +1	-0.3054069 +1	39	40	41	-0.1555
C	11.48810722 +1	36.1888406 +1	17.1215200 +1	1	2	3	-0.0564
C	1.39327317 +1	25.2078443 +1	-129.4100697 +1	45	1	2	-0.1475
C	1.39621734 +1	119.9698030 +1	3.7531995 +1	46	45	1	-0.0084
C	1.60074756 +1	109.3992490 +1	-115.5301005 +1	14	10	9	-0.9563
C	1.40117587 +1	120.8326086 +1	45.4261677 +1	48	14	10	-0.0446
C	1.39965601 +1	119.8574637 +1	-0.7108242 +1	45	46	47	-0.1589
Si	1.87390793 +1	125.9863150 +1	114.4087114 +1	7	3	2	1.8606
H	1.12297199 +1	109.5713894 +1	-76.6715814 +1	1	2	3	0.0923
H	1.12318644 +1	108.8509622 +1	166.5101407 +1	1	2	3	0.0927
H	1.12601104 +1	110.4615017 +1	-74.8111667 +1	2	1	6	0.1412
H	1.12217576 +1	110.2684911 +1	166.9142985 +1	2	1	6	0.1206
H	1.11590657 +1	118.1731962 +1	154.1558321 +1	4	3	2	0.1776
H	1.19739157 +1	104.0826603 +1	-92.5843488 +1	5	4	3	0.0216
H	1.13619618 +1	112.1814740 +1	-164.6272369 +1	5	4	3	0.1604
H	1.13267165 +1	107.6157233 +1	66.8709683 +1	6	1	2	0.0565
H	1.11747481 +1	110.2311587 +1	-177.4411438 +1	6	1	2	0.1051
H	1.11944502 +1	111.1789862 +1	-6.9799237 +1	21	12	11	0.0984
H	1.12118814 +1	110.7408195 +1	113.2439242 +1	21	12	11	0.0982
H	1.12019159 +1	110.4595910 +1	-126.7559115 +1	21	12	11	0.0957
H	1.12173806 +1	111.1701366 +1	-63.2196653 +1	22	9	10	0.1231
H	1.12036945 +1	112.0667900 +1	58.0093636 +1	22	9	10	0.1120
H	1.12222220 +1	109.9176527 +1	177.6432639 +1	22	9	10	0.1001
H	1.11946333 +1	110.9136317 +1	-165.2036992 +1	23	15	16	0.0912
H	1.12108718 +1	110.1598444 +1	-45.2390155 +1	23	15	16	0.0977
H	1.12020499 +1	111.1079184 +1	74.6536307 +1	23	15	16	0.1043
H	1.12200329 +1	109.9305307 +1	-178.5666862 +1	24	18	17	0.0998
H	1.12238582 +1	111.1384222 +1	-59.5142692 +1	24	18	17	0.1293
H	1.12061478 +1	111.8562096 +1	61.7729256 +1	24	18	17	0.1113
H	1.10178711 +1	120.1830167 +1	179.0600587 +1	27	28	29	0.1472
H	1.10105870 +1	120.3571463 +1	179.3411869 +1	28	27	32	0.1561
H	1.10947060 +1	120.1216240 +1	179.4932780 +1	29	28	27	0.1922
H	1.10299485 +1	118.7504770 +1	-6.0435176 +1	31	30	20	0.1323
H	1.10052583 +1	120.0376220 +1	-179.6677937 +1	32	27	28	0.1461
H	1.10181136 +1	120.2328332 +1	-179.6930619 +1	33	34	35	0.1483
H	1.10115366 +1	120.3284291 +1	179.8781182 +1	34	33	38	0.1551
H	1.10915216 +1	119.9706702 +1	179.1430577 +1	35	34	33	0.1875
H	1.10167831 +1	119.2945429 +1	2.1264416 +1	37	36	20	0.1315
H	1.10069941 +1	120.0201859 +1	-179.7022322 +1	38	33	34	0.1490
H	1.10157848 +1	120.0457470 +1	179.3814001 +1	39	40	41	0.1472
H	1.10065749 +1	120.0430643 +1	-179.5550295 +1	40	39	44	0.1484
H	1.10214452 +1	118.8411558 +1	-178.6470995 +1	41	40	39	0.1402
H	1.11495129 +1	119.0767386 +1	-2.4834448 +1	43	42	14	0.1995
H	1.10091340 +1	120.3247997 +1	179.4922701 +1	44	39	40	0.1512
H	1.10176475 +1	120.2413703 +1	179.3724549 +1	45	46	47	0.1488
H	1.10135212 +1	120.3684447 +1	179.5992948 +1	46	45	50	0.1568
H	1.10880349 +1	119.9974277 +1	179.5537264 +1	47	46	45	0.1885
H	1.10275055 +1	118.4822105 +1	-3.6232270 +1	49	48	14	0.1330

```
 H     1.10040223 +1  120.0507294 +1 -179.8587473 +1    50    45    46       0.1484
Cl     6.42372374 +1   35.8746403 +1  -11.0622598 +1     1     2     3      -0.5581
 C     1.97900000 +0   99.3824744 +1 -110.0646720 +1     4     3     2       0.2717
 O     1.82059897 +1   90.5380784 +1 -106.6960983 +1    51    25    14      -0.5245
 C     4.27432879 +1  114.6646027 +1 -154.5194578 +1    94    95     8      -0.0999
 C     3.76911886 +1  130.5866079 +1 -142.4903976 +1    94    95     8      -0.1355
 C     2.49305934 +1  138.1476554 +1 -104.5217624 +1    94    95    25      -0.1134
 C     1.47868714 +1  114.3143670 +1  144.3629937 +1    94    95     1      -0.1385
 C     1.39987451 +1  120.5670095 +1  -28.8276136 +1    99    94    95      -0.0752
 C     1.39354892 +1  120.0792333 +1    0.3933727 +1    96    97    98      -0.1386
 H     1.11679640 +1  117.8987603 +1  142.9299100 +1    94    95    99       0.1234
 H     1.10081909 +1  119.8964647 +1 -179.7429981 +1    96    97    98       0.1439
 H     1.10057530 +1  119.9694846 +1 -179.8328727 +1    97    96   101       0.1449
 H     1.10144094 +1  119.9228837 +1 -179.6953582 +1    98    97    96       0.1360
 H     1.10278926 +1  119.1690074 +1   -1.0094120 +1   100    99    94       0.1626
 H     1.10051541 +1  120.0784745 +1  179.9845587 +1   101    96    97       0.1424
```

The structure **$S_{2.0}$-A** was minimized removing the constraint distance between the two carbon atoms, and the new generated structure was employed as starting point for TS search with TS routine in order to generate the force constants relative to the formation of the new C-C bond. In order to decrease the gradient, a keyword PRECISE was added in the search of the stationary point. However, the gradient value was higher than that accepted for the generation of the force constants, so a keyword LET was added in a FORCE calculation. In this way, the calculation has been performed correctly.

```
___ TS-A-PRECISE.mop_____________________________________________________________
    TS AM1 CHARGE=1  PRECISE
    ricerca del TS a faccia re

 C     0.00000000 +0    0.0000000 +0    0.0000000 +0                         -0.1573
 C     1.51104931 +1    0.0000000 +0    0.0000000 +0     1     0     0      -0.1993
 C     1.49902228 +1  108.0984215 +1    0.0000000 +0     2     1     0       0.3478
 C     1.35100000 +0  123.2632784 +1  -33.0162179 +1     3     2     1      -0.3616
 C     1.50233830 +1  119.8739886 +1   -3.1424326 +1     4     3     2      -0.1284
 C     1.51676846 +1  108.5183301 +1   60.6327775 +1     1     2     3      -0.1639
 O     1.30382938 +1  114.7457548 +1  142.9129158 +1     3     2     1      -0.5118
Cl     4.95889240 +1   10.7608532 +1   94.0029788 +1     1     2     3      -0.5828
 C     9.91737663 +1    6.1641707 +1   27.4095026 +1     1     2     3      -0.2857
 C     1.39957269 +1   48.6180284 +1 -123.5832379 +1     9     1     2      -0.9166
 C     1.44932828 +1  109.5006431 +1  107.9570324 +1    10     9     1       0.0257
 C     1.39561278 +1  111.6883538 +1    1.3434426 +1    11    10     9      -0.3984
 S     1.65636903 +1  112.5827982 +1   -0.1236720 +1     9    10    11       0.6922
 P     1.61869422 +1  124.2292904 +1  176.6576383 +1    10     9    13       3.3065
 C    10.05228771 +1   28.0164101 +1  -40.6757496 +1     1     2     3      -0.3966
 C     1.47361537 +1  131.4418484 +1  174.2349779 +1    11    10     9       0.0118
 C     1.44741318 +1  131.4788315 +1   92.2117946 +1    16    11    10      -0.9293
 C     1.39972570 +1  109.8238203 +1  175.6882031 +1    17    16    11      -0.2686
 S     1.65179230 +1  111.7031917 +1 -177.2393129 +1    15    16    11       0.7038
 P     1.61026705 +1  125.2689999 +1   -9.6431004 +1    17    16    11       3.3031
 C     1.46957572 +1  127.5185387 +1  175.6199365 +1    12    11    10      -0.1653
 C     1.47773987 +1  134.6178691 +1  179.6705428 +1     9    10    11      -0.1873
 C     1.46801400 +1  127.0723240 +1   -0.5920497 +1    15    16    11      -0.1637
 C     1.47721639 +1  134.1801405 +1  177.7645951 +1    18    17    16      -0.1885
 O     1.54103432 +1  109.8830255 +1  125.5936702 +1    14    10     9      -1.1792
 O     1.54070674 +1  106.8617734 +1  -67.2852039 +1    20    17    16      -1.1715
 C     8.83739079 +1   27.7262120 +1 -137.2407614 +1     1     2     3      -0.0569
 C     1.39318139 +1   25.4769823 +1  -49.2748891 +1    27     1     2      -0.1483
 C     1.39537446 +1  119.7530769 +1   55.7813401 +1    28    27     1      -0.0171
 C     1.59951614 +1  112.1987237 +1   54.0023896 +1    20    17    16      -0.9541
 C     1.39897226 +1  121.5675632 +1   42.9743970 +1    30    20    17      -0.0417
 C     1.39898561 +1  120.0294021 +1   -0.7021083 +1    27    28    29      -0.1605
 C     6.38005849 +1   65.4770363 +1  -84.6199540 +1     1     2     3      -0.0526
```

C	1.39411077 +1	41.1357881 +1	69.9606829 +1	33	1	2	-0.1548
C	1.39306877 +1	119.8601407 +1	-104.6157101 +1	34	33	1	-0.0153
C	1.60448025 +1	111.7362456 +1	174.2325828 +1	20	17	16	-0.9570
C	1.39835850 +1	122.8351825 +1	-85.8085980 +1	36	20	17	-0.0314
C	1.39803449 +1	119.7445575 +1	0.0953059 +1	33	34	35	-0.1558
C	9.68939241 +1	34.2479423 +1	70.1464086 +1	1	2	3	-0.0528
C	1.39677285 +1	111.0689220 +1	-70.3046235 +1	39	1	2	-0.1574
C	1.39155409 +1	119.8793310 +1	34.4251829 +1	40	39	1	-0.0310
C	1.60522487 +1	111.2708037 +1	8.9073061 +1	14	10	9	-0.9616
C	1.40273729 +1	118.3789687 +1	79.3616938 +1	42	14	10	-0.0256
C	1.39506030 +1	119.6815777 +1	-0.0998386 +1	39	40	41	-0.1516
C	11.38311881 +1	37.4650605 +1	1.6016885 +1	1	2	3	-0.0564
C	1.39211341 +1	22.0430394 +1	-166.8008226 +1	45	1	2	-0.1478
C	1.39714975 +1	120.0124607 +1	-0.5707943 +1	46	45	1	-0.0161
C	1.59810815 +1	108.0303539 +1	-110.5462167 +1	14	10	9	-0.9638
C	1.40359284 +1	119.9221278 +1	49.3086998 +1	48	14	10	-0.0488
C	1.40071136 +1	119.8566226 +1	-0.6758796 +1	45	46	47	-0.1575
Si	1.85712319 +1	125.1565776 +1	108.0368474 +1	7	3	2	1.8661
H	1.12033728 +1	110.4335137 +1	-60.3286523 +1	1	2	3	0.0864
H	1.12027359 +1	109.9800476 +1	-178.9764541 +1	1	2	3	0.0977
H	1.12507680 +1	111.3599590 +1	-58.8368160 +1	2	1	6	0.1444
H	1.12157001 +1	111.3960684 +1	-178.4808319 +1	2	1	6	0.1213
H	1.11936152 +1	115.1761648 +1	133.1506049 +1	4	3	2	0.1657
H	1.12422647 +1	107.9880876 +1	132.1493787 +1	5	4	3	0.0826
H	1.12439067 +1	109.3117950 +1	-112.4543839 +1	5	4	3	0.1030
H	1.12337310 +1	108.3766030 +1	65.1982548 +1	6	1	2	0.0864
H	1.12097089 +1	109.5251039 +1	-178.4239133 +1	6	1	2	0.0923
H	1.11932982 +1	111.2099271 +1	-9.7969837 +1	21	12	11	0.0991
H	1.12134083 +1	110.6691167 +1	110.4411269 +1	21	12	11	0.0977
H	1.12013345 +1	110.4956053 +1	-129.6270844 +1	21	12	11	0.0951
H	1.12158475 +1	111.2354659 +1	-63.9334277 +1	22	9	10	0.1212
H	1.12035429 +1	112.0567157 +1	57.3177877 +1	22	9	10	0.1100
H	1.12222660 +1	109.9021175 +1	176.8709397 +1	22	9	10	0.1005
H	1.11925841 +1	111.0193103 +1	-172.2157581 +1	23	15	16	0.0910
H	1.12135603 +1	109.9652990 +1	-52.2265815 +1	23	15	16	0.0972
H	1.12038920 +1	111.0829262 +1	67.4647985 +1	23	15	16	0.1040
H	1.12191084 +1	109.9302841 +1	179.2050490 +1	24	18	17	0.1005
H	1.12193557 +1	111.2989661 +1	-61.6813863 +1	24	18	17	0.1252
H	1.12051925 +1	111.7277727 +1	59.5702098 +1	24	18	17	0.1103
H	1.10182170 +1	120.1797320 +1	179.1900962 +1	27	28	29	0.1467
H	1.10103382 +1	120.4339163 +1	179.6873240 +1	28	27	32	0.1560
H	1.11141143 +1	120.0118656 +1	179.5021995 +1	29	28	27	0.1960
H	1.10304532 +1	118.6335931 +1	-5.2380843 +1	31	30	20	0.1317
H	1.10048534 +1	120.0102320 +1	-179.9967854 +1	32	27	28	0.1456
H	1.10165723 +1	120.2610348 +1	-179.7859758 +1	33	34	35	0.1484
H	1.10087785 +1	120.2293290 +1	-179.9257987 +1	34	33	38	0.1516
H	1.10785103 +1	120.0546018 +1	-179.7313934 +1	35	34	33	0.1863
H	1.10189945 +1	119.3666401 +1	3.1716214 +1	37	36	20	0.1343
H	1.10064450 +1	120.0267041 +1	179.9786813 +1	38	33	34	0.1494
H	1.10158801 +1	120.0748134 +1	179.4979705 +1	39	40	41	0.1477
H	1.10074620 +1	120.0491886 +1	-179.3941110 +1	40	39	44	0.1490
H	1.10237057 +1	118.7613954 +1	-178.5088874 +1	41	40	39	0.1415
H	1.10973857 +1	119.0356482 +1	-2.4613092 +1	43	42	14	0.1848
H	1.10111377 +1	120.3330979 +1	179.1941495 +1	44	39	40	0.1551
H	1.10172426 +1	120.3182034 +1	179.4177178 +1	45	46	47	0.1481
H	1.10135244 +1	120.4200011 +1	179.3573094 +1	46	45	50	0.1567
H	1.11418976 +1	119.7298367 +1	178.3734807 +1	47	46	45	0.2012
H	1.10283468 +1	118.3553942 +1	-2.9638979 +1	49	48	14	0.1308
H	1.10041234 +1	120.0167234 +1	-179.5365659 +1	50	45	46	0.1482
Cl	6.20923111 +1	43.0158351 +1	-13.9117394 +1	1	2	3	-0.6163
C	1.98947847 +1	100.6860655 +1	-133.2458872 +1	4	3	2	0.2723
O	1.83321446 +1	99.0408348 +1	-158.7379422 +1	51	25	14	-0.5402
C	4.26687159 +1	116.1092435 +1	-102.2020368 +1	94	95	8	-0.1010
C	3.75808899 +1	134.0360980 +1	-108.7316444 +1	94	95	8	-0.1380
C	2.47656006 +1	143.8649572 +1	117.8876054 +1	94	95	25	-0.1021
C	1.47429239 +1	115.7813262 +1	-104.7765210 +1	94	95	1	-0.1232
C	1.40011213 +1	121.4859348 +1	12.3732943 +1	99	94	95	-0.0782
C	1.39458376 +1	120.0498523 +1	0.0657675 +1	96	97	98	-0.1426
H	1.11890647 +1	115.5621328 +1	-139.4674609 +1	94	95	99	0.1259
H	1.10066162 +1	119.9013676 +1	179.9890191 +1	96	97	98	0.1412
H	1.10034264 +1	120.0059935 +1	-179.9248179 +1	97	96	101	0.1424
H	1.10080380 +1	120.1276748 +1	-179.8278790 +1	98	97	96	0.1364
H	1.10212340 +1	119.2179908 +1	3.3789206 +1	100	99	94	0.1578
H	1.10020073 +1	120.0142494 +1	179.7913441 +1	101	96	97	0.1398

___ TS-A-PRECISE.arc_____

SUMMARY OF AM1 CALCULATION, Site No: 4165

Empirical Formula: C49 H47 O4 Cl2 S2 P2 Si = 107 atoms

TS AM1 CHARGE=1 PRECISE
ricerca del TS a faccia re

GEOMETRY OPTIMISED USING EIGENVECTOR FOLLOWING (TS).
SCF FIELD WAS ACHIEVED

HEAT OF FORMATION	=	-89.25801 KCAL/MOL =	-373.45551 KJ/MOL
TOTAL ENERGY	=	-9678.77376 EV	
ELECTRONIC ENERGY	=	-133114.25670 EV	
CORE-CORE REPULSION	=	123435.48294 EV	
GRADIENT NORM	=	18.59468	
DIPOLE	=	7.40601 DEBYE POINT GROUP:	C1
NO. OF FILLED LEVELS	=	153	
CHARGE ON SYSTEM	=	1	
IONIZATION POTENTIAL	=	10.862788 EV	
HOMO LUMO ENERGIES (EV)	=	-10.863 -2.894	
MOLECULAR WEIGHT	=	924.967	
COSMO AREA	=	641.12 SQUARE ANGSTROMS	
COSMO VOLUME	=	1025.91 CUBIC ANGSTROMS	

MOLECULAR DIMENSIONS (Angstroms)

Atom	Atom	Distance
H 104	H 73	14.62948
H 84	H 78	13.72189
H 88	H 59	11.18354

SCF CALCULATIONS = 364

FINAL GEOMETRY OBTAINED CHARGE

TS AM1 CHARGE=1 PRECISE
ricerca del TS a faccia re

C	0.00000000 +0	0.0000000 +0	0.0000000 +0					-0.1573
C	1.51101939 +1	0.0000000 +0	0.0000000 +0	1	0	0		-0.1993
C	1.49903237 +1	108.1038340 +1	0.0000000 +0	2	1	0		0.3477
C	1.35100000 +0	123.2600851 +1	-33.0119123 +1	3	2	1		-0.3616
C	1.50233566 +1	119.8754852 +1	-3.1422127 +1	4	3	2		-0.1284
C	1.51676229 +1	108.5200241 +1	60.6307889 +1	1	2	3		-0.1639
O	1.30378895 +1	114.7480519 +1	142.9131904 +1	3	2	1		-0.5117
Cl	4.95897879 +1	10.7597836 +1	94.0019198 +1	1	2	3		-0.5827
C	9.91752807 +1	6.1683848 +1	27.4064920 +1	1	2	3		-0.2857
C	1.39957090 +1	48.6175247 +1	-123.5857283 +1	9	1	2		-0.9166
C	1.44932243 +1	109.5017436 +1	107.9589349 +1	10	9	1		0.0258
C	1.39560855 +1	111.6885250 +1	1.3428163 +1	11	10	9		-0.3984
S	1.65636950 +1	112.5829414 +1	-0.1287329 +1	9	10	11		0.6922
P	1.61869130 +1	124.2197377 +1	176.6614864 +1	10	9	13		3.3065
C	10.05241651 +1	28.0179817 +1	-40.6676222 +1	1	2	3		-0.3966
C	1.47361373 +1	131.4409274 +1	174.2337461 +1	11	10	9		0.0118
C	1.44741967 +1	131.4794985 +1	92.2116444 +1	16	11	10		-0.9293
C	1.39972381 +1	109.8236667 +1	175.6874605 +1	17	16	11		-0.2686
S	1.65179016 +1	111.7035556 +1	-177.2388201 +1	15	16	11		0.7038
P	1.61027762 +1	125.2696173 +1	-9.6421813 +1	17	16	11		3.3031
C	1.46957434 +1	127.5183853 +1	175.6210158 +1	12	11	10		-0.1652
C	1.47774055 +1	134.6174383 +1	179.6698974 +1	9	10	11		-0.1873
C	1.46801331 +1	127.0725962 +1	-0.5915887 +1	15	16	11		-0.1637
C	1.47721637 +1	134.1806078 +1	177.7655481 +1	18	17	16		-0.1885
O	1.54102980 +1	109.8812868 +1	125.5928151 +1	14	10	9		-1.1792
O	1.54070967 +1	106.8627665 +1	-67.2841987 +1	20	17	16		-1.1715
C	8.83743708 +1	27.7244145 +1	-137.2332516 +1	1	2	3		-0.0569
C	1.39318084 +1	25.4749803 +1	-49.2729866 +1	27	1	2		-0.1483
C	1.39537617 +1	119.7526056 +1	55.7842688 +1	28	27	1		-0.0171
C	1.59951481 +1	112.1994422 +1	54.0032279 +1	20	17	16		-0.9541
C	1.39896759 +1	121.5678305 +1	42.9733487 +1	30	20	17		-0.0417
C	1.39898226 +1	120.0294872 +1	-0.7020594 +1	27	28	29		-0.1605
C	6.38016595 +1	65.4757538 +1	-84.6136448 +1	1	2	3		-0.0526
C	1.39410994 +1	41.1401330 +1	69.9628374 +1	33	1	2		-0.1548
C	1.39306759 +1	119.8601238 +1	-104.6135130 +1	34	33	1		-0.0153
C	1.60448009 +1	111.7352569 +1	174.2342795 +1	20	17	16		-0.9570
C	1.39835750 +1	122.8356072 +1	-85.8135559 +1	36	20	17		-0.0314
C	1.39803697 +1	119.7443297 +1	0.0951404 +1	33	34	35		-0.1558
C	9.68938577 +1	34.2491459 +1	70.1511018 +1	1	2	3		-0.0528

C	1.39676285 +1	111.0693188 +1	-70.3071691 +1	39	1	2	-0.1574
C	1.39154801 +1	119.8791137 +1	34.4249433 +1	40	39	1	-0.0310
C	1.60522670 +1	111.2702433 +1	8.9062737 +1	14	10	9	-0.9616
C	1.40273895 +1	118.3790305 +1	79.3637428 +1	42	14	10	-0.0257
C	1.39506554 +1	119.6813731 +1	-0.1004513 +1	39	40	41	-0.1516
C	11.38307448 +1	37.4681742 +1	1.6079136 +1	1	2	3	-0.0564
C	1.39211747 +1	22.0421210 +1	-166.8005949 +1	45	1	2	-0.1478
C	1.39715404 +1	120.0127358 +1	-0.5707460 +1	46	45	1	-0.0161
C	1.59810956 +1	108.0305122 +1	-110.5458954 +1	14	10	9	-0.9638
C	1.40359431 +1	119.9219172 +1	49.3061569 +1	48	14	10	-0.0489
C	1.40071275 +1	119.8567019 +1	-0.6752397 +1	45	46	47	-0.1575
Si	1.85712542 +1	125.1481348 +1	108.0445340 +1	7	3	2	1.8661
H	1.12033822 +1	110.4326812 +1	-60.3304571 +1	1	2	3	0.0864
H	1.12027516 +1	109.9797776 +1	-178.9773488 +1	1	2	3	0.0977
H	1.12507867 +1	111.3590550 +1	-58.8377195 +1	2	1	6	0.1444
H	1.12156774 +1	111.3960062 +1	-178.4812094 +1	2	1	6	0.1213
H	1.11935308 +1	115.1784152 +1	133.1578773 +1	4	3	2	0.1657
H	1.12422556 +1	107.9882260 +1	132.1486325 +1	5	4	3	0.0826
H	1.12439161 +1	109.3114391 +1	-112.4553477 +1	5	4	3	0.1030
H	1.12337299 +1	108.3772193 +1	65.2006623 +1	6	1	2	0.0864
H	1.12097208 +1	109.5249859 +1	-178.4211821 +1	6	1	2	0.0923
H	1.11932886 +1	111.2099891 +1	-9.7966922 +1	21	12	11	0.0991
H	1.12134148 +1	110.6689642 +1	110.4411412 +1	21	12	11	0.0977
H	1.12013265 +1	110.4956984 +1	-129.6268546 +1	21	12	11	0.0951
H	1.12158750 +1	111.2354342 +1	-63.9330783 +1	22	9	10	0.1212
H	1.12035398 +1	112.0565471 +1	57.3180393 +1	22	9	10	0.1100
H	1.12222666 +1	109.9022000 +1	176.8711377 +1	22	9	10	0.1005
H	1.11925605 +1	111.0192628 +1	-172.2156089 +1	23	15	16	0.0910
H	1.12135606 +1	109.9654290 +1	-52.2264868 +1	23	15	16	0.0972
H	1.12038857 +1	111.0829737 +1	67.4650561 +1	23	15	16	0.1040
H	1.12190917 +1	109.9302477 +1	179.2047355 +1	24	18	17	0.1005
H	1.12193660 +1	111.2989678 +1	-61.6817535 +1	24	18	17	0.1252
H	1.12051931 +1	111.7278810 +1	59.5699888 +1	24	18	17	0.1103
H	1.10182126 +1	120.1796347 +1	179.1901537 +1	27	28	29	0.1467
H	1.10103695 +1	120.4339778 +1	179.6871492 +1	28	27	32	0.1560
H	1.11141080 +1	120.0119470 +1	179.5020603 +1	29	28	27	0.1960
H	1.10304243 +1	118.6336003 +1	-5.2383639 +1	31	30	20	0.1317
H	1.10048386 +1	120.0103569 +1	-179.9964870 +1	32	27	28	0.1456
H	1.10165725 +1	120.2611410 +1	-179.7859699 +1	33	34	35	0.1484
H	1.10087821 +1	120.2294388 +1	-179.9250473 +1	34	33	38	0.1516
H	1.10785154 +1	120.0545605 +1	-179.7306576 +1	35	34	33	0.1863
H	1.10189987 +1	119.3664433 +1	3.1729374 +1	37	36	20	0.1343
H	1.10064444 +1	120.0266789 +1	179.9777250 +1	38	33	34	0.1494
H	1.10158835 +1	120.0748560 +1	179.4978227 +1	39	40	41	0.1477
H	1.10074523 +1	120.0491824 +1	-179.3942780 +1	40	39	44	0.1490
H	1.10236722 +1	118.7615427 +1	-178.5087695 +1	41	40	39	0.1415
H	1.10973970 +1	119.0356276 +1	-2.4606170 +1	43	42	14	0.1848
H	1.10111698 +1	120.3331196 +1	179.1942876 +1	44	39	40	0.1551
H	1.10172292 +1	120.3182066 +1	179.4178026 +1	45	46	47	0.1481
H	1.10135189 +1	120.4197378 +1	179.3575807 +1	46	45	50	0.1567
H	1.11419157 +1	119.7299379 +1	178.3735199 +1	47	46	45	0.2012
H	1.10283541 +1	118.3554972 +1	-2.9642585 +1	49	48	14	0.1308
H	1.10041168 +1	120.0167732 +1	-179.5368049 +1	50	45	46	0.1482
Cl	6.20922631 +1	43.0164116 +1	-13.9063851 +1	1	2	3	-0.6163
C	1.98956809 +1	100.6900471 +1	-133.2399368 +1	4	3	2	0.2724
O	1.83316650 +1	99.0411746 +1	-158.7339250 +1	51	25	14	-0.5401
C	4.26684174 +1	116.1043996 +1	-102.1942002 +1	94	95	8	-0.1010
C	3.75811995 +1	134.0314778 +1	-108.7273338 +1	94	95	8	-0.1380
C	2.47657937 +1	143.8615241 +1	117.8855814 +1	94	95	25	-0.1021
C	1.47432271 +1	115.7811363 +1	-104.7734643 +1	94	95	1	-0.1232
C	1.40012898 +1	121.4864798 +1	12.3804961 +1	99	94	95	-0.0782
C	1.39459335 +1	120.0481592 +1	0.0657865 +1	96	97	98	-0.1426
H	1.11890370 +1	115.5637447 +1	-139.4664178 +1	94	95	99	0.1258
H	1.10066213 +1	119.9013518 +1	179.9892516 +1	96	97	98	0.1412
H	1.10034315 +1	120.0060068 +1	-179.9248945 +1	97	96	101	0.1425
H	1.10080330 +1	120.1274003 +1	-179.8283298 +1	98	97	96	0.1364
H	1.10212291 +1	119.2179838 +1	3.3794820 +1	100	99	94	0.1578
H	1.10020201 +1	120.0143375 +1	179.7914648 +1	101	96	97	0.1398

___ TS-A-FORCE.mop_____

```
 AM1 CHARGE=1  let force
 ricerca del TS a faccia re

 C     0.00000000 +0    0.0000000 +0    0.0000000 +0                          -0.1573
 C     1.51104931 +1    0.0000000 +0    0.0000000 +0     1     0     0       -0.1993
 C     1.49902228 +1  108.0984215 +1    0.0000000 +0     2     1     0        0.3478
 C     1.35100000 +0  123.2632784 +1  -33.0162179 +1     3     2     1       -0.3616
 C     1.50233830 +1  119.8739886 +1   -3.1424326 +1     4     3     2       -0.1284
 C     1.51676846 +1  108.5183301 +1   60.6327775 +1     1     2     3       -0.1639
 O     1.30382938 +1  114.7457548 +1  142.9129158 +1     3     2     1       -0.5118
Cl     4.95889240 +1   10.7608532 +1   94.0029788 +1     1     2     3       -0.5828
 C     9.91737663 +1    6.1641707 +1   27.4095026 +1     1     2     3       -0.2857
 C     1.39957269 +1   48.6180284 +1 -123.5832379 +1     9     1     2       -0.9166
 C     1.44932828 +1  109.5006431 +1  107.9570324 +1    10     9     1        0.0257
 C     1.39561278 +1  111.6883538 +1    1.3434426 +1    11    10     9       -0.3984
 S     1.65636903 +1  112.5827982 +1   -0.1236720 +1     9    10    11        0.6922
 P     1.61869422 +1  124.2292904 +1  176.6576383 +1    10     9    13        3.3065
 C    10.05228771 +1   28.0164101 +1  -40.6757496 +1     1     2     3       -0.3966
 C     1.47361537 +1  131.4418484 +1  174.2349779 +1    11    10     9        0.0118
 C     1.44741318 +1  131.4788315 +1   92.2117946 +1    16    11    10       -0.9293
 C     1.39972570 +1  109.8238203 +1  175.6882031 +1    17    16    11       -0.2686
 S     1.65179230 +1  111.7031917 +1 -177.2393129 +1    15    16    11        0.7038
 P     1.61026705 +1  125.2689999 +1   -9.6431004 +1    17    16    11        3.3031
 C     1.46957572 +1  127.5185387 +1  175.6199365 +1    12    11    10       -0.1653
 C     1.47773987 +1  134.6178691 +1  179.6705428 +1     9    10    11       -0.1873
 C     1.46801400 +1  127.0723240 +1   -0.5920497 +1    15    16    11       -0.1637
 C     1.47721639 +1  134.1801405 +1  177.7645951 +1    18    17    16       -0.1885
 O     1.54103432 +1  109.8830255 +1  125.5936702 +1    14    10     9       -1.1792
 O     1.54070674 +1  106.8617734 +1  -67.2852039 +1    20    17    16       -1.1715
 C     8.83739079 +1   27.7262120 +1 -137.2407614 +1     1     2     3       -0.0569
 C     1.39318139 +1   25.4769823 +1  -49.2748891 +1    27     1     2       -0.1483
 C     1.39537446 +1  119.7530769 +1   55.7813401 +1    28    27     1       -0.0171
 C     1.59951614 +1  112.1987237 +1   54.0023896 +1    20    17    16       -0.9541
 C     1.39897226 +1  121.5675632 +1   42.9743970 +1    30    20    17       -0.0417
 C     1.39898561 +1  120.0294021 +1   -0.7021083 +1    27    28    29       -0.1605
 C     6.38005849 +1   65.4770363 +1  -84.6199540 +1     1     2     3       -0.0526
 C     1.39411077 +1   41.1357881 +1   69.9606829 +1    33     1     2       -0.1548
 C     1.39306877 +1  119.8601407 +1 -104.6157101 +1    34    33     1       -0.0153
 C     1.60448025 +1  111.7362456 +1  174.2325828 +1    20    17    16       -0.9570
 C     1.39835850 +1  122.8351825 +1  -85.8085980 +1    36    20    17       -0.0314
 C     1.39803449 +1  119.7445575 +1    0.0953059 +1    33    34    35       -0.1558
 C     9.68939241 +1   34.2479423 +1   70.1464086 +1     1     2     3       -0.0528
 C     1.39677285 +1  111.0689220 +1  -70.3046235 +1    39     1     2       -0.1574
 C     1.39155409 +1  119.8793310 +1   34.4251829 +1    40    39     1       -0.0310
 C     1.60522487 +1  111.2708037 +1    8.9073061 +1    14    10     9       -0.9616
 C     1.40273729 +1  118.3789687 +1   79.3616938 +1    42    14    10       -0.0256
 C     1.39506030 +1  119.6815777 +1   -0.0998386 +1    39    40    41       -0.1516
 C    11.38311881 +1   37.4650605 +1    1.6016885 +1     1     2     3       -0.0564
 C     1.39211341 +1   22.0430394 +1 -166.8008226 +1    45     1     2       -0.1478
 C     1.39714975 +1  120.0124607 +1   -0.5707943 +1    46    45     1       -0.0161
 C     1.59810815 +1  108.0303539 +1 -110.5462167 +1    14    10     9       -0.9638
 C     1.40359284 +1  119.9221278 +1   49.3086998 +1    48    14    10       -0.0488
 C     1.40071136 +1  119.8566226 +1   -0.6758796 +1    45    46    47       -0.1575
Si     1.85712319 +1  125.1565776 +1  108.0368474 +1     7     3     2        1.8661
 H     1.12033728 +1  110.4335137 +1  -60.3286523 +1     1     2     3        0.0864
 H     1.12027359 +1  109.9800476 +1 -178.9764541 +1     1     2     3        0.0977
 H     1.12507680 +1  111.3599590 +1  -58.8368160 +1     2     1     6        0.1444
 H     1.12157001 +1  111.3960684 +1 -178.4808319 +1     2     1     6        0.1213
 H     1.11936152 +1  115.1761648 +1  133.1506049 +1     4     3     2        0.1657
 H     1.12422647 +1  107.9880876 +1  132.1493787 +1     5     4     3        0.0826
 H     1.12439067 +1  109.3117950 +1 -112.4543839 +1     5     4     3        0.1030
 H     1.12337310 +1  108.3766030 +1   65.1982548 +1     6     1     2        0.0864
 H     1.12097089 +1  109.5251039 +1 -178.4239133 +1     6     1     2        0.0923
 H     1.11932982 +1  111.2099271 +1   -9.7969837 +1    21    12    11        0.0991
 H     1.12134083 +1  110.6691167 +1  110.4411269 +1    21    12    11        0.0977
 H     1.12013345 +1  110.4956053 +1 -129.6270844 +1    21    12    11        0.0951
 H     1.12158475 +1  111.2354659 +1  -63.9334277 +1    22     9    10        0.1212
 H     1.12035429 +1  112.0567157 +1   57.3177877 +1    22     9    10        0.1100
 H     1.12222660 +1  109.9021175 +1  176.8709397 +1    22     9    10        0.1005
 H     1.11925841 +1  111.0193103 +1 -172.2157581 +1    23    15    16        0.0910
 H     1.12135603 +1  109.9652990 +1  -52.2265815 +1    23    15    16        0.0972
 H     1.12038920 +1  111.0829262 +1   67.4647985 +1    23    15    16        0.1040
 H     1.12191084 +1  109.9302841 +1  179.2050490 +1    24    18    17        0.1005
 H     1.12193557 +1  111.2989661 +1  -61.6813863 +1    24    18    17        0.1252
 H     1.12051925 +1  111.7277727 +1   59.5702098 +1    24    18    17        0.1103
```

```
  H     1.10182170 +1  120.1797320 +1  179.1900962 +1    27    28    29       0.1467
  H     1.10103382 +1  120.4339163 +1  179.6873240 +1    28    27    32       0.1560
  H     1.11141143 +1  120.0118656 +1  179.5021995 +1    29    28    27       0.1960
  H     1.10304532 +1  118.6335931 +1   -5.2380843 +1    31    30    20       0.1317
  H     1.10048534 +1  120.0102320 +1 -179.9967854 +1    32    27    28       0.1456
  H     1.10165723 +1  120.2610348 +1 -179.7859758 +1    33    34    35       0.1484
  H     1.10087785 +1  120.2293290 +1 -179.9257987 +1    34    33    38       0.1516
  H     1.10785103 +1  120.0546018 +1 -179.7313934 +1    35    34    33       0.1863
  H     1.10189945 +1  119.3666401 +1    3.1716214 +1    37    36    20       0.1343
  H     1.10064450 +1  120.0267041 +1  179.9786813 +1    38    33    34       0.1494
  H     1.10158801 +1  120.0748134 +1  179.4979705 +1    39    40    41       0.1477
  H     1.10074620 +1  120.0491886 +1 -179.3941110 +1    40    39    44       0.1490
  H     1.10237057 +1  118.7613954 +1 -178.5088874 +1    41    40    39       0.1415
  H     1.10973857 +1  119.0356482 +1   -2.4613092 +1    43    42    14       0.1848
  H     1.10111377 +1  120.3330979 +1  179.1941495 +1    44    39    40       0.1551
  H     1.10172426 +1  120.3182034 +1  179.4177178 +1    45    46    47       0.1481
  H     1.10135244 +1  120.4200011 +1  179.3573094 +1    46    45    50       0.1567
  H     1.11418976 +1  119.7298367 +1  178.3734807 +1    47    46    45       0.2012
  H     1.10283468 +1  118.3553942 +1   -2.9638979 +1    49    48    14       0.1308
  H     1.10041234 +1  120.0167234 +1 -179.5365659 +1    50    45    46       0.1482
 Cl     6.20923111 +1   43.0158351 +1  -13.9117394 +1     1     2     3      -0.6163
  C     1.98947847 +1  100.6860655 +1 -133.2458872 +1     4     3     2       0.2723
  O     1.83321446 +1   99.0408348 +1 -158.7379422 +1    51    25    14      -0.5402
  C     4.26687159 +1  116.1092435 +1 -102.2020368 +1    94    95     8      -0.1010
  C     3.75808899 +1  134.0360980 +1 -108.7316444 +1    94    95     8      -0.1380
  C     2.47656006 +1  143.8649572 +1  117.8876054 +1    94    95    25      -0.1021
  C     1.47429239 +1  115.7813262 +1 -104.7765210 +1    94    95     1      -0.1232
  C     1.40011213 +1  121.4859348 +1   12.3732943 +1    99    94    95      -0.0782
  C     1.39458376 +1  120.0498523 +1    0.0657675 +1    96    97    98      -0.1426
  H     1.11890647 +1  115.5621328 +1 -139.4674609 +1    94    95    99       0.1259
  H     1.10066162 +1  119.9013676 +1  179.9890191 +1    96    97    98       0.1412
  H     1.10034264 +1  120.0059935 +1 -179.9248179 +1    97    96   101       0.1424
  H     1.10080380 +1  120.1276748 +1 -179.8278790 +1    98    97    96       0.1364
  H     1.10212340 +1  119.2179908 +1    3.3789206 +1   100    99    94       0.1578
  H     1.10020073 +1  120.0142494 +1  179.7913441 +1   101    96    97       0.1398
```

___ TS-A-FORCE.out_____

```
 CALCULATION DONE:
  AM1      - The AM1 Hamiltonian to be used
                 CHARGE ON SYSTEM =     1
   LET      - OVERRIDE SOME SAFETY CHECKS
  FORCE    - FORCE CALCULATION SPECIFIED


 AM1 CHARGE=1  let force
    ricerca del TS a faccia re

             Empirical Formula: C49 H47 O4 Cl2 S2 P2 Si  =   107 atoms
       MOLECULAR POINT GROUP   :   C1
       RHF CALCULATION, NO. OF DOUBLY OCCUPIED LEVELS =  153
           HEAT OF FORMATION =     -89.255079 KCALS/MOLE

           GRADIENT NORM = 143.90085

  ** GRADIENT IS VERY LARGE, BUT SINCE "LET" IS USED, CALCULATION WILL CONTINUE

 [...]

            NORMAL COORDINATE ANALYSIS (Total motion = 1 Angstrom)


    Root No.      1       2       3       4       5       6       7       8

                 1 A     2 A     3 A     4 A     5 A     6 A     7 A     8 A

                -529.1   -74.8   -27.7   -21.0    10.5    18.3    22.5    29.1

  [...]
```

```
            DESCRIPTION OF VIBRATIONS

  VIBRATION    1    1A       ATOM PAIR        ENERGY CONTRIBUTION    RADIAL
  FREQ.      -529.15        C  4 --  C 94          +14.8% (-60.7%)    99.6%
  T-DIPOLE    6.9124        C  4 --  H 56          +13.8% (-58.7%)     1.4%
  TRAVEL      0.1092        C  3 --  C  4          +12.7% (-56.3%)     8.8%
  RED. MASS   4.2568        C 94 --  H102         +12.4% (-55.7%)     0.8%
  EFF. MASS  10.6902        C 94 --  C 99          +10.1% (-50.2%)     2.4%

  VIBRATION    2    2A       ATOM PAIR        ENERGY CONTRIBUTION    RADIAL
  FREQ.       -74.77        C  5 --  C  6          +14.1% (-99.9%)     0.0%
  T-DIPOLE    0.0715        C  4 --  C  5          +12.8% (-99.9%)     0.0%
  TRAVEL      0.0440        C  5 --  H 58          +11.0% (-99.9%)    57.3%
  RED. MASS   1.2804        C  5 --  H 57           +9.6% (-99.9%)    80.7%
  EFF. MASS 465.1000

  VIBRATION    3    3A       ATOM PAIR        ENERGY CONTRIBUTION    RADIAL
  FREQ.       -27.71        C  5 --  C  6          +16.6% (-99.9%)     0.0%
  T-DIPOLE    0.0136        C  1 --  C  6          +15.0% (-99.9%)     0.0%
  TRAVEL      0.0251        C  6 --  H 60          +12.6% (-99.9%)    65.1%
  RED. MASS   1.1036        C  6 --  H 59          +11.2% (-99.9%)    92.1%
  EFF. MASS3869.1782

  VIBRATION    4    4A       ATOM PAIR        ENERGY CONTRIBUTION    RADIAL
  FREQ.       -20.96        C  1 --  C  6           +9.6% (-99.9%)     0.0%
  T-DIPOLE    0.1671        C  1 --  C  2           +7.4% (-99.9%)     0.0%
  TRAVEL      0.0245        C  1 --  H 53           +5.6% (-99.9%)    37.2%
  RED. MASS   0.5910        C  5 --  C  6           +4.9% (-99.9%)     0.0%
  EFF. MASS5352.4691

  VIBRATION    5    5A       ATOM PAIR        ENERGY CONTRIBUTION    RADIAL
  FREQ.        10.46        C 96 --  C101          +5.8% (999.0%)     0.0%
  T-DIPOLE    0.0277        C 97 --  C 98          +5.6% (999.0%)     0.0%
  TRAVEL      0.0204        C 96 --  C 97          +5.3% (999.0%)     0.0%
  RED. MASS   0.4914        C100 --  C101          +5.0% (999.0%)     0.0%
  EFF. MASS9999.9999

 [...]
 [...]

== MOPAC DONE ==
```

APPENDIX

Highly stereoselective metal-free catalytic reduction of imines

Chiral amines are key structural elements of many biologically active compounds, which find application as fragrances, agrochemicals, and pharmaceuticals. Among the different approaches that can be used in order to obtain chiral amines, the reduction of ketoimines represents a powerful and widely used transformation.

Relatively few examples of organocatalytic systems are known for the reduction of imines, reported in paragraph 1.3. In this field, we developed two different families of organic catalysts able to promote the stereoselective reduction of a carbon-nitrogen double bond, allowing to obtain chiral amine compounds in very high yields and often very high enantioselectivity.[110] The reaction is very attractive in view of possible applications to the synthesis of pharmaceutical products, as well as for other fine chemicals. While designing new chiral Lewis basic organocatalysts for the imine reduction, we decided to pursue the highest structural simplicity. Accordingly, the catalysts should be obtained by modification of an inexpensive, commercially available, enantiopure material whose manipulation must be kept to minimum.

In this context, the first class of catalysts was prepared by simple condensation of an aminoalcohol with picolinic acid or its derivatives.[88b] The second class of catalysts was prepared by simple condensation of enantiomerically pure diamines with picolinic acid or its derivatives.[107] The choice of the chiral auxiliary to be connected to the Lewis base is a crucial point for the chemical and stereochemical efficiency of the catalytic

system, and it is under this aspect that the compounds present a character of absolute novelty.

In a one-step procedure, several derivatives were synthesized simply by reaction of a chiral amino alcohol or diamine with picolinoyl chloride or picolinic acid in the presence of condensing agents. Among the different synthesized compounds, (1*R*,2*S*)-ephedrine-derived *N*-picolinoylamide **X1** and *N*-4-chloropicolinoylamide **X2** and the bis(*N*-methyl-*N*-picolinoylamide) of 1,1′-binaphthyldiamine **X3** were selected for this study (Figure 1).[111]

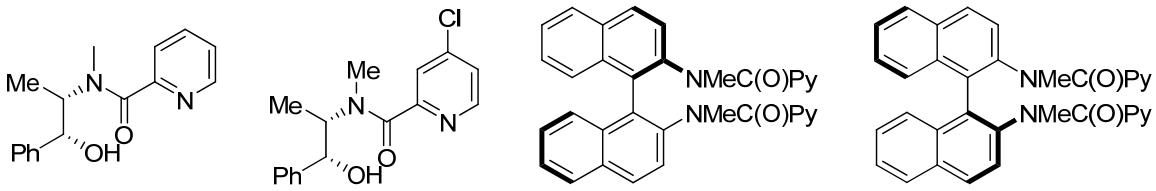

X1 **X2** **(*R*)-X3** **(*S*)-X3**

***Figure 1**: catalysts for stereoselective ketoimine reduction.*

In the reduction of the *N*-benzylimine of acetophenone, by employing 10% of catalyst **X1** at 0°C and 1.5 equiv mol of $HSiCl_3$ in dichloromethane, the product was isolated in 85% yield and 71% ee (Scheme 1).

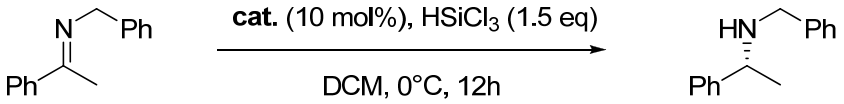

***Scheme 1**: enantioselective reduction of N-Benzylimine.*

Higher performances were obtained with ephedrine-based 4-chloropicolinamide **X2** which promoted the reaction in quantitative yield and 80% ee. Catalyst **(*S*)-X3** promoted the reaction in quantitative yield and 85% ee.

Even if both catalysts **X2** and **X3** showed excellent chemical efficiency and interesting levels of enantioselectivity, the control of the absolute stereochemistry was not satisfactory. In order to improve the selectivity of the process, the trichlorosilane-mediated reduction of acetophenone imines **(*R*)-X4** and **(*S*)-X4** derived from (*R*)- and (*S*)-1-phenylethylamine, respectively, was studied (Scheme 2).[247]

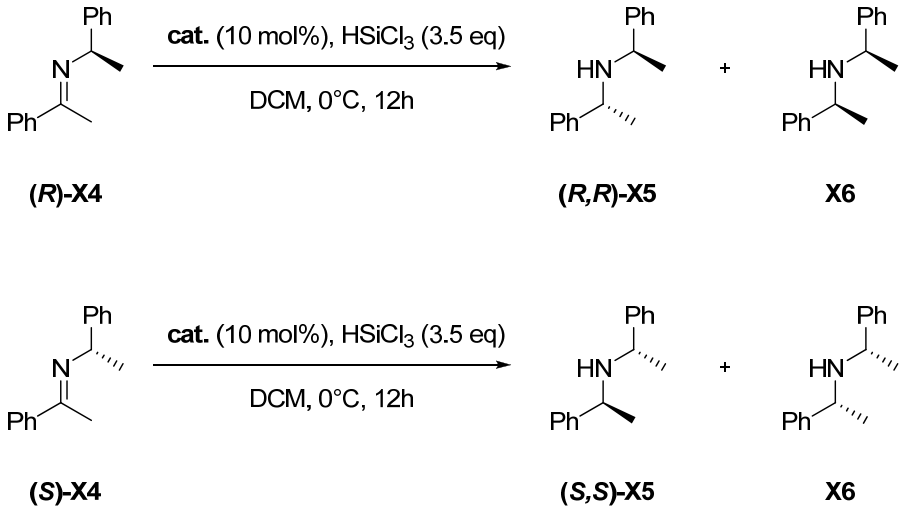

Scheme 2: *stereoselective reduction of imine X4.*

The reaction product is the bis-α-methylbenzylamine, a compound that is enormously employed as chiral base and chiral ligand in numerous reactions.[248] The diastereoselective reduction of these chiral substrates through hydrogenation with different catalytic systems has been investigated.[249] However, no examples of analogous studies with organocatalytic systems have been reported so far.

Therefore, the reduction of imines **(*R*)-X4** and **(*S*)-X4** with 3.5 molar equiv of trichlorosilane and 10 mol% of catalyst was performed in dichloromethane in the presence of either achiral or chiral ligands (Table 1).

entry	cat.	imine	yield (%) of *(R,R)-X5*	*dr X5:X6*
1[c]	-	(*R*)-X4	98	80:20
2	-	(*R*)-X4	37	88:12
3	DMF	(*R*)-X4	72	95:5
4	X2	(*R*)-X4	98	>99:1
5	X2	(*R*)-X4	98	76:24
6	(*R*)-X3	(*S*)-X4	98	95:5
7	(*R*)-X3	(*R*)-X4	98	80:20

[c] Reduction was performed with $NaBH_4$.

Table 1

For the sake of comparison, the reduction of imine **(*R*)-X4** with $NaBH_4$ was accomplished first; in our hands the reaction afforded the products in quantitative yield

and 80:20 **(*R*,*R*)-X5/X6** diastereoisomeric ratio (Table 1, entry 1). In the absence of any organic promoter, trichlorosilane reduced keto-imine **(*R*)-X4** in poor yield; when the reaction was performed in the presence of 2 molar equiv of *N*,*N*-dimethylformamide, chiral amine **X5** was obtained in 72% yield and in 90% diastereoselectivity (entry 3). However, the real improvement was observed when picolinamide **X2** was employed as catalyst; it promoted the reduction in quantitative yield with a total control of the stereoselectivity (Table 1, entry 4). As a demonstration of the presence of a cooperative effect of catalyst **X2** with the (*R*)-methyl benzyl residue at the imine nitrogen, the reduction of imine **(*S*)-4** in the presence of **X2** led to the formation of isomer **(*S*,*S*)-X5** as major product but in only 76:24 isomeric ratio (entry 5).

Also binaphthyl derived bis-picolinamide **X3** efficiently catalyzed the reduction of chiral imines **X4**, although with a lower selectivity. In this case, the matching pair was represented by (*R*)-binaphthyldiamine derivative **X3** and imine **(*S*)-X4** prepared from (*S*)-methylbenzylamine; such a combination allowed us to obtain **(*S*,*S*)-X5** with 90% d.e.

The methodology was extended to the synthesis of an enantiomerically pure secondary amine of either C_1 or C_2 symmetry. For example, the reduction of the (*R*)-*N*-1-β-naphthylethylimine of 2-acetonaphthone **X7** with trichlorosilane and catalyst **X2** was successfully accomplished (eq a, Scheme 3); amine **X8** was obtained at 0°C as single isomer in 98% yield (the reduction of imine **X7** with $NaBH_4$ afforded the product with 78% diastereoselectivity).

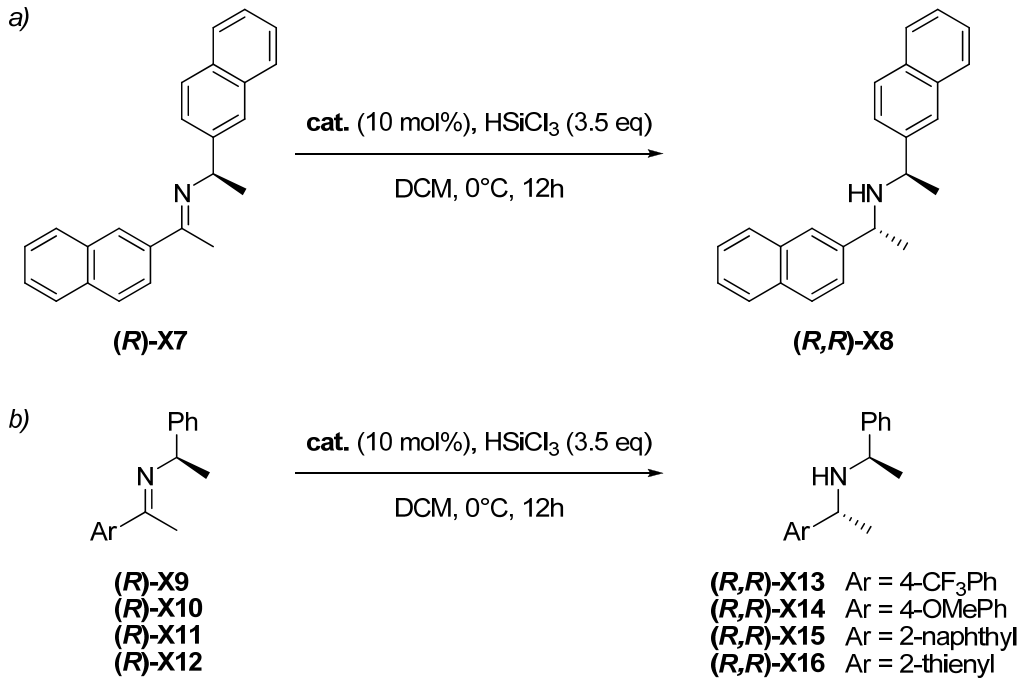

Scheme 3

The general applicability of such a methodology was demonstrated; *N*-α-methylbenzyl- imines of methyl aryl ketones with different electronic properties were effectively reduced to the corresponding secondary amines in quantitative yields, maintaining an absolute control of the stereoselectivity of the process (eq b, Scheme 3). Amines **X13-X15** were all obtained in > 99/1 diastereoisomeric ratio (Table 2).

entry	cat.	Imine	product	yield (%)	*dr*
1[c]	X2	(*R*)-X7	(*R,R*)-X8	98	>99:1
2	X2	(*R*)-X9	(*R,R*)-X13	98	>99:1
3	(*S*)-X3	(*R*)-X9	(*R,R*)-X13	98	>99:1
4	X2	(*R*)-X10	(*R,R*)-X14	98	>99:1
5	X2	(*R*)-X11	(*R,R*)-X15	98	>99:1
6	(*S*)-X3	(*S*)-X11	(*R,R*)-X15	98	>99:1
7	X2	(*R*)-X12	(*R,R*)-X16	98	>99:1

Table 2

It is noteworthy that the correct match pair of **(*R*)-X9** imine and **(*S*)-X3** also afforded the secondary amine as an enantiomerically pure compound. Amine **X13** can be converted to 4-trifluoromethylphenylmethylamine by simple hydrogenation,[250] thus demonstrating the practicability of the approach for the preparation of an enantiomerically pure primary amine. The methodology can also be used for the reduction of heteroaromatic alkyl ketimines; catalyst **X2** promoted the reduction of 2-thienyl methyl ketone-derived imine **X12** in > 99/1 dr (entry 7).

The trichlorosilane-mediated reduction was also applied to imines of dialkyl ketones. Imine **X17** derived from methyl isobutyl ketone was readily reduced in > 98% yield in the presence of both catalysts **X2** and **X3**. By using ephedrine-based catalyst **X2**, and amine **X18**, the direct precursor of (*R*)-isopropylmethylamine, was isolated as an enantiomerically pure compound (Scheme 4).

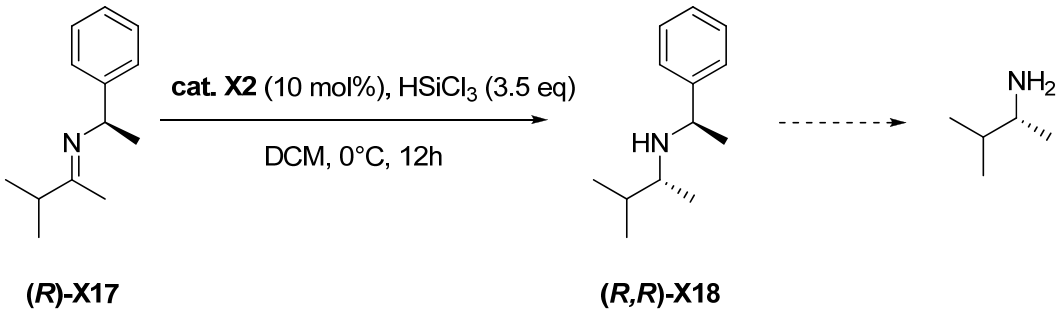

Scheme 4

A model of stereoselection observed in the reaction promoted by catalyst **X2** was proposed: pyridine nitrogen and a CO amidic group of picolinamide would active trichlorosilane by coordination and, in the case of the (*R*)-phenylethylamine-derived imine reduction, a working model of the low energy conformer of *trans*-keto-imine determining the facial selectivity was already proposed.[249] It involves the presence of the imine nitrogen on the same plane with the carbon atom and the hydrogen atom of the stereocenter. Based on these considerations, the sense of the hydrogen attack on the imine *Si*-face determined by the (*R*)-stereocenter of the chiral auxiliary is in accordance with the sense of addition dictated by catalyst **X2**; the cooperative effect of the two chiral elements responsible for the stereoselection explains the sense of the experimentally observed absolute stereochemistry (figure 2).

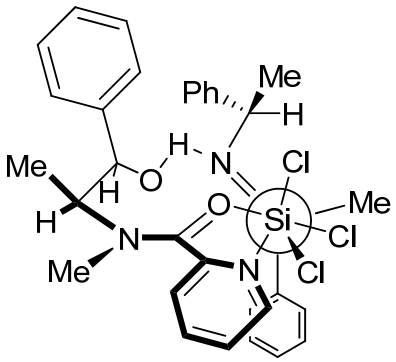

Figure 2: *proposed model of stereoselection.*

Finally, we decided to test our methodology in the preparation of unnatural *R*-amino acids.[248] Very few successful transition-metal-catalyzed hydrogenations of *R*-imino esters were reported.[252] Only one example of organocatalytic ketoimine reduction promoted by phosphoric acid, developed by MacMillan, was known.[253] A very limited

number of cyclic *R*-imino esters were studied, and only one reduction of acyclic imino esters is known.[254]

Catalysts **X2** and **X3** promoted the reduction of *N*-benzyliminoester **X21** in quantitative yield and up to 71% ee. However picolinamide **X2** catalyzed the reduction of chiral imine (***R***)**-X23** at 0°C in dichloromethane to afford the formation of **(*R,S*)-X24** in 73% yield and 91% diastereoisomeric excess (Scheme 5). The use of (1*S*,2*R*)-ephedrine derived catalyst **en-X2** led to the unnatural *R*-aminoester.

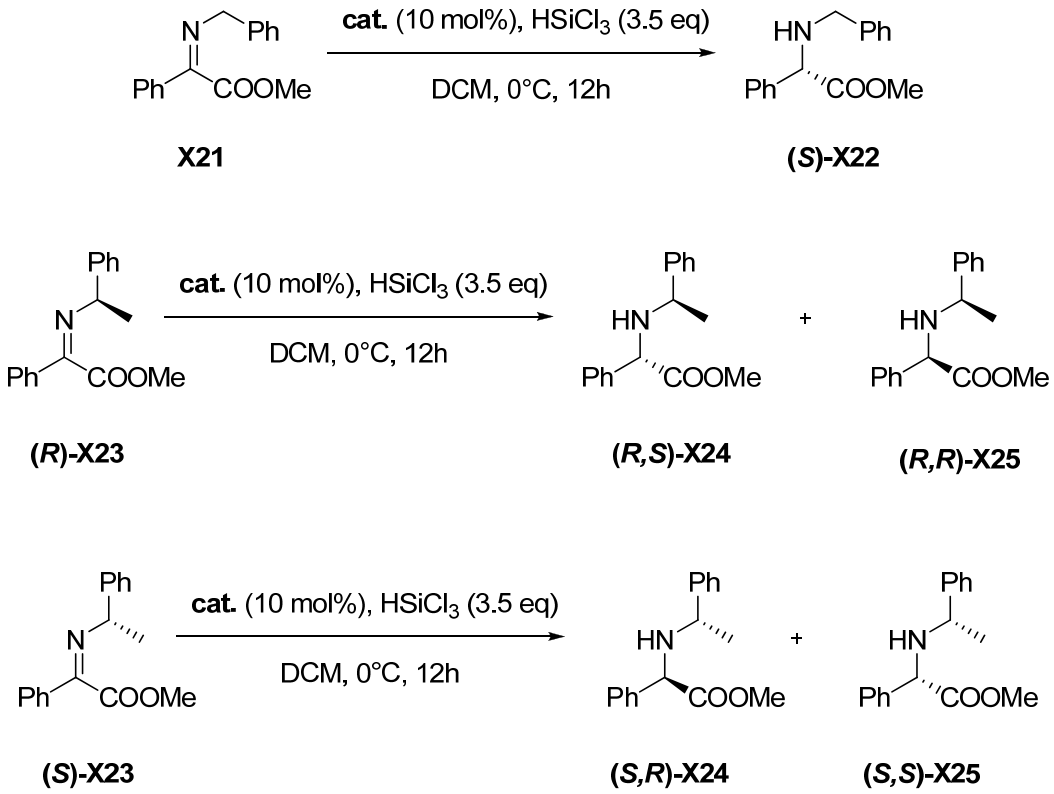

Scheme 5: *stereoselective synthesis of amino esters.*

In conclusion, a highly efficient synthesis of enantiomerically pure primary and secondary amines has been developed. The combination of low cost, easy to make metal-free catalyst and an inexpensive chiral auxiliary permit to reduce keto-imines with different structural features often with total control of the stereoselectivity.

APPENDIX: Experimental section

In this section the synthetic procedures of all products shown in the previous one have been reported. The compounds preserve the numbering established in precedence. For the general information, see Chapter 6.

Synthesis of catalysts

General Procedure A: To a stirred solution of the picolinic acid (1 mol equiv) in chloroform (5 ml/mmol substrate) under nitrogen at 0°C, chloroform solutions of EDC (1.2 mol equiv), and HOBt (1.2 mol equiv), and aminoalcohol (1.2 mol equiv) were added in this order (the volume of each added solution was 1-3 ml; the total final volume of the solution was 8-25 ml). The reaction was stirred at room temperature overnight, and concentrated under vacuum to give the crude product. Purification by flash chromatography afforded the products.

General Procedure B: A stirred solution of the picolinic acid (1 mol equiv) in thionyl chloride (1 ml/mmol substrate) was refluxed for 2 hours, then the solvent was evaporated under vacuum; the residue, dissolved in THF (2 mL) with a few drops of DMF, was added to a solution of chiral aminoalcohol (1 mol equiv) and TEA (3 mol equiv) in THF. The reaction mixture was stirred for 12 hours at reflux. The organic phase was quenched with aqueous saturated solution of $NaHCO_3$ and brine. The organic phase was then dried over Na_2SO_4, filtered and concentrated under vacuum to give the crude product. Purification by flash chromatography afforded the products, as mixture of rotamers.

Synthesis of keto-imines: see paragraph 6.10.4

Reduction of keto-imines: see paragraph 6.10.5

Characterization of products

Catalyst X1 (*Procedure A*)

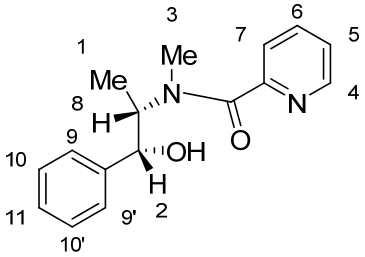

Starting from (1*R*,2*S*)-ephedrine catalyst **X1** was isolated in 70% yield (purification through silica gel, eluent: 99:1 CH_2Cl_2/CH_3OH).

Rotamer 1:

^{1}H-NMR (300 MHz, $CDCl_3$): δ 8.53 (s, 1H, **4**), 7.75 (m, 1H, **6**), 7.49 (m, 1H, **7**), 7.36 (m, 1H, **5**), 7.30-7.25 (m, 5H, **9**, **9'**, **10**, **10'**, **11**), 4.81 (d, *J* = 4.6 Hz, 1H, **2**), 4.35 (s br, 1H, **1**), 2.8 (s, 3H, **3**), 1.33 (d, 3H, **8**).

^{13}C NMR (75 MHz, $CDCl_3$): δ 169, 154.2, 147.3, 141.5, 137.4, 128.2 (2C), 127.4, 126.7 (2C), 124.5, 123.1, 76.1, 58.3, 29.7, 14.5.

Rotamer 2:

^{1}H-NMR (300 MHz, $CDCl_3$): δ 8.53 (s, 1H, **4**), 7.75 (m, 1H, **6**), 7.49 (m, 1H, **7**), 7.36 (m, 1H, **5**), 7.30-7.25 (m, 5H, **9**, **9'**, **10**, **10'**, **11**), 5.09 (s br, 1H, **2**), 4.57 (s br, 1H, **1**), 2.87 (s, 3H, **3**), 1.28 (d, 3H, **8**).

^{13}C NMR (75 MHz, $CDCl_3$): δ 169.8, 154.8, 148.3, 142.1, 137.1, 128.2 (2C), 127.1, 126.3 (2C), 124.5, 124.3, 76.4, 58.6, 35, 11.2.

IR (DCM): $\nu_{C=O}$ = 1725.01 cm^{-1}.

$[\alpha]_D^{25}$ = -19 (solvent: DCM; *c* = 0.55 g/100 mL; λ = 589 nm).

Mass (ESI+): *m*/*z* = $[M+H]^+$ calc for $C_{16}H_{18}N_2O_2$ 271.137, found 271.140,
293.143 $[M+Na]^+$.

Catalyst X2 (*Procedure B*)

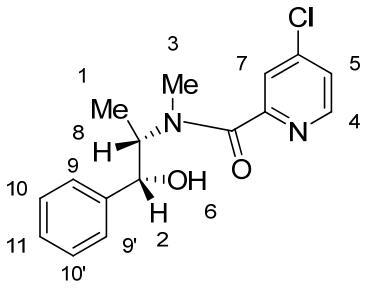

Starting from (1*R*,2*S*) ephedrine and 4-choloropicolinic chloride catalyst **X2** was isolated in 71% yield (purification through silica gel, eluent: 400 mL of 98:2 CH_2Cl_2/MeOH, 600 mL of 95:5 CH_2Cl_2/MeOH, then 400 mL of 9:1 CH_2Cl_2/MeOH)

Rotamer 1:

^{1}H-NMR (300 MHz, $CDCl_3$): δ 8.32 (m, 1H **4**), 7.25 (m, 3H, **5**, **10**, **10'**), 7.23 (m, 1H, **11**), 7.08 (d, J = 6.1 Hz, 2H, **9**, **9'**), 6.48 (s br, 1H, **7**), 4.63 (d, J = 4.0 Hz, 1H, **2**), 4.08 (m, 1H, **1**), 2.86 (s, 3H, **3**), 1.31 (d, J = 6.7 Hz, 3H, **8**).

^{13}C NMR (75 MHz, $CDCl_3$): δ 167.9, 155.4, 148.3, 144.9, 141.7, 128 (2C), 127.6, 126.1 (2C), 124.3, 124.1, 75.2, 58.8, 28.8, 14.2.

Rotamer 2:

^{1}H-NMR (300 MHz, $CDCl_3$): δ 8.30 (m, 1H, **4**), 7.4 (m, 2H, **9**, **9'**), 7.3 (m, 3H, **7**, **10**, **10'**), 7.25 (m, 1H, **5**), 7.23 (m, 1H, **11**), 5.0 (m, 1H, **2**), 4.55 (m, 1H, **1**), 2.80 (s, 3H, **3**), 1.25 (d, *J* = 7 Hz, 3H, **8**).

^{13}C NMR (75 MHz, $CDCl_3$): δ 168.1, 155.8, 149.1, 145, 141.8, 128 (2C), 127.3, 126.1 (2C), 124.3, 123.3, 75.9, 57.6, 34.2, 11.1.

mp = 139-141°C.

IR (DCM): $\nu_{C=O}$ = 1721 cm^{-1}.

$[\alpha]_D^{25}$ = -36.06 (solvent: DCM; *c* = 0.244 g/100 mL; λ = 589 nm).

HRMS Mass (ESI+): *m*/*z* = $[M+Na]^+$ calc for $C_{16}H_{17}ClN_2O_2$ 327.0871, found 327.0869 $[M + Na]^+$.

Catalyst X3 (*Procedure B*)

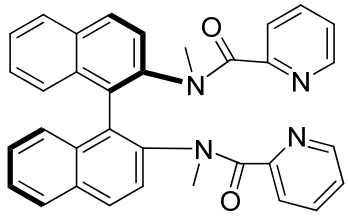

Catalyst **X3** was obtained (76% yield) in the condensation of binaphthyldiamine derivative with picolinoyl chloride. Two sets of signals indicating the presence of two rotamers were detected:

Rotamer 1:

^{1}H-NMR (500 MHz, d_6-DMSO): δ 8.57 (s, *J* = 2.7 Hz, 1H), 7.94 (d, *J* = 8.2 Hz, 2H), 7.81 (s br, 1H) 7.8 (d, 1H), 7.78 (d, 2H), 7.5 (m, 2H), 7.43 (d, *J* = 7.4 Hz, 2H), 7.38 (m, 1H), 7.33 (m, 2H), 7.26 (m, 1H), 7.15 (t, *J* = 7.6 Hz, 2H), 7.06 (d, *J* = 8.8 Hz, 2H), 6.9 (d, *J* = 8.6 Hz, 2H), 2.9 (s, 3H), 2.75 (s, 3H).

^{13}C-NMR (125 MHz, d_6-DMSO): δ 169.8 (2C), 154.8, 148.4, 143.1 (2C), 137.3, 136.5, 134.5 (2C), 131.8 (2C), 129.6 (2C), 128.8 (2C), 128.3 (2C), 128.1 (5C), 127.2 (2C), 126.5 (4C), 125 (2C), 123.5 (2C), 36.9, 36.5.

Rotamer 2:

^{1}H-NMR (500 MHz, d_6-DMSO): δ 8.2 (d, *J* = 4.1 Hz, 1H), 7.94 (d, *J* = 8.2 Hz, 2H), 7.8 (d, 1H), 7.78 (d, *J* = 8.8 Hz, 1H), 7.73 (d, *J* = 8.8 Hz, 2H), 7.5 (m, 2H), 7.43 (d, *J* = 7.4 Hz, 2H), 7.33 (m, 2H), 7.26 (m, 2H), 7.15 (t, *J* = 7.6 Hz, 2H), 6.95 (d, *J* = 8.9 Hz, 2H), 6.85 (d, *J* = 8.6 Hz, 2H), 2.9 (s, 3H), 2.75 (s, 3H).

^{13}C NMR (125 MHz, d_6-DMSO): δ 169.4 (2C), 154.8, 148.6, 142.9 (2C), 137.6, 136.5, 134.3 (2C), 131.5 (2C), 129.5 (2C), 128.7 (2C), 128.3 (2C), 128.1 (5C), 127.2 (2C), 126.5 (4C), 125 (2C), 123.5 (2C), 36.9, 36.5.

mp = 97°C.

IR (DCM): $\nu_{C=O}$ = 1650, 1458, 1380 cm^{-1}.

$[\alpha]_D^{25}$ = +413.9 (solvent: DCM; *c* = 0.244 g/100 mL; λ = 589 nm).

HRMS Mass (ESI+): *m/z* = $[M+H]^+$ calc for $C_{34}H_{26}N_4O_2$ 523.2128 found 523.2146, 545.1939 $[M + Na]^+$.

Bis(1-phenylethyl)amine *(R,R)*-X5

This product is known[255] was purified with a 8:2 hexane/ethyl acetate mixture as eluent.

^{1}H-NMR (300 MHz, $CDCl_3$): δ 7.34-7.20 (m, 10H), 3.55 (q, 2H), 1.31 (d, 6H).

The enantiomeric excess was determined by chiral HPLC with Chiralcel OD-H column [eluent: 99.9:0.1 Hex/IPA; 0.8 mL/min flow rate, detection: 210 nm; t_R 8.1 min (major), t_R 15.5 min (minor).

Bis(1-(naphthalen-2-yl)ethyl)amine *(R,R)*-X8

This product was purified with a 8:2 hexane/ethyl acetate mixture as eluent.

^{1}H-NMR (300 MHz, $CDCl_3$): δ 7.9-7.6 (m, 14H), 3.92 (m, 2H), 1.78 (m, 6H).

^{13}C-NMR (75 MHz, $CDCl_3$): δ 134.1, 132.8, 129.1, 128.9, 127.2, 127.1, 125.0, 124.3, 124.2, 123.9, 56.9, 25.2.

HRMS Mass (ESI+): m/z = $[M+1]^+$ calc for $C_{24}H_{23}N$ 326.1903, found 326.1911, 348.1729 $[M + Na]^+$.

The enantiomeric excess was determined by chiral HPLC with Chiralcel OD-H column [eluent: 99:1 Hex/IPA; 0.8 mL/min flow rate, detection: 210 nm; t_R 4.5 min (minor), t_R 4.7 min (major).

1-phenyl-*N*-(1-(4-(trifluoromethyl)phenyl)ethyl)ethanamine *(R,R)*-X13

This product was purified with a 8:2 hexane/ethyl acetate mixture as eluent.

^{1}H-NMR (300 MHz, $CDCl_3$): δ 7.7-7.2 (m, 9H), 3.7 (m, 1H), 3.55 (m, 1H), 1.5 (d, 6H).

^{13}C-NMR (75 MHz, $CDCl_3$): δ 129.2, 129.0, 127.5, 127.3, 127.0, 126.9, 126.2, 125.0, 57.1, 56.0, 31.2, 25.5, 24.1.

HRMS Mass (ESI+): m/z = $[M+H]^+$ calc for $C_{17}H_{18}F_3N$ 294.1464, found 294.1468.

1-(4-methoxyphenyl)-*N*-(1-phenylethyl)ethanamine *(R,R)*-X14

This product was purified with a 7:3 hexane/ethyl acetate mixture as eluent.

^{1}H-NMR (300 MHz, $CDCl_3$): δ 7.40-7.21 (m, 5H), 7.13 (d, 2H), 6.88 (d, 2H), 3.85 (s, 3H), 3.52 (m, 3H), 1.32 (s, 6H).

^{13}C-NMR (75 MHz, $CDCl_3$): δ 148.0, 139.0, 128.5, 128.3, 127.1, 126.0, 125.8, 118.0, 55.1, 55.0, 54.1, 27.5, 23.1.

HRMS Mass (ESI+): m/z $[M+H]^+$ calc for $C_{17}H_{21}NO$ 256.1696, found 256.1703, 278.1523$[M + Na]^+$.

The enantiomeric excess was determined by chiral HPLC with Chiralcel OD-H column [eluent: 99:1 Hex/IPA; 0.8 mL/min flow rate, detection: 210 nm; t_R 6.5 min (major), t_R 7.4 min (minor).

1-(naphthalen-2-yl)-N-(1-phenylethyl)ethanamine *(R,R)*-X15

This product was purified with a 8:2 hexane/ethyl acetate mixture as eluent.

^{1}H-NMR (300 MHz, $CDCl_3$): δ 7.88-7.81 (m, 3H), 7.63-7.26 (m, 9H), 3.73 (q, 1H), 3.57 (q, 1H), 1.40 (m, 6H).

^{13}C-NMR (75 MHz, $CDCl_3$): δ 138.1, 137.0, 129.0, 128.8, 128.7, 128.0,127.9, 127.5, 126.5, 126.4, 124.4, 123.2, 122.7, 122.5, 55.5, 55.5, 54.1, 25.5, 25.3.

HRMS Mass (ESI+): m/z = $[M+H]^+$ calc for $C_{20}H_{21}N$ 276.1747, found 276.1754, 298.1571$[M + Na]^+$.

1-phenyl-N-(1-(thiophen-2-yl)ethyl)ethanamine *(R,R)*-X16

This product was purified with a 9:1 hexane/ethyl acetate mixture as eluent.

^{1}H-NMR (300 MHz, $CDCl_3$): δ 7.36-7.2 (m, 6H), 6.95-6.8 (m, 2H), 3.83 (q, 1H), 3.71 (q, 1H), 1.41 (d, 3H), 1.33 (d, 3H).

^{13}C-NMR (75 MHz, $CDCl_3$): δ 141.1, 127.2, 126.6, 126.5, 126.3, 125.9,125.8, 123.0, 55.2, 50.1, 25.3, 24.3.

HRMS Mass (ESI+): m/z = $[M+H]^+$ calc for $C_{14}H_{17}NS$ 232.1154, found 232.1161, 254.0980$[M + Na]^+$.

The enantiomeric excess was determined by chiral HPLC with Chiralcel OD-H column [eluent: 99:1 Hex/IPA; 0.8 mL/min flow rate, detection: 210 nm; t_R 5.7 min (major), t_R 6.1 min (minor).

3-Methyl-*N*-(1-phenylethyl)butan-2-amine *(R,R)*-X18

This product is known[256] and it was purified with heptane/EtOAc/NH_4OH = 86:10:4 as eluent.

^{1}H-NMR (300 MHz, $CDCl_3$): 7.31-7.2 (m, 5H), 3.9 (q, 1H), 2.5 (m, 1H), 1.7 (m, 1H), 1.30 (d, 3H), 0.82-0.86 (m, 9H).

The enantiomeric excess was determined by analysis of the acetamide obtained by reaction of the isolated amine with acetic anhydride at room temperature for 12 hours.

The enantiomeric excess was determined by chiral HPLC with Chiralcel OD-H column [eluent: 95:5 Hex/IPA; 0.8 mL/min flow rate, detection: 210 nm; t_R 10.6 min (major), t_R 16.1 min (minor).

Methyl 2-phenyl-2-(1-phenylethylamino)acetate X24

This product is known[257] and it was purified with a 9:1 hexane/ethyl acetate mixture as eluent.

***(R,R)*-X24**

^{1}H-NMR (300 MHz, $CDCl_3$): δ 7.4-7.29 (m, 10H), 4.22 (s, 1H), 3.85 (m, 1H), 3.7 (s, 1H), 1.39 (d, 3H).

***(S,R)*-X24**

^{1}H-NMR (300 MHz, $CDCl_3$): δ 7.4-7.29 (m, 10H), 4.19 (s, 1H), 3.6 (s, 3H), 3.55 (q, 1H), 1.34 (d, 3H).

Bibliography

[01] Anastas P. T., Warner J. C., *Green Chemistry: Theory and Practice,* Oxford University Press: New York, **1998**.

[02] Dalko P. I., Moisan L., *Angew. Chem. Int. Ed.* **2004**, *43*, 5138-5175

[03] (a) Trost M. B., *Science* **1991**, *254*, 1471-1477; (b) Trost M. B., *Angew. Chem. Int. Ed. Engl.* **1995**, *34*, 259-281.

[04] Blaser H.U., *Chem. Comm.* **2003**, 293-296.

[05] (a) Federsel H.- J., *Drug News Perspectives* **2008**, *21*, 193-199; (b) Federsel H.- J., *Acc. Chem. Res.* **2009**, *42*, 671-680.

[06] Blaser H. U., Schmidt, E. (eds.), *Asymmetric Catalysis on Industrial Scale*, Wiley – VCH, Weinheim, **2004**.

[07] von Liebig J., *Justus Liebigs Ann. Chem.* **1860**, *113*, 246-247.

[08] Langenbeck W., *Angew. Chem.* **1932**, *45*, 97-99.

[09] Bredig G., Fiske W. S., *Biochem. Z.* **1912**, *7*, 46.

[10] (a) Pracejus H., *Justus Liebigs Ann. Chem.* **1960**, *634*, 9-22; (b) Pracejus H., Mätje H., *J. Prakt. Chem.* **1964**, *24*, 195-205.

[11] (a) Eder U., Sauer G., Wiechert R., *Angew. Chem. Int. Ed. Engl.* **1971**, *10*, 496-497; (b) Hajos Z. G., Parrish D. R., *J. Org. Chem.* **1974**, *39*, 1615-1621.

[12] Pellissier H., *Tetrahedron*, **2007**, *63*, 9267-9331.

[13] (a) Benaglia M., Puglisi A., Cozzi F., *Chem. Rev.* **2003**, *103*, 3401-3430; (b) Cozzi F., *Adv. Synth. Catal.* **2006**, *348*, 1367-1390.

[14] Ramon D. J., Yus M., *Angew. Chem. Int. Ed.* **2005**, *44*, 1602-1634.

[15] Pellissier H., *Tetrahedron* **2006**, *62*, 1619-1665.

[16] Wasilke J.-C., Obrey S. J., Baker R. T., Bazan G. C., *Chem. Rev.* **2005**, *105*, 1001.

[17] Padwa A., Weingarten M. D., *Chem. Rev.* **1996**, *96*, 223-269.

[18] Berkessel A., Gröger H. (eds.), *Asymmetric Organocatalysis: From Biomimetic Concepts to Applications in Asymmetric Synthesis*, Wiley – VCH, Weinheim, **2005**.

[19] (a) Dalko P. I., Moisan L., *Angew. Chem. Int. Ed.* **2001**, *40*, 3726-3748; (b) Houk K. N., List B. (eds.), "Special Issue: Asymmetric Organocatalysis", *Acc. Chem. Res.* **2004**, *37*, 487-631; (c) Seayad J., List B., *Org. Biomol. Chem.* **2005**, *3*, 719-724; (e) List B., *Chem. Comm.* **2006**, 819-824.

[20] Gaunt M. J., Johansson C. C. C., McNally A., Vo N. T., *Drug Discovery Today* **2007**, *12*, 8-27.

[21] Agami C., Puchot C., Sevestre H., *Tetrahedron Lett.* **1986**, *27*, 1501-1504.

[22] Schmid M. B., Zeitler K., and Gschwind R. M., *Angew. Chem. Int. Ed*. **2010**, *49*, 4997–5003

[23] (a) List B., Lerner R. A., Barbas III C. F., *J. Am. Chem. Soc.* **2000**, *122*, 2395-2396; (b) Northrup A. B., MacMillan D. W. C, *J. Am. Chem. Soc.* **2002**, *124*, 6798-6799.

[24] Notz W., Tanaka F., Watanabe S., Chowdari N. S., Turner J. M., Thayumanavan R., Barbas III C. F., *J. Org. Chem.* **2003**, *68*, 9624-9634.

[25] (a) List B., Pojarliev P., Martin H. J., *Org. Lett.* **2001**, *3*, 2423-2425; (b) Enders D., Seki A., *Synlett.* **2002**, 26-28.

[26] List B., *Acc. Chem. Res.* **2004**, *37*, 548-557.

[27] (a) List B., *J. Am. Chem. Soc.* **2002**, *124*, 5656-5657; (b) Kumaragurubaran N., Juhl K., Zhuang W., Bøgevig A., Jørgensen K. A., *J. Am. Chem. Soc.* **2002**, *124*, 6254.

[28] Brown S. P., Brochu M. P., Sinz C. J., MacMillan D. W. C., *J. Am. Chem. Soc.* **2003**, *125*, 10808-10809.

[29] Vignola N., List B., *J. Am. Chem. Soc.* **2004**, *126*, 450-451.

[30] Brochu M. P., Brown S. P., MacMillan D. W. C., *J. Am. Chem. Soc.* **2004**, *126*, 4108-4109.

[31] Hechavarria Fonseca M. T., List B., *Angew. Chem. Int. Ed.* **2004**, *43*, 3958-3960.

[32] Ahrendt K. A., Borths C. J., MacMillan D. W. C., *J. Am. Chem. Soc.* **2000**, *122*, 4243-4244.

[33] Jen W. S., Wiener J. J. M., MacMillan D. W. C., *J. Am. Chem. Soc.* **2000**, *122*, 9874-9875.

[34] Paras N. A., MacMillan D. W. C., *J. Am. Chem. Soc.* **2001**, *123*, 4370-4371.

[35] Austin J. F., MacMillan D. W. C., *J. Am. Chem. Soc.* **2002**, *124*, 1172-1173.

[36] Paras N. A., MacMillan D. W. C., *J. Am. Chem. Soc.* **2002**, *124*, 7894-7895.

[37] Brown S. P., Goodwin N. C., MacMillan D. W. C., *J. Am. Chem. Soc.* **2003**, *125*, 1192-1194.

[38] Ouellet S. G., Tuttle J. B., MacMillan D. W. C., *J. Am. Chem. Soc.* **2005**, *127*, 32.

[39] (a) Yamaguchi M., Shiraishi T., Hirama M. J., *J. Org. Chem.* **1996**, *61*, 3520-3530; (b) Halland N., Aburel P. S., Jørgensen K. A., *Angew. Chem. Int. Ed.* **2003**, *42*, 661.

[40] (a) Hanessian S., Pham, V., *Org. Lett.* **2000**, *2*, 2975-2978; (b) Halland N., Hazell R. G., Jørgensen K. A., *J. Org. Chem.* **2002**, *67*, 8331-8338.

[41] (a) Huang Y., Walji A. M., Larsen C. H., MacMillan D. W. C., *J. Am. Chem. Soc.* **2005**, *127*, 15051-15053; (b) Marigo M., Schulte T., Franzén J., Jørgensen K. A., *J. Am. Chem. Soc.* **2005**, *127*, 15710-15711.

[42] Dolling U.-H., Davis P., Grabowski E. J. J., *J. Am. Chem. Soc.* **1984**, *106*, 446-447.

[43] (a) O'Donnell M. J., Bennett W. D., Wu S., *J. Am. Chem. Soc.* **1989**, *111*, 2353-2355; (b) O'Donnell M. J., *Acc. Chem. Res.* **2004**, *37*, 506-517.

[44] (a) Lygo B., Wainwright P. G., *Tetrahedron Lett.* **1997**, *38*, 8595-8598; (b) Corey E. J., Xu F., Noe M. C., *J. Am. Chem. Soc.*, **1997**, *119*, 12414-12415.

[45] (a) Ooi T., Doda K., Maruoka K., *J. Am. Chem. Soc.* **2003**, *125*, 9022-9023; (b) Maruoka K, Ooi T., *Chem. Rev.*, **2003**, *103*, 3013-3028.

[46] France S., Guerin D. J., Miller S. J., Lectka T., *Chem. Rev.* **2003**, *103*, 2985-3012.

[47] McDaid P., Chen Y., Deng L., *Angew. Chem. Int. Ed.* **2002**, *41*, 338-340.

[48] (a) Li H., Wang Y., Tang L., Deng L., *J. Am. Chem. Soc.* **2004**, *126*, 9906-9907; (b) Li H., Song J., Liu X., Deng L., *J. Am. Chem. Soc.* **2005**, *127*, 8948-8949.

[49] (a) Li H., Wang Y., Tang L., Wu F., Liu X., Guo C., Foxman B. M., Deng L., *Angew. Chem. Int. Ed.* **2005**, *44*, 105-108; (b) Bella M., Jørgensen K. A., *J. Am. Chem. Soc.* **2004**, *126*, 5672-5673.

[50] Basavaiah D., Rao A. J., Satyanarayana T., *Chem. Rev.* **2003**, *103*, 811-892.

[51] Iwabuchi Y., Nakatani M., Yokoyama N., Hatakeyama S., *J. Am. Chem. Soc.* **1999**, *121*, 10219-10220.

[52] Shi M., Xu Y.-M., *Angew. Chem. Int. Ed.* **2002**, *41*, 4507-4510.

[53] Zhu C., Shen X., Nelson S. G., *J. Am. Chem. Soc.* **2004**, *126*, 5352-5353.

[54] France S., Wack H., Hafez A. M., Taggi A. E., Witsil D. R., Lectka T., *Org. Lett.* **2002**, *4*, 1603-1605.

[55] Papageorgiou C. D., Cubillo de Dios M., Ley S. V., Gaunt M. J., *Angew. Chem. Int. Ed.* **2004**, *43*, 4641-4644.

[56] Read de Alaniz J., Rovis T., *J. Am. Chem. Soc.* **2005**, *127*, 6284-6289.

[57] Wurz R. P., Fu G. C., *J. Am. Chem. Soc.* **2005**, *127*, 12234-12235.

[58] (a) Schreiner P. R., *Chem. Soc. Rev.* **2003**, *32*, 289-296; (b) Pihko P. M., *Angew. Chem. Int. Ed.* **2004**, *43*, 2062-2064.

[59] Jacobsen E. N., Taylor M. S., *Angew. Chem. Int. Ed.* **2006**, *45*, 1520-1543.

[60] (a) Hine J., Linden S. M., Kanagasabapathy V. M., *J. Org. Chem.* **1985**, *50*, 5096-5099; (b) Hine J., Ahn K., *J. Org. Chem.* **1987**, *52*, 2083-2086.

[61] Kelly T. R., Meghani P., Ekkundi V. S., *Tetrahedron Lett.* **1990**, *31*, 3381-3384.

[62] Etter M. C., Urbanczyk-Lipkowska Z., Zia-Ebrahimi M., Panunto T. W., *J. Am. Chem. Soc.* **1990**, *112*, 8415-8426.

[63] Curran D. P., Lung H. K., *Tetrahedron Lett.* **1995**, *36*, 6647-6650.

[64] Schreiner P. R., Wittkopp A., *Org. Lett.* **2002**, *4*, 217-220.

[65] (a) Sigman M. S., Jacobsen E. N., *J. Am. Chem. Soc.* **1998**, *120*, 4901-4902; (b) Vachal P., Jacobsen E. N., *Org. Lett.* **2000**, *2*, 867-870; (c) Wenzel A. G., Jacobsen E. N., *J. Am. Chem. Soc.* **2002**, *124*, 10012-10014; (d) Joly G. D., Jacobsen E. N., *J. Am. Chem. Soc.* **2004**, *126*, 4102-4103; (e) Taylor M. S., Jacobsen E. N., *J. Am. Chem. Soc.* **2004**, *126*, 10558-10559; (f) Taylor M. S., Tokunaga N., Jacobsen E. N, *Angew. Chem. Int. Ed.* **2005**, *44*, 6700-6704.

[66] Okino T., Hoashi Y., Takemoto Y., *J. Am. Chem. Soc.* **2003**, *125*, 12672-12673.

[67] Yamanaka M., Itoh J., Fuchibe K., Akiyama T., *J. Am. Chem. Soc*. **2007**, *129*, 6756-6764.

[68] Reviews about the formation and structure of hypervalent silicon compounds: (a) Tandura S. N., Voronkov M. G., Alekseev N. V., *Top. Curr. Chem* **1986**, *131,* 99; (b) Shklover V. E., Struchov Y.T., Voronkov M. G., *Russ. Chem. Rev* **1989**, *58,* 211; (c) Lukevics E., Pudova O., Sturkovich R., *Molecular Structure of Organosilicon Compounds*; Ellis Horwood: Chichester, **1989**; (d) Holmes R. R., *Chem. Rev* **1996,** *96,* 927.

[69] Gay-Lussac J. L., Thenard L. J., *Mémoires de Physique et de Chimie de la Société d'Arcueil* **1809**, *2,* 17.

[70] (a) Chuit C., Corriu R. J. P., Reye C., Young J. C., *Chem. Rev* **1993**, *93,* 1371; (b) Hosomi A., *Acc. Chem. Res* **1998**, *21,* 200; (c) Furin G. G., Vyazankina O. A., B. Gostevsky A., Vyazankin N. S., *Tetrahedron* **1998**, *44,* 2675.

[71] Rendler S., Oestreich M., *Synthesis* **2005**, *11*, 1727.

[72] Orito Y., Nakajima M., *Synthesis* **2006**, *9*, 1391.

[73] Lewis G. N., *Valence and The Structure of Atoms and Molecules*, Chemical Catalog: New York, **1923**, pp. 141 – 142

[74] Santelli M., Pons J. M., *Lewis Acids and Selectivity in Organic Synthesis*, CRC Press: Boca Raton, FL, **1996**.

[75] (a) Jensen W. B., *The Lewis Acid-Base Concepts*, Wiley-Interscience: New York, **1980**; (b) Jensen W. B., *Chem. Rev.* **1978**, *78*, 1.

[76] Denmark S. E., Beutner G.L., *Angew. Chem. Int. Ed*. **2008**, *47*, 1560.

[77] (a) Musher J. I., *Angew. Chem.* **1969**, *81*, 68; (b) Musher J. I., *Angew. Chem. Int. Ed. Engl.* **1969**, *8*, 54; (c) Curnow O. J., J. *Chem. Educ*. **1998**, *75*, 910.

[78] (a) Gutmann V., *The Donor-Acceptor Approach to Molecular Interactions*, Plenum: New York, **1978**; (b) Gutmann V., *Coord. Chem. Rev.* **1975**, *15*, 207.

[79] Gordon M. S., Carroll M. T., Davis L. P., Burggraf L. W., *J. Phys. Chem*. **1990**, *94*, 8125-8128.

[80] (a) Chuit C., Corriu R. J. P., Reye C., Young J. C., *Chem. Rev*. **1993**, *93*, 1371; (b) Hosomi A., *Acc. Chem. Res*. **1988**, *21*, 200; (c) Furin G. G., Vyazankina O. A., Gostevsky B. A., Vyazankin N. S., *Tetrahedron* **1988**, 44, 2675.

[81] (a) Rendler, S., Oestreich M., *Synthesis* **2005**, *11*, 1727; (b) Orito Y., Nakajima M., *Synthesis* **2006**, *9*, 1391.

[82] For a recent review on hypervalent silicates-mediated reactions see: Benaglia M., Guizzetti S., Pignataro L., *Coord. Chem. Rev.* **2008**, *252*, 492.

[83] (a) Denmark S. E., Wynn T., Beutner G.L., *J. Am. Chem. Soc*. **2002**, *124*, 13405; (b) Denmark S. E., Fan Y., Eastgate M. D., *J. Org. Chem*. **2005**, *70*, 5235.

[84] Rendler S., Oestreich M., *Synthesis* **2005***,* 1727.

[85] For chiral phosphoric acids-mediated reductions see: (a) Connon S. J., *Org. Biomol. Chem.* **2007**, *5*, 3407; (b) Akiyama T., *Chem Rev.* **2007**, *107*, 5744; (c) Terada M., *Chem. Comm.* **2008**, 4098.

[86] Benkeser R. A., Synder D. C. J., *Organomet. Chem*. **1982**, *225*, 107.

[87] Kobayashi S., Yasuda M., Hachiya I., *Chem. Lett.* **1996**, 407.

[88] (a) Iwasaki F., Onomura O., Mishima K., Maki T., Matsumura Y., *Tetrahedron Lett*. **1999**, *40,* 7507; (b) Iwasaki F., Onomura O., Mishima K., Kanematsu T., Maki T., Matsumura Y., *Tetrahedron Lett*. **2001**, *42,* 2525.

[89] Malkov A. V., Mariani A., MacDougal K.N, Kočovský P., *Org. Lett.* **2004**, *6*, 2253.

[90] Malkov A.V., Stončius S., MacDougal K. N., Mariani A., McGeoch G. D., Kočovský P., *Tetrahedron* **2006**, 62, 264.

[91] Malkov A. V., Figlus M., Stončius S., Kočovský P., *J. Org. Chem.* **2009**, *74*, 5839.

[92] Malkov A. V., Vranková K., Sigerson R. C., Stončius S., Kočovský P., *Tetrahedron* **2009**, *65*, 9481.

[93] (a) Malkov A. V., Figlus M., Stoncius S., Kocovský P., *J. Org. Chem.* **2007**, *72*, 1315; (b) Malkov A. V., Figlus M., Kocovský P., *J. Org. Chem.* **2008**, *73*, 3985; (c) for another recoverable system see: Malkov A. V., Figlus M., Prestly M. R., Rabani G., Cooke G., Kočovský P., *Chem. Eur. J.* **2009**, *15*, 9651.

[94] Malkov A. V., Stončius S., Kočovský P., *Angew. Chem. Int. Ed.* **2007**, *46*, 3722.

[95] Malkov A. V., Stončius S., Vranková K., Arndt M., Kočovský P., *Chem. Eur. J.* **2008**, *14*, 8082.

[96] Matsumura Y., Ogura K., Kouchi Y., Iwasaki F., Onomura O., *Org. Lett.* **2006**, *17*, 3789-3792.

[97] Zhou L., Wang Z., Wei S., Sun J., *Chem. Comm.* **2007**, 2977-2979.

[98] Baudequin C., Chaturvedi D. , Tsogoeva S. B., *Eur. J. Org. Chem*. **2007**, 2623.

[99] Wang Z. Y., Wei S., Wang C., Sun J., *Tetrahedron*: *Asymmetr*y **2007**, *18*, 705.

[100] Wang Z., Ye X., Wei S., Wu P., Zhang A., Sun J., *Org. Lett.* **2006**, *5*, 999.

[101] Wang Z., Cheng M., Wu P., Wei S., Sun J., *Org. Lett.* **2006**, *14*, 3045.

[102] Zhang Z., Rooshenas P., Hausmann H., Schreiner P. R., *Synthesis* **2009**, *9*, 1531.

[103] Onomura O., Kouchi Y., Iwasaki F., Matsumura Y., *Tetrahedron Lett*. **2006**, *47*, 3751-3754.

[104] Guizzetti S., Benaglia M., European Patent Application November 30 2007; PCT/EP/2008/010079, Nov. 27, 2008. WO2009068284 (A2)**,** 2009-06-04.

[105] Zheng H., Deng J., Lin W., Zhang X., *Tetrahedron Lett.* **2007**, *48*, 7934.

[106] Guizzetti S., Benaglia M., Annunziata R., Cozzi F., *Tetrahedron,* **2009**, *65*, 6354.

[107] Guizzetti S., Benaglia M., European Patent Appl. n.EP07023240.0, Sept 22, **2008**.

[108] Wang C., Wu X., Zhou L., Sun J., *Chem. Eur. J.* **2008**, *14*, 8789.

[109] Guizzetti S., Biaggi C., Benaglia M., Celentano G., *Synlett* **2010**, 134.

[110] Guizzetti S., Benaglia M., Rossi S., *Org. Lett.,* **2009**, *11*, 2928.

[111] Guizzetti S., Benaglia M., Cozzi F., Rossi S., Celentano G., *Chirality* **2009**, *21,* 233-238.

[112] Guizzetti S., Benaglia M., Celentano G., *Eur. J. Org. Chem.* **2009**, 3683.

[113] Xue Z.-Y., Jiang Y., Yuan W.-C.,. Zhang X.-M, *Eur. J. Org. Chem.* **2010**, 616.

[114] Zheng H.-J., Chen W.-B., Wu Z.-J., Deng J.-G., Lin W.-Q., Yuan W.-C., Zhang X.-M., *Chem. Eur. J.* **2008,** *14*, 9864.

[115] Malkov A. V., Liddon A. J. P. S., Ramírez-López P., Bendová L., Haigh D., Kočovský P., *Angew. Chem. Int. Ed.* **2006**, *45*, 1432.

[116] Pei D., Wang Z., Wei S., Zhang Y., Sun J., *Org. Lett.* **2006**, *25*, 5913.

[117] Pei D., Wang Z., Wei S., Wang M., Sun J., *Adv. Synth. Catal.* **2008**, *350*, 619.

[118] Sugiura M., Sato N., Kotani S., Nakajima M., *Chem. Comm.* **2008**, 4309-4311.

[119] Sugiura M., Kumahara M., Nakajima M., *Chem. Comm.* **2009**, 3585-3587.

[120] Colombo F., Benaglia M., Annunziata R., *Tetrahedron Lett.* **2007,** *46,* 2687.

[121] Ogawa C., Sugiura M., Kobayashi S., *Angew. Chem. Int. Ed***. 2004**, *43*, 6491.

[122] The adddition of allyltrichlorosilane to *N*-acylhydrazones promoted by stoichiometric amount of a chiral sullfoxide was also reported: (a) Kobayashi S., Ogawa C., Konishi H., Sugiura M, *J. Am. Chem. Soc.* **2003**, *125,* 6610; (b) Garcia-Flores F., Flores-Michel L. S., Juaristi E., *Tetrahedron Lett.* **2006**, *47*, 8235. For the use of a chiral allyl silane reagents see Rabbat P. M. A., Corey Valdez S., Leighton J. L., *Org. Lett.* **2006**, *8*, 6119.

[123] For a review on silver catalyzed asymmetric allylation see: Yamamoto H., Wadamoto M., *Chem. Asian J.* **2007**, *2*, 692.

[124] Kiyohara H., Nakamura Y., Matsubara R., Kobayashi S., *Angew. Chem. Int. Ed.* **2006**, *45*, 1615.

[125] Fernandes R. A., Yamamoto H., *J. Org. Chem*. **2004***, 64,* 735.

[126] Denmark S. E., Coe D. M., Pratt N. E., Griedel B.D., *J. Org. Chem.* **1994**, 59, 6161.

[127] (a) Denmark S. E., Fu J., Coe D. M., Su X., Pratt N. E., Griedel B. D., *J. Org. Chem***. 2006,** *71,* 1513-1522; (b) Denmark S. E., Fu J., *J. Am. Chem. Soc.* **2000**, *122,* 12021-12022.

[128] Denmark S. E., Fu J., Lawler M. J., *J. Org. Chem.* **2006**, *71,* 1523-1536.

[129] For a microreview about chiral *N*-oxides in asymmetric catalysis see: Malkov A. V., Kočovský P., *Eur. J. Org. Chem*. **2007**, 29.

[130] Nakajima M., Saito M., Shiro M., Hashimoto S., *J. Am. Chem. Soc.* **1998**, *120,* 6419-6420.

[131] Shimada T., Kina A., Ikeda S., Hayashi T., *Org. Lett.* **2002**, *4,* 2799.

[132] Hrdina R., Valterova I., Hodacova J., Cisarova I., Kotora M., *Adv. Synth. Catal.* **2007**, *349,* 822.

[133] (a) Malkov A.V., Orsini M., Pernazza D., Muir K.W., Langer V., Meghani P., Kocovsky P., *Org. Lett.* **2002,** *4,* 1049; (b) Malkov A.V., Bell M., Orsini M., Pernazza D., Massa A., Herrmann P., Meghani P., Kocovsky P., *J. Org. Chem.* **2003**, *68,* 9659.

[134] Malkov A.V., Bell M., Castelluzzo F., Kocovsky P., *Org. Lett.* **2005**, *7,* 3219.

[135] Malkov A. V., Dufkovà A., Farrugia L., Kocovsky P., *Angew. Chem. Int. Ed.* **2003***, 42,* 3674.

[136] Traverse J. F., Zhao Y., Hoveyda A. H., Snapper M. L., *Org. Lett.* **2005,** *7,* 2799.

[137] Simonini V., Benaglia M., Guizzetti S., Pignataro L., Celentano G., *Synlett,* **2008**, 1061-1065.

[138] (a) Pignataro L., Benaglia M., Cinquini M., Cozzi F., Celentano G., *Chirality* **2005**, *17,* 396; (b) Wong W.-L., Lee C.-S., Leung H.-K., Kwong H.-L., *Org. Biomol. Chem.* **2004**, *2,* 1967.

[139] Chelucci G., Belmonte N., Benaglia M., Pignataro L., *Tetrahedron Lett.* **2007**, *48,* 4037-4041.

[140] Pignataro L., Benaglia M., Annunziata R., Cinquini M., Cozzi F., *J. Org. Chem*. **2006**, *71,* 1458.

[141] Nakajima M., Kotani S., Ishizuka T., Hashimoto S., *Tetrahedron Lett.* **2005**, *46*, 157-161.

[142] Simonini V., Benaglia M., Benincori T., *Adv. Synth. Catal.* **2008**, *350,* 561.

[143] Denmark S. E., Stavenger R. A., *Acc. Chem. Res***. 2000**, *33,* 432.

[144] Denmark S. E., Winter S.B., Su X., Wong K.T., *J. Am. Chem. Soc.* **1996**, *118,* 7604.

[145] Denmark S. E., Pham S. M., *J. Org. Chem.* **2003**, *68,* 5045.

[146] Denmark S. E., Fan Y., *J. Am. Chem. Soc.* **2002**, *124,* 4233.

[147] Nakajima M., Yokota T., Saito M., Hashimoto S., *Tetrahedron Lett.* **2004**, *45,* 61.

[148] Kotani S., Hashimoto S., Nakajima M., *Synlett* **2006**, 1116.

[149] Denmark S. E., Barsanti P. A., Wong K.-T., Stavenger R. A., *J. Org. Chem.* **1998**, *63,* 2428.

[150] Denmark S. E., Barsanti P. A., Beutner G. L., Wilson T.W., *Adv. Synth. Catal.* **2007**, *349,* 567.

[151] Tao B., Lo M. M.-C., Fu G. C., *J. Am. Chem. Soc.* **2001**, *123,* 353

[152] Tokuoka E., Totani S., Matsunaga H., Ishizuka T., Hashimoto S., Nakajima M., *Tetrahedron Asymmetry* **2005***, 16,* 2391.

[153] Pu X., Qi X., Ready J. M,, *J. Am. Chem. Soc.* **2009**, *131*, 10364.

[154] Kobayashi S., Nishio K., *J. Am. Chem. Soc.* **1995**, *117,* 6392.

[155] Nakajima M., Saito M., Hashimoto S., *Tetrahedron Asymmetry* **2002**, *13,* 2449.

[156] (a) Normant H., *Russ. Chem. Rev. (Engl. Transl.)* **1970**, *39*, 457. (b) Reichardt C., *Solvents and Solvent Effects in Organic Chemistry*, VCH: Germany, **1988**.

[157] Luteri G. F., Ford W. T., *J. Org. Chem.* **1977**, *42*, 820.

[158] Denmark S. E, Stavenger R.A., *J. Am. Chem. Soc*. **2000**, 122, 8837-8847.

[159] Denmark S. E., Bui T., *J. Org. Chem.* **2005**, *70*, 10393-10399.

[160] (a) Arcoria A., Ballistreri F. P., Tomaselli G. A., Di Furia F., Modena G., *J. Org. Chem.* **1986**, *51*, 2374. (b) Bortolini O., Di Furia F., Modena G., Schionato A., *J. Mol. Catal.* **1986**, *35*, 47. (c) Wilson S. R., Price M. F., *Synth. Commun*. **1982**, *12*, 657. (d) Iseki K., Kuroki Y., Takahashi M., Kishimoto S., Kobayashi Y., *Tetrahedron* **1997**, *53*, 3513.

[161] Rossi S., *Design and synthesis of chiral Lewis bases and their use in stereoselective reactions,* **2007**.

[162] Lopez F., Minnaard A. J. and Feringa B.L., *Acc. Chem. Res*. **2007**, *40*, 179-188.

[163] (a) Methot J. L., Roush W. R., *Adv. Synth. Catal.* **2004**, *346*, 1035-1050; (b) Ye L.-W., Zhou J., Tang Y., *Chem. Soc. Rev.* **2008**, 37, 1140.

[164] Cowen B. J., Miller S. J., *J. Am. Chem. Soc.* **2007**, *129*, 10988-10989.

[165] For the few examples of organocatalytic reactions with aliphatic amines-*N*-oxides see: (a) Traverse J.F., Zhao Y., Hoveyda A.H., Snapper M.L., *Org. Lett.* **2005**, 7, 3151-3153; (b) Qin B., Liu X., Shi J., Zheng K., Zhao H., Feng X., *J. Org. Chem*. **2007**, *72*, 2374.

[166] (a) Li Y.-M., Kwong F.-Y., Yu W.-Y., Chan A. S. C., *Coord. Chem. Rev*. **2007**, *251*, 2119-2144; (b) Thommen M., Blaser H. U., *Phosphorus Ligands in Asymmetric Catalysis*, **2008**, *3*, 1457-1471.

[167] Grushin V. V., *Chem. Rev*. **2004**, *104*, 1629-1662.

[168] Denmark S. E., Fu J., *Chem. Rev.*, **2003**, *103*, 2763.

[169] Kotani S., Hashimoto S., Nakajima M., *Tetrahedron* **2007**, *63*, 3122-3132.

[170] Nakanishi K., Kotani S., Sugiura M., Nakajima M., *Tetrahedron* **2008**, *64*, 6415.

[171] (a) Carreria E. M., Lee W., Singer R. A., *J. Am. Chem. Soc.* **1995**, *117*, 3649; (b) Ruck R. T., Jacobsen E. N., *J. Am. Chem. Soc.* **2002**, *124*, 2882.

[172] a) Sodeoka M., Tokunoh R., Miyazaki F., Hagiwara E., Shibasaki M., *Synlett* **1997**, 463-466; (b) Yanagisawa A., Matsumoto Y., Nakashima H., Asakawa K., Yamamoto H. J., *J. Am. Chem. Soc.* **1997**, *119*, 9319.

[173] (a) Sakthivel K., Notz W., Bui T., Barbas III C. F., *J. Am. Chem. Soc.* **2001**, *123*, 5260-5267; (b) List B., Pojarliev P., Castello C., *Org. Lett.* **2001**, *3*, 573.

[174] Denmark S. E., Wynn T., *J. Am. Chem. Soc*., **2001**, *123*, 25, 6199-6200.

[175] Denmark S. E., Beutner G. L., *J. Am. Chem. Soc.* **2003**, *125*, 26, 1038-1039.

[176] Denmark S. E, Heemstra Jr J. R., *J. Am. Chem. Soc.* **2006**, *128*, 1028.

[177] Kotani S., Shimoda Y., Sugiura M., Nakajima M., *Tetrahedron Lett*. **2009**, *50*, 4602-4605.

[178] Hamashima Y., Kanai M., Shibasaki M., *J. Am. Chem. Soc.* **2000**, *122*, 7412-7413.

[179] Hamashima Y., Kanai M., Shibasaki M., *Tetrahedron Lett*., **2001**, *42*, 691-694.

[180] Hamashima Y., Sawada D., Nogami H., Kanai M., Shibasaki M., *Tetrahedron* **2001**, *57*, 805-811.

[181] Chemi S.p.a. Via dei Lavoratori, 20092 Cinisello Balsamo, Italy.

[182] Benincori T, Cesarotti E, Piccolo O, Sannicolò F, *J. Org. Chem.* **2000**, *65*, 2043.

[183] For recent ^{29}Si and ^{31}P NMR studies in the field see: Denmark S. E., Eklov B. M., *Chem. Eur. J.,* **2008**, *14*, 234-239.

[184] Halgren T. A., *J. Comput. Chem*, **1996,** *14*, 490.

[185] MOPAC2009, Stewart J. J. P, Stewart Computational Chemistry, Colorado Springs, CO, USA, http://OpenMOPAC.net, 2008.

[186] (a) Yamada Y. M. A., Yoshikawa N., Sasai H., Shibasaki M., *Angew. Chem. Int. Ed.* **1997**, *36*, 1871–1873; (b) Shibasaki M., Yoshikawa N., *Chem. Rev*. **2002**, *102*, 2187–2210; (c) Shibasaki M., Matsunaga S., *Chem. Soc. Rev*. **2006**, *35*, 269–279.

[187] (a) Notz W., Tanaka F., Barbas C. F., *Acc. Chem. Res*. **2004**, *37*, 580–591; (b) Mukherjee S., Yang J. W., Hoffmann S., List B., *Chem. Rev.* **2007**, *107*, 5471.

[188] Bordwell F. G., Fried H. E., *J. Org. Chem*. **1991**, *56*, 4218.

[189] (a) O3Hagan D., *The polyketide metabolites,* E. Horwood: Chichester, UK, **1991**; (b) Pfeifer B. A., Khosla C., *Microbiol. Mol. Biol. Rev*. **2001**, *65*, 106.

[190] Orlandi S., Benaglia M., Cozzi F., *Tetrahedron Lett*. **2004**, *45*, 1747.

[191] (a) Magdziak D., Lalic G., Lee H. M., Fortner K. C., Aloise A. D., Shair M. D., *J. Am. Chem. Soc.* **2005**, *127*, 7284; (b) Lalic G., Aloise A. D., Shair M. D., *J. Am. Chem. Soc.* **2003**, *125*, 2852.

[192] Ricci A., Pettersen D., Bernardi L., Fini F., Fochi M., Herrera R. P., Sgarzani V., *Adv. Synth. Catal*. **2007**, *349*, 1037-1040.

[193] Lubkoll J., Wennemers H., *Angew. Chem. Int. Ed*. **2007**, *46*, 6841.

[194] Alonso D.A., Kitagaki S., Utsumi N., Barbas III C. F., *Angew. Chem*. **2008**, *120*, 4664–4667.

[195] Um P.-J., Drueckhammer D.G., *J. Am. Chem. Soc*. **1998**, *120*, 5605.

[196] Utsumi N., Kitagaki S., Barbas III C. F., *Org. Lett.* **2008**, *16*, 3405-3408.

[197] (a) Kosolapoff G. M., Watson R. M., *J. Am. Chem. Soc.* **1951**, *73*, 4101-4102; (b) Williams R. H., Hamilton L. A., *J. Am. Chem. Soc.* **1952**, *74*, 5418-5420. (c) Quin L. D., Anderson H. G., *J. Org. Chem.* **1966**, *31*, 1206-1209.

[198] Unruh J. D., Christenson J. R., *J. Mol. Catal.* **1982**, *14*, 19-34.

[199] Sun X., Zhou L., Li W., Zhang X., *J. Org. Chem*. **2008**, *73*, 1143-1146.

[200] (a) Hirao T., Masunga T., Ohshiro Y., Agawa T., *Synthesis* **1981**, 56; (b) Hirao T., Masunga T., Yamada N., Ohshiro Y., Agawa T., *Bull. Chem. Soc. Jpn*. **1982**, *55*, 909. For an overview on catalytic carbon-heteroatom bond formations, see: Beletskaya I. P., *Pure Appl. Chem.* **1997**, *69*, 471.

[201] Kalek M., Ziadi A., Stawinski J., *Org. Lett.* **2008,** *10*, 4637-4640.

[202] Gooßen L. J., Dezfuli M. K., *Synlett* **2005**, *3*, 445–448.

[203] Sørensen M. D., Blæhr L. K. A, Christensen M. K., Høyer T., Latini S., Hjarnaac P-J. V., Bjorkling F.B., *Bioorg. Med. Chem.* **2003**, *11,* 5461–5484.

[204] Pensak D. A., *Pure and Applied Chemistry*, **1989**, *61*, 601-603.

[205] Born M., Oppenheimer J. R., *Zur Quantentheorie der Molekeln. Annalen der Physik,* **1927**, *84*, 457-484.

[206] Schrödinger E., *Physical Review*, **1926**, *28*, 1049–1070.

[207] Weiner S. J., Kollman P. A., Case D. A., Singh U. C., Ghio C., Alagona G., Profeta S. Jr., Weiner P., *J. Am. Chem. Soc.* **1984**, *106,* 765-784.

[208] Allinger N. L., Miller M. A, Miller M. T. T., and Wertz D. H., *J. Am. Chem. Soc*. **1971**, *93*, 1637.

[209] Brooks B. R., Bruccoleri R. E., Olafson B. D., States D. J., Swaminathan S., Karplus M., *J. Comp. Chem*. **1983**, *4*, 187-217.

[210] Allinger N. L., *J. Amer. Chem. Soc*. **1977**, *99*, 8127-8134.

[211] Casewit C. J., Colwell K. S., Rappé A.K, *J. Am. Chem. Soc*. **1992***, 114,* 10024.

[212] (a) Allinger N. L., Yuh Y. H., Lii J.-H., *J. Am. Chem. Soc.* **1989**, *111*, 8551-8566; (b) Lii J.-H, Allinger N. L., *J. Am. Chem. Soc.* **1989**, *111*, 8566-8576; (c) Lii J.-H., Allinger N. L., *J. Am. Chem. Soc*. **1989**, *111*, 8576-8582.

[213] Morse P. M., *Phys. Rev*., **1929**, *34*, 57-64.

[214] Burkert U., Allinger N. L., *Molecular Mechanic*s *ACS Monograph*, 177. American Chemical Society: Washington D. C. **1982.**

[215] Eliel E. L., Allinger N. L., Angyal S. J., Morrison G. A., *Conformational Analysis*. Wiley- Interscience: New York, **1965.**

[216] (a) Dinur U., Hagler A.T., *New Approaches to Empirical Force Fields* in *Reviews in Computational Chemistry*, vol. 2; (b) Lipkowitz K. B., Boyd D. B. (Eds.). VCH: New York, **1991** pag. 99-164.

[217] (a) Press W. H., Flannery B. P., Teukolsky S. A., Vetterling W.T., *Numerical Recipes in C,* Cambridge University Press: Cambridge, **1988**; (b) Schlick T., *Optimization Methods in Computational Chemistry* in: *Reviews in Computational Chemistry*, Vol. 3; (c) Lipkowitz, K. B., and Boyd, D. B. (Eds.).VCH: New York, **1992**, pag 1-71.

[218] Ponder J. W., Richards F. M., *J. Comp. Chem*. **1987**, *8*, 1016.

[219] Metropolis N., Ulam S., *Journal of the American Statistical Association* **1949**, *44*, 335–341.

[220] Lennard-Jones J. E., *Trans. Faraday Soc.* **1929**, *25*, 668.

[221] Feller D., Davidson E. R., *Basis Sets for Ab Initio Molecular Orbital Calculations and Intermolecular Interactions* in: *Reviews in Computational Chemistry*, Vol. 1. Lipkowitz, K. B., Boyd, D. B. (Eds.). VCH: New York; **1990**, 143.

[222] www.gaussian.com

[223] Pople J., Beveridge D., *Approximate Molecular Orbital Theory*, McGraw-Hill: New York, **1970**.

[224] Pople J., Beveridge D. L., Dobosh P. A., *J. Chem. Phys.* **1967**, *47*, 2026.

[225] Bingham R. C., Dewar M. J. S., Lo D. H., *J. Am. Chem. Soc.* **1975**, *97*, 1285 and *J. Am. Chem. Soc.* **1975**, *97*, 1307.

[226] Dewar M. J. S., Thiel W., *J. Am. Chem. Soc.* **1977**, *99*, 4899 and 4907.

[227] Dewar M. J. S., Zoebisch E. G, Helay E. F., Stewart J. J. P., *J. Am. Chem. Soc.* **1985**, *107,* 3902-3909.

[228] Stewart J. J. P., *J. Comp. Chem*. **1989**, *10,* 209-220.

[229] Young D., *Computational Chemistry*, Wiley-Interscience, **2001**. pg 342, MOPAC.

[230] Stewart J. J. P., *J. Mol. Modeling* **2007**, *13*, 1173-1213.

[231] www.schrodinger.com.

[232] Ruiz-Gomez G., Iglesias M. J., Ruiz M. S., Lopez-Ortiz F., *J. Org. Chem*. **2007**, *72*, 9704-9712.

[233] Kuznetsov V. F., Jefferson G. R., Yap G. P. A., Alper H., *Organometallics,* **2002**, *21*, 4241.

[234] Stuurman N. F., Conradie J., *J. Organomet. Chem.* **2009**, *694*, 259–268.

[235] Casalnuovo A. L., RajanBabu T. V., Timothy J. A., Ayers A., Warrens T. H., *J. Am. Chem. Soc*. **1994**, *116*, 9869-9882.

[236] (a) Watson D. A., Chiu M., Bergman R. G., *Organometallics* **2006**, *25,* 4731-4733; (b) Driver T. G., Harris J. R., Woerpel K. A., *J. Am Chem Soc.* **2007**, *129*, 3836.

[237] Melegari M., *Studi nel campo della catalisi asimmetrica mediata da complessi di osssazoline chirali e da nuovi fosfinossidi chirali*, **2010**.

[238] Bianchini C., Gatteschi D., Giambastiani G., Rios I. G., Ienco A., Laschi F., Mealli C., Meli A., Sorace L., Toti A., Vizza F., *Organometallics* **2007**, *26*, 726-739.

[239] Wipf P., Jung J.-K., *J. Org. Chem.* **2000**, *65,* 6319-6337.

[240] Yao Q., Sheets M., *J. Org. Chem.* **2006**, *71*, 5384–5387.

[241] Bower J. F., Skucas E., Patman R., Krische M. J., *J. Am. Chem. Soc.* **2007**, *129*, 15134–15135.

[242] Samec J. S. M., Bäckvall J.-E., *J. Chem. Eur.* **2002**, *8*, 2955.

[243] Murahashi S., Imada Y., Kawakami T., Harada K., Yonemushi Y., Tomita N., *J. Am. Chem. Soc*. **2002**, *124*, 2888-2889.

[244] Yenikayaa C., Ogretir C., Berber H., *Journal of Molecular Structure: THEOCHEM* **2005***, 713,* 171–177.

[245] Chaloner P.A., Yenikaya C., Hitchcock P.B., Private Communication to the Cambridge Structural Database, deposition number CCDC-231214. CCDC, 12 Union Road, Cambridge, UK, **2004**.

[246] Thibault M.-H., Fontaine F.-G., *Acta Cryst*. **2007,** E63, o2087-o2088.

[247] Juaristi E., Leon-Romo J. L., Reyes A., Escalante J., *Tetrahedron: Asymmetry* **1999**, *10*, 2441-2495.

[248] Alexakis A., Gille S., Prian F., Rosset S., Ditrich K., *Tetrahedron Lett*. **2004**, *45*, 1449-1451.

[249] Nugent T. C., El-Shazly M., Wakchaure V. N., *J. Org. Chem.* **2008**, *73*, 1297.

[250] Kanai M., Yasumoto M., Kuriyama Y., Inomiya K., Katsuhara Y., Higashiyama K., Ishii A., *Org. Lett*. **2003**, *5*, 1007.

[251] Ma J.-A., *Angew. Chem. Int. Ed*. **2003**, *42*, 4290.

[252] (a) Tang W., Zhang X., *Chem. Rev.* **2003**, *103*, 3029; (b) Shang G., Yang Q., Zhang X., *Angew. Chem. Int. Ed*. **2006**, *45*, 6360.

[253] Ouellet S. G., Walji A., MacMillan D. W. C., *Acc. Chem. Res.* **2007**, *40*, 1327.

[254] Li G., Liang Y., Antilla J. C., *J. Am. Chem. Soc*. **2007**, 129, 5830.

[255] Yamaguchi R., Kawagoe S., Asai C., Fujita K., *Org. Lett.* **2008**, *10*, 181-184.

[256] Nugent T.C., Wakchaure V.N., Ghosh A.K., Mohanty R.R., *Org. Lett*. **2005**, *7*, 4967-4970.

[257] Kanai M., Yasumoto M., Kuriyama Y., Inomiya K., Katsuhara Y., Higashiyama K., Ishii A., *J. Chem. Soc. Perkin Trans I*, **1996**, *10*, 2880.

LIST OF COMMON ABBREVIATIONS

Ac	Acetyl
acac	Acetylacetonate
Ac_2O	Acetic anhydride
AcOEt	Ethyl acetate
AcOH	Acetic acid
aq.	Aqueous
Ar	Aromatic
BINAM	1,1’-binaphthyl-2,2'-diamine
BINAP	2,2’-bis(diphenylphosphanyl)-1,1’-binaphthyl
BINAPO	2,2’-bis(diphenylphosphanyl)-1,1’-binaphthyl *P*-dioxide
BINOL	1,1’-bi-2,2’-naphthol
cat.	Catalyst
°C	Temperature in degrees Centigrade
d	Day (days)
DABCO	1,4-diazabicyclo[2.2.2]octane
DBU	1,8-Diazabicycloundec-7-ene
DCM	dichloromethane
DEA	Diethylamine
DIPA	*N,N*-diisopropyldiamine
DIPEA	*N,N*-diisopropylethyldiamine

DMAP	4-Dimethylaminopyridine
DME	Dimethoxyethane
DMSO	Dimethylsulfoxide
EDC	1-Ethyl-3-(3-dimethylaminopropyl)carbodiimide
ee	Enantiomeric excess
Et	Ethyl
eq	Equivalent (equivalents)
EVE	ethyl vinyl ether
h	Hour (hours)
HMPA	hexamethylphosphoric triamide
HOBt	Hydroxybenzotriazole
IPA	isopropanol alcohol
LDA	Lithium diisopropylamide
m-CPBA	*meta*-Chloroperbenzoic acid
Me_2-BINAM	*N*,*N*-dimethyl-1,1'-binaphthyl-2,2'-diamine
MMP-TetraMe-BITIOPO	2,2',5,5'-TetraMethyl-4,4'-bis(4-Methoxy-3,5-diMethylPhenyl Phoshino)-3,3'-bithiophene P-Oxide
MPP-TetraMe-BITIOPO	2,2',5,5'-TetraMethyl-4,4'-bis(3,5-diMethylPhenylPhoshino)-3,3'-bithiophene P-Oxide
NBS	*N*-Bromosuccinimide
NIS	*N*-Iodosuccinimide
NMM	*N*-methylmorpholine
PMP	*p*-methoxy-phenyl
PMP- TetraMe-BITIOPO	2,2',5,5'-TetraMethyl-4,4'-bis(p-MethoxyPhenylPhosphino)-3,3'-bithiophene P-Oxide
Py	piridine
rac	racemic

RT	Room temperature
TBAF	Tetra-*n*-butylammonium fluoride
TBAI	Tetra-*n*-butylammonium iodide
TEA	Triethylamine
TetraMe-BITIOP	2,2',5,5'-tetramethyl-4,4'-bis(diphenylphosphino)-3,3'-bithiophene
TetraMe-BITIOPO	2,2',5,5'-tetramethyl-4,4'-bis(diphenylphosphino)-3,3'-bithiophene *P*-dioxide
THF	Tetrahydrofurane
TS	Transition state